NUREG/CR–4550
SAND86–2084
Vol. 4, Rev. 1, Part 3

Analysis of Core Damage Frequency: Peach Bottom, Unit 2 External Events

Prepared by
J. A. Lambright, M. P. Bohn, S. L. Daniel, J. J. Johnson, M. K. Ravindra,
P. O. Hashimoto, M. J. Mraz, W. H. Tong, D. A. Brosseau

Sandia National Laboratories
Operated by
Sandia Corporation

Prepared for
U.S. Nuclear Regulatory Commission

AVAILABILITY NOTICE

Availability of Reference Materials Cited in NRC Publications

Most documents cited in NRC publications will be available from one of the following sources:

1. The NRC Public Document Room, 2120 L Street, NW, Lower Level, Washington, DC 20555

2. The Superintendent of Documents, U.S. Government Printing Office, P.O. Box 37082, Washington, DC 20013-7082

3. The National Technical Information Service, Springfield, VA 22161

Although the listing that follows represents the majority of documents cited in NRC publications, it is not intended to be exhaustive.

Referenced documents available for inspection and copying for a fee from the NRC Public Document Room include NRC correspondence and internal NRC memoranda; NRC Office of Inspection and Enforcement bulletins, circulars, information notices, inspection and investigation notices; Licensee Event Reports; vendor reports and correspondence; Commission papers; and applicant and licensee documents and correspondence.

The following documents in the NUREG series are available for purchase from the GPO Sales Program: formal NRC staff and contractor reports, NRC-sponsored conference proceedings, and NRC booklets and brochures. Also available are Regulatory Guides, NRC regulations in the *Code of Federal Regulations*, and *Nuclear Regulatory Commission Issuances*.

Documents available from the National Technical Information Service include NUREG series reports and technical reports prepared by other federal agencies and reports prepared by the Atomic Energy Commission, forerunner agency to the Nuclear Regulatory Commission.

Documents available from public and special technical libraries include all open literature items, such as books, journal and periodical articles, and transactions. *Federal Register* notices, federal and state legislation, and congressional reports can usually be obtained from these libraries.

Documents such as theses, dissertations, foreign reports and translations, and non-NRC conference proceedings are available for purchase from the organization sponsoring the publication cited.

Single copies of NRC draft reports are available free, to the extent of supply, upon written request to the Office of Information Resources Management, Distribution Section, U.S. Nuclear Regulatory Commission, Washington, DC 20555.

Copies of industry codes and standards used in a substantive manner in the NRC regulatory process are maintained at the NRC Library, 7920 Norfolk Avenue, Bethesda, Maryland, and are available there for reference use by the public. Codes and standards are usually copyrighted and may be purchased from the originating organization or, if they are American National Standards, from the American National Standards Institute, 1430 Broadway, New York, NY 10018.

DISCLAIMER NOTICE

NUREG/CR-4550
SAND86-2084
Vol. 4, Rev. 1, Part 3

Analysis of Core Damage Frequency: Peach Bottom, Unit 2 External Events

Manuscript Completed: August 1990
Date Published: December 1990

Prepared by
J. A. Lambright, M. P. Bohn, S. L. Daniel, J. J. Johnson[1], M. K. Ravindra[1], P.O. Hashimoto[1], M. J. Mraz[1], W. H. Tong[1], D. A. Brosseau[2]

Sandia National Laboratories
Albuquerque, NM 87185

Prepared for
Division of Systems Research
Office of Nuclear Regulatory Research
U.S. Nuclear Regulatory Commission
Washington, DC 20555
NRC FIN A1228

---

[1]EQE, Incorporated, San Francisco, CA
[2]ERCE, Inc., Albuquerque, NM

ABSTRACT

The U.S. Nuclear Regulatory Commission is sponsoring probabilistic risk assessments of five operating commercial nuclear power plants as part of a major update of the understanding of risk as provided by the original WASH-1400 risk assessments. In contrast to the WASH-1400 studies, the NUREG-1150 risk assessment will include a detailed analysis of risks due to earthquakes, fires, floods, etc., which are collectively known as "external events" for at least two plants. This report presents the external events probabilistic risk assessment for the Peach Bottom Atomic Power Station, (Unit 2).

In keeping with the philosophy of the internal events analyses for NUREG-1150, which are intended to be "smart" PRAs making full use of all insights gained during the past ten years' developments in risk assessment methodologies, the corresponding external event analyses are being performed by newly-developed methods which are an improvement over past methodologies in terms of completeness and reproducibility and which, in many cases, provide significant simplifications in calculational effort. These methods have been under development at Sandia National Laboratories (SNL) under the sponsorship of the NRC's Division of Systems Research as part of their Dependent Failure Methodology Development Program.

As a first step, an extensive screening analysis was performed which showed that all external events had a negligible contribution except fires and seismic events. Detailed analyses for fire and seismic events were then performed. Final analysis of internal fires resulted in a total (mean) core damage frequency of 1.9E-5 per year. Final analysis of the seismic events resulted in a total (mean) core damage frequency of 7.66E-5 per year using hazard curves developed by Lawrence Livermore National Laboratory (LLNL). The mean seismic core damage frequency was also calculated using hazard curves developed by the Electric Power Research Institute (EPRI) and found to be 3.09E-6 per year. Uncertainty analyses were performed for both fire and seismic events, and dominant components and sources of uncertainty were identified.

CONTENTS

CONTENTS (Continued)

CONTENTS (Continued)

CONTENTS (Continued)

CONTENTS (Continued)

CONTENTS (Continued)

FIGURES

FIGURES

TABLES

TABLES

FOREWORD

This is one of numerous documents that support the preparation of the NUREG-1150 document by the NRC Office of Nuclear Regulatory Research. Figure 1 illustrates the front-end documentation. There are three interfacing programs performing this work: the Accident Sequence Evaluation Program (ASEP), the Severe Accident Risk Reduction Program (SARRP), and the Phenomenology and Risk Uncertainty Evaluation Program (PRUEP). The Zion PRA was performed at the Idaho National Engineering Laboratory and at Brookhaven National Laboratory.

Table 1 is a list of the original primary documentation and the corresponding revised documentation. There are several items that should be noted. First, in the original NUREG/CR-4550 report, Volume 2 was to be a summary of the internal analyses. This report was deleted. In Revision 1, Volume 2 now is the expert judgment elicitation covering all plants. Volumes 3 and 4 include external events analyses for Surry and Peach Bottom, respectively.

The revised NUREG/CR-4551 covers the analysis included in the original NUREG/CR-4551 and NUREG/CR-4700. However, it is different from NUREG/CR-4550 in that the results from the expert judgment elicitation are given in four parts to Volume 2 with each part covering one category of issues. The accident progression event trees are given in the appendices for each of the plant analyses.

Originally, NUREG/CR-4550 was published without the designation "Draft for Comment." Thus, the final revision of NUREG/CR-4550 is designated Revision 1. The label Revision 1 is used consistently on all volumes except Volume 2, which was not part of the original documentation. NUREG/CR-4551 was originally published as a "Draft for Comment" so, in its final form, no Revision 1 designator is required to distinguish it from the previous documentatation.

There are several other reports published in association with NUREG-1150. These are:

NUREG/CR-5032, SAND87-2428, Modeling Time to Recovery and Initiating Event Frequency for Loss of Off-site Power Incidents at Nuclear Power Plants, R. L. Iman and S. C. Hora, Sandia National Laboratories, Albuquerque, NM, January 1988.

NUREG/CR-4840, SAND88-3102, Procedures for External Event Core Damage Frequency Analyses for NUREG-1150, M. P. Bohn and J. A. Lambright, Sandia National Laboratories, Albuquerque, NM, November 1990.

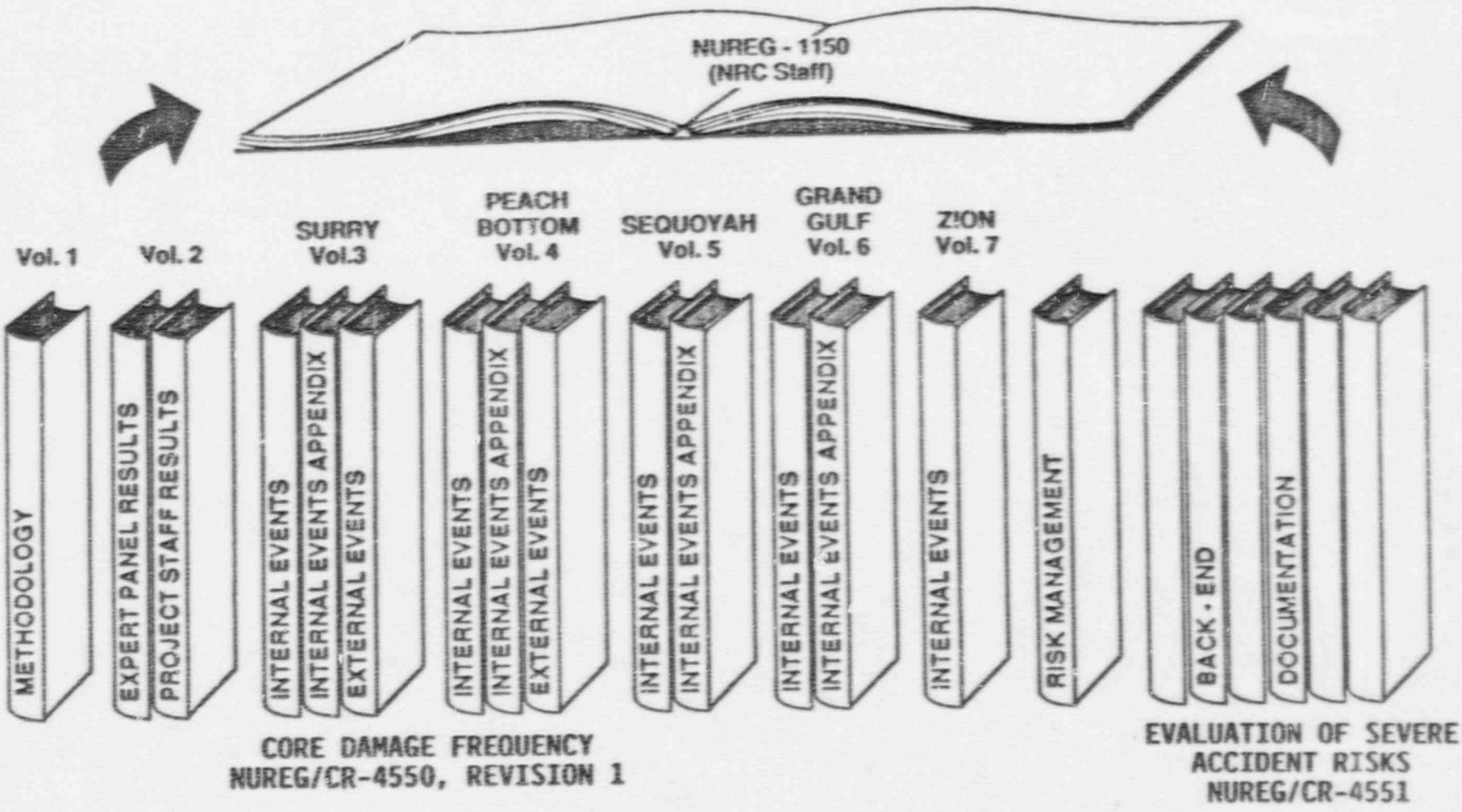

FIGURE 1. DOCUMENTATION FOR NUREG-1150.

Table 1.
NUREG-1150 Analysis Documentation

Original Documentation

NUREG/CR-4550
Analysis of Core Damage Frequency From Internal Events

Volume 1 Methodology
2 Summary (Not Published)
3 Surry Unit 1
4 Peach Bottom Unit 2
5 Sequoyah Unit 1
6 Grand Gulf Unit 1
7 Zion Unit 1

NUREG/CR-4551
Evaluation of Severe Accident Risks and the Potential for Risk Reduction

Volume 1 Surry Unit 1
2 Sequoyah Unit 1
3 Peach Bottom Unit 2
4 Grand Gulf Unit 1
5 Zion Unit 1

NUREG/CR-4700
Containment Event Analysis for Potential Severe Accidents

Volume 1 Surry Unit 1
2 Sequoyah Unit 1
3 Peach Bottom Unit 2
4 Grand Gulf Unit 1

Revised Documentation

NUREG/CR-4550, Revision 1
Analysis of Core Damage Frequency

Volume 1 Methodology
2 Part 1 Expert Judgment Elicit. Expert Panel
Part 2 Expert Judgment Elicit.--Project Staff
3 Part 1 Surry Unit 1 Internal Events
Part 2 Surry Unit 1 Internal Events App.
Part 3 Surry Unit 1 External Events
4 Part 1 Peach Bottom Unit 2 Internal Events
Part 2 Peach Bottom Unit 2 Internal Events App.
Part 3 Peach Bottom Unit 2 External Events
5 Part 1 Sequoyah Unit 1 Internal Events
Part 2 Sequoyah Unit 1 Internal Events App.
6 Part 1 Grand Gulf Unit 1 Internal Events
Part 2 Grand Gulf Unit 1 Internal Events App.
7 Zion Unit 1 Internal Events

NUREG/CR-4551, Evaluation of Severe Accident Risks

Volume 1 Methodology
2 Part 1 Expert Judgment Elicit.--In-vessel
Part 2 Expert Judgment Elicit.--Containment
Part 3 Expert Judgment Elicit.--Structural
Part 4 Expert Judgment Elicit.--Source-Term
Part 5 Expert Judgment Elicit.--Supp. Calc.
Part 6 Expert Judgment Elicit.--Proj. Staff
Part 7 Expert Judgment Elicit.--Supp. Calc.
Part 8 Expert Judgment Elicit.--MACCS Input
3 Part 1 Surry Unit 1 Anal. and Results
Part 2 Surry Unit 1 Appendices
4 Part 1 Peach Bottom Unit 2 Anal. and Results
Part 2 Peach Bottom Unit 2 Appendices
5 Part 1 Sequoyah Unit 2 Anal. and Results
Part 2 Sequoyah Unit 2 Appendices
6 Part 1 Grand Gulf Unit 1 Anal. and Results
Part 2 Grand Gulf Unit 1 Appendices
7 Part 1 Zion Unit 1 Anal. and Results
Part 2 Zion Unit 1 Appendices

NUREG/CR-4772, SAND86-1996, Accident Sequence Evaluation Program Human Reliability Analysis Procedure, A. D. Swain III, Sandia National Laboratories, Albuquerque, NM, February 1987.

NUREG/CR-5263, SAND88-3100, The Risk Management Implications of NUREG-1150 Methods and Results, A. C. Camp et al., Sandia National Laboratories, Albuquerque, NM, December 1988.

A Human Reliability Analysis for the ATWS Accident Sequence with MSIV Closure at the Peach Bottom Atomic Power Station, A-3272, W. J. Luckas, Jr. et al., Brookhaven National Laboratory, Upton, NY, 1986.

A brief flow chart for the documentation is given in Figure 2. Any related supporting documents to the back-end NUREG/CR-4551 analyses are delineated in NUREG/CR-4551. A complete list of the revised NUREG/CR-4550, volumes and parts is given below.

General

NUREG/CR-4550, Volume 1, Revision 1, SAND86-2084, Analysis of Core Damage Frequency: Methodology Guidelines for Internal Events.

NUREG/CR-4550, Volume 2, SAND86-2084, Analysis of Core Damage Frequency from Internal Events: Expert Judgment Elicitation on Internal Events Issues - Part 1: Expert Panel Results, Part 2: Project Staff Results.

Part 1 and 2 of Volume 2, NUREG/CR-4550 are bound together. This volume was not part of the original documentation and was first published in April 1989 and distributed in May 1989 with the title: Analysis of Core Damage Frequency from Internal Events: Expert Judgment Elicitation. In retrospect, a more descriptive title would be: Analysis of Core Damage Frequency: Expert Judgment Elicitation on Internal Events Issues.

SURRY

NUREG/CR-4550, Volume 3 Revision 1, Part 1, SAND86-2084, Analysis of Core Damage Frequency: Surry Unit 1 Internal Events.

NUREG/CR-4550, Volume 3, Revision 1, Part 2, SAND86-2084, Analysis of Core Damage Frequency: Surry Unit 1 Internal Events Appendices.

NUREG/CR-4550, Volume 3, Revision 1, Part 3, SAND86-2084, Analysis of Core Damage Frequency: Surry Unit 1 External Events.

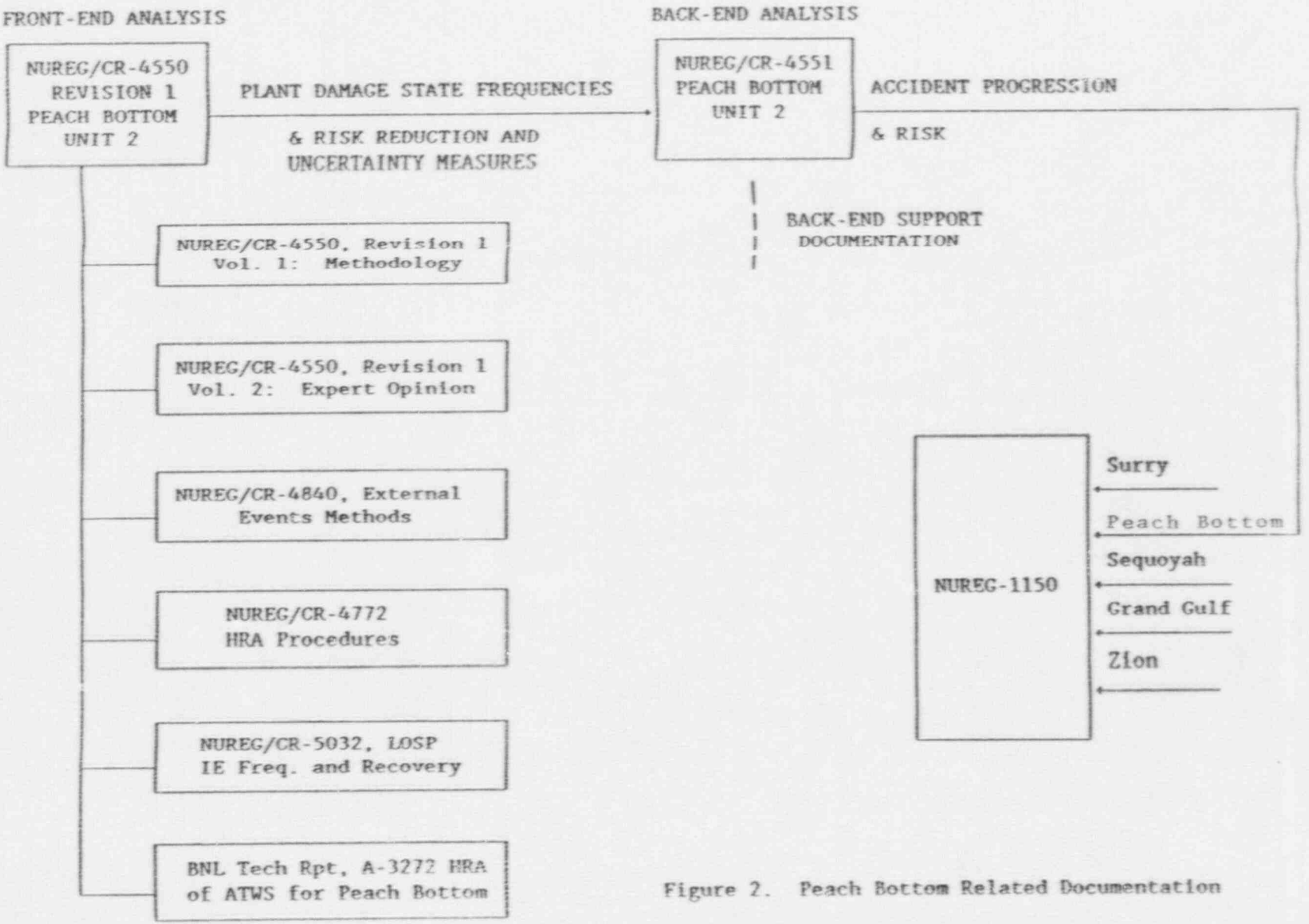

Figure 2. Peach Bottom Related Documentation

Peach Bottom

NUREG/CR-4697, EGG-2464, Containment Venting Analysis for the Peach Bottom Atomic Power Station, D. J. Hansen et al., Idaho National Engineering Laboratory (EG&G Idaho, Inc.) February 1987.

NUREG/CR-4550, Volume 4, Revision 1, Part 1, SAND86-2084, Analysis of Core Damage Frequency: Peach Bottom Unit 2 Internal Events.

NUREG/CR-4550, Volume 4, Revision 1, Part 2, SAND86-2084, Analysis of Core Damage Frequency: Peach Bottom Unit 2 Internal Events Appendices.

NUREG/CR-4550, Volume 4, Revision 1, Part 3, SAND86-2084, Analysis of Core Damage Frequency: Peach Bottom Unit 2 External Events.

Sequoyah

NUREG/CR-4550, Volume 5, Revision 1, Part 1, SAND86-2084, Analysis of Core Damage Frequency: Sequoyah Unit 1 Internal Events.

NUREG/CR-4550, Volume 5, Revision 1, Part 2, SAND86-2084, Analysis of Core Damage Frequency: Sequoyah Unit 1 Internal Events Appendices.

Grand Gulf

NUREG/CR-4550, Volume 6, Revision 1, Part 1, SAND86-2084, Analysis of Core Damage Frequency: Grand Gulf Unit 1 Internal Events.

NUREG/CR-4550, Volume 6, Revision 1, Part 2, SAND86-2084, Analysis of Core Damage Frequency: Grand Gulf Unit 1 Internal Events Appendices.

Zion

NUREG/CR-4550, Volume 7, Revision 1, EGG-2554, Analysis of Core Damage Frequency: Zion Unit 1 Internal Events.

EXECUTIVE SUMMARY

The U.S. Nuclear Regulatory Commission (USNRC) is sponsoring probabilistic risk assessments of five operating commercial nuclear power plants as part of a major update of the understanding of risk as provided by the original WASH-1400 assessments. In contrast to the WASH-1400 studies, at least two of the NUREG-1150 risk assessments will include a detailed analysis of hazards due to earthquakes, fires, floods, etc., which are collectively known as "external events." The two plants for which external events are being considered are Surry and Peach Bottom, a PWR and a BWR respectively. This report presents the results obtained for the Peach Bottom external event core damage frequency assessment.

In keeping with the philosophy of the internal events analyses for NUREG-1150, which are intended to be "smart" PRAs making full use of all insights gained during the past ten years' developments in risk assessment methodologies, the corresponding external event analyses have been performed by newly-developed methods. The methods have been developed under NRC sponsorship and represent, in many cases, both advancements and simplifications over techniques that have been used in past years. They also include the most up-to-date data bases on equipment seismic fragilities, fire occurrence frequencies and fire damageability thresholds. These methods were developed at Sandia National Laboratories under the sponsorship of the USNRC's Division of Systems Research as part of their Dependent Failure Methodology Development Program. The first application of these new methods was to the seismic analysis of six power plants as part of the NRC program for the resolution of Unresolved Safety Issue USI A-45 - Adequacy of Decay Heat Removal Systems. Extension of these methods to fire, flood, etc., has been continuing during recent years.

In contrast to most past external event analyses, wherein rudimentary systems models were developed reflecting each external event under consideration, the NUREG-1150 external event analyses are based on the full internal event PRA systems models (event trees and fault trees) and make use of extensive computer-aided screening to reduce them to accident sequence cut sets important to each external event. This provides two major advantages in that both consistency and scrutability with respect to the internal event analysis is achieved, and the full gamut of random and test/maintenance unavailabilities are automatically included, while only those probabilistically important survive the screening process. Thus, full benefit of the internal event analysis is obtained by performing the internal and external event analyses sequentially.

The external event analysis began with a review of the FSAR, related design documents and the systems descriptions in the internal events PRA. Important components were located on general arrangement drawings. The utility fire study prepared to meet Appendix R of 10CFR50 requirements formed the basis for the initial identification of fire and flood area boundaries and barriers. Shortly thereafter, a plant visit of 3 days

duration was made, involving an integrated team of specialists in the various external events. Based on the plant walkdown and the screening analysis described in Chapter 3, all external hazards were screened out based on probability considerations except for seismic and fire events.

The seismic risk assessment was the critical path item due to the time required to assemble the structural drawings and models. A best estimate structural dynamic response calculation for each building containing equipment important to safety was made using models used in the original design. The results were distributions for floor slab accelerations, and estimates of variability and correlations. Component fragilities were obtained either from a generic data base or derived on a plant specific basis as needed. Dual probabilistic screening methods were used to determine important cut sets while allowing for explicit incorporation of correlation. The seismic hazard itself was obtained by extrapolation from the results of the NRC-sponsored Eastern Seismic Hazard Characterization Program performed at Lawrence Livermore National Laboratory (LLNL) and the industry-sponsored Electric Power Research Institute (EPRI) Seismic Hazard Methodology for the Central and Eastern United States program.

The detailed fire analysis tasks were performed in parallel. Fire initiator frequencies were obtained from an updated historical data set developed at SNL. Partitioning of building fire frequencies (for which data are available) down to sub-area frequencies was based on cable loading, electrical cabinet locations, and transient combustible estimates based on walkdown observations and a transient combustible data base developed at Sandia. Component damage temperatures (rather than auto-ignition temperatures) were based on SNL fire tests. The COMPBRN III code was used to predict component temperatures in fire areas where growth and separation are important considerations. Vital area analyses using the SETS code provided sequence cut sets for quantification, including barrier failure and random failures as appropriate. A fire detection/suppression histogram developed at SNL was used to incorporate firefighting timing into the analysis.

Similar approaches were used for internal and external flood, tornado, winds, etc. A major economy is achieved by analyzing fires and floods together, and seismic, wind and tornado events together, due to the commonality of the analysis processes. For example, it is a minor task to extend the seismic fragility derivations so as to be applicable to wind fragilities. Similar economies arise in the screening steps for fires and floods.

Detailed analysis of internal fires resulted in a total (mean) core damage frequency of 1.95E-5 per year. The detailed seismic analysis resulted in a total (mean) core damage frequency of 7.66E-5 per year using hazard curves developed by Lawrence Livermore National Laboratory. The mean seismic core damage frequency was also calculated using hazard curves developed by the Electric Power Research Institute and found to be 3.09E-6 per year. Uncertainty analyses were performed for both fire and seismic risks, and dominant components and sources of uncertainty were identified.

In general, it was found that only a few accident sequences dominated the results. These were station blackout sequences for both the seismic and fire core damage assessments. For the seismic analysis, it was found that these resulted from failures in the emergency service water (ESW) and emergency cooling water (ECW) systems which provide cooling to the four diesel generators. For the fire analysis, it was found that these sequences resulted from damage to cabling in the emergency switchgear rooms which could cause loss of offsite power and fail the ESW/ECW pumps. It appears that modifications which would lower the contribution of these dominant sequences to core damage frequency could be easily implemented.

1.0 INTRODUCTION

1.1 The NUREG-1150 Risk Analyses

This report describes the Level 1 external events probabilistic risk assessment (PRA) performed for the Peach Bottom Atomic Power Station as part of the NRC-sponsored Accident Sequence Evaluation Program (Ref. 1) power plant risk reevaluations, often referred to as the NUREG-1150 program (after the principal document summarizing the results of the program). In contrast to the original WASH-1400 risk assessments (Ref. 2), both detailed internal and detailed external events risk analyses are being performed in this program.

A Level 1 PRA consists of an analysis of plant design and operation focusing on accident sequences that could lead to core damage, their basic causes, and frequencies. Two kinds of accident initiators are considered for a Level 1 PRA, initiating events that occur within the power plant systems themselves and accident initiators caused by events external to the power plant systems. Examples of external initiators include earthquakes, floods and high winds. The results of both analyses provide assessments of plant safety, design and procedural adequacy, and insights into how the plant functions from the perspective of preventing core damage. This report documents work performed for the Level 1 external events PRA. It describes the methodology used, assumptions, data and models that provide the basis for the work, and the final results.

The methods utilized in the NUREG-1150 external events PRAs represent both advancements, and, in many cases, simplifications over techniques that have been used in past years. They include the most up-to-date data bases on equipment seismic fragilities, fire occurrence frequencies and fire damageability thresholds. In addition, they provide for minimization of execution time and cost reduction through the use of past PRA experience, generic data bases and defensible methodological simplification where possible. A full description of these procedures is given in Bohn and Lambright (Ref. 3). The methods were developed to meet the following objectives:

a. To be consistent with the internal event PRA analyses. The same event trees/fault trees and random, common mode failure and test and maintenance data are used.

b. To be transparent. A standard report format provides the data to enable the reader to reproduce any of the point estimate results.

c. To be realistic. Best estimate data and models are used. All important plant-specific failure modes are analyzed.

d. To be consistent. The external event analyses are intended to be consistent with the internal event analyses due to common generic data, and methodology, and common level of detail.

1.2 The External Event Methodology

The PRA procedures described in this section are based on the following general concepts:

a. The external event analyses are based on the internal event risk assessment plant system models and fault trees, and (other than preliminary data gathering) are not started until the internal events systems analysis (event trees and fault trees) has been finalized.

b. Rigorous and systematic screening of the full range of external events to which the plant could conceivably be exposed (e.g., aircraft crash, external flooding, tornado, extreme wind, etc.) is performed to eliminate early all unimportant contributing events.

c. Simultaneous and coordinated evaluation of all non-negligible external events is performed to minimize data gathering efforts and prevent duplication of effort. For example, building fragilities for extreme winds can be derived directly from seismic fragilities. Also, simultaneous evaluation produces insights into interactions (for example, seismic-fire interactions) not otherwise readily perceived.

d. In the analysis of each types of external event, computer-aided screening techniques and generic failure data are used prior to detailed component failure analysis calculations.

The general steps in the analysis of any external event risk analysis are shown below:

a. Determine the hazard.

b. Model plant and systems.

c. Solve fault trees with screening techniques to determine non-negligible cut sets.

d. Determine responses, fragilities, and correlation for basic events in non-negligible cut sets.

e. Evaluate point estimate sequence and core damage frequencies.

f. Perform uncertainty analysis and sensitivity studies.

These general steps apply to the full range of external events to which a power plant may be exposed. Table 1.1 presents a reasonably complete list of such events. Past PRA experience (Ref. 3) shows that only a very few of these are significant contributors to risk at any given site. In fact, the seismic and fire events are commonly the most important

contributors. In addition, external flooding, tornado or aircraft crashes are less frequent (and usually less significant) contributors.

Simplifications in Step (a), hazard determination, have been identified for both the seismic and fire analyses. Computer-aided screening techniques are used for Step (c) for fire, flood and seismic analyses to reduce the required number of plant-specific component failure calculations. For Step (d), response determination, seismic design fixed-base structural models are utilized in conjunction with an accurate and fully defensible soil-structure interaction model. While not a simplification, this process has been made very efficient by standardization, and use of variabilities and correlation factors derived from previous detailed seismic PRA work. Thus, in each step, defensible simplifications are identified which results, overall, in a cost-effective yet defensible analysis.

The procedures used here have been applied (in whole or in part) to six power plants as part of the U.S. NRC-sponsored Unresolved Safety Issue A-45 resolution program (Ref. 4), and have been applied at the N-Reactor (Ref. 5) and Savannah River (Ref. 6) Department of Energy reactor facilities.

Table 1.1

List of External Events

Major PRA Consideration	Minor PRA Consideration
Seismic	Lightning
Fire	Low Lake/River Level
Internal Flood	Ice Cover
	Avalanche
	Forest Fire
	Industrial Facility Accident
	Landslide
	Meteorite
	Volcanic Activity
	Hail

Occasional PRA Consideration

External flood
Transportation accidents
Pipe line accidents
Aircraft impact
Extreme winds
Tornado

1.3 Steps in the Analysis

1.3.1 Plant Walkdown and Data Gathering

The Peach Bottom external events analysis began with a plant visit in April 1987. The initial visit served as the basis for the initial plant information request submittal. Prior to the first plant visit, the external events team was briefed by the internal events systems analyst as to the general character of safety systems, support systems, system success criteria and critical interdependencies identified to date. In addition, applicable Final Safety Analysis Report (FSAR) sections were reviewed, and a basic set of plant general arrangement drawings were obtained for each team member.

The team consisted of the following personnel:

PRA Project Manager - M. P. Bohn
Team Leader - J. A. Lambright
Structural Fragility Analysts - J. J. Johnson, P. O. Hashimoto
Fire and Flood PRA Analyst - J. A. Lambright
External Event Screening Analyst - R. Ravindra

During the initial walkdown, team members visited all areas containing safety or support equipment except the containment. Two full days were adequate for this initial visit. At the completion of this initial visit, the following had been obtained.

a. A list of components suspected of being vulnerable to seismic damage and requiring site specific fragility analysis.

b. A list of potential secondary seismic structural failures (masonry walls, etc.) and components potentially damaged by these secondary failures.

c. A copy of the civil/structural drawing index for the plant from which needed drawings may be identified.

d. Sketches of typical anchorage details for important tanks, heat exchangers, electrical cabinets, etc.

e. A visual evaluation of structural connectivity of floor slabs, wall-to-ceiling connections, location of diaphragm cut-outs etc., which define load carrying paths. These were to be compared with structural drawings later.

f. For each room or compartment containing essential safety equipment, an identification of fire sources (power cables, pump motors, solvents, etc.), locations of fire barriers, fire/smoke detectors, separation of cable trains, etc., and a list of equipment in the room.

g. For each room or compartment, an identification of flooding sources (tanks, high or low pressure piping), floor drains, pumps, flood walls, flood detectors, etc.

h. A brief list of key plant personnel or utility engineering/licensing personnel to be contacted later if specific questions arose.

Following the initial plant visit, a list of needed drawings and documentation was prepared and sent to the designated plant contact. A second visit to the plant was made by the fire analysis personnel to allow for cable path tracing and verification. This was undertaken after the preliminary fire screening analysis had been performed based on a review of the plant Appendix R submittal. A final plant visit was made in September 1988. During this final visit initial conclusions as to plant vulnerabilities were reviewed with plant personnel, assumptions were verified, and final required data was obtained.

1.3.2 Screening of Other External Events

As mentioned in Section 1.1, the full range of possible external events was considered, but based on the FSAR and the initial plant visit, the vast majority of the external hazards was shown to have negligible impact. The set of general screening criteria which was used is given in the PRA Procedures Guide (Ref. 7) and is summarized as follows:

An external event can be excluded if:

a. The event is of equal or lesser damage potential than the events for which the plant has been designed. This requires an evaluation of plant design bases in order to estimate the resistance of plant structures and systems to a particular external event. For example, it is shown by Kennedy, Blejwas and Bennett (Ref. 8) that safety-related structures designed for earthquake and tornado loadings in Zone 1 can safely withstand a 3.0 psi static pressure from explosions. Hence, if the PRA analyst demonstrates that the overpressure resulting from explosions at a source (e.g., railroad, highway or industrial facility) cannot exceed 3 psi, these postulated explosions need not be considered.

b. The event has a significantly lower mean frequency of occurrence than other events with similar uncertainties and could not result in worse consequences than those events. For example, the PRA analyst may exclude an event whose mean frequency of occurrence is less than some small fraction of those for other events. In this case, the uncertainty in the frequency estimate for the excluded event is judged by the PRA analyst as not significantly influencing the total risk.

c. The event cannot occur close enough to the plant to affect it. This is also a function of the magnitude of the event. Examples of such events are landslides, volcanic eruptions and earthquake fault ruptures.

d. The event is included in the definition of another event. For example, storm surges and seiches are included in external flooding; the release of toxic gases from sources external to the plant is included in the effects of either pipeline accidents, industrial or military facility accidents, or transportation accidents.

These criteria are usually sufficient to exclude all but a few "other" external events. For those remaining, a simple bounding analysis (Ref. 9) will often provide sufficient justification for exclusion. The screening and bounding analyses for Peach Bottom are given in Chapter 3.

1.3.3 Seismic Risk Assessment Methodology

A nuclear power plant is designed to ensure the survival of all buildings and emergency safety systems in a worst-case ("safety shutdown") earthquake. The assumptions underlying this design process are deterministic and subject to considerable uncertainty. It is not possible, for example, to accurately predict the worst earthquake that will occur at a given site. Soil properties, mechanical properties of buildings, and damping in buildings and internal structures also vary significantly. To model and analyze the coupled phenomena that contribute to the total risk of radioactive release requires consideration of all significant sources of uncertainty as well as all significant interactions. Total risk is then obtained by considering the entire spectrum of possible earthquakes and integrating their calculated consequences. This point underscores an important requirement for a seismic PRA; the nuclear power plant must be examined in its entirety, as a system.

A second important aspect which must be addressed in a seismic PRA is that during an earthquake, all parts of the plant are excited simultaneously. Thus, during an earthquake, redundant safety system components experience highly correlated base motion, and there is a high likelihood that multiple redundant components would be damaged if one is. Hence, the planned-for redundancy would be comprised. This "common-cause" failure possibility represents a potentially significant risk to nuclear power plants during earthquakes.

The simplified seismic risk methodology reported here is based, in part, on the results of two earlier NRC-sponsored programs. The first was the Seismic Safety Margins Research Program. In the SSMRP, a detailed seismic risk assessment methodology was developed. This program culminated in a detailed evaluation of the seismic risk at the Zion nuclear power station, Bohn (Ref. 10). In this evaluation, an attempt

was made to accurately compute the responses of all walls and floor slabs in the Zion structures, moments in the important piping systems, accelerations of all important valves, and the spectral acceleration at each safety system component (pump, electrical buss, motor control center, etc.). Correlation between the responses of all components was computed from the detailed dynamic response calculations. The important safety and auxiliary systems functions were analyzed, and fault trees were developed which traced failure down to the individual component level. Event trees related the system failures to accident sequences and radioactive release modes. Using these detailed models and calculations, it was possible to evaluate the seismic risk at Zion, and determine quantitatively the risk importance of the components, initiating events, and accident sequences.

The second is the NRC-sponsored Eastern Seismic Hazard Characterization program (Ref. 11) which performed a detailed earthquake hazard assessment of all sites east of the Rocky mountains. Results of these two programs formed the basis for a number of simplifications used in the seismic methodology reported here.

There are seven steps required for calculating the seismic risk at a nuclear power plant:

a. Determine the local earthquake hazard (hazard cure and site spectra).

b. Identify accident scenarios for the plant which lead to radioactive release (initiating events and event trees).

c. Determine failure modes for the plant safety and support systems (fault trees).

d. Determine the responses (accelerations or forces) of all structures and components (for each earthquake level).

e. Determine fragilities (probabilistic failure criteria) for the important structures and components.

f. Compute the probability of core damage using the information from Steps a through e.

g. Estimate uncertainty in the core damage frequencies.

Only the level of detail differentiates a simplified seismic analysis from a detailed seismic PRA. The seven steps of the NUREG-1150 seismic risk analysis procedure are summarized below.

Step a - Seismic Hazard Characterization

The NUREG-1150 seismic analyses make use of hazard curves obtained from two recent programs aimed at developing sets of hazard curves based on

consistent data bases and assunptions. The first is the Eastern United States Seismic Hazard Characterization Program supported by the USNRC at Lawrence Livermore National Laboratory. The second is the industry-sponsored Seismic Hazard Methodology program performed by the Electric Power Research Institute. In both these programs, hazard curves were developed for all U.S. commercial nuclear power plant sites east of the Rocky Mountains.

Step b - Initiating Events and Event Trees

The scope of NUREG-1150 includes all potential initiating events, including loss of coolant accidents (Vessel Rupture, ALOCA, MLOCA, SLOCA) and transient events. Two types of transients are being considered: those in which the power conversion system (PCS) is initially available (denoted Type T2 transients) and those in which the PCS is failed as a direct consequence of the initiating event (denoted Type T1 transients). The event trees derived for the internal even analyses are utilized.

The reactor vessel rupture and large LOCA event frequencies are based on a Monte Carlo analysis of steam generator and reactor coolant pump support failures. The medium and small LOCA event frequencies are obtained from detailed piping failure calculations performed in the SSMRP.

The frequency of Type T1 transients is based on the probability of seismically-induced loss of offsite power (LOSP). This is the dominant type of transient (for the majority of plants for which LOSP causes loss of main feedwater). The frequency of the Type T3 initiating event is computed from the condition that the sum of the initiating event probabilities must be unity. The hypothesis is that, given an earthquake of reasonable size, at least one of the initiating events will occur.

Step c - Fault Trees

Fault trees for the safety systems at Peach Bottom have been developed in the internal events analysis for random failures only. These fault trees are used with modifications to include basic events for seismic failure modes. The trees are re-solved for pertinent seismic cut sets to be included in the probabilistic calculations. Probabilistic culling is used in resolving these trees in such a way as to assure that important correlated failure modes are not lost.

Step d - Component and Structure Failure Descriptions

Component seismic fragilities are obtained both from a generic fragility data base and from plant-specific fragilities developed for components identified during the plant walkdown.

The generic data base of fragility functions for seismically-induced failures was originally developed as part of the SSMRP (Ref. 10). Fragility functions for the generic categories were developed based on a combination of experimental data, design analysis reports, and an

extensive expert opinion survey. The experimental data utilized in developing fragility curves were obtained from the results of component manufacturer's qualification tests, independent testing lab failure data and data obtained from the U.S. Corps of Engineers extensive SAFEGUARD Subsystem Hardness Assurance Program (Ref. 12). These data were statistically combined with the expert opinion survey data to produce fragility curves for each of the generic component categories as reported in Reference 10. This generic data base was then updated by an evaluation of 19 site-specific seismic PRAs to yield the final generic fragility data base used for the NUREG-1150 seismic PRAs.

Detailed structural fragility analyses were performed for all important safety related structures at the Peach Bottom plant. These were included directly in the risk assessment.

Step e - Seismic Response of Structures and Components

Building and component seismic responses are estimated from peak ground accelerations at several probability intervals on the hazard curve. Three basic aspects of seismic response--best estimates, variability, and correlation--are generated. Zion analysis results from SSMRP (Ref. 10) and simplified methods studies form the basis for assigning scaling, variability and correlation of responses.

In each case, SHAKE code (Ref. 13) calculations are performed to assess the effect of the local soil column (if any) on the surface peak ground acceleration and soil structure interactions. This permits an evaluation of the effects of non-homogenous underlying soil conditions which can strongly affect the building responses.

Fixed base mass-spring (eigen-system) models are either obtained from the plant architect/engineer or are developed from the plant drawings as needed. Using these models one can compute the floor slab accelerations using the CLASSI code (Ref. 14). This code takes a fixed-base eigensystem model of the structure and input-specified frequency dependent soil impedances and computes the structural response (as well as variation in structural response if desired).

Variability in responses (floor and spectral accelerations) is assigned based on the SSMRP results. The recommended uncertainties (expressed as standard deviations of the logarithms of the responses) are shown below:

Quantity	Random
Peak Ground Acceleration	0.25
Floor Zero Period Acceleration	0.35
Floor Spectral Acceleration	0.45

Correlation between component failures is being included explicitly. In computing the correlation between component failures (in order to quantify the cut sets) it is necessary to consider correlations both in the responses and in the fragilities of each component. Inasmuch as

there are no data as yet on correlation between fragilities, the fragility correlations between like components are taken as zero, and the possible effect of such correlation quantified in a sensitivity study. The correlation between responses is assigned according to a set of rules that are explained in Chapter 4.0.

Step f - Probabilistic Failure and Core Damage Calculations

Given the input from the five steps above, the SETS (Ref. 15) code and mean basic event frequencies are used to calculate the required output (mean probabilities of failure, core damage, etc.).

Step g - Estimate Uncertainties

Complete uncertainty distributions are computed for all accident sequences and core damage frequencies using a Monte Carlo approach.

1.3.4 Internal Fire Assessment Methodology

Based on nuclear power plant operating experience over the last 20 years, it has been observed that a typical nuclear power plant will have three to four significant fires over its operating lifetime. Previous probabilistic risk assessments (PRAs) have shown that fires are a significant contributor to the overall core damage frequency, contributing anywhere from 7 percent to 50 percent of the total (considering contributions from internal, seismic, flood, fire, and other events). Because of the relatively high core damage contribution, fires are always examined in detail. An overview of the NUREG-1150 fire PRA methodology is as follows:

A. Initial Plant Visit

Based on the internal event and seismic analyses, the general location of cables and components of the systems of interest is known. The plant visit provides the analyst with a means of seeing the physical arrangements in each of these areas. The analyst will have a fire zone checklist which will aid the screening analysis and in the quantification step.

The second purpose of the initial plant visit is to confirm with plant personnel that the documentation being used is, in fact, the best available information and to get clarification about any questions that might have arisen in a review of the documentation. Also, a thorough review of firefighting procedures is conducted.

B. Screening

It is necessary to select important fire locations within the power plant under investigation having the greatest potential for producing risk-dominant accident sequences. The objectives of location selection are somewhat competing and should be balanced in a meaningful risk assessment study. The first objective is to maximize the possibility that all important locations are analyzed, and this leads to the consideration of a potentially large number of candidate locations. The second objective is to minimize the effort spent in the quantification of event trees and fault trees for fire locations that turn out to be unimportant. A proper balance of these objectives is one that results in an ideal allocation of resources and efficiency of assessment.

The screening analysis is comprised of:

1. Identification of relevant fire zones.

2. Screening of fire zones on probability of the fire-induced initiating events.

3. Screening of fire zones on both order and frequency of cut sets.

4. Numerical evaluation and culling based on probability for each remaining fire zone.

C. Quantification

After the screening analysis has eliminated all but the probabilistically-significant fire zones, quantification of dominant cut sets is completed as follows:

1. Determine temperature response in each fire zone.

2. Compute component fire fragilities.

3. Assess the probability of barrier failure for all remaining combinations of fire zones.

4. Perform a recovery analysis.

Finally, an uncertainty analysis is performed to estimate error bounds on the computed fire-induced core damage frequencies. The Peach Bottom fire analysis is presented in Chapter 5.

1.4 References

1. U.S. Nuclear Regulatory Commission, Reactor Risk Reference Document, NUREG-1150, Vol. 1, February 1987.

2. U.S. Nuclear Regulatory Commission, Reactor Safety Study: An Assessment of Accident Risks in U.S. Nuclear Power Plants, WASH-1400, NUREG-75/014, 1975.

3. M. P. Bohn, and J. A. Lambright, Procedures for External Event Core Damage Frequency Analyses for NUREG-1150, Sandia National Laboratories, Albuquerque, NM, NUREG/CR-4840, November 1990.

4. D. M. Ericson, Jr. et al, Shutdown Decay Heat Removal Analysis: Plant Case Studies and Special Issues, NUREG/CR-5230, SAND88-2375, April 1989.

5. J. A. Lambright and M. P. Bohn, Analysis of Core Damage Frequency Due to External Events at the DOE N-Reactor, SAND89-1147, August 1990.

6. J. A. Lambright, Analysis of Core Damage Frequency Due to Fire at the Savannah River K-Reactor, SAND89-1786, August 1990.

7. U.S. Nuclear Regulatory Commission, PRA Procedures Guide, NUREG/CR-2300, January 1983.

8. Kennedy, R. P., Blejwas, T. E., and D. E. Bennett, Capacity of Nuclear Power Plant Structures to Resist Blast Loadings, NUREG/CR-2462, September 1983.

9. Ravindra, M. K. and Banon, H., Methods for External Event Screening Quantification, NUREG/CR-4839, to be published.

10. M. P. Bohn, et al., Application of the SSMRP Methodology to the Seismic Risk at the Zion Nuclear Power Plant, Lawrence Livermore National Laboratory, Livermore, CA, NUREG/CR-3428, 1983.

11. D. L. Bernreuter, et al., Seismic Hazard Characterization of the Eastern United States: Methodology and Interim Pesults for Ten Sites, NUREG/CR-3756, April 1984.

12. U.S. Army Corps of Engineers, Subsystem Hardness Assurance Report, HNDDSP-72-156-ED.R, Vols I and II, 1975.

13. P. B. Schnabel, J. Lysmer, and H. B. Seed, SHAKE--A Computer Program for Earthquake Response Analysis of Horizontally Layered Sites, Earthquake Engineering Research Center, University of California, Berkeley, CA, EERC 72-12, 1972.

14. H. L. Wong and J. E. Luco, Soil-Structure Interaction: A Linear Continuum Mechanics Approach (CLASSI), Dept. of Civil Engineering University of Southern California, Los Angeles, CA, CE79-03, 1980.

15. R. B. Worrell, SETS Reference Manual, Sandia National laboratories, Albuquerque, NM, SAND83-2675, NUREG/CR-4213, May 1985.

2.0 PLANT DESCRIPTION

2.1 Plant Site and General Characteristics

The Peach Bottom Atomic Power Station occupies 620 acres in York and Lancaster counties of southeastern Pennsylvania, 2.5 miles north of the Maryland-Pennsylvania state line. The plant is 38 miles N-NE of Baltimore, Maryland, and 63 miles W-SW of Philadelphia, Pennsylvania. It is located on the western shore of Conowingo Pond formed by the backwater of Conowingo dam, 9 miles downstream on the Susquehanna River.

The twin BWR units (Peach Bottom Units 2 and 3) of Philadelphia Electric Company are each rated at 1,065 MW. The reactor and generator for both these units were supplied by General Electric Corporation. Bechtel acted as Architect/Engineer/Constructor. The plants began commercial operation in 1974. Unit 1 is a 40 MW decommissioned HTGR and is now in a mothball status. Units 2 and 3 are located approximately 300 ft from the shoreline of Conowingo Pond. In addition to the reactor units, three transmission substations (two of 500 kV and one of 220 kV) represent the dominant features at the plant site.

2.2 Description of Plant Systems

2.2.1 Introduction

This section discusses the system descriptions and system models of the major frontline and support systems identified as important to safety. In addition to the event trees discussed in Section 2.3, component fault trees also developed by the internal events analysts were utilized. Use of the same event trees, fault trees, and accident sequences developed during the internal events analysis ensured consistency between these major studies.

The discussion of the systems that follow includes:

a. A brief functional description of the system with reference to the one-line diagrams that were developed to indicate which components were included in the model;

b. Safety-related success criteria that were applied to the system;

c. Interfaces and safety actuation provisions between the frontline systems and the support systems.

2.2.2 High Pressure Coolant Injection (HPCI) System

The function of the HPCI system is to provide a makeup coolant source to the reactor vessel during accidents in which system pressure remains high (event tree nomenclature--U1).

The HPCI system consists of a single train with motor-operated valves and a turbine-driven pump. Suction is taken from either the Condensate Storage Tank (CST) or the suppression pool (or torus). Injection to the reactor vessel is via a feedwater line. The HPCI pump is rated at 5000 gpm flow with a discharge head of 1135 psig. A simplified schematic of the HPCI system is provided by Figure 2.1. Major components are shown that were modeled in the system fault tree.

The HPCI system is automatically initiated and controlled. Operator intervention is required as follows: (a) to prevent either vessel overfill or continuous system trip/restart cycles, (b) to manually start the system given an auto-start failure, and (c) to set up the system for continuous operation under long-term station blackout conditions. The success criteria for the HPCI system is injection at rated flow to the reactor vessel.

Most of the HPCI system is located in a separate room in the reactor building. Local access to the HPCI system could be affected by either containment venting or containment failure should steam be released to the reactor building area. Room cooling failure is assumed to fail the HPCI pump in 10 hours.

Upon system actuation, HPCI injection valves receive a signal to open and HPCI test valves receive a signal to close. The HPCI system is automatically initiated on the receipt of either a high drywell pressure (2 psig) or low reactor water level (490 inches above vessel zero) signal. The low reactor water level sensors are shared with the RCIC system.

2.2.3 Reactor Core Isolation Cooling (RCIC) System

The function of the RCIC system is to provide a makeup coolant source to the reactor vessel during accidents in which system pressure remains high (event tree nomenclature--U2).

The RCIC system consists of a single train with motor-operated valves and a turbine-driven pump. Suction is taken from either the CST or the suppression pool. Injection to the reactor vessel is via a feedwater line. The RCIC pump is rated at 600 gpm flow with a discharge head of 1135 psig. A simplified schematic of the RCIC system is provided by Figure 2.2. Major components are shown that were modeled in the system fault tree.

The RCIC system is automatically initiated and controlled. Operator intervention is required as follows: (1) to prevent either vessel overfill or continuous system trip/restart cycles, (2) to manually start the system given an auto-start failure, and (3) to set up the system for continuous operation under long-term station blackout conditions. The success criteria for the RCIC system is injection at rated flow to the reactor vessel.

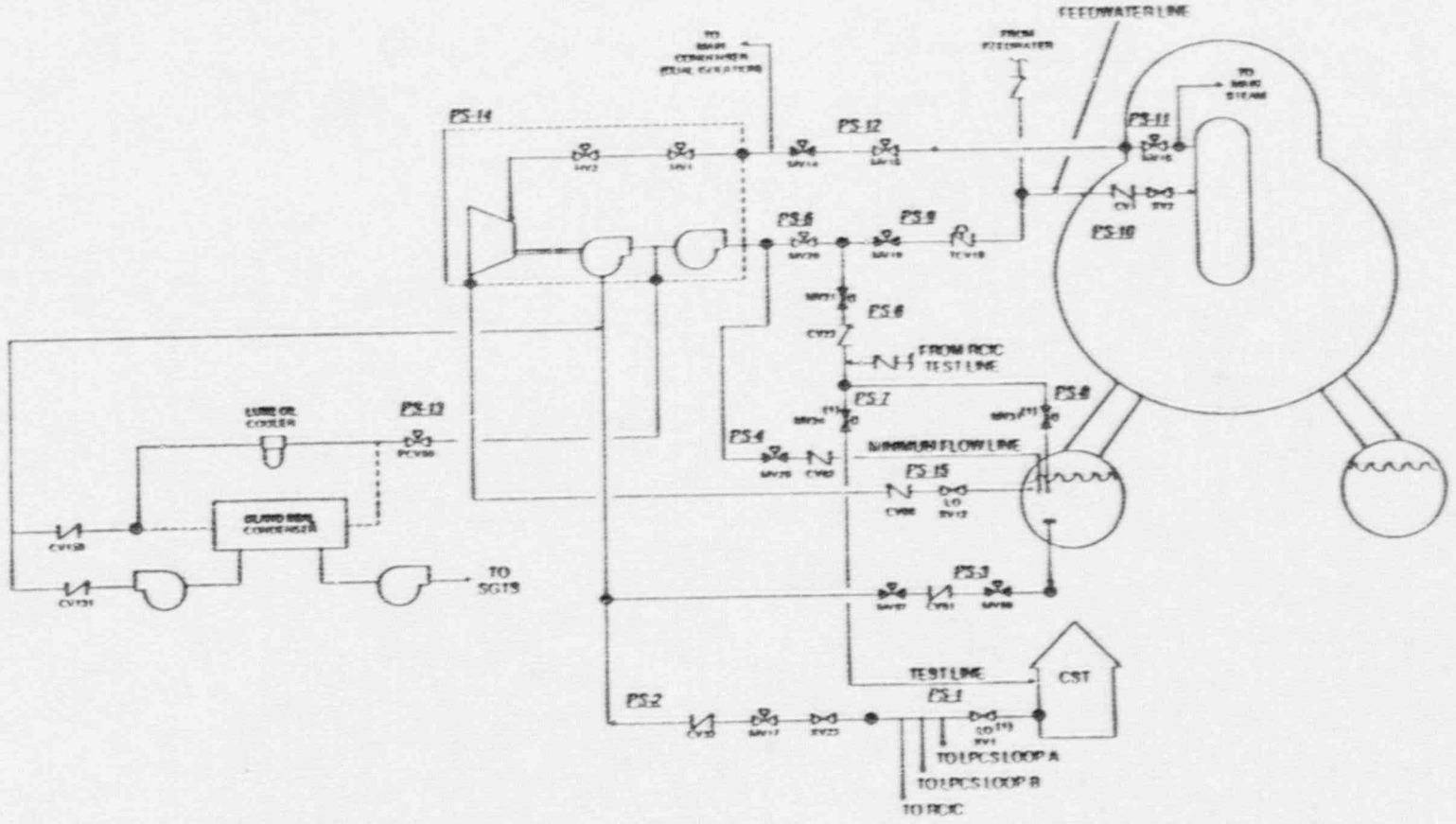

VALVE POSITIONS ARE SHOWN IN THEIR STANDBY MODE
(1) VALVE ALSO SHOWN ON RCIC SCHEMATIC

Figure 2.1 High Pressure Coolant Injection System Schematic.

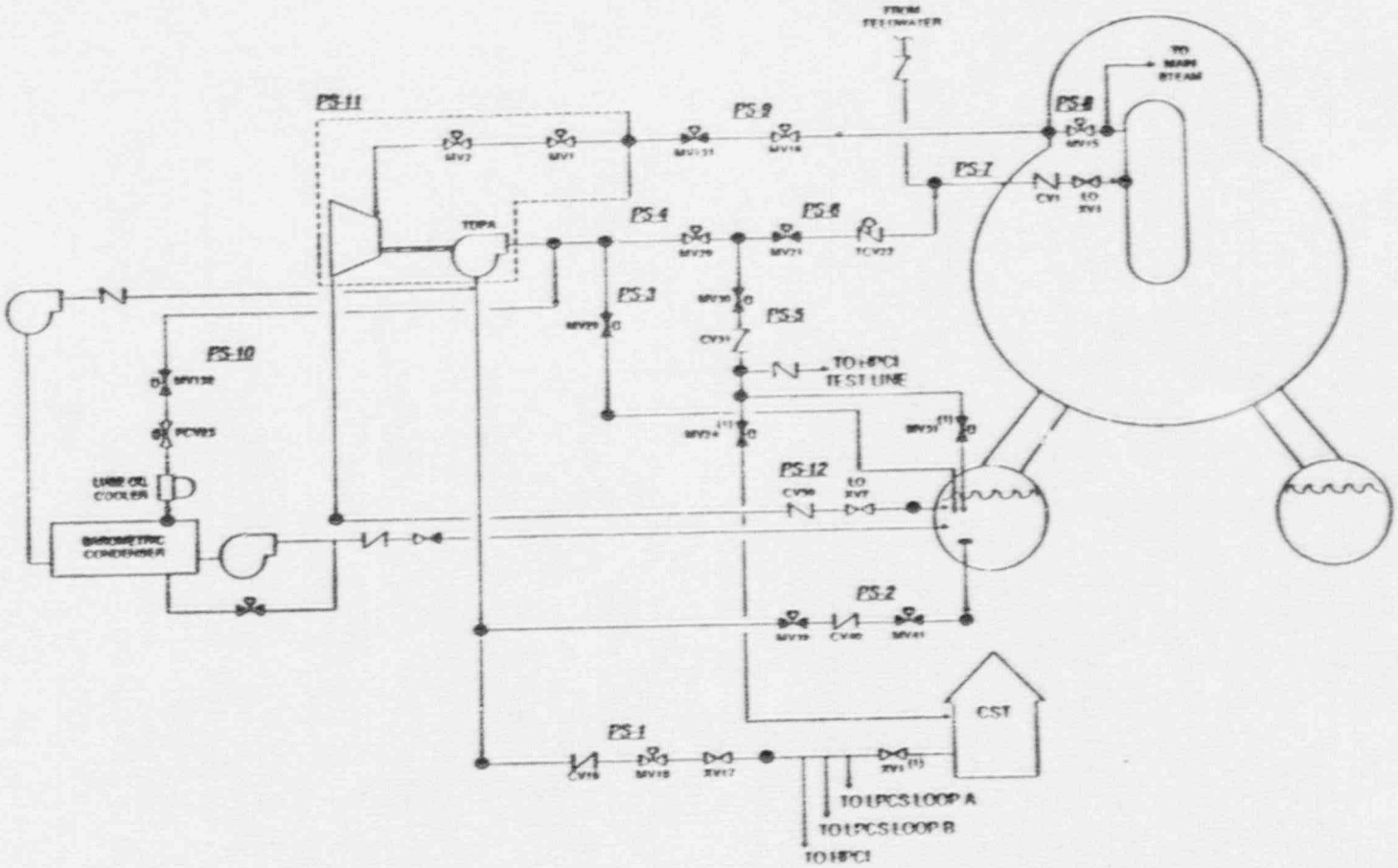

VALVE POSITIONS ARE SHOWN IN THEIR STANDBY MODE
(1) VALVE ALSO LOCATED ON HPCI SCHEMATIC, SEE HPCI SCHEMATIC FOR DEFINITION OF PIPE SEGMENT

Figure 2.2 Reactor Core Isolation Cooling System Schematic

Most of the RCIC system is located in a separate room in the reactor building. Local access to the RCIC system could be affected by either containment venting or containment failure should steam be released to the reactor building area. Room cooling failure is assumed to fail the RCIC pump in 10 hours.

Upon system actuation, RCIC injection valves receive a signal to open and RCIC test valves receive a signal to close. The RCIC system is automatically initiated on the receipt of a low reactor water level signal (490 inches above vessel zero). The low reactor water level sensors are shared with the HPCI system.

2.2.4 Control Rod Drive (CRD) System

The CRD system was modeled as a backup source of high pressure injection (event tree nomenclature--U3-1, CRD Enhanced Mode-2 pumps required, and U3-2, CRD-1 pump required).

The CRD pumps take suction from the condenser hotwell in the Condensate system or the CST. A flow control station is installed downstream of the tap from the Condensate system and ties into the CRD pump suction line before the CRD suction filter. The flow control station will divert 250 gpm from the Condensate system. This will supply the CRD system with the remainder of the water being passed on to the CST. In the event that flow from the Condensate system is interrupted, the CST provides a backup source of water to ensure CRD system operability without operator action being required. A simplified schematic of the CRD system is provided by Figure 2.3.

The CRD pumps, together, can achieve a flow rate of approximately 210 gpm with the reactor fully pressurized and approximately 300 gpm with the reactor depressurized. Two discharge paths are provided for the CRD pumps. One discharge path is through an air-operated valve control station. When instrument air is lost, this path is blocked. With both CRD pumps running and the reactor at nominal pressure, the second discharge path restricts flow, by means of an orifice, to approximately 180 gpm.

Normally one CRD pump is running, with the suction and discharge valves to the standby pump being blocked. Should the operator be required to realign the CRD system as a sole source of early high pressure injection, the standby CRD pump must be placed into operation to achieve sufficient flow to the reactor vessel.

In general, the CRD success criteria (as a sole injection source to the reactor) requires both pumps running and one of the two discharge paths available. If some other injection system has been operating successfully for 6 or more hours following an initiator, the CRD success criteria changes to one pump running and one of two discharge paths available.

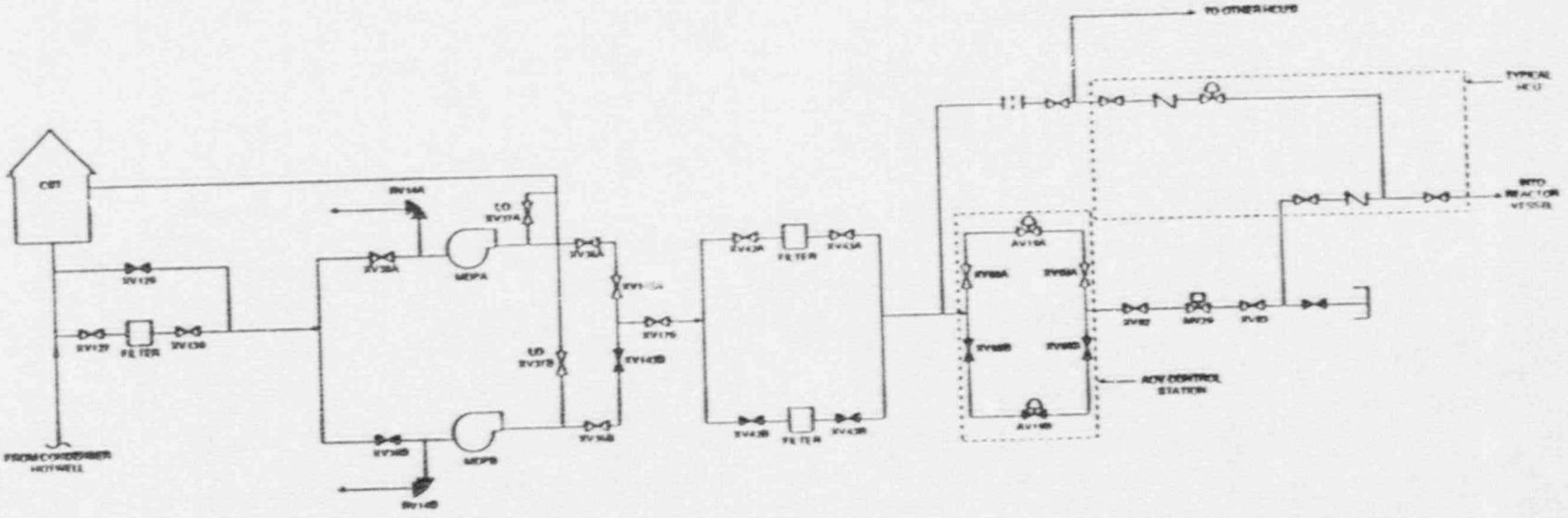

Figure 2.3 Control Rod Drive System Schematic.

Most of the CRD system is located in the turbine building. Any physical impact of accident conditions on the ability of the CRD system to perform its function would be minimal. Since the system is located in a large open area, room cooling failure is not applicable to the CRD pumps. The CRD pumps receive no automatic initiation signals.

2.2.5 Automatic Depressurization System (ADS)

The ADS is designed to depressurize the primary system to a pressure at which the low pressure injection systems can inject coolant to the reactor vessel (event tree nomenclature--X_1, X_2, X_3).

The Automatic Depressurization system (event tree nomenclature--X_1) describes the automatic or, if required, manual operation of the ADS/SRV system to depressurize the primary system. This allows the low pressure injection systems to be used to cool the core. The Manual Depressurization system (event tree nomenclature--X_2) describes manual operation of the ADS/SRV system to depressurize the primary system. This allows the SDC mode of the RHR system to be used. A data value is used for the event tree question, "Do the ADS/SRV valves reopen following containment failure or venting?" (event tree nomenclature--X_3). This is strictly a survivability concern.

The ADS consists of five relief valves capable of being manually opened. Each valve discharges via a tailpipe line through a downcomer to the suppression pool. Relief valve capacity is approximately 820,000 lb/hr. A simplified schematic of the ADS is provided by Figure 2.4.

The ADS is automatically initiated. The operator may manually initiate the ADS or may depressurize the reactor vessel using the six relief valves that are not connected to ADS logic. The operator can inhibit ADS operation if a spurious ADS signal occurs or if the operator desires to do so (as in an ATWS scenario). The success criterion for the ADS is three of five valves opening to depressurize the reactor.

The ADS valves are located inside the containment. ADS performance is not normally affected by accident conditions since the equipment is qualified for accident conditions and the air/nitrogen supply pressure is judged to be sufficiently high to allow valve operation under most containment conditions. However, should containment pressure be excessively high (~85 psig or greater), the valves could not be kept open since the air/nitrogen supply pressure is limited to ~85 psig based on discussions with Philadelphia Electric Company (PECO) personnel indicating the supply is orificed to that limit.

Automatic ADS initiation occurs upon receipt of a low-low reactor water level signal (with an ~8-minute time delay), a low-low level and high drywell pressure signal, or notice that one LPCI or two LPCS pumps are running.

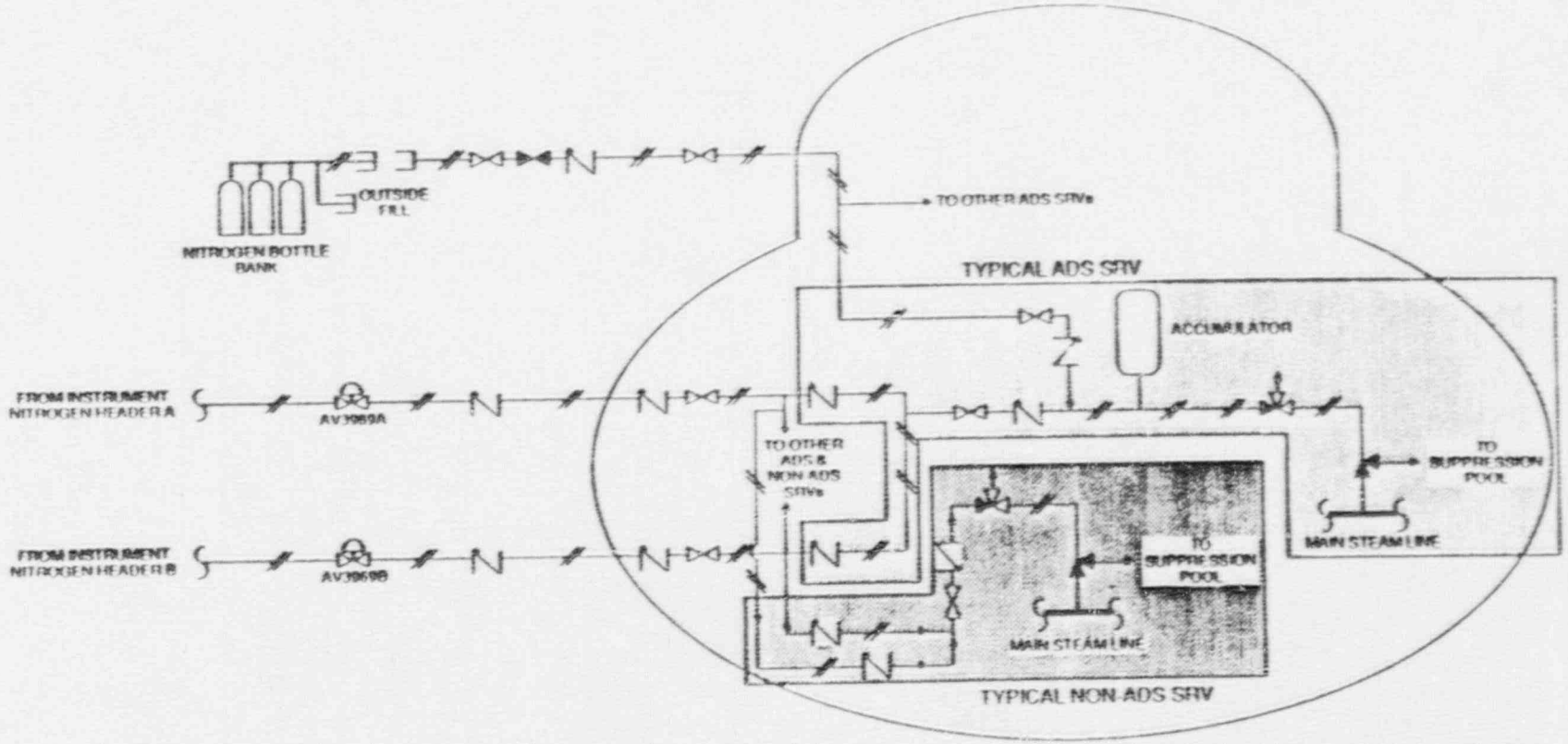

VALVES POSITIONS ARE SHOWN IN THEIR STANDBY MODE

Figure 2.4 Automatic and Manual Depressurization System Schematic.

2.2.6 Low Pressure Core Spray (LPCS) System

The function of the LPCS system is to provide a makeup coolant source to the reactor vessel during accidents in which system pressure is low (event tree nomenclature--V2). The ADS can be used in conjunction with the LPCS system to attain a low enough system pressure for injection to occur.

The LPCS system is a two-loop system consisting of motor-operated valves and motor driven pumps. There are two 50-percent capacity pumps per loop, with each pump rated at 3125 gpm with a discharge head of 105 psig. The LPCS system's normal suction source is the suppression pool. Pump suction can be manually realigned to the CST. A simplified schematic of the LPCS system is provided by Figure 2.5. Major components are shown as well as the pipe segment definitions (e.g., PS-27) used in the system fault tree.

The LPCS system is automatically initiated and controlled. Operator intervention is required to manually start the system given an auto-start failure and to stop the system or manually control flow during an ATWS if required. The success criterion for the LPCS system is injection of flow from any two pumps to the reactor vessel.

Most of the LPCS system is located in the reactor building. Local access to the LPCS system could be affected by either containment venting or failure. Room cooling failure is assumed to fail the LPCS pumps in 10 hours.

Upon the receipt of a LPCS injection signal, start signals are sent to all LPCS pumps, both injection valves are demanded to open, and the test return valves are demanded to close. The LPCS system is automatically initiated on the receipt of either a low-low reactor water level (378 inches above vessel zero) or high drywell pressure (2 psig) and low reactor pressure (450 psig).

2.2.7 Low Pressure Coolant Injection (LPCI) System

The function of the LPCI system is to provide a makeup coolant source to the reactor vessel during accidents in which system pressure is low (event tree nomenclature--V3). The ADS can be used in conjunction with the LPCI system to attain a low enough system pressure for injection to occur. The LPCI system is but one mode of the RHR system and, as such, shares components with other modes.

The RHR system is a two-loop system consisting of motor-operated valves and motor-driven pumps. There are two pump/heat exchanger trains per loop with each pump rated at 10,000 gpm with a discharge head of 450 psig. Cooling water flow to the heat exchangers is not required for the LPCI mode. The LPCI suction source is the suppression pool. A simplified schematic of the LPCI (RHR) system is provided by Figure 2.6. Major components are shown as well as the pipe segment definitions (e.g., PS-19) used in the system fault tree.

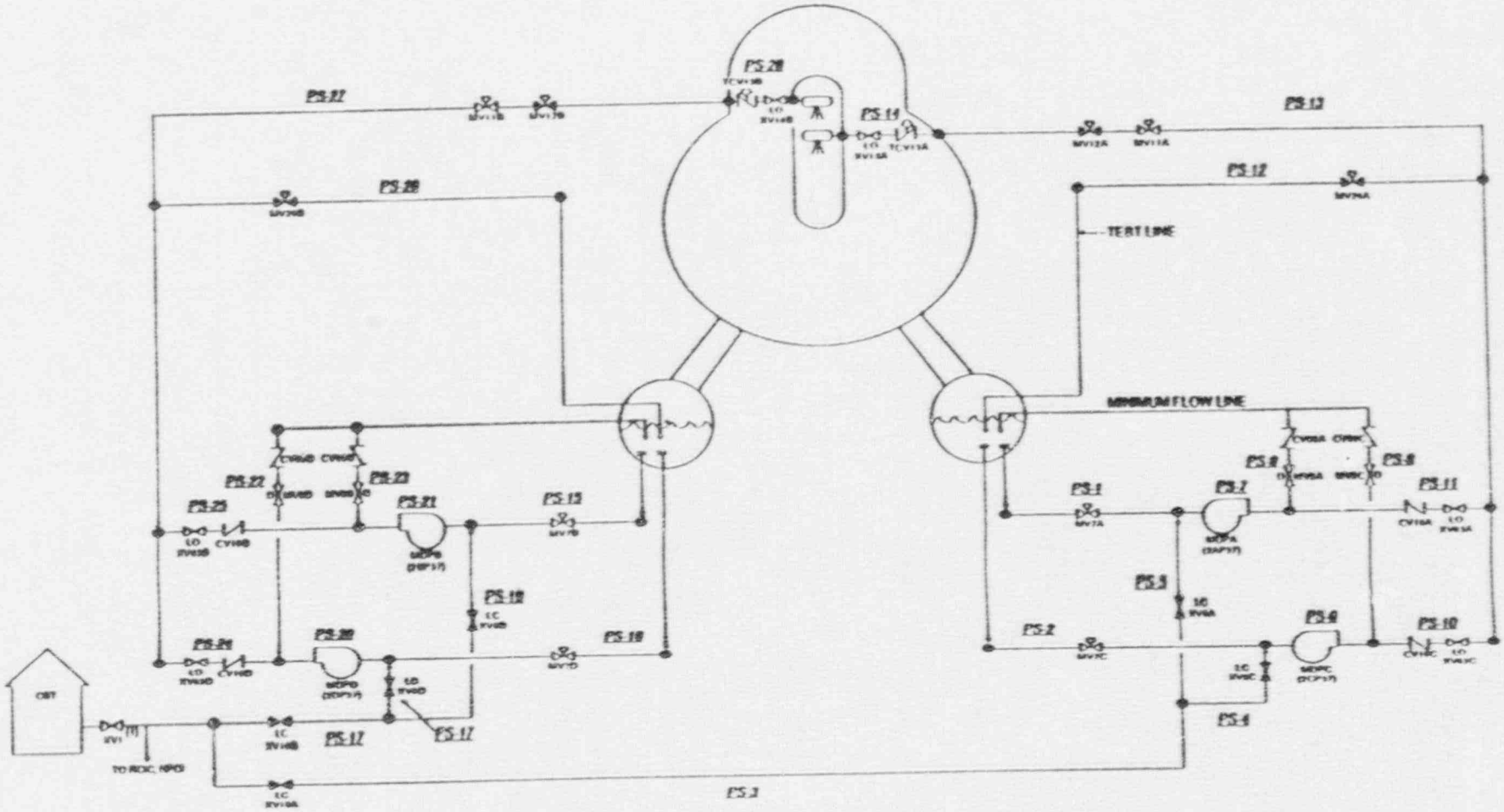

VALVE POSITIONS ARE SHOWN IN THEIR STANDBY POSITION
(1) VALVE ALSO LOCATED ON HPCI SCHEMATIC, SEE HPCI SCHEMATIC FOR DEFINITION OF PIPE SEGMENT

Figure 2.5 Low Pressure Core Spray System Schematic.

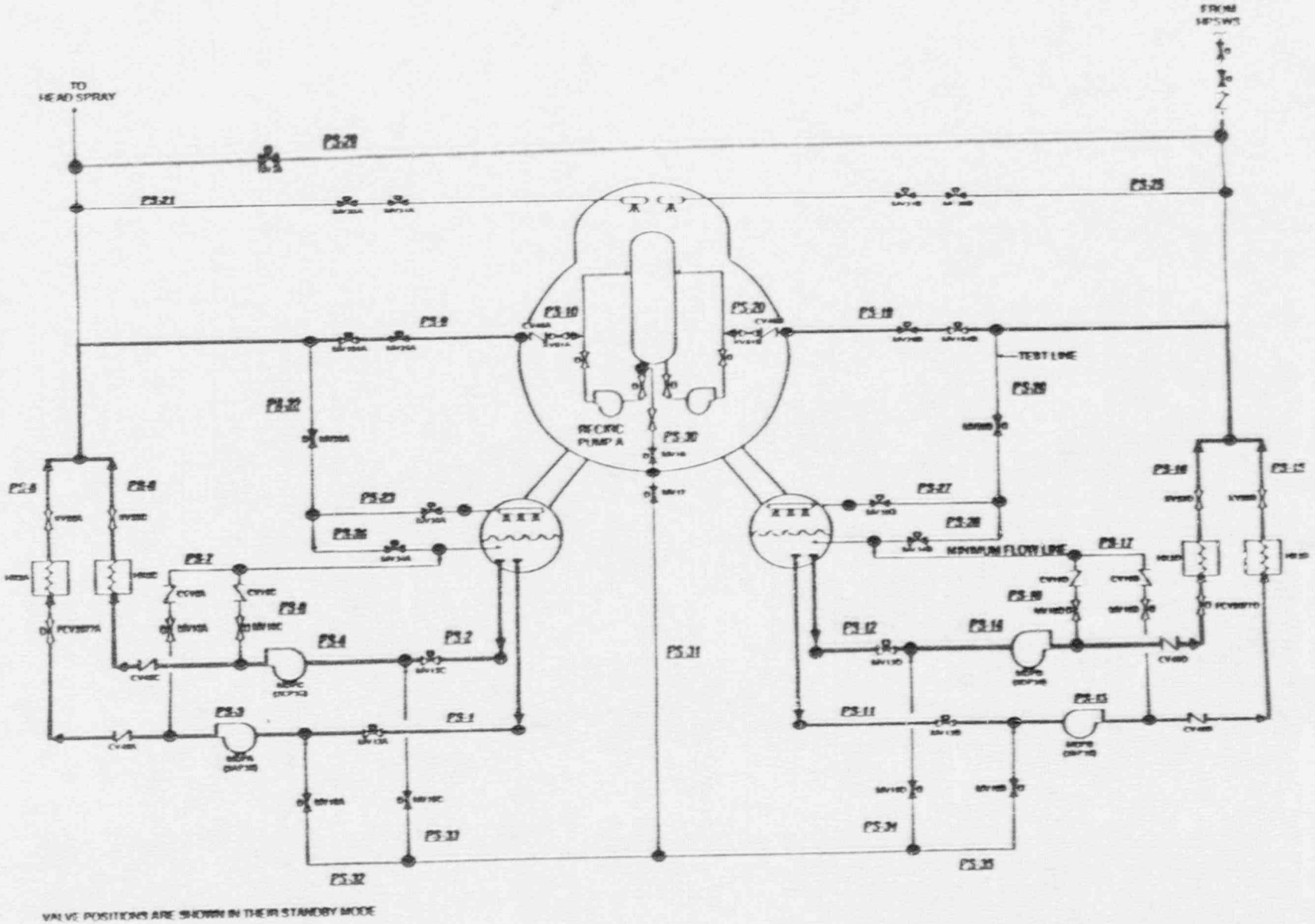

Figure 2.6 Low Pressure Coolant Injection System Schematic.

The LPCI system is automatically initiated and controlled. Operator intervention is required to manually start the system given an auto-start failure and to stop the system or control flow during an ATWS if required. The success criterion for the LPCI system is injection of flow from any one pump to the reactor vessel.

Most of the LPCI system is located in the reactor building. Local access to the LPCI system could be affected by either containment venting or failure. Room cooling failure is assumed to fail the LPCI pumps in 10 hours.

Upon the receipt of a LPCI injection signal, start signals are sent to all pumps, Loops A and B injection valves are subsequently demanded to open when reactor pressure is low enough, and the test return valves are demanded to close. The LPCI system is automatically initiated on the receipt of either a low-low reactor water level (378 inches above vessel zero) or high drywell pressure (2 psig) and low reactor pressure (450 psig).

2.2.8 Residual Heat Removal: Shutdown Cooling (SDC) System

The function of the SDC system is to remove decay heat during accidents in which reactor vessel integrity is maintained (event tree nomenclature--W1). The SDC system is but one mode of the RHR system and, as such, shares components with other modes.

The RHR system is a two-loop system consisting of motor-operated valves and motor-driven pumps. There are two pump/heat exchanger trains per loop, with each pump rated at 10,000 gpm with a discharge head of 20 psid. Cooling water flow to the heat exchanger is required for the SDC mode. The SDC system suction source is one reactor recirculation pump's suction line. A simplified schematic of the SDC (RHR) system is provided by Figure 2.7. Major components are shown as well as the pipe segment definitions (e.g., PS-9) used in the system fault tree. The SDC system is manually initiated and controlled. The success criterion for the SDC system is injection of flow from any one pump/heat exchanger train to the reactor vessel.

Most of the SDC system is located in the reactor building. Local access to the SDC system could be affected by either containment venting or failure. Room cooling failure is assumed to fail the SDC pumps in ten hours.

SDC is initiated after emergency core injection is successful and reactor pressure is low. If an injection signal subsequently occurs, the RHR system will automatically be realigned to the LPCI mode. SDC cannot be initiated if any of the following conditions exist: (a) reactor pressure greater than 225 psig, (b) high drywell pressure (scram pressure), or (c) low reactor water level.

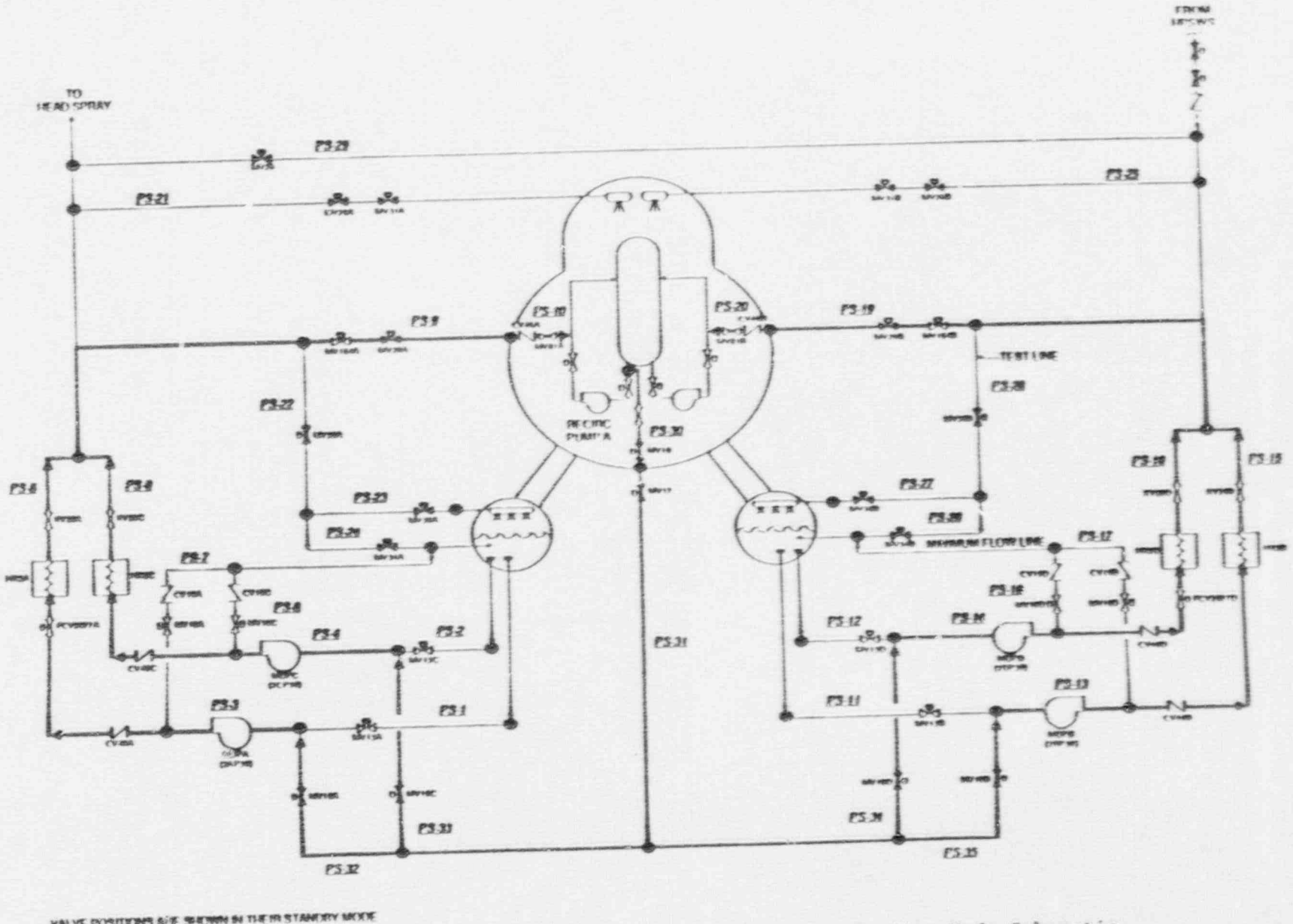

Figure 2.7 Residual Heat Removal System - Shutdown Cooling Mode Schematic.

2.2.9 Residual Heat Removal: Suppression Pool Cooling (SPC) System

The function of the SPC system is to remove decay heat from the suppression pool during accidents (event tree nomenclature--W2). The SPC system is but one mode of the RHR system and, as such, shares components with other modes.

The RHR system is a two-loop system consisting of motor-operated valves and motor-driven pumps. There are two pump/heat exchanger trains per loop, with each pump rated at 10,000 gpm with a discharge head of 20 psid. Cooling water flow to the heat exchanger is required for the SPC mode. The SPC suction source is the suppression pool. A simplified schematic of the SPC (RHR) system is provided by Figure 2.8. Major components are shown as well as the pipe segment definitions (e.g., PS-26) used in the system fault tree. The SPC system is manually initiated and controlled. The success criterion for the SPC system is injection of flow from any one pump/heat exchanger train to the suppression pool.

Most of the SPC system is located in the reactor building. Local access to the SPC system could be affected by either containment venting or failure. Room cooling failure is assumed to fail the RHR pumps in ten hours.

The SPC mode is manually initiated. If an injection signal is generated subsequent to the initiation of the SPC system, the SPC system will automatically realign to the LPCI mode. Besides a time delay, a permissive indicating that the reactor water level is above the shroud (312 inches above vessel zero) must be present prior to aligning to the SPC mode. However, this permissive may be overridden by a switch in the control room.

2.2.10 Residual Heat Removal: Containment Spray (CS) System

The function of the CS system is to suppress pressure in the drywell during accidents (event tree nomenclature--W3). The CS system is but one mode of the RHR system and, as such, shares components with other modes.

The RHR system is a two-loop system consisting of motor-operated valves and motor-driven pumps. There are two pump/heat exchanger trains per loop, with each pump rated at 10,000 gpm with a discharge head of 20 psid. Cooling water flow to the heat exchanger is required for the CS mode. The CS suction source is the suppression pool. A simplified schematic of the CS (RHR) system is provided by Figure 2.9. Major components are shown as well as the pipe segment definitions (e.g., PS-25) used in the system fault tree. The CS system is manually initiated and controlled. The success criterion for the CS system is injection of flow from any one pump/heat exchanger train to the spray ring.

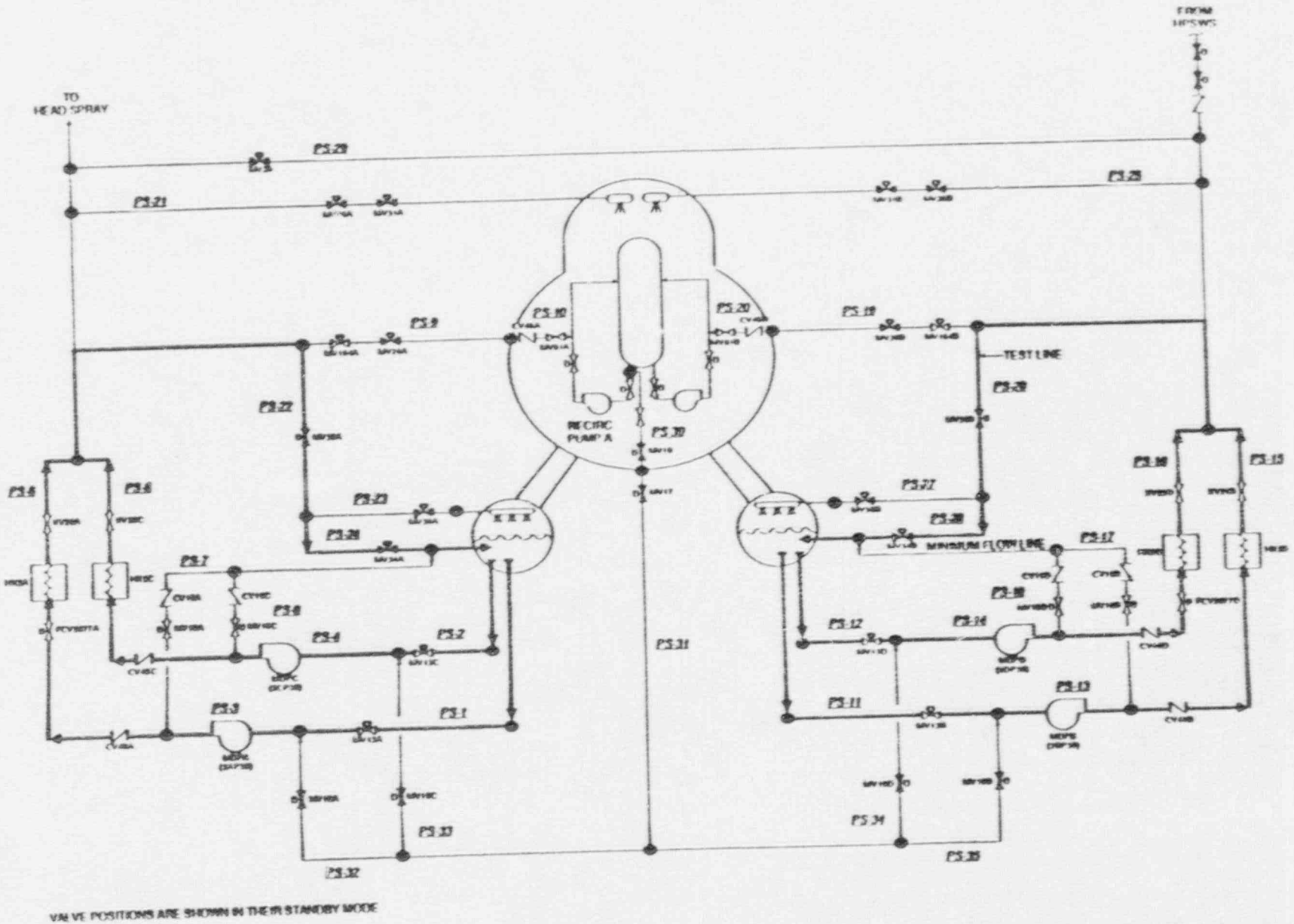

Figure 2.8 Suppression Pool Cooling System Schematic.

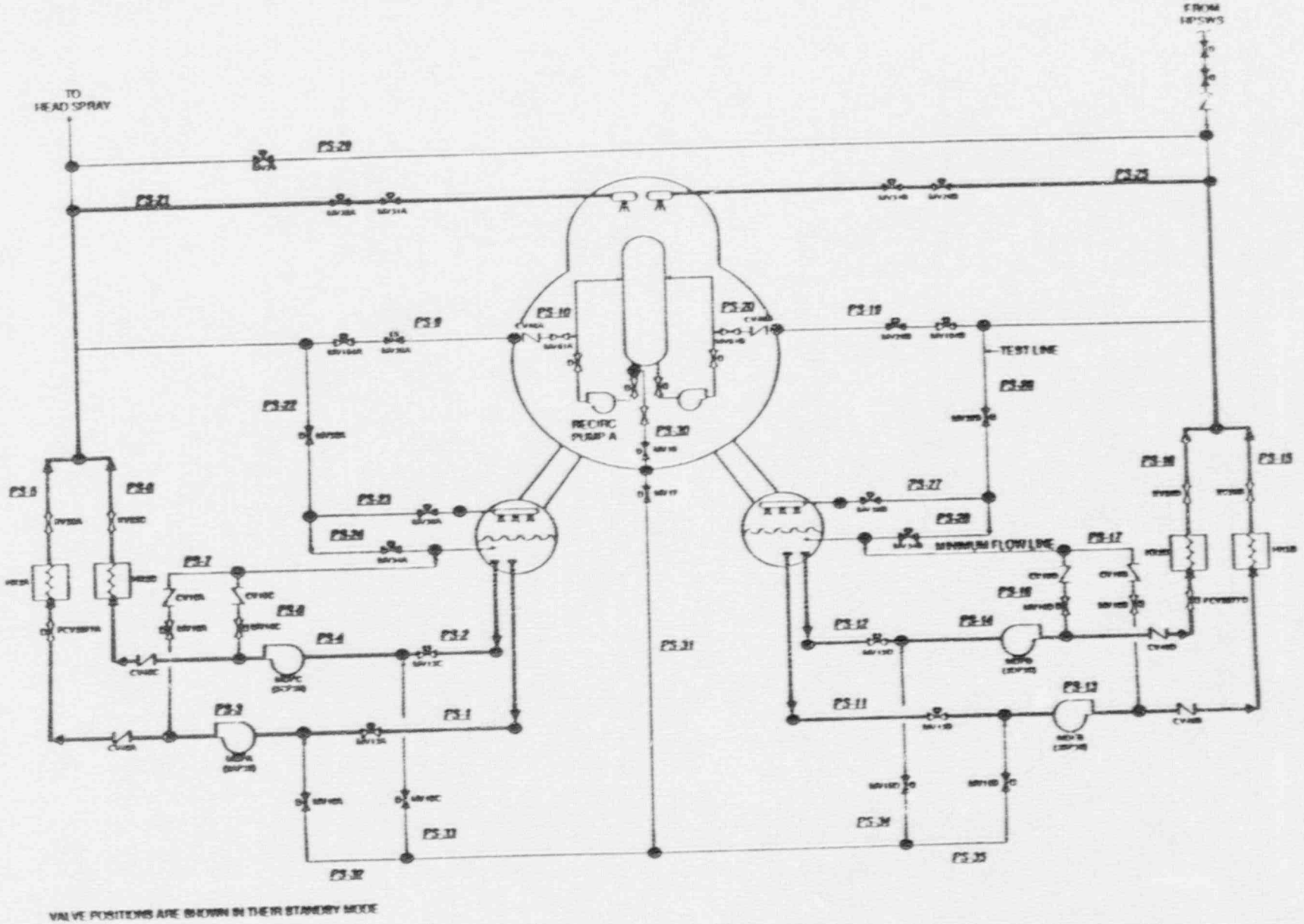

Figure 2.9 Containment Spray System Schematic.

Most of the CS system is located in the reactor building. Local access to the CS system could be affected by either containment venting or failure. Room cooling failure is assumed to fail the CS pumps in ten hours.

Reactor water level above the shroud (312 inches above vessel zero) and high drywell pressure (2 psig) permissive signals must be present before the CS system can be manually initiated. The water level signal can be overridden.

2.2.11 Electric Power System (EPS)

The EPS is designed to provide a diversity of dependable power sources which are physically isolated from each other.

The Peach Bottom station receives power from two separate offsite sources. If both offsite sources are lost, auxiliary power is supplied to both Unit 2 and Unit 3 from four onsite diesel generators shared between the two units. Loads important to plant safety are split and diversified. Station batteries provide control power for specific engineered safeguards and for other required functions when AC power is not available. A simplified schematic of the EPS is provided by Figure 2.10.

Each diesel generator unit consists of a diesel engine, a generator, and the associated auxiliaries mounted on a common base. The continuous rating of the diesel generators is 2600 kW. The engine is rated for a ten percent overload for any two of every 24 hours.

There are two independent 125/250 V DC systems per unit. Each system is comprised of two 125-V batteries, each with its own charger. Each 125-V battery is a lead-calcium type with 58 cells. The chargers are full wave, silicon-controlled rectifiers. The two batteries for each unit are redundant. Loads are diversified between these systems so that each system serves loads which are identical and redundant. Power for larger loads, such as dc motor-driven pumps and valves, is supplied at 250 V from two 125-V sources. Selected batteries from Unit 2 and from Unit 3 are needed to start Diesel Generators 1, 2, 3 and 4, respectively.

E dby diesel generator automatically starts. The diesel generator
ı ed by the operator after determining that continued operation
c al is not required.

the EPS is located in the diesel building and in com-
p lized rooms within the reactor building. Any physical impact of
acc conditions on the ability of the EPS to perform its function would be minimal. It is assumed that room cooling is not required for the ac switchgear or dc battery rooms since the heat loads are small and no sizeable heat loads are near these rooms. Diesel generators are assumed to fail in less than 30 minutes without room cooling although it is recognized that diesel performance would degrade before actual failure of the diesel and provide a warning to the operators that a problem

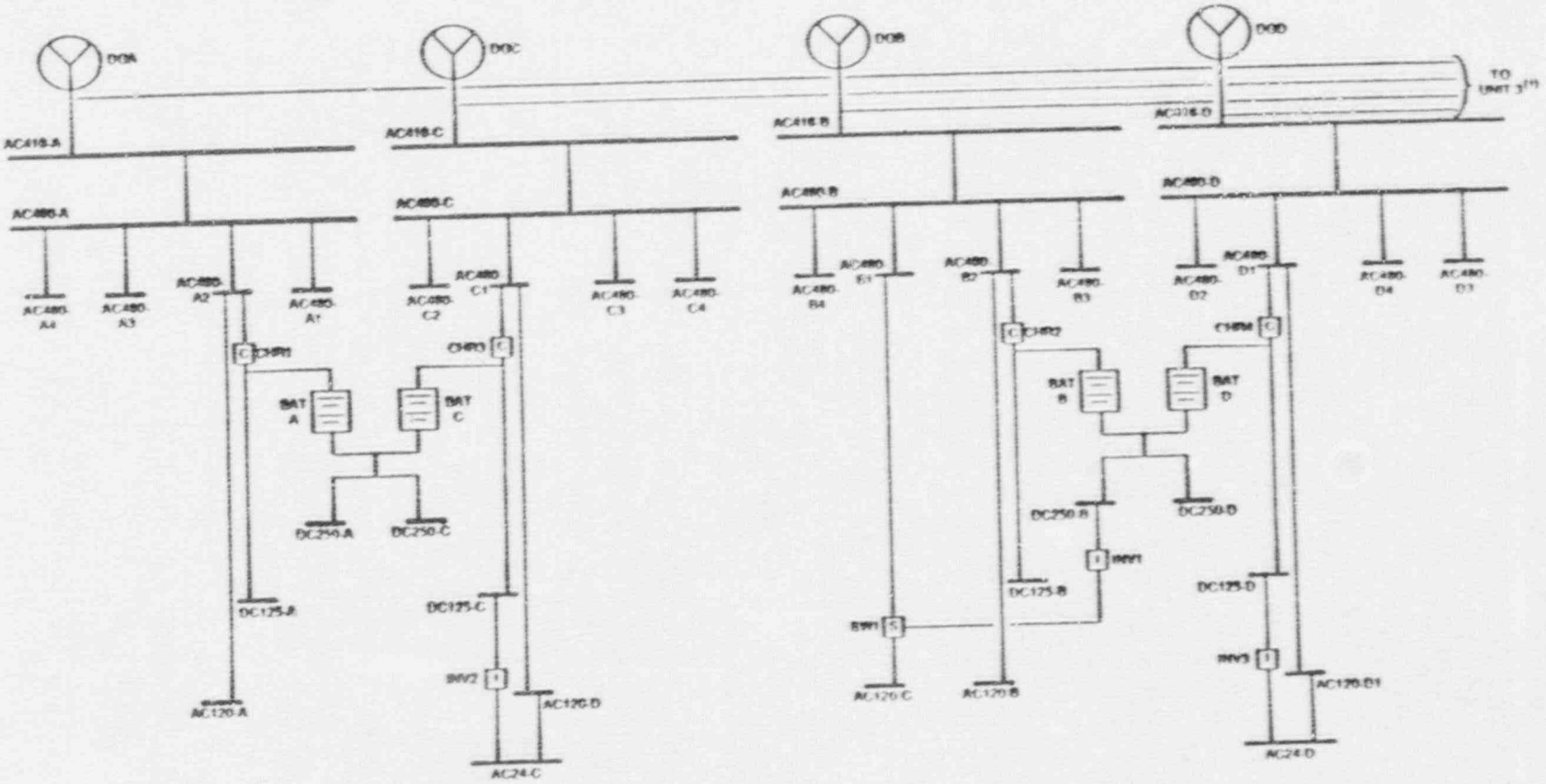

(1) GOES TO UNIT 3 BUSES (DG A, B, C, AND D ARE ARE SHARED BETWEEN UNITS 2 AND 3)

Figure 2.10 Electric Power System Schematic

existed. Possible recovery actions (by opening doors) could therefore take place. Complete failure of the EPS would cause a station blackout. After a total loss of ac power, dc-driven components could operate until the station batteries are depleted (estimated at about 6 hours based on PECO input).

Each standby diesel generator automatically starts on total loss of offsite power, low reactor water level, or high drywell pressure coincident with low reactor pressure. Two sources of offsite power are available to each 4-kV emergency bus. The failure of one offsite power source results in the automatic transfer to the other offsite source. When the diesel generators are demanded, essential loads are automatically sequenced onto the emergency bus. Nonessential 480 V loads are prevented from being automatically sequenced. Each diesel generator can be started locally, but can be electrically connected to its bus only from the main control room.

2.2.12 Emergency Service Water (ESW) System

The function of the ESW system is to provide a reliable supply of cooling water to selected equipment during a loss of offsite power event.

The ESW system is common to both Units 2 and 3. The system has two full capacity pumps installed in parallel. The normal water supply to the suction of the ESW pumps is from Conowingo pond. The pump discharge consists of two headers with service loops to the diesel-engine coolers and selected equipment coolers. The modeled components supplied with cooling water are the LPCS pumps and pump room coolers, the RHR pumps and pump room coolers, the HPCI pump room cooler, and the RCIC pump room cooler. Valves in the supply headers provide loop isolation. A common discharge header directs effluent to Conowingo pond. A simplified schematic of the ESW system is provided by Figure 2.11. Major components are shown as well as the pipe segment definitions (e.g., PS-8) used in the system fault tree.

The ESW pumps are vertical, single-stage, turbine types with an 8000 gpm capacity. Their normal discharge head is 96 ft and their shutoff head is 132 ft.

The cooling for all modeled equipment, with the exception of the diesel generator coolers, is normally provided by the Normal Service Water (NSW) system which operates on offsite ac power only.

Should the preferred flow paths described above be unavailable or the bay level preclude normal flow path operation, the ESW system may also be operated in conjunction with the Emergency Heat Sink (EHS) in a closed or open loop fashion. In the closed loop mode, two ESW booster pumps take return water from various coolers, boost it in pressure, and deliver the water to the emergency cooling tower structure. The booster pumps are horizontal split types, with 8000 gpm flow at a head of 100 psig. One Emergency Cooling Water (ECW) pump then takes suction from the cooling

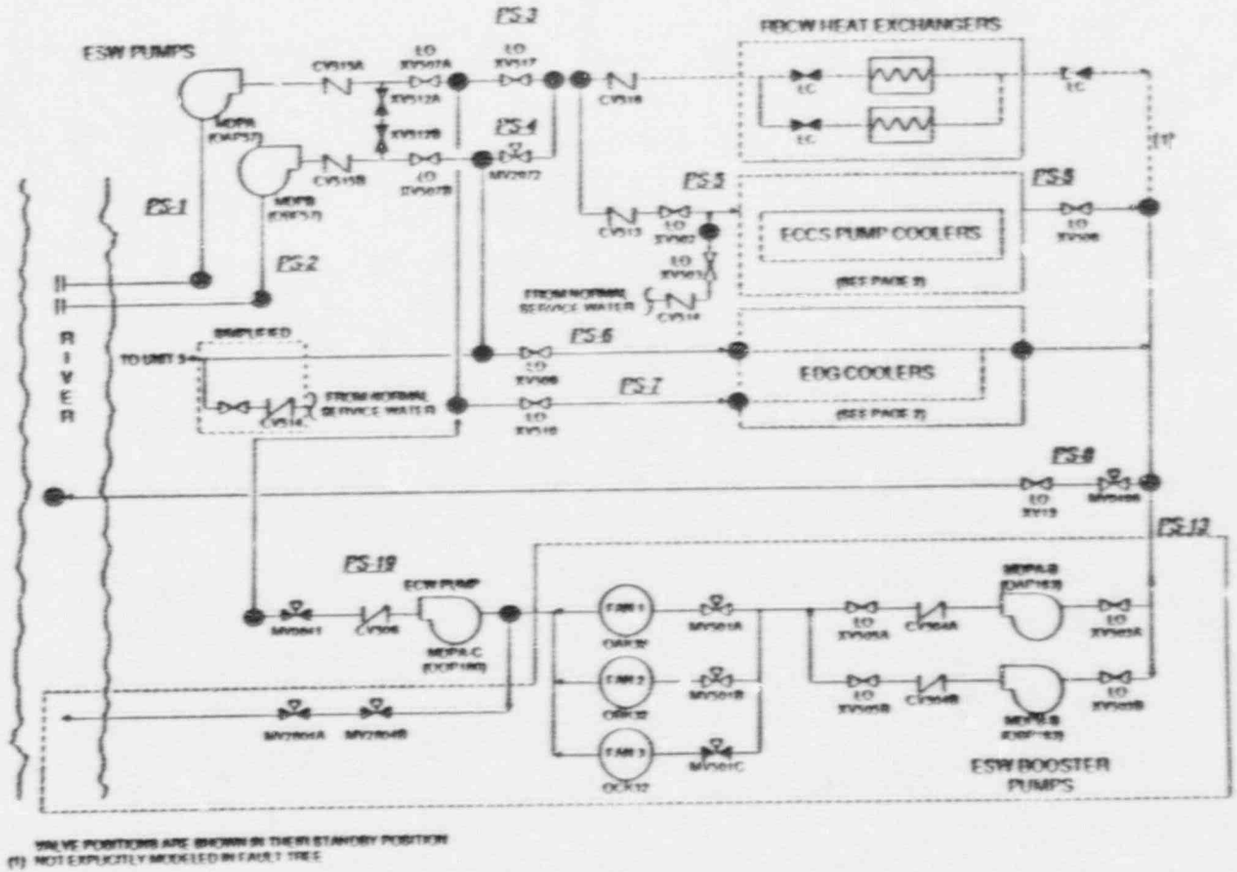

Figure 2.11 Emergency Service Water System Schematic.
(Page 1 of 7)

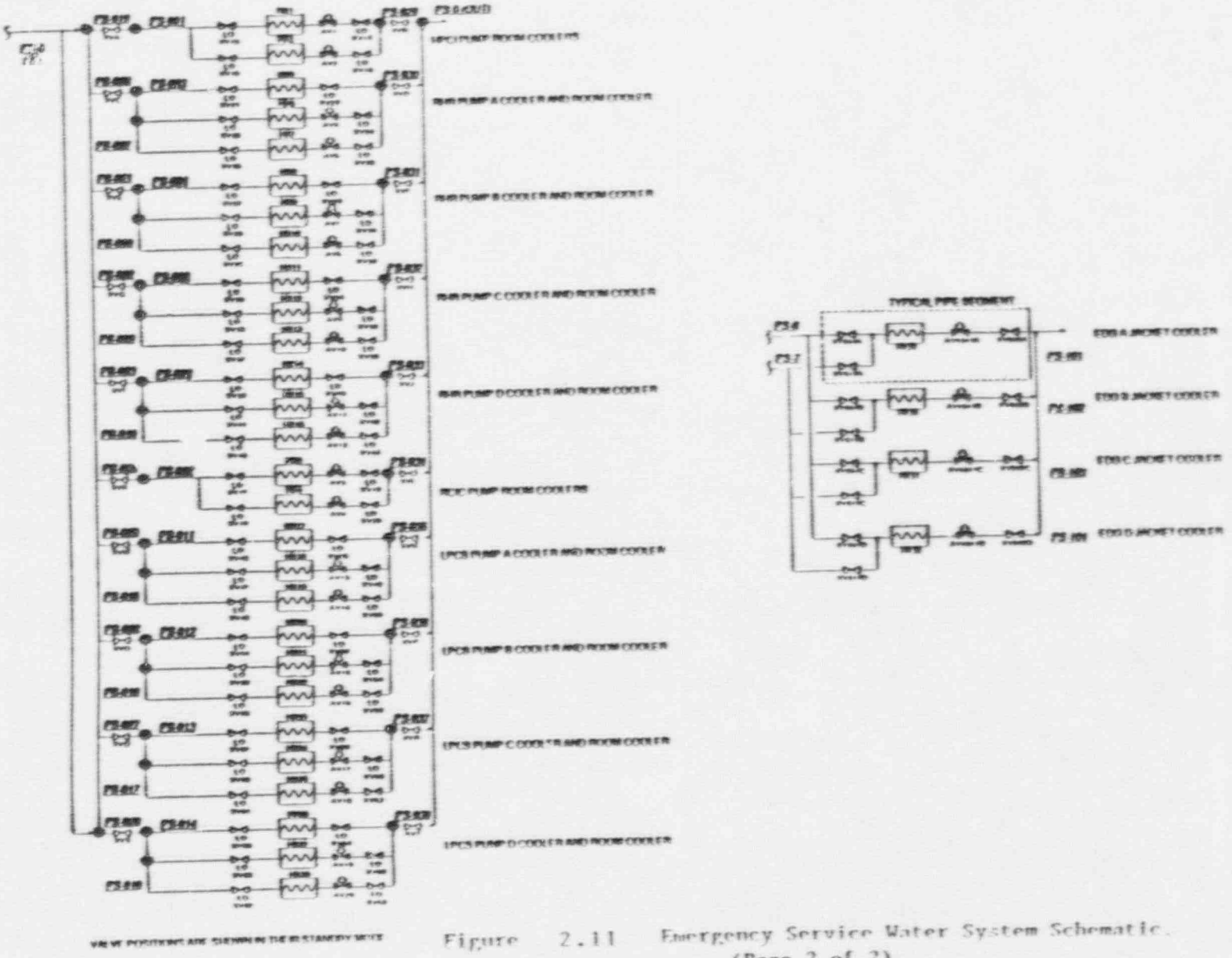

Figure 2.11 Emergency Service Water System Schematic.
(Page 2 of 2)

tower structure. It delivers water through a motor-operated gate valve to the ESW heat loads. The ECW pump and motor are identical to those of the ESW pumps. The only difference between the ECW pump and the ESW pumps is pump column length. While the booster pumps would normally be used in this mode, they are not required since it has been demonstrated by tests that booster pump failure will not fail the cooling function of the ESW. In the open loop mode, the ECW pump delivers water from the cooling tower structure, thru the ESW loads, and back to the bay. There is sufficient water supply in the cooling tower structure to last four days; hence the open loop mode is considered a success path.

Upon system automatic initiation, the operator checks discharge pressure for the two primary ESW pumps. If discharge pressure appears normal, the operator turns off one ESW pump and the ECW pump (the ECW pump also has an automatic trip in ~45 seconds if the discharge pressure is adequate). At some later time, if the operating ESW pump trips and the standby ESW pump fails to start, the operator must manually start the ECW pump. In the EHS closed loop mode, cooling tower fans must be manually started. The success criterion for the ESW system is either of the ESW pumps or the ECW pump supplying cooling water to system heat loads.

Most of the ESW system is located in pump rooms external to the reactor and turbine buildings. Any physical impact of accident conditions on the ability of the ESW system to perform its function would be minimal. Room cooling failure is assumed not to fail the ESW pumps, ESW booster pumps, and ECW pump.

Failure of the ESW system would quickly fail operating diesel generators and potentially fail the LPCS pumps and RHR pumps. The HPCI pump and RCIC pump would fail by a loss of their room cooling 10 hours after a loss of the ESW system if other recovery actions were not taken.

Both ESW pumps and the ECW pump start on a diesel start signal or a LOCA signal (low water level/high drywell pressure). If all three pumps start successfully, the operator will shut off one ESW pump and the ECW pump. If the running ESW pump fails, the other ESW pump will receive an auto start signal on low discharge pressure.

2.2.13 High Pressure Service Water (HPSW) System

The HPSW system is designed to supply cooling water from the ultimate heat sink to the RHR system heat exchangers under post-accident conditions and can provide an additional source of water to the reactor vessel (event tree nomenclature--V_4) through a cross-tie to the RHR injection lines.

The HPSW system consists of four 4500 gpm pumps installed in parallel. The pumps are a vertical multi-stage turbine type with a discharge head of 700 ft. Each pump is sized to the design heat removal capacity of one RHR heat exchanger. Normal water supply to the suction of the pumps is from Conowingo Pond. In the EHS mode of system operation, suction and

discharge comes from the emergency cooling towers. The pump discharge is split into two headers with two pumps in each header. The headers are split by a normally closed, motor-operated gate valve. Each header delivers water to two RHR heat exchangers in parallel. The pump discharge head is sufficient to maintain the HPSW system at a higher pressure than the RHR system, thus precluding leakage of radioactivity and permitting operation in conjunction with the emergency cooling towers. As an injection source to the reactor vessel, the HPSW discharge to RHR injection lines is from the pump B/D header. This connects to the RHR header. A simplified schematic of the HPSW system is provided by Figure 2.12. Major components are shown as well as the pipe segment definitions (e.g., PS-10) used in the system fault tree.

The operator is required to initiate the HPSW system. To initiate the system in the RHR cooling mode, the operator must start the appropriate HPSW pump and open the appropriate motor operated discharge valve depending on which RHR heat exchanger(s) is being used. These discharge valves are arranged with one valve downstream of each of the four RHR heat exchangers. To inject water into the reactor vessel via the RHR system, the operator starts B and/or D HPSW pumps and opens M-176 and M-174.

The success criteria for the HPSW system in the RHR cooling mode is one of four pumps supplying flow to the appropriate one of four heat exchangers. This is based upon the RHR system success criteria. As a last effort injection source, either B or D pump must supply flow through the cross-tie and corresponding RHR injection line under depressurized conditions in the reactor vessel. Pump A or C can be used with operation of a cross-tie valve.

Most of the HPSW system is located in pump rooms external to the reactor and turbine buildings. Any physical impact of accident conditions on the ability of the HPSW system to perform its functions would be minimal except for the injection valves (MV-174, 176) which are in the reactor building and could be affected by harsh environments there. Room cooling failure is assumed not to fail the HPSW pumps.

Failure of the HPSW system in the RHR cooling mode would fail the RHR cooling function. Failure of the HPSW system in the injection mode would fail one source of water for reactor makeup and containment spray. The HPSW system is initiated manually, either locally or from the main control room.

2.2.14 Emergency Ventilation System (EVS)

The objective of the EVS is to maintain suitable temperatures in equipment rooms to preclude component failures.

The EVS cools the following: (1) standby diesel generator rooms, (2) pump structure service water pump rooms, and (3) pump rooms for the RHR, RCIC, HPCI and LPCS pumps. The pump rooms use small individual fan

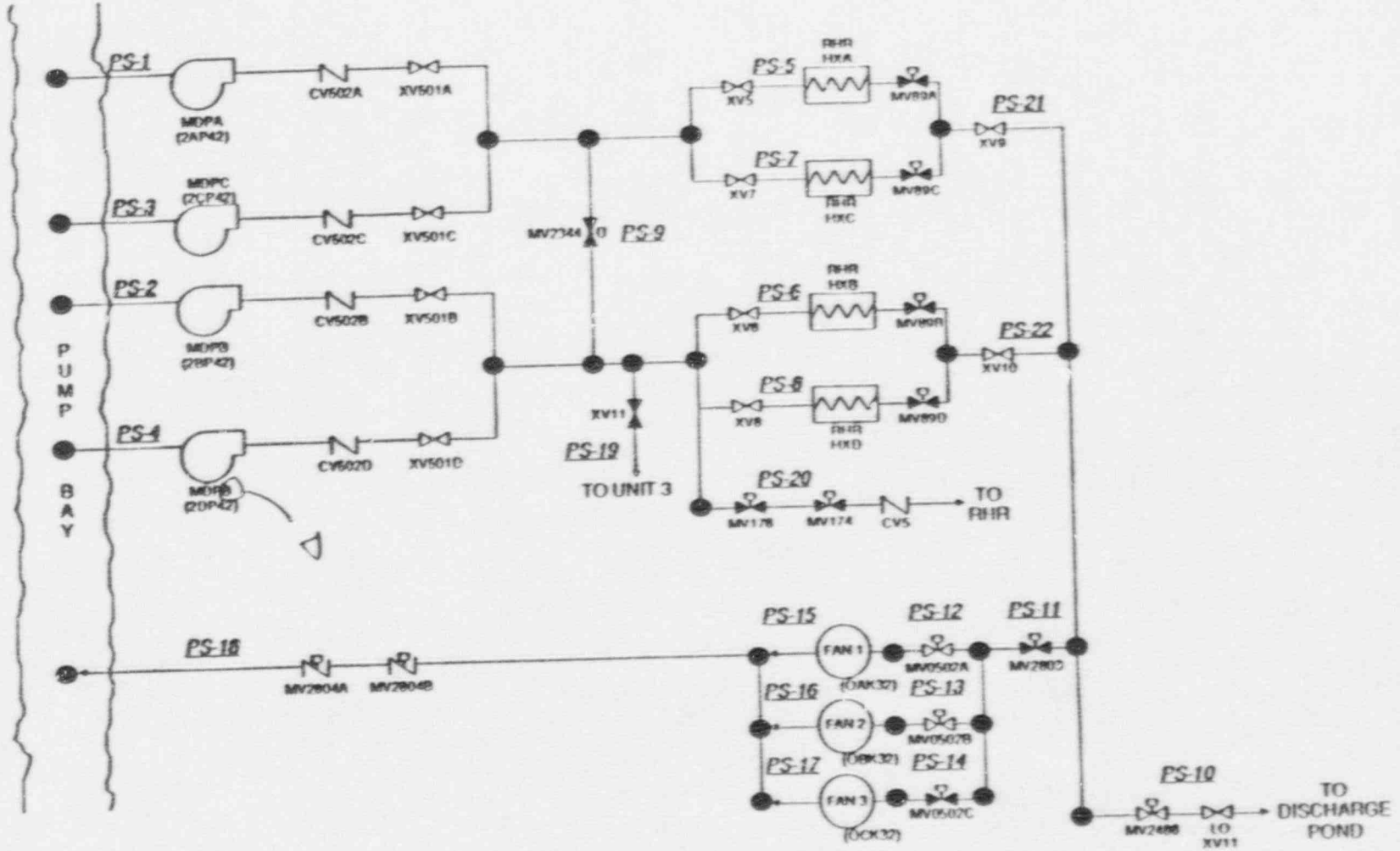

VALVE POSITIONS ARE SHOWN IN THEIR STANDBY MODE

Figure 2.12 High Pressure Service Water System Schematic.

coolers in each room. A simplified schematic of the rest of the EVS is provided by Figure 2.13. Major components are shown as well as the pipe (duct) segment definitions (e.g., PS-4) used in the system fault tree.

The service water pumps, emergency switchgear, and battery rooms are assumed not to require room cooling. Pump room cooling loss for the RHR, RCIC, HPCI, and LPCS pumps is incorporated into the ESW and individual system models. Therefore, the EVS system model does not include ESW, RHR, RCIC, HPCI, and LPCS pump room cooling.

Each standby diesel generator room is provided with ventilation air supply fans and an exhaust relief damper. Diesel generator room cooling requires operation of one of two supply fans. Any physical impact of accident conditions on the ability of the EVS to perform its function would be minimal. It is assumed that failure of the EVS would fail operating diesel generators in less than 30 minutes.

Diesel Generator Room Fans 7, 9, 11, and 13 outside air supply dampers open on 60°F fan discharge temperature and fail open on a loss of instrument air. Diesel Generator Room Fans 7, 9, 11, and 13 room air supply dampers close on 65°F fan discharge temperature and fail closed on a loss of instrument air. Dampers AV27, AV30, AV33, and AV36 open on Fans 7, 9, 11, and 13, starting signals respectively and fail open on a loss of instrument air. Fans 7, 9, 11, 13 automatically start on a diesel generator actuation signal. Fans 8, 10, 12, and 14 automatically start on an automatic start signal of Fans 7, 9, 11, and 13 respectively. Diesel generator room supply fans trip on a carbon dioxide discharge signal except when a LOCA signal is already present.

2.2.15 Instrument Air System (IAS)

The IAS provides a pneumatic supply to support short-term and long-term operations of safety equipment.

The IAS and Service Air System (SAS) consist of three, in parallel, air compressors supplying a common discharge header via individual air receiver tanks, piping, valves, and instrumentation. A fourth air compressor is tied into the SAS header and is common to both units. Two compressors, one IAS and one SAS, normally supply all compressed air requirements. The other IAS compressor serves in a standby capacity. A simplified schematic of the IAS is provided by Figure 2.14. Shown is the tie-in with the Instrument Nitrogen System which is the preferred supply to the MSIVs and ADS/SRVs. In addition to these compressors, the IAS is constantly backed up by two diesel compressors (not shown), and can be served by the Unit 3 IAS/SAS.

Each of the three parallel compressors is a vertical, single-stage, double-acting, non-lubricated, reciprocating compressor rated at 377 SCFM at 100 psig. Each has an aftercooler, moisture separator, and air receiver tank.

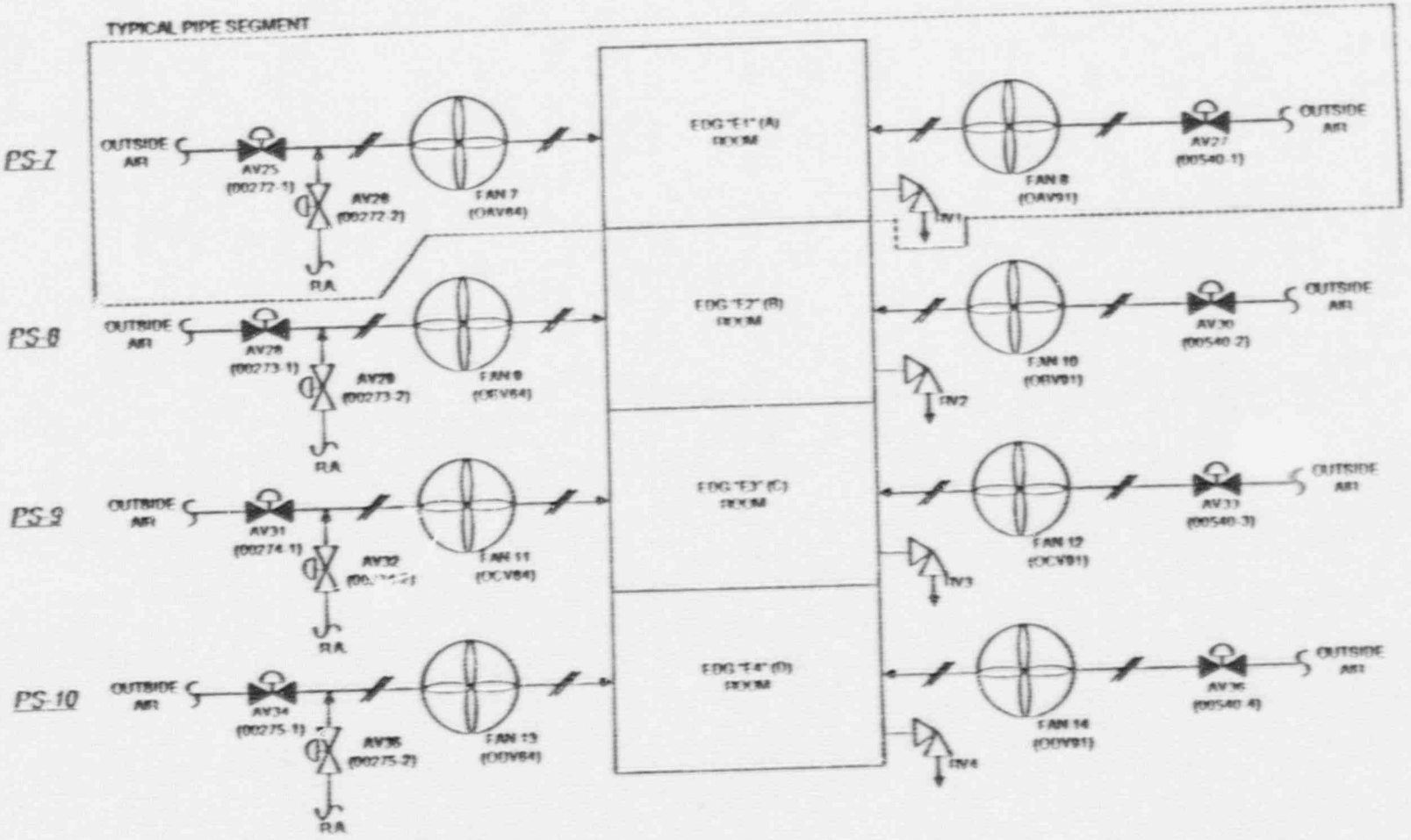

Figure 2.13 Emergency Ventilation System Schematic

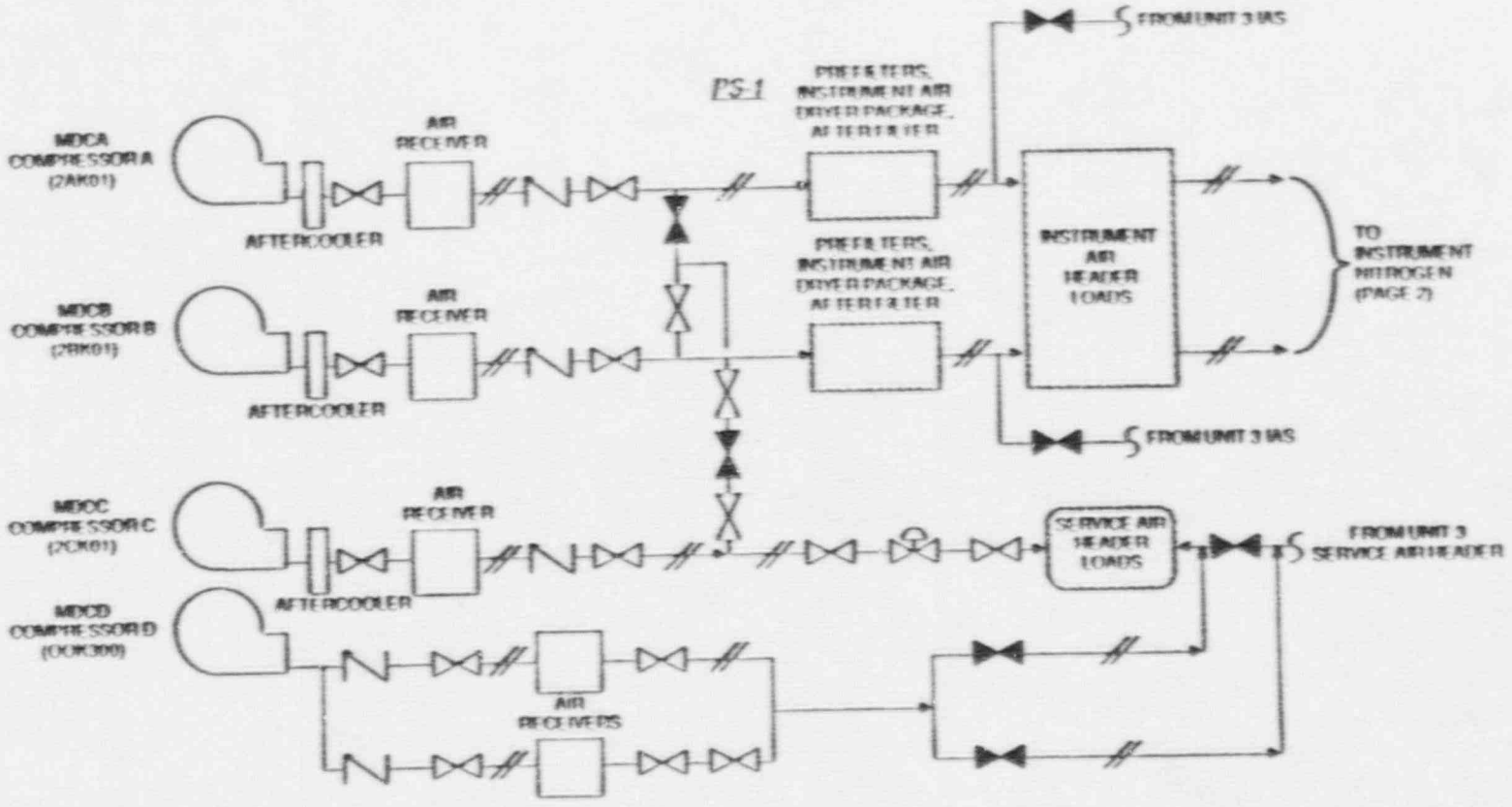

VALVE (DAMPER) POSITIONS ARE SHOWN IN THEIR STANDBY MODE

Figure 2.14 Instrument Air/Nitrogen System Schematic
(Page 1 of 7)

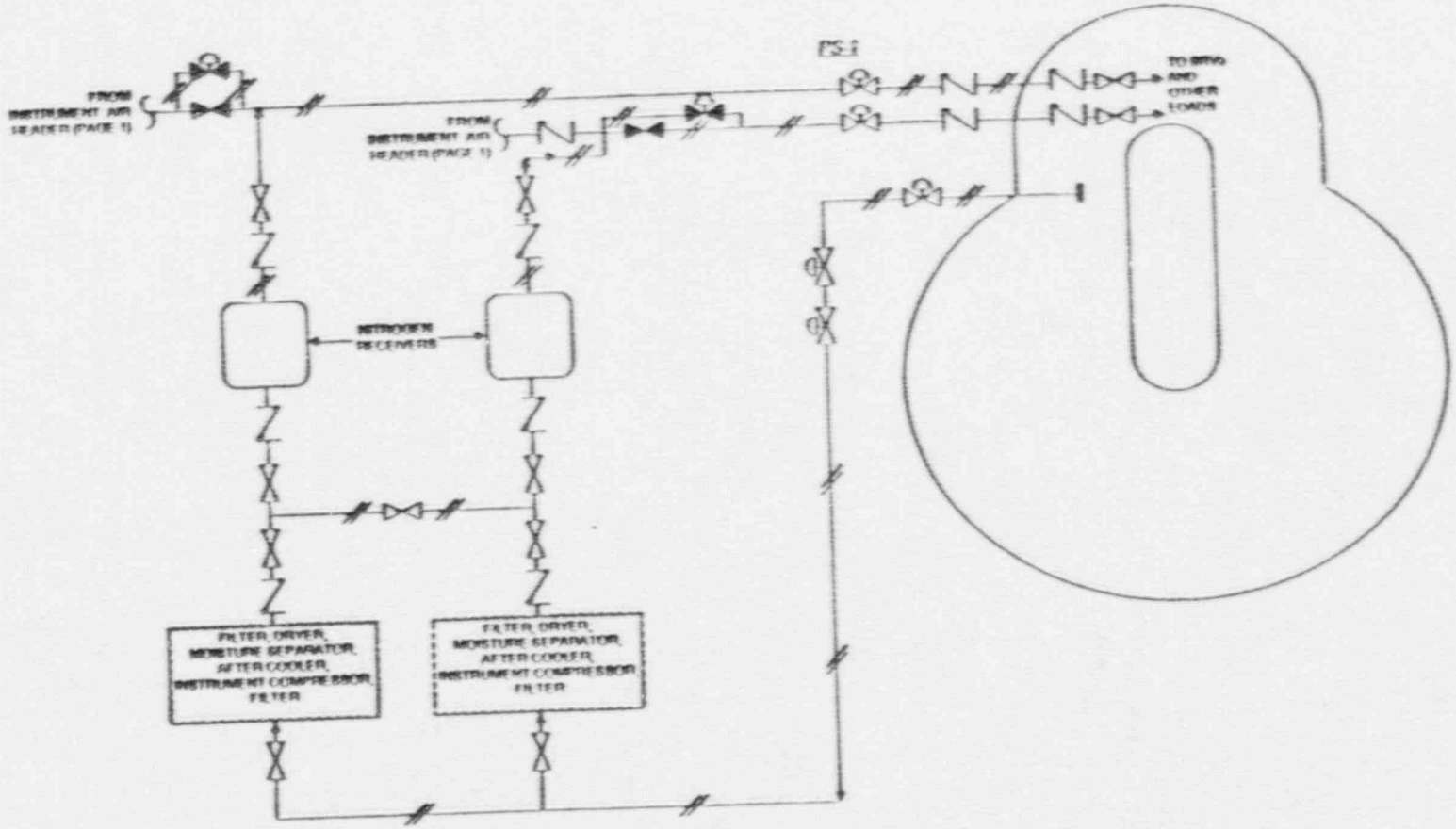

VALVE (DAMPER) POSITIONS ARE SHOWN IN THEIR STANDBY MODE

Figure 2.14 Instrument Air/Nitrogen System Schematic.
(Page 2 of 2)

The standby SAS compressor consists of a non-lubricated compressor, aftercooler, moisture separator, and two receivers. This compressor is rated at 400 scfm at 100 psig.

The IAS supplies clean, dry, oil-free air to EHV and ESW system air valves, the CRD control system, and containment venting air valves and is a backup to the Instrument Nitrogen System. When offsite power is lost, the air compressors trip. The operator is required to manually restart the air compressors when power is restored. The success criterion for the IAS is any one of the compressors supplying air to system pneumatic loads.

Any physical impact of accident conditions on the ability of the IAS to perform its functions would be minimal. Room cooling failure is assumed not to fail the IAS and SAS compressors. Even if this were to occur, the diesel compressors or Unit 3 compressors could serve the necessary loads.

Failure of the IAS does not directly fail any safety systems because (1) accumulators are on the MSIVs and ADS valves, (2) instrument nitrogen is the preferred source to the MSIVs and ADS valves, and (3) other safety systems "fail-safe" on loss of air or have dedicated air bottles.

2.2.16 Condensate System (CDS)

The function of the CDS system is to take condensate from the main condenser and deliver it to the reactor at an elevated temperature and pressure (event tree nomenclature--V1).

The CDS system consists of the condenser hotwell, three condensate pumps, feedwater heaters and associated piping, valves, and controls. The condenser hotwell has a working capacity of approximately 100,000 gallons. The condensate pumps provide the required head to overcome the flow and static resistance of the condensate system, and provide excess over the suction pressure requirements of the feedwater pumps. The reactor vessel must be depressurized to approximately 600 psig in order to use condensate as an injection source without the use of the feedwater pumps. Injection to the reactor vessel is via a feedwater line. The CDS pumps have a 10,870 gpm rated flow head. A simplified schematic of the CDS system is provided by Figure 2.15.

The CDS system is normally running. The success criteria for the CDS system is removal of decay heat (when the reactor has tripped). This can be sufficiently accomplished with only one pump train operational. Virtually all of the CDS system is located in the turbine building.

2.2.17 Primary Containment Venting (PCV) System

When torus and containment sprays have failed to reduce primary containment pressure the PCV is used to prevent a primary containment pressure limit from being exceeded (event tree nomenclature--Y).

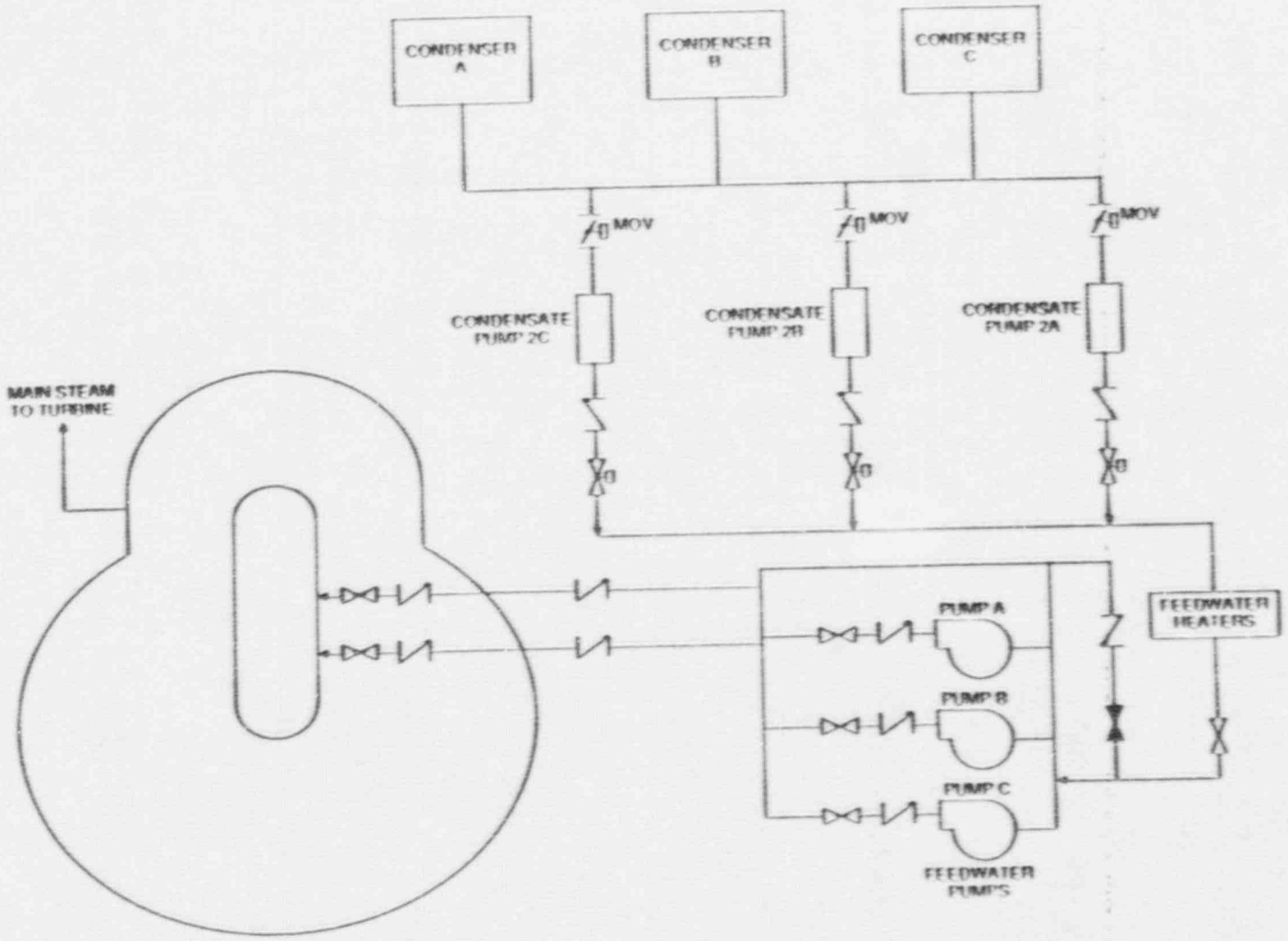

Figure 2.15 Condensate System Schematic.

The preferred primary containment vent paths include: (1) 2-in torus vent to the Standby Gas Treatment System (SGTS), (2) 6-in Integrated Leak Rate Test (ILRT) line from the torus, (3) 18-in torus vent path, (4) 18-in torus supply path, (5) 2-in drywell vent to the SGTS, (6) two 3-in drywell sump drain lines, (7) 6-in ILRT line from the drywell, (8) 18-in drywell vent path, and (9) 18-in drywell supply path. A simplified schematic of the PCV is provided by Figure 2.16.

For decay heat loads alone it is expected that the drywell pressure rise will be relatively slow. PCV success in this case is the 6-in vent path (or larger) being operational.

Current venting procedure requires a vent path to be established if containment pressure rises to 100 psig (PECO is considering changing this to 60 psig). In the case of an ATWS, or if it can be inferred that the suppression pool is being bypassed, the operator is required to directly establish the 18-in vent paths.

2.2.18 Reactor Building Cooling Water (RBCW) System

The function of the RBCW system is to provide a means of cooling auxiliary plant equipment which is located primarily in the reactor building (e.g. recirculation pumps, sump coolers, radwaste, etc.). The RBCW system is a backup for cooling CRD pumps and IAS compressors and aftercoolers should the TBCW be lost.

The RBCW system is a closed loop system consisting of two full-capacity pumps, two full-capacity heat exchangers, one head tank, one chemical feed tank and associated piping, valves, and controls. The RBCW system is designed for an operating pressure of 140 psig. A simplified schematic of the RBCW system is provided by Figure 2.17.

The operator uses RBCW to cool certain critical loads if the TBCW system is lost. The RBCW system usually has one pump continuously operating. Control and instrumentation is designed for remote system startup from the main control room.

The success criteria for the RBCW system is one pump and one heat exchanger train operating, providing sufficient cooling to the loads. The cooling water pumps and heat exchangers are located in the reactor building auxiliary bay. The head tank is located on the reactor building refueling floor. The specific RBCW loads are distributed throughout different areas of the plant.

2.2.19 Turbine Building Cooling Water (TBCW) System

The function of the TBCW system is to provide cooling water to auxiliary plant equipment associated with the power conversion system.

The TBCW system is a closed loop system consisting of two full-capacity pumps, two full-capacity heat exchangers, one head tank, one chemical

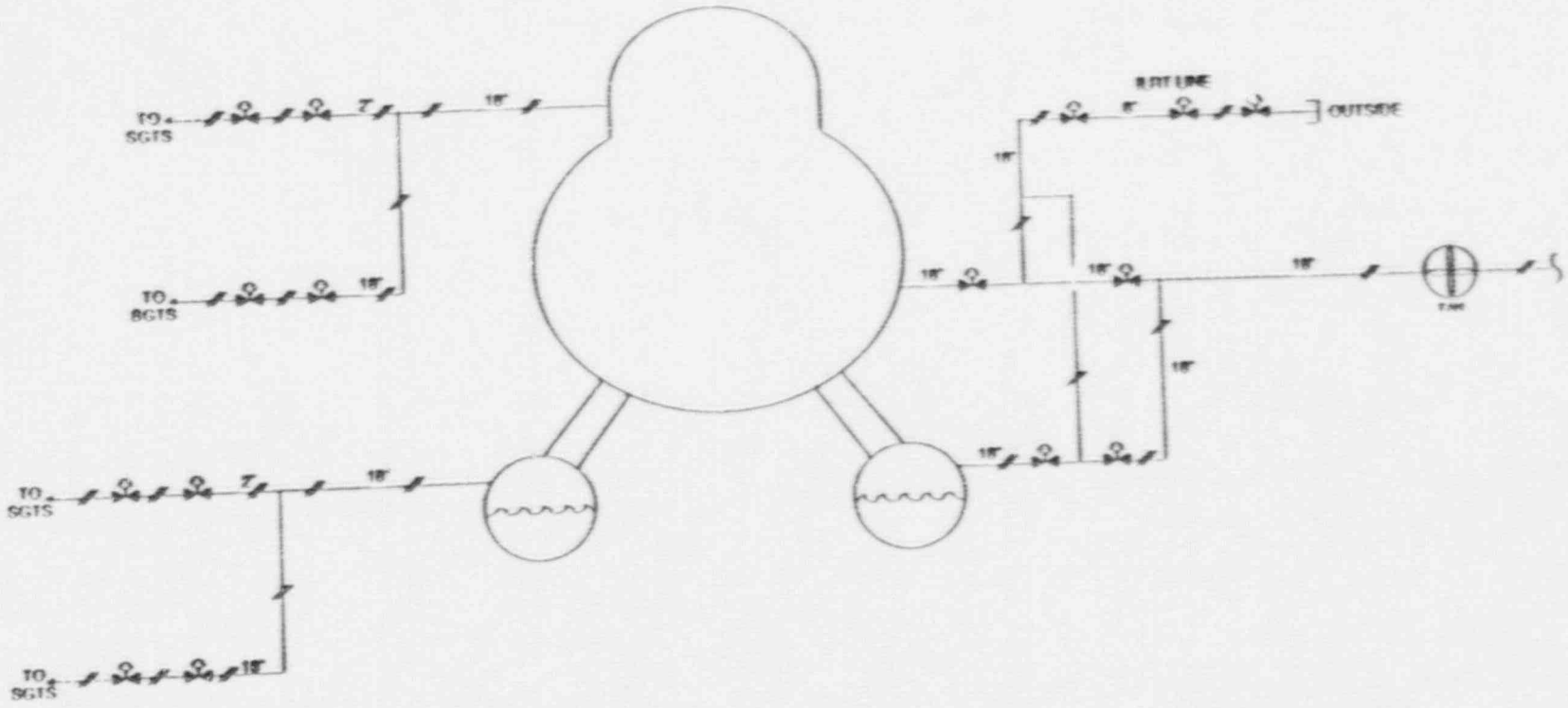

Figure 2.16 Primary Containment Venting System Schematic

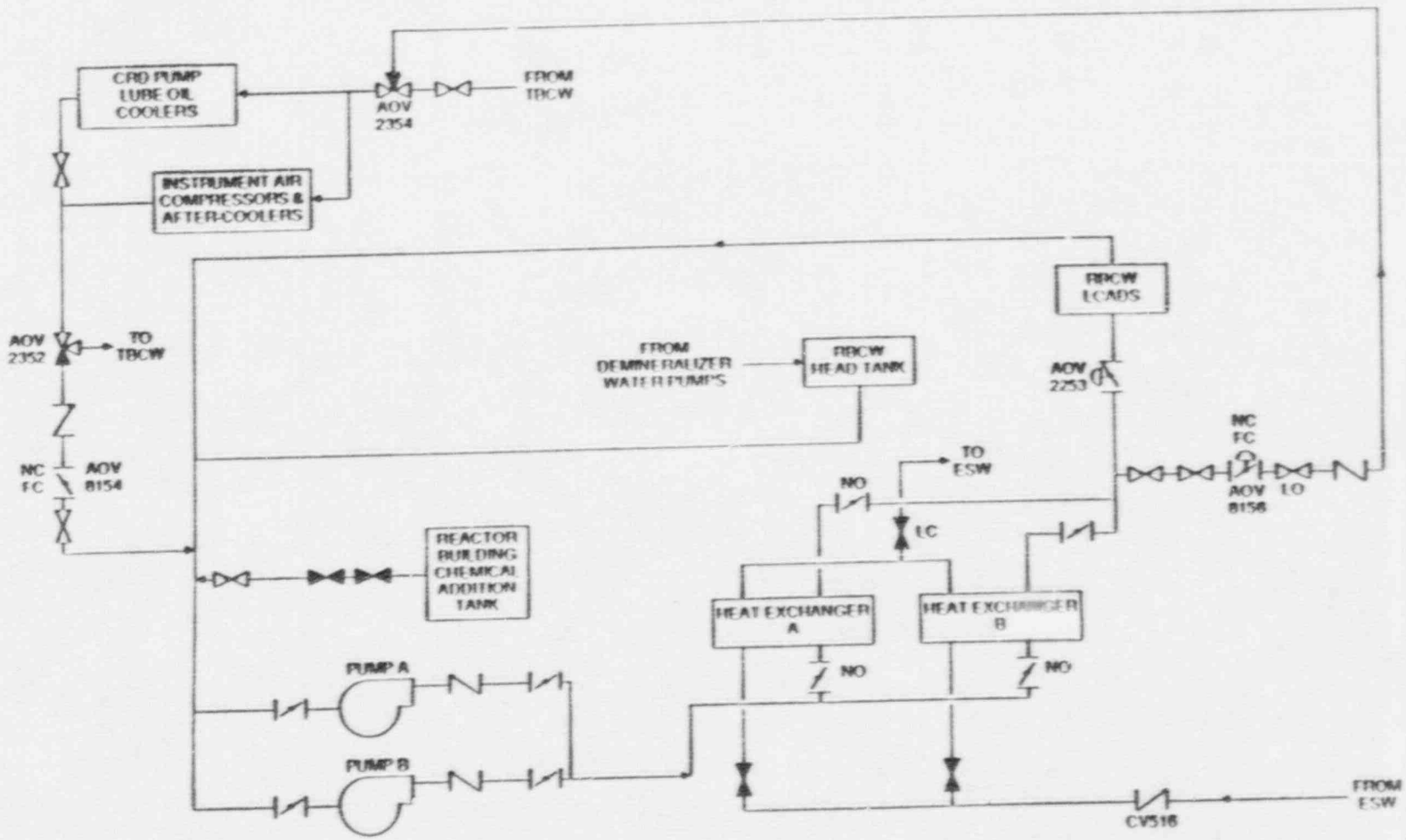

Figure 2.17 Reactor Building Cooling Water System Schematic.

fuel tank and associated piping, valves and controls. A simplified schematic of the TBCW system is provided by Figure 2.18.

The TBCW system is normally running. One pump is required to supply cooling to all TBCW loads. The success criteria for TBCW is one of two pumps and either of the two heat exchangers operating. This will provide sufficient cooling to the TBCW loads.

The majority of the TCW system including the cooling water pumps, heat exchangers and associated piping, valves and controls are located on the turbine building ground floor. The specific TBCW loads are distributed throughout different areas of the plant.

2.3 Event Tree Analysis

Event tree analysis involves the identification of the possible accident sequences for each initiator. This was done using the event tree approach which is commonly used in PRAs. Event trees are logic diagrams at the system level of detail which represent the combinations of system successes and failures forming possible sequences of events following each initiator. The philosophy behind the event tree analysis for Peach Bottom was to depict system successes and failures until the status of the core and containment are safe, vulnerable, or damaged and to display the status of other systems sufficiently to describe the plant damage states applicable to each accident sequence.

The construction of the event trees was performed using the knowledge and experience base already represented by other Boiling Water Reactor (BWR) PRAs and with consideration of the generic event trees created as part of earlier ASEP efforts. Two major expansions of previous BWR event tree work were included, however, in this study:

a. Formal analysis was conducted for more systems capable of core and containment cooling than considered before. Specifically, credit for the Control Rod Drive (CRD) system and the High Pressure Service Water (HPSW) system as injection sources to the reactor vessel was explicitly included in the success criteria and treated in the event trees and accompanying analyses. In addition, the Shutdown Cooling (SDC), Suppression Pool Cooling (SPC), and Containment Spray (CS) modes of the Residual Heat Removal (RHR) system, as well as the latest containment venting procedures (called containment venting in the tree, Y), were explicitly analyzed.

b. The event tree analyses explicitly displayed and covered possible system success and failure paths beyond successful containment venting or containment failure. Therefore, the success or failure probabilities associated with continued core cooling were explicitly and formally analyzed rather than assumed.

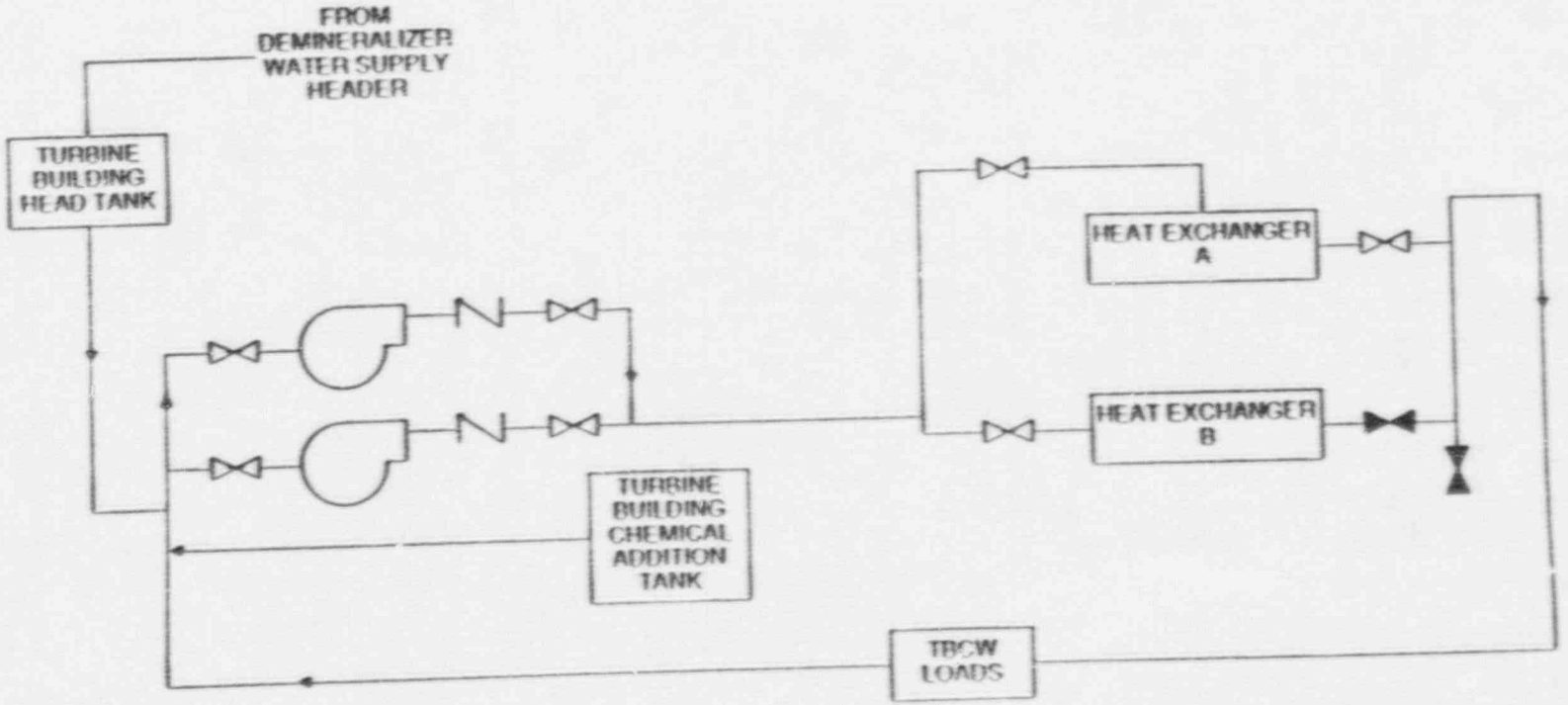

Figure 2.18 Turbine Building Cooling Water System Schematic.

The above expansion features of the event tree analyses provide, in general, more realistic analyses subject to less overall conservatism than previous analyses. However, as will become evident in the following subsections, conservative assumptions were still included in portions of the analyses so that the core damage potential would not be inadvertently underestimated.

Each event tree used in the Peach Bottom-2 external event analysis is presented in subsequent sections. These sections contain specific success criteria considerations, assumptions, and a description of the sequences displayed by each tree. The reader is referred to Section 2.3.8 for the nomenclature used in the event tree headings and resulting sequence identifiers.

2.3.1 General Event Tree Assumptions

There are a number of assumptions which generally apply to the event tree analyses performed for Peach Bottom-2 regardless of the specific initiator being examined. These assumptions are listed below with brief explanations as required:

a. Low Pressure Core Spray (LPCS), Low Pressure Coolant Injection (LPCI), and RHR (all modes) pumps are assumed to fail following successful containment venting or containment failure by overpressure/temperature conditions.

   The suppression pool is assumed to reach near atmospheric saturated conditions shortly after either successful venting or containment failure. Partial boiling of the pool water is assumed to decrease the net positive suction head (NPSH) for the LPCS/LPCI/RHR pumps such that these pumps cavitate, if running, causing subsequent failure.

b. LPCS/LPCI/RHR (all modes) pumps, which use the suppression pool for suction, will successfully operate using pool water at a temperature approaching 350°F (corresponding to saturation conditions near the point of containment failure by overpressure).

   This assumption is based on (a) the corresponding pressure conditions of the containment which will assure adequate NPSH, (b) the pump seals and bearings being cooled by the Emergency Service Water system, (c) the findings of General Electric as reported in Section 5 of Reference 16, and (d) the fact that the RHR pumps normally pump water approaching such temperatures during the early phases of plant shutdown.

c. High Pressure Coolant Injection (HPCI) and Reactor Core Isolation Cooling (RCIC) will fail at pool temperatures of ~210-260°F.

In all the accidents of interest, the HPCI system will eventually switch suction source from the condensate storage tank to the suppression pool automatically on high pool water level. Following procedures at Peach Bottom, the operator switches the RCIC system when he sees HPCI switch. Switching back requires overriding certain circuits and therefore would not normally be performed. If, while the systems are running, the pool water should reach the 210-260°F range (nominally ~230°F), pump failure for both systems is assumed since these pumps are not externally cooled.

d. The CRD system in the enhanced mode (two pumps) is assumed to fail following reactor depressurization for SDC due to low NPSH.

   The CRD system pumps water from the CST in the enhanced mode at approximately 200 gpm, which increases to near 300 gpm following reactor depressurization. The CST level is assumed to be too low at the time of reactor depressurization for SDC to prevent CRD pump cavitation due to insufficient NPSH.

In some event trees, the same event occurs more than once. A system may be successfully utilized in a sequence and later in the same sequence, following containment venting, may fail due to environmental conditions. In this analysis, credit is given for three injection systems (CRD (U4), Condensate (V1), High Pressure Service Water (V4)) to operate following the containment venting event (Y) in many of the event trees. If, in a particular event tree, an injection event has been asked before and after the containment venting event, then these events have different probabilities, although they have the same designation. In this situation, the event asked after containment venting refers to the survivability of the system, or its probability of successfully surviving containment venting. If the event is asked only before containment venting, it refers to a hardware failure. If the event is asked only after containment venting, it refers to hardware failure and survivability.

Core damage in many sequences is described as early or late. Early core damage refers to sequences in which loss of all coolant injection occurs soon after the initiating event and for which recovery is not performed. A late core damage designation is found in the T1 tree for sequences in which station blackout occurs and either HPCI or RCIC is functional. Injection may continue in these sequences for a substantial amount of time before injection fails and core damage occurs. A sequence designated as containment vulnerable indicates conditions (temperature and pressure) in containment which constitute a risk of containment failure unless containment heat removal is effected.

2.3.2 Discussion of Success Criteria

In the following subsections, the system success criteria for each initiator are presented. The identification of initiators and the construction of the corresponding event trees is a very interactive process.

For the most part, the success criteria follow closely those used in the Limerick Probabilistic Safety Study since Limerick and Peach Bottom have similar plant thermal ratings and similar emergency core cooling system designs and capacities. Any specific peculiarities in the criteria are noted for each initiator in subsequent subsections.

2.3.3 Large Loss-of-Coolant-Accident (LOCA) Event Tree

This section contains information on the large LOCA event tree. Success criteria considerations are presented along with the event tree and its description.

2.3.3.1 Success Criteria

A criterion specific to the large LOCA initiator is described below.

For scenarios where core cooling is successful up to the time of containment venting or containment failure: one Condensate, one HPSW, or two CRD pump operation is assumed to be adequate to continue successful core cooling. This is based on the low decay heat loads reached by that time (many hours) and the fact that only small flow rates should be required to maintain sufficient vessel inventory and adequate core cooling.

2.3.3.2 Event Tree

Figure 2.19 displays the event tree for the large LOCA initiator. The following discussions define the event tree headings and describe the sequences presented.

The following event tree headings appear on the tree in the approximate chronological order that would be expected following a large LOCA.

A: Initiating event, large LOCA.

C: Success or failure of the Reactor Protection System (RPS). Success implies automatic scram by the control rods.

LOSP: Success or failure to maintain offsite power.

V2: Success or failure of the LPCS system. Success implies operation of any two of the four LPCS pumps through either or both LPCS injection lines.

V3: Success or failure of the LPCI mode of the RHR system. Success implies operation of one of four LPCI pumps through either LPCI injection line to the reactor vessel.

W1: Success or failure of RHR in the SPC mode. Success implies at least one RHR pump operating in the SPC mode with the appropriate heat exchanger in the loop along with the HPSW system in operation to the ultimate heat sink.

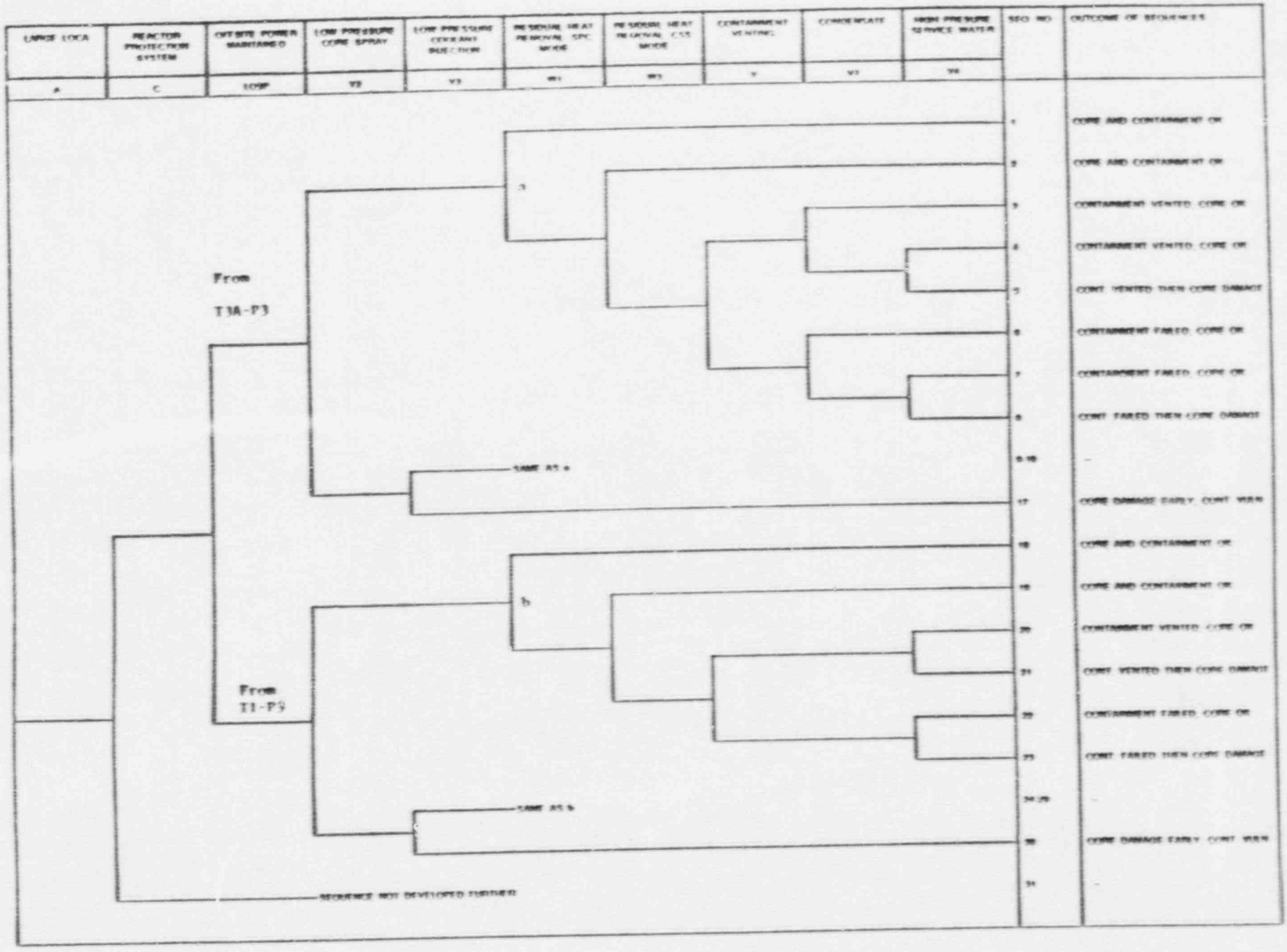

Figure 2.19 Large LOCA Event Tree

W3: Success or failure of RHR in the CS mode. Success implies at least one RHR pump operating in the CS mode with the appropriate heat exchanger in the loop along with the HPSW system in operation to the ultimate heat sink.

Y: Success or failure of containment venting. Success implies that the six-inch integrated leak test line or larger size line is open so as to prevent containment failure by overpressure. As necessary, water makeup is also eventually supplied to the suppression pool.

V1: Success or failure of the Condensate System. Success implies at least one pump operating with sufficient makeup to the condenser hotwell for a continuing water supply.

V4: Success or failure of the HPSW system in the inject mode to the reactor vessel through a LPCI injection line. Success implies manual operation of this injection source such that one HPSW pump successfully provides coolant to the reactor.

The following descriptions refer to the sequences found in Figure 2.19.

SEQUENCE 1 -- $A*\overline{C}*LOSP*V2*\overline{W1}$

Following the large LOCA (A), the RPS successfully inserts the rods into the core (/C). Offsite power remains available (/LOSP). High pressure cooling cannot be utilized because insufficient steam is available to run the turbines and LPCS is initiated to provide core coolant (/V2). The suppression pool temperature is increasing since residual heat from the reactor is being dumped to it. SPC is initiated to provide suppression pool cooling (/W1). With coolant makeup and containment overpressure protection provided, the core and containment are safe.

SEQUENCE 2 -- $A*\overline{C}*LOSP*V2*\overline{W1}*\overline{W3}$

Same as Sequence 1 except containment overpressure protection is provided by the CS mode of RHR (/W3) following the failure of SPC (W1).

SEQUENCE 3 -- $A*\overline{C}*LOSP*V2*\overline{W1}*\overline{W3}*\overline{Y}*\overline{V1}$

Same as Sequence 1 except both SPC (W1) and CS (W3) fail. The subsequent pressure rise in containment is alleviated by containment venting (/Y).

LPCS failure is assumed following containment venting due to insufficient NPSH for the LPCS pumps. The operator then initiates Condensate (/V1) to continue to cool the core.

SEQUENCE 4 -- $\bar{A}*\bar{C}*\overline{LOSP}*\bar{V}2*W1*W3*\bar{Y}*V1*\bar{V}4$

Same as Sequence 3 except HPSW provides core coolant (/V4) subsequent to Condensate failure (V1).

SEQUENCE 5 -- $\bar{A}*\bar{C}*\overline{LOSP}*\bar{V}2*W1*W3*\bar{Y}*V1*V4$

Same as Sequence 4 except HPSW fails (V4) to cool the core. At this point all coolant makeup is lost, which leads to core damage in a vented containment.

SEQUENCES 6 TO 8

Same as Sequences 3 to 5 except containment venting fails (Y) leading to containment failure by overpressurization.

SEQUENCES 9 TO 16

Same as Sequences 1 to 8 except LPCS fails (V2) and LPCI provides initial low pressure coolant injection (/V3).

SEQUENCE 17 -- $\bar{A}*\bar{C}*\overline{LOSP}*V2*V3$

Following the large LOCA (A), the RPS successfully inserts the rods into the core (/C). Offsite power remains available (/LOSP). LPCS and LPCI fail to provide low pressure core cooling, resulting in early core damage.

SEQUENCES 18 TO 19

Same as Sequences 1 and 2 except offsite power is not maintained (LOSP). Onsite power is established which enables LPCS to cool the core (/V2) and SPC (/W1) or CS (/W3) to provide containment overpressure protection.

SEQUENCES 20 TO 21

Same as Sequences 4 and 5 except offsite power is lost (LOSP) and Condensate is therefore not available following successful containment venting.

SEQUENCES 22 TO 23

Same as Sequences 7 and 8 except offsite power is lost (LOSP) and Condensate is therefore not available following failure of containment venting.

SEQUENCES 24 TO 29

Same as Sequences 18 to 23 except LPCI provides initial low-pressure core cooling (/V3) following LPCS failure (V2).

SEQUENCE 30 -- A*$\bar{C}$*LOSP*V2*V3

Same as Sequence 17 except offsite power is also lost (LOSP).

SEQUENCE 31 -- A*C

Following the large LOCA (A), the RPS fails to properly insert the rods into the core (C). The sequence is not developed further due to its low probability.

2.3.4 Intermediate LOCA Event Tree

This section contains information on the intermediate LOCA event tree. Success criteria considerations are presented along with the event tree and its description.

2.3.4.1 Success Criteria

A criterion specific to the intermediate LOCA initiator is described below.

For scenarios where core cooling is successful up to the time of containment venting or containment failure: one Condensate, one HPSW, or two CRD pump operations is assumed to be adequate to continue successful core cooling. This is based on the low decay heat loads reached by that time (many hours) and the fact that only small flow rates should be required to maintain sufficient vessel inventory and adequate core cooling.

2.3.4.2 Event Tree

Figure 2.20 displays the event tree for the intermediate LOCA initiator. The following discussions define the event tree headings and describe the sequences presented.

The following event tree headings appear on the tree in the approximate chronological order that would be expected following an intermediate LOCA. For convenience, high and then low pressure injection systems are shown first, followed by containment-related systems, and finally by systems capable of long-term continued coolant injection.

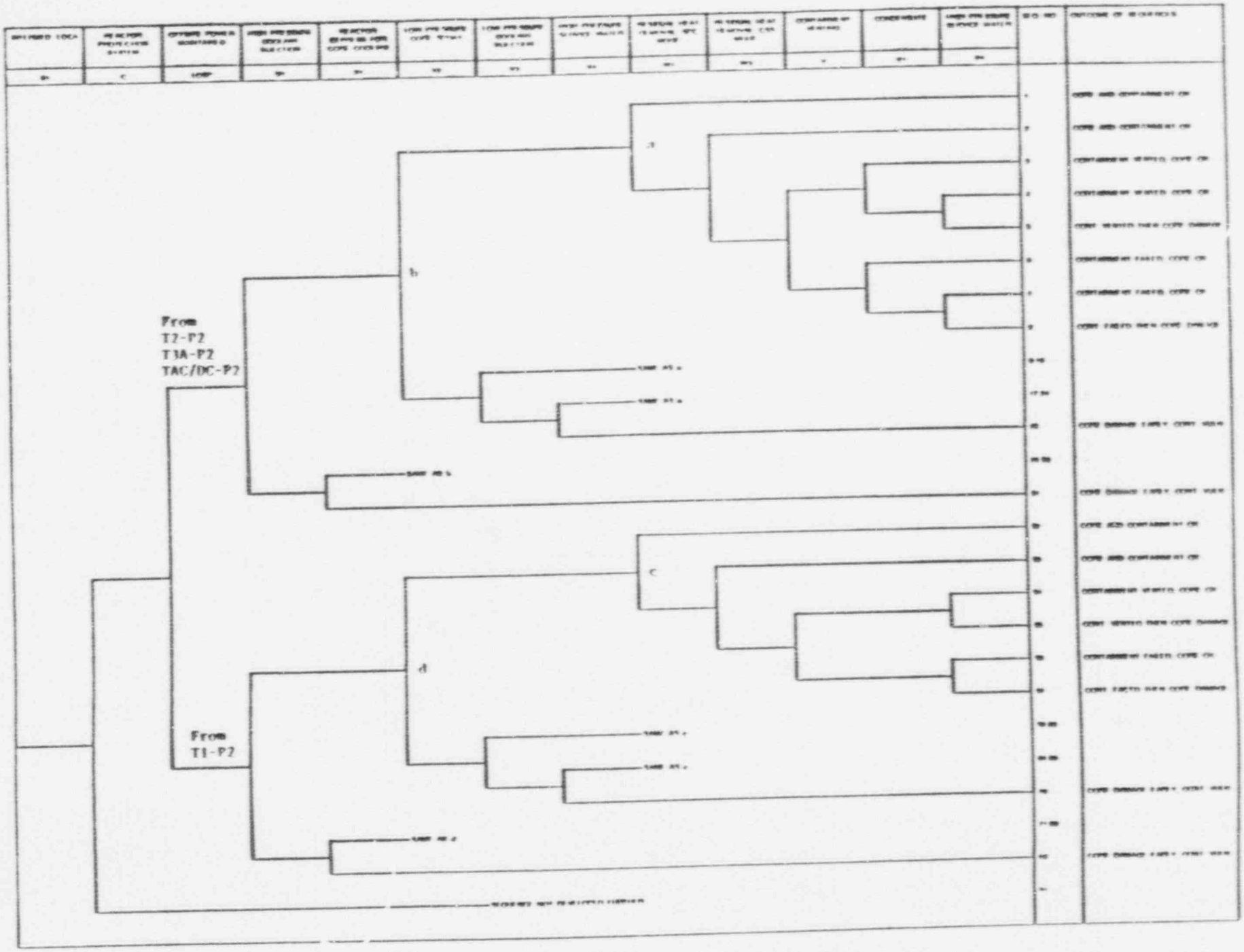

Figure 2.20 Intermediate LOCA Event Tree

S1: Initiating event, intermediate LOCA.

C: Success or failure of the RPS. Success implies automatic scram by the control rods.

LOSP: Success or failure to maintain offsite power.

U1: Success or failure of the HPCI system. Success implies operation of the HPCI system for ~1-2 hours until low primary system pressure causes isolation of HPCI either automatically or manually. U1' refers to the HPCI system without pump room ventilation.

X1: Success or failure of primary system depressurization. Success implies automatic or manual operation of the Automatic Depressurization System (ADS) or manual operation of other SRVs such that three valves or more are opened allowing low pressure injection. An intermediate LOCA may blow the vessel down sufficiently fast to preclude X1 operation.

V2: Success or failure of the LPCS system. Success implies operation of any two of the four LPCS pumps through either or both LPCS injection lines.

V3: Success or failure of the LPCI mode of the RHR system. Success implies operation of one of four LPCI pumps through either LPCI injection line to the reactor vessel.

V4: Success or failure of the HPSW system in the inject mode to the reactor vessel through a LPCI injection line. Success implies manual operation of this injection source such that one HPSW pump successfully provides coolant to the reactor.

W1,W3: Success or failure of the RHR in the SPC mode or CS mode, respectively. Success implies at least one RHR pump operating in either the SPC or CS mode with the appropriate heat exchanger in the loop along with the HPSW system in operation to the ultimate heat sink.

Y: Success or failure of containment venting. Success implies that the six-inch integrated leak test line or larger is open so as to prevent containment failure by overpressure. As necessary, water makeup is also eventually supplied to the suppression pool.

V1: Success or failure of the Condensate system. Success implies at least one pump operating with sufficient makeup to the condenser hotwell for a continuing water supply.

The following descriptions refer to the sequences found in Figure 2.20.

SEQUENCE 1 -- $S1*\overline{C}*LOSP*U1'*\overline{V2}*\overline{W1}$

Following the intermediate LOCA (S1), the RPS successfully inserts the rods into the core (/C). Offsite power remains available (/LOSP) and HPCI (/U1') initially provides core coolant. The primary pressure decreases and steam is lost through the break, which eventually fails HPCI. LPCS is initiated to continue core cooling (/V2). Residual heat from the reactor is being transferred to the suppression pool. SPC is successfully initiated (/W1). With LPCS and SPC providing adequate coolant makeup and containment overpressure protection, the core and containment are safe.

SEQUENCE 2 -- $S1*\overline{C}*LOSP*U1'*\overline{V2}*W1*\overline{W3}$

Same as Sequence 1 except CS (/W3) provides containment overpressure protection following the failure of SPC (W1).

SEQUENCE 3 -- $S1*\overline{C}*LOSP*U1'*\overline{V2}*W1*W3*\overline{Y}*\overline{V1}$

Same as Sequence 1 except SPC (W1) and CS (W3) fail to function, which causes the pressure to increase in containment. Containment venting is successful (/Y) which causes the LPCS pumps to fail due to low NPSH. Condensate is initiated (/V1) for coolant makeup resulting in no core damage in a vented containment.

SEQUENCE 4 -- $S1*\overline{C}*LOSP*U1'*\overline{V2}*W1*W3*\overline{Y}*V1*\overline{V4}$

Same as Sequence 3 except Condensate fails (V1) and HPSW is initiated to supply coolant makeup (/V4).

SEQUENCE 5 -- $S1*\overline{C}*LOSP*U1'*\overline{V2}*W1*W3*\overline{Y}*V1*V4$

Same as Sequence 4 except HPSW fails to provide coolant makeup (V4), resulting in core damage in a vented containment.

SEQUENCE 6 -- $S1*\overline{C}*LOSP*U1'*\overline{V2}*W1*W3*Y*\overline{V1}$

Same as Sequence 3 except containment venting fails (Y) following the loss of containment cooling resulting in a pressure rise in containment which leads to containment failure. This fails LPCS due to low NPSH. Condensate is initiated to provide coolant makeup (/V1). This results in no core damage in a failed containment.

SEQUENCE 7 -- $S1*\overline{C}*\overline{LOSP}*\overline{U1'}*\overline{V2}*W1*W3*Y*V1*\overline{V4}$

Same as Sequence 6 except HPSW provides coolant makeup (/V4) subsequent to Condensate failure (V1).

SEQUENCE 8 -- $S1*\overline{C}*\overline{LOSP}*\overline{U1'}*\overline{V2}*W1*W3*Y*V1*V4$

Same as Sequence 6 except both Condensate (V1) and HPSW (V4) fail to provide coolant makeup resulting in core damage in a failed containment.

SEQUENCES 9 TO 16

Same as Sequences 1 to 8 except early low-pressure coolant makeup is provided by LPCI (/V3) following failure of LPCS (V2).

SEQUENCES 17 TO 24

Same development as Sequences 9 to 16 except HPSW provides early low-pressure coolant makeup (/V4) following LPCI (V3) failure. HPSW asked following containment venting refers to survivability.

SEQUENCE 25 -- $S1*\overline{C}*\overline{LOSP}*\overline{U1'}*V2*V3*V4$

Same as Sequence 1 except all efforts to establish early low-pressure core cooling with LPCS (V2), LPCI (V3) and HPSW (V4) fail, resulting in early core damage in a vulnerable containment.

SEQUENCES 26 TO 50

Same development as Sequences 1 to 25 except HPCI fails to initiate (U1') which requires depressurization of the primary system (/X1) to allow the low-pressure systems to provide coolant makeup.

SEQUENCE 51 -- $S1*\overline{C}*\overline{LOSP}*U1'*X1$

Same as Sequence 1 except HPCI fails to initiate (U1') and depressurization of the primary system is unsuccessful (X1), disabling the low-pressure core coolant systems, leading to early core damage in a vulnerable containment.

SEQUENCES 52 to 57

Same development as Sequences 1 to 8 except offsite power is lost (LOSP) early in the sequence and onsite emergency power is provided by the

diesel generators. Since offsite power is not available, Condensate cannot be asked after the containment venting event, resulting in six sequences instead of eight.

SEQUENCES 58 TO 63

Same development as Sequences 52 to 57 except LPCI provides early coolant makeup (/V3) following LPCS failure (V2).

SEQUENCES 64 TO 69

Same development as Sequences 58 to 63 except HPSW provides early coolant makeup (/V4) following LPCI (V3) failure. HPSW asked following containment venting refers to survivability.

SEQUENCE 70 -- $S1*\bar{C}*LOSP*\bar{\bar{U1}}'*V2*V3*V4$

Following the intermediate LOCA (S1), the RPS successfully inserts the rods into the core (/C). Offsite power is lost (LOSP) and onsite power is established. HPCI provides coolant makeup (/U1') until the pressure in the primary reduces sufficiently to initiate the low-pressure coolant systems. LPCS (V2), LPCI (V3) and HPSW (V4) fail to operate, resulting in early core damage in a vulnerable containment.

SEQUENCES 71 TO 89

Same as Sequences 52 to 70 except HPCI fails to provide early coolant makeup (U1'), followed by successful depressurization (/X1) of the primary system to enable low-pressure systems to initiate.

SEQUENCE 90 -- $S1*\bar{C}*LOSP*U1'*X1$

Following the intermediate LOCA (S1), the RPS successfully inserts the rods into the core (/C). Offsite power is lost (LOSP) and onsite power is established. HPCI fails to provide coolant makeup (U1') followed by unsuccessful primary system depressurization (X1). This disables all low-pressure coolant systems, resulting in early core damage in a vulnerable containment.

SEQUENCE 91 -- S1*C

The RPS does not respond (C) to the intermediate LOCA and the sequence is not developed further due to a low probability.

2.3.5 Small LOCA Event Tree

This section contains information on the small LOCA event tree. Success criteria considerations are presented along with the event tree and its description.

2.3.5.1 Success Criteria

Two criteria specific to the small LOCA initiator are described below:

a. For scenarios in which core cooling has been provided for a period of a few hours or more, two CRD pump operation is considered adequate for continued success of core cooling should the other cooling systems then fail. This is based on the low decay heat levels and relatively small flow rates required by that time to make up for the small break.

b. For scenarios in which core cooling is successful up to the time of containment venting or containment failure, two CRD pumps or depressurization with operation of either one Condensate or one HPSW pump is considered to be adequate to continue successful core cooling.

2.3.5.2 Event Tree

Figure 2.21 displays the event tree for the small LOCA initiators. The following discussions define the event tree headings and describe the sequences presented.

The following event tree headings appear on the tree in the approximate chronological order that would be expected following a small LOCA. For convenience, the Residual Heat Removal (RHR) containment cooling choices are shown early in the tree to decrease the size of the event tree. Otherwise, the tendency is to show high and then low pressure injection systems, followed by containment venting, and finally long-term continued core cooling possibilities.

S2: Initiating event, small LOCA

C: Success or failure of the RPS. Success implies automatic scram by the control rods.

LOSP: Success or failure to maintain offsite power.

Q1: Success or failure of the Power Conversion System (PCS). Success implies operation of the balance of plant by removing heat through at least one Main Steam Isolation Valve (MSIV) with operation of the condenser and circulating water system as well as one feedwater train.

U1: Success or failure of the HPCI system. Success implies operation of the HPCI pump train so as to maintain sufficient coolant injection.

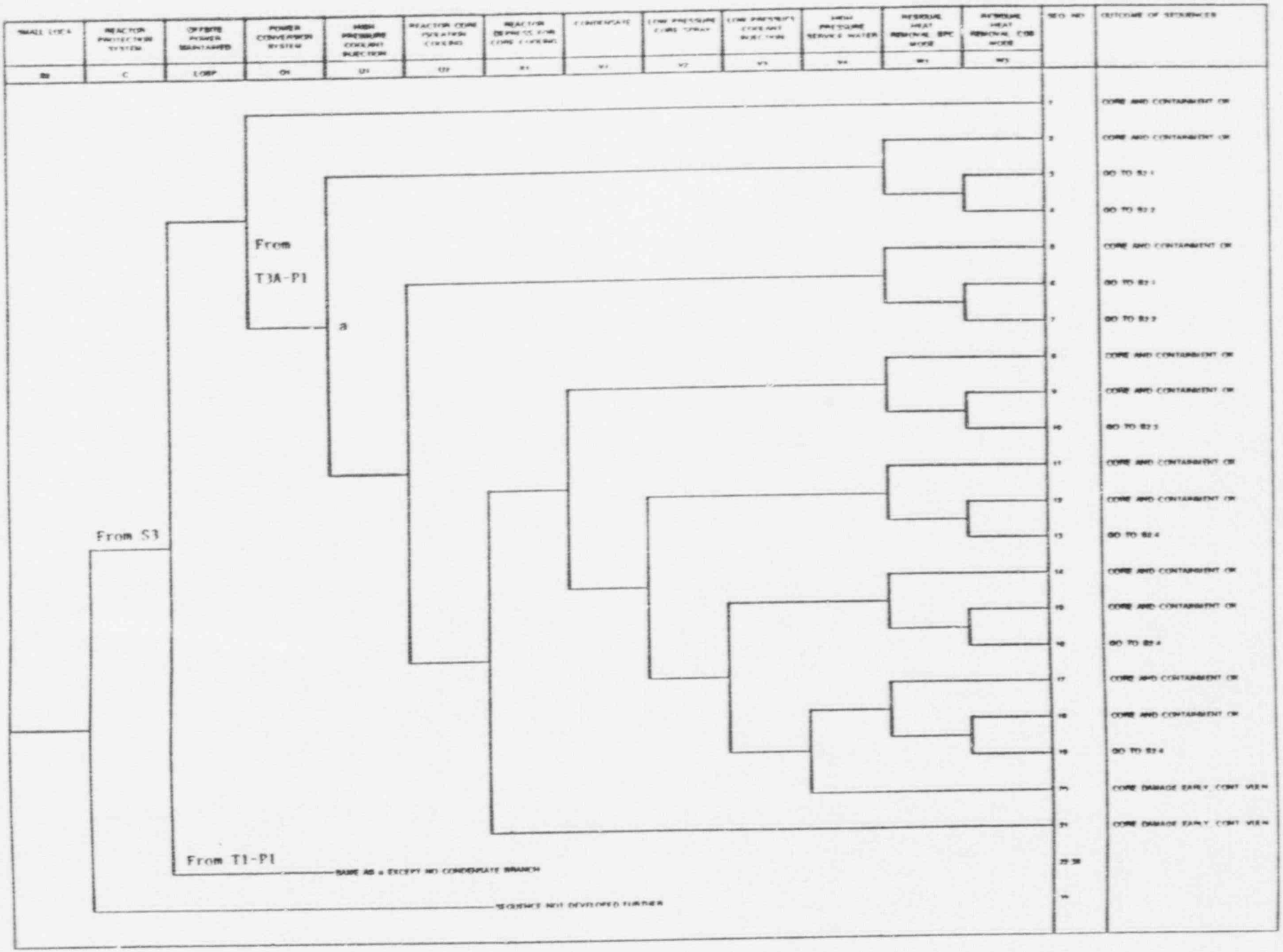

Figure 2.21 Small LOCA Event Tree (Page 1 of 3)

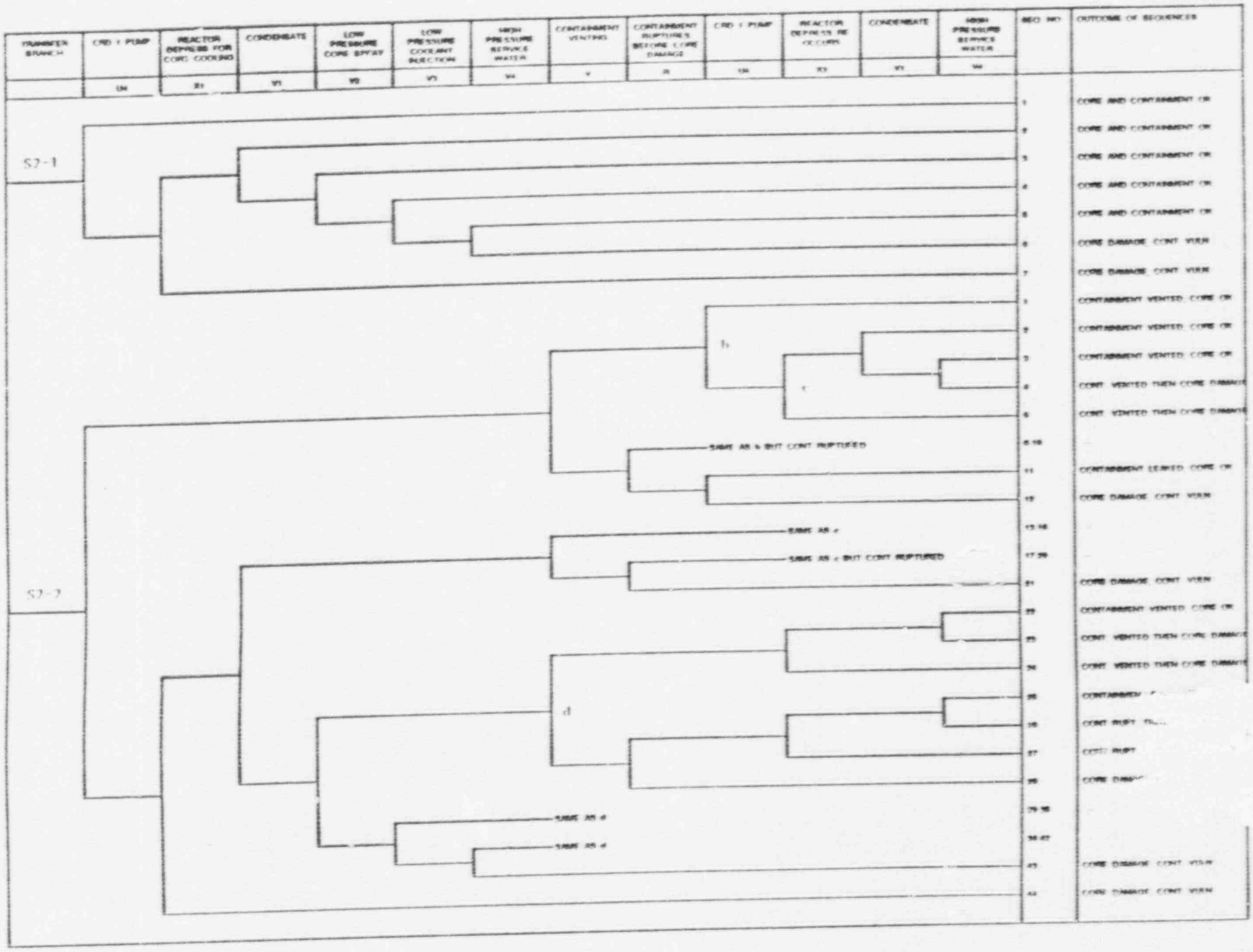

Figure 2.21 Small LOCA Event Tree (Page 2 of 3)

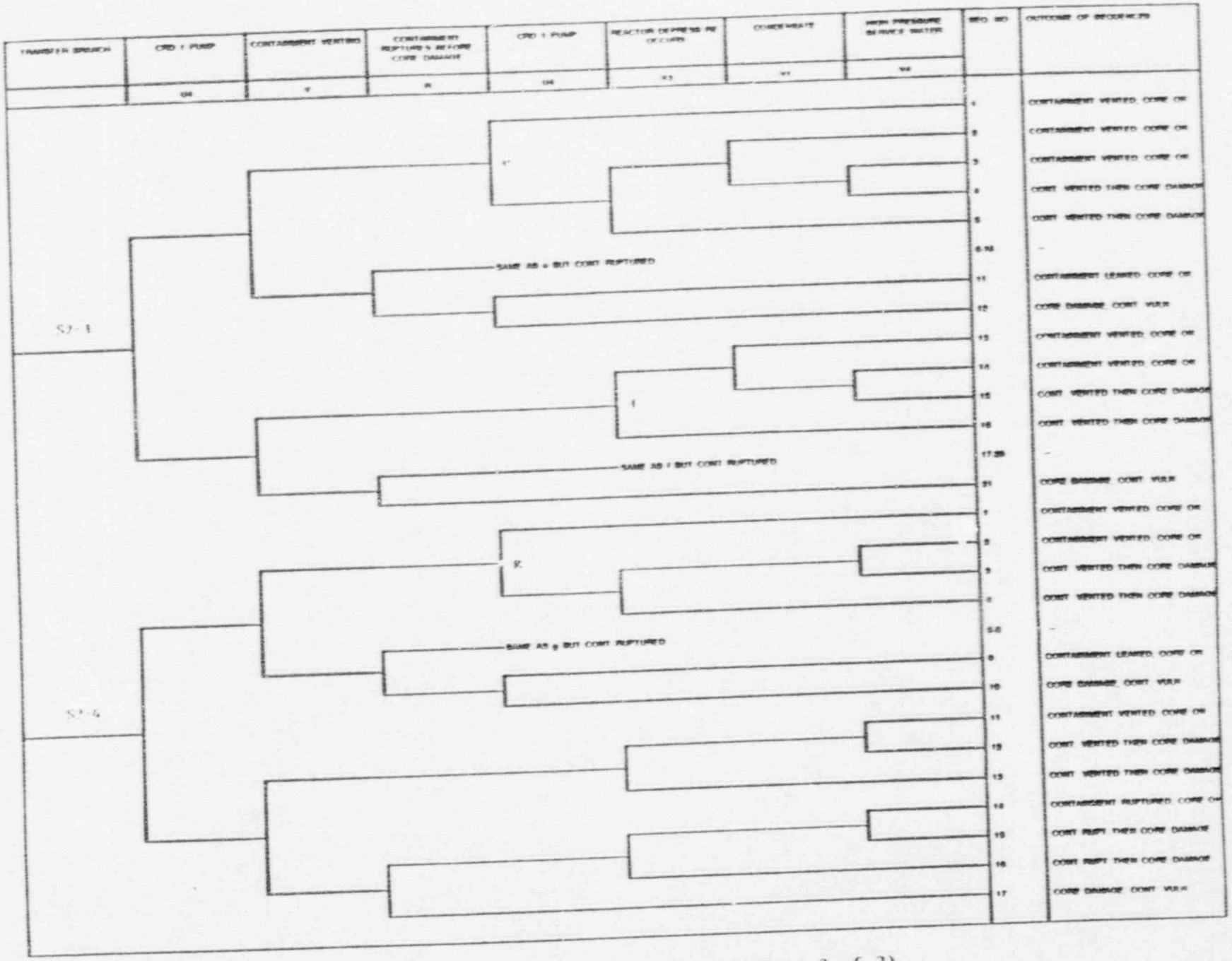

Figure 2.21 Small LOCA Event Tree (Page 3 of 3)

U2: Success or failure of the RCIC system. Success implies operation of the RCIC pump train so as to maintain sufficient coolant injection.

X: Success or failure of primary system depressurization. Success implies automatic or manual operation of the ADS or manual operation of other SRVs such that three valves or more are opened allowing low pressure injection.

V1: Success or failure of the Condensate system. Success implies at least one pump operating with sufficient makeup to the condenser hotwell for a continuing water supply.

V2: Success or failure of the LPCS system. Success implies operation of any two of the four LPCS pumps through either or both LPCS injection lines. Conservative requirement since a small LOCA requires less makeup than two pumps provide.

V3: Success or failure of the LPCI mode of the RHR system. Success implies operation of one of four LPCI pumps through either LPCI injection line to the reactor vessel.

V4: Success or failure of the HPSW system in the inject mode to the reactor vessel through a LPCI injection line. Success implies manual operation of this injection source such that one HPSW pump successfully provides coolant to the reactor.

W1,W3: Success or failure of the RHR system in the SPC mode or CS mode, respectively. Success implies at least one RHR pump operating in either the SPC or CS mode with the appropriate heat exchanger in the loop along with the HPSW system in operation to the ultimate heat sink.

U4: Success or failure of the CRD system as an injection source. Success implies one pump operation.

Y: Success or failure of containment venting. Success implies that the six-inch integrated leak test line or larger size line is open so as to prevent containment failure by overpressure. As necessary, water makeup is also eventually supplied to the suppression pool.

R: Success or failure of the containment to withstand over-pressurization. Success implies the containment ruptures before core damage.

X3: Success or failure of primary system depressurization. Success implies automatic or manual operation of ADS occurs subsequent to an initial depressurization to allow low pressure coolant injection.

The following descriptions refer to the sequences found in Figure 2.21.

SEQUENCE 1 -- $S2*\overline{C}*\overline{LOSP}*\overline{Q1}$

A small LOCA (S2) generates a reactor scram condition and the RPS successfully inserts the rods into the core (/C). Offsite power is maintained (/LOSP) and the PCS functions to remove heat from the core (/Q1), resulting in no core damage in a safe containment.

SEQUENCE 2 -- $S2*\overline{C}*\overline{LOSP}*Q1*\overline{U1}*\overline{W1}$

Same as Sequence 1 except the PCS fails (Q1), HPCI is initiated to provide core coolant (/U1), and SPC provides containment overpressure protection (/W1).

SEQUENCE 3-1 -- $S2*\overline{C}*\overline{LOSP}*Q1*\overline{U1}*W1*\overline{W3}*\overline{U4}$

Same as Sequence 2 except containment overpressure protection fails with SPC (W1) failure and CS (/W3) success. HPCI fails due to high suppression pool temperature reached before CS is initiated and CRD is initiated to provide coolant makeup (/U4).

SEQUENCES 3-2 TO 3-5

Same as Sequence 3-1 except CRD fails (U4) and the primary system is depressurized (/X1) to allow the low-pressure coolant systems to cool the core. Either Condensate (/V1), LPCS (/V2), LPCI (/V3) or HPSW (/V4) functions to cool the core.

SEQUENCE 3-6 -- $S2*\overline{C}*\overline{LOSP}*Q1*\overline{U1}*W1*\overline{W3}*U4*\overline{X1}*V1*V2*V3*V4$

Same as Sequence 3-2 except all low-pressure core coolant systems fail (Condensate, LPCS, LPCI, HPSW) resulting in core damage in a vulnerable containment.

SEQUENCE 3-7 -- $S2*\overline{C}*\overline{LOSP}*Q1*\overline{U1}*W1*\overline{W3}*U4*X1$

Same as Sequence 3-1 except CRD fails to provide coolant makeup (U4) and subsequent primary system depressurization is unsuccessful (X1). Since all low-pressure cooling systems are disabled, core damage results in a vulnerable containment.

SEQUENCE 4-1 -- $S2*\overline{C}*\overline{LOSP}*Q1*\overline{U1}*W1*W3*\overline{U4}*\overline{Y}*\overline{U4}'$

Same as Sequence 2 until both SPC (W1) and CS (W3) fail to provide containment overpressure protection. HPCI eventually trips on high suppression pool temperatures (U1) and CRD is initiated (/U4). High containment pressure is reduced by containment venting (/Y). CRD survives the venting event and continues to provide coolant makeup, resulting in no core damage in a vented containment.

SEQUENCES 4-2 TO 4-3

Same as Sequence 4-1 except CRD does not survive containment venting (U4) and the primary system is depressurized (/X1) to allow Condensate (/V1) or HPSW (/V4) to continue core cooling.

SEQUENCE 4-4 -- $S2*\overline{C}*\overline{LOSP}*Q1*\overline{U1}*W1*W3*\overline{U4}*\overline{Y}*U4'*\overline{X3}*V1*V4$

Same as Sequence 4-3 expect both Condensate (V1) and HPSW (V4) fail to provide core cooling, resulting in core damage in a vented containment.

SEQUENCE 4-5 -- $S2*\overline{C}*\overline{LOSP}*Q1*\overline{U1}*W1*W3*\overline{U4}*\overline{Y}*U4'*X3$

Same as Sequence 4-2 except reactor depressurization is unsuccessful (X3), precluding the use of any low-pressure coolant systems, resulting in core damage in a vented containment.

SEQUENCES 4-6 TO 4-10

Same as Sequences 4-1 to 4-5 except containment venting is unsuccessful (Y) and overpressurization soon causes containment failure. All sequence outcomes are the same except the containment is not vented but failed.

SEQUENCE 4-11 -- $S2*\overline{C}*\overline{LOSP}*Q1*\overline{U1}*W1*W3*\overline{U4}*Y*R*\overline{U4}'$

Same as Sequence 4-1 except containment venting is unsuccessful (Y) and rupture of the containment does not occur (R), although a leak in the containment has developed. CRD survives and continues to provide core coolant resulting in no core damage in a leaking containment.

SEQUENCE 4-12 -- $S2*\overline{C}*\overline{LOSP}*Q1*\overline{U1}*W1*W3*\overline{U4}*Y*R*U4'$

Same as Sequence 4-11 except CRD does not survive the containment overpressurization and leak, resulting in core damage in a leaking containment.

SEQUENCES 4-13 TO 4-16

Same as Sequences 4-2 to 4-5 except CRD does not operate following HPCI failure (U4), the primary system is depressurized (/X1), and Condensate continues core cooling (/V1) prior to venting.

SEQUENCES 4-17 TO 4-20

Same as Sequences 4-13 to 4-16 except containment venting fails (Y) and the containment ruptures (/R).

SEQUENCE 4-21 -- $S2*\overline{C}*\overline{LOSP}*Q1*\overline{U1}*W1*W3*U4*\overline{X1}*\overline{V1}*Y*R$

Same as Sequences 4-17 to 4-20 except the containment does not rupture (R) but only leaks following failure of containment venting. Increasing containment pressure eventually causes closure of the SRVs and a pressure rise in the vessel which precludes low pressure cooling, and core damage results in a leaking containment.

SEQUENCE 4-22 -- $S2*\overline{C}*\overline{LOSP}*Q1*\overline{U1}*W1*W3*U4*\overline{X1}*V1*\overline{V2}*\overline{Y}*\overline{X3}*V4$

A small LOCA (S2) occurs which generates a reactor scram condition and the RPS successfully inserts the rods into the core (/C) Offsite power is maintained (/LOSP) and the PCS fails to remove heat from the core (Q1). HPCI is initiated for coolant makeup (/U1). Containment overpressure protection fails using SPC (W1) and CS (W3), which eventually fails HPCI due to high suppression pool temperatures. CRD fails to supply sufficient makeup (U4) and the primary system is depressurized (/X1). Condensate fails (V1) followed by successful operation of LPCS (/V2) to cool the core. High containment pressure is alleviated by containment venting (/Y), which fails LPCS due to low NPSH. The reactor is again depressurized (/X3) and HPSW continues core cooling (/V4), resulting in no core damage in a vented containment.

SEQUENCE 4-23 -- $S2*\overline{C}*\overline{LOSP}*Q1*\overline{U1}*W1*W3*U4*\overline{X1}*V1*\overline{V2}*\overline{Y}*\overline{X3}*V4$

Same as Sequence 4-22 except HPSW fails to initiate (V4) following containment venting, at which point all coolant makeup is lost, resulting in core damage in a vented containment.

SEQUENCE 4-24 -- $S2*\overline{C}*\overline{LOSP}*Q1*\overline{U1}*W1*W3*U4*\overline{X1}*V1*\overline{V2}*\overline{Y}*X3$

Same as Sequence 4-22 except reactor depressurization following containment venting is unsuccessful (X3), precluding the use of HPSW, resulting in core damage in a vented containment.

SEQUENCES 4-25 TO 4-27

Same as Sequences 4-22 to 4-24 except containment venting is unsuccessful (Y) and the containment ruptures (/R).

SEQUENCE 4-28 -- S2*$\overline{C}$*$\overline{LOSP}$*Q1*$\overline{U1}$*W1*W3*U4*$\overline{X1}$*V1*$\overline{V2}$*Y*R

Same as Sequences 4-25 to 4-27 except the containment does not rupture (R) following containment venting which recloses the SRVs and precludes reactor depressurization and HPSW initiation, resulting in core damage in a leaking containment.

SEQUENCES 4-29 TO 4-35

Same as Sequences 4-22 to 4-28 except LPCS fails (V2) prior to containment venting and LPCI provides coolant makeup (/V3).

SEQUENCES 4-36 TO 4-42

Same as Sequences 4-29 to 4-35 except LPCI also fails (V3) and HPSW provides coolant makeup (/V4) prior to containment venting.

SEQUENCE 4-43 -- S2*$\overline{C}$*$\overline{LOSP}$*Q1*$\overline{U1}$*W1*W3*U4*$\overline{X1}$*V1*V2*V3*V4

Same as Sequences 4-36 to 4-42 except HPSW fails (V4), which leaves no system available for coolant makeup, resulting in core damage in a vulnerable containment.

SEQUENCE 4-44 -- S2*$\overline{C}$*$\overline{LOSP}$*Q1*$\overline{U1}$*W1*W3*U4*X1

Same as Sequence 4-22 until reactor depressurization is unsuccessful (X1) following CRD failure. All low-pressure coolant makeup is now lost, which leads to core damage in a vulnerable containment.

SEQUENCES 5 TO 7

Same as Sequences 2 to 4 except RCIC provides early high-pressure coolant makeup (/U2) following HPCI failure (U1).

SEQUENCES 8 TO 9

A small LOCA (S2) occurs which generates a reactor scram condition and the RPS successfully inserts the rods into the core (/C). Offsite power

is maintained (/LOSP) and the PCS fails to remove heat from the core (Q1). HPCI (U1) and RCIC (U2) fail to provide high-pressure coolant makeup. The reactor is depressurized (/X1) and Condensate successfully provides coolant makeup (/V1). Containment overpressure protection is provided by SPC (/W1) or CS (/W3), resulting in no core damage in a safe containment.

SEQUENCE 10-1 -- $S2*\overline{C}*\overline{LOSP}*Q1*U1*U2*\overline{X1}*\overline{V1}*W1*W3*\overline{U4}*\overline{Y}*\overline{U4}'$

Same as Sequence 8 until SPC (W1) and CS (W3) fail to provide containment overpressure protection, resulting in the eventual loss of Condensate due to high primary system pressure, which occurs after SRVs shut on high containment pressure. CRD is initiated (/U4) to cool the core. High containment pressure is alleviated by venting (/Y). CRD continues to cool the core resulting in no core damage in a vented containment.

SEQUENCES 10-2 TO 10-3

Same as Sequence 10-1 except CRD does not survive containment venting, the reactor is depressurized (/X3), and Condensate (/V1) or HPSW (/V4) provides coolant makeup.

SEQUENCE 10-4 -- $\overline{S2}*\overline{C}*LOSP*Q1*U1*\overline{U2}*\overline{X1}*V1*W1*\overline{W3}*\overline{U4}*Y*\overline{U4}'*X3*V1*V4$

Same as Sequence 10-2 except Condensate (V1) and HPSW (V4) fail, at which point all coolant makeup is lost, resulting in core damage in a vented containment.

SEQUENCE 10-5 -- $S2*\overline{C}*\overline{LOSP}*Q1*U1*U2*\overline{X1}*\overline{V1}*W1*W3*\overline{U4}*\overline{Y}*U4'*X3$

Same as Sequence 10-1 except CRD does not survive containment venting (U4) and reactor depressurization is unsuccessful (X3), leading to core damage in a vented containment.

SEQUENCES 10-6 TO 10-10

Same as Sequences 10-1 to 10-5 except the containment is not vented (Y) and eventually ruptures (/R).

SEQUENCE 10-11 -- $\overline{S2}*\overline{C}*\overline{LOSP}*Q1*U1*U2*\overline{X1}*\overline{V1}*W1*W3*\overline{U4}*Y*R*\overline{U4}'$

Same as Sequence 10-6 until the containment does not rupture but forms a leak, which does not affect CRD operation, resulting in no core damage in a leaking containment.

SEQUENCE 10-12 -- $S2*\overline{C}*\overline{LOSP}*Q1*U1*U2*\overline{X1}*\overline{V1}*W1*W3*\overline{U4}'*Y*R*U4$

Same as Sequence 10-11 except CRD does not operate following the leak in containment (U4), resulting in core damage in a vulnerable containment.

SEQUENCES 10-13 TO 10-14

Same as Sequence 10-1 until CRD fails to initiate (U4) following the loss of Condensate. The containment is vented (/Y) to relieve the pressure and following reactor depressurization (X3), Condensate (/V1) or HPSW (/V4) provides core coolant, resulting in no core damage in a vented containment.

SEQUENCE 10-15 -- $S2*\overline{C}*\overline{LOSP}*Q1*U1*U2*\overline{X1}*\overline{V1}*W1*W3*U4*\overline{Y}*\overline{X3}*V1*V4$

Same as Sequence 10-13 except both Condensate (V1) and HPSW (V4) fail, leaving no system available for coolant makeup, resulting in core damage in a vented containment.

SEQUENCE 10-16 -- $S2*\overline{C}*\overline{LOSP}*Q1*U1*U2*\overline{X1}*\overline{V1}*W1*W3*U4*\overline{Y}*X3$

Same as Sequence 10-13 except reactor depressurization is unsuccessful (X3) following containment venting, which leaves Condensate and HPSW unavailable for coolant makeup, resulting in core damage in a vented containment.

SEQUENCES 10-17 TO 10-20

Same as Sequences 10-13 to 10-16 except containment venting is unsuccessful (Y), leaving the containment overpressurized, resulting in eventual rupture of the containment (/R).

SEQUENCE 10-21 -- $S2*\overline{C}*\overline{LOSP}*Q1*U1*U2*\overline{X1}*\overline{V1}*W1*W3*U4*Y*R$

Same as Sequence 10-17 except (R), and core damage results in a vulnerable containment.

SEQUENCES 11 TO 12

Same as Sequences 8 to 9 except LPCS provides coolant makeup (/V2) following Condensate failure (V1).

SEQUENCE 13-1 -- $S2*\overline{C}*\overline{LOSP}*Q1*U1*U2*\overline{X1}*V1*\overline{V2}*W1*W3*\overline{U4}*\overline{Y}*\overline{U4}'$

Same as Sequence 11 until containment cooling with SPC (W1) and CS (W3) fails. High containment pressure eventually closes the SRVs, which

allows the primary system pressure to increase, resulting in the loss of LPCS (V2). CRD is successfully initiated in the one pump mode (/U4) to continue coolant makeup. Containment overpressure protection is accomplished by containment venting (/Y). CRD continues to provide coolant makeup, resulting in no core damage in a vented containment.

SEQUENCE 13-2 -- $S2*\overline{C}*\overline{LOSP}*Q1*U1*U2*\overline{X1}*V1*\overline{V2}*W1*W3*\overline{U4}*\overline{Y}*U4'*\overline{X3}*\overline{V4}$

Same as Sequence 13-1 except CRD does not survive containment venting (U4), the reactor is depressurized (/X3) to allow HPSW to continue coolant makeup (/V4).

SEQUENCES 13-3 TO 13-4

Same as Sequence 13-2 except either HPSW fails (V4) or reactor depressurization fails (X3), leaving no systems available for coolant makeup, resulting in core damage in a vented containment.

SEQUENCES 13-5 TO 13-8

Same as Sequences 13-1 to 13-4 except containment venting fails (Y) and the containment eventually ruptures (/R).

SEQUENCE 13-9 -- $S2*\overline{C}*\overline{LOSP}*Q1*U1*U2*\overline{X1}*V1*\overline{V2}*W1*W3*\overline{U4}*Y*R*\overline{U4}'$

Same as Sequence 13-5 except (R) but develops a leak. CRD continues to provide coolant makeup, resulting in no core damage in a leaking containment.

SEQUENCE 13-10 -- $S2*\overline{C}*\overline{LOSP}*Q1*U1*U2*\overline{X1}*V1*\overline{V2}*W1*W3*\overline{U4}'*Y*R*U4$

Same as Sequence 13-9 except CRD does not continue to operate following the leak in containment (U4), resulting in core damage in a vulnerable containment.

SEQUENCE 13-11 -- $S2*\overline{C}*\overline{LOSP}*Q1*U1*U2*\overline{X1}*V1*\overline{V2}*W1*W3*U4*\overline{Y}*\overline{X3}*\overline{V4}$

Same as Sequence 13-1 except CRD fails to initiate (U4) following the loss of LPCS. The containment is vented (/Y) and the primary system is depressurized (X3) to allow HPSW to provide coolant makeup (V4), resulting in no core damage in a vented containment.

SEQUENCES 13-12 TO 13-13

Same as Sequence 13-11 except either HPSW fails (V4) or reactor depressurization is unsuccessful (X3), leaving no core coolant system available, resulting in core damage in a vented containment.

SEQUENCES 13-14 TO 13-16

Same as Sequences 13-11 to 13-13 except containment venting fails (Y) and the containment ruptures (/R).

SEQUENCE 13-17 -- $S2*\overline{C}*\overline{LOSP}*Q1*U1*U2*\overline{X1}*V1*\overline{V2}*W1*W3*U4*Y*R$

Same as Sequence 13-14 except (R), causing closure of the SRVs and hence no low pressure cooling, resulting in core damage in a vulnerable containment.

SEQUENCES 14 TO 16

Same as Sequences 11 to 13 except LPCI provides early low-pressure coolant makeup (/V3) following LPCS failure (V2).

SEQUENCES 17 TO 19

Same as Sequences 14 to 16 except HPSW provides early low-pressure coolant makeup (/V4) following LPCI failure (V3).

SEQUENCE 20 -- $S2*\overline{C}*\overline{LOSP}*Q1*U1*U2*\overline{X1}*V1*V2*V3*V4$

Same as Sequence 17 except HPSW fails to operate (V4). At this point all core coolant systems are lost, resulting in early core damage in a vulnerable containment.

SEQUENCE 21 -- $S2*\overline{C}*\overline{LOSP}*Q1*U1*U2*X1$

Following the small LOCA (S2) and successful reactor scram (/C), offsite power is maintained (/LOSP). The PCS fails to remove heat from the core (Q1). Both high-pressure injection systems, HPCI (U1) and RCIC (U2), fail to operate. Depressurization of the reactor is unsuccessful (X1), which leaves no system available for coolant makeup, resulting in early core damage in a vulnerable containment.

SEQUENCES 22 TO 38

Same as Sequences 2 to 21 except offsite power is not maintained (LOSP) early in the sequence. Onsite emergency power is utilized for core

cooling systems, with the exception of the Condensate system, which requires offsite power to operate. All sequence outcomes are the same, except the success paths for Condensate events in the tree are eliminated.

SEQUENCE 39 -- S2*C

The RPS fails to scram the reactor (C) following the small LOCA (S2). This sequence has a low probability and is not developed further.

2.3.6 Loss of Offsite Power Event Tree

This section contains information on the loss of offsite power event tree. Success criteria considerations are presented along with the event tree and its description.

2.3.6.1 Success Criteria

Two criteria specific to the loss of offsite power initiator are described below:

a. For scenarios in which core cooling has been provided for a period of approximately 6 to 8 hours or more, one CRD pump operation is considered adequate for continued success of core cooling. This is based on the low decay heat levels reached by that time with no significant breach of the primary system. While the CRD failure model explicitly treats only the two pump criteria for success, single pump operation was treated as success during these long-term scenarios by eliminating (by hand) failures of the CRD system which would fail only one pump.

b. For scenarios in which core cooling is successful up to the time of containment venting or containment failure, one CRD pump or depressurization with one HPSW pump operation is considered to be adequate to continue successful core cooling.

2.3.6.2 Event Tree

Figure 2.22 displays the event tree for the loss of offsite power initiator. The entire PCS, Feedwater, and Condensate systems are not shown in the tree since loss of offsite power also prevents operation of these systems. Should offsite power be restored, these systems could be used to mitigate the event. The following discussions define the event tree headings and describe the sequences presented.

The following event tree headings appear on the tree in the approximate chronological order that would be expected following a loss of offsite power. For convenience, the RHR containment cooling choices are shown early in the tree to decrease the size of the event tree. Otherwise, the

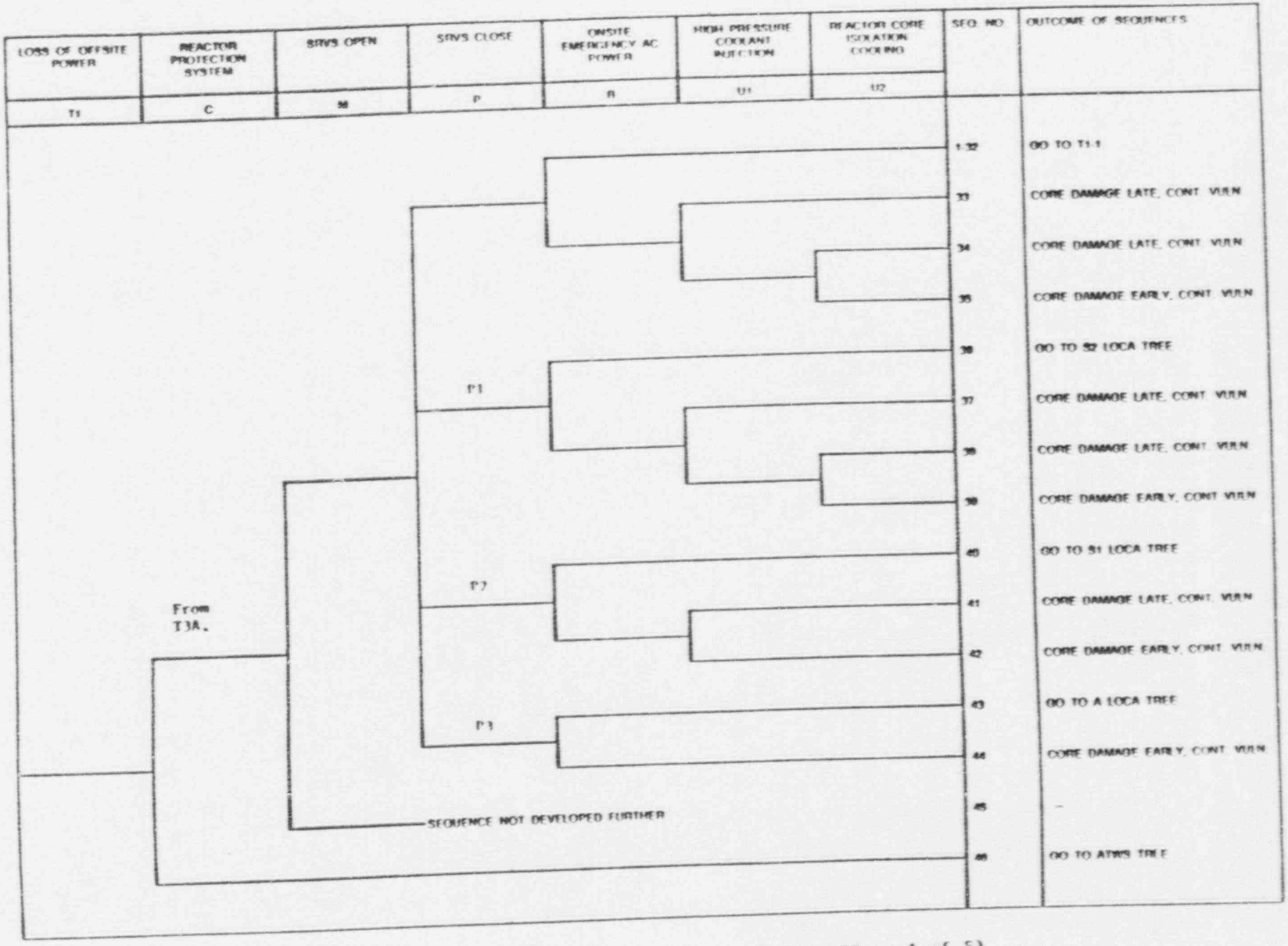

Figure 2.22 Loss of Offsite Power Event Tree (Page 1 of 5)

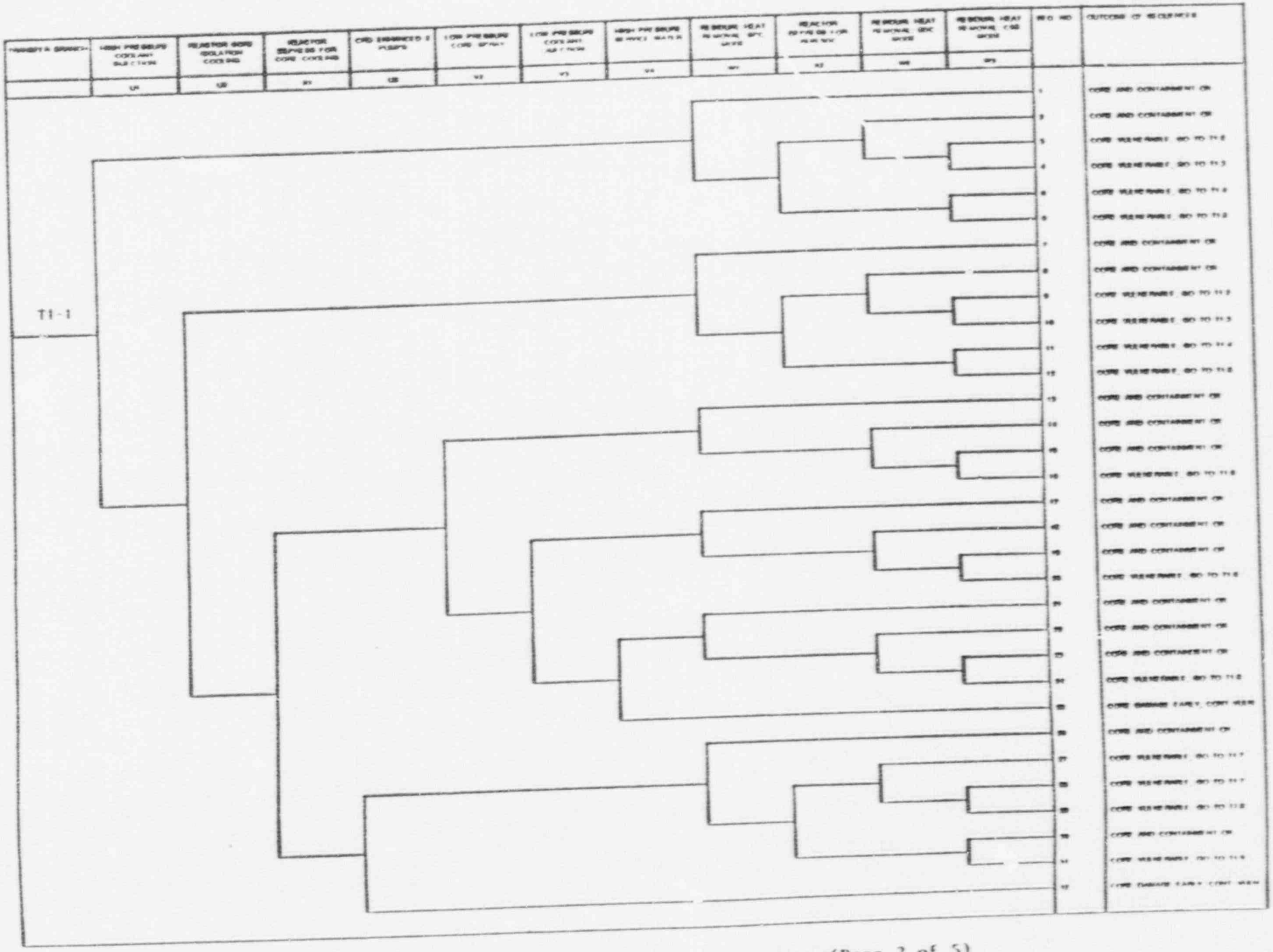

Figure 2.22 Loss of Offsite Power Event Tree (Page 2 of 5)

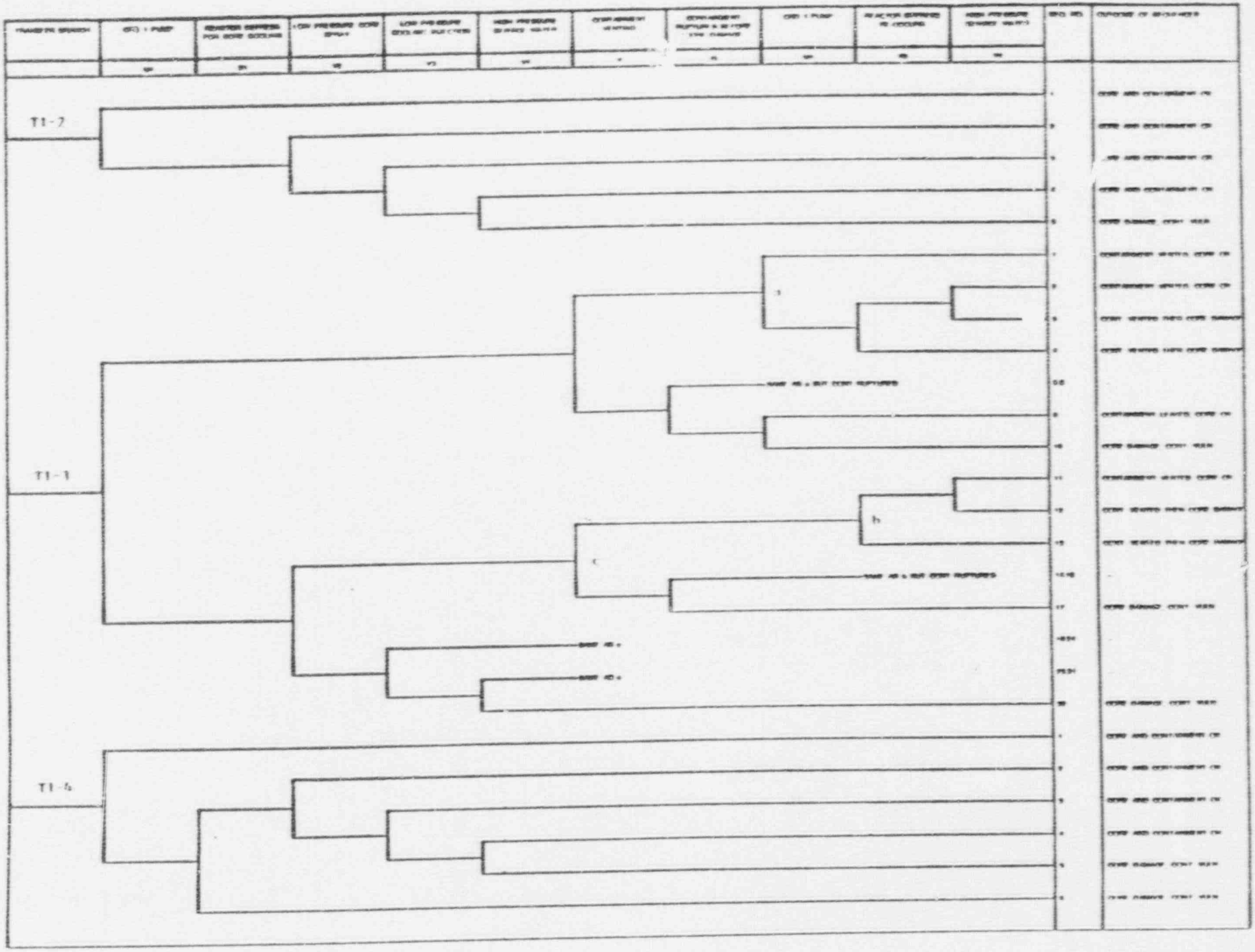

Figure 2.22 Loss of Offsite Power Event Tree (Page 3 of 5)

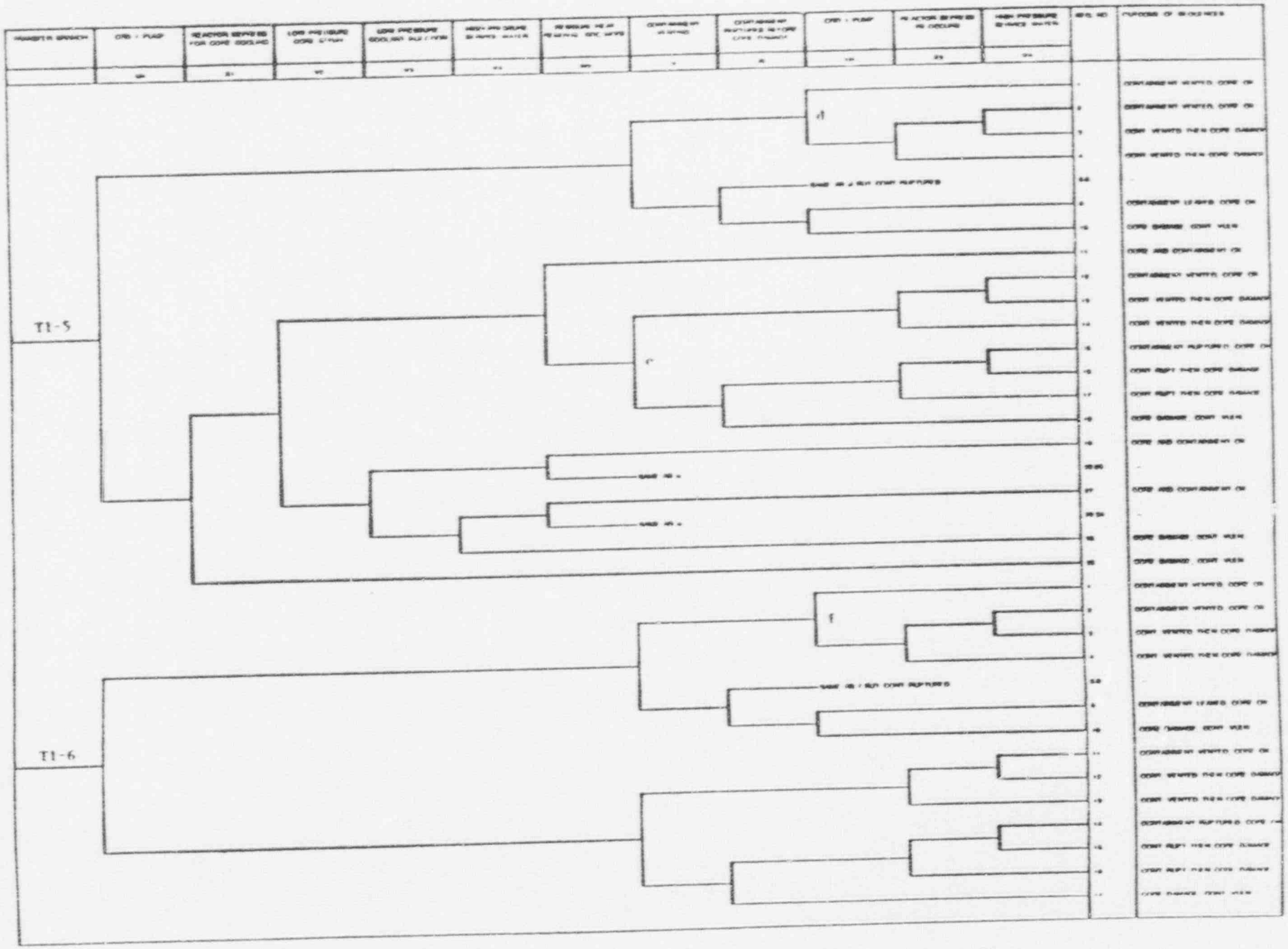

Figure 2.22 Loss of Offsite Power Event Tree (Page 4 of 5)

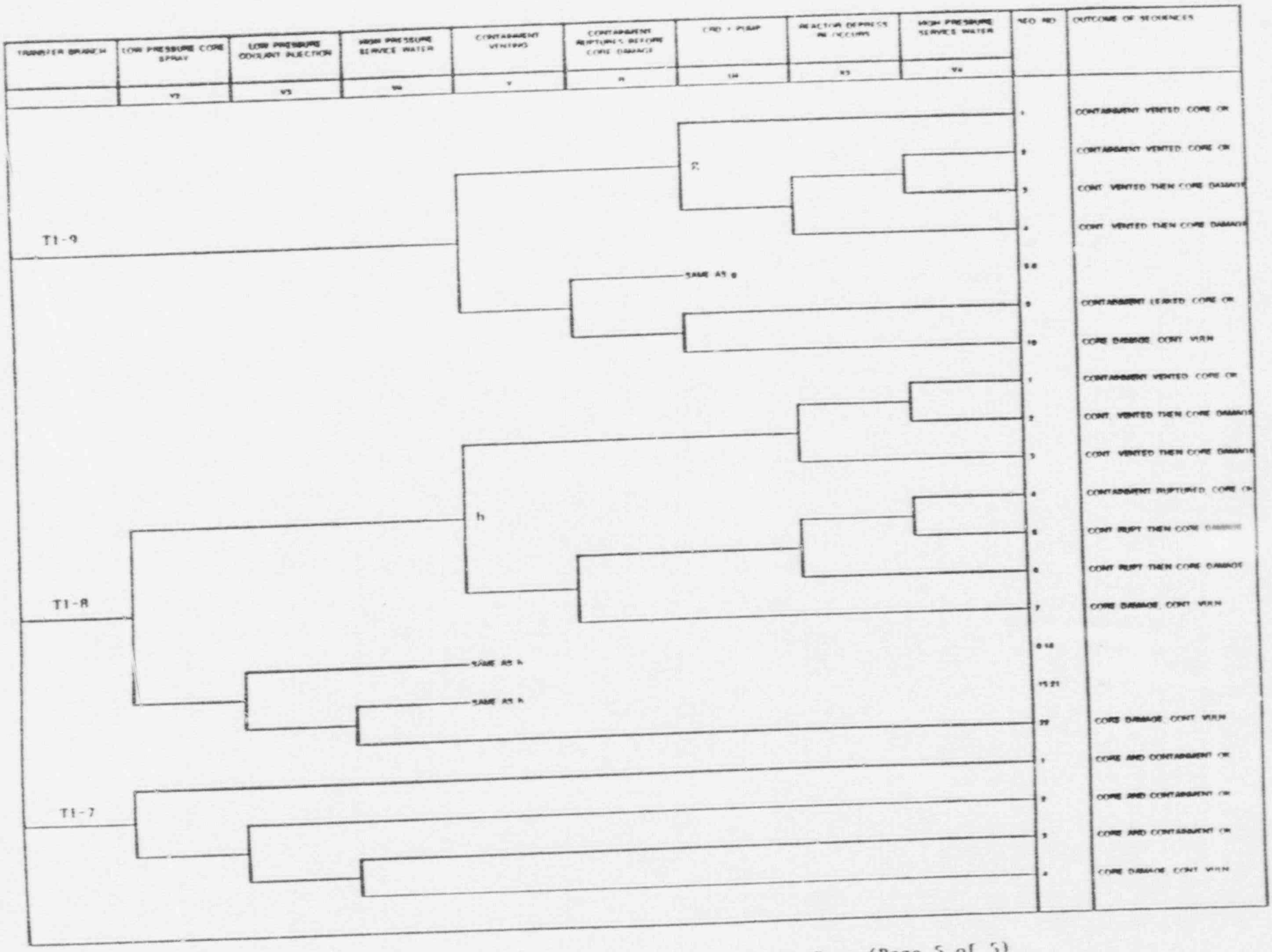

Figure 2.22 Loss of Offsite Power Event Tree (Page 5 of 5)

tendency is to show high and then low pressure injection systems, followed by containment venting, and finally long-term continued core cooling possibilities. In addition, onsite ac power restoration is shown as a specific event so that station blackout sequences can be explicitly depicted.

T1: Initiating event, loss of offsite power.

C: Success or failure of the RPS. Success implies automatic scram by the control rods.

M: Success or failure of Reactor Coolant System (RCS) overpressure protection (if required) by automatic operation of the SRVs. Success implies prevention of RCS overpressure so as to avoid damage to the primary system.

P: Success or failure associated with reclosing of any SRVs which should open in response to reactor vessel pressure rises throughout the sequence. Success implies reclosure of all valves when vessel pressure drops below the closure setpoints. P1, P2 and P3 refer to the failure to reclose one, two and three SRVs, respectively.

B: Success or failure of the onsite ac power system (diesel generators and associated equipment and emergency buses) in response to the loss of offsite power. Success implies operation of at least one emergency ac power division so that ac-powered mitigating systems can be utilized. Failure implies loss of all ac, or station blackout.

U1: Success or failure of the HPCI system. Success implies operation of the HPCI pump train so as to maintain sufficient coolant injection. U1' refers to the HPCI system without pump room ventilation.

U2: Success or failure of the RCIC system. Success implies operation of the RCIC pump train so as to maintain sufficient coolant injection. U2' refers to the RCIC system without pump room ventilation.

X1: Success or failure of primary system depressurization. Success implies automatic or manual operation of the ADS or manual operation of other SRVs such that three valves or more are opened allowing low pressure injection.

U3: Success or failure of the CRD system as an injection source. Success implies two pump operation.

V2: Success or failure of the LPCS system. Success implies operation of any two of the four LPCS pumps through either or both LPCS injection lines.

V3: Success or failure of the LPCI mode of the RHR system. Success implies operation of one of four LPCI pumps through either LPCI injection line to the reactor vessel.

V4: Success or failure of the HPSW system in the inject mode to the reactor vessel through a LPCI injection line. Success implies manual operation of this injection source such that one HPSW pump successfully provides coolant to the reactor.

W1,W2,W3: Success or failure of the RHR system in the SPC, SDC, or CS mode, respectively. Success implies at least one RHR pump operating in any one of the three modes with the appropriate heat exchanger in the loop along with the HPSW system in operation to the ultimate heat sink.

X2: Success or failure of primary system depressurization. Success implies automatic or manual operation of any three of eleven ADS valves to allow the SDC mode of RHR to be initiated.

U4: Success or failure of the CRD system as an injection source. Success implies operation in the one pump mode.

Y: Success or failure of containment venting. Success implies that the six-inch integrated leak test line or larger size line is open so as to prevent containment failure by overpressure. As necessary, water makeup is also eventually supplied to the suppression pool.

B: Success or failure of the containment to withstand over-pressurization. Success implies the containment ruptures before core damage.

X3: Success or failure of primary system depressurization. Success implies automatic or manual operation of ADS occurs subsequent to initial depressurization to allow low pressure coolant injection.

The following descriptions refer to the sequences found in Figure 2.22.

SEQUENCE 1 -- $T1*\overline{C}*\overline{M}*\overline{P}*\overline{B}*\overline{U1}*\overline{W1}$

A loss-of-offsite power occurs (T1) which generates a reactor scram condition and the RPS successfully inserts the rods into the core (/C). The SRVs properly cycle to control reactor pressure (/M, /P) and onsite emergency ac power is established (/B). HPCI is initiated (/U1) for core cooling and SPC is initiated (/W1) for containment overpressure protection, resulting in a safe core and containment.

SEQUENCE 2 -- $T1*\overline{C}*\overline{M}*\overline{P}*\overline{B}*\overline{U1}*W1*\overline{X2}*\overline{W2}$

Same as Sequence 1 but SPC fails to provide containment overpressure protection (W1) and SDC is initiated (/W2) following reactor depressurization (/X2).

SEQUENCES 3-1 TO 3-4

Same as Sequence 2 except SDC fails (W2) and CS continues to provide containment overpressure protection (/W3). HPCI has failed due to high suppression pool temperatures and either CRD (/U4), LPCS (/V2), LPCI (/V3) or HPSW (/V4) continues core cooling.

SEQUENCE 3-5 -- $T1*\overline{C}*\overline{M}*\overline{P}*\overline{B}*\overline{U1}*W1*\overline{X2}*W2*\overline{W3}*U4*V2*V3*V4$

Same as Sequences 3-1 to 3-4 except CRD (U4), LPCS (V2), LPCI (V3) and HPSW (V4) fail, leaving no system available to cool the core, resulting in core damage in a vulnerable containment.

SEQUENCE 4-1 -- $T1*\overline{C}*\overline{M}*\overline{P}*\overline{B}*\overline{U1}*W1*\overline{X2}*W2*W3*\overline{U4}*\overline{Y}*\overline{U4}'$

Same as Sequence 2 except SDC fails (W2), followed by CS failure (W3), leaving the containment without overpressure protection. HPCI eventually fails due to high suppression pool temperatures and CRD is initiated in the one pump mode (/U4). The containment is successfully vented (/Y) and CRD continues to provide core coolant, resulting in no core damage in a vented containment.

SEQUENCE 4-2 -- $T1*\overline{C}*\overline{M}*\overline{P}*\overline{B}*\overline{U1}*W1*\overline{X2}*W2*W3*\overline{U4}*\overline{Y}*U4'*\overline{X3}*\overline{V4}$

Same as Sequence 4-1 except CRD fails during containment venting (U4). Prior to containment venting, due to the loss of containment overpressure protection, high containment pressure forces the SRVs closed and the primary system pressure increases before injection is restored with CRD. The reactor is depressurized (/X3) and HPSW provides core coolant (/V4).

SEQUENCES 4-3 TO 4-4

Same as Sequence 4-2 except HPSW fails (V4), or reactor depressurization prior to HPSW operation is unsuccessful (X3), resulting in core damage in a vented containment.

SEQUENCES 4-5 TO 4-8

Same as Sequences 4-1 to 4-4 except containment venting fails (Y) and the containment ruptures before core damage (/R).

SEQUENCE 4-9 -- $T1*\overline{C}*\overline{M}*\overline{P}*\overline{B}*\overline{U1}*W1*\overline{X2}*W2*W3*\overline{U4}*Y*R*\overline{U4}'$

Same as Sequence 4-8 except the containment does not rupture (R) but develops a leak. CRD continues to operate, resulting in no core damage in a leaking containment.

SEQUENCE 4-10 -- $T1*\overline{C}*\overline{M}*\overline{P}*\overline{B}*\overline{U1}*W1*\overline{X2}*W2*W3*\overline{U4}'*Y*R*U4$

Same as Sequence 4-9 except CRD does not continue to operate (U4) following the containment leak and because of high containment pressure, ADS cannot relieve primary pressure to allow HPSW to operate, resulting in core damage in a leaking containment.

SEQUENCE 4-11 -- $T1*\overline{C}*\overline{M}*\overline{P}*\overline{B}*\overline{U1}*W1*\overline{X2}*W2*W3*U4*\overline{V2}*\overline{Y}*\overline{X3}*\overline{V4}$

Same as Sequence 4-1 except CRD does not operate (U4) following HPCI failure. LPCS is initiated (/V2) to continue core cooling and the containment is eventually vented (/Y). The LPCS pumps then fail due to low NPSH and the reactor is depressurized to allow HPSW to cool the core (/V4), resulting in a safe core in a vented containment.

SEQUENCES 4-12 TO 4-13

Same as Sequence 4-11 except HPSW fails (V4), or depressurization prior to HPSW operation fails (X3), resulting in core damage in a vented containment.

SEQUENCES 4-14 TO 4-16

Same as Sequences 4-11 to 4-13 except containment venting is unsuccessful (Y) and the containment ruptures before core damage (/R).

SEQUENCE 4-17 -- $T1*\overline{C}*\overline{M}*\overline{P}*\overline{B}*\overline{U1}*W1*\overline{X2}*W2*W3*U4*\overline{V2}*Y*R$

Same as Sequence 4-11 except containment venting fails (Y) and the containment does not rupture (R), thereby closing the SRVs due to high containment pressure and preventing low pressure cooling. This results in core damage in a leaking containment.

SEQUENCES 4-18 TO 4-24

Same as Sequences 4-11 to 4-17 except, following LPCS failure (V2), LPCI provides core coolant (/V3) prior to containment venting.

SEQUENCES 4-25 TO 4-31

Same as Sequences 4-18 to 4-24 except, following LPCI failure (V3), HPSW provides core coolant (/V4) prior to containment venting.

SEQUENCE 4-32 -- $T1*\bar{C}*\bar{M}*\bar{P}*\bar{B}*\overline{U1}*W1*\overline{X2}*W2*W3*U4*V2*V3*V4$

Same as Sequence 4-11 except LPCS (V2), LPCI (V3), and HPSW (V4) fail and all core cooling is lost, resulting in core damage in a vulnerable containment.

SEQUENCE 5-1 -- $T1*\bar{C}*\bar{M}*\bar{P}*\bar{B}*U1*W1*X2*\overline{W3}*\overline{U4}$

Same as Sequence 2 except reactor depressurization for SDC is unsuccessful (X2) and CS is initiated to provide containment overpressure protection (/W3). HPCI has failed due to high suppression pool temperatures before CS is established and CRD is initiated to cool the core (/U4), resulting in a safe core and containment.

SEQUENCES 5-2 TO 5-4

Same as Sequence 5-1 except CRD fails to provide coolant injection (U4), the reactor is depressurized (/X1), and LPCS (/V2), LPCI (/V3) or HPSW (/V4) provide core cooling.

SEQUENCES 5-5 TO 5-6

Same as Sequence 5-2 except either reactor depressurization fails (X1) or LPCS (V2), LPCI (V3) and HPSW (V4) fail following depressurization, resulting in core damage in a vulnerable containment.

SEQUENCE 6-1 -- $T1*\bar{C}*\bar{M}*\bar{P}*\bar{B}*\overline{U1}*W1*X2*W3*\overline{U4}*\bar{Y}*\overline{U4}'$

Same as Sequence 5 except CS fails (W3), resulting in the loss of all containment overpressure protection. High suppression pool temperatures fail HPCI, and CRD (1 pump mode) is initiated for core coolant (/U4). Increasing containment pressure is relieved by containment venting (/Y). CRD survives venting and the core is safe in a vented containment.

SEQUENCE 6-2 -- $T1*\bar{C}*\bar{M}*\bar{P}*\bar{B}*\bar{U1}*W1*X2*W3*\bar{U4}*\bar{Y}*U4'*\bar{X3}*\bar{V4}$

Same as Sequence 6-2 except CRD does not survive containment venting, the reactor is depressurized (/X1), and HPSW continues core cooling (/V4).

SEQUENCES 6-3 TO 6-4

Same as Sequence 6-2 except either reactor depressurization fails (X1), or HPSW fails (V4) following reactor depressurization, leading to core damage in a vented containment.

SEQUENCES 6-5 TO 6-8

Same as Sequences 6-1 to 6-4 except containment venting is unsuccessful (Y) and the containment ruptures (/R).

SEQUENCE 6-9 -- $T1*\bar{C}*\bar{M}*\bar{P}*\bar{B}*\bar{U1}*W1*X2*W3*\bar{U4}*Y*R*\bar{U4}'$

Same as Sequence 6-5 except the containment does not rupture (R), but develops a leak. This causes closure of the SRVs and the inability to use low pressure cooling. CRD continues coolant injection, resulting in no core damage in a leaking containment.

SEQUENCE 6-10 -- $T1*\bar{C}*\bar{M}*\bar{P}*\bar{B}*\bar{U1}*W1*X2*W3*\bar{U4}'*Y*R*U4$

Same as Sequence 6-9 except CRD fails (U4) following the containment leak, at which point all coolant makeup is lost, resulting in core damage in a vulnerable containment.

SEQUENCE 6-11 -- $T1*\bar{C}*\bar{M}*\bar{P}*\bar{B}*\bar{U1}*W1*X2*W3*U4*\bar{X1}*\bar{V2}*\bar{W2}$

Same development as Sequence 6-1 until CRD fails to initiate (U4) following HPCI failure. The reactor is depressurized (/X1) to initiate LPCS for coolant injection (/V2). The reactor is sufficiently depressurized to initiate late SDC for containment overpressure protection (/W2), resulting in a safe core and containment.

SEQUENCE 6-12 -- $T1*\bar{C}*\bar{M}*\bar{P}*\bar{B}*\bar{U1}*W1*X2*W3*U4*\bar{X1}*\bar{V2}*W2*\bar{Y}*\bar{X3}*\bar{V4}$

Same as Sequence 6-11 except SDC fails to provide containment overpressure protection (W2), followed by successful venting of the containment (/Y). Coolant injection is restored using HPSW (/V4) following reactor depressurization (/X3), resulting in a safe core in a vented containment.

SEQUENCES 6-13 TO 6-14

Same as Sequence 6-12 except either reactor depressurization fails (X3) or HPSW fails (V4) following reactor depressurization, resulting in core damage in a vented containment.

SEQUENCES 6-15 TO 6-17

Same as Sequences 6-12 to 6-14 except containment venting fails (Y) and the containment ruptures (/R).

SEQUENCE 6-18 -- $T1*\bar{C}*\bar{M}*\bar{P}*\bar{B}*\overline{U1}*W1*X2*W3*U4*\overline{\overline{X1}}*\overline{\overline{V2}}*W2*Y*R$

Same as Sequence 6-11 until containment overpressure protection with SDC fails (W2), followed by failure of containment venting (Y). The containment does not rupture (R), disallowing use of low pressure systems because of closure of the SRVs. Core damage results in a vulnerable containment.

SEQUENCES 6-19 TO 6-26

Same as Sequences 6-11 to 6-18 except LPCI provides coolant makeup (/V3) following failure of LPCS (V2).

SEQUENCES 6-27 TO 6-34

Same as Sequences 6-19 to 6-26 except HPSW provides coolant makeup (/V4) following failure of LPCI (V3).

SEQUENCE 6-35 -- $T1*\bar{C}*\bar{M}*\bar{P}*\bar{B}*\overline{U1}*W1*X2*W3*U4*\overline{X1}*V2*V3*V4$

Same as Sequence 6-11 until LPCS fails (V2) following reactor depressurization, followed by failure of both LPCI (V3) and HPSW (V4), at which point all coolant makeup is lost, resulting in core damage in a vulnerable containment.

SEQUENCE 6-36 -- $T1*\bar{C}*\bar{M}*\bar{P}*\bar{B}*\overline{U1}*W1*X2*W3*U4*X1$

Same as Sequence 6-11 until CRD fails to continue coolant makeup (U4) following HPCI failure. Reactor depressurization fails (X1), which disables all low-pressure core cooling systems, resulting in core damage in a vulnerable containment.

SEQUENCES 7 TO 12

Same as Sequences 1 to 6 except RCIC provides high pressure coolant makeup (/U2) following failure to initiate HPCI (U1).

SEQUENCES 13 TO 15

Same as Sequence 1 until failure to initiate HPCI (U1), followed by failure of RCIC (U2). The reactor is depressurized (/X1) and LPCS is initiated for coolant makeup (/V2). Containment overpressure protection is provided by SPC (/W1), SDC (/W2), or CS (/W3), resulting in a safe core and containment.

SEQUENCES 16-1 TO 16-2

Same as Sequence 13 until SPC fails (W1), followed by failure of SDC (W2) and CS (W3). Without containment overpressure protection, the pressure in containment rises until the SRVs close. Primary system pressure then rises, eventually failing LPCS (V2). CRD is initiated (/U4) for coolant makeup. High containment pressure is relieved by containment venting (/Y). CRD continues to cool the core, or the reactor is depressurized (/X1) and HPSW cools the core (/V4) if CRD does not survive the venting.

SEQUENCES 16-3 TO 16-4

Same as Sequence 16-1 except CRD does not survive containment venting and either reactor depressurization is unsuccessful (X1), or HPSW fails (V4) following reactor depressurization, resulting in core damage in a vented containment.

SEQUENCES 16-5 TO 16-8

Same as Sequences 16-1 to 16-4 except containment venting fails (Y) and the containment eventually ruptures (/R).

SEQUENCE 16-9 -- $T1*\bar{C}*\bar{M}*\bar{P}*\bar{B}*U1*U2*\overline{X1}*\overline{V2}*W1*W2*W3*\overline{U4}*Y*R*\overline{U4}'$

Same as Sequence 16-5 except the containment does not rupture (R) but develops a leak. CRD survives resulting in a safe core in a leaking containment.

SEQUENCE 16-10 -- $T1*\bar{C}*\bar{M}*\bar{P}*\bar{B}*U1*U2*\overline{X1}*\overline{V2}*W1*W2*W3*\overline{U4}'*Y*R*U4$

Same as Sequence 16-9 except CRD does not survive the development of a leak in containment (U4), all coolant systems are lost, and core damage results in a vulnerable containment.

SEQUENCE 16-11 -- $T1*\bar{C}*\bar{M}*\bar{P}*\bar{B}*U1*U2*\bar{X1}*\bar{V2}*W1*W2*W3*U4*\bar{Y}*\bar{X3}*\bar{V4}$

Same as Sequence 16-1 until CRD fails to initiate (U4) following loss of containment overpressure protection. Increasing containment pressure is relieved by containment venting (/Y) and HPSW is initiated to cool the core (/V4) following primary system depressurization (/X1). The core is safe in a vented containment.

SEQUENCES 16-12 TO 16-13

Same as Sequence 16-11 except either HPSW fails to cool the core (V4) or primary system depressurization fails (X1) prior to HPSW operation, resulting in core damage in a vented containment.

SEQUENCES 16-14 TO 16-16

Same as Sequences 16-11 to 16-13 except containment venting fails (Y) and the containment eventually ruptures (/R).

SEQUENCE 16-17 -- $T1*\bar{C}*\bar{M}*\bar{P}*\bar{B}*U1*U2*\bar{X1}*\bar{V2}*W1*W2*W3*U4*Y*R$

Same as Sequence 16-11 until containment venting fails (Y). The containment does not rupture (R) and continues to pressurize, resulting in core damage in a vulnerable containment since the SRVs are forced closed, preventing low pressure cooling.

SEQUENCES 17 TO 20

Same as Sequences 13 to 15 except LPCI provides early core coolant (/V3) following LPCS failure (V2).

SEQUENCES 21 TO 24

Same as Sequences 17 to 20 except HPSW provides early core coolant (/V4) following LPCI failure (V3).

SEQUENCE 25 -- $T1*\bar{C}*\bar{M}*\bar{P}*\bar{B}*U1*U2*\bar{X1}*V2*V3*V4$

Same as Sequences 21 to 24 until HPSW fails (V4), at which point all coolant makeup is lost, resulting in early core damage in a vulnerable containment.

SEQUENCE 26 -- $T1*\bar{C}*\bar{M}*\bar{P}*\bar{B}*U1*U2*X1*\overline{U3}*\overline{W1}$

Same as Sequence 13 until reactor depressurization fails (X1) following failure to initiate high-pressure coolant systems. CRD is initiated in the two-pump mode to provide sufficient injection capacity (/U3). Containment overpressure protection is provided by SPC (/W1), resulting in a safe core and containment.

SEQUENCES 27-1 TO 27-3

Same as Sequence 26 until SPC fails to initiate (W1), the reactor is depressurized (/X2), and SDC provides containment overpressure protection (/W2). Reactor depressurization for SDC increases CRD flow rate which, when considering CST inventory is depleting, is assumed to fail the CRD pumps due to low NPSH. LPCS (/V2), LPCI (/V3) or HPSW (/V4) is initiated for core coolant, resulting in a safe core and containment.

SEQUENCE 27-4 -- $T1*\bar{C}*\bar{M}*\bar{P}*\bar{B}*U1*U2*X1*\overline{U3}*W1*\overline{X2}*\overline{W2}*V2*V3*V4$

Same as Sequence 27-1 until LPCS fails (V2) to initiate after CRD fails, followed by unsuccessful operation of LPCI (V3) and HPSW (V4), resulting in core damage in a vulnerable containment.

SEQUENCES 28-1 TO 28-4

Same as Sequences 27-1 to 27-4 except CS provides containment overpressure protection (/W3) following SDC failure (W2).

SEQUENCE 29-1 -- $T1*\bar{C}*\bar{M}*\bar{P}*\bar{B}*U1*U2*X1*\overline{U3}*W1*\overline{X2}*W2*W3*\overline{V2}*\bar{Y}*\overline{X3}*\overline{V4}$

Same as Sequence 28-1 until CS fails to initiate (W3), at which point all containment cooling is lost. CRD failed due to reactor depressurization for SDC, so LPCS is initiated (/V2) to continue core cooling. Without containment overpressure protection, the pressure in containment is increasing and eventually closes the SRVs. Containment venting (/Y) is successful to relieve containment overpressurization, which fails LPCS due to low NPSH. Since the SRVs are closed, a pressure increase in the primary system begins until the reactor is again depressurized (/X3) and HPSW cools the core, resulting in a safe core in a vented containment.

SEQUENCES 29-2 TO 29-3

Same as Sequence 29-1 except either HPSW fails (V4) or reactor depressurization fails (X3) prior to HPSW operation, leaving no system available for coolant makeup, resulting in core damage in a vented containment.

SEQUENCES 29-4 TO 29-6

Same as Sequences 29-1 to 29-3 except containment venting fails (Y) and the containment eventually ruptures (/R).

SEQUENCE 29-7 -- $T1*\bar{C}*\bar{M}*\bar{P}*\bar{B}*U1*U2*X1*\overline{U3}*W1*\overline{X2}*W2*W3*\overline{V2}*Y*R$

Same as Sequence 29-4 until the containment fails to rupture (R), which precludes HPSW operation because of forced closure of the SRVs. This results in core damage in a vulnerable containment.

SEQUENCES 29-8 TO 29-14

Same as Sequences 29-1 to 29-7 except LPCS fails to initiate (V2) following containment cooling failure and LPCI provides coolant makeup (/V3).

SEQUENCES 29-15 TO 29-21

Same as Sequences 29-8 to 29-14 except LPCI fails to initiate (V3) following containment cooling failure and HPSW provides coolant makeup (/V4).

SEQUENCE 29-22 -- $T1*\bar{C}*\bar{M}*\bar{P}*\bar{B}*U1*U2*X1*\overline{U3}*W1*\overline{X2}*W2*W3*V2*V3*V4$

Same as Sequence 29-11 until LPCS fails (V2) following containment cooling failure. LPCI (V3) and HPSW (V4) also fail to initiate, resulting in core damage in a vulnerable containment.

SEQUENCE 30 -- $T1*\bar{C}*\bar{M}*\bar{P}*\bar{B}*U1*U2*X1*\overline{U3}*W1*X2*\overline{W3}$

Same as Sequence 26 until SPC fails (W1), followed by failure of reactor depressurization for SDC (X2). CS is initiated to provide containment overpressure protection (/W3). Since reactor depressurization was unsuccessful, CRD does not fail, resulting in a safe core and containment.

SEQUENCES 31-1 TO 31-2

Same as Sequence 30 until CS fails (W3), at which point all containment overpressure protection is lost. Eventually containment venting is performed to relieve containment overpressure (/Y). CRD continues to cool the core in the one-pump mode (/U4), or CRD fails on containment venting and HPSW cools the core (/V4), resulting in a safe core in a vented containment.

SEQUENCES 31-3 TO 31-4

Same as Sequence 31-2 except HPSW fails (V4) or reactor depressurization fails prior to HPSW operation (X3), resulting in core damage in a vented containment.

SEQUENCES 31-5 TO 31-8

Same as Sequences 31-1 to 31-4 except containment venting fails (Y) and the containment eventually ruptures (/R).

SEQUENCE 31-9 -- $T1*\bar{C}*\bar{M}*\bar{P}*\bar{B}*U1*U2*X1*\bar{U3}*W1*X2*W3*Y*R*\bar{U4}$

Same as Sequence 31-5 except the containment does not rupture (R) but develops a leak. CRD continues to cool the core, resulting in a safe core in a leaked containment.

SEQUENCE 31-10 -- $T1*\bar{C}*\bar{M}*\bar{P}*\bar{B}*U1*U2*X1*\bar{U3}*W1*X2*W3*Y*R*U4$

Same as Sequence 31-9 except CRD does not survive the containment leak (U4), resulting in core damage in a vulnerable containment.

SEQUENCE 32 -- $T1*\bar{C}*\bar{M}*\bar{P}*\bar{B}*U1*U2*X1*U3$

Same as Sequence 26 until CRD fails to initiate (U3) in the two-pump mode following failure to depressurize the reactor, which leaves no system available for coolant makeup. Early core damage results, with a vulnerable containment.

SEQUENCES 33 TO 34

A loss-of-offsite-power occurs (T1) which generates a reactor scram condition and the RPS successfully inserts the rods into the core (/C). The SRVs properly cycle to control reactor pressure (/M, /P) and onsite emergency power fails to be established (B). HPCI or RCIC is initiated (/U1', /U2') for coolant injection until it fails in the harsh environment or due to battery depletion, and core damage occurs late in a vulnerable containment.

SEQUENCE 35 -- $T1*\bar{C}*\bar{M}*\bar{P}*B*U1'*U2'$

Same as Sequence 34 except RCIC fails to operate (U2') and early core damage results with a vulnerable containment since no other coolant injection is possible without ac power.

SEQUENCE 36 -- $T1*\bar{C}*\bar{M}*P1*\bar{B}$

A loss-of-offsite-power occurs (T1) which generates a reactor scram condition and the RPS successfully inserts the rods into the core (/C). The SRVs open to relieve reactor pressure (/M) but one SRV fails to close (P1), creating a loss-of-coolant accident. Onsite emergency power is established (/B) and the sequence is transferred to the S2 LOCA tree.

SEQUENCES 37 TO 38

Same as Sequence 36 except onsite emergency power is not established (B) and HPCI (/U1') or RCIC (/U2') provides coolant injection until it fails in the harsh environment or due to battery depletion. This results in late core damage in a vulnerable containment.

SEQUENCE 39 -- $T1*\bar{C}*\bar{M}*P1*B*U1'*U2'$

Same as Sequence 37 except both HPCI (U1') and RCIC (U2') fail to provide coolant injection, resulting in early core damage in a vulnerable containment.

SEQUENCE 40 -- $T1*\bar{C}*\bar{M}*P2*\bar{B}$

Same as Sequence 36 except two SRVs fail to close (P2) and the sequence is transferred to the S1 LOCA tree.

SEQUENCES 41 TO 42

Same as Sequence 40 except onsite emergency power is not established (B) and late core damage in a vulnerable containment results if HPCI (/U1) provides temporary coolant injection. If HPCI fails to operate, early core damage results with a vulnerable containment. RCIC does not have enough capacity to provide sufficient coolant in an S1 LOCA situation.

SEQUENCE 43 -- $T1*C*\bar{M}*P3*\bar{B}$

Same as Sequence 40 except three or more SRVs fail to close (P3) and the sequence is transferred to the A LOCA tree.

SEQUENCE 44 -- $T1*\bar{C}*\bar{M}*P3*B$

Same as Sequence 43 except onsite emergency power is not maintained (B) and high pressure coolant systems cannot operate in a large LOCA situation, resulting in early core damage in a vulnerable containment.

SEQUENCE 45 -- T1*$\bar{C}$*M

A loss-of-offsite-power occurs (T1) which generates a scram condition and the RPS successfully inserts the rods into the core (/C). The SRVs do not open to reduce reactor pressure (M). The sequence is not developed further because of its low probability.

SEQUENCE 46 -- T1*C

A loss-of-offsite power occurs (T1) which generates a scram condition and the RPS fails to insert the rods into the core (C). The sequence is transferred to the ATWS tree which was analyzed only in the internal events analysis.

2.3.7 Transient With PCS Initially Available Event Tree

This section contains information on the transient with the PCS initially available event tree. Success criteria considerations are presented along with the event tree and its description.

2.3.7.1 Success Criteria

Transients in which the PCS remains initially available do not represent significant concerns for the plant unless the PCS is subsequently lost while the plant is being shut down. Should the PCS be lost, the sequence of events then proceeds similar to a transient in which the PCS was unavailable from the start. T3A represents all the transients of this type except Inadvertent Open Relief Valve (IORV) events and a loss of feedwater which can have somewhat different effects on plant conditions.

2.3.7.2 Event Tree

The T31 transient event tree is depicted by Figure 2.23 and 2.24. The following discussions define the event tree headings and the sequences.

The events in the tree include:

T31: Initiating event, transient with PCS initially available.

C: Success or failure of Reactor Protection System (RPS). Success implies automatic scram by the control rods.

LOSP1: Success or failure to maintain offsite power. The designation LOSP1 is used instead of LOSP for purposes of computational efficiency within the SETS code.

Q: Continued success or subsequent failure of the PCS. Success implies continued operation of the PCS such that a safe cooldown of the plant is achieved using the PCS.

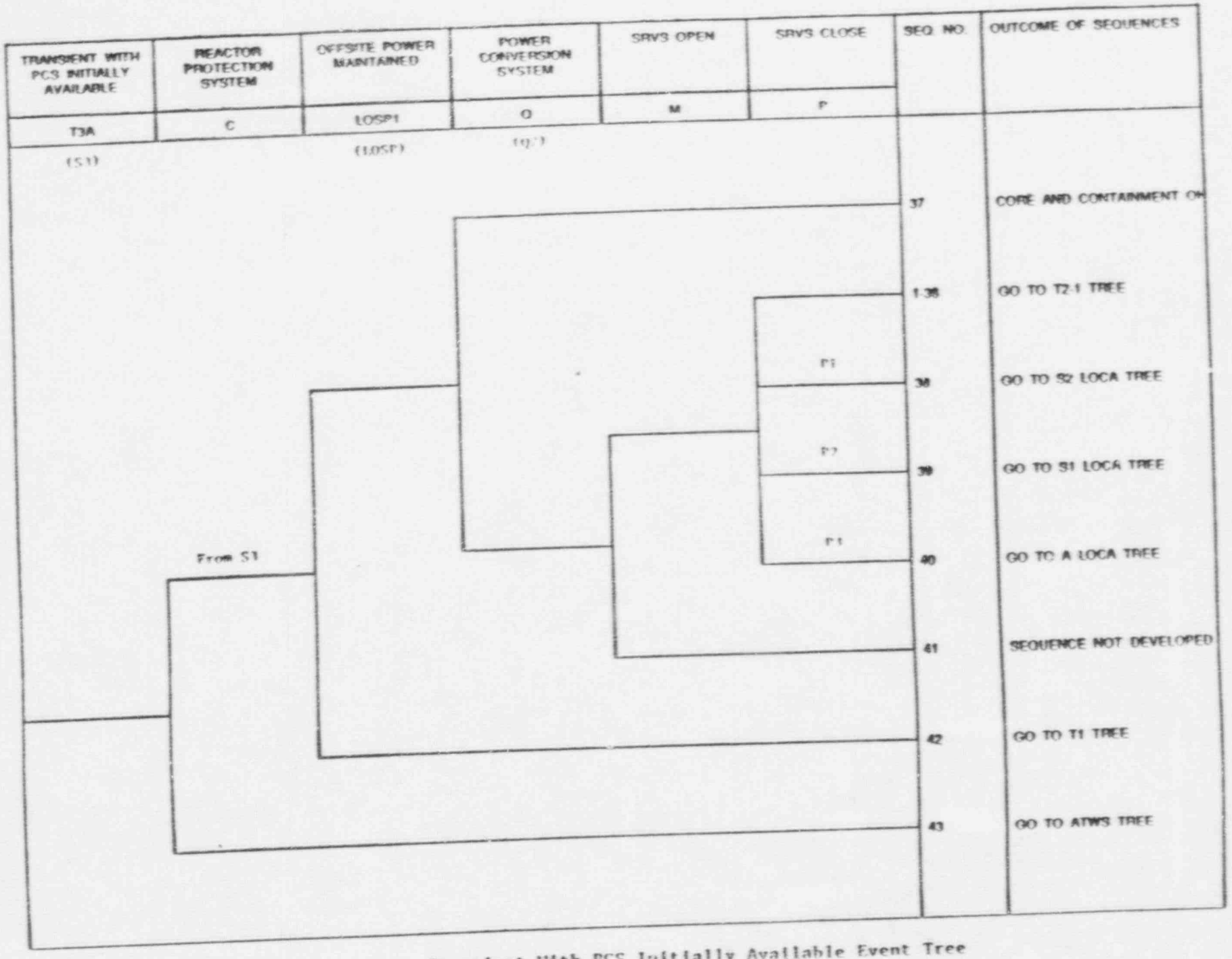

Figure 2.23 Transient With PCS Initially Available Event Tree

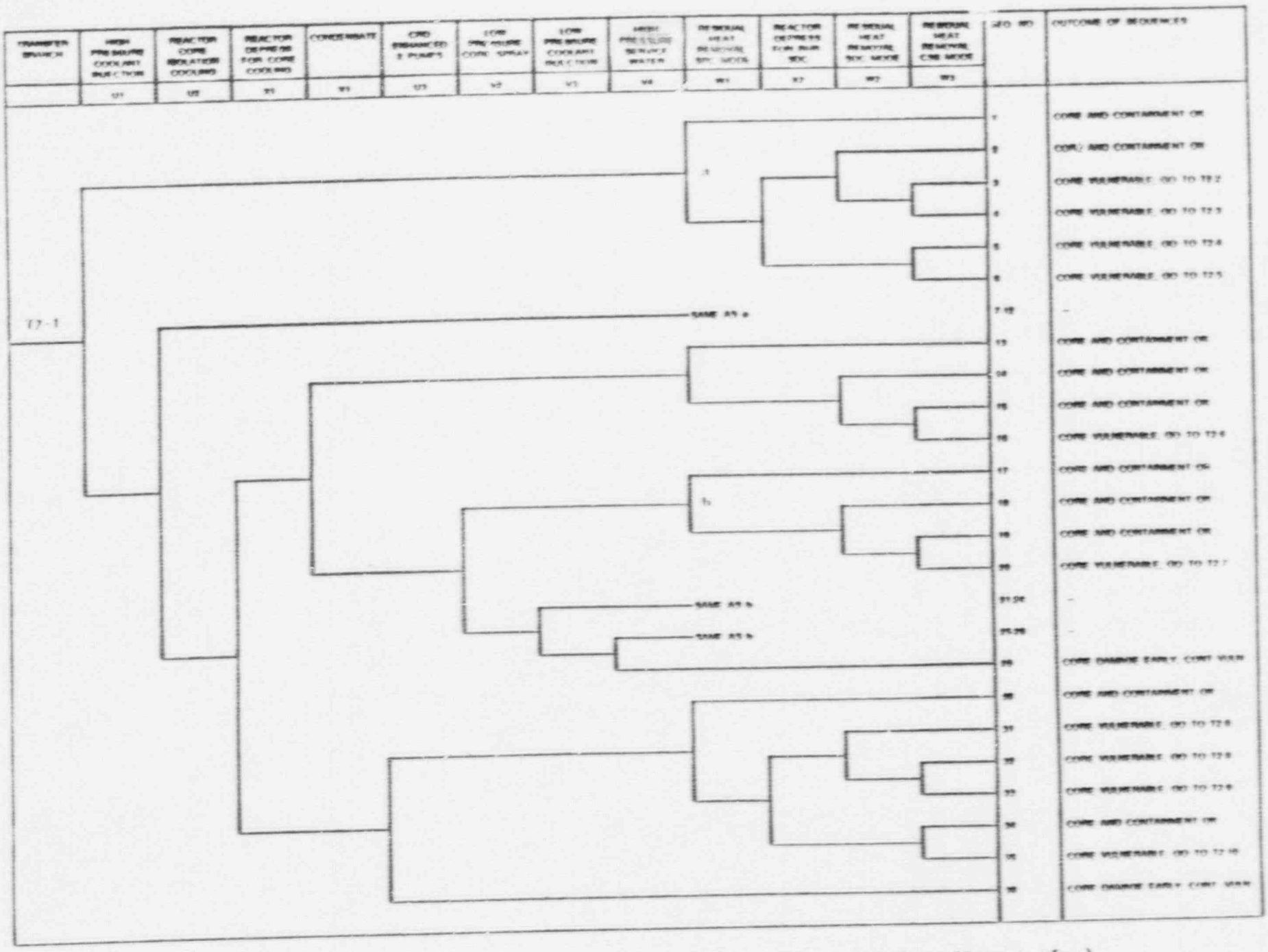

Figure 2.24 Transient Without PCS Initially Available Event Tree (Page 1 of 4)

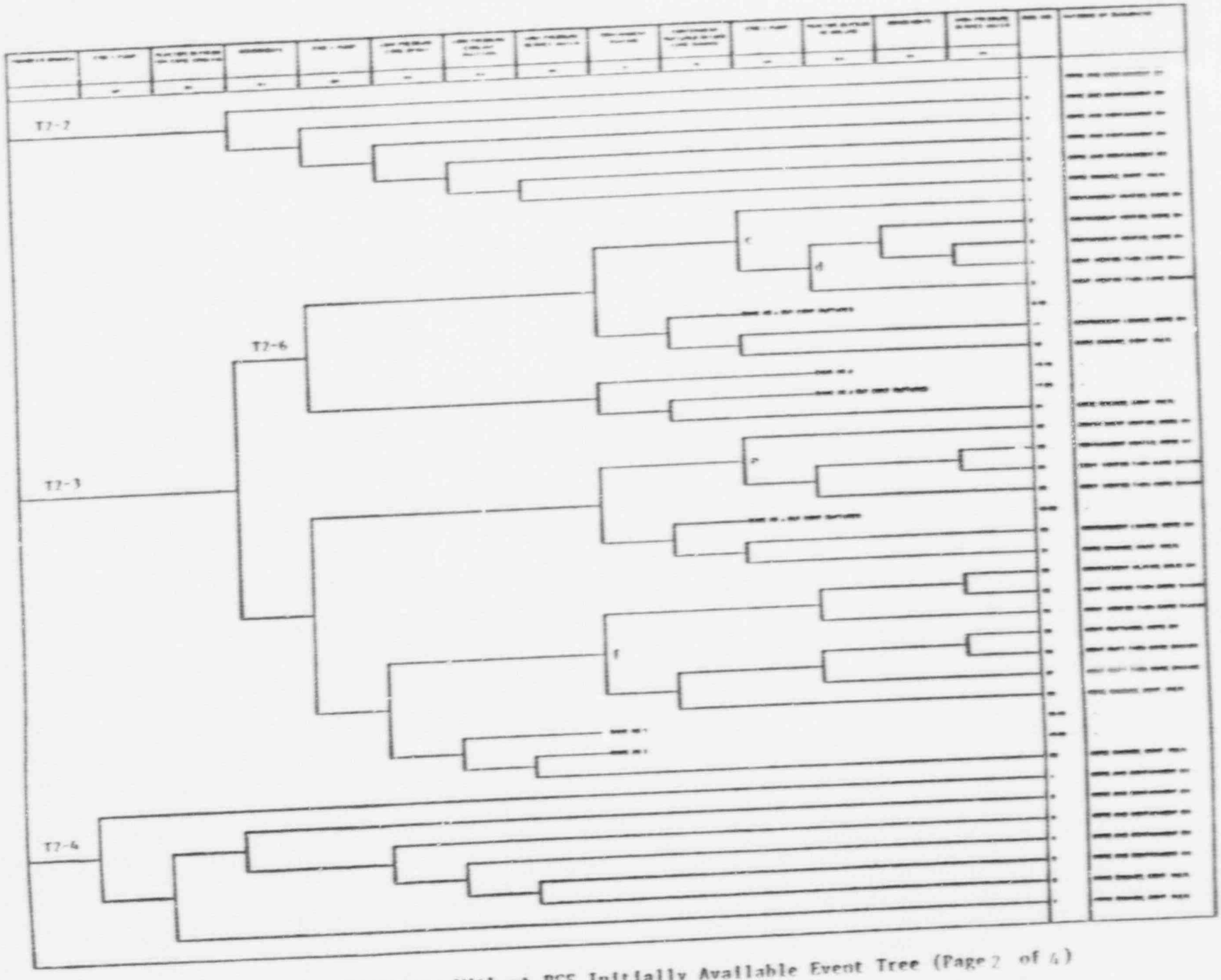

Figure 2.24 Transient Without PCS Initially Available Event Tree (Page 2 of 4)

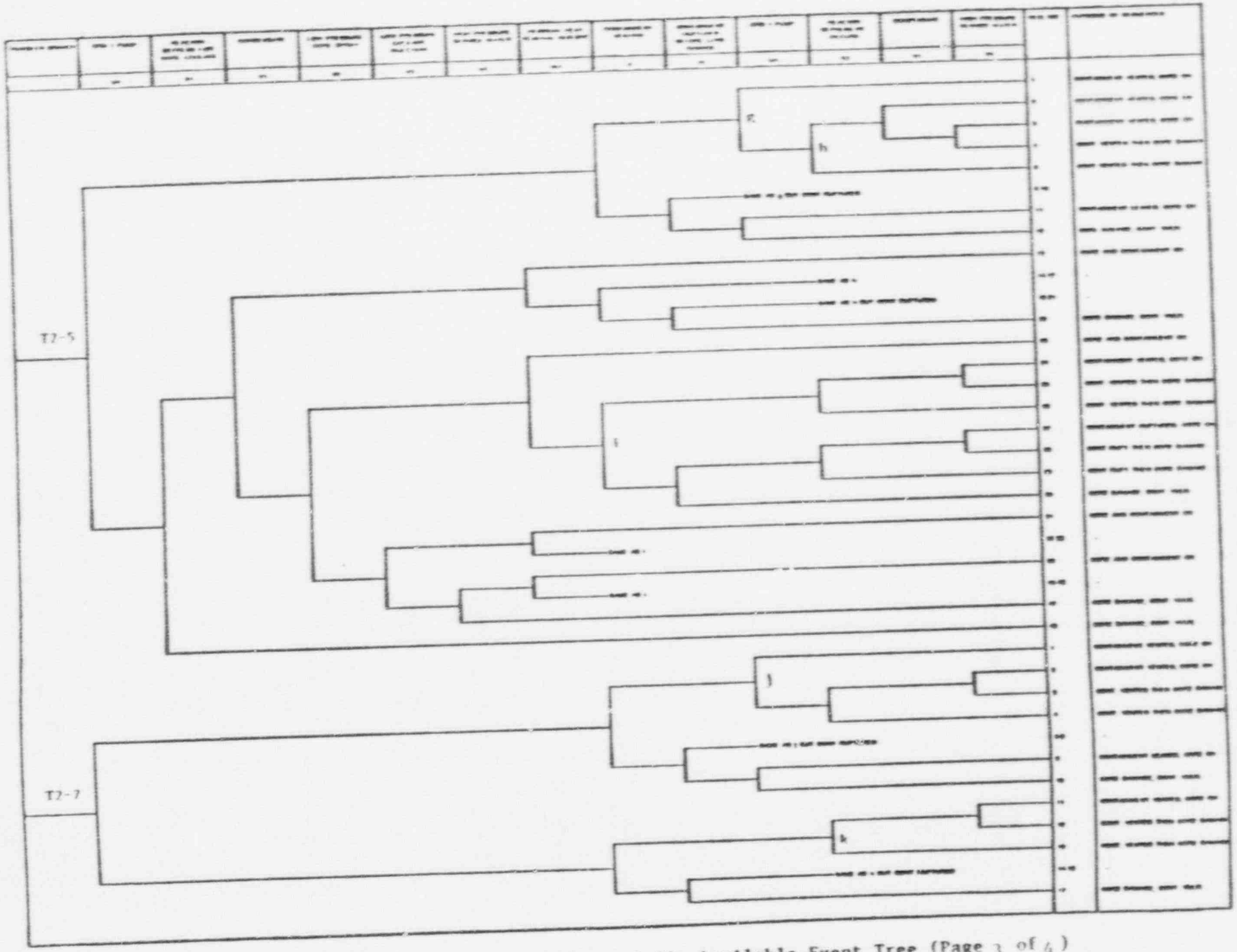

Figure 2.24 Transient Without PCS Initially Available Event Tree (Page 3 of 4)

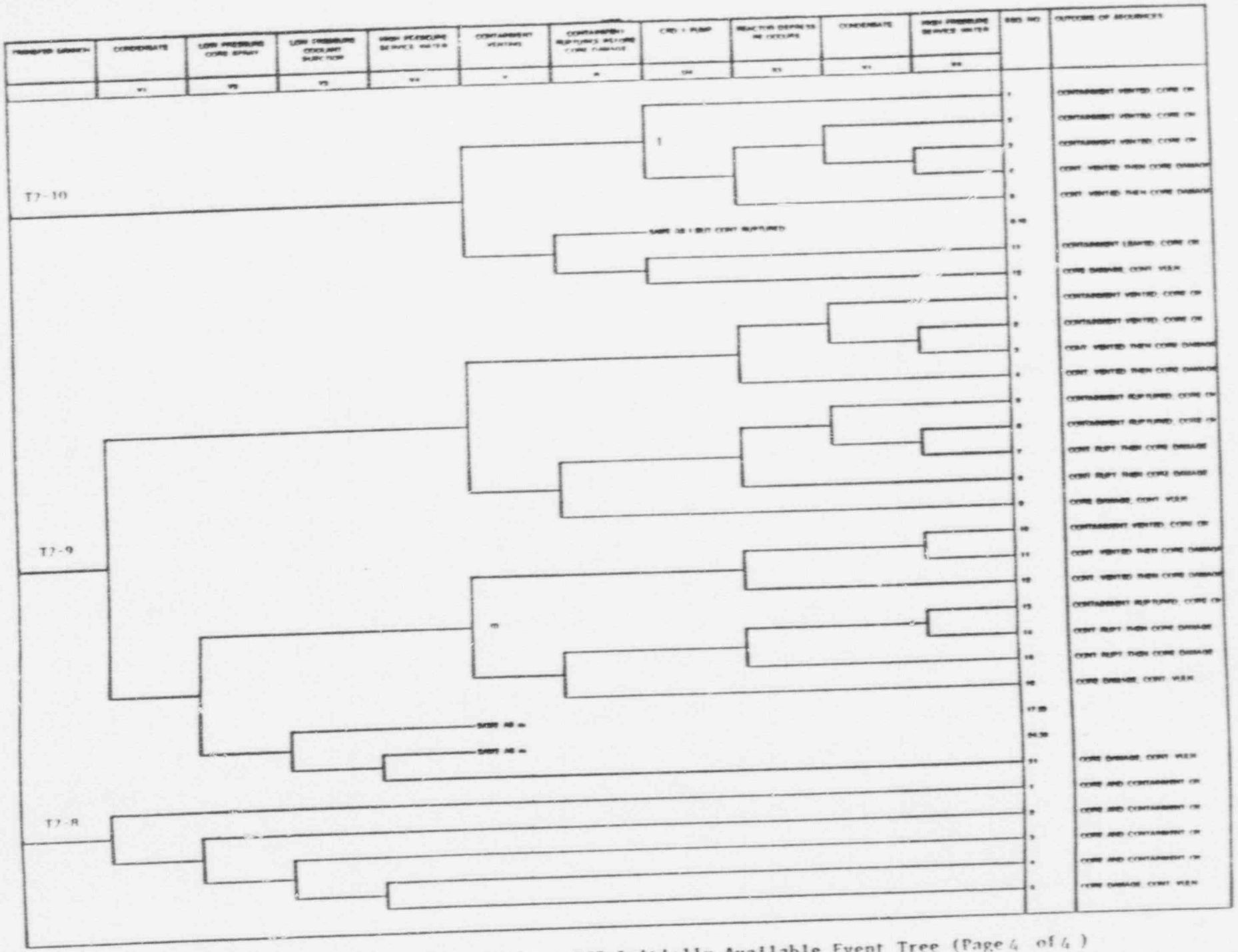

Figure 2.24 Transient Without PCS Initially Available Event Tree (Page 4 of 4)

M: Success or failure of Reactor Coolant System (RCS) overpressure protection (if required) by automatic operation of the SRVs. Success implies prevention of RCS overpressure so as to avoid damage to the primary system.

P: Success or failure associated with reclosing of any SRVs which should open in response to reactor vessel pressure rises throughout the sequence. Success implies reclosure of all valves when vessel pressure drops below the closure setpoints. P1, P2 and P3 refer to the failure of one, two or three or more SRVs to reclose, respectively.

The following descriptions refer to the sequences found in Figure 2.23.

SEQUENCES 1 TO 36 -- T3A*C*LOSP*Q*M*P

A transient occurs with the PCS initially available (T3A) which generates a reactor scram condition and the RPS successfully inserts the rods into the core (/C). Offsite power is maintained (/LOSP1). The PCS fails (Q) and the SRVs properly cycle to control reactor pressure (/M, /P). All sequences then transfer to the T2 tree at the T2-1 branch.

SEQUENCE 37 -- T3A*C*LOSP*Q

Same as initial development of Sequences 1 to 36 except the PCS remains available (/Q), resulting in a safe core and containment.

SEQUENCE 38 -- T3A*C*LOSP*Q*M*P1

Same as initial development of sequences 1 to 36 except one SRV fails to close (P1) and the sequence is transferred to the S2 LOCA tree.

SEQUENCE 39 -- T3*C*LOSP*Q*M*P2

Same as Sequence 38 except two SRVs fail to close (P2) and the sequence is transferred to the S1 LOCA tree.

SEQUENCE 40 -- T3*C*LOSP*Q*M*P3

Same as Sequence 39 except three or more SRVs fail to close (P3) and the sequence is transferred to the A LOCA tree.

SEQUENCE 41 -- T3*C*LOSP*Q*M

Same as initial development of sequences 1 to 36 except the SRVs do not properly open to control reactor pressure (M) and the sequence is not developed further due to low probability.

SEQUENCE 42 -- T3*C*LOSP

A transient occurs with the PCS initially available (T3) and the RPS successfully scrams the reactor (C). Offsite power is not maintained (LOSP) and the sequence is transferred to the T1 tree.

SEQUENCE 43 -- T3*C

A transient occurs with the PCS initially available (T3), the RPS fails to successfully scram the reactor (C), and the sequence is transferred to the ATWS tree. As mentioned previously ATWS sequences were analyzed as part of the internal events analysis.

The following descriptions refer to the Sequences found in Figure 2.24.

SEQUENCES 3-1 to 3-5

Same as Sequence 2 until SDC fails (W2) and CSS is initiated to provide containment overpressure protection (/W3). By the time CSS is initiated, the environment within the containment has failed HPCI. Core coolant is provided by Condensate (/V1), CRD (/U4), LPCS (/V2), LPCI (/V3) or HPSW (/V4), resulting in a safe core and containment.

SEQUENCE 3-6 -- $T2*\bar{C}*\overline{LOSP}*\bar{M}*\bar{P}*\overline{U1}*W1*\overline{X2}*W2*\overline{W3}*V1*U4*V2*V3*V4$

Same as Sequence 3-1 except all low-pressure cooling systems fail (Condensate, CRD (1 pump), LPCS, LPCI, HPSW) which results in core damage in a vulnerable containment.

SEQUENCE 4-1 -- $T2*\bar{C}*\overline{LOSP}*\bar{M}*\bar{P}*\overline{U1}*W1*\overline{X2}*W2*W3*\overline{V1}*\overline{U4}*Y*\overline{U4}'$

Same as Sequence 2 until SDC fails to cool the containment (W2, followed by failure of CSS (W3), resulting in the loss of all containment overpressure protection. HPCI has failed due to the adverse containment environment, and Condensate is initiated for core coolant (/V1). Pressure buildup in containment eventually closes the ADS valves, resulting in a pressure rise in the primary. This higher primary pressure fails the Condensate system, and CRD is initiated to continue core cooling (/U4). Containment venting is performed to relieve high containment pressure (/Y). CRD survives containment venting (/U4') and the core is safe in a vented containment.

SEQUENCES 4-2 to 4-3

Same as Sequence 4-1 except CRD does not survive containment venting. The reactor is depressurized again (/X3) and condensate (/V1) or HPSW (/V4) provide core coolant.

SEQUENCES 4-4 to 4-5

Same as Sequence 4-3 except either reactor depressurization fails (X3), or HPSW fails (V4), which leaves no system available for core coolant, resulting in core damage in a vented containment.

SEQUENCES 4-6 to 4-10

Same as Sequences 4-1 to 4-5 except containment venting fails (Y) and the containment eventually ruptures (/R).

SEQUENCE 4-11 -- $T2*\bar{C}*\overline{LOSP}*\bar{M}*\bar{P}*\overline{U1}*W1*\overline{X2}*W2*W3*\overline{V1}*\overline{U4}*Y*R*\overline{U4}'$

Same as Sequence 4-6 except the containment does not rupture (R) but develops a leak. CRD continues to provide core cooling (/U4').

SEQUENCE 4-12 -- $T2*\bar{C}*\overline{LOSP}*\bar{M}*\bar{P}*\overline{U1}*W1*\overline{X2}*W2*W3*\overline{V1}*\overline{U4}*Y*R*U4'$

Same as Sequence 4-11 except CRD fails (U4') following the leak in containment, leading to core damage in a vulnerable containment.

SEQUENCE 4-13 to 4-16

Same as Sequences 4-2 to 4-5 except CRD fails to initiate (U4) following Condensate failure.

SEQUENCES 4-17 to 4-20

Same as Sequences 4-13 to 4-16 except containment venting fails (Y) and the containment eventually ruptures (/R).

SEQUENCE 4-21 -- $T3*\bar{C}*\overline{LOSP}*\bar{M}*\bar{P}*\overline{U1}*W1*\overline{X2}*W2*W3*\overline{V1}*U4*Y*R$

Same as Sequence 17 until the containment fails to rupture, which inhibits other low-pressure systems from operating, resulting in core damage in a vulnerable containment.

SEQUENCES 4-22 TO 4-23

Same as Sequence 4-1 until Condensate fails to initiate (V1) following containment overpressure protection failure. CRD provides core cooling

(U4) and eventually containment venting is necessary to relieve high containment pressure (Y). CRD survives the venting event, or CRD fails and HPSW continues core cooling, resulting in a safe core in a vented containment.

SEQUENCES 4-24 TO 4-25

Same as Sequence 4-23 except the reactor fails to depressurize (X3) for HPSW, or HPSW fails to initiate (V4), resulting in core damage in a vented containment.

SEQUENCES 4-26 TO 4-29

Same as Sequences 4-22 to 4-25 except containment venting is unsuccessful (Y) and the containment eventually ruptures (R).

SEQUENCE 4-30 -- $T3*\bar{C}*\overline{LOSP}*\bar{M}*\bar{P}*\overline{U1}*W1*\overline{X2}*W2*W3*V1*\overline{U4}*Y*R*\overline{U4}'$

Same as Sequence 4-26 except the containment does not rupture (R) but develops a leak and CRD continues to provide core coolant.

SEQUENCE 4-31 -- $T3*\bar{C}*\overline{LOSP}*\bar{M}*\bar{P}*\overline{U1}*W1*\overline{X2}*W2*W3*V1*\overline{U4}*Y*R*U4'$

Same as Sequence 4-30 except CRD does not survive the containment leak, which leaves no system available for core coolant, resulting in core damage in a vulnerable containment.

SEQUENCE 4-32 -- $T3*\bar{C}*\overline{LOSP}*\bar{M}*\bar{P}*\overline{U1}*W1*\overline{X2}*W2*W3*V1*U4*\overline{V2}*\bar{Y}*\overline{X3}*\overline{V4}$

Same as Sequence 4-22 except CRD does not initiate (U4) after Condensate failure and LPCS is initiated for core coolant (V2). Containment venting is performed to relieve overpressure (Y), which fails LPCS due to low NPSH. The reactor is depressurized again (X3) and HPSW is initiated (V4) to continue core cooling, resulting in a safe core in a vented containment.

SEQUENCES 4-33 TO 4-34

Same as Sequence 4-32 except HPSW fails (V4) or reactor depressurization prior to HPSW initiation fails (X3), resulting in core damage in a vented containment.

SEQUENCES 4-35 TO 4-37

Same as Sequences 4-32 to 4-34 except containment venting fails (Y) and the containment eventually ruptures (R).

SEQUENCE 4-38 -- $T3*\bar{C}*\overline{LOSP}*\bar{M}*\bar{P}*\overline{U1}*W1*\overline{X2}*W2*W3*V1*U4*\overline{V2}*Y*R$

Same as Sequence 4-37 until the containment fails to rupture (R), which forces the SRVs to close thus precluding the use of available core coolant systems, resulting in core damage in a vulnerable containment.

SEQUENCES 4-39 TO 4-45

Same as Sequences 4-32 to 4-38 except prior to containment venting, LPCI provides core coolant (V3) following LPCS failure (V2).

SEQUENCES 4-46 TO 4-52

Same as Sequences 4-39 to 4-45 except prior to containment venting, HPSW provides core coolant (V4) following LPCI failure (V3).

SEQUENCE 4-53 -- $T3*\bar{C}*\overline{LOSP}*\bar{M}*\bar{P}*\overline{U1}*W1*\overline{X2}*W2*W3*V1*U4*V2*V3*V4$

Same as Sequence 4-46 until HPSW fails (V4), which leaves no core coolant system available, resulting in core damage in a vulnerable containment.

SEQUENCES 5-1 TO 5-5

Same as Sequence 2 until depressurization for SDC fails (X2), followed by CS initiation (W3) for containment overpressure protection. HPCI fails prior to CS initiation due to the adverse containment environment. CRD is initiated for core cooling (U4), or, subsequent to CRD failure, the reactor is depressurized (X1) and Condensate (V1), LPCS (V2), LPCI (V3) or HPSW (V4) continues core cooling, resulting in a safe core and containment.

SEQUENCES 5-6 TO 5-7

Same as Sequence 5-2 until reactor depressurization fails (X1) or all low pressure core coolant systems (Condensate, LPCS, LPCI, HPSW) fail to initiate, resulting in core damage in a vulnerable containment.

SEQUENCES 6-1 TO 6-3

Same as Sequence 1 until all containment overpressure protection is lost (SPC, reactor depressurization for SDC, and CS). High suppression pool temperature fails HPCI (U1) and CRD is initiated for core coolant (U4). High containment pressure is relieved by containment venting (Y), and CRD (U4), Condensate (V1) or HPSW (V4) continues core cooling, resulting in a safe core in a vented containment.

SEQUENCES 6-4 TO 6-5

Same as Sequence 6-2 except either reactor depressurization fails (X1) or Condensate (V1) and HPSW (V4) fail, which leaves no system available for core cooling, resulting in core damage in a vented containment.

SEQUENCES 6-6 TO 6-10

Same as Sequences 6-1 to 6-5 except containment venting fails (Y) and the containment eventually ruptures (R).

SEQUENCE 6-11 -- $T3*\bar{C}*\overline{LOSP}*\bar{M}*\bar{P}*\overline{U1}*W1*X2*W3*\overline{U4}*Y*R*\overline{U4}'$

Same as Sequence 6-6 except the containment fails to rupture (R) but develops a leak, resulting in a safe core in a leaking containment.

SEQUENCE 6-12 -- $T3*\bar{C}*\overline{LOSP}*\bar{M}*\bar{P}*\overline{U1}*W1*X2*W3*\overline{U4}*Y*R*U4'$

Same as Sequence 6-11 except CRD does not survive the containment leak (U4), resulting in core damage in a vulnerable containment.

SEQUENCE 6-13 -- $T3*\bar{C}*\overline{LOSP}*\bar{M}*\bar{P}*\overline{U1}*W1*X2*W3*U4*\overline{X1}*\overline{V1}*\overline{W2}$

Same as Sequence 6-1 until CRD fails to initiate (U4) following loss of containment cooling. The reactor is depressurized (X1) and Condensate is initiated for core coolant (V1). Containment overpressure protection is established with SDC (W2), resulting in a safe core and containment.

SEQUENCES 6-14 TO 6-17

Same as Sequences 6-2 to 6-5 except CRD has failed (U4), the reactor is depressurized (X1) and Condensate continues core cooling (V1).

SEQUENCES 6-18 TO 6-21

Same as Sequences 6-14 to 6-17 except containment venting fails (Y) and the containment eventually ruptures (R).

SEQUENCE 6-22 -- $T3*\bar{C}*\overline{LOSP}*\bar{M}*\bar{P}*\overline{U1}*W1*X2*W3*U4*\overline{X1}*\overline{V1}*W2*Y*R$

Same as Sequence 6-13 until SDC fails (W2), followed by failure of containment venting (Y) and containment rupture (R), resulting in core damage in a vulnerable containment.

SEQUENCE 6-23 -- $T3*\bar{C}*\overline{LOSP}*\bar{M}*\bar{P}*\overline{U1}*W1*X2*W3*U4*\overline{X1}*V1*\overline{V2}*\overline{W2}$

Same as Sequence 6-13 except LPCS provides core cooling (V2) following Condensate failure (V1).

SEQUENCE 6-24 -- $T3*\bar{C}*\overline{LOSP}*\bar{M}*\bar{P}*\overline{U1}*W1*X2*W3*U4*\overline{X1}*V1*\overline{V2}*W2*\bar{Y}*\overline{X3}*\overline{V4}$

Same as Sequence 6-23 except SDC fails to provide the containment over-pressure protection (W2) and containment venting is performed (Y), followed by reactor depressurization (X3) and HPSW initiation (V4), resulting in a safe core in a vented containment.

SEQUENCES 6-25 to 6-26

Same as Sequence 6-24 except reactor depressurization prior to HPSW operation is unsuccessful (X3) or HPSW fails to initiate (V4), resulting in core damage in a vented containment.

SEQUENCES 6-27 TO 6-29

Same as Sequences 6-24 to 6-26 except containment venting fails (Y) and the containment eventually ruptures (R).

SEQUENCE 6-30 -- $T3*\bar{C}*\overline{LOSP}*\bar{M}*\bar{P}*\overline{U1}*W1*X2*W3*U4*\overline{X1}*V1*\overline{V2}*W2*Y*R$

Same as Sequence 6-27 except the containment fails to rupture (R), which leaves no system available for core cooling because of forced closure of the SRVs. This results in core damage in a vulnerable containment.

SEQUENCES 6-31 TO 6-38

Same as Sequences 6-23 to 6-30 except LPCI provides core coolant (V3) following failure of LPCS to initiate (V2).

SEQUENCES 6-39 TO 6-46

Same as Sequences 6-31 to 6-38 except HPSW provides core coolant (V4) following failure of LPCI to initiate (V3).

SEQUENCE 6-47 -- $T3*\overline{C}*\overline{LOSP}*\overline{M}*\overline{P}*\overline{U1}*W1*X2*W3*U4*\overline{X1}*V1*V2*V3*V4$

Same as Sequence 6-39 until HPSW fails (V4) and all core cooling is lost, resulting in core damage in a vulnerable containment.

SEQUENCE 6-48 -- $T3*\overline{C}*\overline{LOSP}*\overline{M}*\overline{P}*\overline{U1}*W1*X2*W3*U4*X1$

Same as Sequence 6-13 until depressurization following CRD failure is unsuccessful (X1), precluding the use of low pressure core coolant systems, resulting in core damage in a vulnerable containment.

SEQUENCES 7 TO 12

Same as Sequences 1 to 6 except RCIC provides early high pressure injection to the core (U2) following failure of HPCI to initiate (U1).

SEQUENCES 13 TO 15

A transient occurs with the PCS available (T3) which generates a reactor scram condition and the RFS successfully inserts the rods into the core (C). Offsite power is maintained (LOSP) and the SRVs properly cycle to control reactor pressure (M, P). HPCI (U1) and RCIC (U2) fail to provide high pressure injection, the reactor is depressurized (X1), and Condensate is initiated for core coolant (V1). SPC (W1), SDC (W2) or CS (W3) provide containment overpressure protection, resulting in a safe core and containment.

SEQUENCES 16-1 TO 16-21

Same as Sequences 4-1 to 4-21 except, following failure of HPCI (U1) and RCIC (U2), Condensate provides early core coolant (V1) prior to failure of containment overpressure protection.

SEQUENCES 17 TO 19

Same as Sequences 13 to 15 except LPCS provides early core coolant (V2) following failure of Condensate (V1).

SEQUENCES 20-1 TO 20-2

Same as Sequence 17 until all containment overpressure protection fails (SPC, SDC, CS), which causes increasing containment pressure, eventually closing the SRVs. The primary pressure subsequently increases which fails LPCS, and CRD is initiated to continue core cooling (U4). Containment venting is performed to relieve high containment pressure (Y), and CRD or HPSW continues to cool the core, resulting in a safe core in a vented containment.

SEQUENCES 20-3 TO 20-4

Same as Sequence 20-2 except HPSW fails to initiate (V4) or reactor depressurization prior to HPSW initiation fails (X3), resulting in core damage in a vented containment.

SEQUENCES 20-5 TO 20-8

Same as Sequences 20-1 to 20-4 except containment venting fails (Y) and the containment eventually ruptures (R).

SEQUENCE 20-9 -- $T3*\bar{C}*\overline{LOSP}*\bar{M}*\bar{P}*U1*U2*\overline{X1}*V1*\overline{V2}*W1*W2*W3*\overline{U4}*Y*R*\overline{U4}'$

Same as Sequence 20-5 except the containment fails to rupture and CRD survives, resulting in a safe core in a leaking containment.

SEQUENCE 20-10 -- $T3*\bar{C}*\overline{LOSP}*\bar{M}*\bar{P}*U1*U2*\overline{X1}*V1*\overline{V2}*W1*W2*W3*\overline{U4}*Y*R*U4'$

Same as Sequence 20-9 except CRD does not continue core cooling following the development of a containment leak, resulting in core damage in a leaking containment.

SEQUENCES 20-11 TO 20-13

Same as Sequences 20-2 to 20-4 except CRD fails to initiate (U4) prior to the containment venting event.

SEQUENCES 20-14 TO 20-16

Same as Sequences 20-11 to 20-13 except containment venting fails (Y) and the containment eventually ruptures (R).

SEQUENCE 20-17

Same as Sequence 20-16 except the containment fails to rupture (R), resulting in core damage in a vulnerable containment.

SEQUENCES 21 TO 24

Same as Sequences 17 to 20 except LPCI provides early core coolant (V3) following LPCS failure (V2).

SEQUENCES 25 TO 28

Same as Sequences 21 to 24 except HPSW provides early core coolant (V4) following LPCI failure (V3).

SEQUENCE 29 -- $T3*\bar{C}*\overline{LOSP}*\bar{M}*\bar{P}*U1*U2*\overline{X1}*V1*V2*V3*V4$

Same as Sequence 13 until all low pressure core coolant systems fail (Condensate, LPCS, LPCI, HPSW), which leaves no core coolant system available, resulting in early core damage in a vulnerable containment.

SEQUENCE 30 -- $T3*\bar{C}*\overline{LOSP}*\bar{M}*\bar{P}*U1*U2*X1*\overline{U3}*\overline{W1}$

Same as Sequence 13 until reactor depressurization fails (X1) and CRD is initiated in the enhanced mode (U3) to provide sufficient cooling capacity. SPC is initiated for containment overpressure protection (W1), resulting in a safe core and containment.

SEQUENCES 31-1 TO 31-4

Same as Sequence 30 until SPC fails (W1) and the reactor is depressurized (X2) to initiate SDC (W2). The decreased reactor pressure causes the CRD pump flow to increase, and, considering the CST level is decreasing, the CRD pumps are assumed to fail due to low NPSH. Condensate (V1), LPCS (V2), LPCI (V3) or HPSW (V4) provides core coolant, resulting in a safe core and containment.

SEQUENCE 31-5 -- T3*$\overline{C}$*$\overline{LOSP}$*U1*U2*X1*$\overline{U3}$*W1*$\overline{X2}$*W2*V1*V2*V3*V4

Same as Sequence 31-1 except all low pressure core coolant systems fail (Condensate, LPCS, LPCI, HPSW), resulting in core damage in a vulnerable containment.

SEQUENCES 32-1 TO 32-5

Same as Sequences 31-1 to 31-5 except SDC fails (W2) and CS is initiated for containment overpressure protection (W3).

SEQUENCES 33-1 TO 33-2

Same as Sequence 30 until all containment overpressure protection fails (SPC, SDC, CS), although depressurization for SDC is successful. This depressurization increases the pump flow of CRD which, considering the CST level is continuously decreasing, is assumed to fail the CRD pumps due to low NPSH. Condensate is initiated to continue core cooling (V1). High containment pressure is relieved by containment venting (Y). The reactor is again depressurized (X3) and Condensate (V1) or HPSW (V4) provides core coolant, resulting in a safe core in a vented containment.

SEQUENCES 33-3 TO 33-4

Same as Sequences 33-1 to 33-2 except HPSW fails (V4), or reactor depressurization prior to HPSW initiation fails (X3), resulting in core damage in a vented containment.

SEQUENCES 33-5 TO 33-8

Same as Sequences 33-1 to 33-4 except containment venting fails (Y) and the containment eventually ruptures (R).

SEQUENCE 33-9 -- T3*$\overline{C}$*$\overline{LOSP}$*$\overline{M}$*$\overline{P}$*U1*U2*X1*$\overline{U3}$*W1*$\overline{X2}$*W2*W3*$\overline{V1}$*Y*R

Same as Sequence 33-5 except the containment fails to rupture (R), which leaves no coolant system operable, resulting in core damage in a vulnerable containment.

SEQUENCES 33-10 TO 33-16

Same as Sequences 33-1 to 33-9 except Condensate fails (V1) and LPCS provides core coolant (V2) prior to the containment venting event, which results in two fewer sequences since no success path for Condensate exists subsequent to reactor depressurization (X3).

SEQUENCES 33-17 TO 33-23

Same as Sequences 33-10 to 33-16 except following LPCS failure (V2), LPCI provides core coolant (V3) prior to containment venting.

SEQUENCES 33-24 TO 33-30

Same as Sequences 33-17 to 33-23 except following LPCI failure (V3), HPSW provides core coolant (V4) prior to containment venting.

SEQUENCE 33-31 -- $T3*\overline{C}*\overline{LOSP}*\overline{M}*\overline{P}*U1*U2*X1*\overline{U3}*W1*\overline{X2}*W2*W3*V1*V2*V3*V4$

Same as Sequence 33-1 until Condensate fails (V1), followed by failure of LPCS (V2), LPCI (V3), and HPSW (V4), resulting in core damage in a vulnerable containment.

SEQUENCE 34 -- $T3*\overline{C}*\overline{LOSP}*\overline{M}*\overline{P}*U1*U2*X1*\overline{U3}*W1*X2*\overline{W3}$

Same as Sequence 30 until SPC fails (W1) to provide containment overpressure protection, followed by failure to depressurize the reactor (X2) for SDC. CS is initiated (W3) and CRD continues to function in the enhanced mode, resulting in a safe core and containment.

SEQUENCES 35-1 TO 35-3

Same as Sequence 34 until CS fails (W3), after which all containment overpressure protection is lost, although CRD continues to provide core coolant. High containment pressure is relieved by containment venting (Y), and CRD (U4), Condensate (V1), or HPSW (V4) continues core cooling, resulting in a safe core in a vented containment.

SEQUENCES 35-4 TO 35-5

Same as Sequences 35-3 except HPSW fails (V4) or reactor depressurization prior to HPSW initiation fails (X3), which leaves all core coolant systems unavailable, resulting in core damage in a vented containment.

SEQUENCES 35-6 TO 35-10

Same as Sequences 35-1 to 35-5 except containment venting fails (Y) and the containment eventually ruptures (R).

SEQUENCE 35-11 -- $T3*\bar{C}*\overline{LOSP}*\bar{M}*\bar{P}*U1*U2*X1*\bar{U3}*W1*X2*W3*Y*R*\bar{U4}$

Same as Sequence 35-6 except the containment does not rupture (R) and CRD continues, resulting in a safe core in a vulnerable containment.

SEQUENCE 35-12 -- $T3*\bar{C}*\overline{LOSP}*\bar{M}*\bar{P}*U1*U2*X1*\bar{U3}*W1*X2*W3*Y*R*U4$

Same as Sequence 35-11 except CRD does not operate following the development of a containment leak, resulting in core damage in a vulnerable containment.

SEQUENCE 36 -- $T3*\bar{C}*\overline{LOSP}*\bar{M}*\bar{P}*U1*U2*X1*U3$

Same as Sequence 30 except CRD (two pump mode) fails to initiate to provide core coolant (U3) following failure to depressurize the reactor (X1), which precludes the use of the low pressure core coolant systems, resulting in early core damage in a vulnerable containment.

SEQUENCE 37 -- $T3*\bar{C}*\overline{LOSP}*\bar{M}*P1$

A transient with the PCS available occurs (T3), which generates a reactor scram condition and the RPS successfully inserts the rods into the core (C). Offsite power is maintained (LOSP) and the SRVs properly open to relieve the pressure (M), but one SRV fails to close (P1) and the sequence is transferred to the S2 LOCA tree.

SEQUENCE 38 -- $T3*\bar{C}*\overline{LOSP}*\bar{M}*P2$

Same as Sequence 37 except two SRVs fail to close and the sequence is transferred to the S1 LOCA tree.

SEQUENCE 39 -- $T3*\bar{C}*\overline{LOSP}*\bar{M}*P3$

Same as Sequence 38 except three or more SRVs fail to close and the sequence is transferred to the A LOCA tree.

SEQUENCE 40 -- $T3*\bar{C}*\overline{LOSP}*M$

A transient occurs with PCS available (T3) which generates a reactor scram condition and the RPS successfully inserts the rods (C). Offsite power is maintained (LOSP). The SRVs fail to open to control reactor pressure (M) and the sequence is not developed further due to low probability.

SEQUENCE 41 -- T3*$\overline{C}$*LOSP

Same as Sequence 40 except offsite power is not maintained (LOSP) and the sequence is transferred to the T1 tree.

SEQUENCE 42 -- T3*C

Same as Sequence 40 except the RPS fails to scram the reactor, and the sequence is transferred to the ATWS tree.

2.3.8 Event Tree Nomenclature

Table 2.1 contains a summary of the nomenclature used to identify the systems on the event trees.

Table 2.1

Event Tree Nomenclature

ARI	-	Failure of the Alternate Rod Insertion System
B	-	Failure of all ac power (station blackout)
C	-	Failure of the Reactor Protection System (RPS)
C1	-	Failure of RPS and manual scram
I	-	Failure to inhibit the ADS system
L	-	Failure of operator to isolate S3 "leak"
LOSP,LOSP1	-	Failure to maintain offsite power; Different Designations for this Event are for Different Frequencies
M	-	Failure of Safety Relief Valves (SRVs) to open
P	-	Failure of SRVs to close
P1,P2,P3	-	Failure of one, two or three SRVs to reclose
Q,Q1,Q2	-	Failure of the Power Conversion System (PCS), different designations for this event are for different frequencies
ROD	-	Failure to manually insert the control rods
RPSM	-	Failure of the mechanical RPS
RPSE	-	Failure of the electrical RPS
RPT	-	Failure to trip the recirculation pumps
SCRM	-	Failure to manually scram the reactor
SLC	-	Failure of the Standby Liquid Control System
U1	-	Failure of the High Pressure Coolant Injection (HPCI) system
U1'	-	Failure of HPCI without ventilation
U2	-	Failure of the Reactor Core Isolation Cooling (RCIC) system
U2'	-	Failure of RCIC without recirculation
U3	-	Failure of the Control Rod Drive (CRD) system (2 pump mode)
U4	-	Failure of the Control Rod Drive (CRD) system (1 pump mode)
U4'	-	Failure of CRD to survive containment venting
V1	-	Failure of the Condensate system
V1'	-	Failure of Condensate to survive containment venting
V2	-	Failure of the Low Pressure Core Spray (LPCS) system
V3	-	Failure of the Low Pressure Coolant Injection (LPCI) system
V4	-	Failure of the High Pressure Service Water (HPSW) system as an injection source to the reactor
V4'	-	Failure of HPSW (injection source) to survive containment venting
R	-	Rupture of the containment
W1	-	Failure of the Suppression Pool Cooling (SPC) mode of RHR
W2	-	Failure of the Shutdown Cooling (SDC) mode of the RHR
W3	-	Failure of the Containment Spray (CS) mode of the RHR
X1	-	Failure to depressurize the primary system via SRVs or the Automatic Depressurization System (ADS)
X2	-	Failure to depressurize the primary system to allow SDC to operate
X3	-	Failure to depressurize the primary system subsequent to an initial primary system depressurization
Y	-	Failure of Primary Containment Venting System (including makeup to the pool as required)

3.0 SCOPING QUANTIFICATION STUDY

A scoping quantification study was performed for the Peach Bottom site to determine which external events should be included in the detailed PRA study. This scoping study considered all possible external hazards at the site except for seismic and fire events, since these two events were already scheduled for a detailed risk analysis. The PRA Procedures Guide (Ref. 1) was used as a guideline for systematic identification of all possible external events at the site. Next, an initial screening process was carried out to eliminate as many events as possible from the list. For this purpose, a set of screening criteria was developed and then each external event was examined for possible elimination based on these criteria. After the initial screening process was completed, it was found that the following events could not be screened out based on the general screening criteria:

a. Aircraft Impact
b. External Flooding
c. Extreme Winds and Tornados
d. Industrial or Military Facility Accident
e. Release of Chemicals from On-Site Storage
f. Transportation Accidents
g. Turbine Generated Missiles
h. Internal Flooding

A bounding analysis was done for these events. The degree of sophistication in the bounding analysis for each event depended on whether the event could be eliminated based on only a hazard analysis or whether a complete analysis including hazard determination, fragility evaluation and plant response analysis was required.

This chapter presents the screening and bounding analyses performed for the external hazards at the Peach Bottom site. Section 3.1 is a general description of the plant and its location. Section 3.2 deals with the identification and screening of external events for this site. The external events which required a bounding analysis are discussed in Section 3.3. Section 3.4 summarizes the results of the screening study.

3.1 General Description

3.1.1 The Site

The Peach Bottom Atomic Power Station occupies 620 acres in York and Lancaster counties of southeastern Pennsylvania, 2.5 miles north of the Maryland-Pennsylvania state line. The site is in the Piedmont Physiographic Province of the Appalachian Highlands, 14 miles from the Chesapeake Bay. The plant is located on the western shore of Conowingo Pond, formed by the backwater of Conowingo dam, 9 miles downstream on the Susquehanna River. There is another dam, Holtwood, 6 miles upstream of

the site. There are a number of other dams on the 422-mile-long river from its source in Lake Otsego, New York, to the mouth of the Chesapeake. The Conowingo Pond is surrounded by steep sloping hills up to 300 ft above plant grade (+116.7 ft MSL). The rough hilly terrain continues for 12 to 15 miles from the site and the area is mostly wooded.

The plant is 38 miles N-NE of Baltimore, Maryland, and 63 miles W-SW of Philadelphia, Pennsylvania. Access to the site is from Maryland Route 623, Maryland Route 165 and Pennsylvania Route 74 through Ailston-Peach Bottom link, an all weather bituminous road. There are no other major public roads through the site or near the site. The Maryland and Pennsylvania railroad connects the site by a line from the west.

The land use in the counties surrounding the site is predominantly agricultural with only a few industries, mostly associated with food processing, textiles or tobacco. As the distance from the plant increases, the agricultural activities decrease with concomitant increase in population and industrial activities. As discussed in the FSAR, the estimated 1970 population within 5 miles of the site was less than 6,000, with most of the people concentrated further than 3 miles from the plant. Based on the past population trends, the total population in the 5 mile zone is not likely to change to any significant degree.

The site grade is at 116 feet relative to the Conowingo Datum (C.D.), which is equivalent to 116.7 feet above mean sea level (MSL). The normal elevation of Conowingo Pond is elevation 108.5 feet C.D. but it can vary down to 98.5 feet C.D. Peach Bottom experiences winter temperatures that can go as low as 5°F and summer temperatures reach above 90°F. Severe ice storms are frequent, on an average of once every three years. Winds at the site are considered to be moderate. An analysis of the Philadelphia area records shows that wind speeds above 75 mph are not frequent. A total of 22 tornadoes were observed in a 45 year record. The site is too far inland to be affected by the full force of hurricanes. The annual precipitation has been observed to vary from a minimum of 22.9 inches to a maximum of 55.9 inches. The average annual precipitation recorded at the site from a 25 year record is 45.44 inches.

The Plant

Peach Bottom Units 2 and 3 are twin BWR units, each rated at 1065 MWe. (Unit 1 is a 40 MW decommissioned HTGR and is now in mothball status.) The reactor and generator for both units 2 and 3 were supplied by General Electric Corporation. Bechtel Corp. acted both as Architect/Engineer and Constructor. The plants began commercial operation in 1974. Units 2 and 3 are located approximately 300 feet from the shoreline of Conowingo Pond. In addition to the reactor units, three transmission substations (two 500 kV and one 220 kV) are present at the site.

Each reactor building is a reinforced concrete structure from the foundation (91.6 feet C.D.) up to the refueling floor level (234 feet C.D.). A structural steel framework above this level is covered with metal siding and decking. The reactor building is 150 feet x 150 feet in

plan below elevation 135 feet and 150 feet x 120 feet above this elevation. The foundation supporting both the reactor and primary containment is a monolithic concrete mat on sound rock. Other major structures at the site are the radwaste building, the turbine building and various auxiliary buildings such as a diesel generator building, the stack, the administration building and the water treatment building. Most of the buildings in the complex are founded on solid rock except certain auxiliary buildings (e.g., diesel generator building) which are supported on piles.

The reactor building is a seismic Class I structure designed for a maximum credible earthquake with 0.12 g horizontal peak ground acceleration. Other Class I structures include the turbine building, the control room area (including the switchgear and cable spreading rooms), the radwaste building and the reactor auxiliary bay, the diesel generator building, the circulating water pump structure and the structure housing the service water traveling screens.

The concrete portion of the reactor building and the steel frame above it is designed to withstand full tornado pressure corresponding to 300 mph wind and 3 psi internal pressure. The roof and metal siding of this building is considered expendable since the equipment required for safe shutdown is located in the concrete portion. Wall thicknesses ranging from 2 feet to 3 feet prevent missiles due to tornadoes from penetrating inside the critical areas. Critical portions of reactor auxiliary building, control room area, circulating water pump structure and service water traveling screen structure are also designed for the full force of tornado missiles.

Site Visit

The initial site visit was conducted in March, 1987. The purpose of the site visit was to confirm the information taken from the FSAR which was being used in the scoping quantification study and to collect any new information regarding possible changes in the plant or site conditions which might influence the external hazard screening process. The site visit included a tour of the plant structures as well as a survey of the plant boundary and surrounding areas. Findings from the site visit were:

a. No major changes or deviations from the information in the Peach Bottom FSAR (which could affect the screening process) were found, either for the plant or its surroundings.

b. A survey of the structures in Peach Bottom revealed that a river flood would have to reach elevation 135 feet to overtop the circulating water pump house. However, it was also noted that the pumps are further protected by the steel plates over them.

c. A visual survey of the objects in the plant boundary with a potential to generate tornado missiles was conducted. It confirmed that the likely number of missiles at the site is less than the number which was used in the tornado missile simulation study (Ref. 2) utilized in the bounding analysis process (as discussed in Section 3.3.3).

d. The site visit confirmed that there are no new industries, major airports or pipelines in the vicinity of the site.

3.2 Initial Screening of External Events

An extensive review of information on the site region and plant design was made to identify all external events to be considered. The data in the Peach Bottom FSAR as well as other data obtained from the utility, and information gathered in the site visit were reviewed for this purpose.

A set of screening criteria was utilized to identify those external hazards which could be screened from further consideration based on very general considerations, as described in Section 1.3.2. These criteria, based on those in the PRA Procedures Guide (Ref. 1), are listed again below:

An external event can be excluded from further consideration if:

Criterion 1 The event is of equal or lesser damage potential than the events for which the plant has been designed. This requires an evaluation of plant design bases in order to estimate the resistance of plant structures and systems to a particular external event.

Criterion 2 The event has a significantly lower mean frequency of occurrence than other events with similar uncertainties and could not result in worse consequences than those events.

Criterion 3 The event cannot occur close enough to the plant to affect it. This is also a function of the magnitude of the event.

Criterion 4 The event is included in the definition of another event.

Criterion 5 The event is slow in developing and there is sufficient time to eliminate the source of the threat or to provide an adequate response.

The use of these criteria minimizes the possibility of omitting any significant risk contributors while at the same time reducing the amount of detailed bounding analysis required.

Table 3.1 is a listing of external hazards examined in this study, based on the augmentation of Table 10-1 of the PRA Procedures Guide (Ref. 1). For each external hazard, the applicable screening criteria and a brief description of the basis for the screening (if any) is included on this table.

Table 3.1

Preliminary Screening of External Events for
Peach Bottom Atomic Power Station

Event	Applicable Screening Criteria	Remarks
Aircraft Impact	None	Performed Bounding Analysis.
Avalanche	3	Topography is such that no avalanche is possible.
Biological Events	5	The only biological event which may affect the safety of the plant is fish in the pond, i.e., fish may block flow of water in the intake structure. This event is not considered because there would be adequate warning.
Coastal Erosion	3	Peach Bottom is located on the bank of Susquehanna River, 14 miles upstream of the river mouth where it joins the Chesapeake Bay. There are several flood control dams upstream and downstream of the plant. Therefore, erosion is not a significant concern.
Dam Failure	4	Included in the consideration of external flooding.
Drought	1,5	The flow in the river is well regulated and there would be adequate warning so that remedial action could be taken.
External Flooding	None	Performed Bounding Analysis.
Extreme Winds and Tornadoes	None	Performed Bounding Analysis.

Table 3.1

Preliminary Screening of External Events for
Peach Bottom Atomic Power Station
(Continued)

Event	Applicable Screening Criteria	Remarks
Fog	1	Fog can affect the frequency of occurrence of other hazards such as highway accidents or aircraft landing and take-off accidents. The effects of fog on highway, railway, or barge accidents are implicitly taken into account by assuming a worst possible transportation accident near the site. The effect of fog on aircraft landing or take-off accident rates may be neglected because there are no airports within 5 miles of the site, i.e., only in-flight accidents contribute to aircraft hazard at the site.
Forest Fire	1,3	There are no forests in the immediate vicinity of the plant; i.e., the site has been cleared.
Frost	1	Loads induced on structures due to frost are much lower than snow and ice loads, i.e., frost loads can be safely neglected in the plant hazard analysis.
Hail	1	Hail is less damaging than the tornado missiles. Therefore, hail is not considered further in the scoping study.
Tide, High Lake Level or High River Stage	4,5	Included under external flooding.

Table 3.1

Preliminary Screening of External Events for
Peach Bottom Atomic Power Station
(Continued)

Event	Applicable Screening Criteria	Remarks
High Summer Temperature	1	As mentioned under drought, it is possible to safely shut down the plant because of sufficient warning time. Therefore, high temperatures on record are indirectly included under drought conditions.
Hurricane	1,4	The effects are included under flooding and tornado events.
Ice Cover	1, 4	Plant structures and systems are designed for the ice effects.
Industrial or Military Facility Accident	None	Performed Bounding Analysis.
Internal Flooding	None	Performed Bounding Analysis.
Landslide	3	Detailed stability analyses were performed at the site preparation stage to confirm the safety of the slopes in the west and north sides of the site; hence, no landslide is expected.
Lightning	1	Plants are usually designed for lightning.
Low Lake or River Water Level	1,5	The condition should not occur because of the regulated flow in the river; also, there will be adequate warning so that remedial action could be taken.
Low Winter Temperature	1,5	Thermal stresses and embrittlement are insignificant. These are covered by design codes and standards for plant design. Generally, there is adequate warning about ice on the ultimate heat sink (i.e., river) so that remedial action could be taken.

Table 3.1

Preliminary Screening of External Events for
Peach Bottom Atomic Power Station
(Continued)

Event	Applicable Screening Criteria	Remarks
Meteorite	2	This event has a very low probability of occurrence. A study by Solomon (Ref. 3) showed that the probability of a meteorite impacting any nuclear power plant in the U.S. is negligible, and therefore meteorites need not be considered.
Pipeline Accident	3	There are no pipelines in the vicinity of the Peach Bottom site.
Intense Precipitation	4	Included under external flooding.
Release of chemicals From On-Site Storage	None	Performed Bounding Analysis.
River Diversion	3	The river is well regulated.
Sand Storm	3	This is not relevant for this region.
Seiche	4	Included under external flooding.
Seismic Activity	None	Included in External Event Analysis.
Snow	1	Roofs of all structures are designed for a snow load of 30 psf. Load combinations other than those involving snow load, however, govern the design. Therefore, snow loads can be excluded from further study.
Soil Shrink-Swell Consolidation	1	Plant structures are all designed for the effects of consolidation. Such effects occur over a long period and do not pose a hazard during plant operation, i.e., the plant can be safely shut down if needed.

Table 3.1

Preliminary Screening of External Events for
Peach Bottom Atomic Power Station
(Continued)

Event	Applicable Screening Criteria	Remarks
Storm Surge	4	Included under External Flooding.
Transportation Accidents	None	Performed Bounding Analysis.
Tsunami	2,3	Peach Bottom is inland; tsunamis are rare on the East coast.
Toxic Gas	4	Included under transportation accidents, on-site chemical release, and industrial and military facility accidents.
Turbine-Generated Missiles	None	Performed Bounding Analysis.
Volcanic Activity	3	The site is not close to any active volcanos.
Waves	3	The site is located on Conowingo Pond formed in the river by the Conowingo Dam; it is not subjected to severe wave action.

In summary, the findings of the preliminary screening are as that, aside from seismic and fire events, which have already been included in the detailed external event risk analyses, the following events were identified for a bounding study:

a. Aircraft Impact
b. External Flooding
c. Extreme Winds and Tornados
d. Industrial or Military Facility Accident
e. Release of Chemicals from On-Site Storage
f. Transportation Accidents
g. Turbine Generated Missiles
h. Internal Flooding

The bounding analyses performed for these events are discussed in Section 3.3.

3.3 Bounding Analyses

The bounding analyses for the external events which could not be screened out by the general criteria as described above are given in this section. The probabilistic models used in these bounding analyses integrate the randomness and uncertainty associated with loads, response analysis, and capacities to predict the annual frequency of the plant damage from conservative models. If the mean frequency computed with a conservative model is predicted to be sufficiently low (e.g., less than 10^{-6}/year), the external event may be eliminated from further consideration. The bounding analyses thus provide a second screening of the external hazards, allowing additional hazards to be deleted from further consideration, and identifying those remaining external events which need to be analyzed in detail as part of the PRA.

In addition to calculating and screening on a best estimate frequency of core damage, the uncertainties in hazard and component fragilities may be used to find the high confidence (95 percent) bounds on the frequency of core damage. However, such an uncertainty analysis is required only if the best estimate of the core damage frequency of the external event leads to a value which is close to the (usual) mean rejection frequency of 10^{-6}/year.

Often, simplifications in the above analyses are introduced. As an example, in case of aircraft impact, back-face (inside) scabbing of the exterior barrier walls of safety-related structures can be assumed to result in core damage even though, actually, a suitable combination of component failures is necessary to lead to this damage state. However, if the resulting frequency of core damage computed with the conservative model is sufficiently small, no further consideration is required.

In addition, for some external events, it is possible to perform a bounding analysis without performing a structural response analysis. In effect, one shows that the frequency of exceeding the design loads is

very small, and thus infers that the hazard can be neglected due to the conservatism in the design process. These, and other simplifications are utilized as appropriate in the following bounding analyses.

3.3.1 Aircraft Impact

As assessment of the risk from aircraft crashes into the Peach Bottom structures is presented in this section. The analysis is based on plant location relative to nearby airports and airways. It was concluded that plant damage due to aircraft crash is not a significant event for Peach Bottom.

One approach to bounding the risk due to aircraft crashes is based on the US NRC Standard Review Plan. According to this Standard Review Plan, the probability of aircraft accide s resulting in unacceptable radiological consequence is less than approximately 10^{-7} per year if all the following conditions are met:

a. The plant-to-airport distance D is between 5 and 10 statute miles, and the projected annual numbers of flight operations is less than 500 D^2, or the plant-to-airport distance D is greater than 10 statute miles, and the projected number of flight operations is less than 1,000 D^2;

b. The plant is at least 5 statute miles from the edge of military training routes, including low-level training routes, except for those associated with a usage greater than 1,000 flights per year, or where activities (such as practice bombing) may create an unusual stress situation.

c. The plant is at least 2 statute miles beyond the nearest edge of a federal airway, holding pattern, or approach pattern.

The Standard Review Plan requires that a detailed review of aircraft impact risk be performed if the above requirements are not met or if sufficiently hazardous military activities are identified.

In the present case, there are four airports within 10 statute miles of the Peach Bottom Station (Table 3.2) two intended for public but limited use, and two are private, restricted. There is also reported to be a small private airport in Corryville. None of these has any regular traffic. There are no military airports within 10 miles of the site. Therefore, the requirements regarding the location of airports of the Standard Review Plan are satisfied.

However, the requirements with respect to location relative to FAA controlled airways were not met. In fact, the centerlines of two airways (Victor 3 and Victor 93E) intersect within one mile of the site. This Norris intersection is used for change of airways by aircraft using a radio navigation facility. The airways extend about 4 miles on either

Table 3.2

Airports Within 10 Miles of the
Peach Bottom Atomic Power Station

Airport	Tanglewood	Conowingo	Tuff	Delta
Distance (statute mi)	6 1/2	7	4	4
Direction (true north)	36°	140°	272°	226°
Elevation (ft)	680	380	465	540
Type	Public Use	Public Use	Private, Restricted	Private, Restricted

side of their centerlines and carry commercial and general aviation traffic between 3,000 feet and 18,000 ft. The air traffic on Victor 3 passes directly above the station in an E-NE and W-SW direction. All of the traffic on these airways is expected to conform to the Federal Aviation Administration regulations concerning the minimum low altitudes, i.e., all aircraft must fly at least 1,000 feet above the tallest object in the corridor.

Aircraft flying at 9,000 feet and below are normally single- and twin-engine light aircraft whereas those flying above this level are mostly three- and four-engine heavy commercial jet aircraft. The annual inflight crash rates for different types of aircraft are given in Table 3.3. The crash rates for commercial jets is very low compared to single-engine and twin-engine aircraft. As there are no data on the number of flights in these airways for different types of aircraft, a bounding analysis is performed to show that aircraft impact is unlikely or if it occurs, is unlikely to lead to core melt.

Capacities of Category I structures against aircraft impact are determined by using the formulas which have been developed for impact of non-deformable missiles on reinforced concrete walls and panels. It can be assumed that the engine and part of the aircraft body represent the non-deformable missile. Since the plant is designed for a spectrum of tornado-generated missiles, the walls provide some structural resistance against aircraft impact. Typically, if a plant has been designed against an automobile-missile impact as a result of tornadoes, it can withstand a single-engine aircraft impact. Based on formulas which have been developed from full scale and model impact tests, any reinforced concrete

Table 3.3

Annual In Flight Crash Rates (Crash/mile)

Aircraft Type	5th Percentile	50th Percentile	95th Percentile
Single-Engine	1.91×10^{-7}	2.27×10^{-7}	2.70×10^{-7}
Twin-Engine	5.54×10^{-8}	7.14×10^{-8}	9.20×10^{-8}
Commercial	6.95×10^{-10}	1.39×10^{-9}	2.76×10^{-9}

structure with walls at least 18 in. thick may be excluded from the impact analysis for single-engine aircraft.

This criterion will exclude all of the safety-related buildings, e.g., the reactor building which has 2 feet to 3 feet thick walls. A single-engine aircraft could cause damage to the reactor building if it crashes into the metal superstructure above elevation 234 feet C.D. However, there is no safety-related equipment in this area and the slab thickness (at elevation 234 ft) will ensure against penetration. The main control room complex is located well inside the turbine building and the event of crashing aircraft reaching the control room complex after traversing the turbine building is improbable. In addition, the control room itself is designed for tornado missiles. The crash of an aircraft may sometimes damage the outdoor equipment but such impacts do not directly lead to a core melt. As an example, the crash might damage the two service water pumps in the cribhouse. The loss of the normal service water system is not a significant contributor since an additional redundant source (in the emergency cooling tower) is located on the hill adjacent to the main plant structure. Thus, any risk due to light airplane crash at Peach Bottom can be discounted.

For commercial aircraft, in order to have an acceptable bounding frequency of 10^{-6}/year, the minimum number of flights likely to achieve this value must be shown to be much larger than the likely traffic on this route. The probability per year, P, of an aircraft crash into the plant from an aviation corridor passing near the site is given by

$$P = C\ N\ A/W$$

where

- P = Probability of aircraft strike/year
- C = Inflight crash rate per mile for a given type of aircraft using the airway
- N = Number of movements or flights per year of aircraft along a given flight pattern
- A = Effective target area of critical portions of the plant
- W = Width of airway

The effective target area A is computed based on the base area of the Units 2 and 3, plus the radwaste building and additional areas accounting for the possibility of skidding of an aircraft after hitting the ground, as well as taking into consideration structures in the shadow areas of structures. The numerical values assumed here allow for an aircraft hitting up to 100 feet short of a structure and sliding into it. The exposed area is calculated by assuming a 30° angle of attack for the approaching aircraft. Units 2 and 3 are the largest structures, and they shield a large part of adjacent structures. Thus, for example, the shielded structures are protected against any aircraft hitting the reactor dome. The area is calculated for four different directions of aircraft travel and the maximum value is chosen. Due to the complexity of the site plan, such area computations necessarily involve some approximations. The target area is conservatively estimated to be 7.7×10^{-3} sq. miles which is increased to 9.0×10^{-3} to account for other small structures on the site. The number of flights/year, corresponding to a bounding probability value of 1×10^{-6}/year, is thus estimated to be 639,488, which is equivalent to 1,752 flights/day. As the data on the number of actual flights through the corridor is not available, some conservative arguments, as explained below, are made to show that this number can be considered to be much larger than the possible number of flights in this flight corridor.

The Federal Aviation Administration (FAA), which operates and maintains the National Airspace System, allocates and regulates the use of airspace. It designates air traffic hubs, which denote the cities and standard metropolitan areas requiring aviation services. These hubs overwhelmingly dominate the traffic in the United States and are classified as large, medium or small. Philadelphia is one such large hub near the Peach Bottom site.

The number of aircraft handled at any hub is officially designated as the number of air operations at the hub plus IFR overflights. The number of air operations is two times the number of aircraft departures, assuming that the number of departures is equal to the number of landings. IFR overflights are those flights originating outside the local Air Route Traffic Control Center and passing through the area without landing. Conservatively, we assume that Philadelphia results are also valid for Peach Bottom and the total number of aircraft handled there is equal to the number passing over the Peach Bottom site. The statistics (FAA Statistical Handbook of Aviation, Ref. 4) for the Philadelphia hub show that 122,002 air operations were performed there in one year.

As there is no local data for IFR overflights it is conservatively computed from national data. For the United States, there are seven aviation zones, and a total of 953,251 overflights/year were handled for air carriers in these zones. Three of these zones cover the Eastern Seaboard. Therefore, assume that 3/7 of the overflights/year belong to Eastern Seaboard and all these flights pass over the Peach Bottom site. This gives the total traffic at this hub to be approximately 1,453 flights/day, which is still lower than the value of 1,752 flights/day required to reach the probability of core damage due to aircraft impact at the 10^{-6} level.

3.3.2 External Flooding

The Peach Bottom Atomic Power Station is located on the west side of the Conowingo Reservoir which is formed in the Susquehanna River by the Conowingo Dam, located 9 miles downstream. Holtwood dam, located about 6 miles upstream from the Peach Bottom site, forms the upper limit of Conowingo Reservoir. The Muddy Run Pumped Storage Generating Plant is located about 4 miles upstream on a tributary entering the reservoir on the eastern side.

The Susquehanna River and its tributaries form the major drainage system of southeastern Pennsylvania. The total drainage area is 27,500 square miles of which 6,270 square miles are in south central New York, 20,950 square miles in central Pennsylvania, and 280 square miles in northeastern Maryland, with 27,000 square miles above the Peach Bottom site. The flow in the Susquehanna River is regulated by a series of dams upstream and downstream of the plant site. Therefore, precipitation and snow melting, failure of the Holtwood dam and wave run-up are the main sources of external flooding at the site.

The observed peak flows on the Susquehanna River at Harrisburg from 96 observation years have ranged from a minimum of 127,000 cfs to a maximum of 1,020,000 cfs. The maximum recorded flood occurred on June 24, 1972, when a peak flow of 1,020,000 cfs was measured. The second largest flood occurred in 1936 with a discharge of 740,000 cfs. A chronological listing of other known floods at Harrisburg is given in Table 3.4.

Table 3.4

Chronological List of Flood Peak Discharges
for Susquehanna River at Harrisburg, Pennsylvania

Year	Date	Discharge (cfs)	Year	Date	Discharge (cfs)
1786	Oct. 5	482,000	1933	Aug. 25	269,000
1846	Mar. 15	482,000	1934	Dec. 2	242,000
1865	Mar. 15	573,000	1935	July 11	187,000
1868	Mar. 18	417,000	1936	Mar. 19	740,000
1886	Jan. 6	385,000	1937	Jan. 24	231,000
1889	June 2	654,000	1938	Dec. 20	178,000
1891	Feb. 19	408,000	1939	Feb. 23	210,000
1892	April 5	270,000	1940	April 2	418,000
1893	May 5	324,000	1941	April 7	244,000

Table 3.4 (Concluded)

Chronological List of Flood Peak Discharges
for Susquehanna River at Harrisburg, Pennsylvania

Year	Date	Discharge (cfs)	Year	Date	Discharge (cfs)
1894	May 22	613,000	1942	May 24	290,000
1895	April 11	230,000	1943	Jan. 1	412,000
1896	April 1	265,000	1944	May 9	212,000
1897	Mar. 26	180,000	1945	Mar. 5	252,000
1898	Mar. 24	315,000	1946	May 29	494,000
1899	Mar. 6	228,000	1947	April 7	214,000
1900	Mar. 2	238,000	1948	April 16	308,000
1901	Nov. 28	249,000	1949	Jan. 1	220,000
1902	Mar. 3	449,000	1950	Nov. 27	416,000
1903	Mar. 2	276,000	1951	April 1	226,000
1904	Mar. 8	298,000	1952	Mar. 13	324,000
1905	Mar. 21	306,000	1953	Mar. 26	216,000
1906	Dec. 4	210,000	1954	Mar. 3	242,000
1907	Mar. 15	247,000	1955	Mar. 6	177,000
1908	Mar. 20	297,000	1956	Mar. 1[illegible]	338,000
1909	May 2	297,000	1957	April 7	250,000
1910	Mar. 3	332,000	1958	April 9	281,000
1911	Jan. 16	178,000	1959	Jan. 24	230,000
1912	April 4	249,000	1960	April 2	382,000
1913	Mar. 28	402,000	1961	Feb. 27	392,000
1914	Feb. 30	358,000	1962	April 2	270,000
1915	Mar. 26	286,000	1963	Mar. 28	249,000
1916	Mar. 29	379,000	1964	Mar. 12	484,000
1917	Mar. 29	155,000	1965	Feb. 11	136,000
1918	Mar. 16	288,000	1966	Feb. 15	265,000
1919	May 23	294,000	1967	Mar. 17	182,000
1920	May 13	423,000	1968	Mar. 24	202,000
1921	Nov. 30	278,000	1969	April 8	127,000
1922	Mar. 9	192,000	1970	April 4	343,000
1923	Mar. 6	261,000	1971	Mar. 1	224,000
1924	April 8	324,000	1972	June 24	1,020,000
1925	Feb. 13	379,000	1973	Feb. 4	209,000
1926	Nov. 17	323,000	1974	Dec. 29	105,000
1927	Mar. 23	208,000	1975	Sept. 27	529,000
1928	May 2	252,000	1976	Feb. 19	239,000
1929	Mar. 17	235,000	1977	Oct. 10	254,000
1930	Feb. 28	177,000	1978	Mar. 24	252,000
1931	Mar. 31	153,000	1979	Mar. 7	416,000
1932	April 2	245,000	1980	Mar. 23	205,000

The water elevation attained in the vicinity of the Peach Bottom Plant during the second largest flood of March 1936 is reported by local residents to be about elevation +111.5 feet C.D. As per the FSAR, backwater computations utilizing high water marks recorded upstream and downstream from the site by the U.S. Geological Survey have estimated the 1936 flood level of +113 ft C.D. The maximum flow of record of about 1,020,000 cfs is thought to have reached around +116 ft. C.D., which is also the plant grade elevation.

As a first approach, a simplified analysis was conducted to assess the probability distribution of flooding at the site based on the stream gage data. Three different commonly-used distributions, i.e., log normal, Type I Extreme Value and Log-Pearson Type III were investigated for this purpose. The flood discharge corresponding to a return period of one million years was found from these distributions. The respective resulting values were 2,248,950 cfs, 1,702,639 cfs and 3,140,837 cfs. (Note that the third distribution investigated is from the Hydrology Subcommittee Bulletin 17B in Ref. 25. However, the outlier and weighted skew adjustments - which would reduce this particular estimate - recommended in Reference 25 were not applied for this level of analysis). Two of the three estimates might be expected to equal or exceed the 135 foot elevation level to which all critical equipment and structures are protected against flood. Hence, this approach could not be used to definitely screen out the possibility of non-negligible risk from external floods.

As an alternative approach, the maximum credible flood based on local conditions was estimated using PMF methodology as reported in the FSAR. The probable maximum flood (PMF) at the site was determined by the U.S. Corps of Engineers using probable maximum precipitation data over the Susquehanna River watershed above Harrisburg, PA. The assumption of simultaneous rainfall over such a large area (24,100 square miles) is very conservative and resulted in a probable maximum flood estimate of 1,750,000 cfs at the site.

Holtwood dam, upstream of the site, is a gravity structure and is unlikely to fail completely. However, should a complete failure of this dam take place, there is estimated to be an instantaneous additional flow of 200,000 cfs. The most severe combination of maximum probable flood, failure of Holtwood dam and wind-generated waves acting simultaneously was assumed so as to produce a maximum flooding elevation of 131.5 feet at the site.

As per the FSAR, a study of surge propagation in the reservoir for the probable maximum flood indicated a transient wave height of 0.5 ft at the site. Superimposing the height of the transient wave on the steady state backwater profile produces a maximum level of +132 ft at the site. The height of the wind generated waves was computed using the greatest average fetch. From a consideration of the surrounding conditions, recorded wind velocity, wind direction, effect of topography, and time required for waves to develop, a wind-generated wave height of 1.8 ft was computed. Superimposing 1.8 ft of wind-generated waves yields a peak of elevation of 133.8 ft C.D.

The critical equipment, systems, and structures essential to a safe shutdown of the reactor are flood protected to elevation +135 ft C.D. Watertight doors are provided for all the critical structures, including the reactor building, main control room complex, switchgear room, diesel generator building, service water pump structures, etc., up to an elevation of +135 ft C.D., leaving a margin of 1.2 ft. All penetrations in the exterior walls, including conduits, are sealed to ensure leak tightness necessary for plant safety. In addition, an emergency service water pump is located in the emergency cooling tower structure. These plant design features and extremely conservative assumptions in all phases of analysis leads us to conclude that the contribution of flooding to overall plant risk is negligible.

3 3.3 Extreme Winds and Tornadoes

Extreme winds resulting from tornadoes, hurricanes or wind storms can present a threat to nuclear power plants. The winds associated with hurricanes and storms are, however, less intense and lower in magnitude than those associated with tornadoes at the design-basis level (Figure 3.1, taken from Ref. 5). Also, Peach Bottom is well inland making the hurricane effects minimal. Hence, it is sufficient to consider only the risk to the structures due to tornadoes. This section describes the analysis of Peach Bottom structures for the effects of tornadoes.

Assuming a Poisson process for occurrence of tornadoes, the probability of a tornado striking the structures during time T with a velocity exceeding V* may be written as:

$$P\,[\text{strike by tornado with } V \geq V^*] = \nu T\, E[V(A_I) \geq V^*(A_I)]$$

where ν is the mean arrival rate per unit area per year for the site, $V(A_I)$ is the velocity in an area A_I which will be defined below and $E(.)$ is the expectation operator taken over all tornado parameters.

Figure 3.2 shows a rectangular structure with dimension A and B. Assume that this structure is approached by a tornado which travels at an angle as measured from the side B. Also, let us assume that this tornado travels a touchdown distance equal to L and the damage is limited to width W during the lifetime of the tornado. Knowing the above information, one can define an area A_I where any tornado initiated in this area would strike the structure. Here, the point of initiation for the tornado is assumed to be the mid-point of width W, but in general the following results are not dependent on this assumption. The area A_I is shown in the lower part of Figure 3.2. Using simple geometry, it is observed that A_I is made up of four distinct regions.

a. The sum of the areas denoted by T_1 and T_2, which is equal to the total tornado damage area WL.

b. The area denoted by P, which is equal to HL where H is the projection of the structure on a line which is perpendicular to the tornado path.

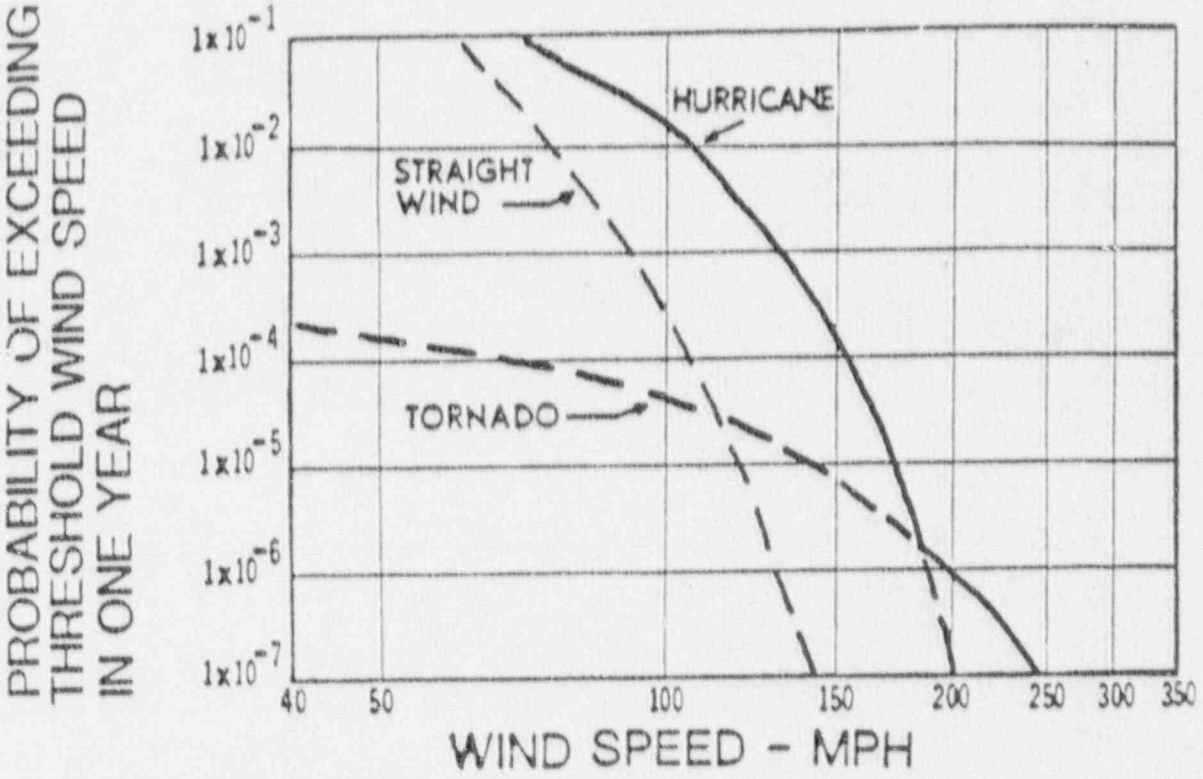

Note: Relative positions of straight wind and hurricane probability models could be interchanged depending on site.

Figure 3.1 Typical tornado, hurricane and straight wind hazard probability models (Kimura and Budnitz, 1987)

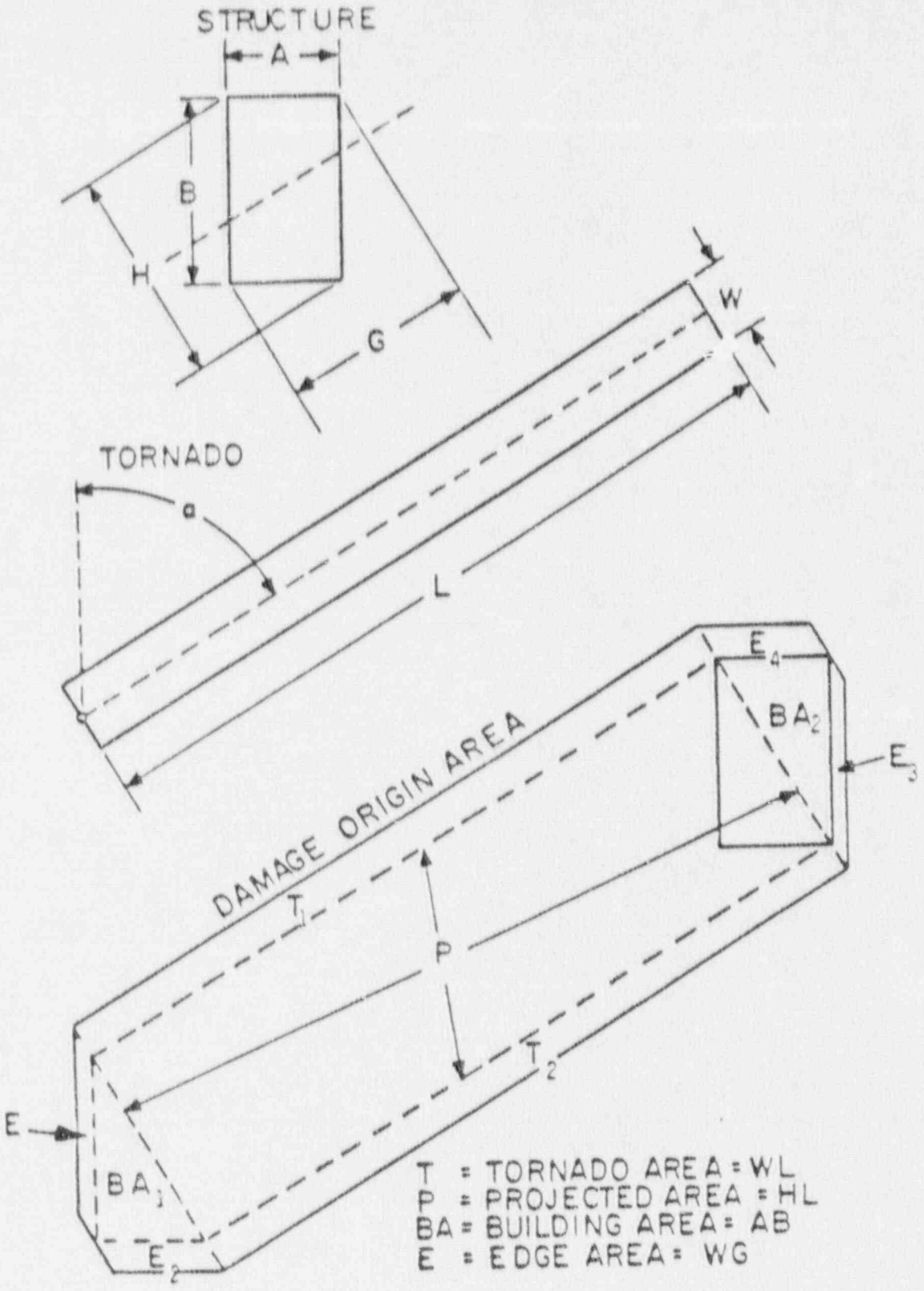

Figure 3.2 Tornado parameters and damage origin area definition

c. The area denoted by areas BA_1 and BA_2 added to the structure area AB.

d. The areas denoted by E_1, E_2, E_3 and E_4 added to WG, where G is the projection of the structure on the tornado path.

Therefore, it is observed that the tornado will strike the structure if it is initiated within an area A_I given by

$$A_I = WL + HL + WG + AB$$

The first term in this equation is the tornado damage area whereas the next two terms provide for any intersection between the tornado and the structure. Finally, the last term is the area of the structure itself. Thus, the tornado hazard curves for a site are expected to depend on the size of the structure as well as the damage area of the tornado. For typical structures, the last two terms may be neglected and A_I may be written as

$$A_I = WL + HL$$

where WL is the area for a point structure and HL is the lifeline term which also contributes to the probability of a tornado strike.

In general, one must integrate the results over the probability distribution of angle α for all possible tornado strikes. For this scoping study, angle α was conservatively chosen such that it would maximize the second term in the equation, i.e., H was chosen as the maximum projection length of the structure. A matrix formulation for calculating the annual frequency of tornado strikes with $V \geq V^*$ is presented here, based on the procedure described in Reinhold and Ellingwood (Ref. 6).

This model includes the following elements:

a. Variation of tornado intensity with occurrence; tornado occurrences decrease rapidly with increased intensity,

b. Correlation of width and length of damage area; longer tornadoes are usually wider,

c. Correlation of area and intensity; stronger tornadoes are usually larger than weaker tornadoes,

d. Variation in tornado intensity along the damage path length; tornado intensity varies throughout its life cycle, and

e. Variation of tornado intensity across the tornado width path.

In this model, the occurrence of tornadoes in this model is assumed to have a Poisson distribution, i.e., the probability distribution of tornado inter-arrival times is assumed to be exponential. Given that a tornado has occurred at the site, the conditional probability of the tornado intensity scale is then based on historical data. Next, for each tornado intensity scale, one determines the average (expected) value of

tornado area (WI.) and tornado path length (L). Thus, one can calculate the expected value of area A_I for each tornado intensity scale. Assuming that the maximum tornado wind velocity for each intensity scale is the mid-point of the velocity scale as reported in Table 3.5, the probability of a tornado strike with maximum wind speeds exceeding a given velocity V* is equivalent to the probability of that tornado being initiated in the area A_I. As an example, an F3 tornado in Table 3.5 would correspond to a maximum wind velocity of 182 mph. Also, one can calculate a corresponding A_I area for F3 tornadoes. Therefore, the probability of exceeding 182 mph winds at the site is equivalent to the probability of an F3 tornado occurring in the corresponding A_I at the site. However, the problem is complicated by the fact that an F3 tornado does not exhibit the same level of damage along its path. A detailed description of the probabilistic model and its application to the Peach Bottom site is given next.

Table 3.5

Velocity, Length, Width and Area Scales

Scale No.	Fujita - F Velocity Scale (mph)	Pearson - P Length Scale (mi)	Pearson - P Width Scale (mi)	Area Scale (mi^2)
0	72	1.00	0.010	0.001
1	73-112	1.00-3.15	0.010-0.31	0.001-0.009
2	113-157	3.16-9.99	0.032-0.099	0.010-0.099
3	158-206	10.0-31.5	0.100-0.315	0.100-0.999
4	207-260	31.6-99.9	0.316-0.999	1.000-9.999
5	261-318	100-315	1.00-3.15	10.00-99.99
6	319-380	316-999	3.16-9.99	100.0-999.9

The Peach Bottom site is located in Pennsylvania, which belongs to tornado region I (Figure 3.3) according to the scheme proposed by Markee et al. (Ref. 7) or region C (Figure 3.4) as per Twisdale and Dunn (Ref. 8). The tornado occurrence rates for these regions are 4.12×10^{-4}/square mile/year and 3.37×10^{-4}/square mile/year, respectively (Table 3.6). These occurrence rates have been corrected for possible unreported tornadoes in sparsely populated areas. The specific frequency in the local region around the Peach Bottom site can be estimated from Figure 3.5, which gives the number of tornadoes occurring in the United States by 1° box (i.e., an area enclosed by one degree latitude-longitude lines) from 1954 to 1983 as recorded by National Severe Storms Forecast Center (Ref. 9). As Peach Bottom is located in one of the four shaded squares

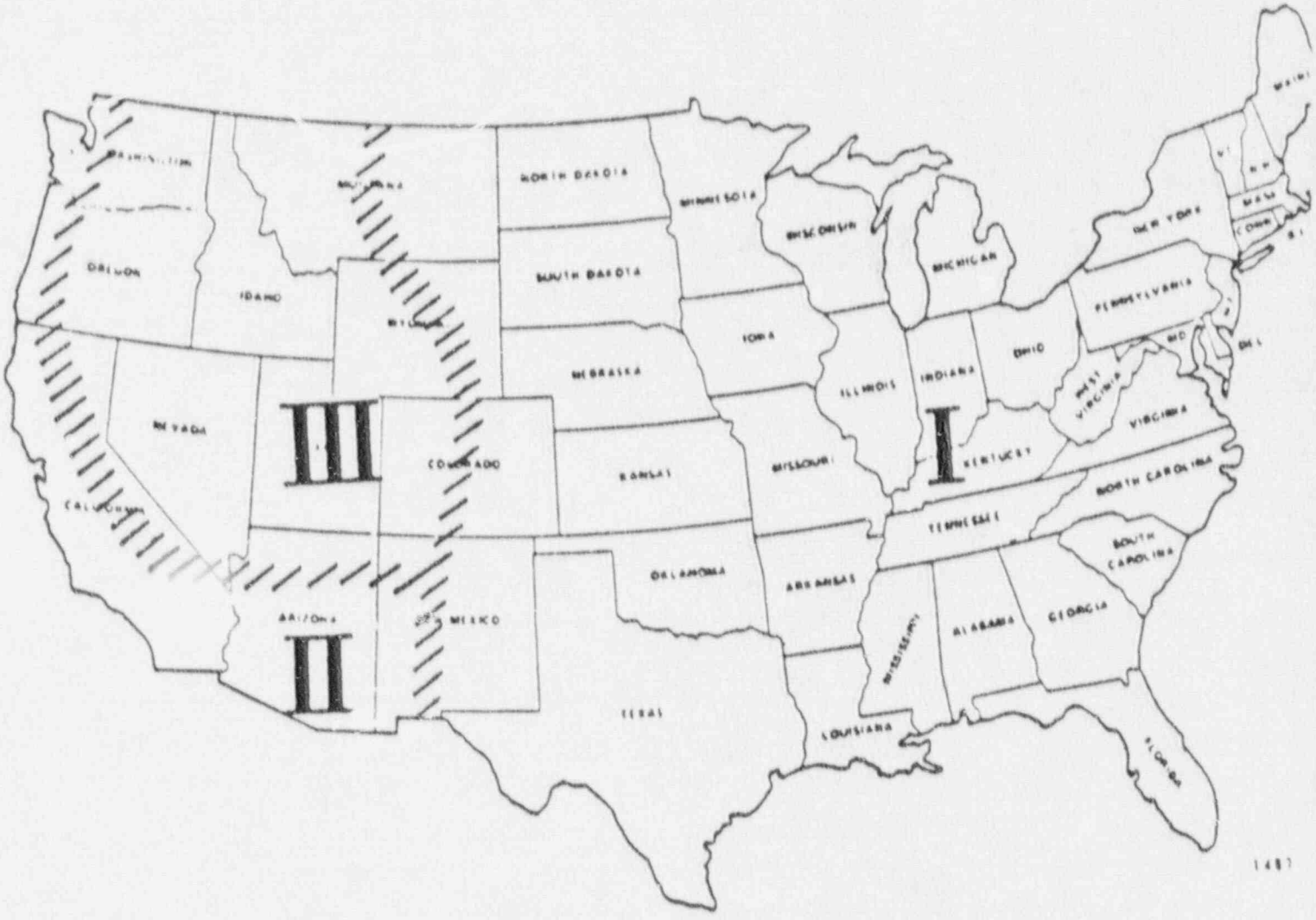

Figure 3.3 Tornado risk regionalization scheme proposed in WASH-1300.

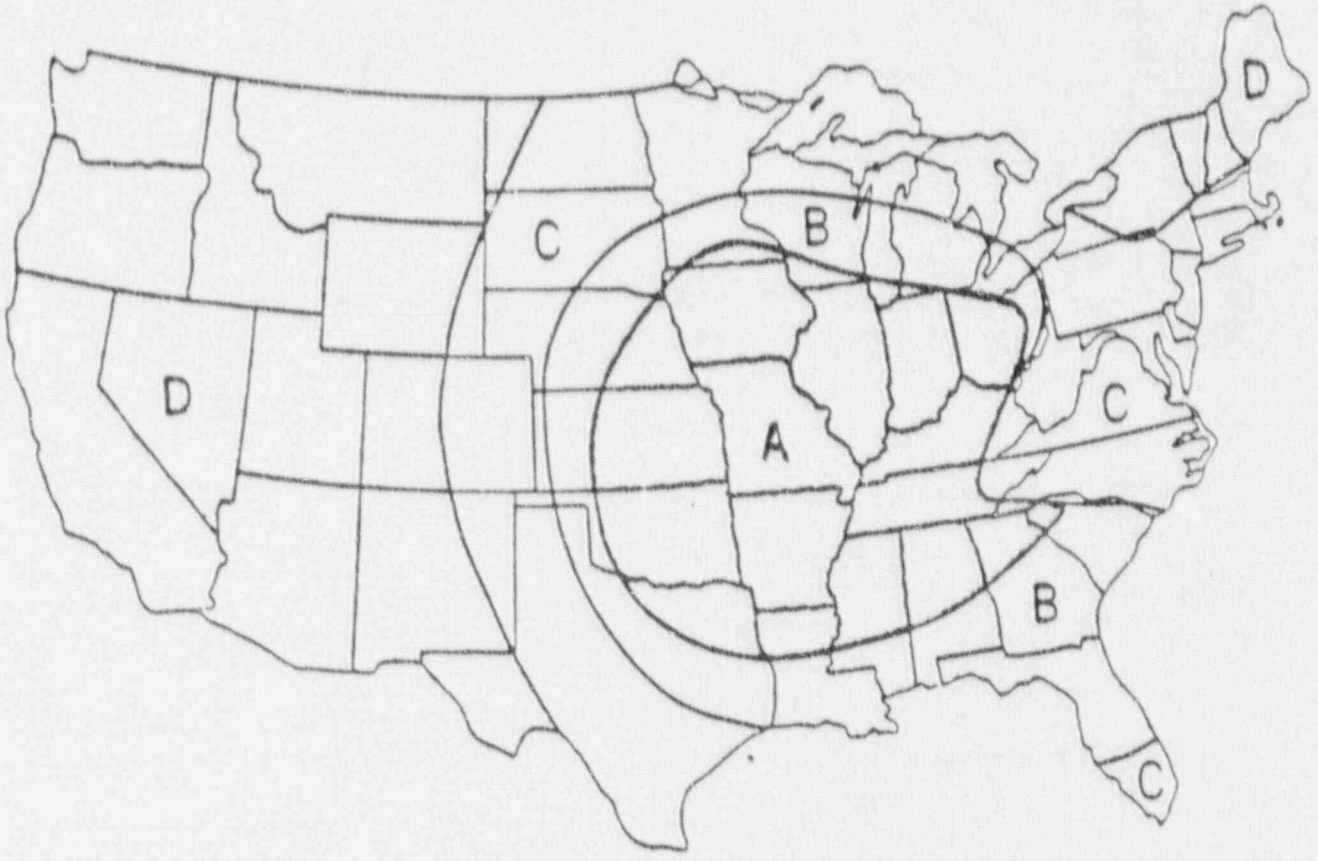

Figure 3.4 Tornado risk regionalization scheme proposed by Twisdale and Dunn (1983)

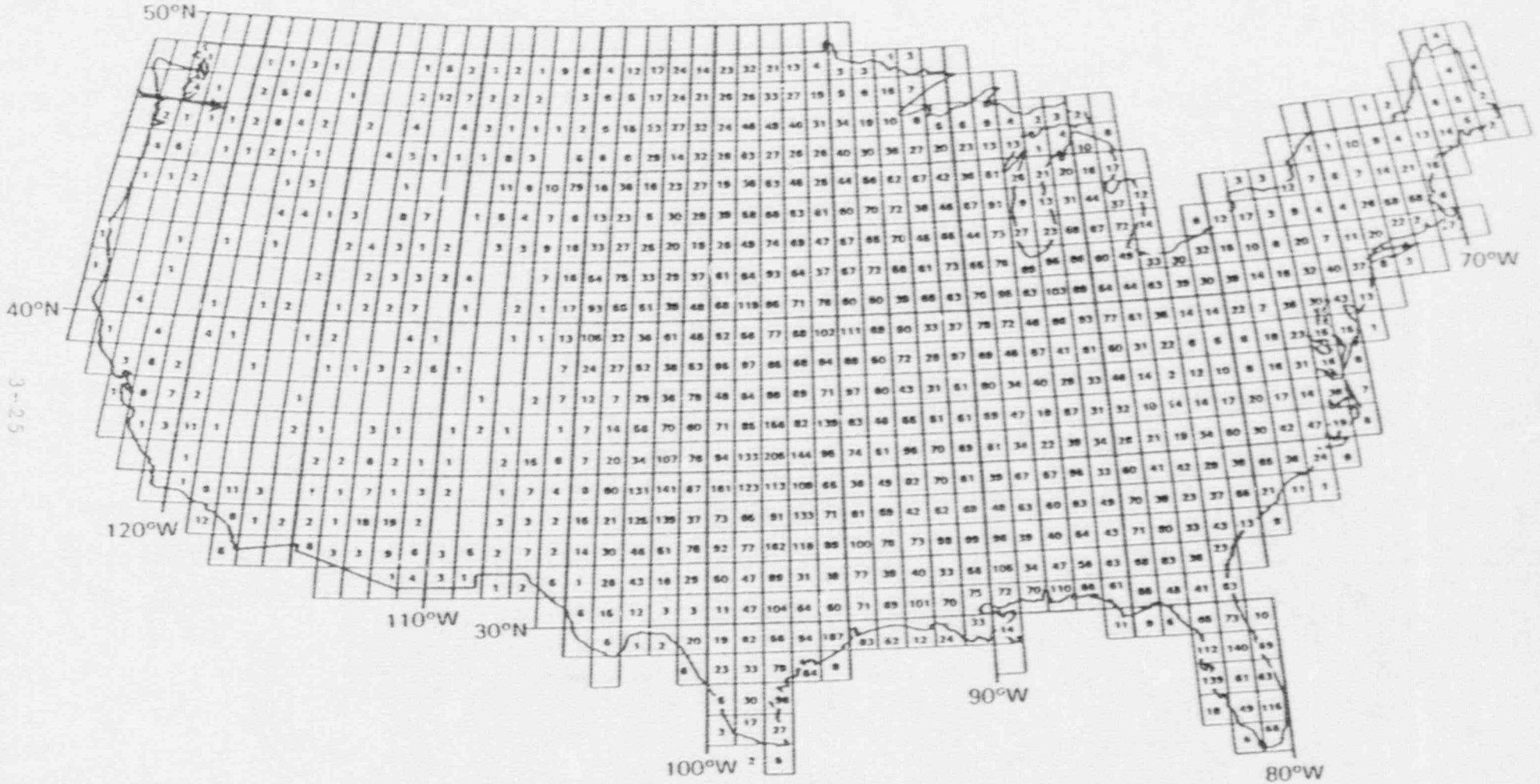

Fig. 3.5 Number of Tornadoes in U.S. by 1° Box (1954-1983)

in the Figure 3.5, the highest value of 43 is used to calculate the frequency. The area of each square is 4780 cos θ, where θ is the latitude of the center of the square. Assuming $\theta = 40°$, the site specific frequency of tornado occurrence is computed to be 3.91×10^{-4}/square mile/year.

To be conservative, the value of 4.12×10^{-4}/square mile/year given by Markee et al. (Ref. 7) is, however, used in further analysis. The probabilities of occurrence of different intensities (F0 to F6) are given (Table 3.6) by:

F_0	F_1	F_2	F_3	F_4	F_5	F_6

$$(OI) = (0.2227 \quad 0.3785 \quad 0.2576 \quad 0.1016 \quad 0.0324 \quad 0.0066 \quad 0.0009)$$

where the F-scale intensities depend on the qualitative assessment of the worst damage that occurs during a tornado, based on actual observations or computation of pressure required to cause the observed damage. Thus, each row of the Table 3.6 gives the conditional probability of each F-scale intensity tornado given that a tornado has occurred. Each tornado intensity scale is also associated with a velocity scale, a length scale, a width scale and an area scale as shown in Table 3.5.

Next, the average or the expected values of tornado area and tornado path length are determined in order to compute the expected value of area A_I for each tornado intensity scale. Assuming that the maximum tornado wind velocity for each intensity scale is the mid-point of the velocity reported in Table 3.5, the probability of a tornado strike with maximum wind speeds exceeding a given velocity V* is equivalent to the probability of that tornado being initiated in the area A_I. As an example, a F3 tornado in Table 3.5 would correspond to a maximum velocity of 182 mph. Also, one can calculate a corresponding A_I area for F3 tornadoes. Therefore, the probability of exceeding 182 mph winds at the site is equivalent to the probability of an F3 tornado occurring in the corresponding A_I at the site.

For the present study, the expected value of tornado damage area WL is required for each value in the intensity scale. These average areas may be calculated from historical measured damage areas of observed tornadoes, i.e., an area-intensity relationship for tornadoes is to be obtained. Table 3.7 shows a matrix of area-intensity relationships for all tornadoes based on 10,240 tornadoes (Ref. 10). Each row of this table shows the percentages of each F-scale intensity tornado which were classified according to area classification in Table 3.5. Since F6 tornadoes have not been observed in the past, the last row in Table 3.7 represents engineering judgment (Ref. 6). Representing the average of area scales in Table 3.5 by a vector (AA) and the matrix in Table 3.7 (A_IM), the vector of expected values of areas for each F-scale intensity (A_I) may be written as

$$(A_I) = (A_IM)\ (AA)$$

Table 3.6

Regional Tornado Occurrence - Intensity Relationships
Corrected for Direct Classification Errors and Random Encounter Errors
(Each Row in the Table is the Vector IO)

Region	F Scale	Corrected Probability of Occurrence at Each F-Scale Intensity						
		F0	F1	F2	F3	F4	F5	F6
Fig. 3.3	I	.2227	.3785	.2576	.1016	.0324	.0066	.009
9								
	II	.3610	.3116	.2198	.0912	.0147	.0015	.000
2								
	III	.3044	.4421	.1730	.0681	.0112	.0012	.000
1								
Fig. 3.4	A	.1658	.3379	.3122	.1322	.0413	.0093	.001
3								
	B	.2263	.3527	.2785	.1040	.0312	.0063	.000
8								
	C	.2830	.3611	.2426	.0856	.0225	.0047	.000
6								
	D	.3034	.3799	.2436	.0622	.0096	.0011	.000
1								

Region	Regional Occurrence Rates Corrected for Unreported Tornadoes (occurrences per square mile per year)
Fig. 3.3	I 4.12×10^{-4}
	II 2.67×10^{-5}
	III 1.35×10^{-5}
Fig. 3.4	A 5.18×10^{-4}
	B 6.98×10^{-4}
	C 3.37×10^{-4}
	D 3.53×10^{-5}

Using (AA) = [0.001 0.0055 0.055 0.55 5.5 55 555] and $(A_I M)$ as the matrix of Table 3.7, the mean tornado areas (square miles) for each F-scale intensity are obtained as

$$F_0 \quad F_1 \quad F_2 \quad F_3 \quad F_4 \quad F_5 \quad F_6$$

$$(A_I) = [0.30 \quad 0.72 \quad 1.8 \quad 4.3 \quad 8.5 \quad 15.7 \quad 18.9]$$

Another characteristic of a tornado is that its intensity does not stay constant along its path and the tornado is usually at its highest intensity only for a fraction of the time it is active. This resulted from the fact that intensity scales are assigned to a tornado based on

Table 3.7

Intensity-Area Relationship Including Corrections
For Direct Observation and Random Encounter Errors ($A_I M$ Matrix)

Actual Maximum Tornado State	Percentage of Tornadoes With Indicated Area Classification					
	A0	A1	A2	A3	A4	A5
F0"	.155	.421	.269	.125	.029	.0016
F1"	.057	.255	.355	.259	.071	.003
F2"	.022	.139	.303	.368	.155	.013
F3"	.009	.070	.210	.376	.289	.046
F4"	.003	.033	.123	.299	.435	.107
F5"	.001	.017	.068	.216	.461	.237
F6"	.001	.012	.049	.185	.458	.295

the most severe observed damage. Figure 3.6 shows a hypothetical F4 tornado with variation of intensity along its path. Table 3.8 shows a matrix (VWL) giving corrections for the combined variation of tornado intensity along its path length and across its path width. Each column of matrix (VWL) in Table 3.8 shows the proportion of each F-scale damage in the area (WL) for a tornado which has been assigned an intensity scale based on the most severe observed damage from the analysis of 149 tornadoes (Ref. 6). As an example, F3 tornadoes are expected to inflict F3 damage on only 2.7 percent of the total damage area. In fact, 61.5 percent of the damage inflicted by a F3 tornado is expected to be very light (F0).

The probabilities of tornado strike associated with a point structure A_I = WL (Figure 3.3) for each F-scale intensity tornado are obtained from

$$P\ [\{V(A_I,WL)\} \geq \{V^*\}] = \nu\ \{C_1\} = \nu\{VWL\}\ \{A_I.OI\}$$

where $\{V^*\}$ is taken to be the mid-point of tornado velocity scales in Table 3.5, i.e., $\{V^*\}$ = (72 93 135 182 234 290 349) and matrix VWL is as defined above. $\{A_I.OI\}$ is a vector where its elements are the expected values of tornado areas times the occurrence-intensity rates assuming that the whole tornado corresponds to the classified intensity.

$$\{A_I.OI\} = \{0.0668\ \ 0.2725\ \ 0.4639\ \ 0.4369\ \ 0.2754\ \ 0.1036\ \ 0.017\}$$

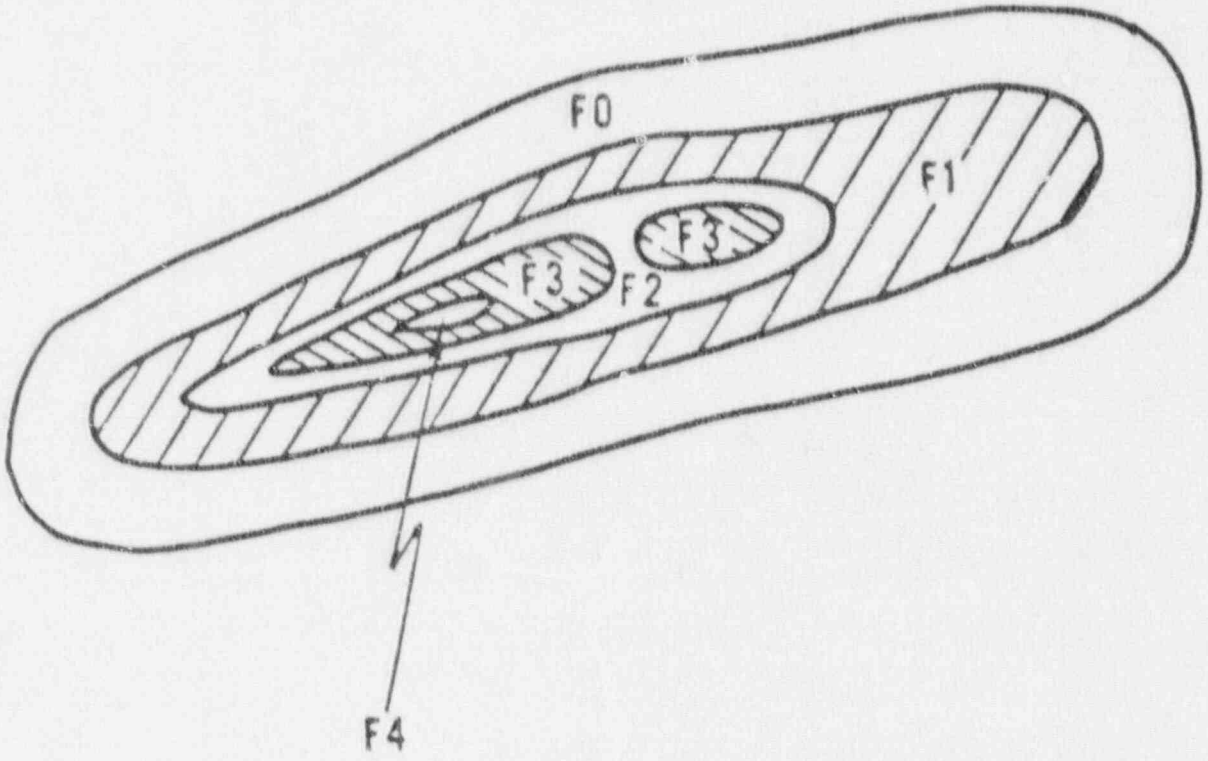

Figure 3.6 Sketch of hypothetical F4 tornado illustrating variation of intensity

Table 3.8

Variation of Tornado Intensity Along Path Length and Across Path Width (VWL Matrix)

Local Tornado State	True Maximum Tornado State						
	F0"	F1"	F2"	F3"	F4"	F5"	F6"
F0*	1.000	.743	.658	.615	.637	.632	.625
F1*	0	.257	.248	.267	.234	.236	.238
F2*	0	0	.094	.091	.093	.088	.089
F3*	0	0	0	.027	.028	.033	.033
F4*	0	0	0	0	.008	.009	.011
F5*	0	0	0	0	0	.002	.003
F6*	0	0	0	0	0	0	.001

The vector (C_1) is

$$(C_1) = (1.09 \quad 0.39 \quad 0.122 \quad 2.35 \times 10^{-2} \quad 3.3 \times 10^{-3} \quad 1 \times 10^{-4} \quad 1.7 \times 10^{-5})$$

There is additional contribution to the probability of the tornado wind speeds exceeding a certain value due to the lifeline term which depends on the tornado length and is independent of tornado width. Table 3.9 shows a matrix of intensity-length relationship (LIM) where each row of the matrix is the fraction of tornadoes with a given F-scale intensity which were observed to have length scales according to Table 3.5. This matrix was based on an analysis of 7953 tornadoes between 1971 to 1979 (Ref. 6). The expected value of tornado length for each F-scale intensity tornado (LI) may then be computed from

$$(LI) = (LIM) \bullet (LL)$$

where (LL) is the vector of mid-point length scales from Table 3.6, i.e., (LL) = (1.0 2.08 6.58 20.8 65.8 208 658) and the length-intensity vector is

$$(LI) = (1.53 \quad 3.01 \quad 4.76 \quad 9.15 \quad 18.8 \quad 26.9 \quad 30.1)$$

Table 3.9

Intensity Length Relationship Including Corrections for Direct Observation and Random Encounter Errors (LIM Matrix)

Actual Maximum Tornado State	Percentage of Tornadoes With Indicated Area Classification					
	PL0	PL1	PL2	PL3	PL4	PL5
F0"	.801	.115	.069	.014	.001	0
F1"	.590	.219	.140	.046	.005	0
F2"	.436	.249	.212	.093	.010	0
F3"	.272	.226	.268	.195	.038	.001
F4"	.141	.152	.272	.326	.090	.019
F5"	.079	.113	.197	.444	.131	.036
F6"	.058	.101	.155	.496	.147	.043

Since a tornado intensity varies along its length, one needs to establish a relationship between the total length for a given F-scale tornado and the percentages of total length which were observed to have different F-scale intensities. Such a relationship is shown in terms of the matrix of variation of intensity along length (VL) in Table 3.10 where each column of the matrix lists the percentages of total tornado length with different F-scale intensities. This matrix was based on the analysis of 149 tornadoes.

Thus, the contribution of the lifeline term to the probability of exceedance of a wind speed [V*] of the site may be written as

$$P\ [(V(A_I, WH)) \geq (V^*)] = \nu\ (C_2) = \nu\ (VL) \bullet (LI \bullet OI)\ H$$

Where H is a characteristic length of a structure and (V*) is again taken to be the mid-point of velocity scales for each F-scale tornado as shown in Table 3.5, i.e.,

$$(V^*) = (72 \quad 93 \quad 135 \quad 182 \quad 234 \quad 290 \quad 349)$$

Table 3.10

Variation of Intensity Along Length
Based on Percentage of Length Per Tornado (VL Matrix)

Local Tornado State	Recorded Tornado State						
	F0"	F1"	F2"	F3"	F4"	F5"	F6"
F0	1.000	.383	.180	.077	.130	.118	.100
F1	0	.617	.279	.245	.131	.125	.110
F2	0	0	.541	.310	.248	.236	.160
F3	0	0	0	.368	.234	.236	.160
F4	0	0	0	0	.257	.187	.200
F5	0	0	0	0	0	.172	.150
F6	0	0	0	0	0	0	.160

The vector (LI • OI) is obtained by multiplying each term of the length-intensity vector (LI) by the occurrence-intensity vector (OI), i.e.,

$$(LI \bullet OI) = (0.3407 \quad 1.1393 \quad 1.2262 \quad 0.9296 \quad 0.6091 \quad 0.1775 \quad 0.0271)$$

Combining the point strike and the lifeline terms and using the Poisson arrivals for tornadoes, the annual probability of exceedance for each F-scale velocity may be written as

$$(P\ [F \geq F_i]) = (P\ [V \geq V^*]) = \nu\ [(C_1) + (C_2)\ H]$$

where ν is occurrence rate for region I ($= 4.12 \times 10^{-4}$/year/square mile).

Figure 3.7 shows the resulting tornado hazard curves for the Peach Bottom site for lifeline lengths of 100, 300 and 500 feet. Category I structures at Peach Bottom are built adjacent to each other. The dimension of a prototype structure which models unit 2, unit 3 and the auxiliary building is 150 ft x 450 ft. Assuming that a tornado approaches the plant at a 45° angle to one of the sides, the maximum lifeline length of the structure is calculated to be 474 ft. From Figure 3.7, the annual probability of exceedance of the design basis tornado

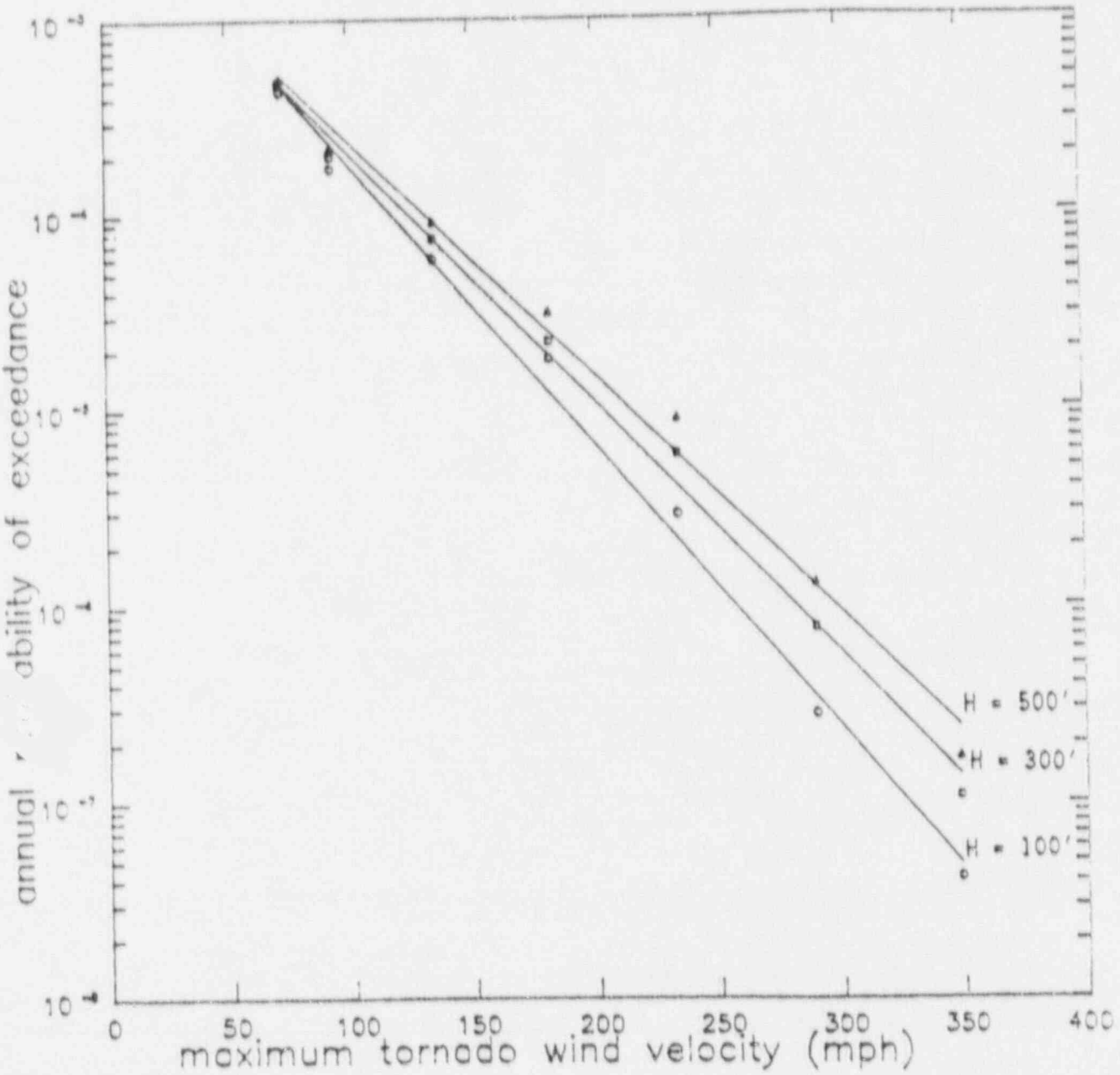

Figure 3.7 Tornado hazard curves for Peach Bottom site

windspeed of 300 mph for a characteristic length of 474 feet is approximately 9×10^{-7}. Thus, it is concluded that the structural failure due to tornado wind pressure is not a significant contributor to overall plant risk.

Tornado missile hazard can be eliminated on the basis of the thickness of the reinforced concrete walls provided for enclosures containing safety related components. Several empirical expressions have been suggested for non-deformable missile impact on reinforced concrete walls. In all the studies performed to date, it has been concluded that the amount of reinforcement is not an important factor in calculating the scabbing thickness or perforation thickness of a reinforced concrete wall. The most widely used formulas for determination of minimum wall thickness required to prevent scabbing are the Chang's formula (Ref. 11) and the modified National Defense Research Committee (NDRC) formula. Based on these, a wall thickness of 18 in to 20 in is found to prevent scabbing of concrete walls due to tornado missiles. The wall thickness of the important Peach Bottom structures are as follows:

Reactor Buildings, Unit 2 and 3	24 inches. to 40 inches.
Radwaste Auxiliary Building	24 inches. to 36 inches.
C.W. Pump Concrete Superstructure	24 inches. to 31 inches.
Diesel Generator Building	24 inches.

These structures are also protected by missile-proof doors and baffle walls. The control building is in the middle of turbine building and is also designed for missiles.

Additionally, it can be argued that given the occurrence of a tornado, the tornado missile damage is a low probability event because a combination of multiple component failures must occur for the missile to cause any damage. The event sequence includes the missile injection and then transport, missile impact and barrier damage of Category I structures and then appropriate component failures. This conclusion was confirmed in a detailed study by Twisdale and Dunn (Ref. 1) who performed a simulation study for a typical nuclear power plant to obtain tornado missile impact probabilities and probability distributions of missile velocities. They used a total of 65,550 potential missiles which could be injected from different zones near the plant. Since most of these missiles represent objects which would be available during construction of a plant, the total number of missiles used in the study is expected to be conservative for the Peach Bottom site. In fact, the site visit verified that the potential missile population at Peach Bottom is a small fraction of the number used in the above study.

Deformable tornado missiles, namely wood planks and automobiles were included in the design of Category I structures. The velocity used for wood planks in the design was 300 mph which is higher than the suggested

velocity by the Standard Review Plan. On the other hand, the automobile impact velocity used in the design was 50 mph which is lower than the value used in Standard Review Plan. The results of the above simulation study show that for a given tornado, the probability of an automobile impacting any of the structures in the plant with a velocity greater than 57 mph is less than 10^{-8} per year. Due to inherent conservatisms in design, it may be concluded that the capacity of structures is such that they will withstand an automobile impact less than 57 mph and the automobile impact's contribution to the plant risk would be less than 10^{-8} per year. The only deformable tornado missile which was not specifically considered in the plant design is the utility pole. However, based on the full-scale tornado missile impact tests conducted by EPRI (Ref. 12), utility poles are not expected to cause any damage to the 12-in-thick reinforced concrete walls. Therefore, based on the conservative bounding analysis performed in this study, it is concluded that non-deformable tornado missiles as well as deformable missiles are not significant contributors to the plant risk.

In summary, the probability of structural failure resulting from tornado strikes on the Peach Bottom structures shows that the probability of a tornado striking the plant structures with wind speeds in excess of 300 mph is of the order of 9×10^{-7} per year. Even if the plant structures are assumed to fail at the design value, the contribution of the tornado events to the plant risk is negligibly small. Finally, the thickness for the exterior walls of various safety related structures have been shown to be adequate for any potential damage from tornado missiles.

3.3.4 Industrial or Military Facility Accidents

There are three possible effects from an industrial accident near the site: (1) incident over-pressure on plant structures due to an explosion, (2) seepage of toxic chemical fumes into the control room, which could incapacitate the operators, and (3) flammable vapor clouds leading to a fire hazard at the site. Industrial accidents at distances farther than 5 miles to the site are not expected to cause significant over-pressure loads on the plant structures because all the Category I structures are designed for tornado wind loads, with a minimum capacity of 3 psi against blast loads. Similarly, release of the chemicals stored or situated at distances greater than 5 miles need not be considered as an external hazard. This is due to the fact that if a release occurs at such a distance, atmospheric dispersion will dilute and disperse the incoming plume to such a degree that there would be sufficient time for the control room operators to take appropriate action.

According to the Peach Bottom FSAR, the area surrounding the site is principally rural and agricultural. There are only a few industrial units within 10 miles of the plant and these are listed in Table 3.11. None of these units deal with hazardous materials in significant quantities. The only chemical and fertilizer unit is a small 21 person operation, farther than 5 miles from the site. Therefore, the probability of accidents in nearby industrial facilities leading to core melt is judged to be negligible.

Table 3.11

Companies Located Within 10 Miles of the
Peach Bottom Site*

Company Name	Type of Industry
Fawn Grove Manufacturing Company	Sewing Factory
H.E. Shallcross & Sons	Butcher
Wiley Manufacturing Company	Ship Building
Blue Ridge Flooring Company	Saw Milling, Flooring
C.D. Miller	Lumber Manufacturing, Saw Milling
Maryland Green Marble Corporation	Maryland Verde Antique Marble Green Marble Chips
Maryland Lava Company	Lava Insulation, Special Insulators, Pilot Tips
Miller Chemical & Fertilizer Corporation	Chemicals, Fertilizer
McCorquodale Color Card Company	Color Charts
Whitefore Packing Company	Epoxy and Lava Products
Petti Frocks, Inc., Assoc.	Canned Foods
R. Roberts & Son	Fuel Tanks, Refuse Containers
B. G. S. Jourdan & Sons	Canned Tomatoes
The Susquehanna Electric Company	Hydro Electric Plant
Star Printing Company	Printing
Weldom Packing Company	Canned Foods
Snyder Packing Company	Canned Foods
Philadelphia Electric Company	Nuclear Power Generating Station
Pennsylvania Power & Light Company	Hydro Electric Plant

*Companies with less than 10 employees have not been reported.

3.3.5 Release of Chemicals from On-Site Storage

According to Regulatory Guide 1.78 (Ref. 13), the maximum quantities of different chemicals that can be stored on-site at specified distances are based on leak-tightness of the control room. If the quantity exceeds the limits of the Regulatory Guide, automatic detectors must be installed so that the control room is isolated. If the plant design meets these requirements, it is judged that the probability of chemical release in excessive concentration combined with the malfunction of the detectors (if any) is very small. However, if the Regulatory Guide limits are exceeded, a detailed risk analysis such as that described in the Limerick

Severe Accident Risk Assessment (Ref. 14) must be performed to analyze the consequence of release of these chemicals, their dispersion and subsequent build-up in the control room. Discussions with plant personnel indicated that only the normal amount of hazardous chemicals expected at any nuclear power plant site (chlorine, ammonia, etc.) were present at Peach Bottom. Given this, and the fact that no previous risk assessment has ever shown a frequency of impact on personnel in the control room greater than 10^{-7} per year, the risk due to release of on-site chemicals at Peach Bottom can be discounted.

As regards the movement of trucks with hazardous materials within the plant exclusion area, it is infrequent and controlled. Moreover, the consequences of a release are not important for core melt since only a limited amount of hazardous material can be carried in each shipment. Thus, this hazard can also be discounted for Peach Bottom.

3.3.6 Transportation Accidents

A transport accident near the site can pose risk in one of the following ways: (1) a chemical explosion due to a transportation accident may cause damage to Category I structures and safety-related equipment due to pressure loading and missile impacts, and (2) toxic chemicals which are spilled in a transportation accident may drift into the control room and cause incapacitation of the operators. Transportation modes considered in this section include highways, railroads and river traffic. The risk from air transport was covered in Section 3.3.1.

A chemical explosion near the plant structures may cause over-pressure, dynamic pressures, blast-induced ground motion, or blast-generated missiles. However, from previous research in this area, it has been determined that over-pressures would be the controlling consideration for explosions resulting from transportation accidents (Regulatory Guide 1.91, Ref. 15). An accident over-pressure at the site can also occur because of explosions of a vapor cloud drifting towards the structures. This type of explosion involves complex phenomena which depend on the material involved, combustion process, and topographical and meteorological conditions. According to a study by Eichler and Napadensky (Ref. 16), present theoretical and empirical knowledge is too limited to quantitatively evaluate realistic accidental vapor cloud explosion scenarios. However, vapor cloud explosions are implicitly included in the TNT equivalents which are used to represent transportation accidents. According to the Regulatory Guide 1.91 (Ref. 15), chemical explosions which would result in free-field over-pressures of less than 1 psi at the site do not need to be considered in the plant design. Based on experimental data on hemispherical charges of TNT, a 1 psi pressure would be translated into a safe distance R (feet) which is defined as:

$$R > kw^{1/3}$$

where k = 45 and w is an equivalent weight of TNT charge. The maximum probable equivalent TNT charge is stipulated to be 50,000 lbs for a highway truck, 132,000 lbs for a single railroad boxcar, and 5,000 tons for a river barge.

Route 74 is 3 miles from the site. Assuming a maximum specified TNT charge of 50,000 lbs, the safe distance from the plant is 45 $(50,000)^{1/3}$ = 1,657 feet, which is less than 3 miles. There is a railroad about 1.75 miles from the Peach Bottom site, where a collision between a truck and a train occurred in 1987. Considering the maximum postulated equivalent TNT charge of 132,000 lbs, the leak overpressure at the site will be 2.2 psi. However, as the plant is designed for the design basis tornado loading, the probability of core damage due to highway and railroad accidents is expected o be negligible. As Conowingo Pond is used only by a moderate number of boaters and fishermen for recreational purposes, the possibility of barge explosion on the pond is discounted.

A toxic chemical spill near the site would pose a danger to the plant if toxic chemicals penetrate into the control room through air intakes. This could happen if (a) large quantities of toxic chemicals are released, (b) there are favorable wind conditions which would cause a drift of chemicals towards the control room air intakes at excessive concentrations, and (c) there are no detection systems and air isolation systems in the control room.

Regulatory Guide 1.78 provides detailed guidelines for the safety analysis for release of toxic gases in transportation accidents. It is possible to exclude chemicals on the basis of frequency of transportation criterion but this data is not available. The weights of hazardous chemicals that require consideration in control room evaluation for a 50 mg/m^3 toxic limit and Pasquill stability Category F for a range of distances from the control room to the accident and for three different control room ventilation systems are specified (Table 3.12).

The main control room is in the central portion of the turbine building. Since it is inside the turbine building, it can be reasonably assumed to have leakage characteristics of (at least) a Type B control room. Moreover, site conditions are such that there are steep hills rising up to 300 feet all around the plant site. Thus, any accidental release of chemicals on a transportation route has a low probability of reaching the site. Based on Table 3.12, the maximum permissible weight of hazardous chemical on Route 74, at least 3 miles from the site, range from a maximum of 3,700,000 to 33,000 lbs, depending on the type of control room environment. For Type B, it is 780,000 lbs. Since the transportation on the highways is by trucks, and the maximum load carried by a single truck is smaller than this limit, chemical release from highway accident can be eliminated from consideration. Similar arguments applied to rail traffic show that chemical release from this transportation mode is not a governing factor. As there is no transportation of chemicals by barges, this possibility is discounted.

Table 3.12

Weights of Hazardous Chemicals That Require
Consideration in Control Room Evaluations
(for 50 mg/m³ Toxic Limit and Pasquill Stability Category F)

Distance From Control Room (Miles)	Weight (lbs)		
	Type A Control Room	Type B Control Room	Type C Control Room
< 0.3	100	100	100
0.3 to 0.5	9,000	2,300	100
0.5 to 0.7	35,00	8,800	400
0.7 to 1.0	120,000	20,000	1,000
1 to 2	270,000	52,000	2,500
2 to 3	1,300,000	280,000	13,000
3 to 4	3,700,000	780,000	33,000
4 to 5	8,800,000	1,400,000	60,000

Type A Control Room - A tight control room having low leakage construction features and the capability of detecting at the fresh air intake those hazardous chemicals stored or transported near the site. Detection of the chemical and automatic isolation of the control room are assumed to have occurred. An air exchange rate of 0.015 per hour is assumed (0.015 of the control room air by volume is replaced with outside air in one hour). The control volume is defined as the volume of the entire zone serviced by the control room ventilation system. The assumption that the air exchange rate is less than 0.015 per hour requires verification by field testing.

Type B Control Room - Same as Type A, but with an air exchange rate of 0.06 per hour. This value is typical of a control room with normal leakage construction features. The assumption that the air exchange rate is less than 0.06 per hour requires verification by field testing.

Type C Control Room - A control room that has not been isolated, has no provision for detecting hazardous chemicals, and has an air exchange rate of 1.2 per hour.

3.3.7 Turbine Generated Missiles

Failures of large steam turbines in both nuclear and fossil-fueled power plants, although rare, have occurred occasionally in the past. These failures have occurred because of one or more of the following broad classes of reasons: (1) metallurgical and/or design inadequacies, (2) environmental effects, (3) out-of-phase or generator field failures and (4) failures of overspeed protection systems. The failures have resulted in loss of blades, disk cracking, rotor and disk rupture and even missiles. Interior missiles are highly energetic and have the potential to damage safety-related structures housing critical components.

Based on a total of 2,500 years of operation in nuclear power plants, only four failures have occurred: Calder Hall (1958), Hinkley Point (1969), Shippingport (1974), and Yankee Rowe (1980). Missiles were produced in the Hinkley Point and Calder Hall failures. Although the causative mechanisms of these failures have been identified and are generally corrected in the modern plants, there is no assurance that turbine failures will not occur in the future. Recent discovery of widespread stress corrosion cracking in the disks and rotors of operating nuclear turbines has revived the industry's interest in the issue of such failures.

Turbines rotate at 1,800 rpm with the low-pressure (LP) and high-pressure (HP) sections on a contiguous shaft. The LP sections have blade hubs (called "wheels" or "disks") shrunk onto the rotor. Depending on the manufacturer and rated capacity of the turbine, there could be ten to 16 disks on each LP section. The disks are massive components each weighing between 4 and 8 tons. These disks, because of their relatively large radius, are the most highly stressed spinning components in the interior. With the interior unit running at less than 120 percent of the rated speed, the disks are stressed well below the yield strength of material so that failures can be caused only by undetected material flaws that may be aggravated by stress corrosion and fatigue. At 180 percent of the rated speed, the disks are stressed at or above their ultimate strength so that they burst into fragments. At intermediate speeds (i.e., 120 to 180 percent), rupture of disks may be caused by a combination of flaws and weaker material in the disks.

Turbine missiles are spinning, irregular fragments with weights in the range of 100 to 8,000 pounds, and velocities in the range of 30 ft/sec to 800 ft/sec. It is conventional to discuss two types of turbine missile trajectories: low trajectory missiles (LTM) and high trajectory missiles (HTM). The low trajectory missiles are those which are ejected from the turbine casing at a low angle toward a barrier protecting an essential system. High trajectory missiles are ejected vertically (almost) upward through the interior casing and may strike critical targets by falling on them. The customary ballistic distinction between LTM and HTM is the

initial elevation angle (ϕ) of the missile (LTM is for $\phi < 45°$ and HTM is for $\phi > 45°$). Turbine manufacturers have specified that the maximum deflection angle for the missiles produced in the burst of the last disk on the rotor is 25°. Based on this, the NRC has defined a low trajectory missile strike zone in the Regulatory Guide 1.115 (Ref. 17) and recommended that the essential systems be located outside this LTM strike zone. If a turbine missile impacts a barrier enclosing a safety-related component, interest lies in knowing if the missile perforates or scabs the barrier to cause sufficient damage to the component. Using empirical formulas for scabbing derived on the basis of the full scale and model tests, it is estimated that concrete barriers should be at least 4 feet thick to prevent scabbing. The need for providing such barriers depends on the probability of turbine failure and the arrangement of safety-related components with respect to interior missile trajectories. In the design of a nuclear power plant, the designers have many alternative approaches for treating the potential effects of turbine failures (Sliter, Chu and Ravindra, Ref. 18). These approaches can be grouped as: (1) prevention of turbine failure, (2) prevention of missiles, (3) prevention of strike on critical components, and (4) performance of probabilistic analysis to demonstrate that the probability of turbine missile damage is acceptably low.

The probability of serious damage from turbine missiles to a specific system in the plant is calculated as (Ref. 19):

$$P_4 = P_1 P_2 P_3$$

where:

P_1 = probability of turbine failure leading to missile generation

P_2 = probability of missiles striking a barrier which encloses the safety system given that the missile(s) have been generated

P_3 = probability of unacceptable damage to the system given that one or more missiles strike the barrier

In practice, the evaluation of P_4 should include consideration of different speed conditions, distribution of missiles and all the safety-related components and systems in the plant.

Turbine missile damage in the older plants was usually considered on the basis of a deterministic safety review according to RG 1.115 (Ref. 17) and SRP 2.2.3 (Ref. 20), i.e., the probability of unacceptable damage from turbine missiles (P_4) was implicitly shown to be less than 10^{-7} per year. The new guidelines concerning safety of nuclear power plants against turbine missile strikes are best summarized in NUREG-1068 (Ref. 21) which is a review of the Limerick PRA. The following paragraphs have been reproduced from NUREG-1068 describing the NRC position on calculating the probability of turbine missile damage.

In the past, analyses for construction permit and operating licer e review assumed the frequency of missile generation (P_1) to be approximately 10^{-4} per turbine year, based on the historical failure rate. The strike probability (P_2) was estimated (SRP 3.5.1.3) based on postulated missile sizes, shapes, and energies, and on available plant-specific information such as turbine placement and orientation, number and type of intervening barriers, target geometry, and potential missile trajectories. The damage probability (P_3) was generally assumed to be 1.0. The overall frequency of unacceptable damage to safety-related systems (P_4), which is the sum ove targets of the product of these frequencies, evaluated for compliance with the NRC sa ety objective. This logic places the regulatory emphasis on the strike probability. That is, having established an individual plant safety objective of about 10^{-7} per year, or less, for the probability of unacceptable damage to safety-related systems as a result of turbine missiles, this procedure requires that P_2 P_3 be less than or equal to 10^{-3}.

Although the calculation of strike probability (P_2) is not difficult in principle, for the most part reducing it to a straightforward ballistics analysis presents a problem in prac ice. The problem stems from the fact that numerous modeling approximations and simplifying assumptions are required to make tractable the incorporation into acceptable models of available data on the (1) properties of missiles, (2) interactions of missiles with barriers and obstacles, (3) trajectories of missiles as they interact with or perforate (or are deflected by) barriers, and (4) identification and location of safety-related targets. The particular approximations and assumptions made tend to have a large effect on the resulting value of P_2. Similarly, a reasonably accurate specification of the damage probability (P_3) is no simple matter because of difficulty of defining the missile impact energy required to make given safety-related systems unavailable to perform their safety function, and the difficulty of postulating sequences of events that would follow a missile-producing turbine failure.

Because of the uncertainties involved in calculating P_2, the NRC staff concludes that P_2 analyses are "ball park" or "order of magnitude" type calculations only. Based on simple estimates for a variety of plant layouts, the strike and damage probability product can

be reasonably taken to fall in a characteristic narrow range that is dependent on the gross features of turbine-generator orientation because (1) for favorably oriented turbine generators, P_2 P_3 tend to lie on the range 10^{-4} to 10^{-3}, and (2) for unfavorably oriented turbine generators, P_2 P_3 tend to lie in the range 10^{-3} to 10^{-2}. For these reasons (and because of weak data, controversial assumptions, and modeling difficulties), in the evaluation of P_4, credit is given for the product of the strike and damage probabilities of 10^{-3} for an unfavorably oriented turbine, and no calculations are required.

According to NRC staff, the safety objective with regard to turbine missiles is best expressed in terms of criterion applied to the missile generation frequency which requires the demonstrated value of turbine missile generation frequency (P_1) be less than 10^{-5} for initial start-up and that corrective action be taken to return P_1 to this value if it should become greater than 10^{-5} during operation.

The frequency of unacceptable damage to safety-related structures, systems and components as a result of turbine missiles is acceptably low (i.e., less than 10^{-7} per year) provided that the above criterion on turbine missile generation is met. This criterion is to be met by the maintenance of an appropriate in service inspection and testing program on the turbine throughout the plant's life as discussed in detail in the Limerick SARA.

From the preceding paragraphs, it is seen that the emphasis is on turbine maintenance and in-service inspection to assure a value of the frequency of turbine missile generation (P_1) less than 10^{-5} per year. Then, based on a minimum P_2 P_3 value of 10^{-2} per year, turbine missiles can be excluded from external events analysis.

Peach Bottom station has turbine generators manufactured by General Electric Corporation (GE). According to the Peach Bottom FSAR, GE has established the probability of high trajectory missile generation at 1×10^{-8} per year. Based on historical failure data (Bush, Ref. 19), the probability of turbine missile generation has been calculated to be approximately 10^{-4} per year. Also, Patton et al. (Ref. 22) conducted a comprehensive study which estimated the probabilities of turbine missile generation at operating speed and overspeed as 1.2×10^{-4} per year and 4.4×10^{-4} per year, respectively. These estimates are several orders of magnitude higher than those reported by GE. Recent discovery of stress corrosion incidents in the operating GE turbine-generators (Southwest Research Institute, Ref. 23) suggest that P_1 values are not as low as what the manufacturers have estimated.

Assuming the estimates made by GE to be the lower bounds (i.e., 5th percentile), the estimates by Patton et al. (Ref. 22) as the upper bounds (i.e., 95th percentile) and the uncertainty in P_1 values to be modeled by lognormal distribution, the estimate of annual probability of turbine missile generation will be 1.4×10^{-5}.

But, damage due to turbine missiles in a favorably oriented turbine is almost entirely due to the high trajectory missiles. The P_2 P_3 probability estimate of 10^{-3} per year which was accepted by the NRC staff is judged to be conservative. Therefore, the probability of turbine missile damage in plants which have favorably oriented turbines is conservatively estimated to be in the order of 10^{-7} per year or better and a bounding analysis is not required.

These conclusions will, however, depend on the turbine maintenance and in-service inspection to assure a value of P_1 of at least 10^{-5} per year. According to the letter of October 9, 1986 (Ref. 24), from Philadelphia Electric Company (PECO) to NRC (Docket No. 50-277, 50-278) it is stated that PECO plans to implement a turbine inspection program based upon the methodology described in a proprietary GE report applied to Peach Bottom using plant-specific data, and which leads to an inspection interval of 6 operating years. This methodology has been reviewed and approved by the NRC, and implementation of it is, therefore, assumed to assure a value for P_1 of 10^{-5}/year or better.

3.3.8 Internal Flooding

3.3.8.1 Introduction

A nuclear power plant contains many potential sources of flooding and flood locations. In order to make the analysis of these floods tractable, a process was defined to identify candidate sources and critical flooding areas and to estimate their contribution to core damage frequency if required. The general process consists of the following steps:

a. Identification of important flood sources and critical flooding areas during the initial plant walkdown. Critical areas can be thought of as those plant areas where flooding could not only result in a plant trip but also damage safety-related equipment needed to mitigate the effects on any flood-induced plant transient.

b. Definition of all initiating events which have the potential to be flood-induced for each flood source in each critical area. This step of the analysis results in identifying the spectrum of potential flood rates and is also used in quantification of initiating event frequencies.

c. Perform a screening analysis. The screening analysis is comprised of the following steps:

   1. Eliminate all plant areas not identified either by the initial plant walkdown or by computer mapping of critical equipment.

   2. Perform a computer-aided vital area analysis which identifies critical areas for further consideration and which allows for the incorporation of random failures (i.e., failures not related to the flood itself) as well as all flood-related damage. This is a similar process to what occurs in the fire analysis so the reader can refer to Chapter 5 for details on this procedure. This step resulted in flood zone singles, singles with randoms, and double combinations that are listed in Table 3.13.

   3. Screen on frequency for each remaining critical area flood scenario. For Peach Bottom this step resulted in elimination all remaining flood areas and scenarios under consideration. Details of the reasons why each of the Table 3.13 areas were screened from further consideration are given in Section 3.3.8.2.

d. Quantify core damage sequences for each remaining flood scenario.

e. Perform an uncertainty analysis utilizing the TEMAC computer code for all remaining scenarios.

3.3.8.2 Screening of Areas for Internal Flooding

As described above, a complete vital area analysis was performed for all the areas within the plant and for all the potential flood-induced accident sequences identified as part of a review of all internal events accident initiators. This analysis identified those singles, singles in conjunction with random failures, or multiple areas (with or without random failures) which, if all equipment in the zone is assumed to be failed by the flood, results in the occurrence of an accident scenario. The results for Peach Bottom are shown in Table 3.13. The zones themselves are defined in Table 5.3 of Chapter 5. The fire zones of that Table 5.3 correspond directly with the flood zones of Table 3.13. In addition, the equipment located in each fire zone is described in Appendix D. Table 3.13 presents all the zones that survived the screening analysis and these are the zones which were analyzed for the possible occurrence of floods in this section. Note that the same zone (for example, Zone 2) can occur either as a single or as a single plus random in different accident sequences. (Of course, the same zone cannot occur as a single and as a single plus random in the same

Table 3.13

Peach Bottom Flooding Vital Area Analysis Summary

Single Zone	Single Zone Plus Randoms	Double Zones	
Zone 2	Zone 2	Zone 5	Zone 6S
Zone 6S	Zone 4	25	50
Zone 25	Zone 32	6S	50
Zone 50	Zone 34	6N	50
	Zone 35	25	37
	Zone 36	25	39
	Zone 37	36	37
	Zone 38	36	38
	Zone 39		
	Zone 48		
	Zone 50		

accident sequence or it would be non-minimal). As can be seen, a total of only fourteen zones survived the screening process. Four zones were identified as singles, while eleven zones in conjunction with random failures were identified. Note that each of these zones in general was associated with a number of different random failures, so each zone itself could actually occur in a number of different single plus random cut sets. Finally, eight combinations of two zones (again, some in combination with random failures) were identified. In the following, each one of these zones or zone plus random failure combinations are analyzed to determine any potential non-negligible flooding scenarios.

Zones 32-39 Emergency Switchgear Rooms

These eight zones are all on the 135 foot elevation of the control/power structure and consist of the individual emergency switchgear rooms for both units. These rooms contain no water sources and the scenarios involved require random failures in addition to flood-induced failures within the room. In each case the vulnerability occurs because of potential for flood-induced loss of offsite power in conjunction with flood-induced damage within the cabinets themselves. The cable associated with loss of offsite power runs across the top of the room over the cabinets and may run down both ends of the bank of cabinets. The flood zone directly above these eight areas is the cable spreading room and it also has no water sources. The only potential source of water for all these rooms is water coming from the hallway outside each of these zones. In the case of the hallway on the radwaste building side there are no water sources. Also, there are stairs at each end of the hallway so water cannot build up in the hallway. On the Turbine Building hallway side, there are both stairways and open grates. Hence, any water that happened to occur in these hallways would preferentially go down the stairways rather than under the locked doors leading into the emergency switchgear rooms. Given that there are no local water sources and there is a preferential pathway leading away from the flood zones, flooding in these areas is highly unlikely.

Zone 25 Cable Spreading Room and Control Room

The cable spreading room is on elevation 150 directly above the emergency switchgear and the control room is directly above the cable spreading room. The cable spreading room has no water sources within the room and no water fire suppression systems in the room. Cable trays in the cable spreading room are at least 6 feet above the floor. The doors from the cable spreading room face onto a hallway adjacent to the Turbine Building. There is a water sprinkler system outside the doors of the cable spreading room but there are both stairways and elevators in that hallway immediately adjacent. Hence, the shafts would direct the water down and away from the cable spreading room. Similarly, for the control room, there are no water sources either above the control room or in areas to the side. There is water associated with air handling units in an area adjacent to the control room but there are no doorways between the two areas through water can travel. On the Turbine

Building side of the control room there is both an elevator and stairs; therefore, any water that would occur in that hallway would be directed downward. Given these physical considerations there is a negligible possibility of flooding in either the cabling spreading room or the control room.

Zone 50 Turbine Building

The Turbine Building would constitute a single vital area analysis cut set if a flood could disable both the instrument air system (located at the end of the building) and a variety of safety-related control and power cables routed in conduits which run vertically down a wall at the center of the building. Elevation 116 is the critical elevation for these two groups of components and conduits. However, there is 280 feet of horizontal separation between the instrument air system and the power conduits of interest. There is also a variety of hatchways and grills on this elevation which would direct water through the floor and down to lower levels. Hence, there is virtually no possibility of an internal flood occurring which could damage both the instrument air system and the control power cables.

Zone 6S Reactor Building on both the 135 and 165 Elevation

Contained in this area are cables, instruments, and actuators which could result in failure of the HPCI, RCIC, and ADS systems. There are a number of water sources at elevation 165 including small pumps and heat exchangers associated with the radwaste cooling system and the regenerative heat exchanger systems. The ADS system cables and actuators are on elevation 165 while the HPCI and RCIC cables and actuators are on elevation 135. There is a horizontal separation of greater than 100 feet between the ADS location and the HPCI, RCIC system locations. In addition, there is a large open floor hatch on elevation 135 which would direct any water accumulating in that area down to lower elevations. Given the configuration of these systems and the fact that the ADS system (from an accident sequence viewpoint) is a backup to the HPCI and RCIC systems, flooding in this zone can be eliminated from further consideration.

Zone 2 Multiple Elevations of Reactor Building

This flood area is on multiple elevations of the Reactor Building. The only area containing critical equipment in this fire zone is the hallway adjacent to the emergency switchgear room areas (discussed as part of zones 32 &8). The same arguments used there demonstrate that flooding in this area is a negligible risk contributor.

Zone 4 Elevation 89 of the Reactor Building

This area contains the HPCI and RCIC systems as well as cables for the off-site power. The vital area analysis showed that the simultaneous loss of HPCI, RCIC and off-site power would result in a transient

accident sequence. However, the off-site power trunk cables are inside conduit embedded in concrete and hence would not be vulnerable to any flood within the room. Thus, flooding in this area could not give rise to this particular accident sequence and thus flooding in this area need not be further considered.

Zone 48 Unit 2 Side of Circulating Water Pump House at Elevation 112 feet

This structure contains all the high pressure service water pumps as well as one of the three emergency service water pumps. Cabling for an additional emergency service water pump is also located in this area. As will be seen in Chapter 4 and 5, all three of the emergency service water pumps must simultaneously fail in order to lead to an accident sequence (by virtue of loss of cooling to the diesel generators). There are two scenarios identified in these vital area cut sets. The first involves flood-induced failure of ESW pumps A and B in conjunction with random failure of the ECW pump located in the emergency cooling tower at a significantly higher elevation (elevation 153 feet). However, in order to fail both pumps, water would have to reach the level of the cabling of the one pump. This cabling, however, is attached to the ceiling. In addition, water cannot build up in this area due to the fact that the openings for the ESW pump shafts go directly down to the forebay and, hence, a number of natural direct drainage paths exist.

The second potential scenario would involve failure of all four high pressure service water pumps which are in this fire zone in conjunction with another random failure. Again, due to the direct drainage available from the pump floors back down into the bay, it is not deemed possible that the water could build up to the level acquired to damage all four of the high pressure service water pumps. Therefore, internal flooding in this area is viewed as a negligible event.

3.3.8.3 Reactor Building Drainage and Subsystem

As mentioned above, all the flood-induced vital areas identified in the vital area analysis were screened out by knowledge of the location of the equipment within the room and knowledge of drainage paths and/or water sources. The final question that must be addressed is: given the water sources at various levels within the building, what would be the consequences of the water draining down through hatchways, stairways, etc. into the lower elevation of the building and into the sump area. Peach Bottom does have a sump which is both alarmed and contains a sump pump and which is connected to the various pump rooms and other areas containing water sources within the plant via drains. It might be possible in some cases for the sump to fill up and water to back into the HPCI or RCIC areas and lose those two systems. However, as mentioned earlier, the ADS system (which is a backup for the HPCI and RCIC) is located at elevation 165 and could not be affected by such a scenario.

Also, another source of high pressure injection water exists in the CRD system which is also located away from this area. Therefore, with

random failure of these two systems required to make any sump back-up flood scenario valid, any postulated scenario would be probabilistically insignificant.

3.4 Summary

The scoping quantification study considered all possible external events at the site except for seismic and fire events, since these two events were included in a detailed external events analysis. The PRA Procedures Guide (Ref. 2), suitably augmented with other available information, was used as a guideline for identification of all possible external events at the Peach Bottom site. Next, an initial screening process was carried out to eliminate events not applicable to Peach Bottom from the list. For this purpose, a set of screening criteria was developed and then each external event was examined for possible elimination based on these criteria. After the initial screening process was completed, the following events were found to be potential contributors to the plant risk.

a. Aircraft Impact
b. Extreme Winds and Tornadoes
c. External Flooding
d. Industrial or Military Facility Accident
e. Release of Chemicals from On-Site Storage
f. Turbine Generated Missiles
g. Transportation Accidents
h. Internal Flooding

The degree of sophistication in the bounding analysis for each event depended on whether the event could be eliminated based on only a hazard analysis or a complete analysis including hazard analysis, fragility evaluation and plant response analysis. The detailed plant response analysis was conservatively neglected in evaluating the impact of these external events.

The risk due to an aircraft striking the plant structures and causing unacceptable radiological consequences was screened out on the basis of the probability of strike and the design of different structures.

Evaluation of the potential for flooding as a result of the most conservative combination of Probable Maximum Flood (computed from conservative estimates of probable maximum precipitation), failure of Holtwood dam and wind-generated waves showed that the essential structures in the plant are located much above the probable maximum surge level and the risk of flooding is negligibly small.

Tornadoes and tornado missile impacts were eliminated on the basis of a detailed computation of tornado strike probability of 9×10^{-7}/year and other features of plant structures and components designed to withstand the effects of a Design Basis Tornado.

The information available from Philadelphia Electric Company on the frequency of turbine disk inspection was used as the basis to assume the safety of essential plant structures from damage due to turbine missiles.

Finally, explosions due to transportation accidents and both on-site and off-site chemical release have a low probability of affecting the site.

Thus, all external hazards except fire and seismic events were found to be negligible contributors to the risk of core damage at the Peach Bottom plant. Detailed evaluations of fire and seismic events are contained in the remainder of this report.

3.5 References

1. Twisdale, L. A., and W. L. Dunn, Tornado Missile Simulation and Design Methodology, Vol. 1, Research Triangle Institute, NP-2005, August 1981.

2. USNRC, PRA Procedures Guide, NUREG/CR-2300, January 1983.

3. Soloman, K. A., et al., Estimate of the Hazards to a Nuclear Reactor From the Random Impact of Meteorites, UCLA, ENG-7426, March 1974.

4. FAA, Statistical Handbook of Aviation, 1982.

5. Budnitz, R. J., and C. Y. Kimura, Evaluation of External Hazards to Nuclear Power Plants in the United States, NUREG/CR-5042, December 1987.

6. Reinhold, T. A., and B. Ellingwood, Tornado Damage Risk Assessment, USNRC, NUREG/CR-2944, September 1982.

7. Markee, E. J., J. G. Beckerley, and K. E. Sanders, Technical Basis for Interim Regional Tornado Criteria, U.S. Government Printing Office, Washington, WASH-1300, May 1974.

8. Twisdale, L. A., et al., Probabilistic Analysis of Turbine Missile Risks, EPRI Report NP-2749, February 1983.

9. Ramsdell, J. V., and G. L. Andrews, Tornado Climatology of the Contiguous United States, Pacific Northwest Laboratory, Richland, Washington, NUREG/CR-4461, PNL-5697, March 1986.

10. Schaefer, J. T., D. L. Kelley, and R. F. Abbey, "Tornado Track Characteristics and Hazard Probabilities," in Proceedings of the Fifth International Conference on Wind Engineering, Pergamon Press, New York, 1980.

11. Chang, W. S., "Impact of Solid Missiles on Concrete Barriers," Journal of the Structural Division, ASCE, 107, No. ST2, pp. 257-271 (1981).

12. Stephenson, A. E., Full Scale Tornado-Missile Impact Tests, EPRI Report, RP-399, August 1976.

13. USNRC, Regulatory Guide 1.78, Assumptions for Evaluating Habitability of Nuclear Power Plant Control Room During a Postulated Hazardous Chemical Release, U.S. AEC Directorate of Regulatory Standards, June 1974.

14. NUS Corporation, Severe Accident Risk Assessment, Limeric Generation Station, Philadelphia, Pennsylvania, prepared for NUS Corporation, Philadelphia Electric Company, 1983.

15. USNRC Regulatory Guide 1.91, Evaluation of Explosions Postulated to Occur on Transportation Routes Near Nuclear Power Plants, USNRC Office of Standards Development, Revision 1, February 1978.

16. Eichler, T. V., and H. S. Napadensky, Accidental Vapor Phase Explosions on Transportation Routes Near Nuclear Power Plants, USNRC, NUREG/CR-0075, May 1978.

17. USNRC Regulatory Guide 1.115 - Protection Against Low Trajectory Turbine Missiles, Rev. 1, July 1977.

18. Sliter, G. E., B. Chu, and M. K. Ravindra, "EPRI Research on Turbine Missile Effects in Nuclear Power Plants," in Transactions of 7th International Conference on Structural Mechanics in Reactor Technology, Paper J815, Chicago, Illinois, 1983, pp. 403-409.

19. Bush, S. H., "Probability of Damage to Nuclear Components Due to Turbine Failure," Nuclear Safety, 14, No. 3 (1973).

20. USNRC Standard Review Plan for the Review of Safety Analysis Reports for Nuclear Power Plants, NUREG-0800 LWR Edition, USNRC, Office of Nuclear Reactor Regulations, Washington, DC, July 1981.

21. Azarm, M. A., et al., A Review of the Limerick Generating Station Severe Accident Risk Assessment, NUREG/CR-3493, July 1984.

22. Patton, E. M., et al., Probabilistic Analysis of Low-Pressure Steam Turbine Missile Generation Events, Battelle Pacific Northwest Laboratories, EPRI NP-2749, August 19[illegible].

23. Southwest Research Institute, Steam Turbine Disk Cracking Experience, Vol. 2: Data Summaries and Discussion, prepared for Electric Power Research Institute, EPRI NP-2429, June 1982.

24. Philadelphia Electric Company, letter of October 9, 1986, to NRC, Docket #50-277, 50-278.

25. U. S. Geological Survey, Guidelines for Determining Flood Flow Frequency, Hydrology Subcommittee Bulletin 17B, 1982.

4.0 SEISMIC PRA

A detailed seismic risk assessment was performed for the Peach Bottom Plant. This analysis utilized dynamic response calculations for all important structures, a generic seismic fragility data base for components, and detailed component fragility derivations for a number of components identified during the plant visit as falling outside the generic data base. Hazard curves developed by the USNRC sponsored Seismic Hazard Characterization Program at Lawrence Livermore National Labs and by the Electric Power Research Institute were used. Mean values of accident sequence and core damage frequencies were obtained using a Monte Carlo approach. Each of these aspects of seismic risk are described in the following subsections.

4.1 Seismicity and Hazard Curves

The earthquake hazard at a given power plant site is characterized by a hazard curve and a site ground motion spectra. The hazard curve is a frequency plot which gives the probability of exceedance (per year) of different peak ground accelerations. The site response spectra describes the relative frequency content of the earthquakes expected at the site, and also the influence of the local soil column and layering in modifying the earthquake frequencies transmitted to the site.

4.1.1 General Considerations

For a given site, the hazard curve is derived from a combination of recorded earthquake data, estimated earthquake magnitudes of known events for which no data are available, review of local geological investigations, and use of expert judgment from seismologists and geologists familiar with the region in question. The region around the site (say within 100 km) is divided into zones, each zone having an (assumed) uniform mean rate of earthquake occurrence. This mean occurrence rate is determined from the historical record, as is the distribution of earthquake magnitudes. Then, for the region under consideration, an attenuation law is determined which relates the ground acceleration at the site to the ground acceleration at the earthquake source, as a function of the earthquake magnitude. The uncertainty in the attenuation law is specified by the standard deviation of the data (from which the law was derived) about the mean attenuation curve. These four pieces of information (zonation, mean occurrence rate and magnitude distribution for each zone, and attenuation law) are then combined statistically to compute the hazard curve.

The low level of seismic activity and the lack of instrumental records make it difficult to carry out seismic hazard analyses for the central and eastern United States using historic data alone. To augment the data base, current methodologies make use of the judgment of experts familiar with the area under consideration.

Approaches used to generate the subjective input, to assure reliability by feedback loops and cross-checking, and to account for biases and modes of judgment are described in detail in Bernreuter (Ref. 1).

4.1.2 Hazard Curves Used For Peach Bottom

The hazard curves used in the NUREG-1150 PRAs were taken from two sources. The first set of curves was obtained from the USNRC-sponsored Eastern U.S. Seismic Hazard Characterization Program (Reference 1) being performed by Lawrence Livermore National Laboratories (LLNL). From this program one can obtain a median hazard curve and an estimate of the distribution about the median curve. This is shown in Figure 4.1 where the mean, the median, the 15th percentile and 85th percentiles are shown. According to the principal investigator of this program, the distribution about the median is nearly log normal so for use in the NUREG-1150 analyses a log normal distribution was fit using the median and mean curves. From this fit any particular percentile curve of the hazard curve family can be computed. Table 4.1 lists the numerical values used in fitting the LLNL hazard curves.

A second set of hazard curves was obtained from the industry-sponsored Electric Power Research Institute's Seismic Hazard Methodology Development program for the Eastern United States (Reference 2). The corresponding curves are shown in Figure 4.2. These were also fit with a log normal model. The numerical values used in fitting the EPRI curves are listed in Table 4.2.

Note that the mean hazard curves of Figure 4.1 and 4.2 are near or above the 85th percentile hazard curves shown. The mean hazard curve will be found to drive the calculation of mean core damage frequency estimates as demonstrated in Section 4.4.

The two sets of hazard curves shown in Figures 4.1 and 4.2 are significantly different, both in regard to location of the mean curve as well as to the range of uncertainty about the median curve. This is not too surprising inasmuch as the emphasis of the two programs was somewhat different. The EPRI program focussed on very detailed geological studies of the sites in question, and resulted in a somewhat finer zonation of each site. However, only three attenuation (ground motion) models were used. Further, while a number of teams of seismological and geological experts were assembled, each team was proscribed to reach a consensus on the final hazard curve families developed by that team.

By contrast, in the LLNL program, considerable emphasis was placed on the full range of attenuation models, and rather than a number of teams, a total of 11 seismicity experts and 5 ground motion experts were individually polled, and a set of 2750 hazard curves were developed for each site by considering each expert's input equally likely. The

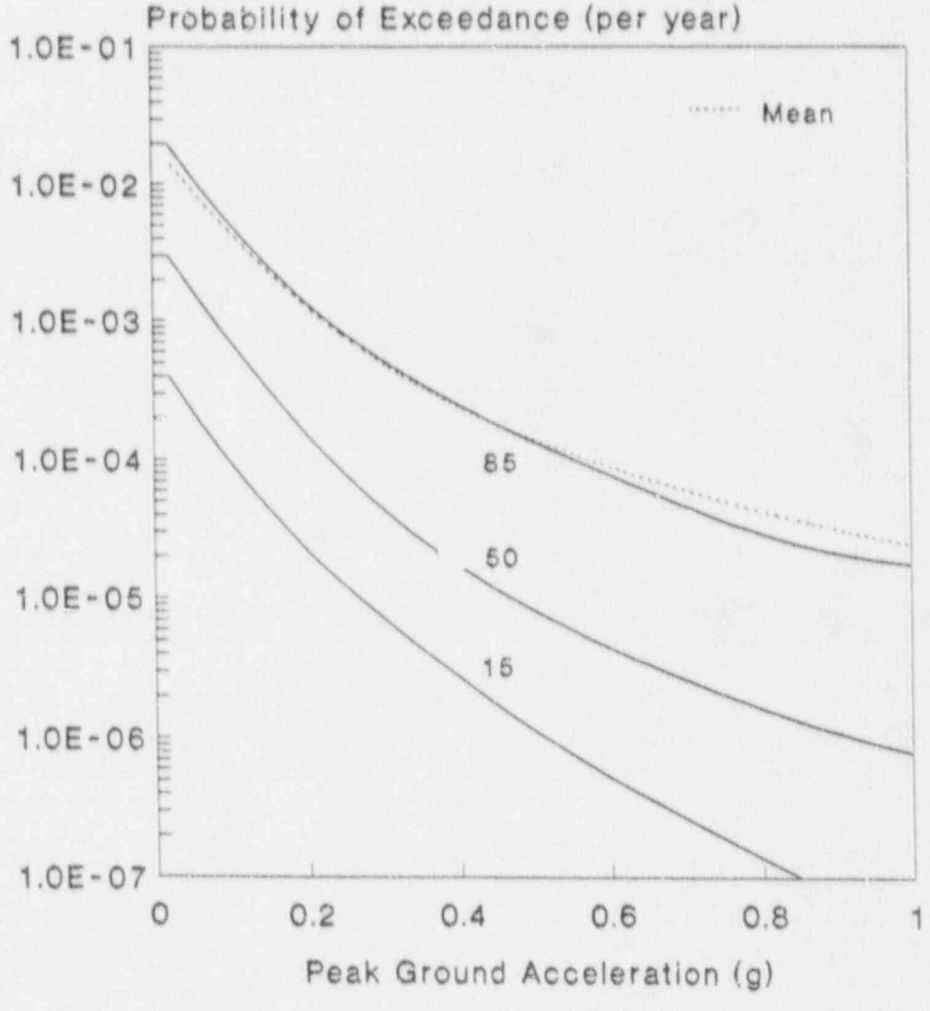

Figure 4.1 Peach Bottom LLNL Hazard Curves: Mean, Median, 85th and 15th Percentile Curves

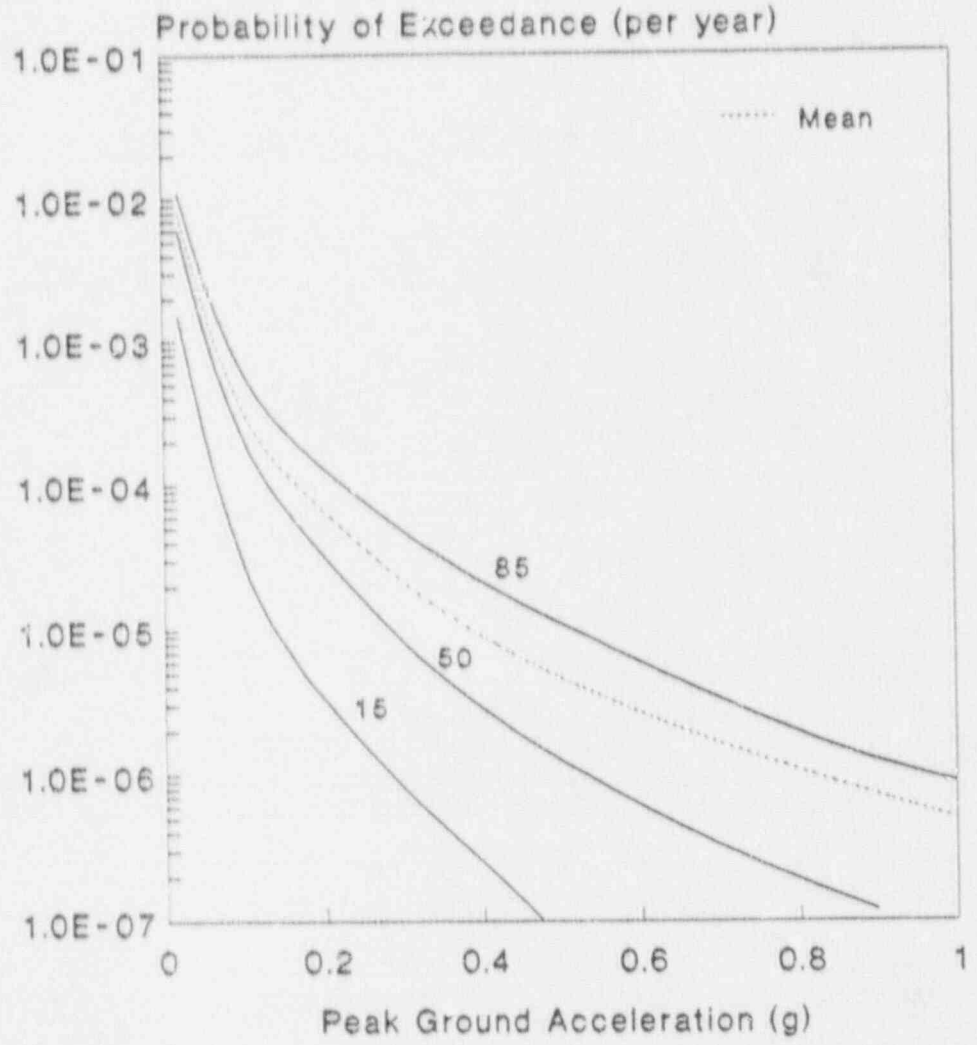

Figure 4.2 Peach Bottom EPRI Hazard Curves: Mean, Median, 85th and 15th Percentile Curves

Table 4.1

LLNL Mean and Median Hazard Curve CCDF Values

PGA(g)	Median Hazard Curve $P_{exceedance}$ per year	Mean Hazard Curve $P_{exceedance}$ per year
0.15	2.76E-4	1.98E-3
0.30	3.89E-5	4.58E-4
0.45	1.11E-5	1.79E-4
0.60	4.35E-6	8.89E-5
0.75	2.03E-6	5.05E-5
0.90	1.07E-6	3.14E-5
1.05	5.96E-7	2.08E-5
1.20	3.58E-7	1.44E-5

Table 4.2

EPRI Mean and Median Hazard Curve CCDF Values

PGA(g)	Median Hazard Curve $P_{exceedance}$ per year	Mean Hazard Curve $P_{exceedance}$ per year
0.15	6.77E-5	1.21E-4
0.30	7.33E-6	1.95E-5
0.45	1.79E-6	6.14E-6
0.60	5.96E-7	2.62E-6
0.75	2.38E-7	1.31E-6
0.90	1.19E-7	7.15E-7
1.05	5.96E-8	4.77E-7
1.20	5.96E-8	2.98E-7

curves developed in this process encompass somewhat more uncertainty than those produced by the EPRI process, and the increased uncertainty leads to higher probabilities of non-exceedence for the LLNL mean curve peak ground acceleration values than are obtained from the EPRI distributions.

At this time, the methods used to generate both sets of hazard curves are viewed by the U.S. NRC staff as being equally credible. As such, calculations of the seismic core damage and plant damage state frequencies at Peach Bottom are presented for both sets of hazard curves in this report.

4.2 Response Calculations

4.2.1 Introduction

As previously described, seismic probabilistic risk assessments (PRAs) can be considered in a series of steps: seismic hazard characterization, seismic response of structures and components, structure and component failure descriptions, plant logic models, and probabilistic failure calculations. Section 4.2 deals with the frequency characteristics of the free field ground motion (an element of the seismic hazard characterization) and the seismic response of structures and components.

In a seismic PRA of a nuclear power generating plant's safety systems, only the components affecting the operation of the systems and those structures housing or supporting these components need to be analyzed. Plant logic models identify the components. Plant general arrangement and mechanical drawings are then used to locate the components and identify the relevant supporting structures. For the Peach Bottom Atomic Power Station, the specific safety-related components are housed in the Reactor Building, the Turbine Building, the Radwaste Turbine structure, the Diesel Generator structure, the circulating water pump house, and the Emergency Cooling Tower (ECT). Figure 4.3 illustrates the general plant layout showing relative location of these structures.

Seismic PRAs require as input best-estimate (median-centered) structural response, variations of response and correlation of response. A seismic PRA considers earthquakes over the entire range of the seismic hazard curve; hence, seismic responses must be determined over this range. Often, seismic response determined as part of the plant design process is available. However, this data reflects the conservatism associated with the seismic design analysis methodology and considers only low seismic excitation levels.

To determine structural response at the higher excitation levels required by a seismic PRA, either the design analyses must be extrapolated or reanalyses of the structures must be made. For this study, analytical models of each structure identified above as housing safety-related

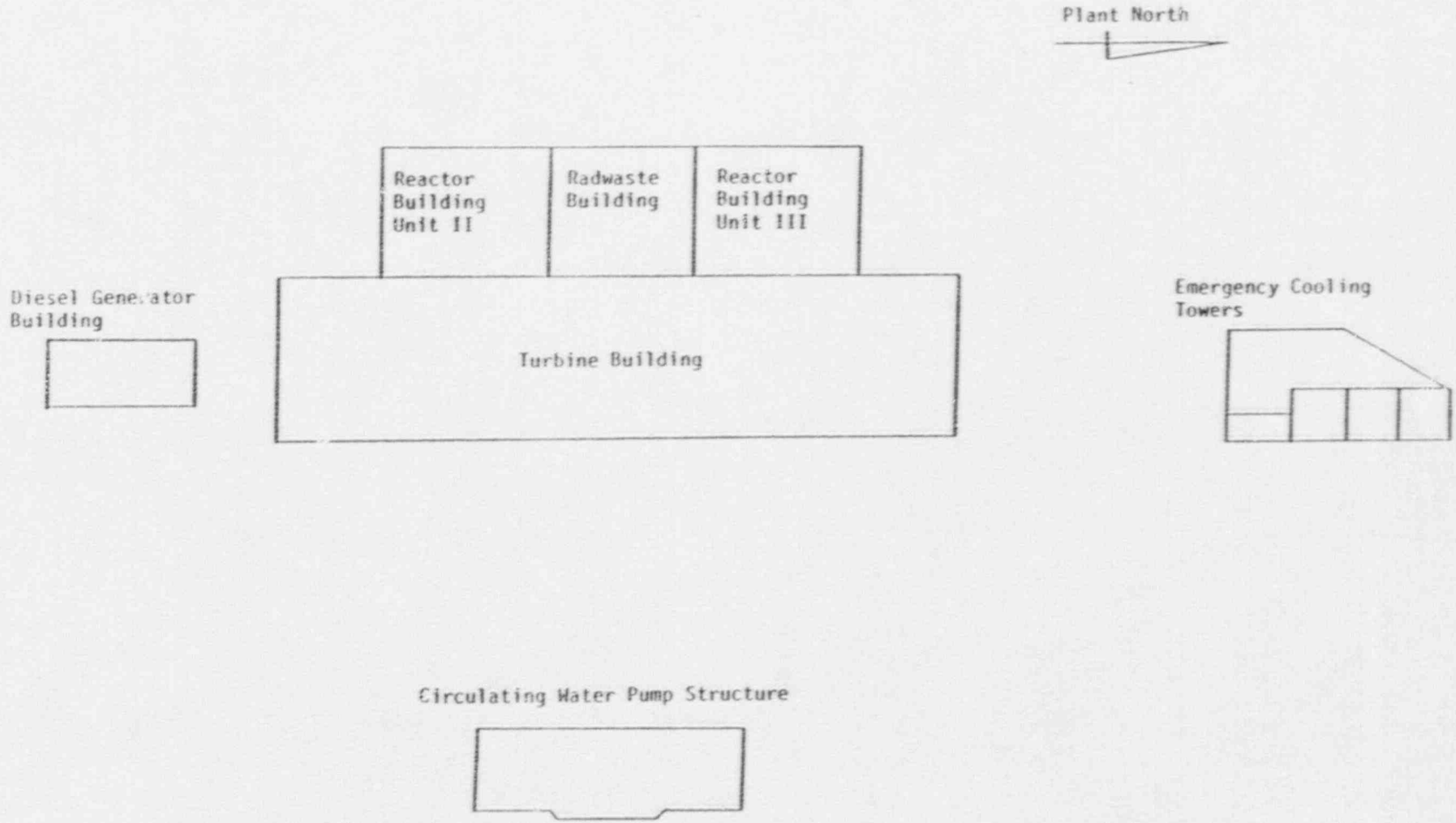

Figure 4.3. Peach Bottom Power Station General Arrangement

components were developed and used in a probabilistic response analysis to determine the best-estimate seismic response of these structures.

The balance of this section will describe and summarize:

- site and seismic characteristics
- probabilistic response analysis of each structure
- in-structure responses which define the response of safety-related components

4.2.2 Site and Seismic Characteristics

4.2.2.1 Site Description

The Peach Bottom Power Station site is characterized as a rock site (Reference 3). An outcrop zone of Peters Creek Schist exists throughout the site. Peters Creek Schist is a metamorphosed sedimentary rock of precambrian or early Paleozoic age. The outcropping zone is exposed 12 mi along the banks of the Susquenhanna River, 35 mi to the northeast, and 20 mi to the southwest. Original site topography was characterized by rugged heavily wooded terrain. The elevation ranges from 400 ft (west) to 110 ft (near Conowingo Pond) sloping steeply to the east toward the river. Overburden is a residual sandy silt and gravel derived by weathering of the underlying schist. Depth of the overburden varies from 10 to 60 ft, predominantly at 15 ft below original grade. All structures at the Peach Bottom Power Station are founded on sound rock, and hence, all structure analyses were performed using fixed-base models of the structures.

4.2.2.2 Earthquake Definition

The objective of the initial portion of the investigation was to define the input motion for the probabilistic response analyses of the structures.

The safe shutdown earthquake (SSE) for the Peach Bottom site is defined to have a peak horizontal ground acceleration of 0.12 g. Three seismic excitation levels were considered as defined by their peak ground acceleration in the horizontal direction--0.12 g (1 SSE), 0.24 g (2 SSE), 0.36 g (3 SSE). They are denoted acceleration ranges 1, 2, and 3 in subsequent discussions. These excitation levels were treated explicitly--input motions and probabilistic response for other levels defined by the hazard curve can then be interpolated from the results. A suite of ten earthquake time histories was defined and scaled to each of the three excitation levels for the analyses. Each of the acceleration time histories are recorded motions of actual earthquakes from rock sites. A total of five recorded earthquake acceleration time histories were selected and listed in Table 4.3. For the purpose of the analyses

a total of 10 input acceleration time histories in each orthogonal horizontal direction was created by rotation of the two recorded horizontal components. The median acceleration response spectrum of the ten horizontal components is shown in Figure 4.4 with median responses from a larger number of rock sites reported in Reference 4. The comparison shows frequency content and amplification for the median response of the ten components in each horizontal direction adequately represent expected motion at the Peach Bottom Power Station.

In general, soil properties such as shear modulus and damping are a function of soil strain and consequently a function of excitation level, i.e., acceleration ranges 1, 2, and 3 as defined above. With higher excitation levels, soil shear modulus tends to decrease while soil damping tends to increase. However, for the Peach Bottom Power Station rock site no difference between the low strain and strain compatible properties exists due to the rock nature of the site.

Table 4.3

Selected Free-Field Acceleration Time Histories for Probabilistic Response Analysis

Site	Date
Pacoima Dam	February 9, 1971
Castaic	February 9, 1971
Temblor	June 27, 1966
Helena	October 31, 1935
Taft, Lincoln School Tunel	July 21, 1952

4.2.3 Probabilistic Response Analysis

This section describes the probabilistic response analyses performed for each structural model. In each analysis, ten earthquake acceleration time histories were considered for each component direction of the 3-D models, and ten dynamic structural response calculations were performed for each structure of interest.

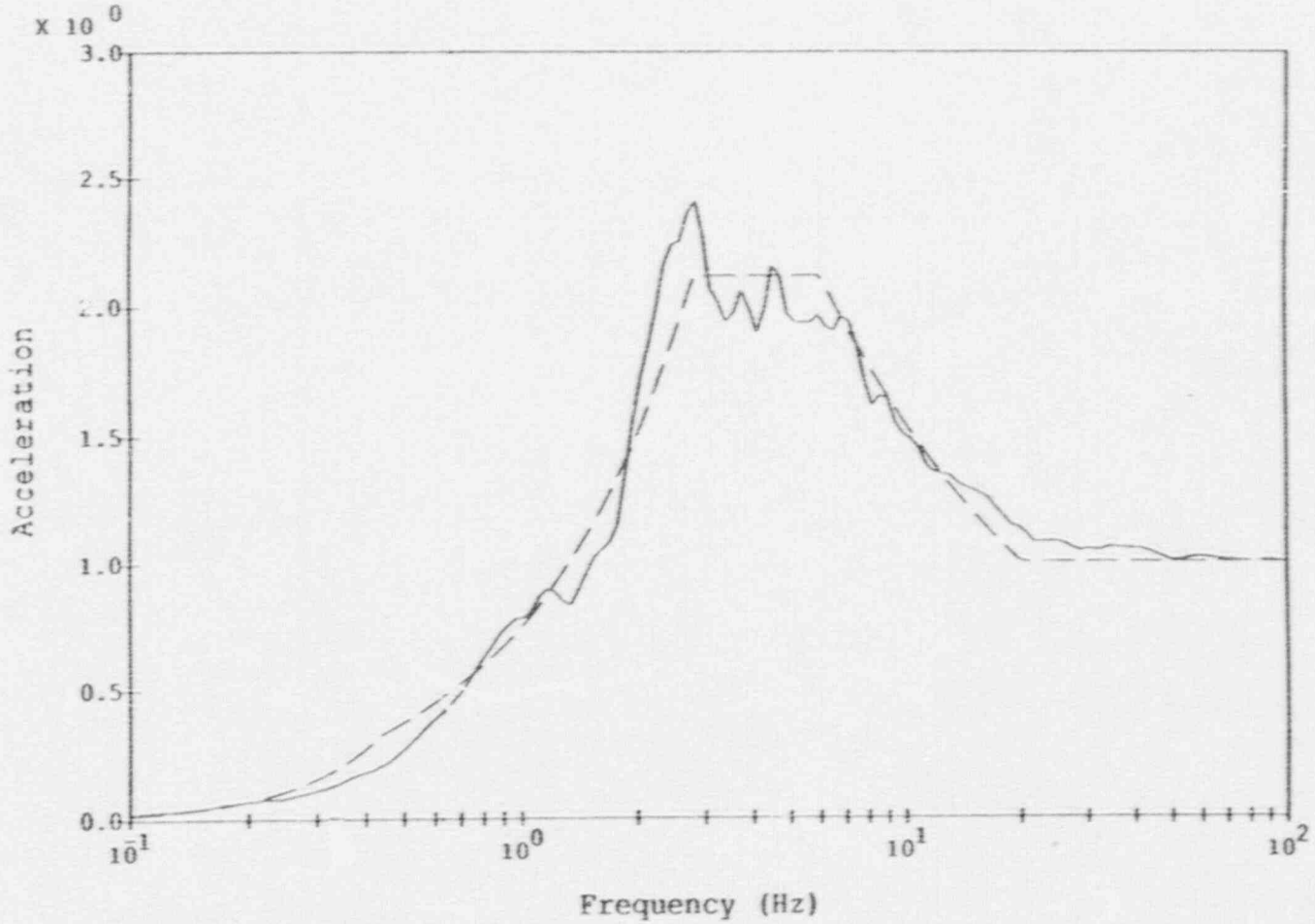

Legend:

Median of 10 Comp. _____

Rock 50% — — — — —

Notes:

All spectra calculated at 5% damping

Acceleration in units of g

Figure 4.4 Peach Bottom Power Station Median Free-Field Input Motion Compared to Median Rock Spectra from WASH-1255 (Ref. 12)

Specification of the free-field ground motion includes specifying its frequency characteristics, spatial variation, and control point. The frequency characteristics and spatial variation of the free-field motion were discussed above. The elevation at which the free-field is specified for each structure is the control point. Generally, this would be the existing free surface for the Peach Bottom Power Station Site. However, it is the base of the foundations which are founded on the bedrock regardless of elevation.

Structural dynamic characteristics are described by their fixed-base eigensystem and modal damping factors. Eigensystems (fundamental modes of vibration, natural frequencies and eigenvectors) are determined from fixed-base lumped mass finite element models. Beam elements represent stiffness between floor levels located at the shear centroid of the reinforced concrete walls or diagonal steel bracing, including shear deformation. The contribution to lumped mass at each floor level is from the half height of the wall above and below, floor slab, and equipment at that floor. Nominal values of structure damping were taken to be 0.07, 0.085, and 0.10 (fractions of critical damping) for the three seismic acceleration ranges considered. These were based on published damping values and assumed stress levels achieved.

The procedure is to perform a series of deterministic analyses, each simulating an earthquake occurrence, including variability in seismic input, soil-structure interaction, and in-structure representation. The seismic input variability is normally introduced by considering an ensemble of earthquake motions. For this study, the five earthquake motions described earlier were used. A series of ten earthquake simulations for each acceleration range were performed, with each acceleration range using the identical free-field input motion as a starting point. Structure response variability is introduced through a limited number of parameters--structure frequency and modal damping. (Since this is a rock site, no soil column variability had to be considered.) Variability in structure dynamic behavior is modeled by treating structure frequency and modal damping as random variables. Parameter variations in each step of the response analysis were selected to represent random variability, and not to include modeling uncertainty. The assumed parameter variability corresponds to that determined in the SSMRP (Ref. 5). The parameter values for each of the ten simulations were selected from the probability distributions by dividing the distributions into equally probable segments, sampling from each segment and combining the samples using a Latin hypercube experimental design. The responses calculated from the simulations were combined to estimate median responses conditional on the occurrence of an earthquake described by a particular hazard curve parameter, e.g., peak ground acceleration.

For each acceleration range the median instructure acceleration response spectra from the ten free-field input motions were calculated at 5 percent damping at the mass centroid of each floor elevation and for each translational component direction.

The structures for which best-estimate dynamic responses were computed based on the 10 selected time histories are shown in Table 4.4 along with their lowest natural (fixed-based) frequencies in each direction. Each structure considered is described below.

Reactor Building. The reactor building is a reinforced concrete structure from its foundation at elevation 91 ft to the refueling floor at elevation 234 ft. Above the refueling floor elevation exists a structural steel superstructure with metal siding and decking. The building is nominally 150 ft by 150 ft in plan below elevation 135 ft and 150 ft by 120 ft in plan above this level. A reinforced concrete mat foundation supports the primary containment and internal structure. The foundation mat rests on sound rock.

Figure 4.5 shows the 3-D fixed base model used to calculate the nominal eigenvalues and eigenvectors of the reactor building containment and internal structure. A structural model provided by the utility consisted of a single stick model providing overall response of the structure. An internal structure model is coupled with the utility model directly at its base and through equivalent stabilizer stiffnesses at elevation 195'-0". The internal structure model includes the reactor vessel pedestal, sacrificial shield wall, and reactor pressure vessel for determining stiffness and mass properties.

Radwaste/Turbine Building. The radwaste/turbine building is a reinforced concrete structure, rectangular in plan supported on a reinforced concrete mat at elevation 91.5 ft and extending in height to elevation 191 ft. The foundation mat rests on sound rock.

Figure 4.6 shows the 3-D fixed base model used to calculate the nominal eigenvalues and eigenvectors of the reactor building containment and internal structure developed for this effort. The radwaste building foundation is tied to the adjacent turbine building foundation. In addition both structures share lateral force resisting systems. Stiffness and mass contributions from the turbine building are incorporated in the structural model to the extent structural details and load paths dictate. Outriggers and massless beams transfer motion from the center of mass of the common structures to the center of the radwaste building control room.

Circulating Water Pump Structure. The circulating water pump structure is a reinforced concrete structure, rectangular in plan supported on a reinforced concrete mat at elevation 79.83 ft and extending in height to elevation 130.5 ft. The foundation mat rests on sound rock.

Figure 4.7 shows the 3-D fixed base model used to calculate the nominal eigenvalues and eigenvectors of the circulating water pump structure. The structural model developed for this effort consists of lumped

Table 4.4 Peach Bottom Structural Models

Structure	Freq(Hz)	Dir	% Mass
Reactor Building	7.1	N-S	68
	7.6	E-W	71
	18.5	Vert	72
Radwaste/Turbine Building	9.3	N-S	81
	11.4	E-W	57
	24.5	Vert	70
Circulating Water Pump Structure	13.4	N-S	86
	20.6	E-W	70
	46.0	Vert	57
Emergency Cooling Tower	9.7	N-S	36
	10.4	E-W	79
	19.3	N-S	61
	27.0	Vert	79
Diesel Generator Building	17.5	N-S	99
	21.8	E-W	97
	47.7	Vert	92

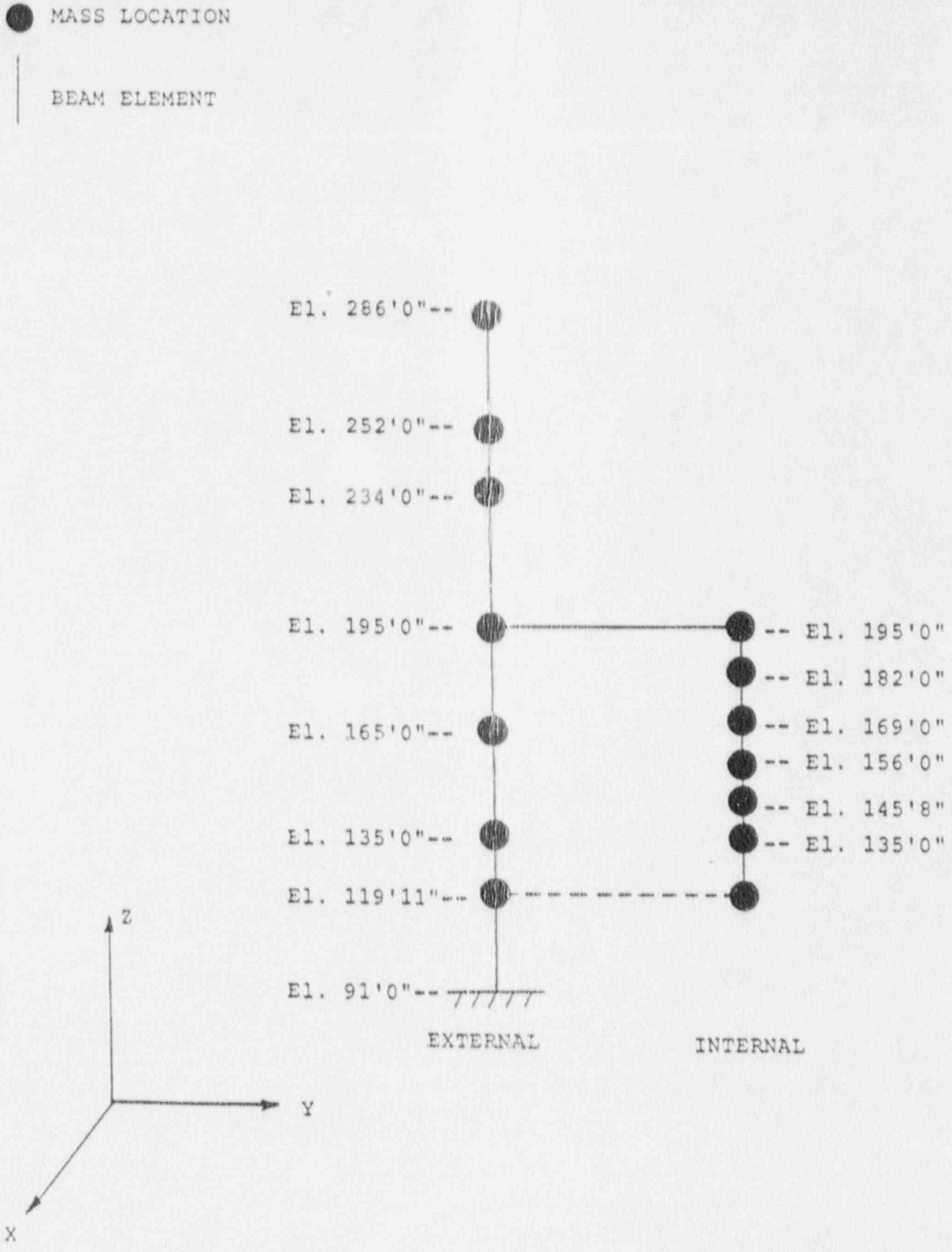

Figure 4.5 Peach Bottom Atomic Power Station Reactor Building Structural Model

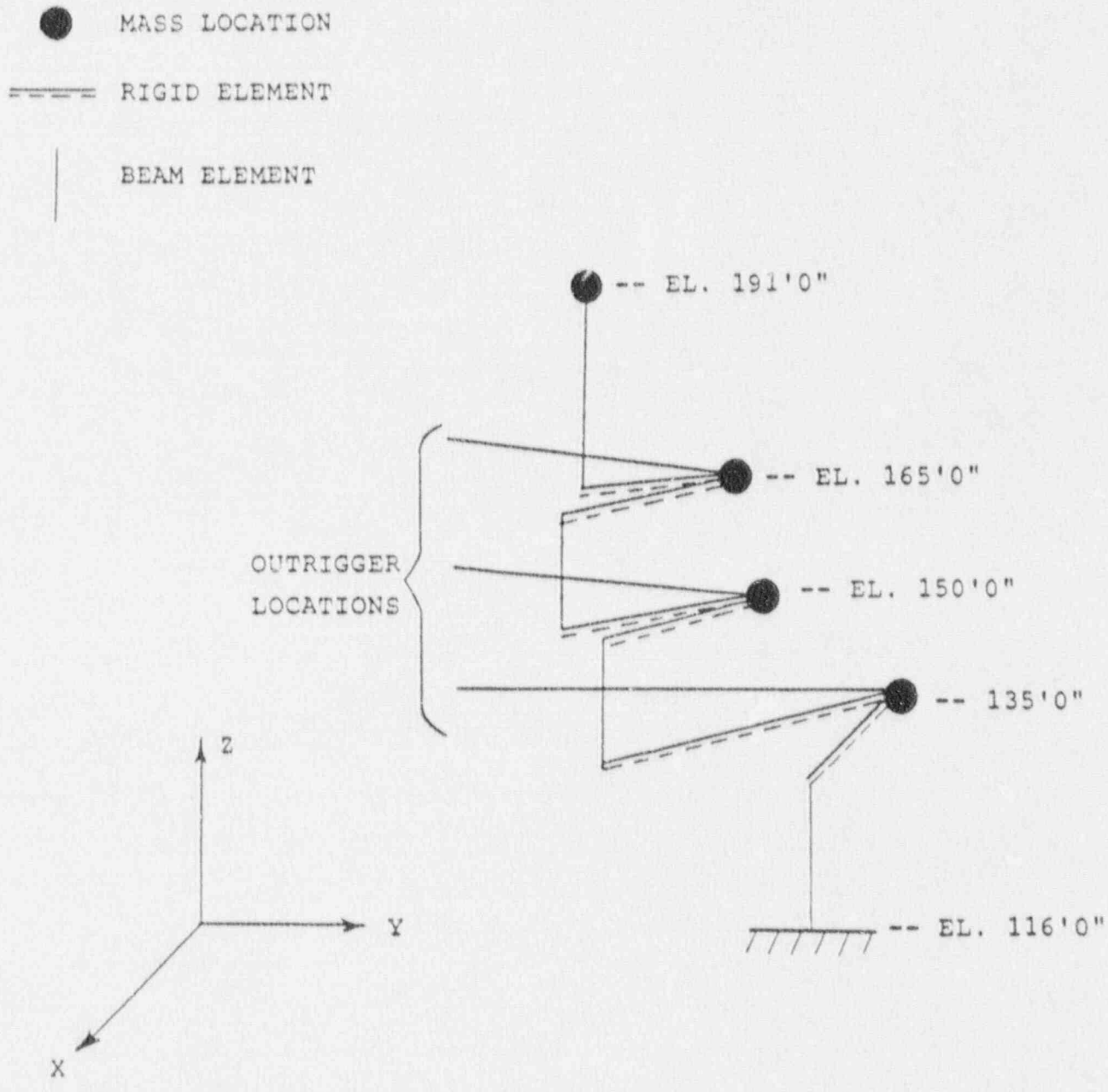

Figure 4.6 Peach Bottom Atomic Power Station Radwaste/ Turbine Building

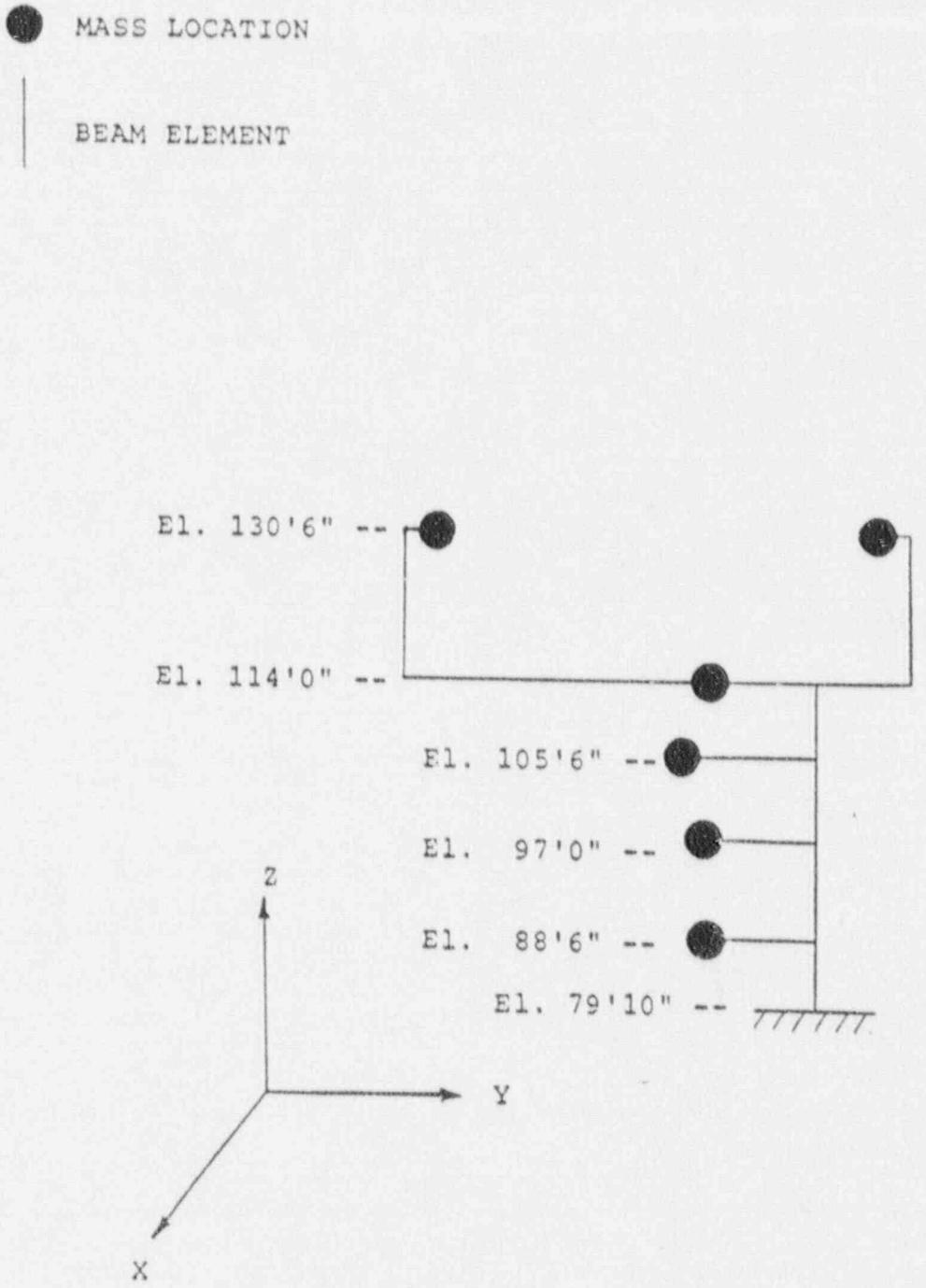

Figure 4.7 Peach Bottom Atomic Power Station
Circulating Water Pump Structure

masses located at the mass centroid of the floor levels, and beam elements representing the stiffness between floor levels. Included in the masses are structure, water (normal water level elevation 109'-0") and equipment weight. Effective water mass was taken as the rigid tank impulsive fluid mass.

Emergency Cooling Tower. The emergency cooling tower is a reinforced concrete structure, rectangular in plan supported on a reinforced concrete mat at elevation 118 ft and extending in height to elevation 202 ft. The foundation mat rests on sound rock.

Figure 4.8 shows the 3-D fixed-base model used to calculate the nominal eigenvalues and eigenvectors of the emergency cooling tower provided by the utility. This model was used without any modifications.

Diesel Generator Building. The diesel generator building is a reinforced concrete structure, rectangular in plan supported on a reinforced concrete mat with shear walls at various elevations and extending in height to elevation 162 ft. The foundation footings rest on sound rock.

Figure 4.9 shows the 3-D fixed-base model used to calculate the nominal eigenvalues and eigenvectors of the diesel generator building provided by the utility with the following modification. Portions of the structure below elevation 127 ft were not included in the model since this portion of the structure is rigid and founded on sound rock. Therefore, the free-field input motion rock outcrop is applied at elevation 127 ft.

Response Results

For each of these structures, the dynamic structural response for each of the ten suites of time histories was computed at each of the three earthquake excitation levels. From the computed time history responses at the different floor levels, response spectra were generated. As examples of the output, the computed response spectra for the 2SSE acceleration range for each structure are shown in Figures 4.10 through 4.14. In each figure, spectra in the E-W, N-S and vertical directions are shown. Each spectra plot has several building elevations (corresponding to major floor slabs). Similar spectra are given in Appendix A for the other acceleration ranges. Taken together, the spectra at the three different acceleration ranges provide all the response input needed for the seismic PRA.

4.2.4 Safety-Related Component Responses

The in-structure spectra presented in the previous section are used to determine safety-related component response. Assuming that the dynamic characteristics of a given component can be represented by a single dominant mode of vibration, the component response can be approximated by the spectral acceleration of the appropriate in-structure spectra at the frequency of the dominant mode.

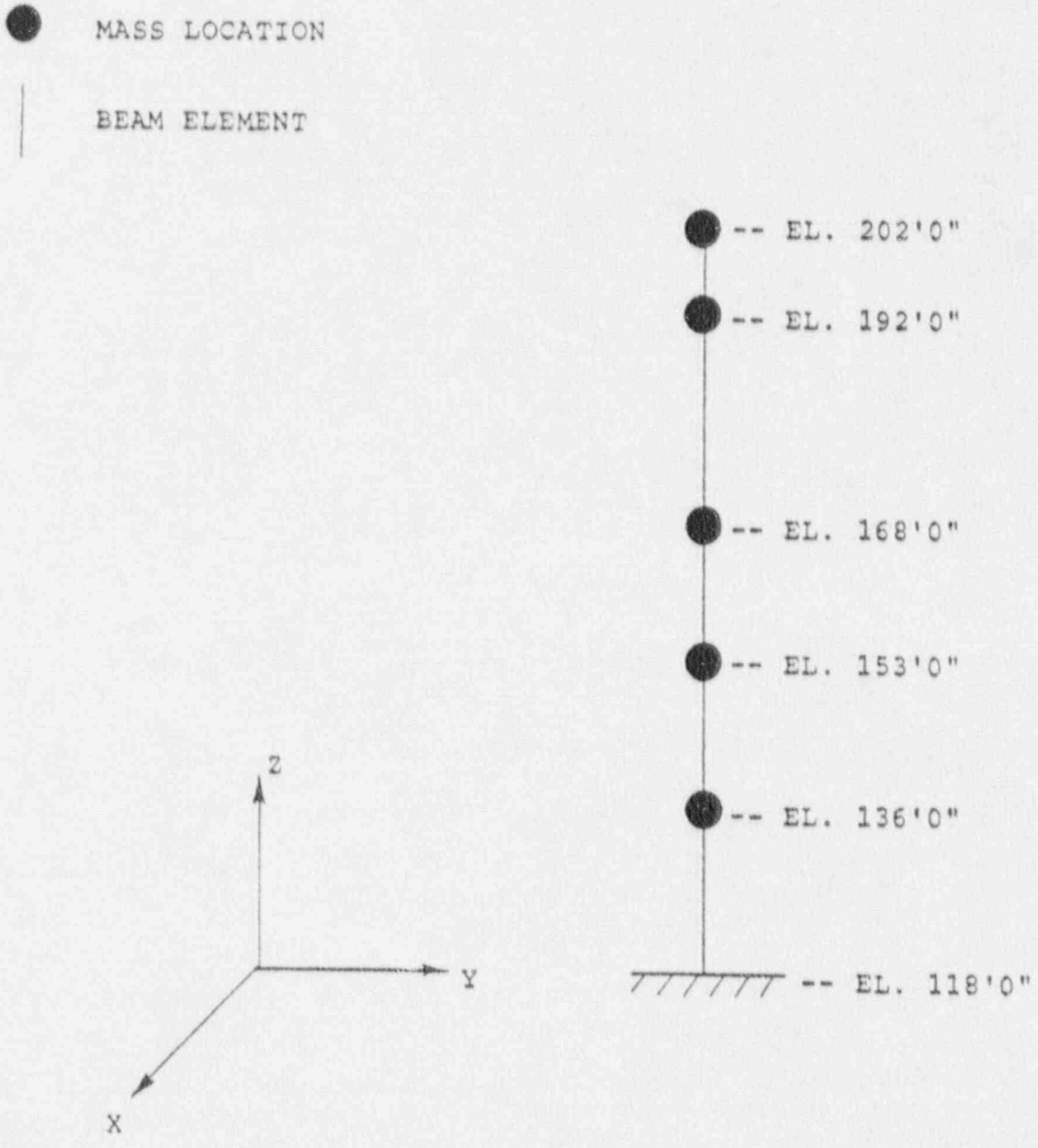

Figure 4.8 Peach Bottom Atomic Power Station Emergency Cooling Towers Structural Model

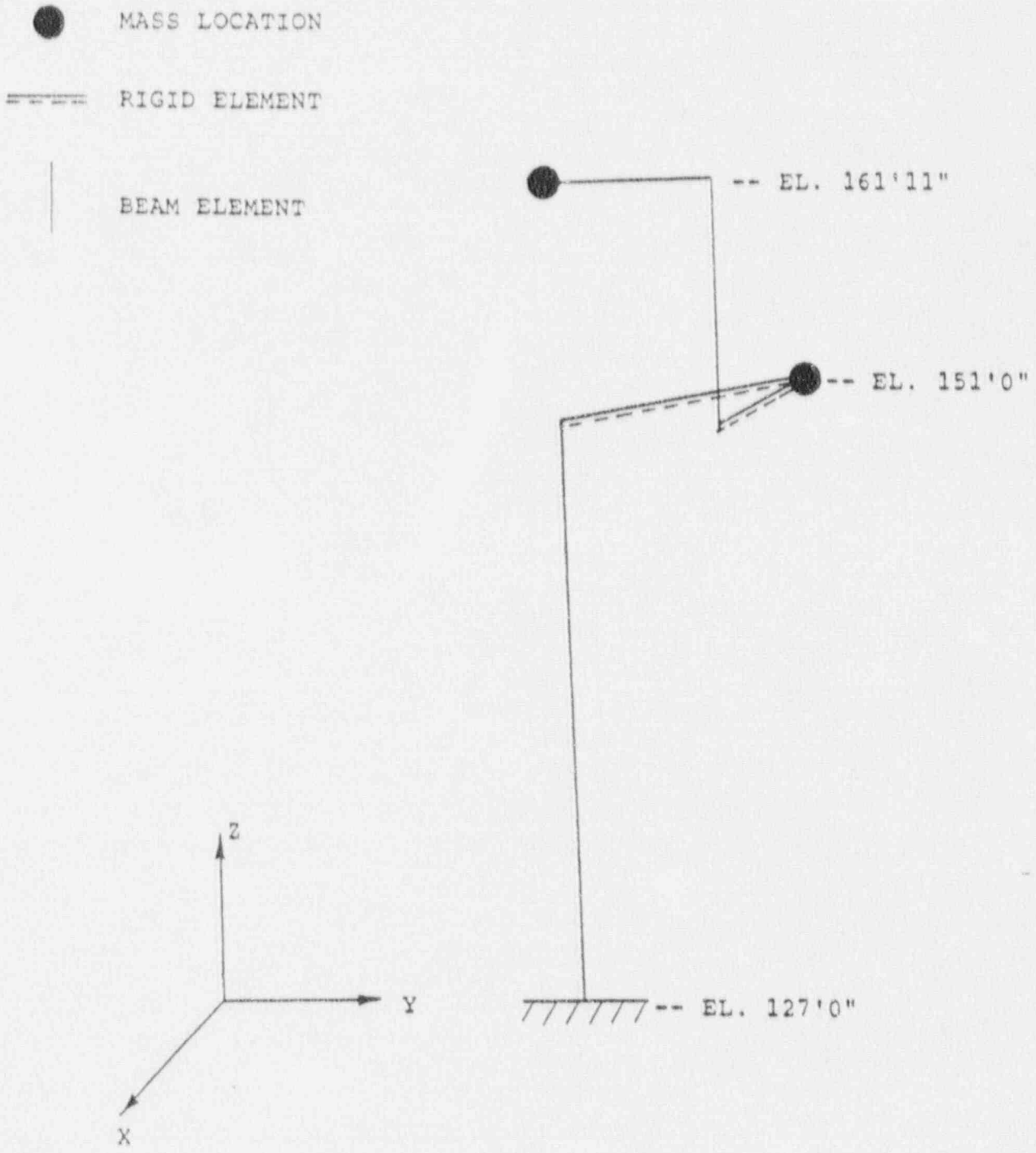

Figure 4.9 Peach Bottom Atomic Power Station Diesel Generator Building Structural Model

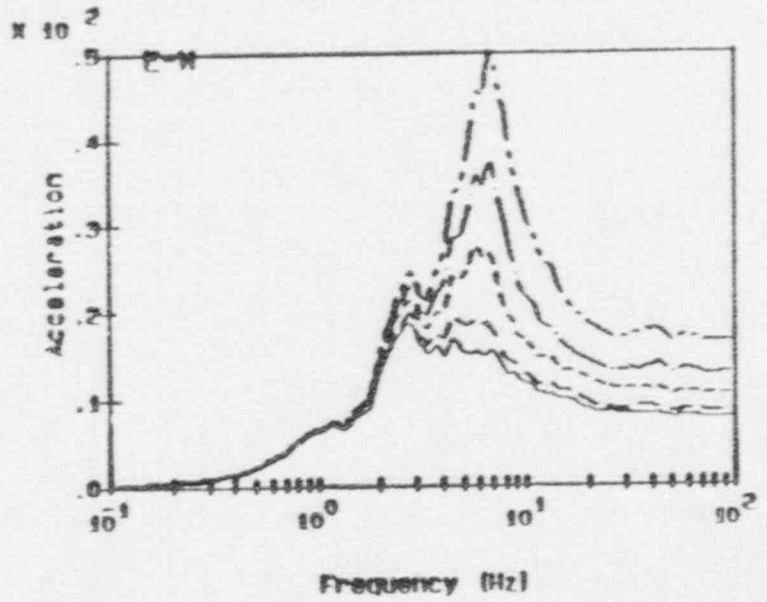

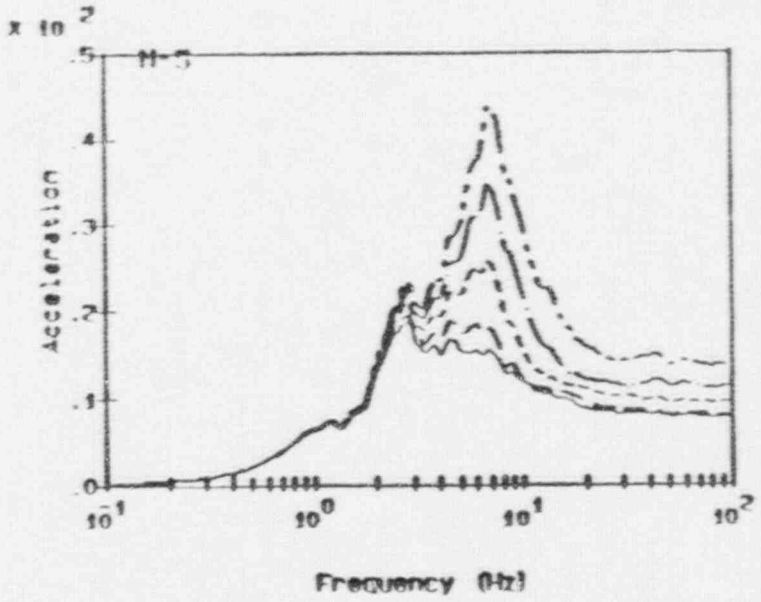

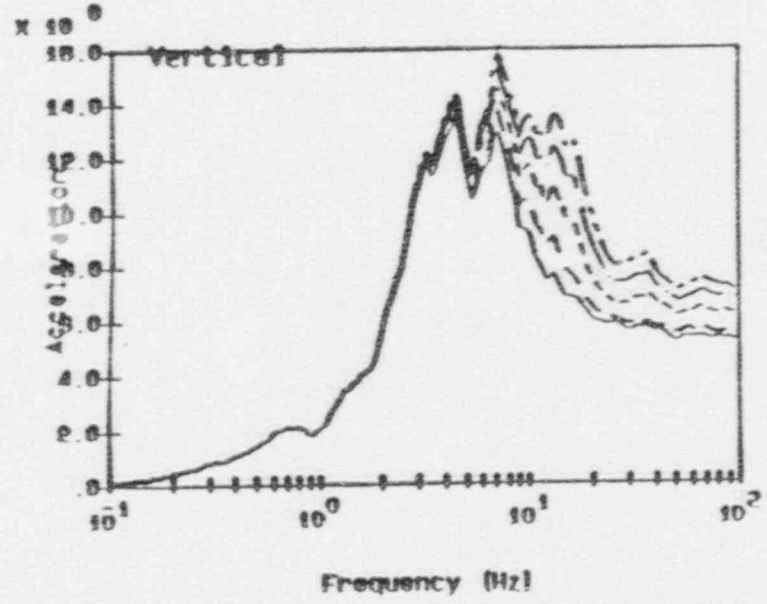

Legend:

free-field
el 135°-0°
el 165°-0°
el 195°-0°
el 234°-0°

Notes:

accelerations in units of ft/s/s
spectra calculated at 5% damping

Figure 4.10a Peach Bottom Atomic Station Reactor/Containment Bldg
Instructure Responses for Acceleration Range 2

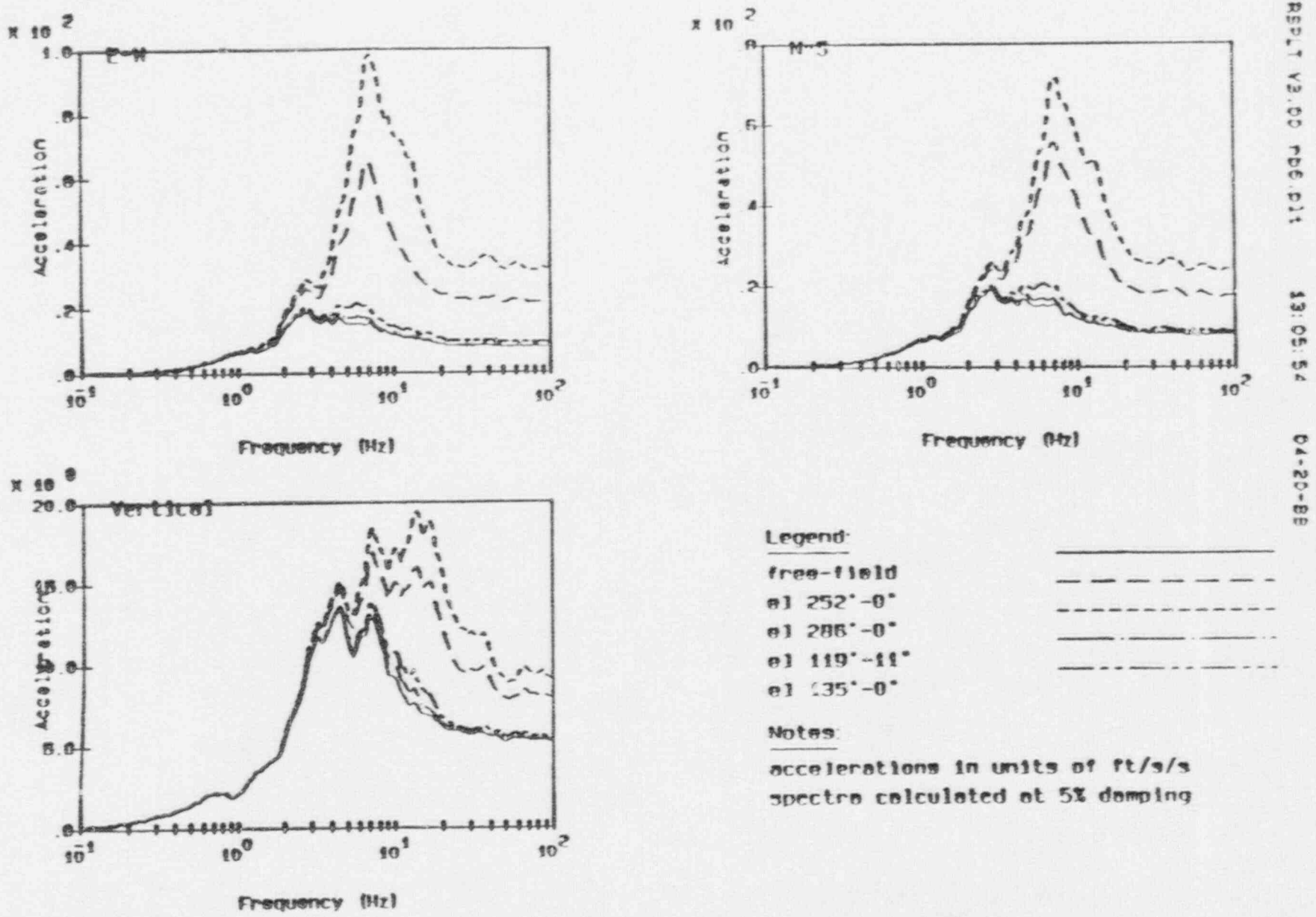

Figure 4.10b Peach Bottom Atomic Station Reactor/Containment Bldg
Instructure Responses for Acceleration Range 2

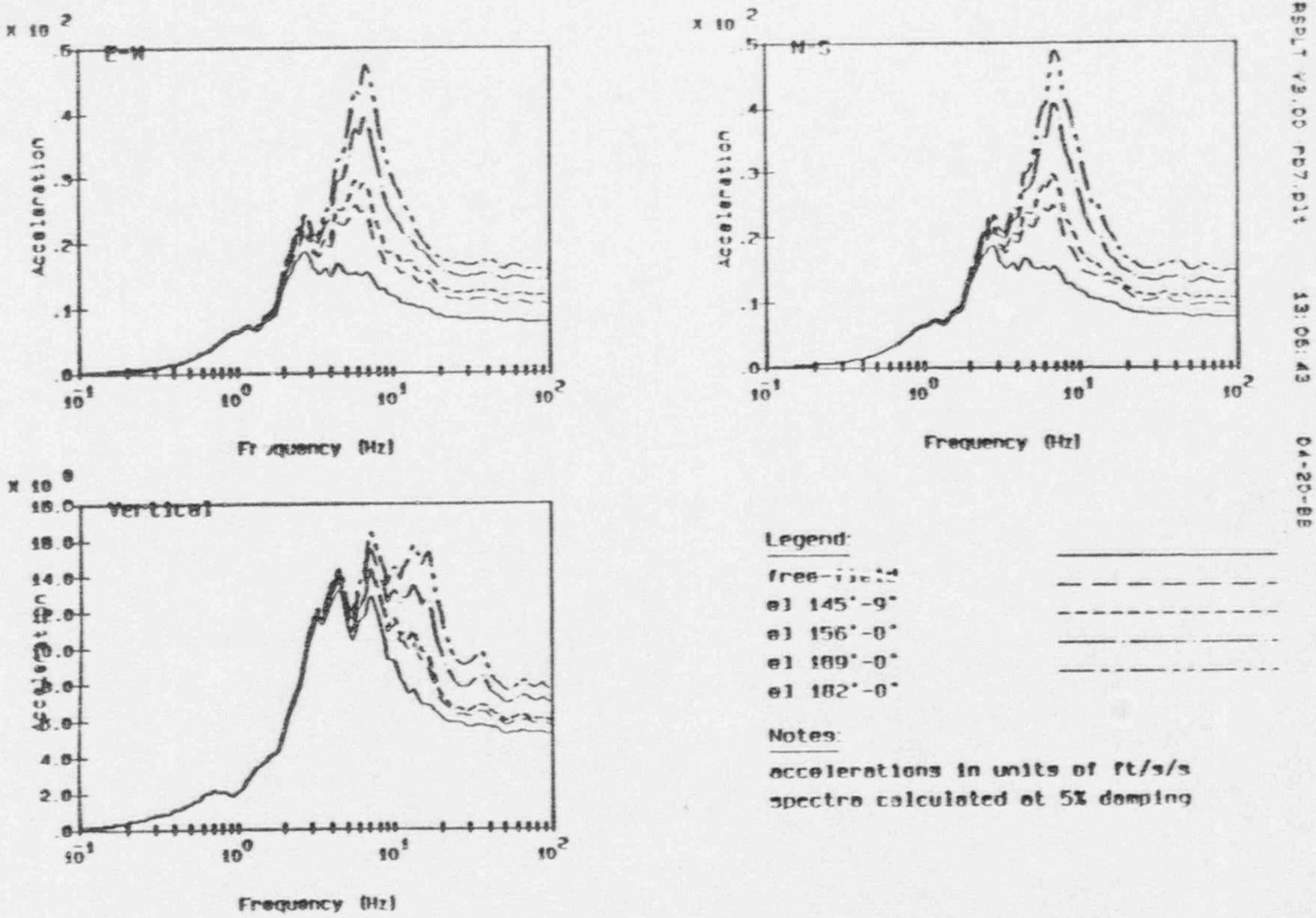

Figure 4.10c Peach Bottom Atomic Station Reactor/Containment Bldg Instructure Responses for Acceleration Range 2

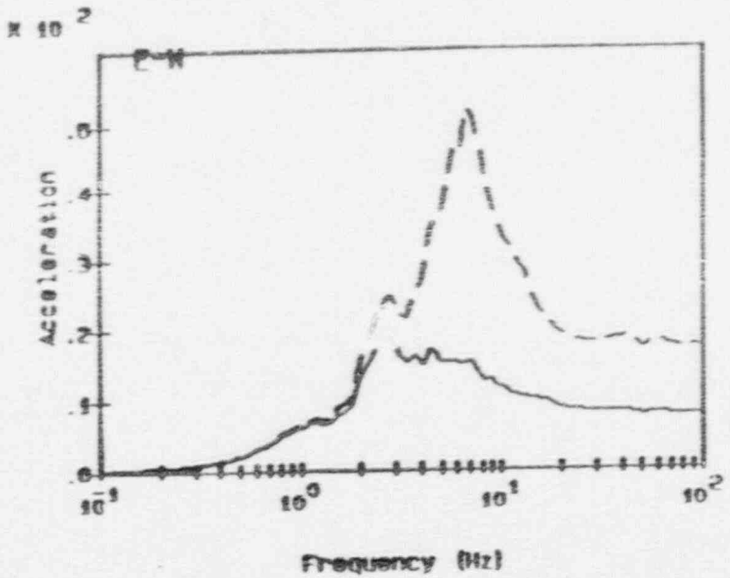

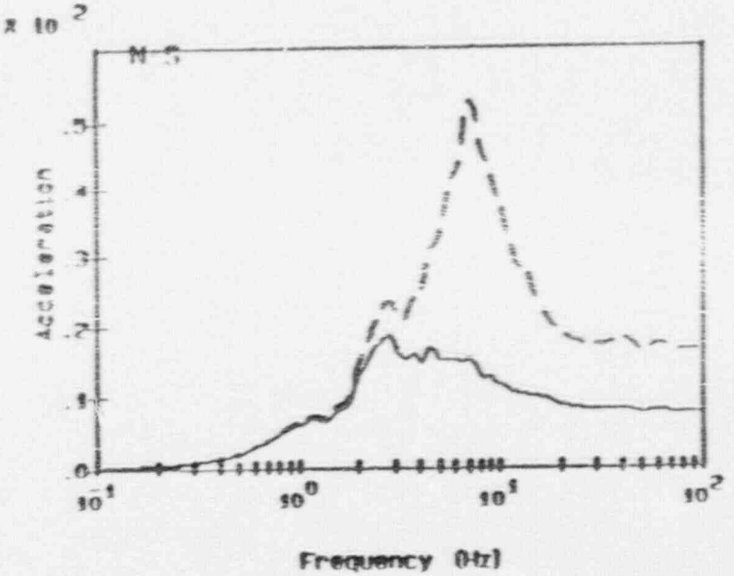

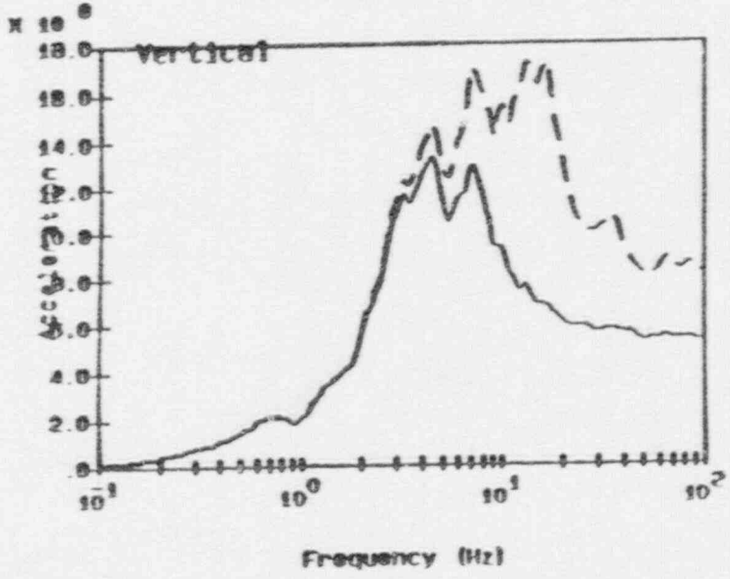

Legend:

free-field ——————————

el 195'-0" — — — — — — —

Notes:

accelerations in units of ft/s/s

spectra calculated at 5% damping

Figure 4.10d Peach Bottom Atomic Station Reactor/Containment Bldg Instructure Responses for Acceleration Range 2

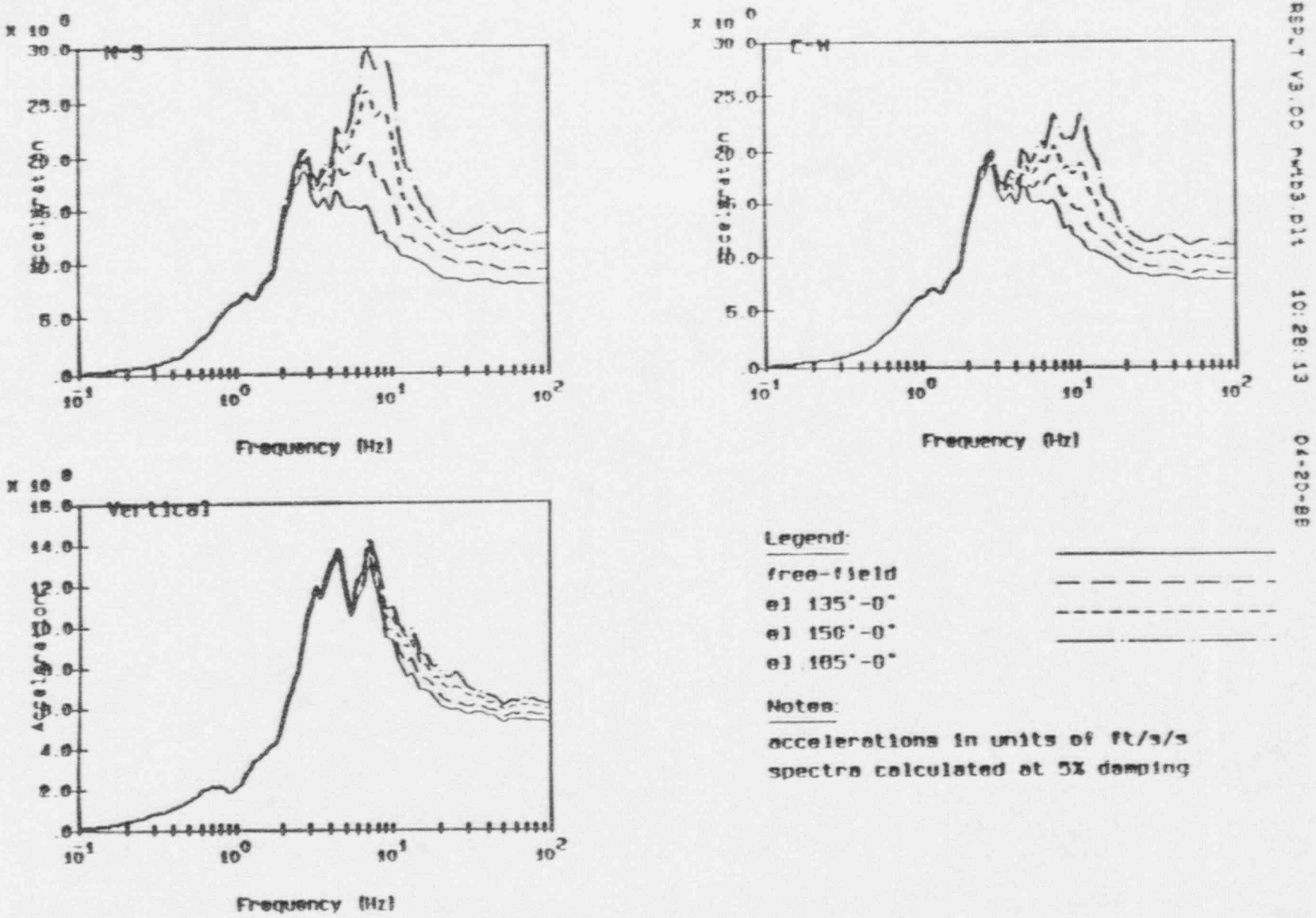

Figure 4.11a Peach Bottom Atomic Station Radwaste/Turbine Building Instructure Responses for Acceleration Range 2

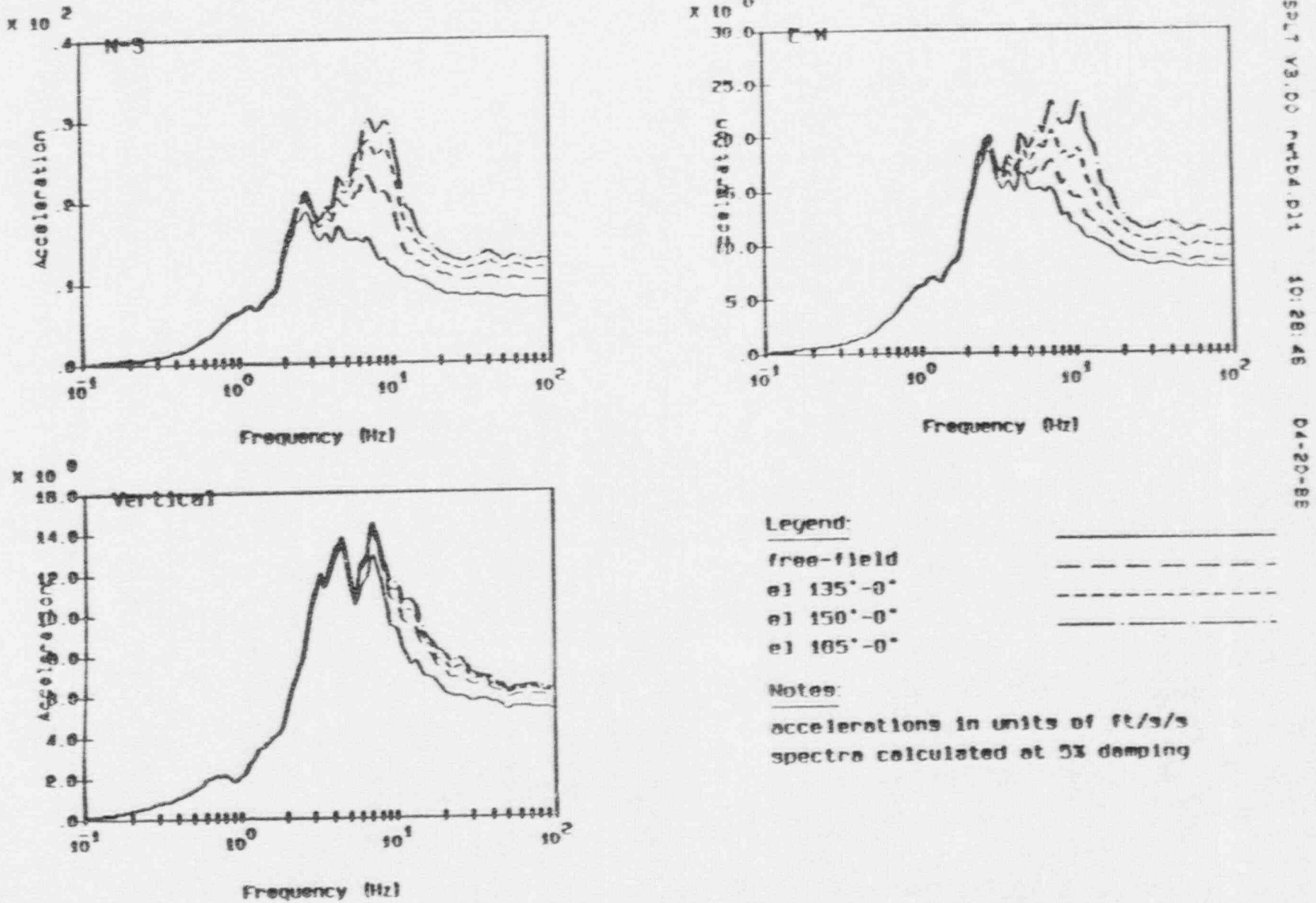

Figure 4.11b Peach Bottom Atomic Station Radwaste/Turbine Building Instructure Responses for Acceleration Range 2

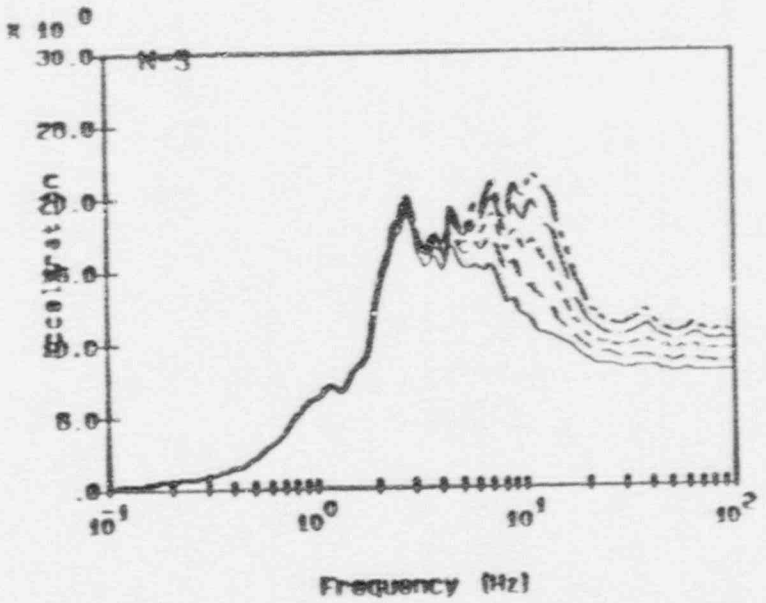

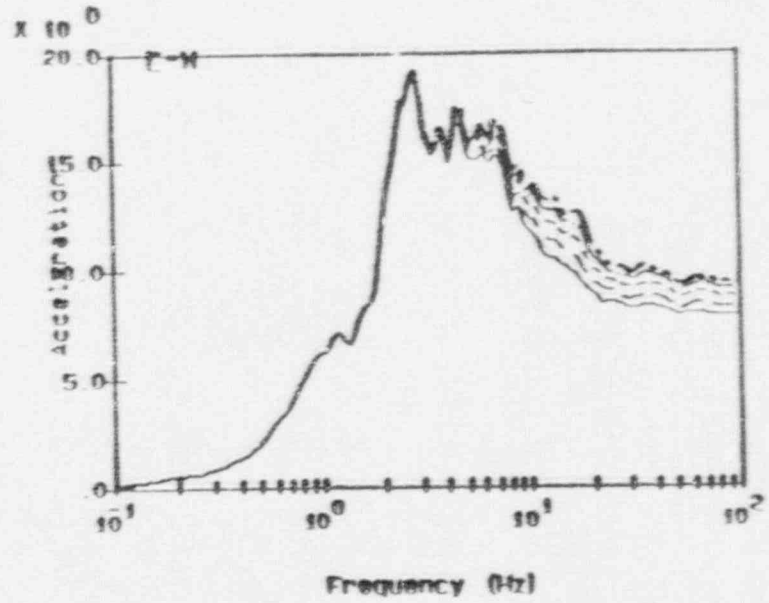

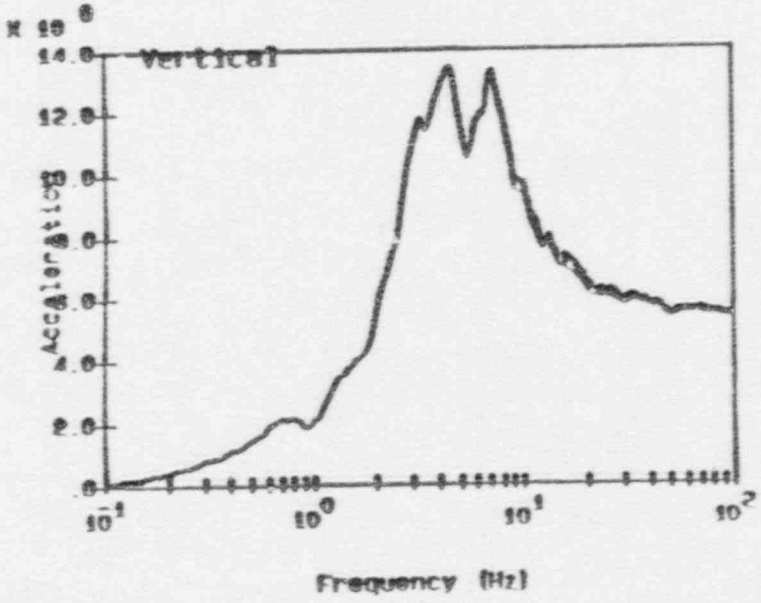

Legend:

free-field

el 88' - 6"

el 97' - 0"

el 105' - 8"

el 114' - 0"

Notes:

accelerations in units of ft/s/s

spectra calculated at 5% damping

Figure 4.12a Peach Bottom Atomic Station Circulating Water Pump Bldg Instructure Responses for Acceleration Range 2

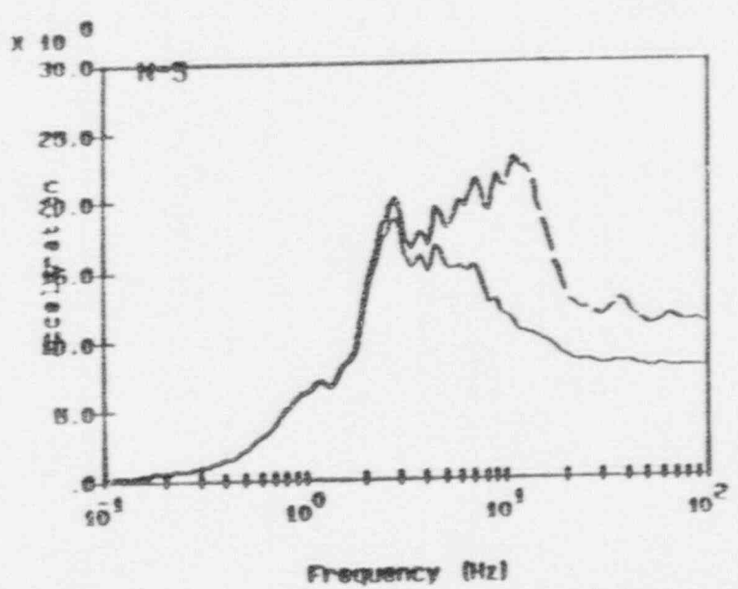

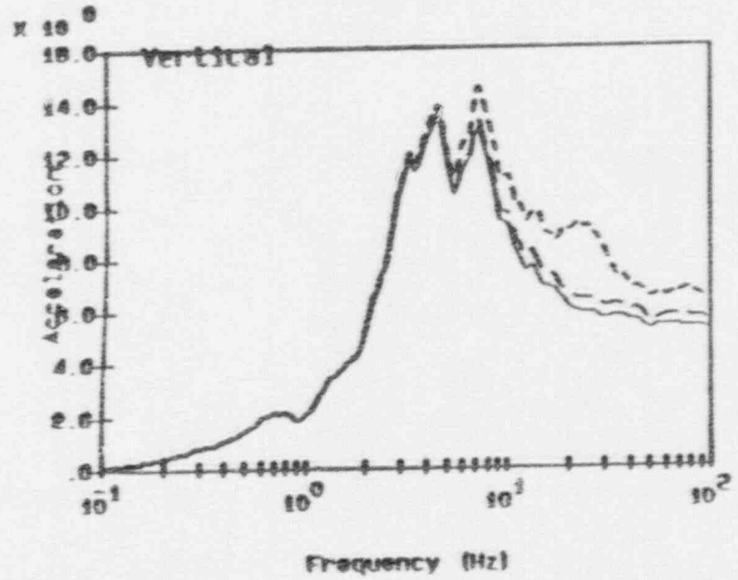

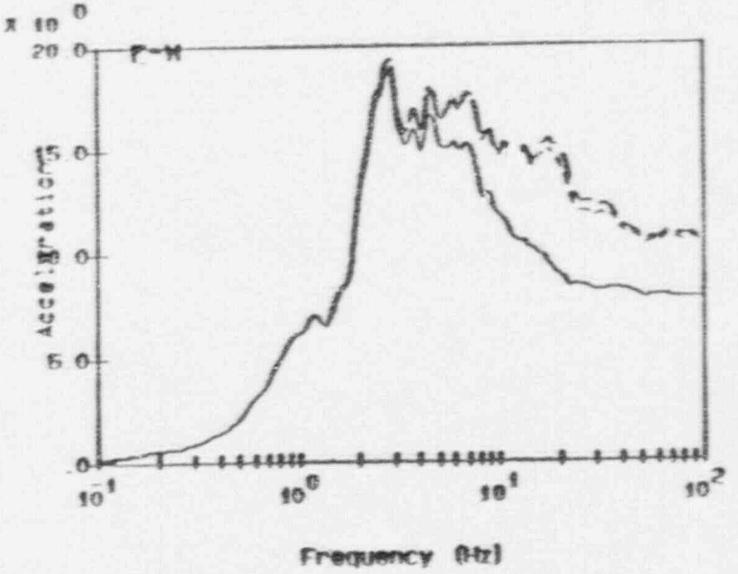

Legend:

free-field

el 130'6" (#17)

el 130'6" (#20)

Notes:

accelerations in units of ft/s/s

spectra calculated at 5% damping

Figure 4.12b Peach Bottom Atomic Station Circulating Water Pump Bldg Instructure Responses for Acceleration Range 2

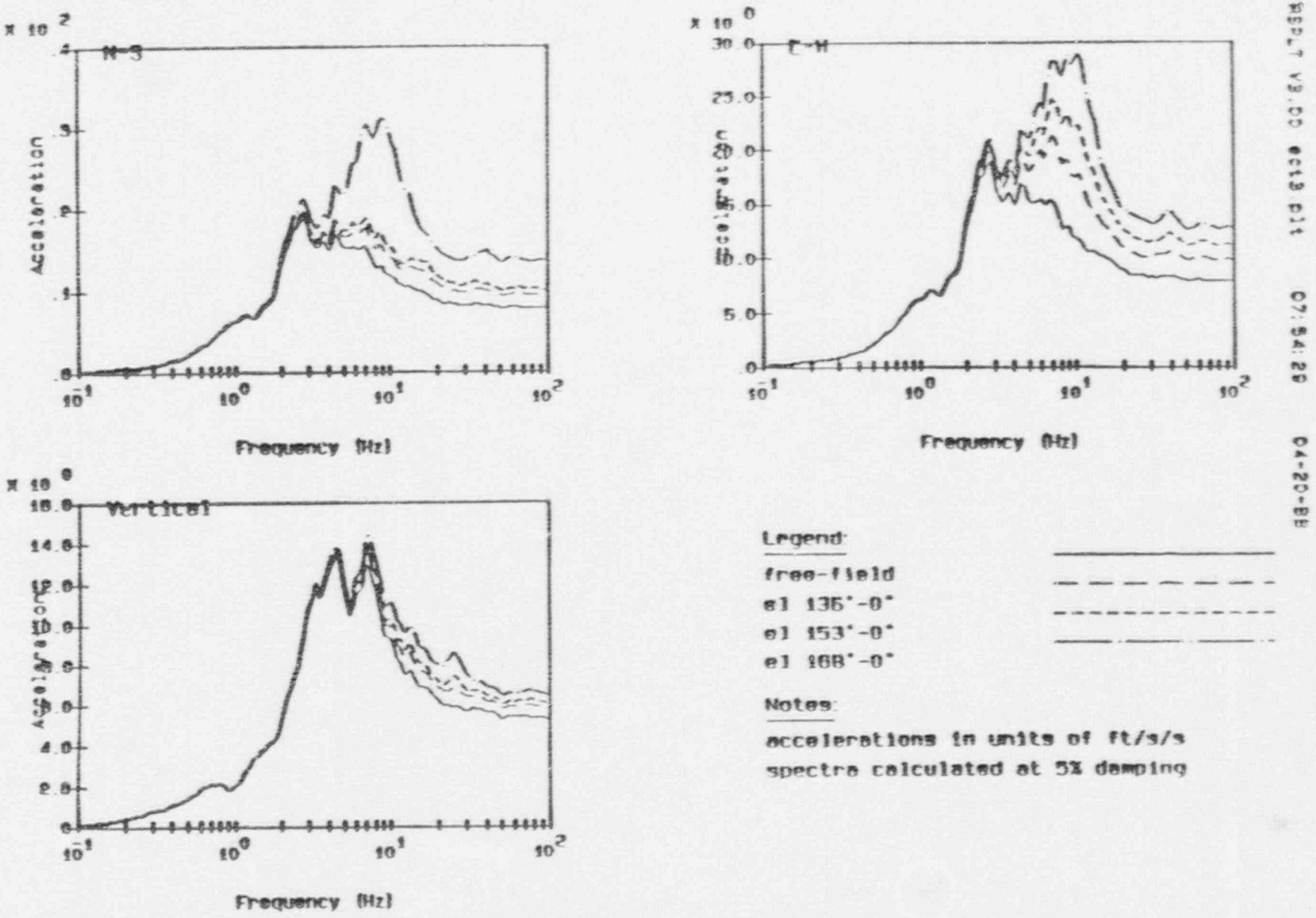

Figure 4.13a Peach Bottom Atomic Station Emergency Cooling Towers
Instructure Responses for Acceleration Range 2

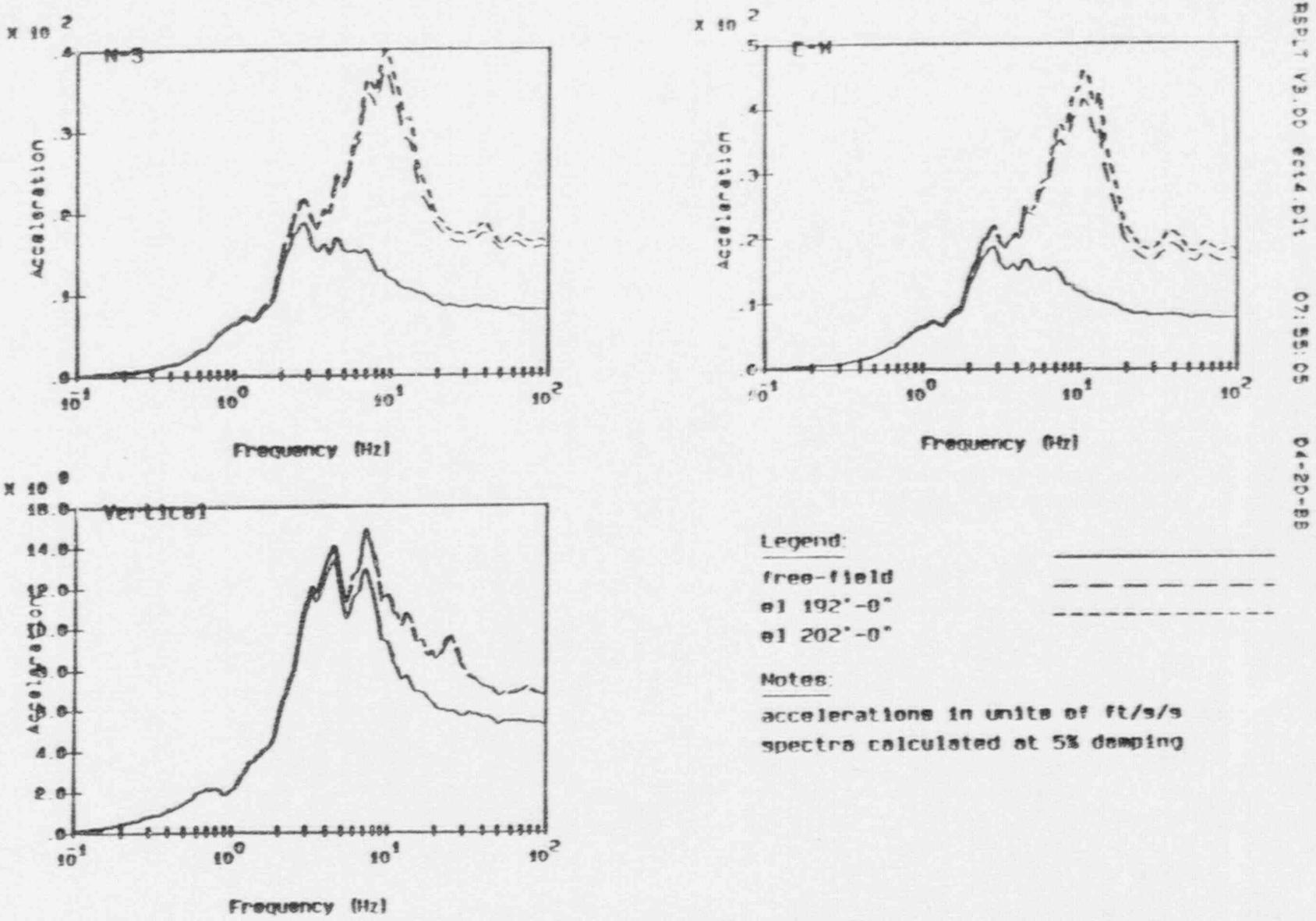

Figure 4.13b Peach Bottom Atomic Station Emergency Cooling Towers
Instructure Responses for Acceleration Range 2

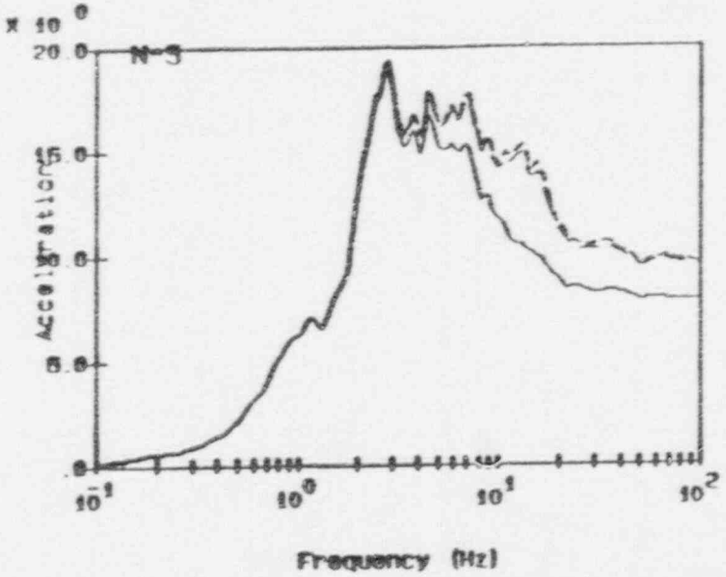

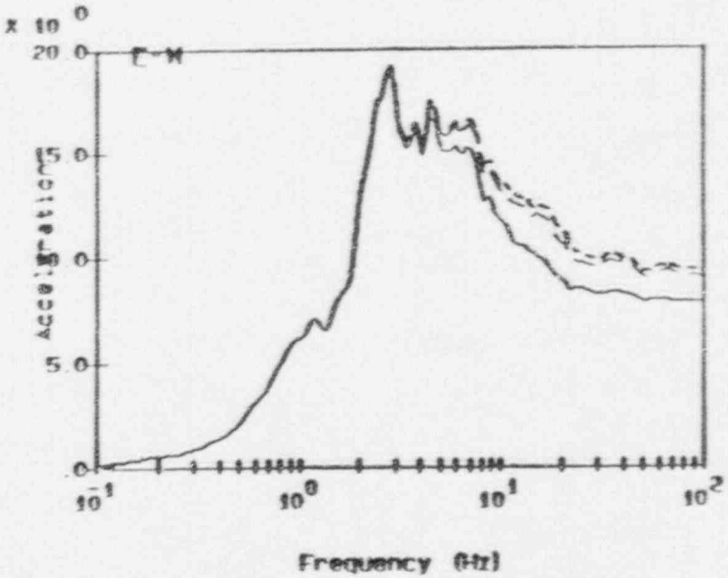

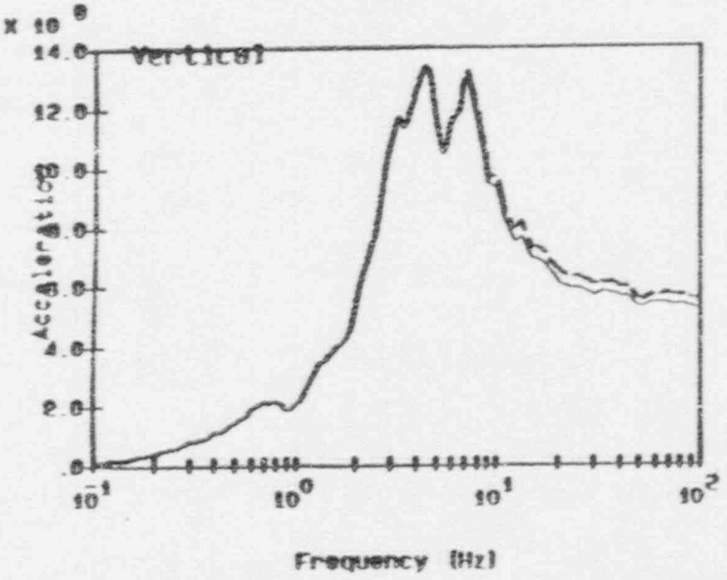

Legend:

free-field

el 151°-0"

el 161°-11"

Notes:

accelerations in units of ft/s/s

spectra calculated at 5% damping

RSPLT V3.00 0692 011 08:35:34 04-20-88

Figure 4.14 Peach Bottom Atomic Station Diesel Generator Building
Instructure Responses for Acceleration Range 2

Thus, at each structural location, numerical response values at different frequencies or frequency ranges are computed directly from these spectra. These ranges span the probable natural frequencies of the components housed at that location. The median zero period acceleration response is calculated from the ten values given by the probabilistic response analysis assuming a lognormal distribution. The median response over a frequency range is computed over the range from the median spectra given by the ten earthquake simulations. Given the natural frequency of the component of interest, the appropriate frequency interval and component response is then defined. Numerical values of the median component responses for the three levels of ground motion (1 SSE, 2 SSE, and 3 SSE) taken from these spectra are presented in Appendix B.

4.2.4.1 Responses in Terms of Peak Ground Acceleration (PGA)

The responses in Appendix B are given at three peak ground acceleration values (0.12 g, 0.24 g, and 0.36 g). One could directly interpolate between these three values to obtain any specified response at any arbitrary value of peak ground acceleration.

However, a more direct approach which greatly simplifies computation of the component failure probabilities is to compute the average ratio between the median PGA and the median response spectral acceleration at each specified component location. Figures 4.15 through 4.19 are plots of the response location accelerations in each building (at various building elevations) versus PGA. It can be seen that a linear relation exists up to free field accelerations of 0.4 g or greater. Furthermore, for those curves which show significant non-linearity at higher acceleration levels, the linear relation provides a conservative estimate of the local response.

From these figures, ratios between the various responses and PGA were determined, as listed in Table 4.5. (Note that not all responses listed in Appendix B are included on this table, as not all floor slabs supported critical components identified on the seismic fault trees.) Using these response amplification ratios, the local spectral acceleration response at any floor level of any of the buildings can be computed at any PGA level.

4.2.4.2 Variability in Response

Variability in responses (floor and spectral accelerations) was assigned based on SSMRP results (Ref. 5). Confidence bounds were computed for the final core melt probabilities using both random (irreducible) and systematic (modeling) uncertainties. The uncertainties (expressed as standard deviations of the logarithms of the responses) are shown below:

Quantity	Random	Systematic
Peak Ground Acceleration	0.25	See cross-reference table in Appendix C
Floor Zero Period Acceleration	0.35	
Floor Spectral Acceleration	0.45	

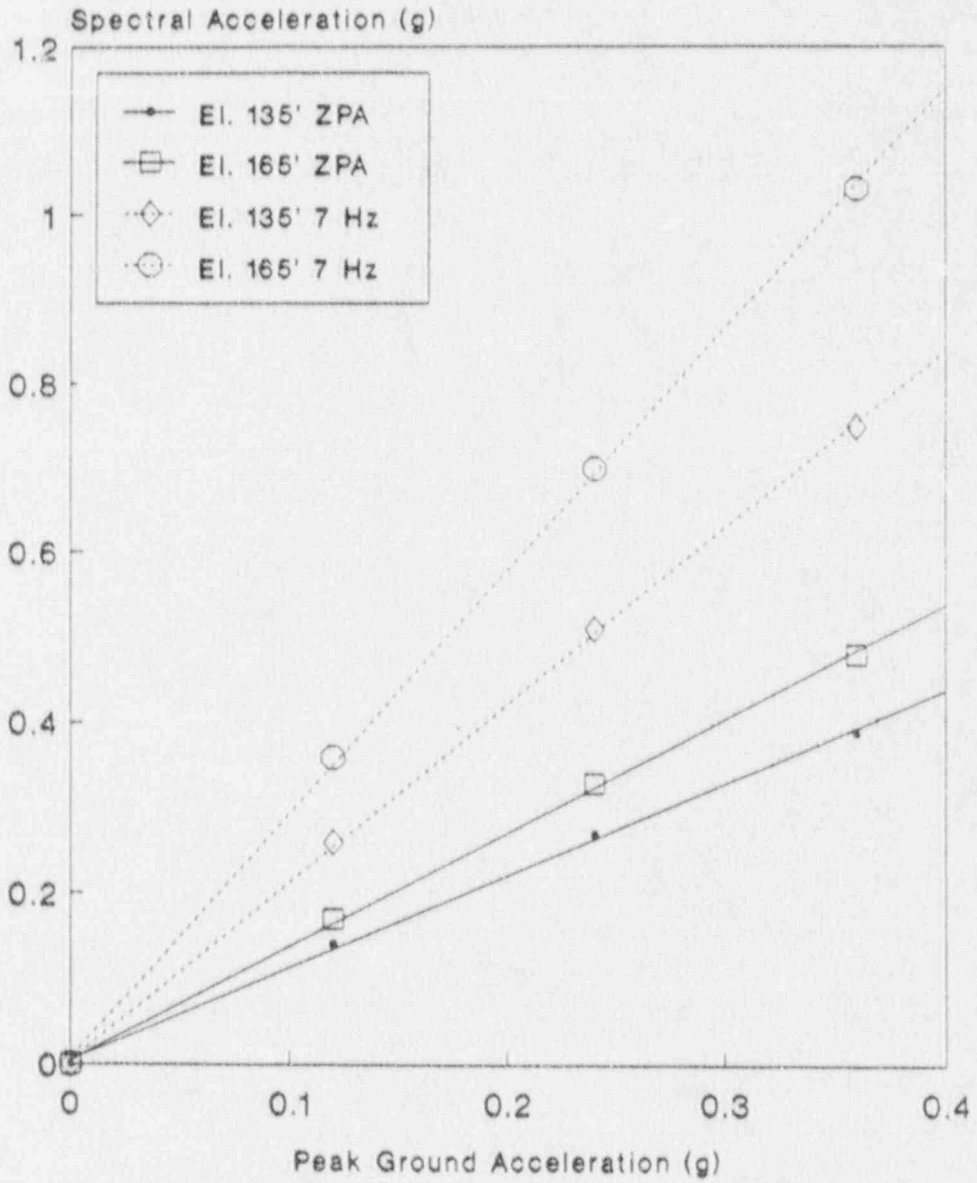

Figure 4.15 Median Responses for Reactor Building

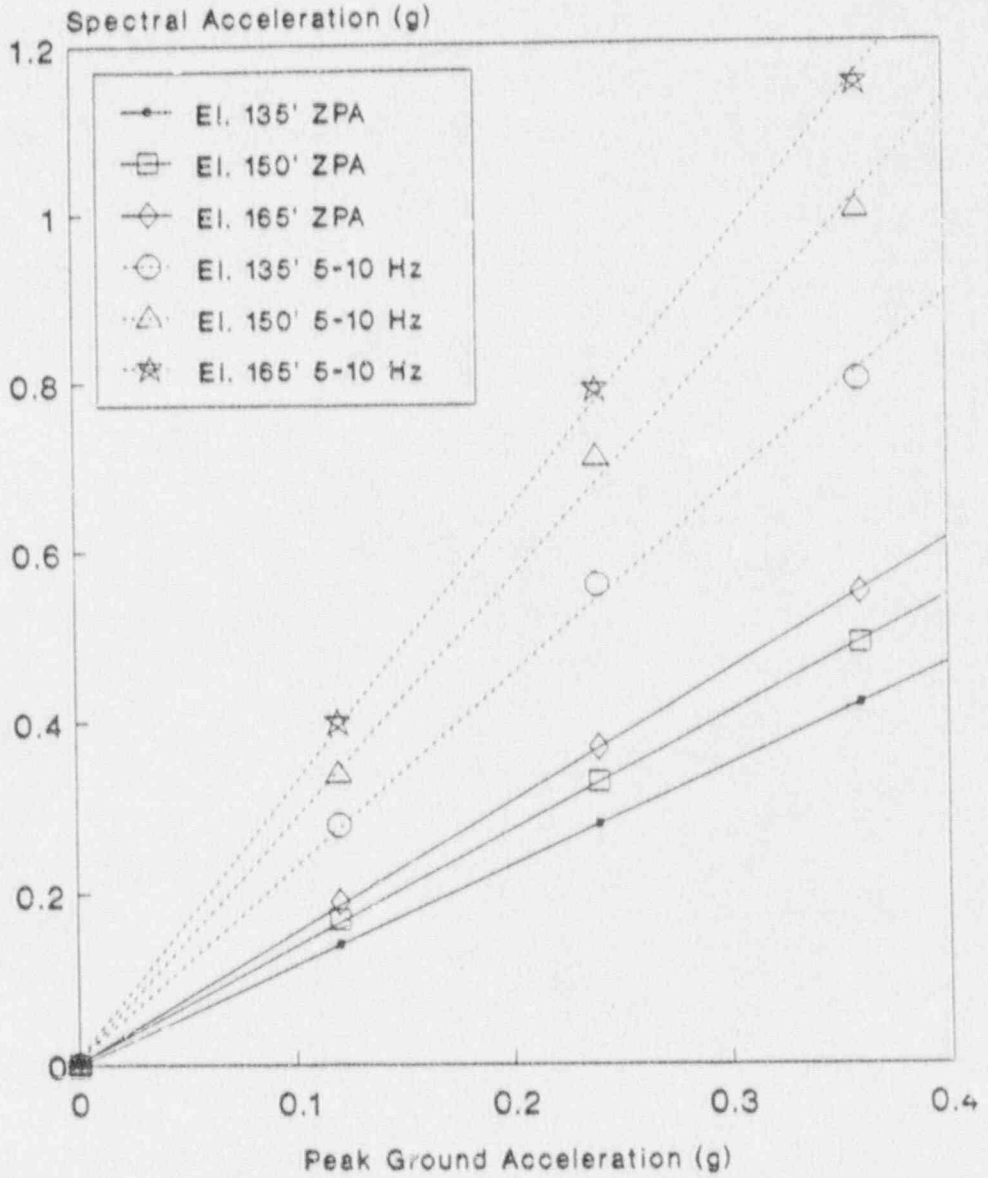

Figure 4.16 Median Responses for Radwaste/Turbine Building

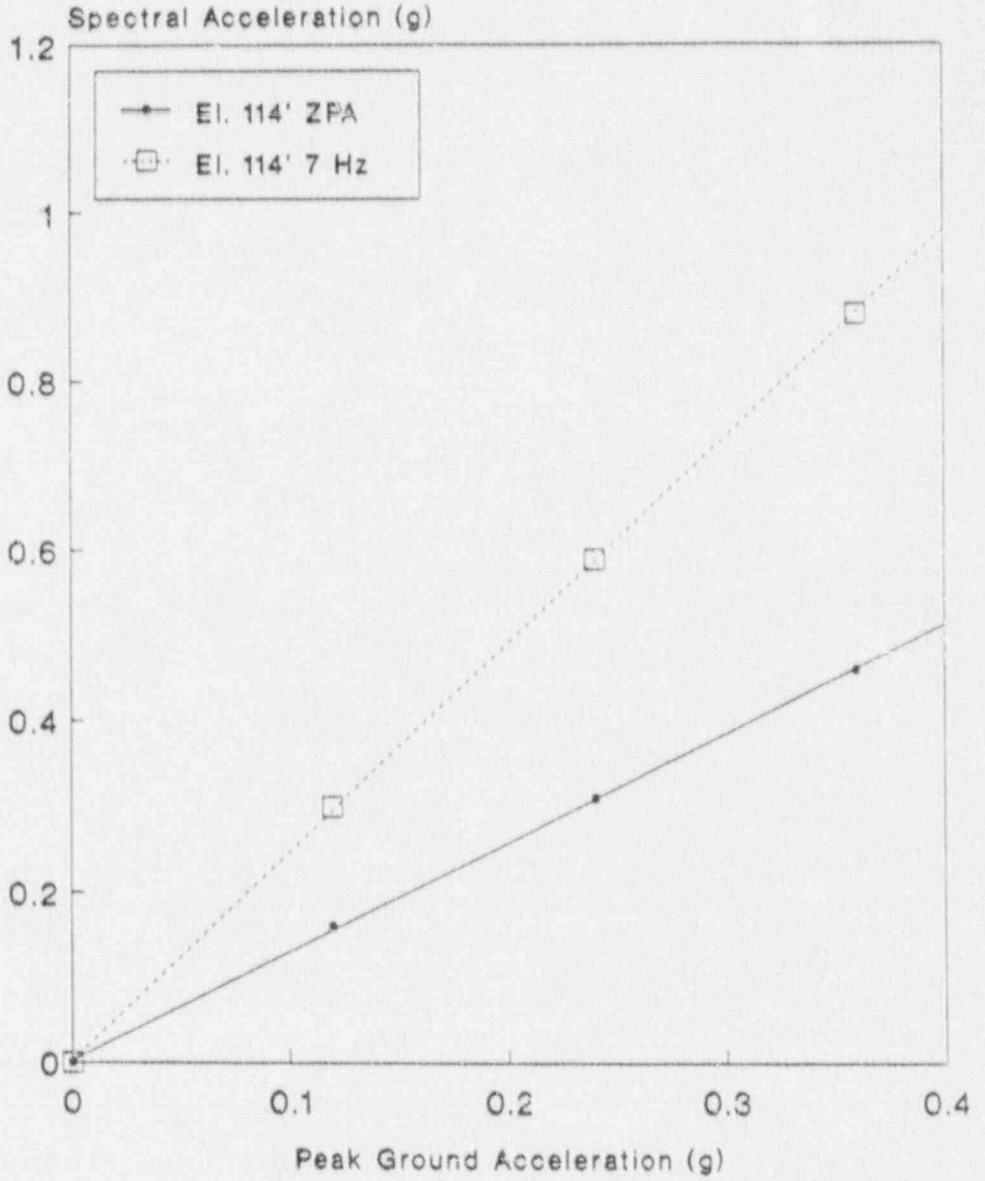

Figure 4.17 Median Responses for Circulating Water Pump Structure

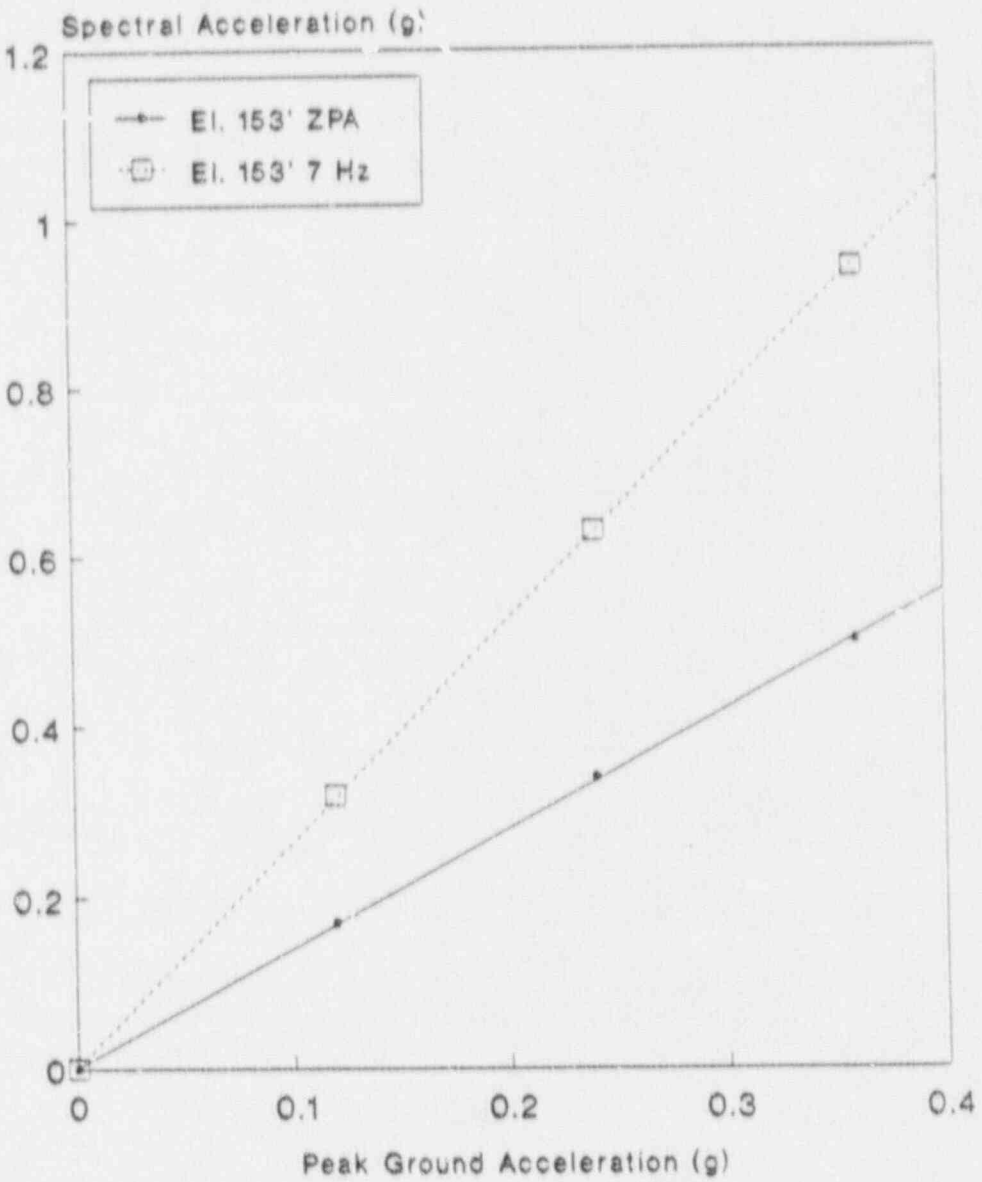

Figure 4.18 Median Response for Emergency Cooling Towers

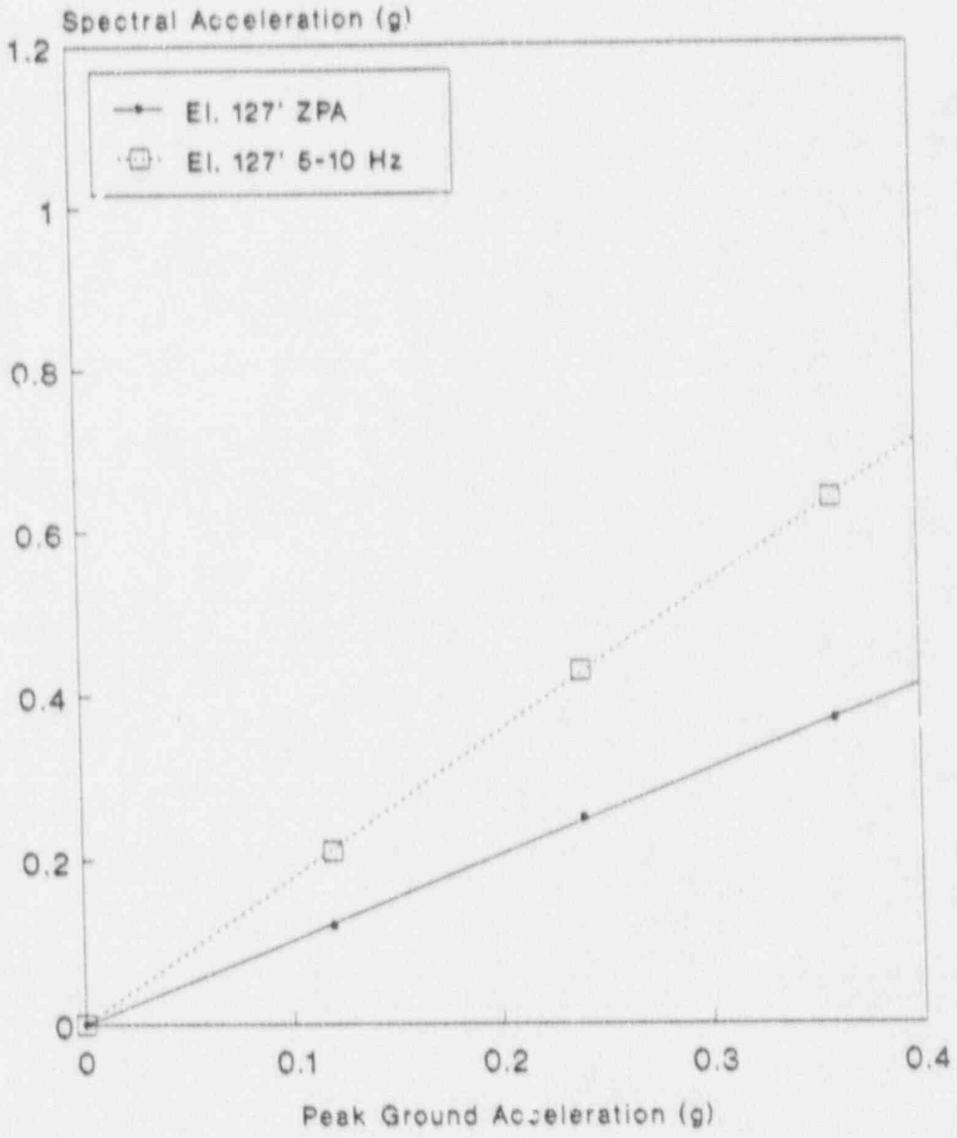

Figure 4.19 Median Responses for Diesel Generator Building

Table 4.5

Peach Bottom Seismic Response Locations

Response Number	Location	Elevation	Frequency	Multiple of PGA
1	Free Field		ZPA	1.0
2			2-5 Hz	2.08
3			5	1.9
4			5-10	1.78
5			7	1.9
6	CS	135'	ZPA	1.2
7			5-10	2.5
8		150'	ZPA	1.4
9			5-10	3.0
10		165'	ZPA	1.6
11			5-10	3.3
12	RB	91'	ZPA	1.0
13			5-10	1.8
14			7	1.8
15			5	1.8
16		116'	ZPA	1.1
17			7	2.1
18		135'	ZPA	1.1
19			7	2.1
20		165'	ZPA	1.3
21			7	3.0
22	DG	127'	ZPA	1.0
23			5-10	1.8
24			5	1.8
25	TB	116'	ZPA	1.0
26			7	1.9
27	CWPS	114'	ZPA	1.3
28			7	2.4
29	ECT	153'	ZPA	1.4
30			7	2.6
31			5	2.6

4.2.4.3 Correlation

In computing the probability of cut sets involving correlated component failures, it is necessary to determine the correlations both in the responses and in the fragilities of each pair of components in the cut set. Once this is done, the correlation coefficient between any two component failures is computed from the expression

$$\rho = \frac{\beta_{R1}\beta_{R2}}{\sqrt{\beta_{R1}^2 + \beta_{F1}^2}\sqrt{\beta_{R2}^2 + \beta_{F2}^2}}\rho_{R1R2} + \frac{\beta_{F1}\beta_{F2}}{\sqrt{\beta_{R1}^2 + \beta_{F1}^2}\sqrt{\beta_{R2}^2 + \beta_{F2}^2}}\rho_{F1F2}$$

in which

ρ = correlation coefficient between the failure of components 1 and 2

$\beta_{R1,\ R2}$ = standard deviation of the logarithms of the responses of components 1 and 2

$\beta_{F1,\ F2}$ = standard deviations of the logarithms of the fragilities of components 1 and 2

ρ_{R1R2} = correlation coefficient between responses of components 1 and 2

ρ_{F1F2} = correlation coefficient between the fragilities of components 1 and 2

This relation shows that the correlation between the failure of any two components depends not only on the correlations between the respective responses and fragilities, but also on the variances in the responses and fragilities.

With the correlation between the failure events in the cut set known, the evaluation of the cut set probability is performed by evaluating the multivariate probability distribution for the cut set. Methods for evaluating such correlated cut sets are described in Reference 3 of Chapter 1 of this report.

The pairwise correlations between the responses are assigned according to the rules on Table 4.6. Using the rules given and the definitions of the responses given on Table 4.5, the response correlation matrix shown in Table 4.7 results.

Inasmuch as there are no data as yet which prove or disprove correlation between fragilities, the fragility correlations between both like and unlike components were taken as zero.

In general, there exists some degree of correlation between any two components excited by the same earthquake by virtue of the common ground motion. However, it is not necessary to compute correlated failure probabilities when the degree of correlation between the failure events is small (e.g., less than 0.25) as the result will be very close to the uncorrelated value. By examining the response and (in general) the fragility correlations, it is possible to identify those pairs of components for which correlation effects may be neglected, and those for which correlation must be considered. In general, it is found that correlation between like components (identical components which are sensitive to the same spectral acceleration) in the same location should always considered as they are usually the most significant. However, while correlations between two unlike components can (in principle) exist, these are usually of lesser significance, and can usually be neglected, especially when dealing with components located on different floors of a building or in seperate buildings.

For Peach Bottom, a review of the response correlation table (Table 4.7) in conjunction with the fact that fragility correlations are taken as zero allowed screening of the components for those groups of components which should be assigned correlation. For unlike components, it was found that only correlation between the 4kV busses and the 125 volt busses had any potential significance. By contrast, a number of identical components in the same location were found to be significantly correlated. These components are shown below:

- 4 kV busses
- 125 volt busses
- diesel generators
- ESW motor driven pumps

For the components identified above, the correlation coefficient was computed and a proper evaluation of the correlated pairs of failures occurring in the various cut sets was made during quantification of the accident sequences.

Table 4.6

Rules for Assigning Response Correlation
ρ_{R1R2}

1.	Components on the same floor slab, and sensitive to the <u>same</u> spectral frequency range (i.e., ZPA, 5-10 Hz, or 10-15 Hz) will be assigned response correlation = 1.0.
2.	Components on the same floor slab, sensitive to <u>different</u> ranges of spectral acceleration will be assigned response correlation = 0.5.
3.	Components on different floor slabs (but in the same building) and sensitive to the <u>same</u> spectral frequency range (ZPA, 5-10 Hz or 10-15 Hz) will be assigned response correlation = 0.75.
4.	Components on the ground surface (outside tanks, etc.) shall be treated as if they were on the grade floor of an adjacent building.
5.	"Ganged" valve configurations (either parallel or series) will have response correlation = 1.0.
6.	All other configurations will have response correlation = 0.

Table 4.7

Correlation Coefficients Between Responses - Peach Bottom

	1	2	3	4	5	6	7	8	9	10	11	12	13	14	15	16	17	18	19	20	21	22	23	24	25	26	27	28	29	30	31
1	1	.5	.5	.5	.5																										
2		1	.5	.5	.5																										
3			1	.5	.5																										
4				1	.5																										
5					1																										
6						1	.5	.75		.75																					
7							1		.75		.75																				
8								1	.5	.75																					
9									1		.75																				
10										1	.5																				
11											1																				
12												1	.5	.5	.5	.75															
13													1																		
14														1			.75														
15															1																
16																1	.5	.75		.75											
17		Table is Symmetric															1		.75		.75										
18																		1	.5	.75											
19																			1		.75										
20																				1	.5										
21		All correlations zero																			1										
22		except those shown.																				1	.5	.5							
23																							1	.5							
24																								1							
25																									1	.5					
26																										1					
27																											1	.5			
28																												1			
29																													1	.5	.5
30																														1	.5
31																															1

4.3 Seismic Fragilities

Component failure is taken as either loss of pressure boundary integrity or loss of operability. Failure (fragility) is characterized by a cumulative distribution function which describes the probability that failure has occurred given a value of loading. Loading may be described by local spectral acceleration or moment, depending on the component and failure mode. The fragilities are related to the appropriate local response to permit an accurate assessment of the effects of common-cause seismic failures in the evaluation of the accident sequences.

4.3.1 Generic Fragilities

A generic data base of fragility functions for seismically-induced failures was developed in the SSMRP (Ref. 6). As a first step, all components were grouped into generic categories. For example, all motor operated valves located on piping with diameters between 2-1/2 and 8 inches were placed into a single generic category, and similarly, all motor control centers were placed into another generic category.

Fragility functions for the generic categories were developed based on a combination of experimental data, design analysis reports, and an extensive expert opinion survey. The experimental data utilized in developing fragility curves were obtained from the results of component manufacturer's qualification tests, independent testing lab failure data and data obtained from the U.S. Corps of Engineers extensive SAFEGUARD Subsystem Hardness Assurance Program. These data were critically examined for applicability and then statistically combined with the expert opinion survey data to produce the fragility curves for the generic component categories.

Finally, a review of more recent site-specific component fragilities contained in the Lawrence Livermore data base (Ref. 11) was made. Based on these reviews, several of the SSMRP generic fragilities in Reference 6 were updated.

The final generic categories and the corresponding fragility medians and uncertainties are shown in Tables 4.8 and 4.9. These fragilities are used as the starting point in the simplified seismic PRA. As in the use of any generic data base, one must be cognizant of the source of the data and the equipment to which it applies. An important aspect of using this data is to examine the equipment in the plant being analyzed and compare it with the data base for which the generic fragilities were developed. Any deviation is noted and examined carefully, and new site-specific fragilities developed as necessary.

Fragilities for electrical components represent a special problem in that there is a wide variety of electrical gear found within a plant. Typically, all this gear is enclosed in switchgear cabinets or motor control centers. The two lowest failure modes that were identified in the SSMRP fragility data base were relay chatter and inadvertent trip of circuit breakers. Virtually all electrical switchgear and motor control

Table 4.8

Generic Component Categories

Fragility Category	Component Class	Typical Components	Frequency (Hz)
1	LOSP	Ceramic Insulators	ZPA
2	Relays		5-10
3	Circuit Breakers		5-10
4	Batteries		ZPA
5	Battery Racks		ZPA
6	Inverters		5-10
7	Transformers	4 kV to 480 V and 480 to 120 V	10
8	Motor Control Centers	Control for ESF Pumps and Valves	5-10
9	Aux. Relay Cabinets		5-10
10	Switchgear (Inc. Transformers, Buses & Breakers)	416 V and 480 V	5-10
11	Cable Trays		ZPA
12	Control Panels and Racks	RPS Process Control	5-10
13	Local Instruments	Misc. Pressure & Temperature Sensors	5-35
14	Diesel Generators	4160 ac Emergency Power Units	22
15	Horizontal Motors	Motor-Generator Sets	ZPA
16	Motor-Driven Pumps and Compressors	AFWS, RHR, SIS, Charging Pumps, Lube Oil Pumps, Diesel Starting Compressors	7
17	Large Vertical, Centrifugal Pumps (Motor-Drive)	Service Water Pumps	5
18	Large Motor-Operated Valves (>10")		ZPA
19	Small Motor-Operated Valves (<10")		ZPA
20	Large Pneumatic/Hydraulic Valves	Includes MSIV, ADP, and PORV	ZPA
21	Large Check and Relief Valves		ZPA
22	Miscellaneous Small Valves (<8")		ZPA
23	Large Horizontal Vessels & Heat Exchangers	Pressurizer Relief Tank, CCW Heat Exchangers	ZPA

Table 4.8

Generic Component Categories (Concluded)

Fragility Category	Component Class	Typical Components	Frequency (Hz)
24	Small to Medium Heat Exchangers and Vessels	Boron Injection Tank	20
25	Large Vertical Storage Vessels with Formed Heads	RHR Heat Exchanger, Accumulator Tank	ZPA
26	Large Vertical Flat-Bottomed Storage Tanks	CST, RWST	
27	Air Handling Units	Containment Fan Coolers	5

Table 4.9

Generic Component Fragilities, in units of gravity (g)

Category	Generic Component	Median*	β_R	β_U
1	Ceramic insulators	0.25	0.25	0.25
2	Relays	4.00	0.48	0.75
3	Circuit breakers	7.63	0.48	0.74
4	Batteries	0.80	0.40	0.39
5	Battery racks	2.29	0.31	0.39
6	Inverters	2.00	0.26	0.35
7	Dry transformers	8.80	0.28	0.30
8	Motor control centers	7.63	0.48	0.74
9	Auxiliary relay cabinets	7.63	0.48	0.74
10	Switchgear	6.43	0.29	0.66
11	Cable trays	2.23	0.34	0.19
12	Control panels and racks	11.50	0.48	0.74
13	Local instruments	7.68	0.20	0.35
14	Diesel generators	1.00	0.25	0.31
15	Horizontal motors	12.10	0.27	0.31
16	Motor-driven pumps and compressors	2.80	0.25	0.27
17	Large vertical centrifugal pumps	2.21	0.22	0.32
18	Large motor-operated valves (>10 in.)	6.50	0.26	0.60
19	Small motor-operated valves (<10 in.)	4.83	0.26	0.35
20	Large pneumatic/hydraulic valves	6.50	0.26	0.35
21	Large relief, manual, and check valves	8.90	0.20	0.35
22	Misc. small valves	12.50	0.33	0.43
23	Large horizontal vessels and heat exchangers	3.0	0.30	0.53
24	Small to medium vessels and heat exchangers	1.84	0.25	0.45
25	Large vertical vessels with formed heads	1.46	0.20	0.35
26	Large vertical tanks with flat bottoms	0.45	0.25	0.29
27	Air handling units	6.90	0.27	0.61

β_R - random uncertainty
β_U - systematic uncertainty
All medians in terms of spectral acceleration (g's) at 5% damping.

centers in a nuclear power plant include these two types of components, so these two fragilities were used as the generic failure modes for electrical gear in the SSMRP analysis. Relay chatter is the lowest failure mode and, if included blindly in a risk analysis, would be the dominant failure. Because, in many cases, circuits are protected by time delay circuits and because, in most cases, chatter of relays would not cause a change in the state of a system being controlled, the NUREG -1150 analyses chose not to include relay chatter as a failure mode for electrical gear but rather to include circuit breaker trip as the lowest functional failure mode.

4.3.2 Site-Specific Component Fragilities

During the plant walkdown, a number of components were identified as not fitting in the generic fragility data base. These components were later examined for their importance in the system fault trees models, and for those playing a role in the systems analysis, site-specific fragilities were derived. The resulting site-specific fragilities are shown on Table 4.10.

The 4kV switchgear are critical in that both onsite and offsite AC power are distributed through them. They were found to be anchored with fillet welds into steel imbedded in the floor and a fragility analysis was required to assess the capacity of the welds. The diesel generator day tank is a vertical tank held by 5/8 inch bolts and is critical to the continued operation of the diesel generators in the event of loss of offsite power. The HPCI room cooler was found to be anchored to an I beam frame with small welds at its corners. Failure of this cooler would result in long term failure of the HPCI pump (approximately 10 hours). The condensate storage tank plays a role as a suction source for the high pressure injection systems. The tank itself is a vertical water storage tank anchored with six bolts to a mounting pad. Such tanks often have relatively low seismic capacity. However, the tank itself is surrounded by a water tight dike and so credit was given for the possibility that, if the CST failed, water would still be available since it would be contained by the dike. A calculation was made to verify that the level of the water after tank failure was such that suction could still be maintained. Thus, the fragility of the condensate storage tank was based on the fragility of the water tight dike as listed in Table 4.11.

It should be noted that in each case the items identified had less margin than typical in the generic fragility data base. However, in each case, the median capacity of the component was well above that required for the SSE.

4.3.3 Site Specific Building Fragilities

4.3.3.1 Method of Fragility Evaluation

The fragilities of Peach Bottom Unit 2 structures were generated using

Table 4.10

Peach Bottom Site Specific Fragilities

Component	Failure Mode	M_F	β_R	β_U	Response No.
4KV Switchgear	Anchor weld failure	3.30	0.15	0.25	7 (5-10Hz)
DG Day Tank	Anchorage Failure	0.95	0.15	0.20	22 (ZPA)
HPCI Room Cooler	Weld Failure	4.42	0.15	0.25	13 (5-10HZ)
Condensate Storage Tank	Anchorage/Building	Fragility Based on Dike, See Table 4.11			
RWST	Unanchored	Not on Fault Trees			

Table 4.11

Summary of Structural Fragilities

Structure	Element	A_m(g)	β_R	β_U	Effect of Failure
Reactor Building	N-S, E-W Shear Walls	1.6	0.16	0.27	Vessel Rupture Initiating Event
Radwaste/Turbine Building	Roof Diaphragm	1.2	0.10	0.23	Cause SBO and loss of all actuation. Modeled as initiating event, and failure event in LOCA sequences
Radwaste/Turbine Building	N-S Shear Walls	1.5	0.13	0.25	
Diesel Generator Building	E-W Shear Walls	1.9	0.06	0.21	Negligible
Circulating Water Pump Structure	N-S Shear Walls	2.3	0.11	0.28	Negligible
Emergency Cooling Tower	Columns, EL 153' to EL 163'	0.55	0.11	0.21	Basic event in ESW system. Screened out due to redundancy
Turbine Building	---	0.50	0.11	0.21	Fails PCS, ECW pump cables, instrument air, and condensate system. Modeled as a a failure event in T1, T3 and LOCA sequences.
Various	Block Walls	1.5	0.13	0.24	Negligible
Watertight Dike	Surrounds CST	1.0	0.04	0.17	Failure mode of CST. Screened out due to redundancy.

1. β_R and β_U do not include response variability.

the basic methodology described in Reference 1, with certain modifications. The fragility of a structure can be expressed in terms of its peak ground acceleration capacity, A, as follows:

$$A = A_m e_R e_U$$

In this formulation, A_m is the median peak ground acceleration (PGA) capacity, and e_R and e_U are random variables with unit median, representing the inherent randomness about the median and the uncertainty in the median value. The variables e_R and e_U are assumed to be lognormally distributed with logarithmic standard deviations β_R and β_U, respectively. The properties of the lognormal distribution are presented in Reference 2.

For convenience, the median peak ground acceleration capacity, A_m, was formulated as the product of three times the SSE peak ground acceleration, A_{3SSE} = 0.36 g for Peach Bottom site, and a median factor of safety against this ground motion level, F_m. Thus, the median peak ground acceleration capacity can be expressed as:

$$A_m = F_m A_{SSE}$$

The median factor of safety, F_m, was in turn expressed as the product of the following two median factors of safety:

a. The median strength factor, F_s, which is defined as the ratio of the median structure strength to the mean (approximate median) structure loads for three times the SSE ground motion input.

b. The median inelastic energy absorption factor, F_u, which accounts for the ability of the structure to withstand seismic loads in excess of those corresponding to yield through ductile, nonlinear response.

The loads from the three times SSE ground motion input were used since ten percent damping was assigned to the structures for this case. This damping was estimated to be a median value for reinforced concrete structures at yield.

The strength and inelastic energy absorption factors have associated logarithmic standard deviations, β_s and β_u. From the properties of the lognormal distribution, the logarithmic standard deviation associated with the total factor of safety is calculated as follows:

$$\beta^2 = \left(\beta_s^2 + \beta_u^2 \right)^{1/2}$$

These variabilities are composed of randomness and uncertainty, which are defined as follows:

a. Randomness consists of variabilities that cannot be reduced by more detailed evaluation or data collection.

b. Uncertainty consists of variabilities resulting from lack of knowledge.

The only source of random variability reported in this section results from the effect of certain earthquake characteristics on the structure inelastic energy absorption capability. Uncertainties result from variables such as material strength, member capacity, member ductility, etc.

Structure seismic response contributes additional variability to the structural fragilities. Logarithmic standard deviations for seismic response variability are not included in the values reported in this section, as they are included in the responses directly.

4.3.3.2 Development of Structural Capacity Factors

The Peach Bottom structural fragilities are expressed in terms of factors which account for structure ultimate strength and inelastic energy absorption capability. This section describes the development of these factors. The reader is referred to Reference 6 for more details of the process.

Structure Element Ultimate Strengths

Two major considerations are involved in the determination of the ultimate strengths of individual structural elements. One is the definition of the strengths of the materials composing the members. The other is the determination of the ultimate strength capacities of the structural members given the type of loading, material strength, member configuration, etc.

The Peach Bottom plant specific material strength data were not available. The following values, which were used in the fragility evaluation, were estimated based upon data from other nuclear power plants (Ref. 6):

Concrete Compressive Strength

Minimum Specified (psi)	Median (psi)	β
3000	4900	0.17
4000	6000	0.15

Steel Reinforcement Yield Strength

Grade	Median (ksi)	β
40	49	0.10
50	55	0.10
60	69	0.07

The median ultimate strength capacities of the structural elements were found using the median material strengths and member configurations (i.e., geometry, reinforcement, etc.) in conjunction with available predictive formulation or approaches. The approaches and formulations used were those appropriate for the type of element (i.e., shear wall, reinforced concrete cylinder, etc.) and loading (i.e., shear, flexure, etc.). They were typically found to provide essentially median-centered capacities when compared to the results of available experimental testing. For example, the predictive equations used to determine the median ultimate strengths of the Peach Bottom shear walls subjected to in-plane shear and flexure are presented in Reference 7.

Median strength factors, F_{sm}, were calculated for individual structural elements as follows:

$$F_{sm} = \frac{V_{um,i}}{V_{3SSE,i}}$$

$V_{um,i}$ = Median ultimate strength for element i

$V_{3SSE,i}$ = Median load due to 3 x SSE ground motion input for element i

The median strength factor for a structure was generally taken to be the lowest value of the individual elements composing its primary seismic load-resisting system. This is slightly conservative if the structural elements are ductile and redundant. In certain cases, load redistribution among such structural elements was considered when determining the structure strength factor.

Variability of the structural element ultimate strengths was considered to be composed of uncertainty since it is associated with a lack of knowledge. Uncertainty attributed to material strength was based upon the estimated variabilities listed above. Comparisons of the predicted strength capacities to the available test results provided estimates of the uncertainty in the predictive strength formulations. Additional uncertainty attributable to variabilities associated with other sources, such as member geometry, reinforcement spacing, openings, workmanship, differences between field and laboratory conditions, accuracy of the predicted load distributions, etc., were also included.

Structure Inelastic Energy Absorption

The ability of a structure to withstand seismic levels in excess of those corresponding to yield through ductile, nonlinear response was accounted for by the inelastic energy absorption factor, F_u. This factor was based upon the Riddell-Newmark response deamplification factor, ϕ_u (Ref. 8).

The median inelastic energy absorption factor, F_{um}, corresponding to some ductility ratio, μ, is given by the following equation:

$$F_{um} = \frac{S_{ae}}{S_{au}}$$

S_{ae} = Median elastic spectral acceleration for median structure damping at the dominant structure frequency

S_{au} = Deamplified spectral acceleration at the dominant structure frequency

For frequencies in the amplified acceleration range (between about 2 Hz and 7 Hz) of the Peach Bottom median ground response spectrum:

$$S_{au} = \phi_u S_{ae} > S_{ahf}$$

$$\phi_u = (p\mu - q)^{-r}$$

$$p = q + 1$$

$$q = 3.0\ \beta^{-0.30}$$

$$r = 0.48\ \beta^{-0.08}$$

β = System damping

For frequencies greater than the frequency at which the median spectral acceleration returns to the peak ground acceleration (about 33 Hz):

$$S_{au} = S_{ahf} = \mu^{-0.13}\ PGA$$

PGA = Peak ground acceleration

The Riddell-Newmark response deamplification factor was based upon a series of nonlinear analyses utilizing single-degree-of-freedom (SDOF) fixed base models subject to time histories of large magnitude, long duration earthquakes. Nonlinear response of the Peach Bottom structures would be expected to differ from the response calculated using these deamplification factors for the following reasons:

a. The Peach Bottom structures are typically multi-degree-of-freedom (MDOF) systems.

b. Small magnitude earthquakes are expected for the Peach Bottom site.

To account for these differences, an effective ductility, μ_e, was used in the equations above.

The system ductility, μ_{sys}, for use with the Riddell-Newmark deamplification factor is a measure of the nonlinearity throughout the structure.

For fixed-base SDOF structures, the system ductility is equal to the story drift ductility, μ_{st}. However, for MDOF structures, the system ductility may be less than the story ductility if the ratio of the story demand to story capacity is not uniform through the structure.

The system ductility, μ_{sys} can be related to the story ductility by a factor M.

$$\mu_{sys} = \left[\frac{\mu_{st} - 1}{M}\right] + 1$$

The story ductility for typical nuclear plant shear walls is estimated to be about five. Values for the factor M were estimated on a case-by-case basis for the Peach Bottom 2 structures with guidance from the following bounding values:

a. M = 1 for fixed base SDOF structures or MDOF structures with uniform nonlinearity.

b. M = 2 for fixed base structures with highly concentrated nonlinearities.

The Riddell-Newmark response deamplification factors were based only on large magnitude earthquakes. It is well known that lower magnitude earthquakes are not as damaging to structures and equipment as higher magnitude earthquakes with the same peak ground acceleration (Ref. 9). The lower magnitude earthquakes have lower energy content and shorter durations which develop fewer strong response cycles. Structures are able to withstand larger deformations (i.e., higher ductility) for a few cycles compared to the larger number of cycles resulting from longer duration events.

Earthquake magnitude effects were accounted for by using an effective ductility, μ_e, in the Riddell-Newmark response deamplification factor approach. The effective ductility was calculated as follows:

$$\mu_e = 1.0 + C_D(\mu_{sys} - 1.0)$$

where the duration coefficient, C_D, is a function of the earthquake magnitude and μ_{sys} is the previously defined system ductility.

The results of the analyses performed in Reference 9 were used to provide estimates of the duration coefficient, C_D, as a function of earthquake magnitude. For earthquakes having magnitudes ranging from 4.5 to 6.0, a duration coefficient of 1.4 was determined to be appropriate by correlating the inelastic energy absorption factor from the Riddell-Newmark formulation to the results of Reference 9. Similarly, a duration coefficient of 0.7 was estimated for earthquake magnitudes in the 6.5 to 7.5 range. A duration coefficient of 1.3 was estimated for the Peach Bottom structures. This is a representative value for eastern United States nuclear plants.

It should be noted that, for purposes of this study, structures are considered to fail functionally when inelastic deformations of the structure under seismic load are estimated to be sufficient to potentially interfere with the operability of safety-related equipment attached to the structure. The element and system ductility limits chosen for structures are estimated to correspond to the onset of significant structural damage. For many potential modes of failure, this is believed to represent a conservative bound on the level of inelastic structural deformation which might interfere with the operability of components housed within the structure. It is important to note that considerably greater margins of safety against structural collapse are believed to exist for these structures than many cases reported within this study. Thus, the structural element capacities reported herein should not be inferred as corresponding to structure collapse.

4.3.4 Structure Fragilities Derived For Peach Bottom Structures

The fragilities derived for the Peach Bottom structures are listed in Table 4.11. In general, several potential failure modes were investigated for each structure. Fragilities for the governing failure modes are reported. These failure modes are typically associated with structural failure which would result in damage to the safety-related equipment located in the building.

In developing the capacity factors, structural wall and beam resultant forces were determined from the dynamic response models. The building's structural dynamic characteristics are described by their fixed base eigensystem and modal damping factors. Eigensystems, fundamental modes of vibration and eigenvectors, are determined from fixed base lumped mass finite element models. Beam elements represent stiffness between floor levels located at the shear centroid of the reinforced concrete walls or diagonal steel bracing, including shear deformation. The contribution to lumped mass at each floor level is from the half height of the wall above and below, floor slab, and equipment at that floor. Nominal values of structure damping were taken to be 0.07, 0.085, and 0.10 (fractions of critical damping) for the three seismic acceleration ranges considered here. These were based on published damping values and assumed stress levels achieved. Failure odes for each structure are described below.

Reactor Building

The reactor building houses the nuclear steam supply system, primary containment, and auxiliary systems. It is founded on rock at elevation 91 feet-6 inches. The reactor building is isolated from adjacent structures above elevation 116 feet-0 inches by 0.5-inch-thick gaps. The seismic load-resisting system consists of reinforced concrete walls and slabs up to the refueling floor at elevation 234 feet-0 inch. The superstructure above the refueling floor consists of structural steel framing, siding, and roof deck. The concrete shield wall that encloses the drywell is integral with the reactor building structure. The reactor

pedestal and sacrificial shield wall are founded on fill concrete within the drywell. The stabilizer truss connected to the top of the sacrificial shield wall provides lateral support for these internal structures.

The following structural elements were investigated for seismic-induced failure:

a. N-S shear walls
b. E-W shear walls
c. Diaphragms
d. Drywell shield wall
e. Reactor pedestal
f. Sacrificial shield wall
g. Stabilizer truss

Seismic capacity of the reactor building was found to be governed by failure of the N-S or E-W shear walls. Resistance to lateral seismic loads is provided mainly by the exterior shear walls and the drywell shield wall. Failures of these walls are expected to be initiated at elevation 135 feet-0 inch. Median PGA capacities in both the N-S and E-W directions were determined to be 1.6 g. Shear wall failure corresponds to gross structural failure and is expected to cause damage to equipment located throughout the entire reactor building, including components housed within the drywell.

Radwaste/Turbine Building

The radwaste building and the immediately adjacent portion of the turbine building were constructed integral with each other and are thus considered a single structure. The radwaste building is located between the reactor buildings for Units 2 and 3. It houses various components of the radwaste system, the standby gas treatment system, and associated equipment. The turbine building portion houses the control room, cable spreading room, switchgear rooms, and battery rooms. The radwaste/turbine building is founded on rock. The seismic load-resisting system consists of reinforced concrete shear walls and slabs. It is separated from adjacent buildings above elevation 116 feet-0 inch by a 0.5-inch-thick gap.

A number of shear walls and diaphragms were evaluated. The roof diaphragm was found to have the lowest seismic capacity, with a median PGA capacity of 1.2 g. The roof over the radwaste building is either metal deck or 1 foot-6 inches-thick concrete slab. The roof over the control room is a 2 feet-6 inches-thick concrete slab. E-W seismic inertial loads from the radwaste/turbine building roof are delivered by the slabs to the main shear walls on Column Lines 18, 19.6, 21.4, and 23. Because the Column Line 19.6 and 21.4 walls are integral with the 1 foot-6 inches roof slab for lengths of only 27 feet each, load transfer capability is limited, and in-plane slab shear failure will initiate at these locations. Because this failure mode has some ductility, the

seismic loads will redistribute to the Column Line 18 and 23 walls. Load transfer to these walls is limited by their in-plane flexural capacity. This failure mode is localized, and will result in damage to equipment located between elevation 165 feet-0 inch and the roof, which includes the control room.

Gross structural failure is expected to result from failure of the N-S shear walls. The median PGA capacity for this failure mode was calculated to be 1.5 g. Damage to equipment located throughout the radwaste/turbine building is expected to result.

Diesel Generator Building

The diesel generator building houses the emergency diesel generators and associated components. The lateral load-resisting system consists of reinforced concrete shear walls and slabs. The bottom floor of the diesel generator building is typically at elevation 127 feet-0 inch, which is approximately at grade. Shear walls below grade were designed to transmit lateral loads down to bedrock. The central portion of the building is supported by piles driven to bedrock. The piles were intended to support gravity loads only.

The seismic capacities of several shear walls and diaphragms above grade were evaluated. Potential seismic-induced failure of the shear walls below grade is not expected to result in a loss of function of equipment components housed within the building. Failure of the diesel generator building was found to be governed by failure of the E-W shear walls. A median PGA capacity of 1.9 g was calculated. This failure mode is expected to result in gross structural failure with damage to equipment located throughout the building.

Circulating Water Pump Structure

The central portion of the circulating water pump structure (CWPS) houses the Seismic Class I emergency and high-pressure service water systems. The remainder of the structure houses the service and circulating water systems. The CWPS is founded on rock. Lateral load-resisting systems for Class I portions of the building consist of reinforced concrete shear walls and slabs. The superstructures over the circulating and service water pumps are constructed of precast concrete panels and structural steel frames. They were not evaluated since their failure will not damage Class I equipment.

Selected shear walls and diaphragms were evaluated. Seismic capacity of the CWPS was found to be governed by failure of the N-S shear walls. A median PGA capacity of 2.3 g was calculated. This failure mode corresponds to gross structural failure and damage to equipment located throughout the building.

Emergency Cooling Tower

The emergency cooling tower contains the fans and associated components for the emergency heat sink. It is founded on rock. The water reservoir below elevation 153 feet-0 inch is enclosed by the bottom slab, exterior walls, and precast roof panel with concrete fill. The three cells containing the fans are enclosed by concrete walls.

N-S seismic load from the cells above elevation 163 feet-0 inch is transferred to the structure below elevation 153 feet-0 inch by a number of reinforced concrete columns. The lateral load capacity of these columns is limited by their bending strength. Column failure was estimated to have a median PGA capacity of 0.55 g based upon approximate calculations. This capacity is low compared with other Peach Bottom 2 structure capacities for the following reasons:

a. The upper elevations of the emergency cooling tower experience significant ground motion amplification.

b. The columns have relatively low resistance against lateral loads.

The column failure fragility is assumed to correspond to gross structural failure and damage to equipment located throughout the emergency cooling tower. This assumption may be conservative if function of critical equipment can be maintained despite this structural damage.

Turbine Building

The following components included in the systems analysis are located in Seismic Class II portions of the turbine building:

a. Control rod drive water pumps.
b. Instrument air compressors.

Design of Seismic Class II structures was based upon the 1967 Uniform Building Code requirements for Seismic Zone I locations. Because the components above are not Class I systems, detailed calculation of turbine building structural fragilities was judged to be unwarranted. The fragility listed in Table 4.11 was estimated and may be conservative.

Block Walls

Block walls at Peach Bottom are typically reinforced. Seismic reevaluation of the Peach Bottom block walls was performed in response to I & E Bulletin 80-11 as described in Reference 10. A limited number of walls were seismically retrofitted. Most of the remaining walls were found to be acceptable by criteria comparable to current licensing criteria. The remaining walls were qualified by alternative criteria. This latter group of walls was judged to be the most seismically vulnerable. The

block walls in the cable spreading room were selected from this group for fragility evaluation. Their capacities were analyzed to account for the actual ultimate strength and inelastic energy absorption capability against out-of-plane bending. A median PGA capacity of 1.5 g was calculated. The fragility listed in Table 4.11 is appropriate for the cable spreading room walls and is probably conservative for other block walls located throughout the plant. Table 1 of Reference 10 identifies Class I components that may be damaged by block wall failure.

Watertight Dike

The refueling water and condensate storage tanks are enclosed by a watertight dike which consists of reinforced concrete cantilever walls and exterior walls of adjacent building structures. The purpose of the dike is to retain water in the event the tanks fail. The tanks themselves are lightly anchored or unanchored. Water must be available to the RCIC and HPCI systems for a maximum of about eight hours. After this duration, battery depletion will cause failure of these systems even if water is still available. Only water above the 5-foot level can be drawn.

The dike was evaluated assuming that it was completely filled with water at the initiation of the earthquake. This may be fairly conservative since some time duration is necessary to build up sufficient response to fail the tanks and totally evacuate their contents. After this period, the earthquake ground motion may not have sufficient energy content to fail the dike walls, or may have stopped altogether.

Much of the dike consists of lengths of cantilever walls separated by seismic gaps. Dike failure was postulated to occur at the southeast corner, where outward movement of the east wall could open the gap and cause a leak path. The maximum permanent displacement at the top of the wall was limited to one inch. This is only a very approximate and probably conservative estimate on the leak area sufficient to cause loss of water to RCIC and HPCI. Sufficient data is available to determine a more accurate estimate of the limiting displacement if a more refined estimate is needed.

Out-of-plane failure of the dike wall at the critical location was evaluated. Resistance against structure inertial and fluid hydrodynamic loads was determined. The available ductility was reduced to account for ratcheting since the wall deforms in the outward direction only. A (conservative) median peak ground acceleration capacity of 1.0 g was determined.

4.4 Core Damage and Risk Computations

In the event of an earthquake or any other abnormal condition at a nuclear power plant, the plant safety systems act to bring the plant to a safe shutdown condition. In this step of the risk analysis process, we identify the possible paths that a nuclear plant would follow, given that an earthquake-related event has occurred which causes shutdown. These

paths involve an initiating event and a success or failure designation for systems affecting the course of events, and are referred to as accident sequences.

4.4.1 Initiating Events

The seismic analysis performed for Peach Bottom is based on the same set of event trees developed for the internal event analyses of the plant. The initiating events considered are:

a. Reactor Vessel Rupture (ECCS ineffective)

b. Large LOCA

c. Medium LOCA

d. Small LOCA

e. Radwaste/Turbine Building (RWT)

f. Transient Type 1 (LOSP)

g. Transient Type 3 (PCS initially available)

Note that one structure failure has been included in the list of initiating events. This RWT failure can cause a loss of offsite power as well as system failures and thus was included explicitly in the hierarchy of initiating events.

The reactor vessel rupture event was computed based on the probability of failure of the supports of the reactor vessel itself. A generic fragility for support failure of a BWR vessel was constructed from data given in a review of site specific BWR risk analyses as given in Reference 11. No pipe failures or failure of the recirculation pump supports were considered, because information provided by the internal events analysts indicated that even failure of both recirculation lines could be handled by the existing ECCS capability at Peach Bottom.

The frequency for the large LOCA event was computed based on the failure of the supports of the recirculation pumps. Again, values of the support failure fragility parameters for these pumps were taken from a review of site specific PRAs performed for BWRs. Failures of the piping (steam outlet, feedwater inlet or recirculation lines) were not included as a review of their capacity showed that they were significantly higher than the pump support failures and hence, would make negligible contribution to the initiating event frequency. (In addition, three or more stuck open safety relief valves result in a break size equivalent to a large LOCA and this also serves effectively as an initiator by transfer from the transient event trees directly to the large LOCA tree.)

The small and medium LOCA initiating events were computed based on the failure of piping in the reactor coolant loop. The fragility for the

pipe failures was generated from the calculations of piping failures for pipes considered in the SSMRP Zion analysis. These distributions are shown in Figure 4.20. The independent variable for this figure is peak ground acceleration, with a random variability of 0.25. These distributions were input in log normal form for the analysis. (In addition, transfers from the transient tree based on stuck open relief valves are considered. Two stuck open relief valves are equivalent to a medium LOCA whereas one stuck open relief valve is equivalent to a small LOCA.)

The Type 1 transient initiating event was based on the probability of loss of offsite power (LOSP). This has been found to be the dominant source of such transients in all seismic PRAs to date (wherein LOSP results in loss of the main feedwater system).

In computing the frequency of the initiating events, a hierarchy between them must be established. The order of this hierarchy is such that, if one initiating event occurs, the occurrence of other initiating events further down the hierarchy are of no consequence. For example, if a large LOCA occurs, we are not concerned if a small LOCA or transient occurs. Thus, the most serious initiating event is assumed to be the RVR event. The probability of the large LOCA event is then computed as the probability of the anchorage failures causing the large LOCA times the complement of the RVR initiating event, and similarly, for the MLOCA, SLOCA and T1 events. The RWT building failure was put above the T1 (LOSP) transient inasmuch as this building failure results in loss of offsite power and causes station blackout, loss of all actuation, and loss of the control room. Figure 4.21 illustrates the hierarchy in an event tree format and shows the expressions used to calculate the initiating event frequencies. Implicit in the hierarchy definition is the requirement that events in the hierarchy above a given initiating event cannot occur in the accident sequence for that event. For example, LOSP can occur as a basic event in any of the LOCA or RWT sequences, but cannot occur as a basic event in the T_3 accident sequences.

With the hierarchy established, the Type 3 initiating event probability is computed from the condition that the sum of the initiating event probabilities considered must be unity. The hypothesis is that, given an earthquake of reasonable size, at least one the initiating events will occur. At the least, we expect the operator to manually SCRAM the plant given an earthquake above the operating basis earthquake (OBE) level.

Numerical values for the initiating events at various earthquake levels are given in Section 4.4.5. Numerical values for the parameters of the fitted distributions are listed in Appendix C.

4.4.2 Event Trees

The event trees developed for the internal event analyses were used directly, so as to be able to compare the final core melt frequencies due to seismic and internal events on a common basis. The internal event

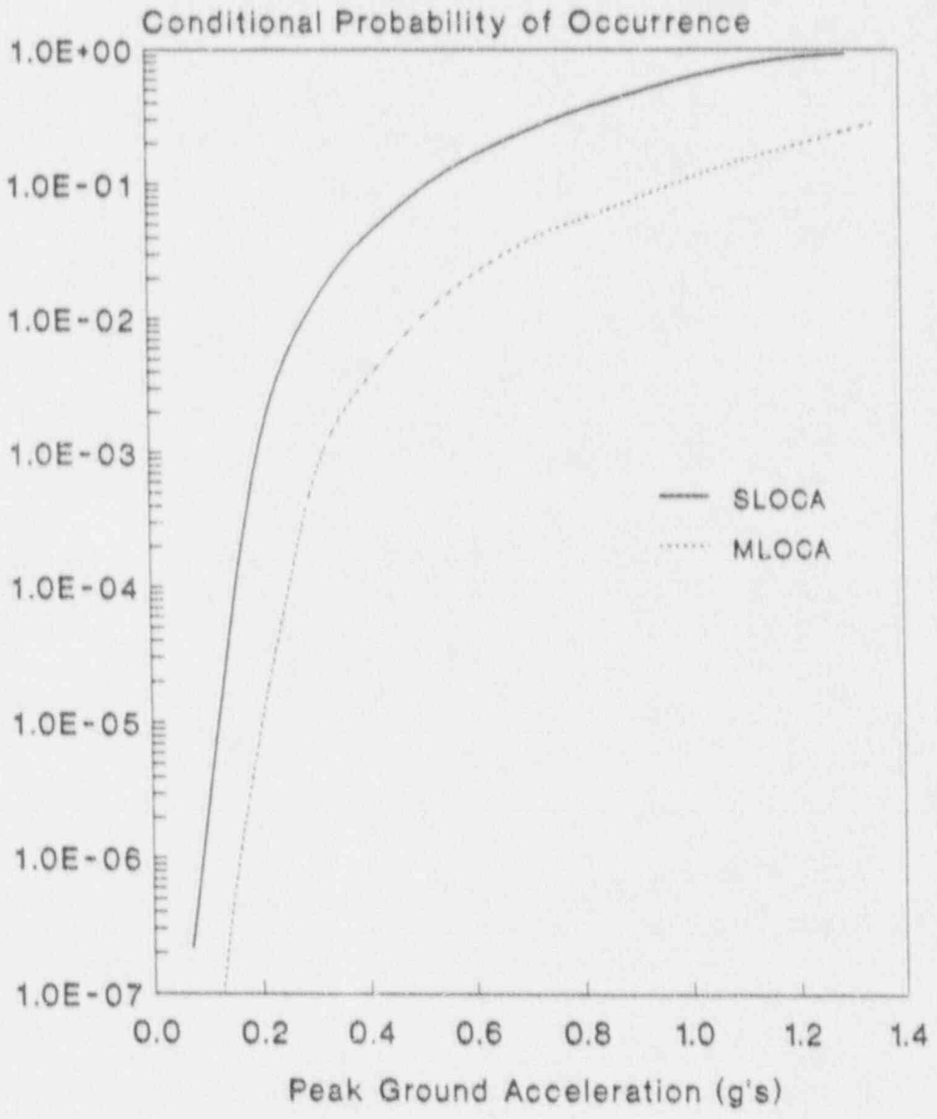

Figure 4.20 Frequencies of Pipe Breaks Causing Medium and Small LOCAS Derivec From SSMRP Piping Calculations

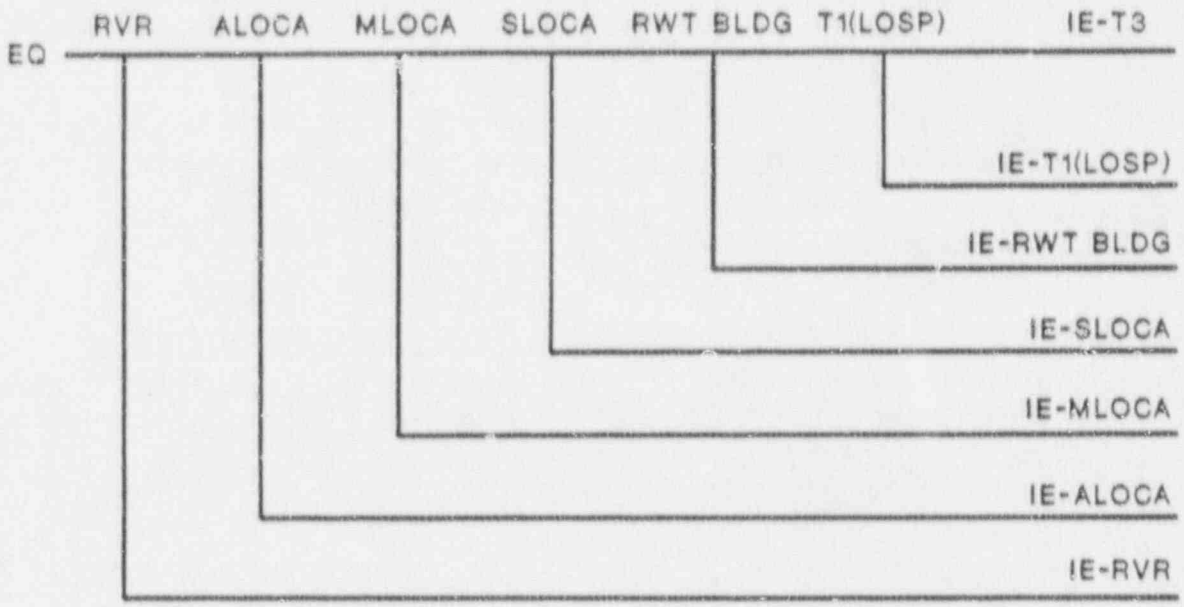

$$P(IE\text{-}RVR) = P(RVR)$$

$$P(IE\text{-}ALOCA) = P(ALOCA)*\overline{P(RVR)}$$

$$P(IE\text{-}ALOCA) = P(MLOCA)*\overline{P(ALOCA)}*\overline{P(RVR)}$$

$$P(IE\text{-}SLOCA) = P(SLOCA)*\overline{P(MLOCA)}*\overline{P(ALOCA)}*\overline{P(RVR)}$$

$$P(IE\text{-}RWT) = P(RWT)*\overline{P(SLOCA)}*\overline{P(MLOCA)}*\overline{P(ALOCA)}*\overline{P(RVR)}$$

$$P(IE\text{-}LOSP) = P(LOSP)*\overline{P(RWT)}*\overline{P(SLOCA)}*\overline{P(MLOCA)}*\overline{P(ALOCA)}*\overline{P(RVR)}$$

$$P(IE\text{-}T3) = 1.0 - P(IE\text{-}RVR) - P(IE\text{-}ALOCA) - P(IE\text{-}MLOCA) - P(IE\text{-}SLOCA) - P(IE\text{-}RWT) - P(LOSP)$$

Figure 4.21 Initiating Event Hierarchy Event Tree

trees used for all external events analyses were presented in Section 2.3. They are repeated here for ease of subsequent discussion as Figures 4.22 through 4.26.

The RWT building failure event identified as causing an initiator does not have a separate event tree. The accident sequences which result from this building failure can be identified from the existing LOSP event tree described in Section 2.3. The failure of the RWT structure causes both loss of off-site power, loss of the control room, and failure of the cabling to the ESW and ECW pumps, which results in station blackout. In addition, loss of all actuation fails HPCI and RCIC. In this case, since both on-site AC power as well as HPCI (U_1) and RCIC (U_2) are failed, four essentially identical sequences result.

$$RWT\text{-}1 = T_1CMPBU_1U_2 = (RWT) \cdot CMP$$

$$RWT\text{-}2 = T_1CMP_1BU_1U_2 = (RWT) \cdot CMP_1$$

$$RWT\text{-}3 = T_1CMP_2BU_1U_2 = (RWT) \cdot CMP_2$$

$$RWT\text{-}4 = T_1CMP_3BU_1U_2 = (RWT) \cdot CMP_3$$

These sequences differ only by the fraction of safety relief valves which fail to close (zero, one, two, or three or more), and all have early failure of HPCI and RCIC and station blackout, leading to early core damage and vulnerable containment. Although all four sequences result in early core damage with the containment being vulnerable, they were kept separate for the purposes of the containment and consequence analysis.

Finally, assignment of the accident sequences and their cut sets to the different damage states was performed by examination of the cut sets in both the accident sequences and the containment system sequences, as will be described later.

4.4.3 Failure Modes of Safety Systems

To determine failure modes for the plant safety systems, fault tree methodology is used. This methodology systematically identifies all groups of components in a system which, if they failed simultaneously, would result in failure of that system.

Construction of a fault tree begins by identifying the immediate causes of system failure. Each of these causes is then examined for more fundamental causes, until one has constructed a downward branching tree, at the bottom of which are failures not further reducible, i.e., failures of mechanical or electrical components due to all causes such as structural failure, human error, maintenance outage, etc. These lowest order failures on the fault tree are called basic events. Failures of basic events due to seismic ground motions, random failures, human error, and test and maintenance outages are included in the seismic analyses.

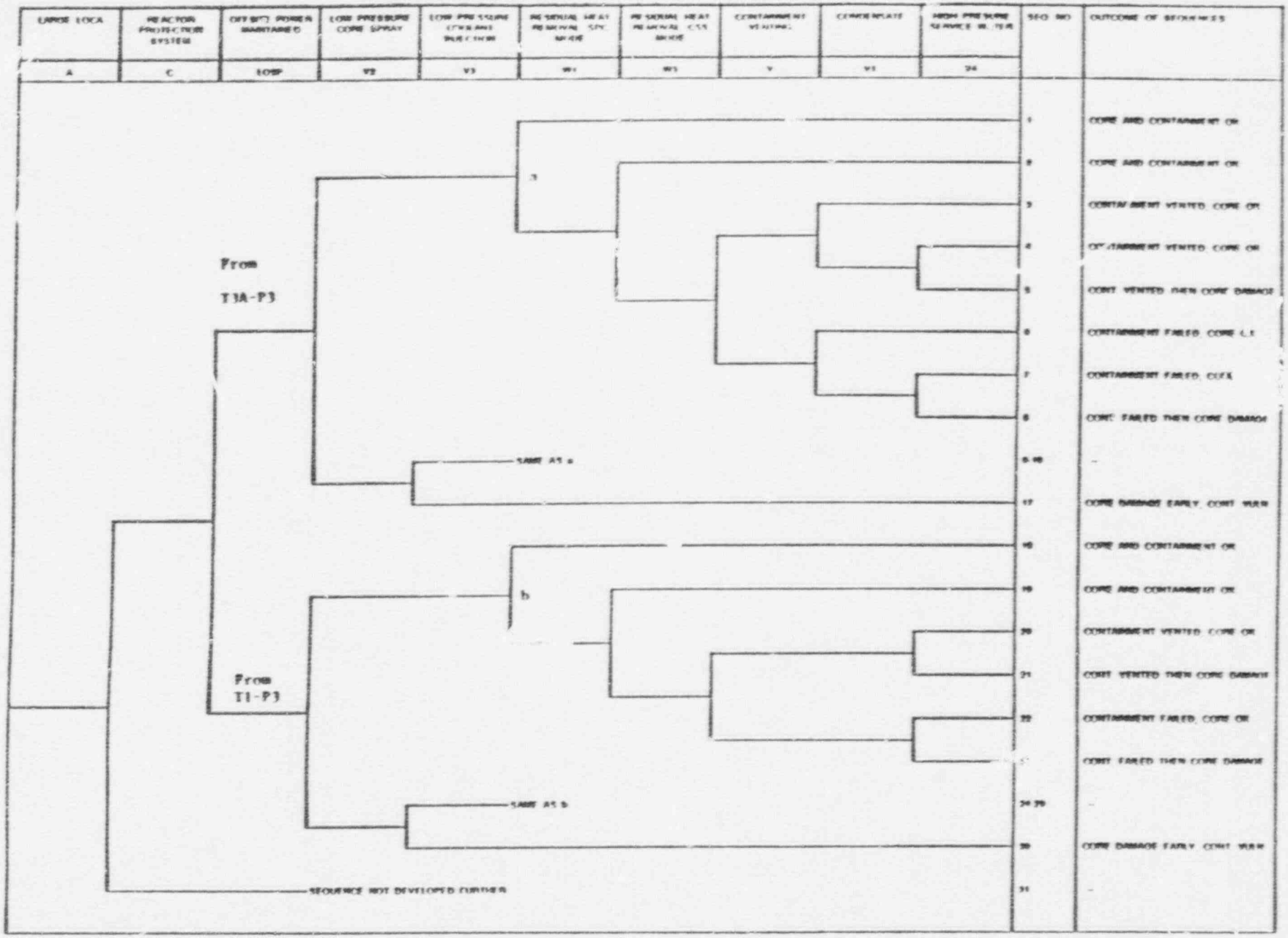

Figure 4.22 Large LOCA Event Tree

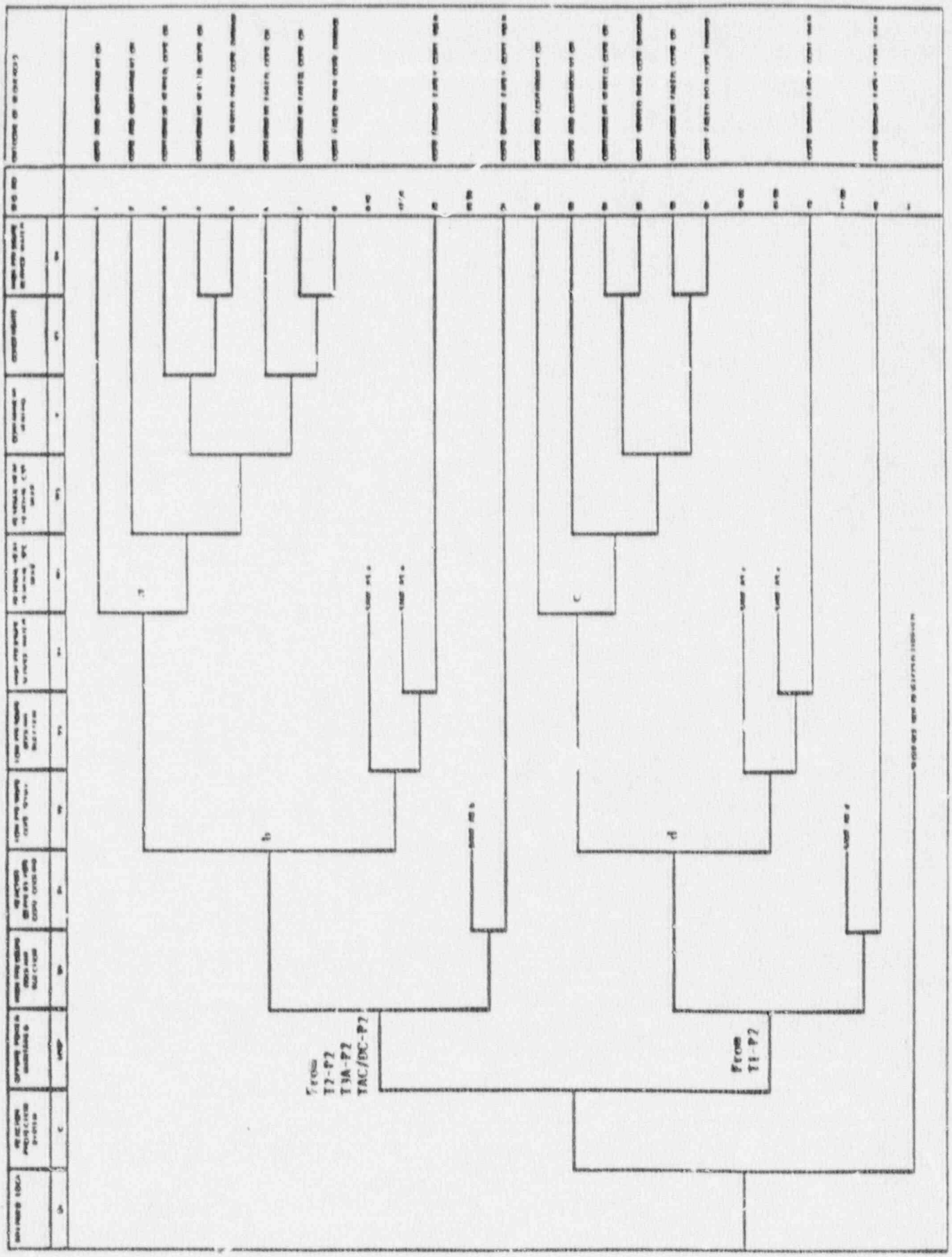

Figure 4.23 Medium LOCA Event Tree

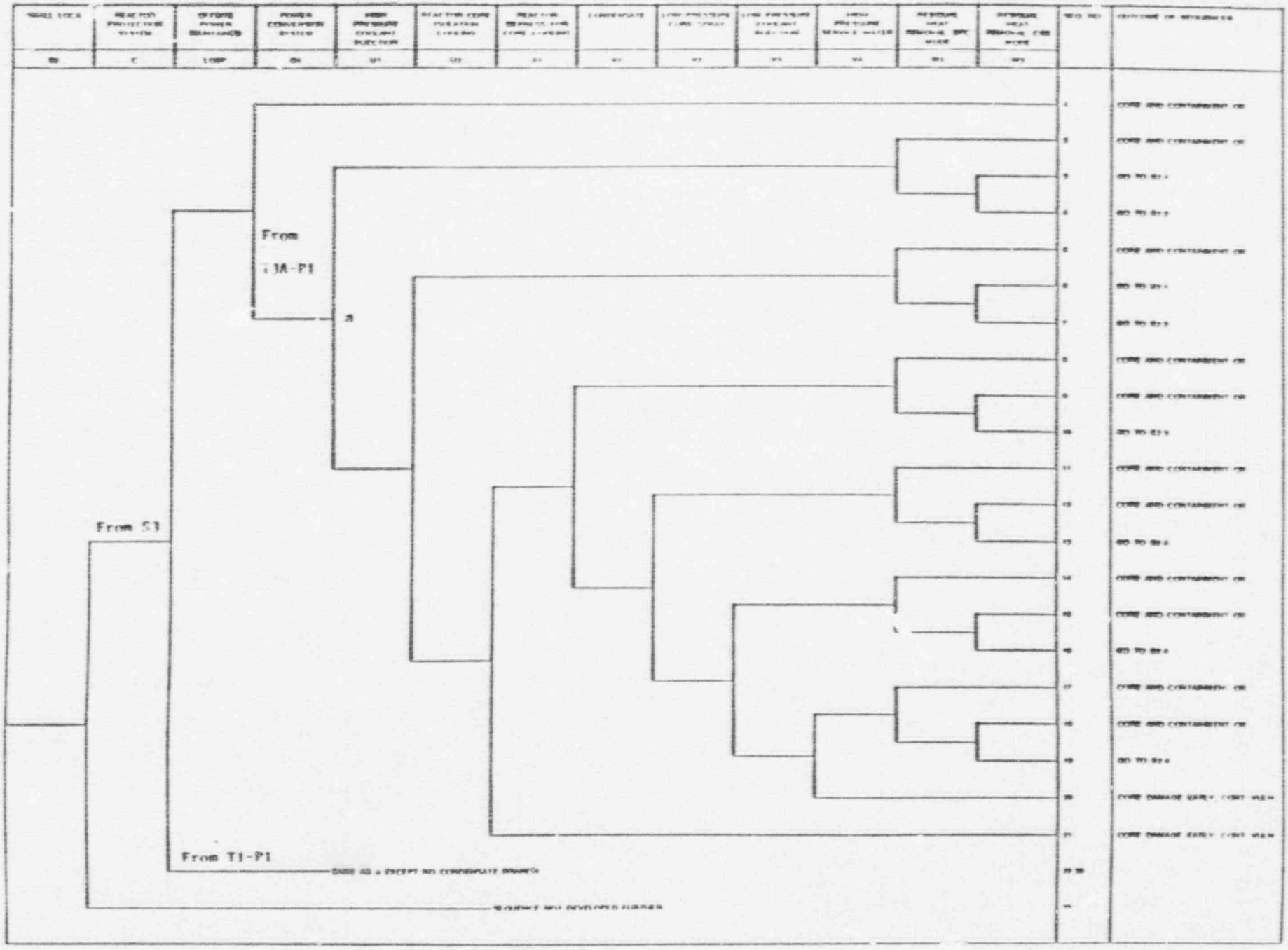

Figure 4.24. Small LOCA Event Tree

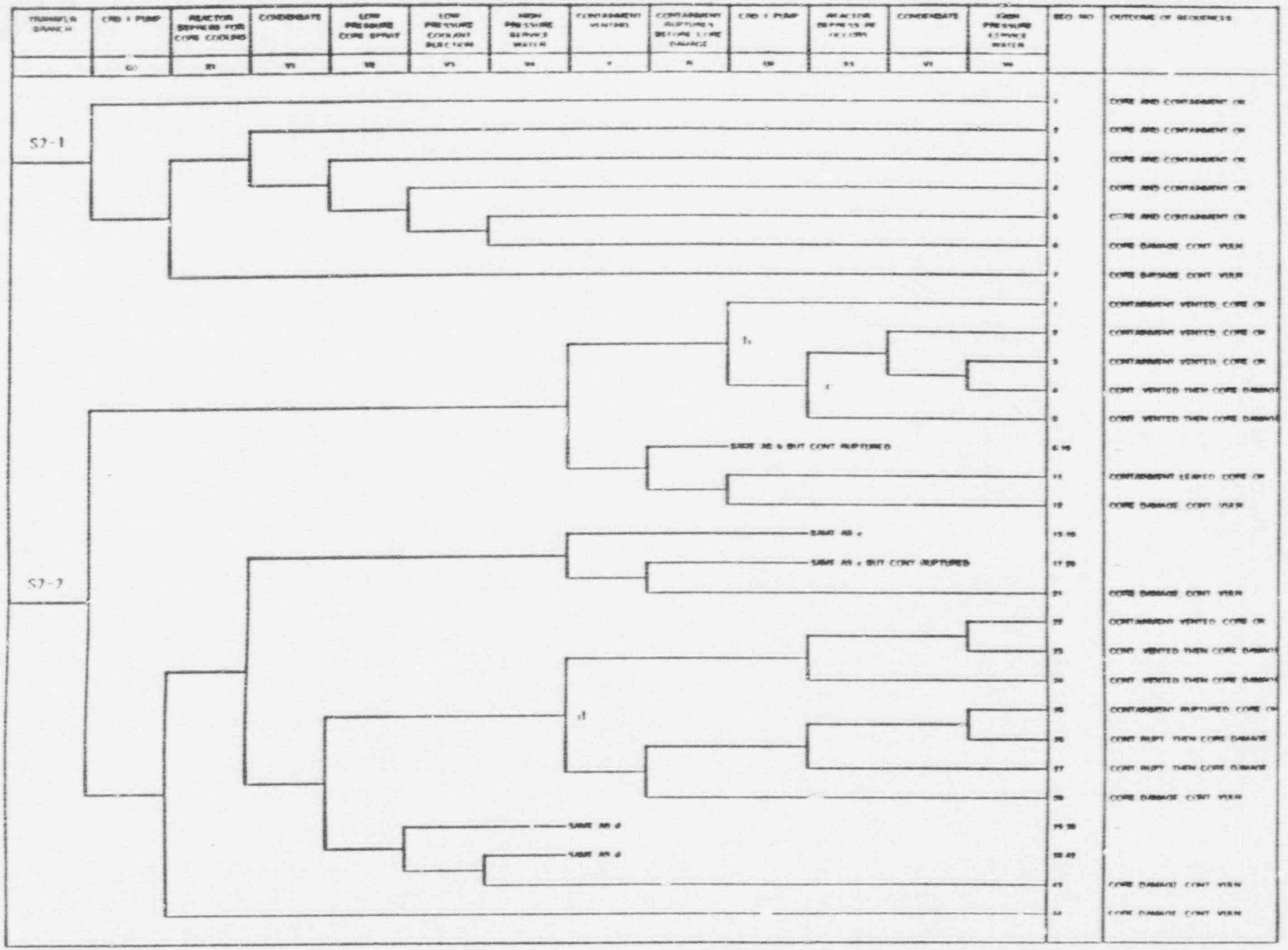

Figure 4.24. Small LOCA Event Tree (Cont'd)

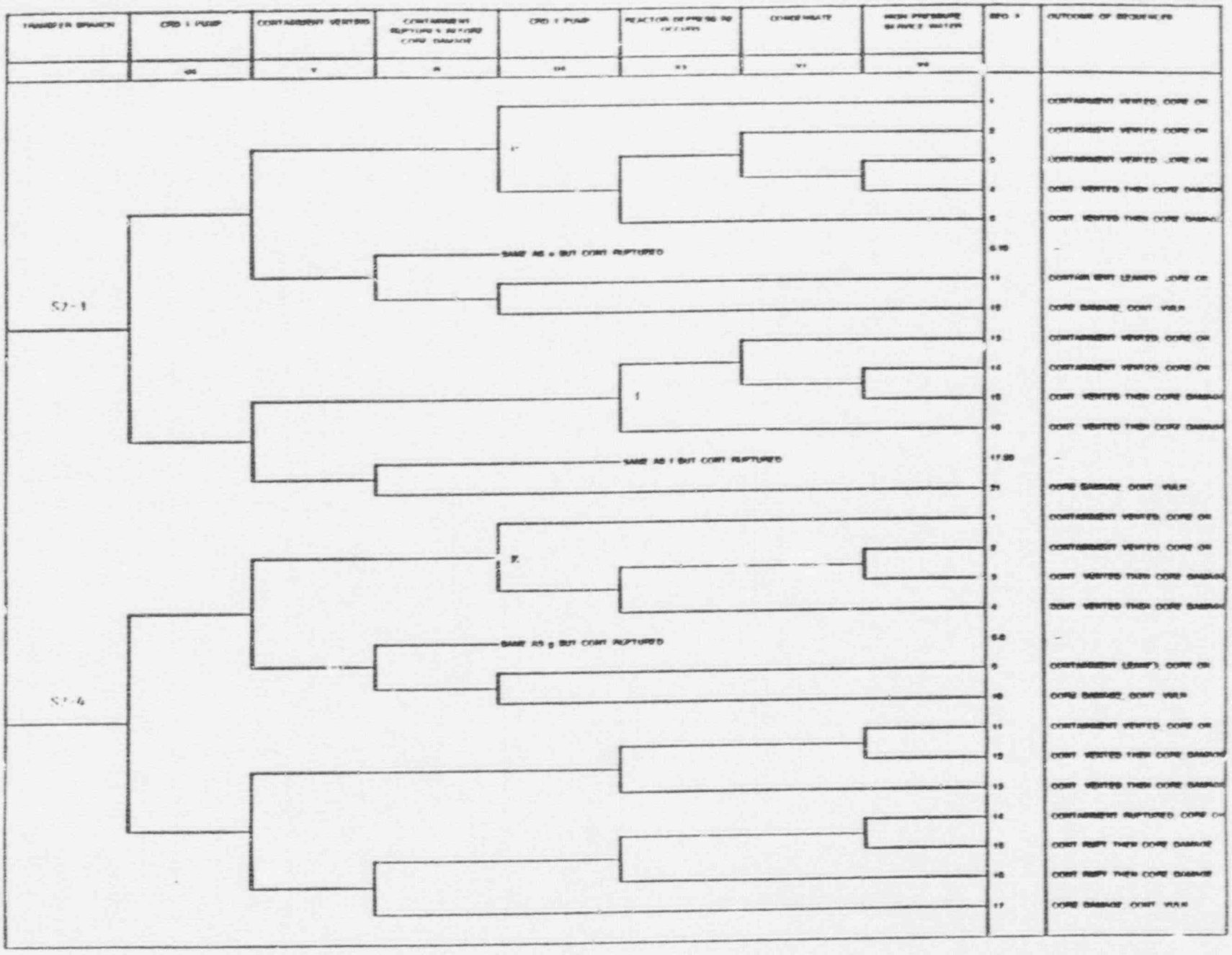

Figure 4.24. Small LOCA Event Tree (Concluded)

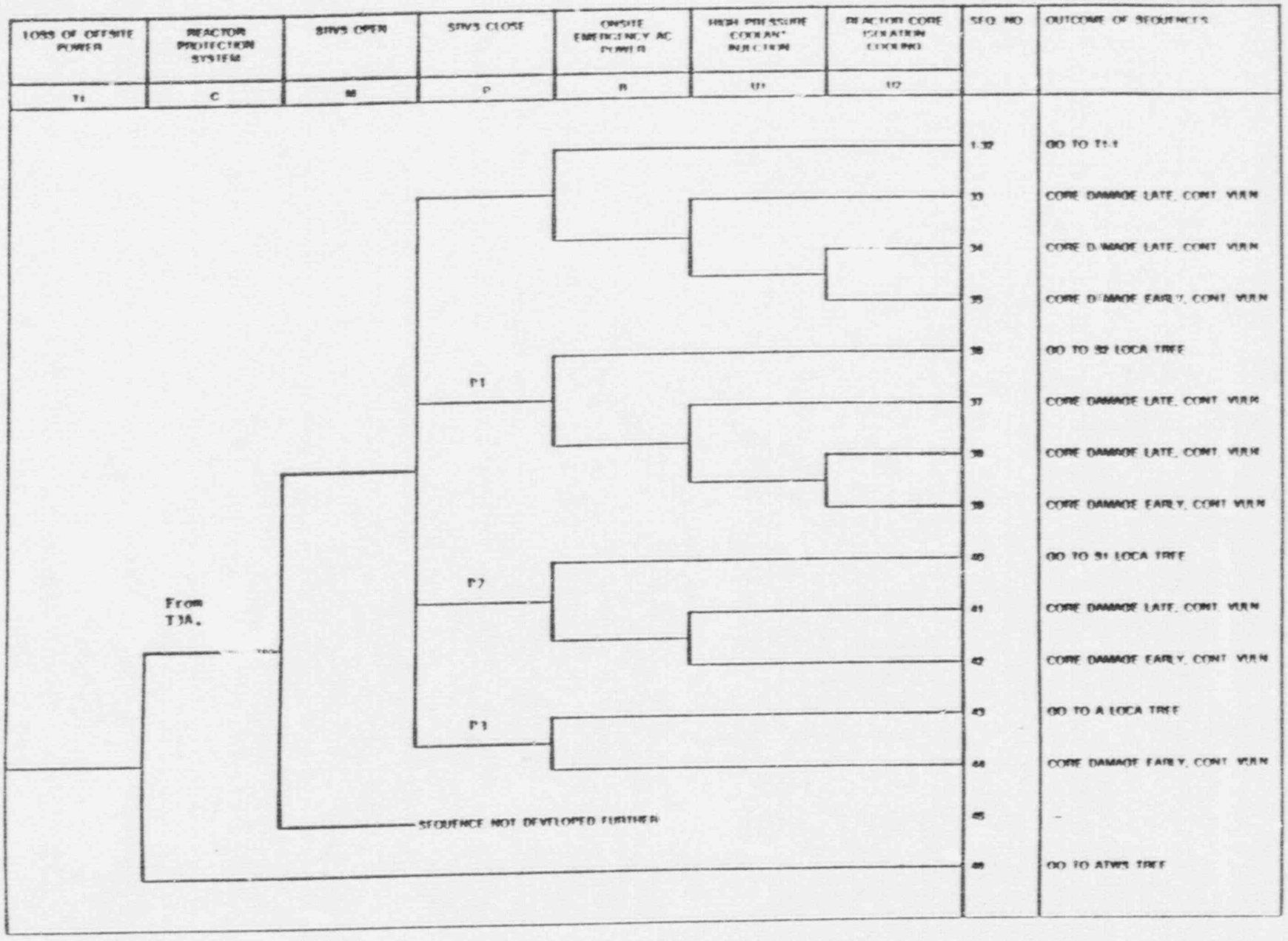

Figure 4.25. T_1 (Loss of Offsite Power) Event Tree

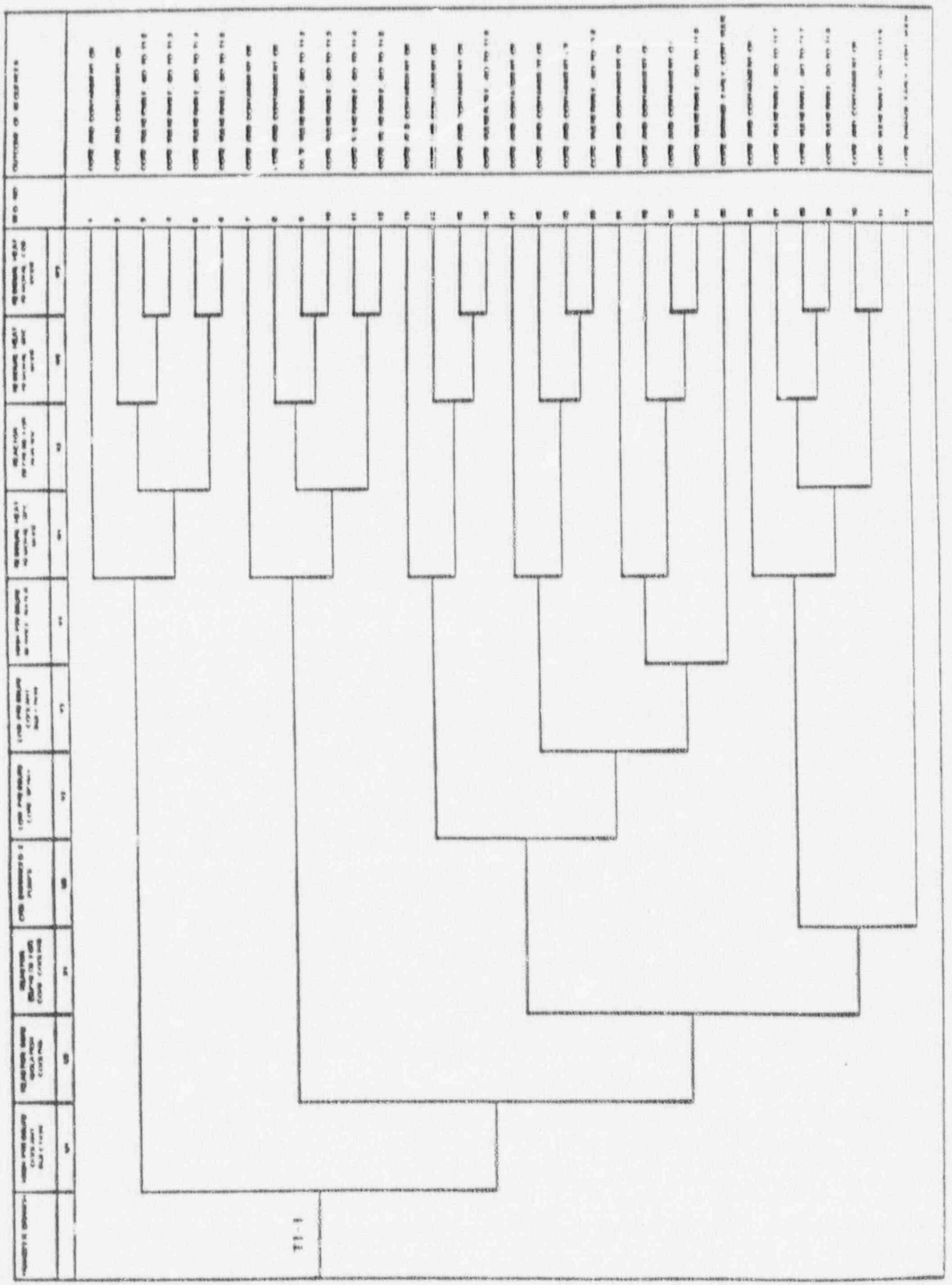

Figure 4.25. T_1 (Loss of Offsite Power) Event Tree (Cont'd)

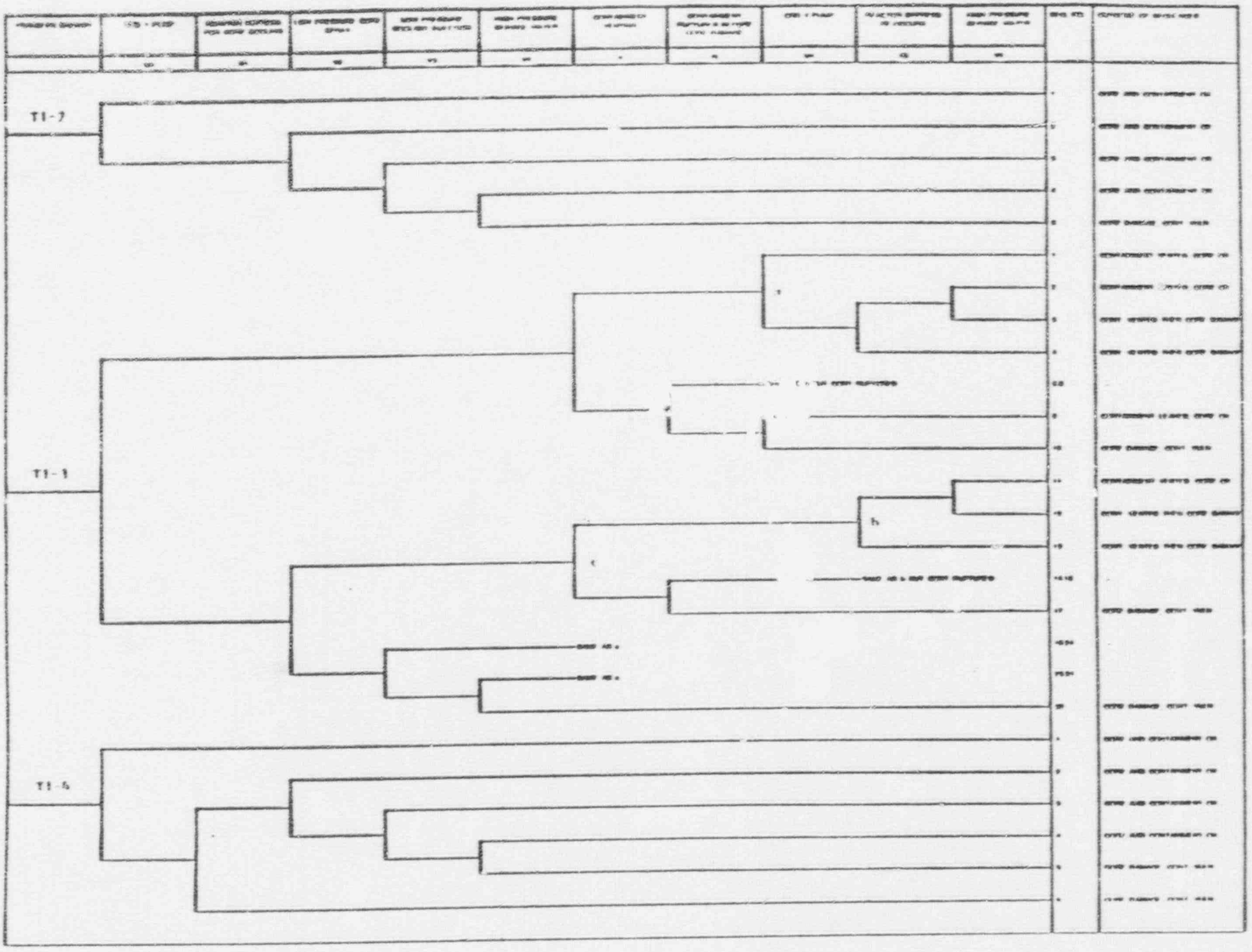

Figure 4.25. T_1 (Loss of Offsite Power) Event Tree (Cont'd)

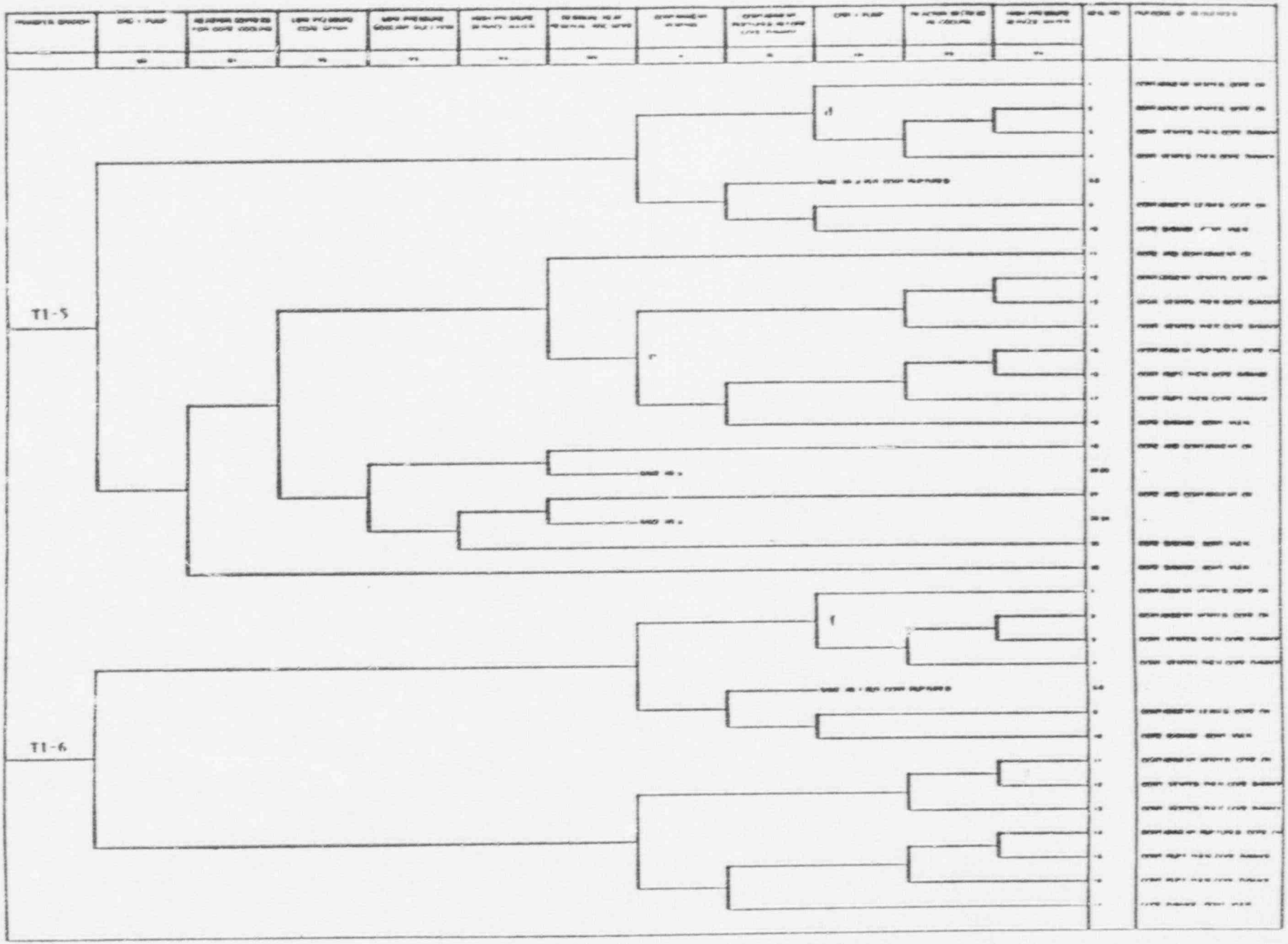

Figure 4.25. T_1 (Loss of Offsite Power) Event Tree (Cont'd)

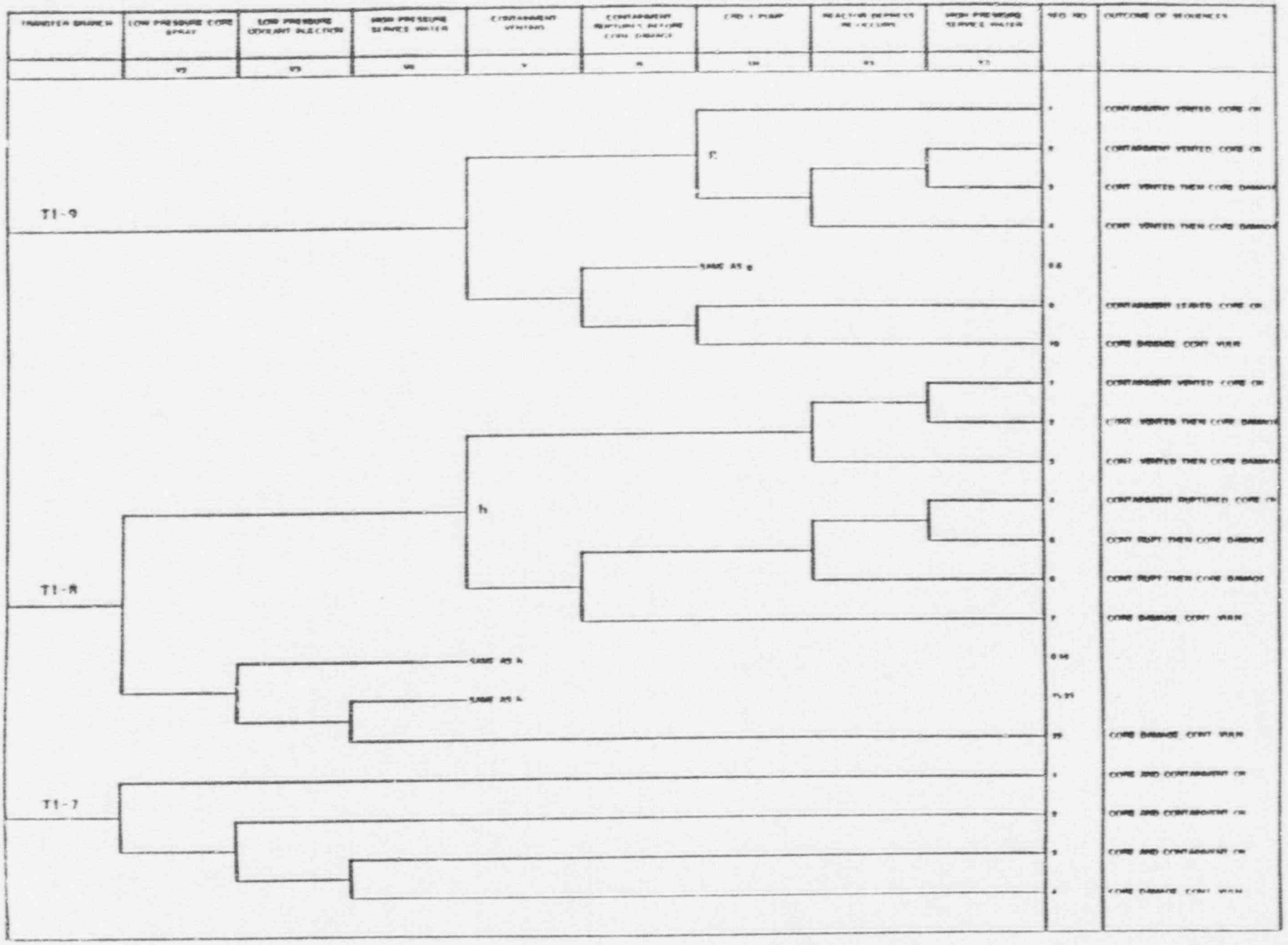

Figure 4.25. T_1 (Loss of Offsite Power) Event Tree (Concluded)

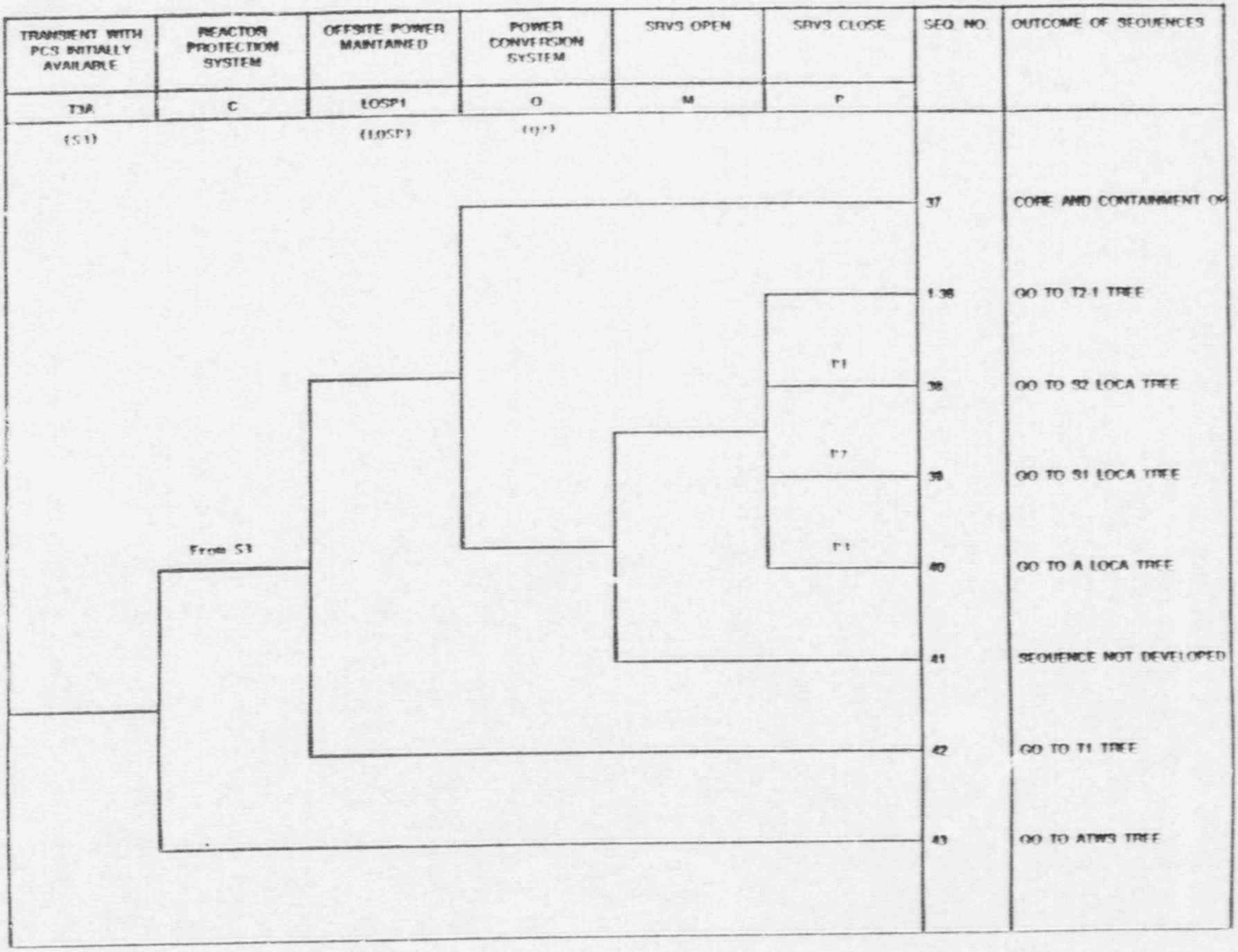

Figure 4.26. T_3 Transient (PCS initially available) Event Tree

The main difference between an internal event fault tree for a safety system and an external event fault tree is that consideration must be given to the physical location of the components, because the physical location determines to what extent secondary failures become important. Examples of this would be secondary failures due to local masonry wall collapse or due to a high temperature/steam environment from a broken steam line. Hence, in performing the seismic analyses, the locations of all important pieces of equipment must be determined from the general arrangement drawings for the plant, and then a systematic examination for secondary failure possibilities is made during the plant walkdown.

As stated earlier, the internal event PRA fault trees form the basis for the fault trees used in the seismic analysis. This allows for a consistent level of detail between internal and external event analyses, and assures the consistent inclusion of random and test/maintenance outage unavailabilities in the seismic analysis.

Since the internal event fault trees are assumed to exist and seismic failure modes are to be added, one must modify the internal event fault trees to include:

a. Local structural failures (block walls, cranes, etc.)

b. Failure of critical passive components (tanks, cable tray failures, and pipes) often missing in internal events analysis.

This is accomplished in several ways. First, the secondary or passive failure event can be added directly to the fault tree structure and the "gate" definition data file modified. Alternatively, the fragility definition of a relatively strong component on the tree may be redefined in terms of the (relatively weaker) associated secondary failure. Finally, events globally affecting a safety system or an accident sequence (such as building failure or liquefaction) can be added directly to the top event of the Boolean expression for the system failure or for the accident sequences.

4.4.4 Accident Sequence Evaluation

Accident sequence probabilities are used in determining the frequencies of core damage and of radioactive release for a given release category. Core damage frequency is defined as the sum of the frequencies of all accident sequences leading to core damage.

A. General Considerations

Each accident sequence consists of groups of events (successes or failures of safety systems) which must occur together. The failure of each safety system can be represented in terms of minimal cut sets, which are groups of component failures which will cause the safety system to fail. These cut sets and the accident sequences are combined together so

that every accident sequence can be expressed in a Boolean expression of the form

$$ACC_j = IE_j \ [C_1C_2C_3 \text{ or } C_4C_5 \text{ or } \ldots \text{ or } C_iC_jC_k]$$

in which IE_j is the initiating event and the C_i are basic events (i.e., failure of individual components) identified on the system fault trees. If at least one of the component failure groups $C_iC_jC_k$ occurs, then the accident sequence occurs. Computation of each accident sequence probability consists of determining the probability of each cut set, and then combining them to get the accident sequence probability.

Each basic event seismic failure probability is computed assuming that the response and fragility distributions are in log normal form. Calculations in the SSMRP showed that responses were reasonably fit by log normal distributions. The limited data on fragilities can be fit with log normal distributions as well as any other type. Hence, for convenience the log normal distribution is used for both. The equation used to calculate seismic failure frequencies is given as

$$P_f = \Phi \left[\frac{\ln \left(m_R / m_F \right)}{\sqrt{\beta^2_{FR} + \beta^2_{RR}}} \right]$$

where

Φ is the standard normal distribution function.

m_R, m_F are the medians of response and fragility functions

β_{FR}, β_{RR} are the corresponding random variabilities.

Note that the use of log normal distributions is not essential to the calculation process used in these calculations, and, in fact, any arbitrary pair of distributions could be used for the responses and fragilities provided they are physically meaningful and supported by the data available.

When the individual basic failure events in a cut set $C_iC_jC_k$ are not independent, correlation between the basic events must be explicitly included. When only two of the basic events are correlated the joint probabilities may be computed directly by the use of tables. When more than two basic events in a cut set are correlated, numerical multiple integration is used (such as contained in the SEISIM code developed in the SSMRP).

Finally, the accident sequences defined above are a function of peak ground acceleration, and as such, are conditional on the hazard curve.

They are subsequently unconditioned by integrating these sequences over the hazard curve as described subsequently.

B. Accident Sequence Quantification

Quantification of the accident sequences is a multi-step procedure involving several levels of screening. In the first step, the SETS code is used to evaluate all potential accident sequences using point estimate input screening values for all the seismic failure events (and using the internal events point estimate failure values for all random events). The same fault trees used by the internal events analysis are solved here with additions as noted in Section 4.4.3. The seismic screening values are taken as some conservative estimate, usually the component failure probabilities evaluated at three times the SSE. A dual probabilistic culling criterion is used in this culling process. This dual criterion is used in recognition of the fact that potentially large correlations can exist between basic events in the same cut set due to the pervasive nature of the seismic input motion. The result of this screening step is a reduced set of Boolean equations describing each of the safety and support systems.

In the second step, again utilizing the SETS code, these Boolean equations are merged together to form the accident sequences, again as defined for the internal events analysis. At this stage, truncation is performed based both on the order of the cut sets as well as the probability of the cut sets. The result of this step is Boolean equations describing each accident sequence and containing all the important seismic and random failure events.

The final step involves the actual quantification of the accident sequences. These accident sequence expressions are utilized both to compute point estimates of the accident sequence frequencies and to perform the uncertainty analysis calculations. A cross reference table is set up which relates each component to a component ID number, its random point estimate and error factor value, and to its associated seismic fragility category and seismic response category. This cross reference table thus provides all the information required to compute the probability of failure of any basic event (random or seismic or combined) at any peak ground acceleration level. The cross reference table for Peach Bottom is presented in Appendix C.

Finally, a complete uncertainty analysis is performed on the dominant accident sequences (and on the dominant cut sets in each accident sequence) as determined in the point estimate evaluations. A true Monte Carlo analysis was used for the NUREG-1150 studies. Thus, the expression for the unconditional accident sequence frequencies (and for core damage frequency), shown as below:

$$ACC_j = \int P(ACC_j, PGA) f_{eq}(PGA) d(PGA)$$

where

$P(ACC_j, PGA)$ is the conditional accident sequence frequency as a function of PGA, and

$f_{eq}(PGA)$ is the probability distribution function for the hazard curve,

is randomly sampled varying the hazard curve parameters, the random failure frequencies, and the seismic response and fragility parameters. From the accumulated values of accident sequence frequency and core damage frequency, exact statistics on their distributions are directly obtainable.

Note that in performing the uncertainty analyses, full correlation between random samples taken from each response category and from each fragility category was enforced. This is correct, and consistent with the philosophy utilized in the internal event NUREG-1150 uncertainty calculations.

In addition to the full uncertainty analysis (which produces exact mean values and exact percentiles of the distributions of the accident sequences and total core damage frequency) a "mean point estimate" is computed. The mean point estimate is useful for illustrating various intermediate results (conditional accident sequence frequencies, initiating event frequencies, etc.) which explain the flow of the calculations, for demonstrating convergence of the numerical integration, and for performing sensitivity studies in a cost-effective manner. Specifically, the mean point estimate is used to understand the contributions of the various basic events to the total frequencies and to understand the contributions to the total uncertainty bands.

The mean point estimate is computed by using the mean random failure frequencies, the mean seismic hazard curve, and mean values for the seismic failure event frequencies in evaluating the accident sequences. Only one re-evaluation of the accident sequences is required. These mean point estimates will be seen to be nearly equal to the exact mean values of the accident sequence and core damage frequencies as obtained in the uncertainty analysis. This is to be expected because mean values probabilistically add to yield the mean value of each accident sequence (conditional on the hazard), and the only difference between the true mean and the mean point estimate has to do with integration of the conditional accident frequencies over the hazard curve. Experience has shown, however, that the difference between these is very small.

4.4.5 Base Case Peach Bottom Results

This section presents the results of the base case seismic risk analysis for the Peach Bottom Nuclear Power Plant. The base case is our best estimate of the current configuration of the plant and its emergency procedures. In particular, the seismic component failure probabilities

were taken from the generic fragility data base (Table 4.9), the site-specific component fragilities from Table 4.10, and the building fragilities were given in Table 4.11. As described earlier, a total of seven initiating events and five event trees were used for the seismic analysis.

A total of 22 accident sequences survived the seismic screening process. These 22 sequences are presented in Table 4.12 along with identification of the Boolean sequences that were solved for each accident sequence. (The number of Boolean expressions solved using the SETS code is less than the number of accident sequences because several accident sequences may utilize the same Boolean expression even though the initiating event may be different.) Also identified on this table are the complement expressions which must be included in the numerical sequence quantification at high PGA levels for which success probabilities may be significantly less than unity. The multiplier expression column lists those events specified by algebraic equations rather than by Boolean logical expressions. The analytical equations used for calculating the multipliers, the Boolean sequences, and the complement factors are presented in Appendix C. Table 4.13 describes the abbreviations used for the accident sequences in Table 4.12.

These 22 non-negligible accident sequences resulting from the screening process were fully re-quantified using best-estimate random failures and best estimate seismic fragilities and responses plus associated variabilities. The total mean core damage frequency for the Peach Bottom base case was computed to be 7.66E-5 per year using the LLNL hazard curve and 3.09E-6 per year using the EPRI hazard curve. The mean contributions of the accident sequences are shown on Table 4.14 for both hazard curves. Percentiles of the frequency distributions from the Monte Carlo analysis are shown on Tables 4.15 and 4.16. (Relative importance of the basic events to these results is presented in the point estimate results presented later.)

Based on this final quantification, five dominant sequences were identified. These dominant sequences are :

Accident Sequence	Contribution (LLNL Hazard)	Contribution (EPRI Hazard)
T1-33	48%	52%
ALOCA-30	24%	22%
RVR-1	11%	11%
RWT-1	9%	6%
S1LOCA-70	4%	6%

The percentage contributions were taken from the Monte Carlo uncertainty results on Table 4.14. Note that the same dominant accident sequences were obtained from the two different hazard curves. Further, it will be seen later that the order of the major basic event contributors is the same. A description of the top seven accident sequences follows.

Table 4.12

Seismic Accident Sequences

	Accident Sequence		Multiplier Expression	Boolean Expression	SETS ID No.	Complement Factor
	Vessel Rupture					
1.	RVR-1		1	1	N/A	1
	Large LOCA					
2.	ALOCA-17	$A\ \overline{C}\ \overline{LOSP}\ V_2V_3$	1	BOOL 5	N/A	$\overline{C}$
3.	ALOCA-30	$A\ \overline{C}\ LOSP\ V_2V_3$	1	BOOL 4+RWT	N/A	$\overline{C}$
	Intermediate LOCA					
4.	S1 LOCA-25	$S_1\ \overline{C}\ \overline{LOSP}\ \overline{U_1}\ V_2V_3V_4$	1	BOOL 6	N/A	$\overline{CU_1LOSP}$
5.	S1-LOCA-70	$S_1\ \overline{C}\ LOSP\ \overline{U_1}\ V_2V_3V_4$	1	Bool 4		
6.	S1 LOCA-80	$S_1\ \overline{C}\ LOSP\ U_1\ X_1$	1	RWT	N/A	$\overline{CU}_1$
	Small LOCA					
7.	S2 LOCA-2-44	$S_2\ \overline{C}\ \overline{LOSP}\ Q_1\overline{U}_1W_1W_3U_4X_1$	1	BOOL 7	N/A	$\overline{C}$
8.	S2 LOCA-42	$S_2\ \overline{C}\ LOSP\ U_1U_2X_1$	1	RWT	N/A	$\overline{C}$
	Radwaste/Turbine Building					
9.	RWT-1	$RWT\ \overline{C}\ \overline{M}\ \overline{P}\ B\ U_1\ U_2$	1	1	N/A	$\overline{CMP}$
10.	RWT-2	$RWT\ \overline{C}\ \overline{M}\ P_1\ B\ U_1\ U_2$	1	1	N/A	$\overline{CMP}_1$
11.	RWT-3	$RWT\ \overline{C}\ \overline{M}\ P_2\ B\ U_1\ U_2$	1	1	N/A	$\overline{CMP}_2$
12	RWT-4	$RWT\ \overline{C}\ \overline{M}\ P_3\ B\ U_1\ U_2$	1	1	N/A	$\overline{CMP}_3$

Table 4.12

Seismic Accident Sequences (Concluded)

	Accident Sequence	Multiplier Expression	Boolean Expression	SETS ID No.	Complement Factor
	LOSP Transient				
13.	T1-25	$T_1\overline{CMPB}U_1U_2X_1V_2V_3V_4$	1	$BU_1U_2X_1V_2V_3V_4$	$\overline{CMBX_1P}$
14.	T1-32	$T_1\overline{CMPB}U_1U_2X_1U_3$	1	$BU_1U_2X_1U_3$	$\overline{CMBP}$
15.	T1-33	$T_1\overline{CMPBU_1}$	1	BU_1 · BOOL 4	$\overline{CMU_1P}$
16.	T1-36 to S2-41	$T_1\overline{CMP_1B}$ $U_1U_2X_1V_2V_3V_4$	P_1	$BU_1U_2X_1V_1V_2V_3V_4$	$\overline{CMBX_1}$
17.	T1-36 to S2-42	$T_1\overline{CMP_1B}$ $U_1U_2X_1$	P_1	$BU_1U_2X_1$	$\overline{CMB}$
18.	T1-40 to S1-70	$T_1\overline{CMP_2}BU_1V_2V_3V_4$	P_2	$BU_1X_1V_2V_3V_4$	$\overline{CMBX_1U_1}$
19.	T1-40 to S1-80	$T_1\overline{CMP_2}BU_1X_1$	P_2	BU_1X_1	$\overline{CMB}$
20.	T1-43 to ALOCA-30	$T_1\overline{CMP_3}BV_2V_3$	P_3	BV_2V_3	$\overline{CMB}$
	Transient with PCS Initially Available				
21.	T3A-1 to T2-1-29	T_{3A} $\overline{C}$ $\overline{LOSP}$ Q_R $\overline{MP}$ $U_1U_2X_1U_3$	Q	$U_1U_2X_1U_3$	$\overline{C\ LOSP\ P}$
22.	T3A-1 to T2-1-36	T_{3A} $\overline{C}$ $\overline{LOSP}$ Q_R $\overline{MP}$ $U_1U_2\overline{X}_1V_1V_2V_3V_4$	Q	$U_1U_2X_1V_1V_2V_3V_4$	$\overline{C\ LOSP\ P\ X_1M}$

Table 4.13

Safety Systems Nomenclature

ARI	-	Failure of the Alternate Rod Insertion System
B	-	Failure of all ac power (station blackout)
C	-	Failure of the Reactor Protection System (RPS)
C1	-	Failure of RPS and manual scram
I	-	Failure to inhibit the ADS system
L	-	Failure of operator to isolate S3 "leak"
LOSP,LOSP1	-	Failure to maintain offsite power; Different Designations for this Event are for Different Frequencies
M	-	Failure of Safety Relief Valves (SRVs) to open
P	-	Failure of SRVs to close
P1,P2,P3	-	Failure of one, two or three SRVs to reclose
Q,Q1,Q2	-	Failure of the Power Conversion System (PCS), different designations for this event are for different frequencies
ROD	-	Failure to manually insert the control rods
RPSM	-	Failure of the mechanical RPS
RPSE	-	Failure of the electrical RPS
RPT	-	Failure to trip the recirculation pumps
SCRM	-	Failure to manually scram the reactor
SLC	-	Failure of the Standby Liquid Control System
U1	-	Failure of the High Pressure Coolant Injection (HPCI) system
U1'	-	Failure of HPCI without ventilation
U2	-	Failure of the Reactor Core Isolation Cooling (RCIC) system
U2'	-	Failure of RCIC without recirculation
U3	-	Failure of the Control Rod Drive (CRD) system (2 pump mode)
U4	-	Failure of the Control Rod Drive (CRD) system (1 pump mode)
U4'	-	Failure of CRD to survive containment venting
V1	-	Failure of the Condensate system
V1'	-	Failure of Condensate to survive containment venting
V2	-	Failure of the Low Pressure Core Spray (LPCS) system
V3	-	Failure of the Low Pressure Coolant Injection (LPCI) system
V4	-	Failure of the High Pressure Service Water (HPSW) system as an injection source to the reactor
V4'	-	Failure of HPSW (injection source) to survive containment venting
R	-	Rupture of the containment
W1	-	Failure of the Suppression Pool Cooling (SPC) mode of RHR
W2	-	Failure of the Shutdown Cooling (SDC) mode of the RHR
W3	-	Failure of the Containment Spray (CS) mode of the RHR
X1	-	Failure to depressurize the primary system via SRVs or the Automatic Depressurization System (ADS)
X2	-	Failure to depressurize the primary system to allow SDC to operate
X3	-	Failure to depressurize the primary system subsequent to an initial primary system depressurization
Y	-	Failure of Primary Containment Venting System (including makeup to the pool as required)

Table 4.14
Accident Sequence and Total Core Damage Mean Frequencies (1/yr)

	Accident Sequence	Mean Frequency LLNL Hazard	Mean Frequency EPRI Hazard
1	RVR-1	8.92E-6	3.27E-7
2	ALOCA-17	1.23E-7	6.99E-9
3	ALOCA-30	1.84E-5	6.70E-7
4	S_1LOCA-25	2.02E-8	5.49E-10
5	S_1LOCA-70	6.67E-6	1.85E-7
6	S_1LOCA-80	6.72E-7	2.27E-8
7	S_2LOCA-2-44	2.86E-7	6.43E-9
8	S_2LOCA-42	1.20E-6	4.90E-8
9	RWT-1	2.76E-6	1.75E-7
10	RWT-2	2.94E-7	1.86E-8
11	RWT-3	6.26E-9	3.87E-10
12	RWT-4	6.26E-10	3.87E-11
13	T1-25	2.98E-7	6.45E-9
14	T1-32	1.18E-10	2.63E-12
15	T1-33	3.69E-5	1.61E-6
16	T1-36 to S2-41	2.86E-8	6.20E-10
17	T1-36 to S2-42	1.11E-11	2.50E-13
18	T1-40 to S1-70	1.27E-10	3.27E-12
19	T1-40 to S1-80	5.67E-13	1.40E-14
20	T1-43 to ALOCA-30	2.53E-7	1.14E-8
21	T3A-1 to T2-1-29	1.45E-9	2.94E-11
22	T3A-1 to T2-1-36	4.48E-10	8.18E-12
	TOTAL	7.66E-5	3.09E-6

Table 4.15

Base Case Accident Sequence Frequency Distribution Percentiles (LLNL Hazard)

No.	Sequence	Mean	Var	5%	50%	95%
1	RVR-1	8.92E-6	4.01E-09	1.64E-10	1.46E-07	2.66E-05
2	ALOCA-17	1.23E-7	3.68E-12	3.77E-13	5.40E-10	2.35E-07
3	ALOCA-30	1.84E-5	1.08E-08	1.05E-09	4.55E-07	6.79E-05
4	S_1LOCA-25	2.02E-8	4.59E-15	5.64E-15	2.95E-11	2.33E-08
5	S_1LOCA-70	6.67E-6	7.06E-10	3.29E-10	1.40E-07	1.67E-05
6	S_1LOCA-80	6.72E-7	1.54E-11	9.73E-12	1.08E-08	1.22E-06
7	S_2LOCA-2-44	2.86E-7	5.52E-13	9.33E-13	9.95E-10	3.35E-07
8	S_2LOCA-42	1.20E-6	4.26E-11	3.32E-11	2.68E-08	3.59E-06
9	RWT-1	2.76E-6	4.31E-10	4.72E-11	3.83E-08	8.12E-06
10	RWT-2	2.94E-7	4.88E-12	5.02E-12	4.08E-09	8.64E-07
11	RWT-3	6.26E-9	2.12E-15	1.05E-13	8.50E-11	1.80E-08
12	RWT-4	6.26E-10	2.12E-17	1.05E-14	8.50E-12	1.80E-09
13	T1-25	2.98E-7	1.40E-12	3.99E-16	9.60E-11	1.97E-07
14	T1-32	1.18E-10	6.48E-20	1.06E-15	1.30E-12	1.81E-10
15	T1-33	3.69E-5	5.38E-08	1.35E-08	1.69E-06	1.21E-04
16	T1-36 to S2-41	2.86E-8	1.29E-14	3.83E-17	9.21E-12	1.89E-08
17	T1-36 to S2-42	1.11E-11	5.87E-22	1.19E-16	1.26E-13	1.73E-11
18	T1-40 to S1-70	1.27E-10	1.59E-19	3.58E-16	7.46E-13	2.26E-10
19	T1-40 to S1-80	5.67E-13	1.54E-24	1.59E-17	8.16E-15	8.45E-13
20	T1-43 to ALOCA-30	2.53E-7	7.24E-12	2.18E-13	2.36E-09	6.57E-07
21	T3A-1 to T2-1-29	1.45E-9	7.92E-18	6.25E-15	3.71E-12	1.16E-09
22	T3A-1 to T2-1-36	4.48E-10	4.91E-19	1.21E-15	1.49E-12	4.58E-10
	TOTAL	7.66E-5	1.34E-07	5.33E-08	4.41E-06	2.72E-04

Table 4.16

Base Case Accident Sequence Frequency Distribution Percentiles (EPRI Hazard)

No.	Sequence	Mean	Var	5%	50%	95%
1	RVR-1	3.27E-07	1.95E-12	1.69E-11	2.16E-08	1.37E-06
2	ALOCA-17	6.99E-09	5.10E-15	1.09E-13	8.67E-11	1.60E-08
3	ALOCA-30	6.70E-07	5.12E-12	2.34E-10	6.92E-08	3.09E-06
4	S_1LOCA-25	5.49E-10	1.17E-17	1.98E-15	4.93E-12	1.53E-09
5	S_1LOCA-70	1.85E-07	4.70E-13	9.30E-11	2.10E-08	7.93E-07
6	S_1LOCA-80	2.27E-08	1.41E-14	6.76E-13	1.51E-09	7.59E-08
7	S_2LOCA-2-44	6.43E-09	1.05E-15	2.51E-13	1.82E-10	2.27E-08
8	S_2LOCA-42	4.90E-08	5.87E-14	2.45E-12	3.78E-09	2.00E-07
9	RWT-1	1.75E-07	1.62E-12	7.83E-12	5.97E-09	5.32E-07
10	RWT-2	1.86E-08	1.83E-14	8.34E-13	6.36E-10	5.66E-08
11	RWT-3	3.87E-10	7.95E-18	1.74E-14	1.32E-11	1.18E-09
12	RWT-4	3.87E-11	7.95E-20	1.74E-15	1.32E-12	1.18E-10
13	T1-25	6.45E-09	2.82E-15	4.41E-17	1.20E-11	1.58E-08
14	T1-32	2.63E-12	1.03E-22	1.00E-16	1.88E-13	1.27E-11
15	T1-33	1.61E-06	3.36E-11	8.06E-09	2.89E-07	6.01E-06
16	T1-36 to S2-41	6.20E-10	2.60E-17	4.23E-18	1.15E-12	1.51E-09
17	T1-36 to S2-42	2.50E-13	8.97E-25	1.36E-17	1.84E-14	1.18E-12
18	T1-40 to S1-70	3.27E-12	1.81E-22	1.01E-16	1.07E-13	1.37E-11
19	T1-40 to S1-80	1.40E-14	2.78E-27	3.78E-18	1.26E-15	5.34E-14
20	T1-43 to ALOCA-30	1.14E-08	4.16E-15	7.80E-15	2.50E-10	3.25E-08
21	T3A-1 to T2-1-29	2.94E-11	2.56E-20	1.78E-15	6.54E-13	9.50E-11
22	T3A-1 to T2-1-36	8.18E-12	1.27E-21	3.84E-16	2.42E-13	3.31E-11
	TOTAL	3.09E-06	7.61E-11	2.30E-08	7.07E-07	1.27E-05

Description of Dominant Accident Sequences

The dominant accident sequences can be understood after reviewing the basic dependencies at Peach Bottom. Peach Bottom has three systems of high pressure injection (HPCI, RCIC, and CRD). Both HPCI and RCIC are steam-driven and dependent only on DC battery power for actuation and control. Given failure of the high pressure injection systems, there are both automatic and manual means of depressurizing the system. There are then four potential means of cooling the core at low pressure (condensate, LPCS, LPCI, and via the HPSW systems). The low pressure systems all require AC motive power.

Peach Bottom has four diesel generators (shared) and four station batteries (per unit) and thus, a high degree of redundancy is available in the onsite AC power system. The diesel generators, however, are dependent on the emergency service water system for cooling. Loss of this cooling is assumed to result in early failure of the diesel generators.

Successful operation of any one of the three pumps (two ESW and one ECW) will provide the necessary cooling to all four diesel generators as well as all emergency room cooling and all emergency pump cooling. Thus, failure of these three pumps together would result in loss of all diesels as well as loss of all room and emergency pump cooling. ESW pump A takes power from diesel generator B while ESW pump B takes power from diesel generator C. Lastly, the ECW pump takes AC power from diesel generator D. Thus, any appropriate combination of electrical bus failure, diesel generator failure, and emergency cooling water pump failure will result in loss of all three diesels and, in conjunction with loss of offsite power, will result in station blackout. In addition, failure of the turbine building is assumed to fail the power and control cables to the ECW pump and thus constitutes a means of failing one of the three pumps. These dependencies result in the vast majority of the cut sets computed in the dominant sequences for Peach Bottom as described below.

Sequence T_1-33 is a LOSP transient in which onsite power (B) fails but the HPCI system (U1) succeeds. Thus, the high pressure injection system succeeds initially and will continue functioning until battery depletion occurs or until the HPCI and RCIC pumps fail due to loss of room cooling. Thus the sequence involves station blackout (SBO) and late core damage with the containment being vulnerable. The dominant cut sets are given in Bool(4) and all cut sets constitute the failure of the ESW system. Note that the failure of the ESW system also fails the low pressure systems LPCI and LPCS.

Sequence ALOCA-30 is a large loss of coolant break in conjunction with LOSP and loss of the low pressure LPCI and LPCS systems. The surviving cut sets in this sequence are again due to Bool(4) each of which causes a failure of the emergency service water cooling which fails the diesels. Hence, this is a large LOCA in conjunction with station blackout. Note

that the Radwaste-Turbine Building also makes a contribution to this sequence. Dominant cut sets are all failures of the ESW system, which with LOSP, results in station blackout. Hence, the low pressure injection systems are without power. The result is SBO, early core damage with a vulnerable containment.

Sequence RVR-1 is the hypothesized failure of the reactor vessel supports leading to an uncoolable configuration (i.e., the ECCS is ineffective in providing cooling to the core). This event leads directly to core damage, and no mitigating safety systems need be considered (except for containment post accident pressure control and radiation removal in the consequence analysis).

Sequence S1 LOCA-70 is an intermediate break LOCA with loss of offsite power. In this case, HPCI succeeds long enough until the system is depressurized to the point where low pressure injection could be utilized. However, since a station blackout situation exists there is no motive power for any of the low pressure injection systems. The result is station blackout, early core damage, and a vulnerable containment.

Sequence RWT-1 is a transient sequence brought about by the failure of the Radwaste/Turbine Building as an initiator. Both HPCI and RCIC high pressure injection systems fail due to the loss of actuation and control. The result is a station blackout with no high pressure injection leading to early core damage and vulnerable containment.

Sequence S2 LOCA-42 is a small break LOCA in conjunction with loss of offsite power and immediate failures of both HPCI and RCIC high pressure systems as well as failure to depressurize due to the RWT failure. The result is SBO, early core damage and containment vulnerability.

Sequence S1 LOCA-80 is an intermediate break LOCA in conjunction with loss of offsite power, failure of HPCI, and failure to depressurize the system (X_1). The logical cut set causing immediate failure of HPCI and X_1 is the Radwaste/Turbine Building failure. Failure to depressurize results from the station blackout situation. The result is SBO, early core damage and a vulnerable containment.

Mean Point Estimates Using LLNL Hazard Curves

As described earlier, the mean point estimate is based on using the mean values for all variables. The mean initiating event frequencies at different PGA values are given in Table 4.17. As can be seen, at the lower earthquake levels the transient sequence initiating events dominate, and as the earthquake acceleration level increases, the LOCA initiators increase until, finally, at the highest earthquake levels, there is a contribution from the reactor vessel rupture (RVR) event. Also note that, at each earthquake level, the initiating events sum to 1.0. Values of the dominant accident sequence mean conditional frequencies at various earthquake levels are presented in Table 4.18. These are the values that are subsequently integrated over the hazard curve to obtain the unconditional accident sequence frequencies.

Table 4.17

Mean Initiating Event Frequencies (LLNL Hazard)

IE	0.23g	0.37g	0.53g	0.68g	0.83g	0.98g	1.12g
1	3.4E-05	1.9E-03	1.5E-02	5.4E-02	1.3E-01	2.3E-01	3.4E-01
2	6.8E-03	5.3E-02	1.4E-01	2.5E-01	3.3E-01	3.8E-01	3.8E-01
3	9.4E-04	1.1E-02	3.6E-02	6.7E-02	8.9E-02	9.6E-02	8.9E-02
4	1.1E-02	6.5E-02	1.4E-01	1.8E-01	1.8E-01	1.5E-01	1.1E-01
5	5.6E-05	3.2E-03	1.9E-02	4.1E-02	5.2E-02	4.7E-02	3.3E-02
6	4.1E-01	6.9E-01	6.0E-01	4.0E-01	2.2E-01	1.0E-01	4.2E-02
7	5.7E-01	1.8E-01	4.5E-02	9.6E-03	1.8E-03	3.3E-04	5.6E-05

Table 4.18

Mean Dominant Accident Sequence Frequencies (LLNL Hazard)
(Conditional on Hazard)

ACC	0.23g	0.37g	0.53g	0.68g	0.83g	0.98g	1.12g
1	3.4E-05	1.9E-03	1.5E-02	5.4E-02	1.3E-01	2.3E-01	3.4E-01
2	5.5E-07	1.8E-04	1.5E-03	2.7E-03	2.2E-03	1.2E-03	5.0E-04
3	8.4E-07	1.3E-03	4.3E-02	2.0E-01	3.3E-01	3.8E-01	3.8E-01
4	2.8E-09	4.6E-06	8.4E-05	2.5E-04	2.9E-04	1.9E-04	9.5E-05
5	9.4E-08	2.4E-04	1.0E-02	5.2E-02	8.7E-02	9.6E-02	8.9E-02
6	2.2E-08	3.2E-05	9.5E-04	6.0E-03	1.7E-02	3.0E-02	3.9E-02
7	6.0E-07	1.7E-04	1.1E-03	1.6E-03	1.0E-03	4.3E-04	1.4E-04
8	2.6E-07	1.9E-04	3.6E-03	1.6E-02	3.5E-02	4.9E-02	5.0E-02
9	5.0E-05	2.9E-03	1.7E-02	3.7E-02	4.7E-02	4.2E-02	3.0E-02
10	5.4E-06	3.0E-04	1.8E-03	4.0E-03	5.0E-03	4.5E-03	3.2E-03
11	1.1E-07	6.4E-06	3.8E-05	8.3E-05	1.0E-04	9.3E-05	6.7E-05
12	1.1E-08	6.4E-07	3.8E-06	8.3E-06	1.0E-05	9.3E-06	6.7E-06
13	4.4E-08	1.1E-05	1.3E-04	4.8E-04	8.4E-04	9.3E-04	7.5E-04
14	1.4E-10	2.9E-09	1.5E-07	7.5E-07	9.4E-07	7.9E-07	5.5E-07
15	8.9E-05	1.7E-02	1.7E-01	2.9E-01	1.9E-01	9.1E-02	3.8E-02
16	4.3E-09	1.0E-06	1.3E-05	4.6E-05	8.1E-05	8.9E-05	7.2E-05
17	1.4E-11	2.8E-10	1.5E-08	6.9E-08	9.1E-08	7.8E-08	5.4E-08
18	1.4E-11	1.3E-09	3.8E-08	3.3E-07	1.1E-06	1.8E-06	1.9E-06
19	5.6E-14	3.3E-10	1.7E-09	3.0E-09	3.0E-09	2.2E-09	1.3E-09
20	1.2E-10	1.5E-07	1.3E-05	3.1E-04	2.5E-03	1.0E-02	2.6E-02
21	7.1E-09	1.2E-06	6.6E-06	8.1E-06	4.4E-06	1.4E-06	3.4E-07
22	2.2E-09	3.3E-07	2.0E-06	3.1E-06	2.1E-06	8.7E-07	2.5E-07

Table 4.19 presents the mean core damage contributions for each accident sequence based on the LLNL hazard curve, for each of the seven integration intervals of the hazard curve. (Integration over the hazard curve was performed from 0.15 g to 1.20 g and in the uncertainty analysis computations, integration increments of 0.025 g were utilized. However, for explanatory purposes the results presented here are based on an integration increment of 0.1 g.) The right hand column presents the total contribution of each accident sequence to the total core damage frequency of 8.82E-5. This is very close to the Monte Carlo estimate of mean core damage frequency of 7.66E-5 computed using the same accident sequence equations in the uncertainty analysis. As can be seen, the incremental contributions from the LOCA events do not become significant until the higher acceleration levels. The reactor vessel rupture sequence does not make a significant contribution until the highest PGA increment.

An important thing to note from Table 4.19 is the sum of the accident sequence contributions at each earthquake level, as shown at the bottom of each column on the table. The contributions are seen to be small at the first increment, increasing to a maximum at the fourth earthquake increment, and then decreasing at higher earthquake levels. This indicates that the bulk of the risk is occurring in the range of 0.45 g to 0.90 g which roughly corresponds to the range of 4-7 SSE. Further, this shows that the bulk of the risk has been captured by integrating over the range 0.12 g to 1.20 g.

Mean Point Estimates Using EPRI Hazard Curves

Tables 4.20 through 4.22 presents similar results for the mean point estimate case using the EPRI hazard curves. In this case a total core damage frequency of 3.02E-6 per year was computed. Similar comments with respect to the variation of initiating event frequencies and accident sequence frequencies with earthquake level as described for the LLNL mean point estimate case apply.

4.4.6 Base Case Importance Studies

A. Basic Event Importance to Mean Values

The importance of the basic seismic failure events was evaluated by setting the seismic failure probability of each dominant component to zero (one at a time) in the mean point estimate calculation, which gives a measure of the net reduction in total core damage frequency that would result if that component would never fail due to seismic shaking.

Results of these calculations for both sets of hazard curves are shown in Table 4.23, and the results are both qualitatively and quantitatively similar. (Note that the sum of the risk reduction percentages do not and should not equal unity, since many of the important components occur together in the same cut sets, and hence a zero failure probability of one component causes the entire cut set to vanish.)

Table 4.19

Mean Core Damage Contributions at Intervals of PGA (LLNL Hazard)

ACC	0.15-0.30g	0.30-0.45g	0.45-0.60g	0.60-0.75g	0.75-0.90g	0.90-1.05g	1.05-1.20g	TOTAL
1	5.1E-08	5.2E-07	1.4E-06	2.1E-06	2.4E-06	2.4E-06	2.2E-06	1.1E-05
2	8.3E-10	4.9E-08	1.4E-07	1.1E-07	4.2E-08	1.2E-08	3.2E-09	3.5E-07
3	1.3E-09	3.6E-07	3.9E-06	7.6E-06	6.2E-06	4.0E-06	2.4E-06	2.5E-05
4	4.3E-12	1.3E-09	7.6E-09	9.6E-09	5.5E-09	2.1E-09	6.0E-10	2.7E-08
5	1.4E-10	6.7E-08	9.2E-07	2.0E-06	1.7E-06	1.0E-06	5.7E-07	6.2E-06
6	3.4E-11	8.8E-09	8.6E-08	2.3E-07	3.3E-07	3.2E-07	2.5E-07	1.2E-06
7	9.1E-10	4.6E-08	1.0E-07	6.1E-08	2.0E-08	4.5E-09	9.0E-10	2.3E-07
8	4.0E-10	5.2E-08	3.3E-07	6.3E-07	6.8E-07	5.1E-07	3.2E-07	2.5E-06
9	7.6E-08	8.0E-07	1.5E-06	1.4E-06	9.0E-07	4.4E-07	1.9E-07	5.4E-06
10	8.1E-09	8.5E-08	1.6E-07	1.5E-07	9.6E-08	4.7E-08	2.0E-08	5.7E-07
11	1.7E-10	1.8E-09	3.4E-09	3.2E-09	2.0E-09	9.9E-10	4.3E-10	1.2E-08
12	1.7E-11	1.8E-10	3.4E-10	3.2E-10	2.0E-10	9.9E-11	4.3E-11	1.2E-09
13	6.8E-11	3.0E-09	1.2E-08	1.8E-08	1.6E-08	9.8E-09	4.8E-09	6.4E-08
14	2.2E-13	8.0E-13	1.4E-11	2.9E-11	1.8E-11	8.3E-12	3.5E-12	7.3E-11
15	1.4E-07	4.8E-06	1.5E-05	1.1E-05	3.7E-06	9.6E-07	2.4E-07	3.6E-05
16	6.5E-12	2.8E-10	1.2E-09	1.8E-09	1.5E-09	9.4E-10	4.6E-10	6.2E-09
17	2.1E-14	7.7E-14	1.3E-12	2.7E-12	1.7E-12	8.2E-13	3.4E-13	7.0E-12
18	2.1E-14	3.7E-13	3.4E-12	1.3E-11	2.1E-11	1.9E-11	1.2E-11	6.8E-11
19	8.5E-17	9.3E-14	1.6E-13	1.1E-13	5.7E-14	2.4E-14	8.3E-15	4.5E-13
20	1.8E-13	4.2E-11	1.2E-09	1.2E-08	4.7E-08	1.1E-07	1.6E-07	3.3E-07
21	1.1E-11	3.3E-10	6.0E-10	3.1E-10	8.4E-11	1.5E-11	2.2E-12	1.4E-09
22	3.3E-12	9.1E-11	1.8E-10	1.2E-10	4.0E-11	9.2E-12	1.6E-12	4.5E-10
	2.8E-07	6.8E-06	2.3E-05	2.5E-05	1.6E-05	9.8E-06	6.4E-06	8.82E-05

Table 4.20

Mean Initiating Event Frequencies (EPRI Hazard)

IE	0.23g	0.37g	0.53g	0.68g	0.83g	0.98g	1.12g
1	3.4E-05	1.9E-03	1.5E-02	5.4E-02	1.3E-01	2.3E-01	3.4E-01
2	6.8E-03	5.3E-02	1.4E-01	2.5E-01	3.3E-01	3.8E-01	3.8E-01
3	9.4E-04	1.1E-02	3.6E-02	6.7E-02	8.9E-02	9.6E-02	8.9E-02
4	1.1E-02	6.5E-02	1.4E-01	1.8E-01	1.8E-01	1.5E-01	1.1E-01
5	5.6E-05	3.2E-03	1.9E-02	4.1E-02	5.2E-02	4.7E-02	3.3E-02
6	4.1E-01	6.9E-01	6.0E-01	4.0E-01	2.2E-01	1.0E-01	4.2E-02
7	5.7E-01	1.8E-01	4.5E-02	9.6E-03	1.8E-03	3.3E-04	5.6E-05

Table 4.21

Mean Accident Sequence Frequencies (per year) Conditional on Hazard (EPRI Hazard)

ACC	0.23g	0.37g	0.53g	0.68g	0.83g	0.98g	1.12g
1	3.4E-05	1.9E-03	1.5E-02	5.4E-02	1.3E-01	2.3E-01	3.4E-01
2	5.5E-07	1.8E-04	1.5E-03	2.7E-03	2.2E-03	1.2E-03	5.0E-04
3	8.4E-07	1.3E-03	4.3E-02	2.0E-01	3.3E-01	3.8E-01	3.8E-01
4	2.8E-09	4.6E-06	8.4E-05	2.5E-04	2.9E-04	1.9E-04	9.5E-05
5	9.4E-08	2.4E-04	1.0E-02	5.2E-02	8.7E-02	9.6E-02	8.9E-02
6	2.2E-08	3.2E-05	9.5E-04	6.0E-03	1.7E-02	3.0E-02	3.9E-02
7	6.0E-07	1.7E-04	1.1E-03	1.6E-03	1.0E-03	4.3E-04	1.4E-04
8	2.6E-07	1.9E-04	3.6E-03	1.6E-02	3.5E-02	4.9E-02	5.0E-02
9	5.0E-05	2.9E-03	1.7E-02	3.7E-02	4.7E-02	4.2E-02	3.0E-02
10	5.4E-06	3.0E-04	1.8E-03	4.0E-03	5.0E-03	4.5E-03	3.2E-03
11	1.1E-07	6.4E-06	3.8E-05	8.3E-05	1.0E-04	9.3E-05	6.7E-05
12	1.1E-08	6.4E-07	3.8E-06	8.3E-06	1.0E-05	9.3E-06	6.7E-06
13	4.4E-08	1.1E-05	1.3E-04	4.8E-04	8.4E-04	9.3E-04	7.5E-04
14	1.4E-10	2.9E-09	1.5E-07	7.5E-07	9.4E-07	7.9E-07	5.5E-07
15	8.9E-05	1.7E-02	1.7E-01	2.9E-01	1.9E-01	9.1E-02	3.8E-02
16	4.3E-09	1.0E-06	1.3E-05	4.6E-05	8.1E-05	8.9E-05	7.2E-05
17	1.4E-11	2.8E-10	1.5E-08	6.9E-08	9.1E-08	7.8E-08	5.4E-08
18	1.4E-11	1.3E-09	3.8E-08	3.3E-07	1.1E-06	1.8E-06	1.9E-06
19	5.6E-14	3.3E-10	1.7E-09	3.0E-09	3.0E-09	2.2E-09	1.3E-09
20	1.2E-10	1.5E-07	1.3E-05	3.1E-04	2.5E-03	1.0E-02	2.6E-02
21	7.1E-09	1.2E-06	6.6E-06	8.1E-06	4.4E-06	1.4E-06	3.4E-07
22	2.2E-09	3.3E-07	2.0E-06	3.1E-06	2.1E-06	8.7E-07	2.5E-07

Table 4.22

Mean Core Damage Contributions From Dominant Accident Sequences
(EPRI Hazard)

	0.15-0.30g	0.30-0.45g	0.45-0.60g	0.60-0.75g	0.75-0.90g	0.90-1.05g	1.05-1.20g	TOTAL
1	3.4E-09	2.5E-08	5.3E-08	7.1E-08	7.5E-08	5.4E-08	6.1E-08	3.4E-07
2	5.6E-11	2.3E-09	5.3E-09	3.6E-09	1.3E-09	2.8E-10	8.9E-11	1.3E-08
3	8.5E-11	1.7E-08	1.5E-07	2.6E-07	1.9E-07	8.9E-08	6.8E-08	7.8E-07
4	2.9E-13	6.1E-11	3.0E-10	3.3E-10	1.7E-10	4.6E-11	1.7E-11	9.2E-10
5	9.6E-12	3.2E-09	3.6E-08	6.9E-08	5.2E-08	2.3E-08	1.6E-08	2.0E-07
6	2.3E-12	4.2E-10	3.3E-09	7.9E-09	1.0E-08	7.2E-09	7.0E-09	3.6E-08
7	6.1E-11	2.2E-09	3.9E-09	2.1E-09	6.1E-10	1.0E-10	2.5E-11	9.0E-09
8	2.7E-11	2.5E-09	1.3E-08	2.2E-08	2.1E-08	1.2E-08	8.9E-09	7.9E-08
9	5.1E-09	3.8E-08	6.0E-08	4.9E-08	2.8E-08	1.0E-08	5.4E-09	2.0E-07
10	5.4E-10	4.1E-09	6.4E-09	5.2E-09	3.0E-09	1.1E-09	5.7E-10	2.1E-08
11	1.1E-11	8.5E-11	1.3E-10	1.1E-10	6.2E-11	2.2E-11	1.2E-11	4.3E-10
12	1.1E-12	8.5E-12	1.3E-11	1.1E-11	6.2E-12	2.2E-12	1.2E-12	4.3E-11
13	4.5E-12	1.4E-10	4.7E-10	6.3E-10	5.0E-10	2.2E-10	1.3E-10	2.1E-09
14	1.5E-14	3.8E-14	5.4E-13	9.8E-13	5.6E-13	1.9E-13	9.7E-14	2.4E-12
15	9.0E-09	2.3E-07	5.8E-07	3.8E-07	1.1E-07	2.2E-08	6.8E-09	1.3E-06
16	4.3E-13	1.4E-11	4.5E-11	6.0E-11	4.8E-11	2.1E-11	1.3E-11	2.0E-10
17	1.4E-15	3.7E-15	5.2E-14	9.1E-14	5.4E-14	1.9E-14	9.7E-15	2.3E-13
18	1.4E-15	1.8E-14	1.3E-13	4.3E-13	6.4E-13	4.3E-13	3.5E-13	2.0E-12
19	5.7E-18	4.5E-15	6.1E-15	3.9E-15	1.8E-15	5.3E-16	2.3E-16	1.7E-14
20	1.2E-14	2.0E-12	4.7E-11	4.1E-10	1.5E-09	2.4E-09	4.6E-09	8.9E-09
21	7.2E-13	1.6E-11	2.3E-11	1.1E-11	2.6E-12	3.4E-13	6.1E-14	5.4E-11
22	2.2E-13	4.4E-12	7.1E-12	4.0E-12	1.3E-12	2.1E-13	4.5E-14	1.7E-11
	1.8E-08	3.2E-07	9.1E-07	8.7E-07	5.0E-07	2.2E-07	1.8E-07	3.02E-06

Table 4.23

Dominant Component Contributions to Mean Core Damage Frequency Ranked by Risk Reduction Potential

Component	Percent Reduction if not Failed	
	LLNL Hazard	EPRI Hazard
Ceramic Insulators	48%	52%
ESW/ECW Pumps	31%	34%
Diesel Generator	24%	26%
Turbine Building	14%	16%
4kV Busses	12%	13%
Radwaste/Turbine Building	8%	8%
RV Recirculation Pumps Supports	7%	7%
RV Skirt Support	1%	1%

All other components and structures less than 1%

It can be seen that the largest reduction occurs for ceramic insulators. This occurs, of course, because the ceramic insulators are the basis for the loss of off-site power and all the T_1 transient sequences. The ESW and ECW pumps together have a risk reduction potential of about 30 percent. This reduction potential is large because these pumps provide all the emergency service water cooling to the diesel generators, to all the room cooling (except the diesel generator enclosures) and also provide all emergency pump cooling. The Turbine Building has a significant risk reduction potential because its failure would serve to fail the cables to the ECW pump. The importance of the Turbine Building may be overestimated due to the conservative estimate of its median failure capacity. The 4kV buses have a significant risk reduction potential inasmuch as all off-site power and on-site emergency power is fed through these busses. The Radwaste/Turbine Building failure, as noted earlier, is both an initiator and houses the control room and all the emergency switchgear rooms. Thus, its failure would have a significant impact on the overall core damage frequency. The reactor vessel recirculation pumps and the reactor vessel supports have significant reduction potential due to the fact that they are used to model the reactor vessel rupture initiating event and the large LOCA initiating event. All other components and structures had risk reduction potentials of less than 1 percent.

B. Basic Event Uncertainty Contribution to Overall Uncertainty

The relative contribution of uncertainties in the hazard curve, the seismic responses and the seismic fragilities (the β_u's) to the uncertainty in the overall core damage frequency was ascertained. The results of these comparisons (for both sets of hazard curves) are shown on Tables 4.24 and 4.25. The base case mean, 95 percent and 50 percent core damage frequencies are shown in the first column. The second column shows the corresponding values with the hazard curve fixed at its mean value (i.e., with no modeling uncertainty). For the LLNL hazard curve case it can be seen that the error factor (EF) associated with these results is only 2.6 whereas the corresponding error factor for the base case was 61.7. Similarly, for the EPRI hazard curve case, the base case error factor was 18.0 while with no uncertainty in the hazard curve, the error factor is reduced to 3.0. Clearly, the hazard curve is contributing the vast majority of the uncertainty to the base case results.

The third column shows the calculation wherein all the fragility and response modeling uncertainties are simultaneously set to zero. For the LLNL hazard curves, the error factor 53.1. For the EPRI hazard curves, the corresponding error factor is 14.0. These results show that the reduction in response and fragility uncertainties has little effect on the overall core damage uncertainty (no matter which set of hazard curves is used).

These results show quite clearly that the uncertainty in the hazard curve is the dominant factor which determines the uncertainty of the core

Table 4.24

Comparison of Contributions of Modeling Uncertainty in Response, Fragility and Hazard Curves to Core Damage Frequency
LLNL Hazard

P_{cm}	Base Case	Hazard $\beta_U = 0$	$\beta_{FU} = 0$ $\beta_{RU} = 0$
Mean	7.66E-5	8.62E-5	7.92E-5
95%	2.72E-4	1.89E-4	3.12E-4
50%	4.41E-6	7.21E-5	5.88E-6
$\frac{P_{cm}(95\%)}{P_{cm}(50\%)}$	61.7	2.6	53.1

Table 4.25

Comparison of Contributions of Modeling
Uncertainty in Response, Fragility and Hazard
Curves to Core Damage Frequency
EPRI Hazard

P_{cm}	Base Case	Hazard $\beta_U=0$	$\beta_{FU}=0$ $\beta_{RU}=0$
Mean	3.09E-6	3.04E-6	3.02E-6
95%	1.27E-5	7.23E-6	1.27E-5
50%	7.07E-5	2 39E-6	9.07E-7
$\frac{P_{cm}(95\%)}{P_{cm}(50\%)}$	18.0	3.0	14.0

damage frequency. Further, this emphasizes the fact that it is the mean hazard curve which determines the (true) mean estimate of core damage frequency as obtained from an uncertainty analysis, as was shown earlier in the discussion of the mean point estimate case. Again, this shows the dominant influence of the hazard curve uncertainty (which determines the mean hazard curve) in determining the (true) mean core damage frequency.

C. Effect of Hazard Curve Discretization

All the results discussed so far have been based on a model of the hazard curve uncertainty in which the variation is assumed to be log normal (at each value of PGA). The principal investigator of the Eastern US Seismic Hazard Characterization Program has indicated that this uncertainty distribution is approximately log normal, and this was substantiated by the calculated mean hazard curve shown earlier. However, the log normal distribution does have an extended tail. To assess the potential effect of contributions from the tail of the assumed distribution an alternate approach was taken.

In this study, a family of ten hazard curves was generated from the assumed log normal distribution corresponding to confidence levels of 5 percent, 15 percent, ...95 percent. Each of these ten curves is assumed to be equally weighted. Using this family of curves the Monte Carlo uncertainty analysis was repeated which resulted in a reduced mean value of core damage frequency. This reduction in core damage frequency is due to both eliminating the tails of the distribution and due to a shift in the mean hazard curve.

Table 4.26 compares the LLNL mean hazard curve ordinates derived from the family of discrete hazard curves used above with the mean hazard curve obtained from the full log normal distribution model. As can be seen from this table, the mean hazard curve is somewhat less for the discrete family. Repeating the Monte Carlo analysis with the discrete family of hazard curves gave a mean core damage frequency of 4.14E-5 per year as compared to the base case value of 7.66E-5. Thus, a 46% reduction has resulted from truncating the tails of the LLNL hazard curve description.

Table 4.27 compares the EPRI mean hazard curve ordinance derived from the family of discrete hazard curves with the full log normal distribution model. Again, repeating the Monte Carlo analysis resulted in a mean core damage frequency of 2.5E-6 as contrasted to the base case result of 3.02E-6. Thus, in this case, a 17% reduction results.

From these results, one would infer that the use of a limited number of discrete hazard curves results in a reduction in computed core damage frequencies from 17% to 46%, and that the reduction is due to the reduction in the mean hazard curve which results from cutting off the tails of the full hazard curve distribution. From a PRA perspective, a 30% reduction, while not insignificant, would not affect the conclusions resulting from a seismic PRA. Thus, one would conclude that knowledge of

Table 4.26

Comparison of LLNL Mean Hazard Curve Probabilities From Ten Discrete Hazard Curves and From Hazard Curve with Assumed Log Normal Distribution

PGA	10 Discrete Curves Mean Hazard Probability	Full Distribution Mean Hazard Probability
0.15 g	1.19E-3	1.98E-3
0.30 g	2.26E-4	4.58E-4
0.45 g	7.74E-5	1.79E-4
0.60 g	3.47E-5	8.89E-5
0.75 g	1.82E-5	5.05E-5
0.90 g	1.06E-5	3.14E-5
1.05 g	6.56E-5	2.08E-5
1.20 g	4.35E-6	1.44E-5

Table 4.27

Comparison of EPRI Mean Hazard Curve Probabilities From Ten Discrete Hazard Curves and From Hazard Curve with Assumed Log Normal Distribution

PGA	10 Discrete Curves Mean Hazard Probability	Full Distribution Mean Hazard Probability
0.15 g	1.11E-4	1.21E-4
0.30 g	1.60E-5	1.95E-5
0.45 g	4.65E-6	6.14E-6
0.60 g	1.85E-6	2.62E-6
0.75 g	8.94E-7	1.31E-6
0.90 g	4.77E-7	7.15E-7
1.00 g	2.98E-7	4.77E-7
1.20 g	1.79E-7	2.98E-7

the exact form of the tails of the hazard curve distribution (as determined by the LLNL hazard curve development process) is not essential to a robust understanding of the plants seismic risk and vulnerabilities.

4.4.7 Summary

This chapter has presented the seismic risk results for the Peach Bottom Plant using both industry-sponsored (EPRI) and NRC-sponsored (LLNL) hazard curve estimates. The differences between these sets of hazard curves resulted in a significant difference in computed total core damage frequency (7.66E-5 per year for the LLNL hazard curves and 3.09E-6 per year for the EPRI hazard curves). This rather significant difference is expected to bound the seismic risk at Peach Bottom.

However, the seismic risk was found to be dominated by relatively few accident sequences and the same dominant accident sequences were found using both sets of hazard curves. Furthermore, it was found that the relative contribution of individual component failures was the same (both qualitatively and quantitatively) for both sets of hazard curves. Thus, insights as to important contributors to risk at Peach Bottom and to the identification of important accident scenarios are relatively robust and did not depend on the particular hazard curves chosen.

The dominant accident sequences primarily involve station blackout situations which resulted from loss of cooling water to the emergency diesel generators. A variety of different component failures were identified which led to this situation, with failures of the emergency service water and emergency cooling water systems being the most important.

Finally, a sensitivity study in which the continuous lognormal uncertainty model for the hazard curves was replaced by a discrete family of hazard curves (and, hence, the extreme tails of the lognormal distribution were truncated) was made. This study showed that the tails of the hazard curve distribution did not dominate the core damage frequency results obtained.

4.5 References

1. D. L. Bernreuter et al., Seismic Hazard Characterization of 69 Nuclear Plant Sites East of the Rocky Mountains, NUREG/CR-5250, October 1988.

2. Electric Power Research Institute, Seismic Hazard Methodology for the Central and Eastern United States, EPRI NP-4726, Vols 1-10, July 1986

3. Peach Bottom Power Station, Updated Final Safety Analysis Report, Section 2.0, June 1983.

4. N. M. Newmark, A Study of Vertical and Horizontal Earthquake Spectra, WASH-1255, 1973.

5. M. P. Bohn et al., Application of the SSMRP Methodology to the Seismic Risk at the Zion Nuclear Power Plant, Lawrence Livermore National Laboratory, Livermore, CA, UCRL-53483, NUREG/CR-3428, 1983.

6. L. E. Cover, et al., Handbook of Nuclear Power Plant Seismic Fragilities, NUREG/CR-3558, December 1983.

7. D. A. Wesley, and P. S. Hashimoto, Seismic Structural Fragility Investigation for the Zion Nuclear Power Plant, NUREG/CR-2320, October 1981.

8. R. Riddell, and N. M. Newmark, Statistical Analysis of the Response of Nonlinear Systems Subjected to Earthquakes, University of Illinois, UILU-ENG 79-2016, August 1979.

9. R. P. Kennedy, et al., Engineering Characterization of Ground Motion - Task I: Effects of Characteristics of Free-Field Motion on Structural Response, NUREG/CR-3805, May 1984.

10. "Report on the Re-Evaluation of Concrete Masonry Walls in Response to NRC I & E Bulletin 80-11 for the Peach Bottom Atomic Power Station Units 2 and 3," prepared for Philadelphia Electric Company by Bechtel Power Corporation, 1982.

11. R. D. Campbell, et al., Compilation of Fragility Information From Available Probabilistic Risk Assessments, Lawrence Livermore National Laboratory Report UCID-20571 Rev. 1, September 1988.

12. N. M. Newmark, A Study of Vertical and Horizontal Earthquake Spectra, U. S. Nuclear Regulatory Commission WASH-1255, 1973.

5.0 PEACH BOTTOM FIRE ANALYSIS

5.1 Introduction

The objective of the analysis reported here was to estimate the contribution of fire-induced events to core damage and plant damage state frequencies. The overall fire-induced core damage frequency for Peach Bottom Unit 2 was found to be 1.95E-5 per year. The various fire area contributions are given in Table 5.1. The accident sequences these scenarios mapped into are listed in Table 5.2.

Based on plant operating experience over the last 20 years, it has been observed that typical nuclear power plants will have three to four significant fires over their operating lifetime. Previous probabilistic risk assessments (PRAs) have shown that fires are a significant contributor to the overall core damage frequency, contributing anywhere from 7 percent to 50 percent of the total (considering contributions from internal, seismic, flood, fire, and other events). Because of the relatively high core damage contribution, fires need to be examined in more detail.

An overview of the simplified fire PRA methodology is as follows:

A. Initial Plant Visit

Based on the internal event and seismic analyses, the general location of cables and components of the systems of interest is known. The plant visit provides the analyst with a means of seeing the physical arrangements in each of these areas. The analyst will have a fire zone checklist which will aid the screening analysis and in the quantification step. The second purpose of the initial plant visit is to confirm with plant personnel that the documentation being used is, in fact, the best available information and to get clarification about any questions that might have arisen in a review of the documentation. Also, a thorough review of firefighting procedures is conducted.

B. Screening

It is necessary to select important fire locations within the power plant under investigation having the greatest potential for producing risk-dominant accident sequences. The objectives of location selection are somewhat competing and should be balanced in a meaningful risk assessment study. The first objective is to maximize the possibility that all important locations are analyzed, and this leads to the consideration of a potentially large number of candidate locations. The second objective is to minimize the effort spent in the quantification of event trees and fault trees for fire locations that turn out to be unimportant. A proper balance of these objectives is one that results in an ideal allocation of resources and efficiency of assessment.

The screening analysis is comprised of:

Table 5.1

Dominant Peach Bottom Fire Area Core Damage Frequency Contributors

Fire Area	Core Damage Frequency (/yr) Mean	5th Percentile	50th Percentile	95th Percentile
Emergency Switchgear Room 2A	7.4E-7	4.6E-10	1.6E-7	3.0E-6
Emergency Switchgear Room 2B	3.6E-6	3.5E-9	2.0E-6	1.3E-5
Emergency Switchgear Room 2C	4.7E-6	4.2E-9	2.2E-6	1.7E-5
Emergency Switchgear Room 2D	7.4E-7	4.6E-10	1.6E-7	3.0E-6
Emergency Switchgear Room 3A	7.4E-7	4.6E-10	1.6E-7	3.0E-6
Emergency Switchgear Room 3B	7.4E-7	4.6E-10	1.6E-7	3.0E-6
Emergency Switchgear Room 3C	7.4E-7	4.6E-10	1.6E-7	3.0E-6
Emergency Switchgear Room 3D	8.1E-7	5.3E-10	1.7E-7	3.3E-6
Control Room	6.2E-6	4.2E-10	1.4E-6	8.0E-6
Cable Spreading Room	6.7E-7	9.1E-9	1.7E-7	2.3E-6
Total	2.0E-5	1.1E-6	1.2E-5	6.4E-5

Table 5.2

Dominant Accident Sequence Core Damage Frequency Contributors

Sequence	Fire Area	Mean Core Damage Frequency (/yr)
$T_1BU_1U_2$	Emergency Switchgear Room 2A	7.4E-7
	Emergency Switchgear Room 2B	3.6E-6
	Emergency Switchgear Room 2C	3.6E-6
	Emergency Switchgear Room 2D	7.4E-7
	Emergency Switchgear Room 3A	7.4E-7
	Emergency Switchgear Room 3B	7.4E-7
	Emergency Switchgear Room 3C	7.4E-7
	Emergency Switchgear Room 3D	8.1E-7
$T_3U_1U_2X_1U_3$	Control Room	6.2E-6
	Cable Spreading Room	6.7E-7
$T_1\overline{BU}_1W_1\overline{X}_2W_2$ $W_3U_4V_2\overline{V}_3Y$	Emergency Switchgear Room 2C	8.1E-7
$T_1\overline{BU}_1W_1\overline{X}_2W_2$ $W_3U_4\overline{V}_2Y$	Emergency Switchgear Room 2C	2.7E-7

1. Identification of relevant fire zones. Those Appendix R identified fire zones which had either safety-related equipment or power and control cables for that equipment were identified as requiring further analysis. This group of fire zones (areas) is briefly described in Section 5.2 All safety components within these fire areas are given in Appendix D.

2. Screen fire zones on probable fire-induced initiating events. Determination of the fire frequency for all plant locations and determination of the resulting fire-induced initiating events and "off-normal" plant states is delineated in Sections 5.3 and 5.4 respectively.

3. Screen fire zones on both order and frequency of cut sets.

4. Each fire zone remaining is numerically evaluated and culled on frequency.

The screening methodology (Section 5.5) describes how reduction of the initial group of locations from Section 5.2 to the ten remaining with contributions to core damage frequency of greater than 10^{-8}/yr was accomplished.

C. Quantification

After the screening analysis has eliminated all but the probabilistically-significant fire zones, quantification of dominant cut sets is completed as follows:

1. Determine temperature response in each fire zone.

2. Compute component fire fragilities. The latest version of the fire growth code COMPBRN with some modifications, as described in Section 5.6, was used to calculate fire propagation and equipment damage. A description of these results for steps 1 and 2 is given in Section 5.6. These fire calculations were only performed for the fire areas that survived the screening analysis.

3. Assess the probability of barrier failure for all remaining combinations of fire zones. A barrier failure analysis was conducted for those combinations of two adjacent fire zones which, with or without additional random failures, remained after the screening analysis. The methodology to assign barrier failure probability to the fire zone combinations is described in Section 5.7.

4. Perform a recovery analysis. In similar fashion as in the internal event analysis recovery of non-fire related random failures was addressed. Appropriate modifications to recovery probabilities were made as described in Section 5.8.

5. An uncertainty analysis is performed to estimate error bounds on the computed fire-induced core damage frequencies. As in the internal events analysis, the TEMAC code was utilized in the uncertainty analysis described in Section 5.9.

In Section 5.10 a detailed description of all fire scenarios with contributions to core damage frequency of greater than 10^{-8} per year and their associated fire areas is given. Distributions and description of all factors used in the final quantification of all fire areas are delineated.

5.2 Fire Locations Analyzed

The plant areas (fire zones) are listed in Table 5.3. A list of components contained in each of these fire zones is given in Appendix D. Table 5.3 also provides a brief physical description of each fire zone.

These lists of components as well as cable-traced vital components formed the basis of the computer-aided fire area screening analysis. All other fire areas not included in Table 5.3 were screened, as they did not contain either vital equipment or cabling for that equipment.

5.3 Initiating Event Frequencies

Data on fires in Light Water Reactors have been analyzed in several studies (Ref. 1,2,3). Although they have been done independently, they have some common aspects. For example, almost all studies have used License Event Report (LER) data from the Nuclear Regulatory Commission (NRC). All have reported the overall frequency of fires at approximately 0.16 per reactor year on a plant-wide basis.

To determine fire initiating event frequencies, there are two kinds of information needed: (1) the number of fire incidents that have occurred in specific compartments during commercial operation, and (2) the number of compartment years that the nuclear industry has accumulated. Most of the data for the first part comes from reports of insurance inspectors to American Nuclear Insurers (ANI), although other sources are also used, e.g., the U.S. Nuclear Regulatory Commission. While the NRC requires the reporting of fires that in some way affect the safety of the plant, the ANI has more stringent requirements in that all fire events must be reported. Compartment years are computed by adding the age of all compartments (within a certain category of compartments) of units that were in commercial operation by the end of June 1985. The age is defined as the time between first commercial operation and the end of June 1985 (or date of decommissioning). The combination of specific fire locations and compartment age is given in Table 5.4. Even though fire events that occurred when the plant was shutdown were used, an event was only included if it could be postulated that it also might occur when the plant was at power. Eight areas are typically found in nuclear power plants. These are (1) the control room, (2) cable spreading room, (3)

Table 5.3

Peach Bottom Fire Areas Containing Safety Related Components

Fire Area	Physical Description
1	Unit 2--A and C RHR Heat Exchanger and Pump Rooms (Elev. 91'-6" and 116'-0"); Stairwell No. 26 (Elev. 135'-0" to 234'-0").
2	Unit 2--B and D RHR Heat Exchanger and Pump Rooms (Elev. 91'-6" and 116'-0"). Unit 3--A and C RHR Heat Exchanger and Pump Rooms (Elev. 91'-6" and 116'-0"); Reactor Recirculation Pump M-G Set Room (Elev. 135'-0"); Stairwell No. 25 (Elev. 91'-6" to 135'-0"). Units 2 and 3--HPCI Pump Rooms, Reactor Sump Pump Rooms, RCIC Pump Areas (Elev. 88'-0"); Cooling Water Equipment Rooms (Elev. 116'-0"). Radwaste Building--Standby Gas Treatment Room, Waste Sludge Pump Room, Waste Sludge Tank Room, Floor Drain Collector Tank and Waste Collector Tank Room, Spent Resin Pump Room, Spent Resin Tank Room, Chemical Waste Tank Room, Core Pump Room, Tank and Pump Area (Elev. 91'-6"); Waste Surge Tank Room (Elev. 108'-0"); Condensate Tank Rooms, Condensate Pump Rooms, Filter Holding Pump Room, Corridor, Laundry Room, Chemical and Funnel Storage, Demineralizer Room, Filter Rooms (Elev. 116'-0"); Medical Station, Radwaste Control Room, Emergency Switchgear Room Corridor, Filter Room Personnel Decontamination Station, Radwaste Baling and Trash Compactor Area (Elev. 135'-0"); Hopper Compartments, Sample Tank and Pump Room, Radwaste H&V Equipment Compartment (Elev. 150'-0"); Centrifuges, Absorbent Feeder Rooms, Radwaste Exhaust Fan Rooms (Elev. 165'-0"); Stairwell No. 34 (Elev. 91'-6" to 165'-0").
4	Unit 2--Stairwell No. 24 (Elev. 91'-6" to 135'-0"); Recirculation Pump M-G Set Room (Elev. 135'-0").
5	Unit 2--A, B, and C Core Spray Pump Rooms (Elev. 91'-6"); Stairwell No. 18 (Elev. 91'-6" to 116'-0"); Torus Area (Elev. 92"-6"); North and South Vacuum Breaker Areas (Elev. 116'-0").
6N	Unit 2 - North CRD Equipment Area, North Isolation Valve Compartment, Drywell Access, Corridors (Elev. 135'-0").

Table 5.3

Peach Bottom Fire Areas Containing Safety Related Components
(Continued)

Fire Area	Physical Description
6S	Unit 2--South CRD Equipment Area, Neutron Monitoring Room, South Isolation Valve Compartment (Elev. 135'-0"); Cleanup Recirculation Pump Rooms, Regen Heat Exchanger Room, Non-Regen Heat Exchanger Room, Transfer Pump Room, Backwash Receiving Tank Room, Operating Area, Isolation Valve Compartment (Elev. 165'-0"); Stairwell No. 30 (Elev. 165'-0" to 180'-0"); Valve Compartments (Elev. 180'-0"); Reactor Building Ventilating Equipment Area, Prefilter and HEPA Filter Compartments, Laydown Area, Filter-Demineralizer Compartments, Holding Pump Compartments, Source Storage and Calibration (Elev. 195'-0"); Steam Separator and Steam Dryer Storage Pit (Elev. 209'-0"); Reactor Building Fan Room (Elev. 214'-0"); New Fuel Storage (Elev. 217'-0"); Washdown Area (Elev. 234'-0").
17	Unit 2--MSIV Room (Elev. 135'-0")
18	Unit 2--Drywell Area (Elev. 116'-0")
19	Unit 2--Control Rod Drive Area (Elev. 116'-0")
25	Cable Spreading Room (Elev. 150'-0"), Computer Room (Elev 150'-0"), Radwaste Building Fan Room, Control Room, Instrument Lab, Shop, Offices (Elev. 165'-0").
30	Battery Room 268 (Elev. 135'-0").
31	Battery Room 266 (Elev. 135'-0").
32	Emergency Switchgear Room 261 (Elev. 135'-0").
33	Emergency Switchgear Room 267 (Elev. 135'-0").
34	Emergency Switchgear Room 265 (Elev. 135'-0").
35	Emergency Switchgear Room 263 (Elev. 135'-0").
36	Emergency Switchgear Room 226 (Elev. 135'-0").
37	Emergency Switchgear Room 231 (Elev. 135'-0").

Table 5.3

Peach Bottom Fire Areas Containing Safety Related Components
(Concluded)

Fire Area	Physical Description
38	Emergency Switchgear Room 217 (Elev. 135'-0").
39	Emergency Switchgear Room 227 (Elev. 135'-0").
40	Battery Room 225 (Elev. 135'-0").
41	Battery Room 218 (Elev. 135'-0")
43	Diesel Generator Building Bay D (Elev. 127'-0" and 151'-0").
44	Diesel Generator Building Bay C (Elev. 127'-0" and 151'-0").
45	Diesel Generator Building Bay B (Elev. 127'-0" and 151'-0").
46	Diesel Generator Building Bay A (Elev. 127'-0" and 151'-0").
47	Unit 3--Pump Structure HPSW and ESW Room (Elev. 112'-0").
48	Unit 2--Pump Structure HPSW and ESW Room (Elev. 112'-0").
50	Turbine Building
51	Emergency Cooling Towers; Platform (Elev. 125'-0"); Switchgear Rooms, Cooling Water Pump Room (Elev. 153'-0").
54	Diesel Generator Building Cardox Room (Elev. 127'-0").

Table 5.4

Statistical Evidence of Fires in LWRs
(As of June 1985)

Area	Number of Fires r	Number of Compartment Years T
Control Room	3	681.0
Cable Spreading Room	2	747.3
Diesel Generator Room	37	1600.0
Reactor Building	15	847.5
Turbine Building	21	654.2
Auxiliary Building	43	673.2
Electrical Switchgear Room	4	1346.4
Battery Room	4	1346.4

diesel generator room, (4) reactor building, (5) turbine building, (6) auxiliary building, (7) electrical switchgear room, and (8) battery room. In most plants, the first three areas and the electrical switchgear and battery rooms are single compartments while the other three are typically large buildings. A listing of all generic data used for each of these eight areas is given in Appendix E.

To obtain fire zone specific initiating frequencies, a partitioning method is required. Partitioning allows the analyst to subdivide the frequency of fire occurrence from a large building (e.g., auxiliary building) to a specific room or area within that building. Also, further partitioning can occur within a specific room or area. One method of partitioning is comprised of ratioing the areas of fire zones within a building (e.g., auxiliary building). The assumption here is that the probability of fire occurrence is dependent only upon the amount of area a fire zone contains. Another method of partitioning would look at each fire zone and analyze factors important to probability of fire initiation. These factors are the amount of electrical components and cabling, the fire loading, whether the fire zone is controlled, and how often the fire zone is occupied.

The fire events and operating years for the eight plant areas were obtained using the fire data base developed by Wheelis (Ref. 4). To determine operating years for electrical switchgear and battery rooms, auxiliary building operating years were doubled. A survey of all U.S. light water reactors indicated that there is an average of 2.25 trains of emergency switchgear and their associated batteries per plant. However, it is known that some plants such as Surry locate both trains of their emergency switchgear in one fire zone. So it was assumed that an average number would be close to two per plant.

To aid partitioning within a large building or within a specific fire zone in that building, a checklist was used on the initial plant visit to determine the most probable fire initiating sources. Also, data on past fire occurrences were thoroughly reviewed. For instance, control room and electrical switchgear room data indicate that fires have only occurred in electrical cabinets/switchgears. Therefore, area ratios were developed based on cabinet/switchgear area within these respective areas. Since transient combustile-initiated fires have never occurred, they were eliminated from further consideration.

The generic fire occurrence data was updated using a method developed by Iman (Ref. 5) to determine plant-specific fire occurrence frequencies.

This Bayesian approach models the incidence rate for each plant relative to the incidence rates of all other plants, and the posterior distribution is found for the incidence rate for each plant.

For this analysis the gamma distribution is used as a model, although many other distributions could be used.

In this way plant-specific fire initiating event frequencies and distributions were developed. Table 5.5 lists the Peach Bottom Unit #2 specific fire initiating event frequencies for the three types of fire areas with contributions to core damage frequency of greater than 10^{-8} per year.

Peach Bottom Unit #2 had no recorded fire occurrences in any of these three areas (cable spreading room, control room, electrical switchgear room). Even though Unit #2 and #3 share a common cable spreading room and Unit #3 had one cable spreading room fire event, this event was not considered applicable. A relay fire occurred that never spread beyond its associated cabinet and there is at least sixty feet separation to the nearest critical cable runs for Unit #2.

5.4 Determination of Fire-Induced "Off-Normal" Plant States

One of the most critical steps in a fire analysis is to determine on a plant-specific basis which of a wide range of possible initiating events have the potential to be induced by a fire occurrence.

As in the NUREG-1150 internal events analysis, a comprehensive list of initiators was identified for further study. It is known from a review of previous fire PRAs that only a limited set of initiating events have the potential to be significant contributors to fire-induced core damage frequency. Typically, initiating events such as large or medium LOCAs caused directly by the fire have not been analyzed because the vulnerabilities of a piping system or tanks to fire events are considered insignificant.

Table 5.6 lists the initiating events that were analyzed during the screening process and provides a brief explanation as to why a particular initiating event was included for further study.

Some events such as loss of either an AC or DC bus were eliminated from further consideration. In the case of a fire-related failure of 4.1kV AC switchgear a loss of offsite power would also occur; therefore, this initiator was quantified using the loss of offsite power event tree. Fire-related failures of a DC bus were eliminated due to bounding arguments. The frequency of such a fire-induced event was at least one order of magnitude below the frequency used in the internal event analysis and no other safety equipment would be affected if the fire was contained within the applicable fire zones. Therefore, loss of a DC bus was not studied further.

Table 5.5

Peach Bottom Fire Initiating Event Frequencies (/yr)

Fire Area	Mean	5th Percentile	50th Percentile	95th Percentile
Control Room	2.3E-3	1.2E-7	2.1E-3	6.2E-3
Cable Spreading Room	8.1E-3	1.0E-5	4.2E-3	2.9E-2
Electrical Switchgear Room	2.7E-3	6.2E-6	2.6E-3	5.5E-3

Table 5.6

Peach Bottom Fire-Induced Initiating Events Analyzed

Initiating Event	Comments
Loss of Offsite Power	Offsite power trains J57 and J58 were found to be routed through common areas.
Transient With PCS Initially Available	Similar to the seismic methodology; if no other initiator could occur it was assumed that the operator would manually scram the plant.
Transient-Induced Large, Medium, and Small LOCAs	The probability of one or more stuck-open relief relief valves was sufficiently high ($>10^{-4}$ yr) to require further analysis.

V-sequence events were thoroughly addressed in the Peach Bottom Appendix R submittal. After careful review of both the internal events analysis and safety system schematics, no additional credible mechanisms which were not covered in the Appendix R submittal were identified. Therefore, this type of sequence was eliminated from further consideration.

As was previously mentioned small, medium, or large LOCAs caused directly by a fire were eliminated due to no credible fire-related failure mechanism for either piping or tanks being identified.

The same fault trees and event trees that were used in the internal events analysis were utilized in the fire analysis. Thus, the level of analytical detail was consistent with the level in the internal event analysis.

Consideration of the initiating events listed in Table 5.6 led to analysis of approximately six hundred event sequences.

5.5 Detailed Description of the Screening Analysis

A comprehensive screening analysis is required to reduce the number of potential fire-induced scenarios to only those which have the potential to be probabilistically significant to core damage frequency.

The screening analysis is composed of the following five steps:

Step 1. Identification of Relevant Fire Zones

Fire zones containing equipment or cables associated with safety-related systems which mitigate the effects of the unscreened fire-induced "off-normal" plant states were identified. All other fire zones were then eliminated from further analysis. This resulted in the fire zones which are described in Section 5.2.

Step 2. Screen Fire Zones on Frequency of Significant Fire

Fire initiating event frequencies were developed utilizing the data base developed by Wheelis (Ref. 4) and updated to plant specific frequencies using the methodology developed by Iman (Ref. 5). A fire zone with a fire frequency shown to be less than 10^{-6} per year was not considered further.

Even if the frequency of fire occurrence in a fire zone is greater than the screening value, some initiators (e.g., LOCA) may still be eliminated from consideration. The sum of all initiators given a fire occurrence is always one. However, some of initiator frequencies may be sufficiently small such that fire occurrence in conjunction with that initiator is below the screening cutoff value. In this way, even if a fire zone is

not eliminated from consideration, some of the potential fire-induced initiators may be.

For instance, in the electrical switchgear rooms where loss-of-offsite power occurred, transients with PCS initially available were eliminated from further consideration.

Step 3. Screen Fire Zones Based on Fire Area Analysis

The remaining fire zones underwent a fire area analysis (location mapping) of components as well as control and power cables for a limited set of "vital" components that were located within these areas. This information resulted in a transformation block used in conjunction with the SETS computer code (Refs 6,7) to solve all front line systems and then all of the identified sequences (Table 5.6) of Section 5.4.

Fire occurrence frequency for each zone was set to 1.0 and, given a fire, all components within that zone were assumed to fail. The output of this process was accident cut sets which included fire zone combinations as well as random failures (i.e., not fire-related).

Truncation of cut sets at a random failure probability of 10^{-4} was accomplished, which is equivalent to truncation of internal event cut sets at approximately 10^{-8} since the fire frequency is arbitrarily set for screening purposes to 1.0.

Cut sets which required three or more fire zones were eliminated. This was deemed appropriate since these cut sets imply the failure of two or more three-hour rated fire barriers. Cut sets which contained two fire zones were screened on the following three criteria: (1) no adjacency between zones, (2) no penetrations in the adjacency between zones, and (3) if there were penetrations by numerical culling with barrier penetration failure set to a screening value of 0.1. It is known from previous fire barrier analyses that typical failure rates are on the order of 10^{-2} to 10^{-3}. Therefore, this screening value has been set high enough to ensure potentially important fire zone combinations are not lost.

One additional important piece of information gained from these cut sets was identification of the remaining plant locations where zone to zone barriers needed to be analyzed. Dominant cut sets which contained adjacent fire zones were analyzed for barrier failure in the quantification process.

Step 4. Cull Fire Zones on Probability

Cut sets not eliminated in the first three screening steps were resolved with as-calculated fire-zone-specific initiating event frequencies.

Also, operator recovery of non-fire-related random failures was included. For screening purposes only all short term (less than 24 hour) recovery actions (of non-fire failures) were increased from their respective internal events probabilities by a factor of five to allow for the

additional confusion of the fire situation occurring in conjunction with other random failures. If recovery actions were long term (greater than 24 hours) no modification to internal event probabilities were deemed appropriate. It is felt that by this time the fire will be extinguished and any spurious signals will have terminated in open circuits.

It must be noted that steps 3 and 4 of the screening process reduced the number of cut sets under consideration by at least two orders of magnitude. Also, there were only a few remaining sequences which had not been screened.

Step 5. Confirmatory Plant Visit

For the remaining fire zones all fire-related failure scenarios were identified. A scenario can be thought of as a combination of one or more fire-related equipment failures within a fire zone with or without additional non-fire-related (random) failures outside of the fire area. These failure combinations must minimally lead to core damage. Each fire zone can have one or more scenarios depending on the equipment combinations which must fail due to the fire in that particular area. A second plant visit was then conducted to determine which of these scenarios were valid based upon cable or equipment locations within a particular fire zone. For instance, if a given scenario required the fire-related failure of cabling for components A and B and it could be shown that these cables were always separated by greater than 40 ft. within a room of sufficient size to preclude buildup of a hot gas layer, or one of the component's cabling was in a 3-hr rated fire wrap, then these types of scenarios were eliminated from further consideration. Past experience with fire code calculations, which is discussed in the following section, and fire testing, provided much of the basis for assessing the validity of the scenarios.

About one-half of the remaining cut sets (scenarios) were eliminated as a result of this confirmatory plant visit. Most of these scenarios were associated with cables routed in conduit on the 116 foot elevation of the turbine building and cabling in the circulating water pump structure. Three-hour rated cable wraps for emergency service water pump B cabling precluded short-term fire related failure which was necessary for these scenarios to be valid.

Those scenarios remaining after screening on physical location of components or their associated cabling within a fire zone was determined were subject to fire propagation calculations to determine equipment damage. It must be noted for the cable spreading room that the exact location of a particular component's cabling could not be determined. In this case a best estimate of cable routing was used.

5.6 Fire Propagation Modeling

The COMPBRN fire growth code (Ref. 8) was used to calculate fire propagation and equipment damage. COMPBRN was developed specifically for use in nuclear power plant fire PRAs. The code calculates the time to

damage critical equipment given that a fire has started. This failure time is then used in conjunction with experiential information on fire suppression in nuclear power plants to obtain the probability or frequency that a given fire will cause damage which leads to core damage before the fire can be suppressed. The latest version of the code, COMPBRN III (Ref. 9), with some additional modifications, was used for the calculations.

COMPBRN follows a quasi-static approach to simulate the process of fire during the pre-flashover period in an enclosure. COMPBRN uses a zone model, breaking the fire environment into three zones: flame/plume, hot gas layer, and ambient (see Figure 5.1). Simple fire and heat transfer models and correlations are employed to predict the thermal environment as a function of time. The thermal response of various targets in the fire scenario is modeled to predict the amount of time for a fire to damage or ignite critical equipment. The critical equipment is generally taken to be a cable tray carrying cables necessary for safe shutdown of the plant, although other critical components such as pumps may be modeled.

The original version of COMPBRN, now referred to as COMPBRN I, has been used to calculate damage times in the majority of fire PRAs to date. However, the code calculations are thought to be ultra-conservative due to the neglect of heat losses from the targets. A critical assessment of the code detailing this and other problems has been performed (Ref. 10). In response to these problems with COMPBRN I, two later versions of the code were developed: COMPBRN II and COMPBRN III (Ref. 9). Neither of the later versions of the code has been extensively validated or compared to data, but presumably represent various degrees of improvement.

As a part of a recent study (Ref. 3) on nuclear power plant fire risk assessment, the latest version of the code (COMPBRN III) was selected to requantify fire damage times from several fire PRAs. Initial attempts to use COMPBRN III in the requantification resulted in the observation of problems, with and nonphysical behavior of, the code. Many of the code calculations could not be explained on a physical basis. As a result, an effort was undertaken to identify problem areas and to suggest and implement modifications to the code which make the code predictions more reasonable on a physical basis. It was this modified version of the COMPBRN code which was used to provide the fire propagation analysis for this report. References 3 and 11 provide detailed discussions of the problems noted and recommended modifications for the COMPBRN III code. The following is a brief listing of the major problems which were identified and addressed in the modified version of the code:

a. An error, and nonconservative assumption, exists in the forced ventilation hot gas layer model, predicting low hot gas layer temperatures.

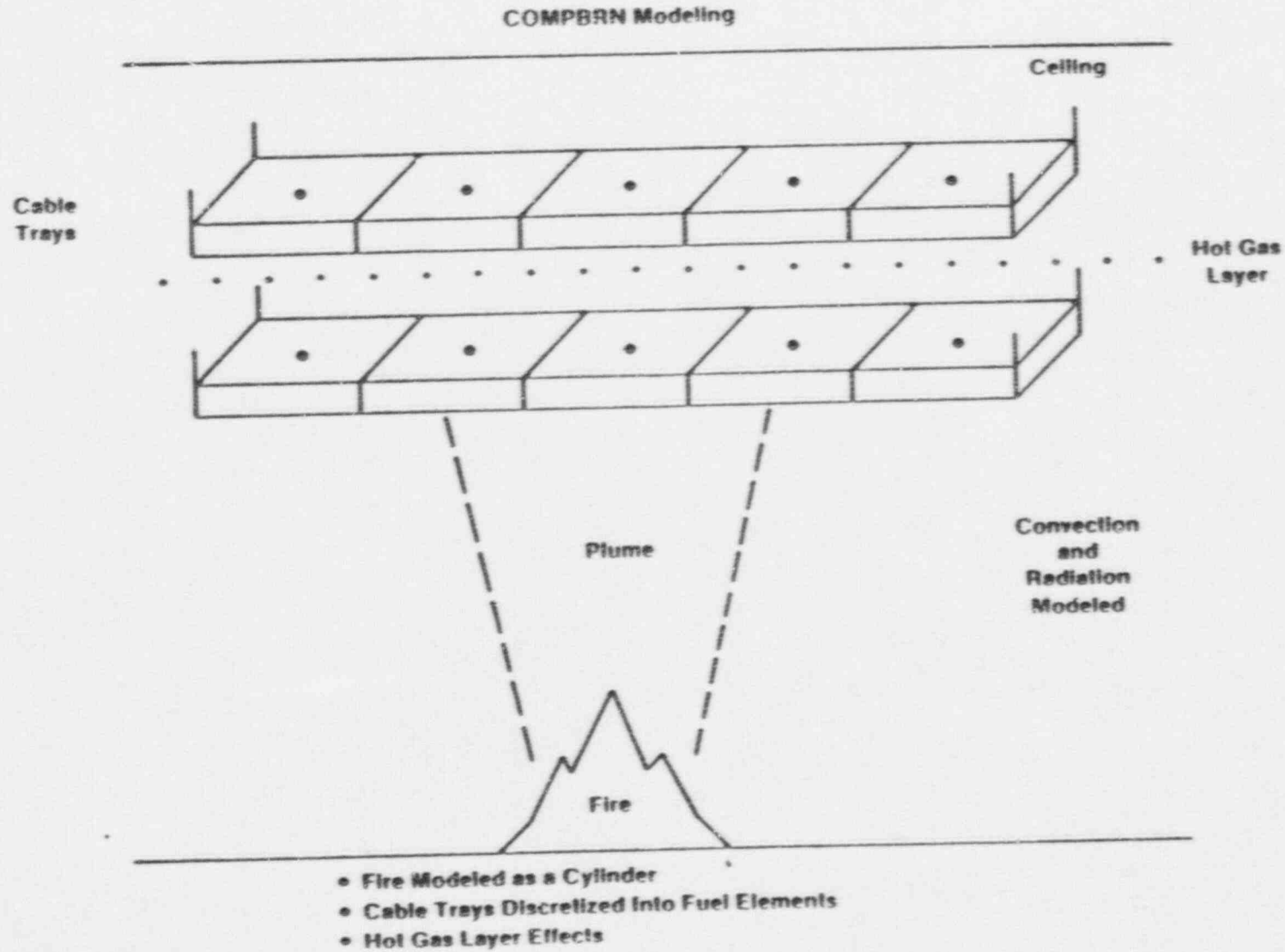

Figure 5.1 COMPBRN Zone Model

b. Radiative heat transfer directly above the flame is not modeled, yielding cooler temperatures directly above the flame than off to the side of the flame.

c. Two errors in the calculation of view factors overpredict the heat radiated to targets to the side as compared to objects directly above the flame.

d. Only convective heat transfer, and not the dominant radiative heat transfer for objects directly engulfed in the flame, is modeled. Time to ignition is highly non-physical.

e. The conduction algorithm is unstable, often resulting in premature termination of the code, especially for cases involving objects in the flame or thermal response of barriers.

f. The mass burning rate of burning objects is underpredicted due to lack of thermal feedback modeling.

g. Cable insulation ignition and damage failure threshold criteria are not currently well understood and the results are quite sensitive to the input parameters chosen.

Both small and large fires were postulated in the calculations. A small fire was assumed to be 2 ft. (.61 m) in diameter and consist of 1 gallon (3.8 l) of oil. A large fire was assumed to be 3 ft (.91 m) in diameter and consist of 10 gallons (38 l) of oil. Analysis of a data based on transient combustible fuel sources found at nuclear power plants (Ref. 12) indicates that oil sources less than or equal to 1 gallon (3.8 l) were found approximately 70 percent of the time. Oil sources larger than this were found roughly 30 percent of the time. A similar partitioning between small and large quantities in terms of heat content (BTU or KJ) can be made for other credible transient combustible sources such as solvents or trash paper. Again, analysis indicates that a 70/30 partitioning between small and large fuel sources is appropriate (within ± 10 percent). It can also be shown that 10 gallons (38 l) of oil bounds any large solvent or trash paper combustible source in terms of heat content and is, therefore, an appropriate upper bound on transient combustible fuel source size.

A walkdown of the Peach Bottom Plant was performed to obtain vital information for the COMPBRN calculations. This information included the location of critical equipment and cable trays, separation between redundant trains, types of cable present, and any shielding or fire barriers which may be present. Several "pinch points" were identified where critical cables from redundant trains passed from one room to another, or where cables for important plant safety and support systems were routed through the same area in close proximity. Some of the cabling was enclosed in conduit or in rectangular aluminum busways. However, because of its low melting point this aluminum was neglected in the COMPBRN calculations to be conservative. Similarly, in several cases the power cables to critical pumps were routed in metal sleeves. In the

COMPBRN calculations, these cables were assumed to be incapable of igniting. However, damage was assumed to occur when the surface temperature reached the temperature corresponding to cable failure.

Cable insulation ignition and damage thresholds are currently not well known (Ref. 13). For this study, a cable insulation ignition temperature of 773°K (932°F) was assumed along with a damage temperature of 623°K (662°F). For the large fire simulations these thresholds are not as critical to the fire damage time calculations because of the intensity of the flames.

A list of input parameters for the COMPBRN calculations is shown in Table 5.7. These parameters were selected to represent typical qualified cable insulation. It was assumed that the cabling in the areas of interest included typical brands of nuclear qualified cable insulation materials, such as Rockbestos Firewall III, Brand Rex, or Okonite. Because of the good flame resistance properties of these cables, no self-ignited (electrically initiated) cable tray fires were postulated.

The COMPBRN results are shown in Table 5.8 for the critical areas. Summary discussions of each fire area are provided in Sections 5.6.1 through 5.6.14. A number of scenarios were considered for many of these areas. In a number of cases, a "zone of influence" was determined for the equipment and fire sizes modeled. In other words, the fire location was varied in the COMPBRN models to determine the maximum distance the fire could be away from the critical equipment and still cause damage. The times to damage increase exponentially as the fire distance increases. The numbers given in the table represent the combination of greatest distance and longest times to damage. Using these results, the floor area in which a fire would have to occur to damage critical cables can be estimated. An area ratio can then be calculated by dividing this area by the total floor area of the room. This reduction factor can then be multiplied by the initiating frequency to estimate the frequency of fires which occur in a critical portion of a given room.

It should be noted that a small fire, except for zone of influence cases, does not yield damage in most of the areas. Prior experience with COMPBRN shows that a small fire must be very close to its target to yield damage. Large fires, however, can and do yield damage in most of the areas. In large open rooms, the larger fire must still be within about 3 feet horizontally of the target cable trays (assuming typical tray heights). The major exception is in small closed rooms (like the switchgear rooms) in which a hot gas layer rapidly develops. Since Peach Bottom is divided into small fire zones, hot gas layer effects were sometimes important. Thus, for the majority of COMPBRN runs, room parameters were used in order to simulate a model of the hot gas layer. For these cases, damage occurs sooner, due to the increased thermal input from the hot gases.

Table 5.7

Modified COMPBRN III Input Parameters

Cable Insulation Parameters	
Density	1715 kg/m^3
Specific Heat	1045 J/kg-K
Thermal Conductivity	0.092 W/m-K
Heat of Combustion	1.85-2.31E-7 J/kg
Combustion Efficiency	0.6-0.8
Critical Temperature	
Piloted Ignition	773°K
Spontaneous Ignition	773°K
Damage	623°K
Surface Controlled Burning Rate	0.0001-0.0075 kg/m^2-S
Burning Rate Radiation Augmentation	1.86E-7 kg/J-m^2
Radiative Fraction	0.3-0.5
Smoke Attenuation Factor	1.4
Reflectivity	0.1-0.3
Oil Parameters	
Density	900 kg/m^3
Specific Heat	2100 J/kg-K
Heat of Combustion	4.67E7 J/kg
Combustion Efficiency	0.9
Surface Controlled Burning Rate	0.06
Radiative Fraction	0.3-0.5
Mass of Oil	3.4-34.0 kg

Table 5.8

Time to Damage Critical Cables

Area	Scenario	Small Fire	Large Fire
Room 262/147	LOSP, cables Area of Influence	Inf 4 min,.5m	Inf 8 min, 1.5m
Cable Spreading Room	Critical cables	3 min,.6m	5-7 min 1.8m
Switchgear Rooms:			
Area 32, Rm 261	LOSP Switchgear fire	Inf 8-9 min	4 min NA
Area 33, Rm 267	LOSP Switchgear fire	Inf 8-9 min	5-8 min* NA
Area 34, Rm 265	LOSP Switchgear fire	Inf 8-9 min	3 min NA
Area 35, Rm 263	LOSP Switchgear fire	Inf 8-9 min	5-8 min* NA
Area 36, Rm 226	LOSP Switchgear fire	Inf 8-9 min	5-8 min* NA
Area 37, Rm 231	LOSP ESW pumps and swgr ESW pumps not swgr Switchgear fire	Inf Inf NA 8-9 min	5-8 min* 4 min NA NA
Area 38, Rm 217	LOSP Switchgear fire	Inf 8-9 min	3 min NA
Area 39, Rm 227	LOSP ESW pumps and swgr ESW pumps not swgr Switchgear fire	Inf Inf NA 8-9 min	3 min 6 min NA NA
Area 44, C Diesel	Both ESW cables	4 min,0.8 min	8 min 1.5m
Area 46, A Diesel	Both ESW cables	4 min,0.8m	8 min 1.5m
Area 48, HPSW	All pumps	Inf	Inf
Area 50, Rm 126	LPCS A and B LPCS C and D	Inf Inf	2 min Inf

* - Required a slightly larger fire (.91m x .91m)

The fire data base indicates there have been several cases where switchgear either exploded or otherwise ignited, resulting in a fire. The question was posed as to the possible effects of such a fire in the switchgear rooms and how to model it. There are open cable trays directly above each of the cabinets which would be vulnerable to ignition given a fire in the cabinet below. All of the switchgear cabinets have open ventilation louvers at the bottom and openings in the tops of each of eight cubicles through which cable conductors pass and are routed to the overhead cable trays. The resulting chimney effect would easily promote propagation of flames from within the cabinet through the top penetration and up to the cable trays. The possibility of fire propagation and damage to the offsite power trains would then be a consideration.

To model switchgear fires which result in open flames above the cabinets themselves, an oil pool fire 2-feet (0.61 m) in diameter was modeled on top of the switchgear cabinet directly below the open cable tray. This fire would simulate the ignition of the cables penetrating the cabinet and possibly the overhead tray, given a fire in the cabinet itself. Thus, the effect of ignition of the cables entering the switchgear cabinets, along with the overhead cable trays, on the two offsite power trains in the immediate vicinity could be examined.

For the switchgear in fire areas 32-39, the two offsite power trains were damaged in 8 to 9 minutes after roughly 3 gallons of fuel had burned. This relatively small fire was capable of such results due to its proximity to the offsite power trains and to the additional heat input which results as the cables above the switchgear cabinets ignite and the flames propagate along the cable tray.

It was found during some of the simulations that the COMPBRN results can be very sensitive to the location of the ceiling midpoint and wall midpoint. In some cases, fires initially located directly under the ceiling midpoint had to be located elsewhere in the room, or the calculated ceiling temperatures were unrealistically high, resulting in unrealistic radiative heat fluxes to the cable trays of interest. In other cases, similar behavior was observed when a wall was modeled. For these cases, the wall was divided into several sections to more realistically calculate the wall thermal response.

5.6.1 Fire Area 2: Room 262/147

5.6.1.1 Results

The first scenario in this area involved damage to both the offsite power trains and critical cables located in a tray between those trains. No postulated fire, large or small, can simultaneously damage this equipment.

The second scenario consisted of determining the "zone of influence" of fire damage around the critical cable tray. A small fire will damage these cables in 4 minutes from a distance of 0.5 m either side of the

midpoint of the cable tray. The large fire will cause damage in 8 minutes from 1.5 meters.

5.6.1.2 Discussion

This fire area involves a limited section of a long hallway corridor approximately 1.2 meters wide and 3.5 meters high. The equipment of interest includes offsite power cable raceways and other critical cables of nonspecific location within the area. It was assumed that the critical cables are all in a bunched configuration in one overhead cable tray between the two offsite power trains. Since this long corridor is open at its ends to other plant areas, it was determined that use of parameters to simulate hot gas layer effects would be overly conservative and non-physical given the narrowness of the room.

5.6.2 Cable Spreading Room

5.6.2.1 Results

One scenario was analyzed, assuming all critical cables are located in the lower middle tray of a typical section of the cable trays in the cable spreading room. The zone of influence for the small fire is 0.6 meters with damage in 3 minutes. The larger fire will damage the target cables in 5-7 minutes from a distance of $\pm$1.8 meters.

5.6.2.2 Discussion

Modeling of the critical cables in this area involves an estimate as to the location of the cables associated with certain equipment in the control room above. It was assumed that the critical cables penetrate down from the control room to the lowest middle cable tray in a nested 3 by 3 matrix of cable trays, and then run horizontally around the room and out to the respective plant equipment. Exact cable tray relational dimensions were obtained from plant drawings to model the 9-tray array. The fire was moved either side of the critical lower middle tray to determine the zone of influence. Though ignition did occur, the important consideration was the time to damage the target cable tray. The actual propagation of the flames down the length of the cable trays was not developed in detail, though such propagation would probably occur with the postulated fire. The primary concern was the time required to fail certain system equipment whose failure leads to core damage.

5.6.3 Fire Area 32: Room 261

5.6.3.1 Results

As discussed above, a small fire within and on top of the switchgear themselves will cause damage to both trains in 8-9 minutes. These results apply to the other eight switchgear rooms and, therefore, will not be repeated. A large fire will damage both offsite power trains in 4 minutes.

5.6.3.2 Discussion

Since all of the switchgear rooms are relatively small and closed, it was deemed appropriate to model the effects of a hot gas layer, which significantly contributes to the target heat load given a fire. One of the largest uncertainties with these rooms was the actual ventilation flow, both before and during a fire. Based on plant input and the effectiveness of door seals and fire dampers that are isolated upon fire detection, it was considered appropriate to assume 1 air change per hour for forced ventilation.

In Room 261, the fire was placed between the point of closest approach of the offsite power trains, at the end of the switchgear near the wall. A technique to segment the wall to more realistically model radiation from the wall was adopted, in this and other similar scenarios involving fires in close proximity to walls.

5.6.4 Fire Area 33: Room 267

5.6.4.1 Results

A fire approximately 25 percent larger than is typically modeled, as discussed above, was used here to yield damage in 5 to 8 minutes to both offsite power trains.

5.6.4.2 Discussion

The large fire was placed at a location midway between the offsite power trains, which are approximately 4.0 meters apart. The overhead cable tray above the switchgear cabinets was modeled also, though its distance from the oil pool on the floor had no consequence regarding time to damage.

5.6.5 Fire Area 34: Room 265

5.6.5.1 Results

Damage to both offsite power trains occurs within 3 minutes in this room for a large fire.

5.6.5.2 Discussion

The modeling of this fire area was similar to the other switchgear rooms with one exception. There is a cable tray which spans the room over the floor space between the offsite power trains. When the large fire is modeled immediately below the tray, its cables are ignited early in the simulation and provide additional heat input towards damaging the offsite power cables.

5.6.6 Fire Area 35: Room 263

5.6.6.1 Results

Similar to Fire Area 33, the larger fire will damage the offsite power cables in 5 to 8 minutes.

5.6.6.2 Discussion

This room, though quite similar to Room 267, had slightly different geometry than the latter with respect to relative placement of the overhead trays. As a result, damage will occur more quickly because of additional heat input from the tray, which will eventually ignite, even though it is not located immediately above the flames.

5.6.7 Fire Area 36: Room 226

5.6.7.1 Results

The larger fire results in damage in 5 to 8 minutes.

5.6.7.2 Discussion

This room was quite simple to model as it did not involve any overhead trays for the pool fire on the floor. The 4-meter separation of the offsite power trains was the only parameter of interest.

5.6.8 Fire Area 37: Room 231

5.6.8.1 Results

This area involved three scenarios. The first, LOSP, yielded results the same as Fire Area 35 due to identical geometries and modeling considerations (this includes the earlier discussions regarding small fires and switchgear fires).

For the scenario involving both ESW pump cabling in conduit and the "B" HPSW switchgear, damage occurs in 4 minutes with a large fire. The postulated small fire cannot damage all of this equipment.

The scenario involving the ESW pumps and not the switchgear does not apply as the switchgear is damaged in 2 to 4 minutes, regardless of how the switchgear is modeled or where the fire is located. Thus, this scenario is "impossible" to meet.

5.6.8.2 Discussion

The ESW cables were located high in the room though separate trains were in close enough proximity to yield damage to both with a large fire simulation. The actual switchgear location and damage parameters were not accurately known; however, sensitivity analyses were performed to determine the effect of varying fire locations, switchgear geometry, and material vulnerability. Damage to the switchgear came readily due to its

face area exposed to the radiant heat from the flame, in addition to convective and hot gas layer effects.

5.6.9 Fire Area 38: Room 217

5.6.9.1 Results

A large fire will cause damage in 3 minutes in this room.

5.6.9.2 Discussion

The modeling of this room was similar to Fire Area 32, but included an additional overhead cable tray which ignited. The geometry and distances were similar but different enough to change the final results slightly. Using a segmented wall model for the wall adjacent to the fire, and taking into account some shielding due to the congestion in the part of the room modeled, somewhat increased the time to damage.

5.6.10 Fire Area 39: Room 227

5.6.10.1 Results

This area included the same three scenarios discussed for Fire Area 37. The geometry for the LOSP scenario was identical to Fire Area 38 and will not be discussed further.

For the scenario involving the ESW cables and HPSW switchgear, the large fire will damage all equipment in 6 minutes.

As in Fire Area 37, the third scenario--ESW cables and not the switchgear--was not possible to meet as the switchgear is damaged first.

5.6.10.2 Discussion

For the two scenarios involving the ESW cables in conduit and the HPSW switchgear, there are significant differences in geometry and in the models used from those in Fire Area 37. The same comments apply as those mentioned in Section 5.6.8, including the fact that there is more separation between the ESW cable conduit, which is the primary reason for the increased time to damage over that noted for Fire Area 37.

5.6.11 Fire Area 44: "C" Diesel Bay

5.6.11.1 Results

For the ESW conduit mounted on the wall, a large fire will cause damage to both trains in 8 minutes from a distance of 1.5 meters, defining the outer bounds of the zone of influence and area ratio for the fire area.

The small fire will cause damage in 4 minutes from 0.8 meters.

5.6.11.2 Discussion

This model involves a relatively simple case of redundant cables in conduit running along a wall at slightly different elevations. No hot gas layer was modeled due to the size and ventilation of the room, which would tend to minimize such effects.

5.6.12 Fire Area 46: "A" Diesel Bay

See the previous section for the "C" diesel bay as the results and discussion are identical.

5.6.13 Fire Area 48: HPSW Pumps

5.6.13.1 Results

No fire, large or small, will damage all of the power cables or motors associated with these four pumps.

5.6.13.2 Discussion

This scenario involves four vertical pumps, motors, and associated power supply cables mounted along the wall in a large, closed, but well ventilated room. The ventilation rate was kept low for conservatism and cases both using and ignoring hot gas layer effects were simulated. The shielding effects of the inner pump motors for heat transmitted from the fire (located between them) to the outer pumps was analyzed. Fire location was varied to eliminate the shielding effects. None of the models resulted in conditions adequate to damage all of the pumps with the postulated fire sizes.

5.6.14 Fire Area 50: Room 126

5.6.14.1 Results

A large fire will damage both LPCS B cable runs in 2 minutes. The small fire will not damage both trains.

The LPCS C and LPCS D cable runs were sufficiently high and separated to eliminate the possibility of damage to both trains by a small or large fire.

5.6.14.2 Discussion

This fire area contains numerous cables from safety related equipment. The cable in conduit runs for LPCS A and B are vertical and about 3 meters apart immediately adjacent to a wall. Despite the separation, a large fire will easily damage these cables. Modeling was relatively simple and involved the wall and no hot gas layer effects. In the case involving the C and D LPCS cable conduit runs, the distance above the

floor and separation distance together were sufficient to prevent damage from a large fire placed anywhere between them. The vertical section along the wall and the "bend" in the conduit run about 4.5 meters off the floor were modeled, along with the oil pool fire.

It was noted that a number of the cable runs in this vicinity are encased in 3-hour rated fire barriers which eliminated consideration of a number of potential fire vulnerabilities.

5.7 Barrier Failure Analysis

In the unscreened cut sets where a potential for barrier failure had been identified, the barrier failure probability was estimated using barrier failure rates developed as described below.

Barriers were grouped into three types: (1) fire doors, security doors, water-tight doors, and [illegible] curtains; (2) fire dampers and ventilation dampers; and (3) penetration seals and fire walls. The data base contains 628 records from when construction began on any given plant to the end of June 1985. The number of barriers of each type at a plant is required to estimate the rate at which a specific component fails. The number is not known precisely for each plant, but a nominal figure that has been estimated for each barrier type is given in Table 5.9.

The statistical uncertainty of each estimate, reflecting sampling variation and plant-to-plant variation, is represented by 90 percent confidence bounds. These estimates and confidence bounds are given in Table 5.10 where units of both estimates and bounds are failures/year.

During the confirmatory plant visit scenarios which required barrier failure had those barriers inspected. No plant-specific vulnerabilities which would require modification of generic barrier failure rates were noted as a result of this inspection. After multiplying barrier failure rates by the number of penetrations at each appropriate fire zone adjacency and utilizing the probabilities developed in screening step 5, all remaining barrier failure scenarios did not survive the 10^{-8} per year frequency screening criteria.

Table 5.9

Approximate Number of Barriers at a Plant

Type	Nominal
1	150
2	200
3	3000

Table 5.10

Estimates of Single Barrier Failure Rates

Barrier Type	Barriers/ Unit	Estimate	5% Confidence Bound	95% Confidence Bound
1	150	7.4E-3	0.0	2.4E-1
2	200	2.7E-3	0.0	2.2E-1
3	3000	1.2E-3	0.0	3.7E-2

5.8 Recovery Analysis

For those remaining cut sets which survived the screening process and where the COMPBRN code predicted fire damage would occur, recovery of random failures and credit for extinguishment of the fire before the COMFBRN-predicted time to fire damage was applied.

Recovery of random failures (non-fire related) was treated in a similar fashion as in the internal events analysis. All operator recovery actions that were used in the internal events analysis were inspected for use where appropriate on the remaining cut sets. If a sequence was long term (greater than 24 hours), two recovery actions were allowed. In short term (less than 24 hours) sequences only one recovery actions was allowed. This recovery action was chosen if the possibility of multiple recovery actions was present and on a hierarchy based on recovery probabilities established by the internal events analysts. For short term sequences recovery action probabilities were modified when deemed appropriate.

In the areas where firefighting activity takes place, no credit was given for local recovery actions until after the fire was extinguished. In non-affected areas, local recovery was allowed for valve manipulation or pump operation when damage to power cabling of an applicable component had not occurred.

In conjunction with human factors analysts and the "Handbook of Human Reliability Analysis With Emphasis on Nuclear Power Plant Applications" (Ref. 14), any additional recovery actions not developed by the internal events recovery procedure were quantified. Only one additional recovery action was added for the Peach Bottom analysis. This recovery action was necessitated by failure of control cabling either in the cable spreading room or control room requiring control of the plant from the remote shutdown system. Even though explicit procedures were in place for this situation, a high stress recovery probability was applied. This was

deemed appropriate due to timing of the sequence (less than one hour) and the fact that some amount of time would be required to make the decision to abandon the control room and man the remote shutdown stations.

The probability of manual non-suppression of a fire before the COMPBRN predicted time to damage was quantified using the Wheelis data base (Ref. 4) which contained information on 69 fire events which had time to suppression associated with them. As part of the Fire Risk Scoping Study (Ref. 3) a distribution was fit to this data. A probability of non-suppression was then associated with any COMPBRN-predicted time to fire damage.

The probability of automatic non-suppression of a fire was quantified consistent with Reference 15. No modification to generic reliability values was deemed appropriate for the cable spreading room.

5.9 Uncertainty Analysis

Distributions on fire frequency, fire suppression probability, fire code calculations, random failure probability, barrier failure probability, and operator recovery actions, were used to generate uncertainties on fire core damage frequencies.

The uncertainty of these values was propagated through the accident sequence models using two computer codes. A Latin Hypercube Sampling (LHS) algorithm was used to generate the samples for all of the parameter values (Ref. 16). The Top Event Matrix Analysis Code (TEMAC) was used to quantify the uncertainty of the accident sequence equation using the parameter value samples generated by the LHS code (Ref. 17).

LHS is a constrained Monte Carlo technique which forces all parts of the distribution to be sampled. The LHS code is also flexible in that it can sample a variety of random variable distributions. Furthermore, parameter distributions for similar events were correlated. For example, if two similar components (e.g., MOV XX-FTO and MOV YY-FTO) are modeled from the same probability distribution, then the sampling of these two distributions is perfectly correlated, meaning the same value is used for both events in a given sample member. For basic events which are modeled with very similar but slightly different distributions (e.g., MOV XX fails to remain closed for 100 hours and MOV YY fails to remain closed for 200 hours), the LHS code permits an induced correlation between the samples. However, LHS does not allow the correlation coefficient for this case to be equal to 1.0. LHS did permit sampling with a coefficient of 0.99 in these cases

TEMAC uses the LHS parameter samples and the accident sequence equations (cut sets) as input to quantify the core damage estimates. TEMAC generates a sample of the accident sequence frequency, a point estimate of the frequency, and various importance measures and ranking for the base events.

Uncertainty on fire initiating event frequency was developed when the generic fire frequencies were updated using Peach Bottom specific data.

This process which was briefly discussed in Section 5.3 is covered in more detail in Reference 5.

Uncertainty on fire non-suppression probabilities ($Q(T_B)$) was addressed by modification of COMPBRN predicted time to damage. The COMPBRN-predicted time to damage and its associated non-suppression curve probability were taken to be a best estimate of a maximum entropy distributed variable. Fifteen minutes were added and subtracted from the COMPBRN-predicted time to allow for uncertainty in its result and the uncertainty in the probability of non-suppression distribution. These probabilities were taken as a minimum and maximum of the maximum entropy distribution respectively.

Uncertainty associated with the fire size estimate factor (f_s) was developed utilizing information associated with an I&E inspector report (Ref. 12) on a survey of different types of combustiles and their amounts found in nuclear power plants. Two fire sizes, a large and small fire were modelled as described in Section 5.6. These fire sizes (BTU content) were compared to the distributions on possible fire sizes developed for the different combustibles from the I&E data. The best estimate for percentage of fires that were either large or small was taken from an average of the different types of combustibles for an equivalent BTU level fire modelled by COMPBRN. This probability was assumed to be the best-estimate value of a maximum entropy distribution. Maximum and minimum probabilities for this distribution were assumed to be based on one individual type of combustible with either the maximum or minimum percentage corresponding to applicable fire size (BTU rating).

Random failure events and operator recovery actions were treated identically as in the internal events analysis. Uncertainties and types of distributions were not modified for the fire analysis.

All other factors and their associated uncertainties are not common to all fire sequences and will be addressed individually in the appropriate subsections of Section 5.10.

5.10 Description of Unscreened Fire-Induced Core Damage Scenarios and Their Associated Fire Areas

5.10.1 Introduction

This section will describe the fire scenarios and their associated fire zones which are listed in Table 5.1. All other fire zones and all adjacent fire zone combinations dropped below 10^{-8} per year after either operator recovery of non-fire related failures, COMPBRN code calculations, or barrier failure probabilities were applied.

5.10.2 Control Room

Two scenarios in the control room remained after screening, both based on a single transient sequence ($T_{3A}U_1U_2X_1U_3$).

These scenarios both assumed abandonment of the control room due to smoke from a cabinet fire. Credit was given for quick extinguishment of the fire within the applicable cabinet since the control room is continually manned. None of the three control room fires in the data base led to abandonment of the control room. It was assumed that only one in ten fires would not be extinguished before sufficient smoke was generated to force abandonment of control room. This factor (f_R) was taken to be the best estimate of a maximum entropy distribution. As an upper bound it was assumed that the next control room fire that occurred would force abandonment and thus the probability would be one-fourth. As a lower estimate it was assumed that only one in one hundred control room fires would lead to abandonment. Sandia large-scale enclosure tests (Ref. 17) have demonstrated that smoke has engulfed a mocked up control room due to a cabinet fire within 6 to 8 minutes from time to ignition even with ventilation rates of up to 10 room changes per hour. Therefore, these estimates on abandonment probability given a cabinet fire are deemed to be reasonable.

Because of the cabinet configuration within the Peach Bottom control room and based on Sandia cabinet fire tests (Ref. 18) the postulated fire was assumed not to spread and damage any components outside of the cabinet where initiation occurred. The penetrations to all Peach Bottom control room cabinets were through the bottom to the cable spreading room below. Also, these cabinets had enclosed backs and tops. In Sandia cabinet fire tests cabinets had open backs and enclosed tops. Even in this configuration fire did not spread to adjacent cabinets. Therefore, the cabinet area ratio factor (f_A) was considered to be known fairly accurately. As a lower bound it was assumed that only one half of the applicable cabinet could initiate a sufficiently large fire. An upper bound estimate assumed that all cabinet areas could initiate the fire but also that a transient fire at a maximum of one foot away from the cabinet in all exposed directions could cause the same damage to the cabinet and fire-initiated smoke release. In both control room scenarios the fire was assumed to totally disable the functions of the cabinet where initiation occurred.

Both fire scenarios assumed that the remote shutdown system was independent of the control room. This assumption is potentially non-conservative in that the possibility exists that subtle interactions between the remote shutdown panels and the control room are still present. As part of the Fire Risk Scoping Study (Ref. 3), an exhaustive cable tracing effort yielded a number of subtle interactions between one plant's control room and remote shutdown panel.

Area ratios for fire involvement only considered total cabinet area in the control room. This is based on fire data which illustrates the fact that the only control room fires to date have occurred in control cabinets.

5.10.2.1 Control Room Scenario 1

The first scenario postulates fire initiation interior to the RCIC cabinet which, due to subsequent smoke release, forces abandonment of the control room. Procedures require that the reactor be manually scrammed, thus resulting in a T_3 transient sequence. The RCIC system (U_2) is not independent of the control room since it is not part of the remote shutdown system and is assumed to fail given a fire in its control cabinet. The CRD system (U_3) is also not part of remote shutdown system and thus no credit is given for its utilization. The HPCI (U_1) and ADS (X_1) systems are part of the remote shutdown panel but are failed due to operator error.

The core damage equation is as follows:

$$\phi_{cm} = \lambda_{CR}\ f_A\ R_{op}\ f_R$$

where

ϕ_{CM} = fire-induced core damage frequency for Control Room Scenario 1

λ_{cr} = frequency of control room fires

f_A = area ratio of the RCIC cabinet to total cabinet area within the control room

R_{op} = probability that operators will fail to recover the plant from the remote shutdown panel

f_R = probability that smoke will force abandonment of the control room given a fire occurrence

Table 5.11 gives the values of each of these factors as well as their associated distribution and upper and lower bounds.

For all lognormal- and gamma-distributed variables in Table 5.11 and the following tables of Section 5.10, the lower bound and upper bound are the 5th and 95th percentiles of the distribution while the best estimate is the mean value.

5.10.2.2 Control Room Scenario 2

The second fire scenario in the control room assumes that the fire is initiated in any other cabinet than the RCIC.

As in the first scenario subsequent smoke release forces abandonment of control room. Credit was given for the RCIC system automatically cycling to control reactor level even though it is not controlled from the remote shutdown panel. Therefore, the RCIC system (U_2) must randomly fail which adds the Q_{RCIC} term in the core damage equation. As in the first scenario the reactor is manually scrammed (T_3) and the HPCI system (U_1) and ADS system (X_1) are failed due to operator error at the remote shutdown panel. Also, no credit is given for the CRD system (U_3) since it is not part of the remote shutdown panel.

Table 5.11

Control Room Fire Scenario 1 Factors and Distributions

Factor	Distribution	Lower Bound	Best Estimate	Upper Bound
λ_{CR}	Gamma	1.2E-7	2.3E-3	6.2E-3
f_A	Maximum entropy	0.01	0.02	0.028
R_{op}	Maximum entropy	6.4E-?	0.064	0.64
f_R	Maximum entropy	0.01	0.1	0.25

The core damage equation is as follows:

$$\phi_{cm} = \lambda_{CR} (1 - f_A) R_{op} Q_{RCIC} f_R$$

where

o_{CM} = fire-induced core damage frequency for Control Room Scenario 2

λ_{CR} = frequency of control room fires

$(1-f_A)$ = area ratio of all cabinets other than RCIC to total cabinet area

R_{op} = probability that operators will fail to recover the plant from the remote shutdown panel

Q_{RCIC} = random failure of the RCIC system (non-fire related failure)

f_R = probability that smoke will force abandonment of the control room given a fire occurrence

Table 5.12 gives the probabilities of each of these factors as well as their associated distribution and upper and lower bounds.

5.10.3 Cable Spreading Room

One scenario involving the cable spreading room survived the screening process, the transient sequence ($T_{3A}U_1U_2X_1U_3$). This scenario requires the fire-related failure of control power for the HPCI, RCIC, ADS and CRD systems. Credit was given for independence of the remote shutdown system from the cable spreading room. Exact cable locations were unknown.

Table 5.12

Control Room Fire Scenario 2 Factors and Distributions

Factor	Distribution	Lower Bound	Best Estimate	Upper Bound
λ_{CR}	Gamma	1.2E-7	2.3E-3	6.2E-3
$(1-f_A)$	Maximum entropy	0.49	0.98	1.0
R_{op}	Maximum entropy	6.4E-3	0.064	0.64
Q_{RCIC}	Lognormal	(EF=5)	5.0E-2	
f_R	Maximum entropy	0.01	0.1	0.25

However, knowing the cabinet locations within the control room which is directly above the cable spreading room and that cables run directly out the bottom of associated cabinets, an accurate approximation of cable routing for the cable spreading room was obtained. The area ratio within the cable spreading room was based on the location where the control cables for HPCI, RCIC, and ADS intersected with those for the CRD system directly below its cabinet, and continuing to the west wall. Given a transient there is also a probability that one or more relief valves may stick open. These sequences were analyzed but did not survive screening. Therefore, the factor P_1 accounts for the fact that, given a transient, no stuck-open relief valves will occur approximately 90 percent of the time.

The automatic CO_2 system within the cable spreading room was analyzed to determine whether generic reliability data needed to be modified. This system requires that two smoke detectors from different zones within the cable spreading room detect the fire for system activation to occur. Since the smoke detectors are fast-acting, and provide thorough detector coverage of the area, no modifications to CO_2 system reliability data was deemed appropriate. Thus, the term in core damage equation Q_{auto} reflects the probability that the automatic CO_2 system will not suppress the postulated fire.

The percentage of time that personnel are in the cable spreading room is known. The factor $Q(\tau_g)$ take this percentage into account, and gives credit for manual extinguishment of the fire before the automatic CO_2 system would be actuated.

Two sizes of fires were postulated under the cable trays of interest. The COMPBRN results discussed in Section 5.6 were used to develop area ratios for both the large and small fires.

Abandonment of the control room is assumed based on operators being unable to control the safety systems that received fire damage. Thus, according to procedure the reactor will be manually scrammed leading to a (T_3) transient. The RCIC system (U_2) and CRD system (U_3) receive fire damage to their control systems and are not independent of the cable spreading room. Therefore, both systems are assumed to fail. As was the case for the control room fire scenarios, operator error fails the HPCI system (U_1) and ADS system (X_1).

The core damage equation is as follows:

$$\phi_{CM} = \lambda_{CSR}\, Q(\tau_G)\, Q_{AUTO}\, R_{op}\, P_1 \times [f_{A1}\, f_{S1} + f_{A2}\, f_{S2}]$$

where

ϕ_{CM} = fire-induced core damage frequency for the cable spreading room

λ_{CSR} = frequency of cable spreading room fires

$Q(\tau_G)$ = that percentage of fires that are not manually suppressed before automatic detection occurs

Q_{AUTO} = probability that the automatic CO_2 system will not suppress the fire

R_{op} = probability that operators will fail to recover the plant from the remote shutdown panel

P_1 = percentage of initiating event frequency where one or more stuck-open relief valves does not occur

f_{A1} = area ratio within the cable spreading room for a large fire

f_{S1} = that percentage of fires which are in the "large" category

f_{A2} = area ratio within the cable spreading room for a small fire

f_{S2} = that percentage of fires that are in the "small" category

Table 5.13 gives the values of each of these factors as well as their associated distribution and upper and lower bounds.

5.10.4 Emergency Switchgear Rooms 2A, 2D, 3A, 3B, and 3C

For all five of these fire areas a similar scenario occurred. This sequence (T_1BU_1) was a station blackout caused by a fire-induced loss of offsite power and a random loss of the emergency service water system

Table 5.13

Cable Spreading Room Fire Scenario Factors and Distributions

Factor	Distribution	Lower Bound	Best Estimate	Upper Bound
λ_{CSR}	Gamma	1.2E-6	3.5E-3	7.9E-3
$Q(f_S)$	Maximum entropy	0.60	0.87	1.0
Q_{AUTO}	Maximum entropy	4.0E-3	0.04	0.4
R_{op}	Maximum	6.4E-3	0.064	0.64
P_1	Pt. value		0.90	
f_{A1}	Maximum entropy	0.031	0.062	0.15
f_{A2}	Maximum entropy	0.014	0.027	0.068
f_{S1}	Maximum entropy	0.19	0.3	0.67
f_{S2}	Maximum entropy	0.33	0.7	0.81

(ESW). This random (failure not related to the fire itself) loss of emergency service water caused a station blackout because emergency service water provides cooling for all four diesel generators. Thus, the emergency onsite power system (B) failed. Emergency service water also provides room cooling for the HPCI system (U_1). The HPCI system will fail in approximately 10 to 12 hours due to either loss of room cooling or battery depletion caused by the station blackout.

These areas are all similar in that the primary source of fire is electrical switchgear within the fire area. Therefore, the fire frequency was developed for electrical switchgear rooms, and area ratios for only the cabinet area within the room. A valid mechanism for spread of fire outside these cabinets was required to develop a hot gas layer which would fail offsite power. A plant-specific look at these switchgear revealed that, in the case of all breaker cubicles, many small cables passed through the top at one penetration and that this penetration was inadequately sealed. Because there are ventilation

slots at the bottom of the cabinets, a chimney effect could occur given a fire. It was assumed that there would be a 50 percent chance of the fire exiting the top. Furthermore, a cable run exists directly above these penetrations which would add more fuel to the fire.

This fire scenario requires that the cable run directly above the 4160V switchgear ignite to add sufficient fuel to form a hot gas layer covering the entire room, which then fails offsite power trunks J57 and J58. The area ratio factor (f_A) was therefore taken as the ratio of 4160V switchgear area to total cabinet area within the fire area. A measurement of this ratio yielded a best estimate of 0.9 for this maximum entropy variable. As a lower bound, only the centermost cubicle was postulated as being capable of failing offsite power, resulting in an area ratio of 0.1. For an upper bound it was assumed that the most probable source of fire was the high-voltage 4160V cubicles, and not the other lower voltage cabinet. This led to an upper bound of 1.0.

The percentage of cabinet fires (f_s) large enough to exit the top of cubicle was approximated as unity, based on Sandia fire testing experience. Thus, a tight maximum entropy distribution for the severity ratio factor was postulated.

The percentage of fires $Q(\tau_G)$ that are manually extinguished before requisite damage occurs was evaluated as described in Section 5.9.

The term that represents random failure of the emergency service water system Q_{ESW} can be represented by the following equation:

$$Q_{ESW} = \text{ACP-DGN-FR-EDGB} * \text{ACP-DGN-FR-EDGC} * \text{DGHWNR16HR} * \text{ESW-XHE-FO-EHS} + \text{ESW-CCF-LF-AOVS}.$$

These random failure basic events were developed as part of the internal events analysis of Peach Bottom and are identical except for the postulated mission time of the emergency diesel generators. A sixteen-hour mission time was assumed for the diesel generators because offsite power trunks J57 and J58 were irrecoverably lost due to fire damage. Peach Bottom station blackout procedures specify that, given failure of the emergency diesel generators, portable generators are to be transported to the site. It is felt that a portable generator would be in place within 24 hours, and cabling would be run to provide some core cooling to prevent core damage. Failure of the diesel generators at sixteen hours and subsequent boiloff from the core would lead to core damage in approximately 24 hours, if portable power and core cooling were not in place.

The core damage equation is as follows:

$$\phi_{CM} = \lambda_{SGR}\ f_A\ f_S\ Q(\tau_G)\ Q_{ESW}\ f_R$$

where

ϕ_{CM} = fire-induced core damage frequency for each of the five switchgear rooms 2A, 2D, 3A, 3B, 3C

λ_{SGR} = frequency of switchgear room fires

f_R = that percentage of fires that exit the top of a switchgear cubicle

f_A = ratio of 4160V switchgear to total cabinet area within the fire area

$Q(\tau_G)$ = that percentage of fires that are manually suppressed before requisite damage occurs

Q_{ESW} = random failure of the emergency service water system

Table 5.14 gives the values of each of these factors as well as their associated distribution and upper and lower bounds.

Table 5.14

Emergency Switchgear Rooms Fire Scenario Factors and Distributions

Factor	Distribution	Lower Bound	Best Estimate	Upper Bound
λ_{SGR}	Gamma	5.8E-6	2.7E-3	5.7E-3
f_A	Maximum entropy	0.1	0.9	1.0
f_S	Maximum entropy	0.9	0.99	1.0
$Q(\tau_G)$	Maximum entropy	0.52	0.77	1.0
f_R	Maximum entropy	0.05	0.5	1.0

'0.5 Emergency Switchgear Rooms 3D and 2B

The identical scenario to that described in Section 5.10.4 occurs, however, some fire-related failures of the ESW also occur. For emergency switchgear room 3D the fire fails power to the ECW pump, while for room

2B power is failed to ESW pump A. These fire-related failures coupled with additional random failures lead to a loss of ESW system, and consequently, station blackout.

Therefore, the only modification to core damage equation of Section 5.10.4 is to the Q_{ESW} term. For emergency switchgear room 3D:

$$Q_{ESW} = \text{ACP-DGN-FR-EDGB} * \text{ACP-DGN-FR-EDGC} * \text{DGHWNR16HR} + \text{ESW-CCF-LF-AOVS},$$

while for emergency switchgear room 2B:

$$Q_{ESW} = \text{ESW-CKV-C515A} + \text{ESW-CCF-LF-AOVS} + \text{ACP-DGN-FR-EDGC} * \text{ACP-DGN-FR-EDGD} * \text{DGHWNR16HR}.$$

5.10.6 Emergency Switchgear Room 2C

Three scenarios survived screening for emergency switchgear room 2C. The first was the station blackout scenario described in Section 5.10.5 with fire-related failure of offsite power and ESW pump B. The other two sequences were $T_1BU_1W_1X_2W_2W_3U_4V_2V_3Y$ and $T_1BU_1W_1X_2W_2W_3U_4V_2Y$. For these last two cases station blackout does not occur and other random failures lead to long-term core damage scenarios. The core damage equation for all three scenarios is identical to that in Section 5.10.4, except Q_{ESW} is replaced with Q_{RANDOM} for the latter two long-term sequences to reflect different random failures necessary for core damage.

5.10.6.1 Scenario 1

The only difference from Section 5.10.5 arises in the Q_{ESW} term because of slightly different fire-induced damage.

$$Q_{ESW} = \text{ESW-CKV-C515B} + \text{ESW-CCF-LF-AOVS} + \text{ACP-DGN-FR-EDGB} * \text{ACP-DEN-FR-EDGD} * \text{DGHWNR16HR}.$$

5.10.6.2 Scenario 2

Scenario 2 is a long-term (approximately 30 hr) core damage sequence. The HPCI system (U_1) and LPCI system (V_3) succeed, but core damage eventually occurs due to failure of all modes of the RHR system (W_1,W_2,W_3). Fire-related failures are to offsite power, 4160VAC bus C, and indirectly to 24VAC bus C. This fire-induced damage fails the suction path logic to the SDC system (W_2), and one of two injection paths for the SPC system (W_1) and CS system (W_3). Additional random failures to the emergency diesel generator fail the other injection path for the SPC and CS systems. Containment venting is failed by loss of the instrument air system cooling, which given a loss-of-offsite power fails the TBCW system. The alternate cooling system (RBCW) is never aligned due to random failure RBC-XHE-FO-SWCH. The CRD system (U_4) is also failed due to a failure to switch cooling.

The terms (λ_{SGR}, f_R, f_s, f_R, $Q(\tau_G)$ and their associated distributions are identical to the scenario described in Section 5.10.5.

The term Q_{RANDOM} for scenario 2 is described by the following equation:

$$Q_{RANDOM} = RBC\text{-}XHE\text{-}FO\text{-}SWCH * [ACP\text{-}DGN\text{-}FR\text{-}EDGD* DEHWNR30HR + ACP\text{-}DGN\text{-}LP\text{-}EDGD * DGHWNR30HR + ACP\text{-}DGN\text{-}TE\text{-}EDGD * DGHWNR30HR + DCP\text{-}DGN\text{-}MA\text{-}EDGD * DGMANR30HR + DGACTD * DGACTNR30HR].$$

The core damage equation is as follows:

$$\phi_{CM} = \lambda_{SGR}\ i_A\ f_S\ Q(\tau_G)\ f_R\ Q_{RANDOM}$$

where all factors have been previously defined.

Table 5.14 gives the values of each of the terms as well as their associated distributions.

5.10.6.3 Scenario 3

As was the case for scenario 2 long-term (approximately 30 hrs) core damage occurs. The HPCI system (U_1) and LPCS system (V_2) succeed but core damage eventually occurs due to failure of all modes of the RHR system (W_1,W_2,W_3). The CRD system (U_4) and containment venting system (Y) fail for identical reasons as in scenario 2. However, fire-related damage to emergency bus C fails one injection side of SPC, CS, and SD systems and random failures fail the other injection path. The core damage equation is identical to Section 5.10.6.2. The only modification is the equation for the term Q_{RANDOM}.

$$Q_{RANDOM} = RBC\text{-}XHE\text{-}FO\text{-}SWCH * [LPI\text{-}PTF\text{-}RE\text{-}LOOPB + ESF\text{-}LOG\text{-}HW\text{-}RHRB].$$

5.11 Conclusion

The overall fire-induced core damage frequency for Peach Bottom Unit 2 was found to be 1.95E-5 per year. The dominant contributing plant areas are the (a) control room, (b) emergency switchgear room 2C, and (c) emergency switchgear room 2B. These three areas comprise 75% of the total fire risk.

In the case of the control room, a general transient occurs with smoke-induced abandonment of the area. Failure to control the plant from the remote shutdown panel results in core damage.

For the two emergency switchgear rooms, a fire-induced loss of offsite power and failure of one train of the ESW occurs. Random failure of other two ESW trains results in station blackout and core damage.

5.12 References

1. Seabrook Station Probabilistic Safety Assessment, Section 9.4, Public Service Company of New Hampshire and Yankee Atomic Electric Company, December 1983.

2. Severe Accident Risk Assessment Limerick Generating Station, Chapter 4, Main Report, Philadelphia Electric Company, Report #4161, April 1983.

3. J. A. Lambright, S. P. Nowlen, V. F. Nicolette, and M. P. Bohn, Fire Risk Scoping Study: Current Perception of Unaddressed Fire Risk Issues, Sandia National Laboratories, Albuquerque, NM, SAND88-0177, NUREG/CR-5088, December 1988.

4. W. T. Wheelis, Users Guide for a Personal-Computer-Based Nuclear Power Plant Fire Data Base, Sandia National Laboratories, Albuquerque, NM, SAND86-0300, NUREG/CR-4586, August 1986.

5. R. L. Iman, S. C. Nora, Modeling Time to Recovery and Initiating Event Frequency for Loss of Off-Site Power Incidents at Nuclear Power Plants, Sandia National Laboratories, Albuquerque, NM, SAND87-2428, NUREG/CR-5032, January 1988.

6. R. B. Worrell, SETS Reference Manual, Sandia National Laboratories, Albuquerque, NM, SAND83-2675, NUREG/CR-4213, May 1985.

7. D. W. Stack, A SETS User's Manual for Accident Sequence Analysis, Sandia National Laboratories, Albuquerque, NM, SAND83-2238, NUREG/CR-3547, January 1984.

8. N. O. Siu, COMPBRN - A Computer Code for Modeling Compartment Fires, University of California, UCLA-ENG-8257, NUREG/CR-3239, May 1983.

9. V. Ho, N. O. Siu, G. Apostolakis, COMPBRN III - A Computer Code for Modeling Compartment Fires, University of California, UCLA-ENG-8524, November 1985.

10. C. Ruger, J. L. Boccio, and M. A. Azarm, Evaluation of Current Methodology Employed in Probabilistic Risk Assessment (PRA) of Fire Events at Nuclear Power Plants, Brookhaven National Laboratory, NUREG/CR-4229, May 1985.

11. V. F. Nicolette, S. P. Nowlen, J. A. Lambright, Observations Concerning the COMPBRN III Fire Growth Code, Sandia National Laboratories, Albuquerque, NM, SAND88-2160C, April 1989.

12. W. T. Wheelis, Transient Combustible Fuel Sources Found at Nuclear Power Plants (Data), Letter Report, Sandia National Laboratories, Albuquerque, NM, July 1984.

13. V. F. Nicolette, and S. P. Nowlen, A Critical Look at Nuclear Qualified Electrical Cable Insulation Ignition and Damage Thresholds, SAND88-2161, paper accepted for presentation at Operability of Nuclear Systems in Normal and Adverse Environments, Lyon, France, September 18-22, 1989.

14. A. D. Swain, H. E. Guttman, Handbook of Human Reliability Analysis with Emphasis on Nuclear Power Plant Applications, Sandia National Laboratories, Albuquerque, NM, SAND80-0200, NUREG/CR-1278, August 1983.

15. M. P. Bohn, and J. A. Lambright, Procedures for External Event Core Damage Frequency Analyses for NUREG-1150, Sandia National Laboratories, Albuquerque, NM, NUREG/CR-4840, November 1990.

16. R. L. Iman, M. J. Shortencarrier, A FORTRAN 77 Program and User's Guide for the Generation of Latin Hypercube and Radom Samples for Use with Computer Models, Sandia National Laboratories, Albuquerque, NM, SAND83-2365, NUREG/CR-3024, March 1984.

17. R. L. Iman, M. J. Shortencarrier, A User's Guide for the Top Event Matrix Analyses Code (TEMAC), Sandia National Laboratories, Albuquerque, NM, SAND86-0960, NUREG/CR-4598, August 1986.

18. An Experimental Investigation of Internally Ignited Fires in Nuclear Power Plant Cabinets, Part II - Room Effects Tests, SAND86-0336, NUREG/CR 4527/V2, Albuquerque; Sandia National Laboratories, October 1988.

19. An Experimental Investigation of Internally Ignited Fires in Nuclear Power Plant Control Cabinets, Part I - Cabinet Effects Tests, SAND86-0336, NUREG/CR-4527/V1, Albuquerque: Sandia National Laboratories, April 1987.

APPENDIX A

STRUCTURAL FLOOR SPECTRA FOR PEACH BOTTOM

PEACHBOTTOM STRUCTURAL MODELS

Structure	Freq (Hz)	Dir	% Mass
Reactor Building	7.1	N-S	68.6
	7.6	E-W	71
	18.5	VERT	72
Radwaste/Turbine Building	9.3	N-S	81
	11.4	E-W	57
	24.5	VERT	70
Circulating Water Pump Structure	13.4	N-S	86
	20.6	E-W	70
	46.0	VERT	57
Emergency Cooling Tower	9.77	N-S	36.5
	10.41	E-W	79
	19.32	N-S	61.7
	27.0	VERT	79
Diesel Generator Building	17.5	N-S	99
	21.83	E-W	97
	47.7	VERT	92

MASS OF STRUCTURES

Building	MASS (Kip-s^2/ft)		
	X	Y	VERT.
RCB	2859.	2859.	2859.
RWTB	1610.	1610.	1610.
CWPS	1485.	1485.	979.8
ECT	1309.	1309.	1309.
DGB	313.4	313.4	313.4

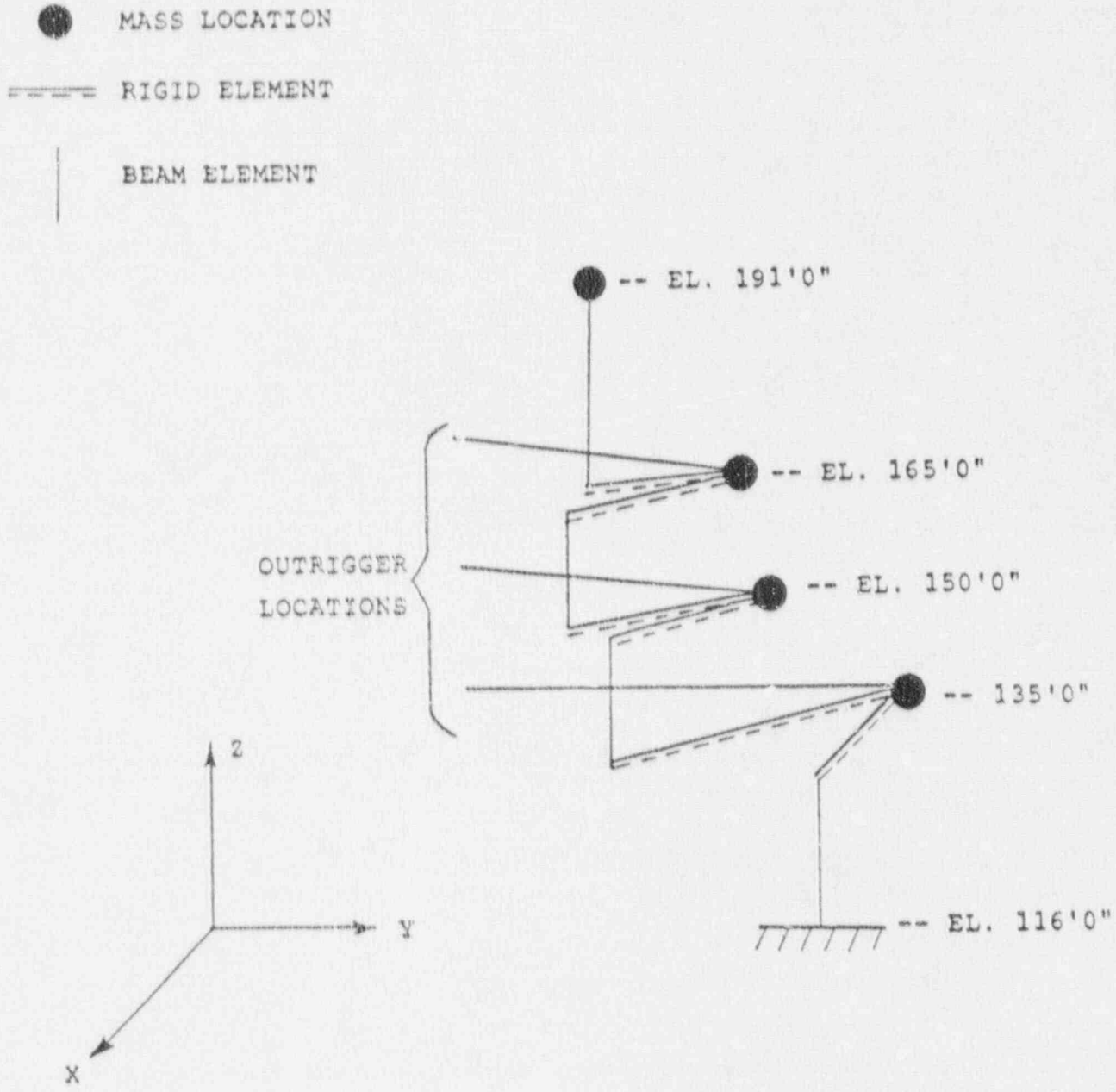

Fig. 1 Peach Bottom Power Station Rad-Waste and Turbine Building

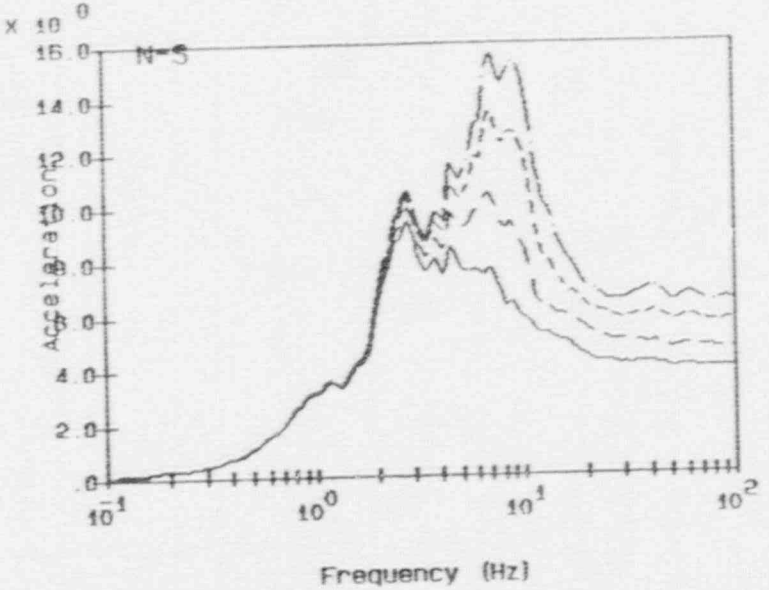

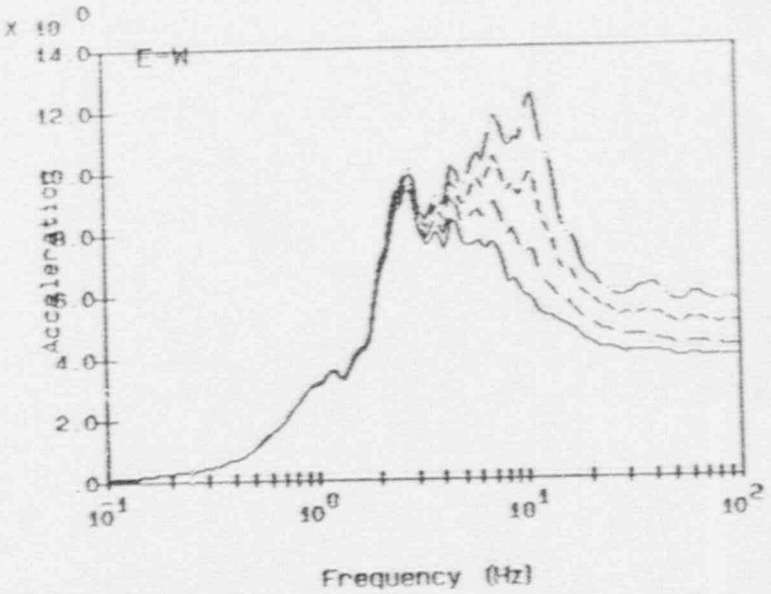

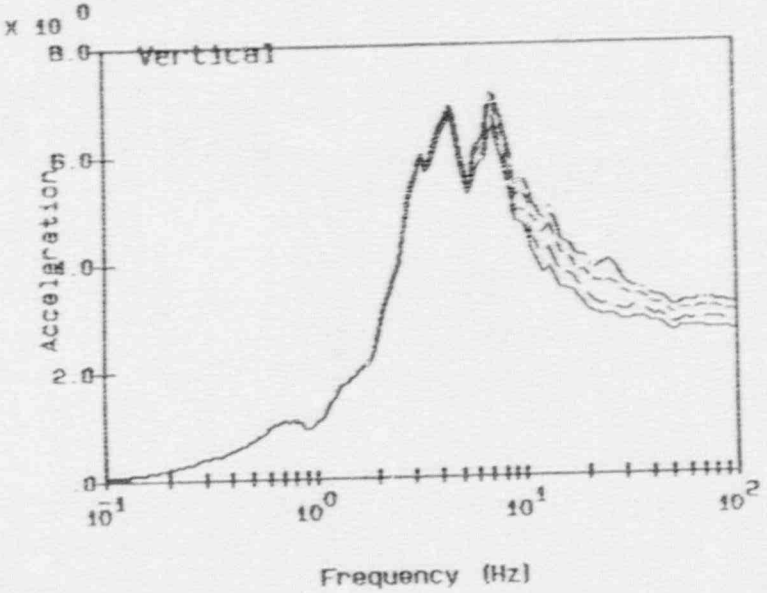

Legend:

free-field
el 135°-0°
el 150°-0°
el 165°-0°

Notes:

accelerations in units of ft/s/s
spectra calculated at 5% damping

BSPLT V3.00 Plot 10:14:08 04-20-88

A-4

Fig. 2a Peach Bottom Atomic Power Station Radwaste/Turbine Building
Instructure Responses for Acc. Range 1

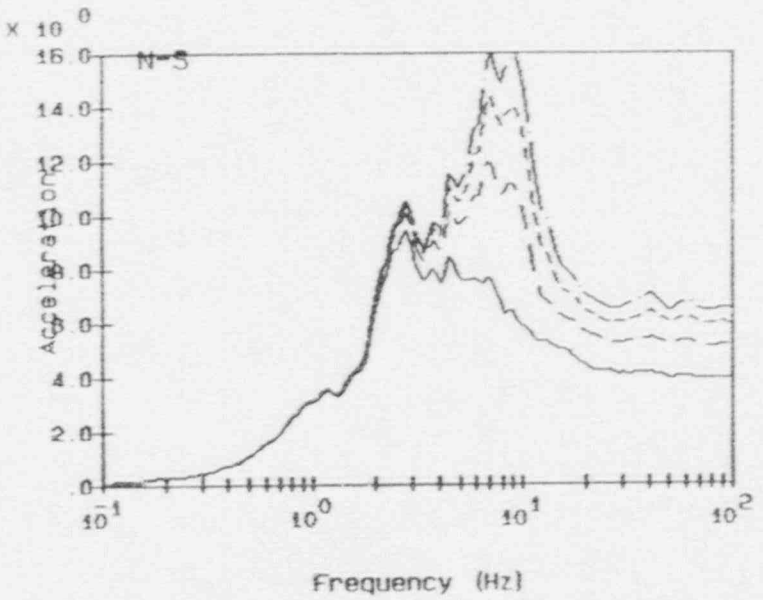

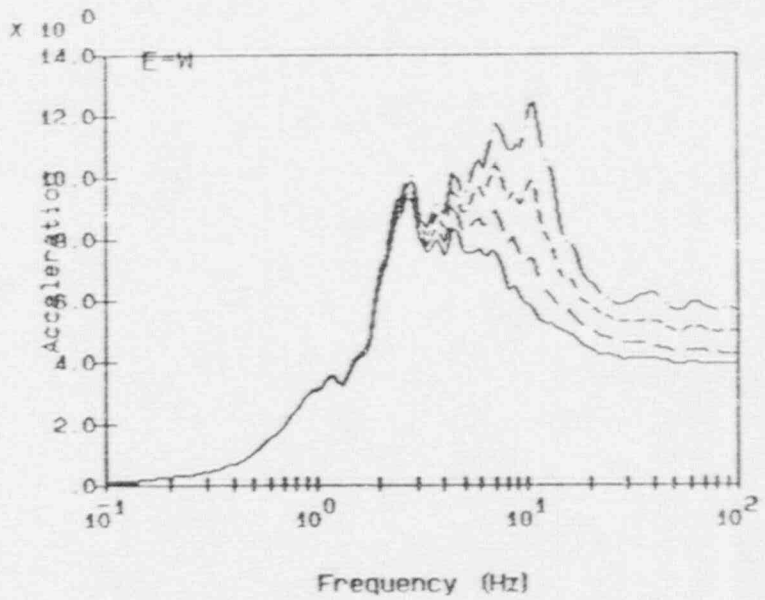

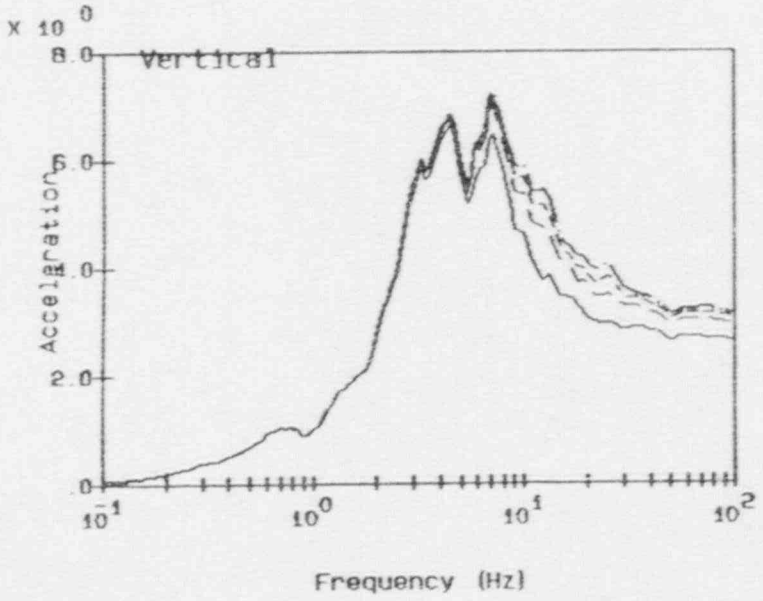

RESPLT V3.00 rwtb2.plt 10:14:51 04-20-88

Legend:

free-field

el 135°-0°

el 150°-0°

el 165°-0°

Notes:

accelerations in units of ft/s/s

spectra calculated at 5% damping

A-5

Fig. 2b Peach Bottom Atomic Power Station Radwaste/Turbine Building(outrigger) Instructure Responses for Acc. Range 1

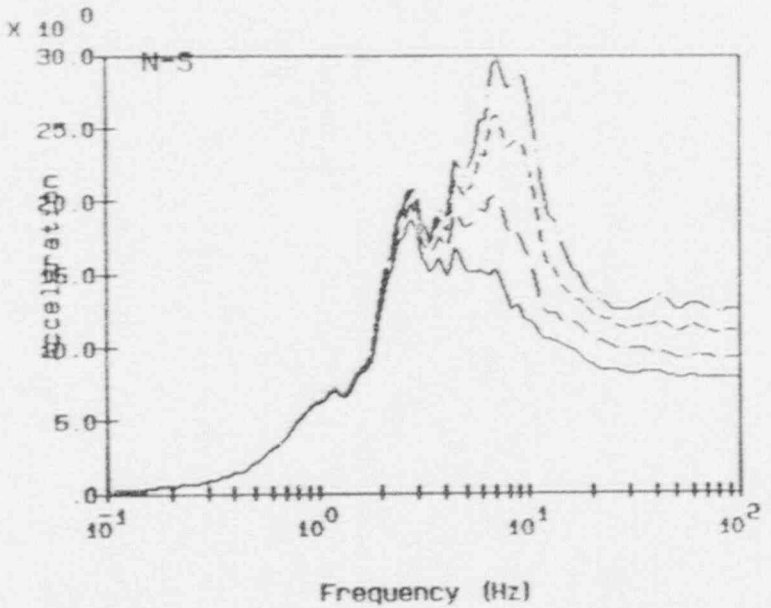

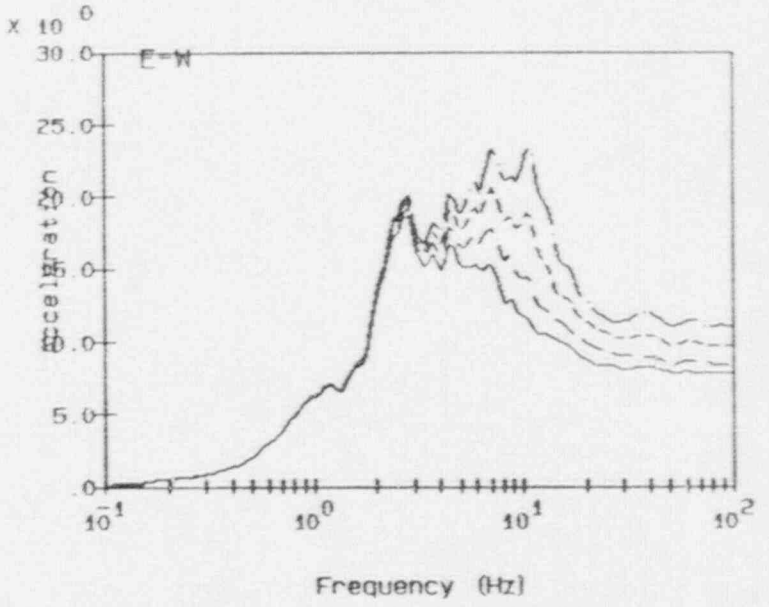

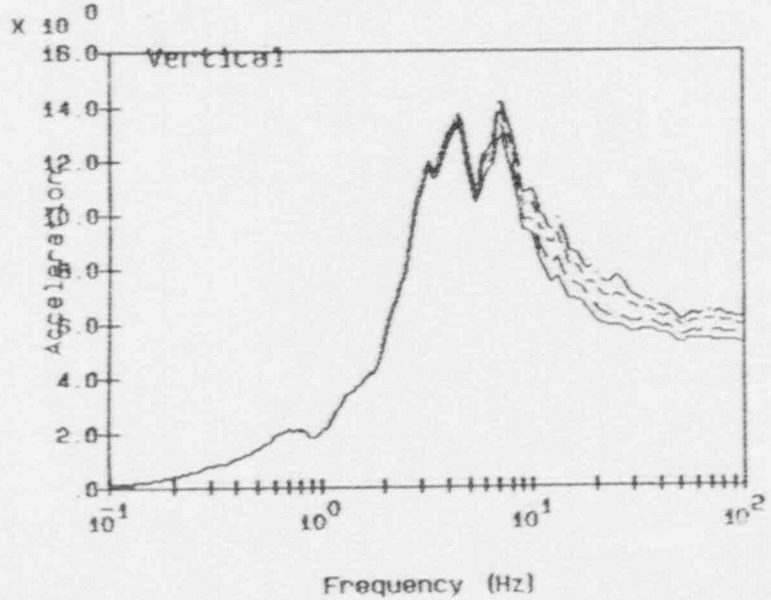

Legend:

free-field
el 135°-0°
el 150°-0°
el 165°-0°

Notes:

accelerations in units of ft/s/s
spectra calculated at 5% damping

RSPLT V3.00 rwtb3.plt 10:28:13 04-20-88

A-6

Fig. 3a Peach Bottom Atomic Power Station Radwaste/Turbine Building Instructure Responses for Acc. Range 2

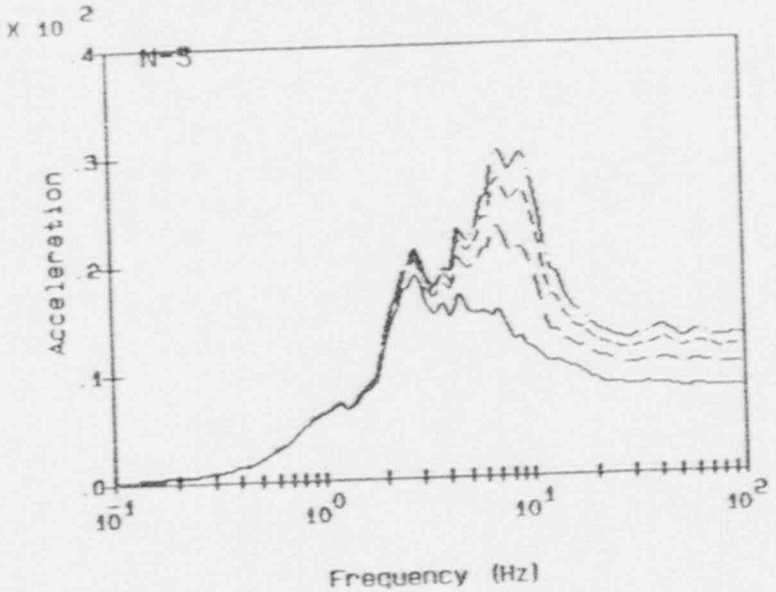

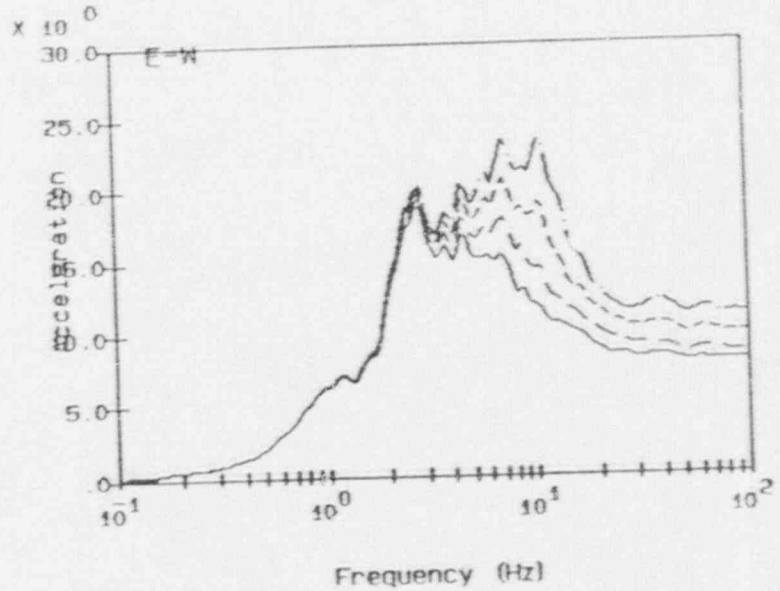

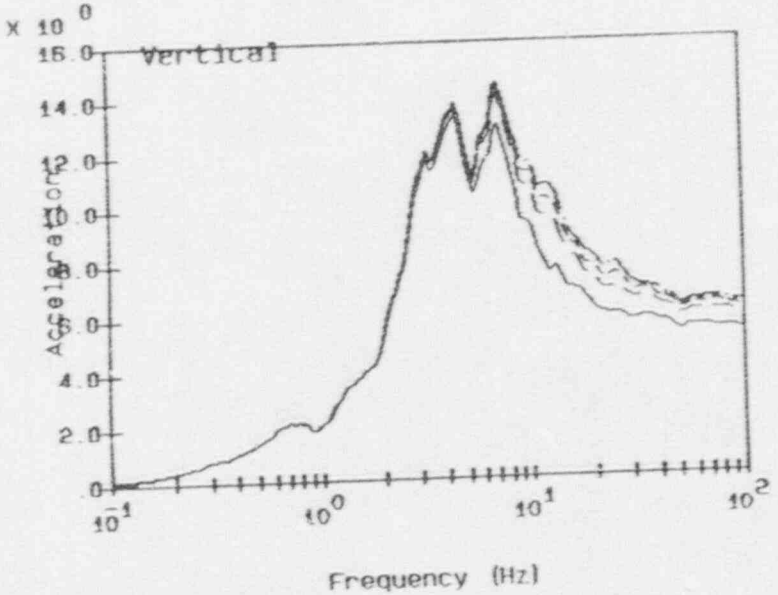

RESPLT V3.00 rwtb4.plt 10:28:48 04-20-88

Legend:

free-field

el 135°-0°

el 150°-0°

el 165°-0°

Notes:

accelerations in units of ft/s/s

spectra calculated at 5% damping

Fig. 3b Peach Bottom Atomic Power Station Radwaste/Turbine Building (outrigger) Instructure Responses for Acc. Range 2

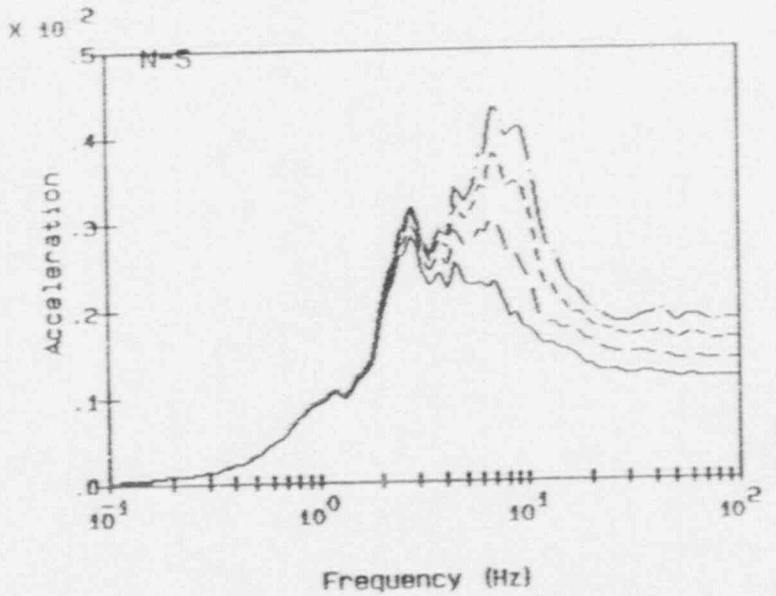

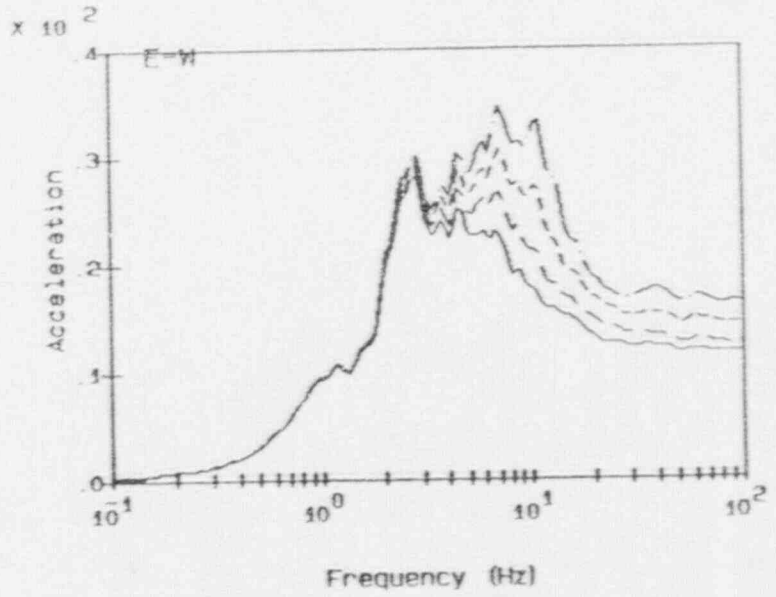

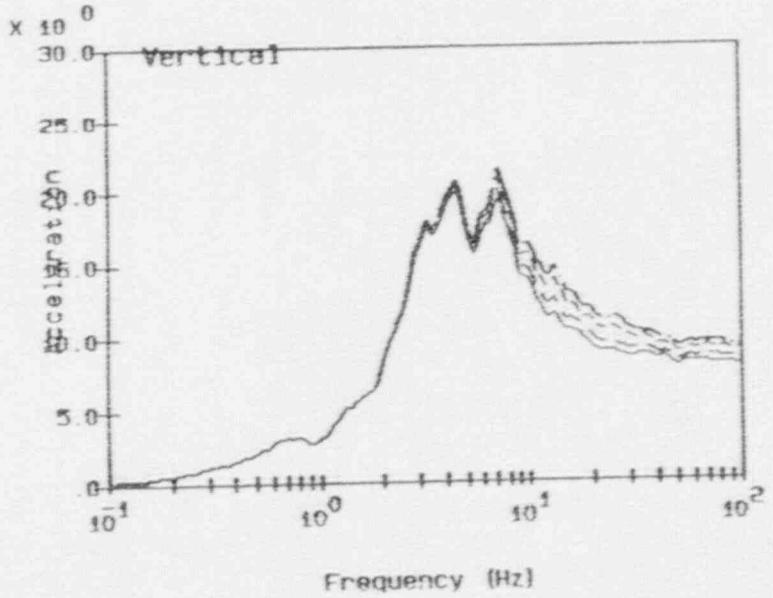

RSPLT V3.00 rwtb5.plt 10:38:54 04-20-88

Legend:

free-field

el 135°-0°

el 150°-0°

el 165°-0°

Notes:

accelerations in units of ft/s/s

spectra calculated at 5% damping

A-8

Fig. 4a Peach Bottom Atomic Power Station Radwaste/Turbine Building
Instructure Responses for Acc. Range 3

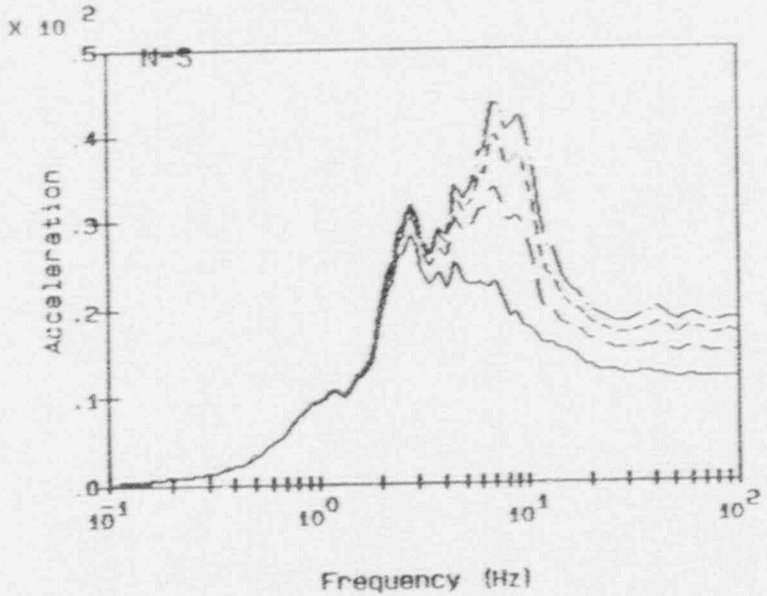

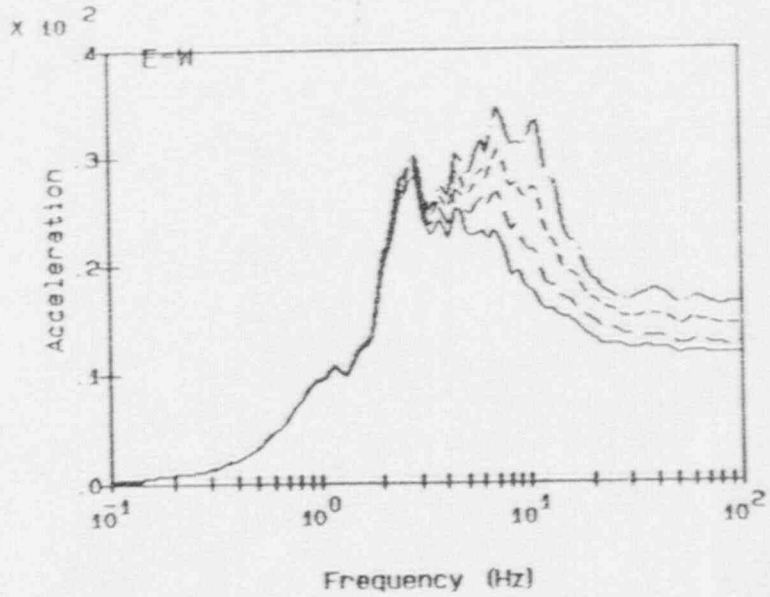

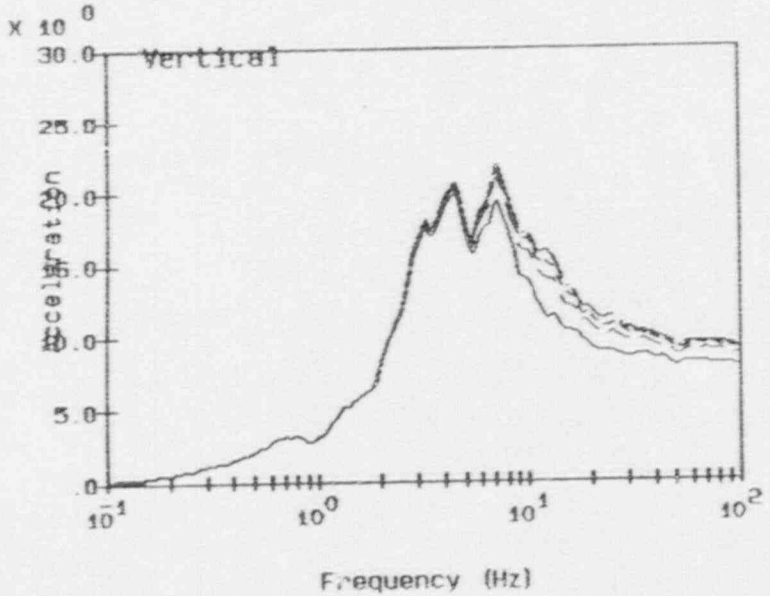

Legend:

free-field
el 135°-0°
el 150°-0°
el 165°-0°

Notes:

accelerations in units of ft/s/s
spectra calculated at 5% damping

RESULT V8.00 rwtb6.plt 10:38:32 04-20-88

A-9

Fig. 4b Peach Bottom Atomic Power Station Radwaste/Turbine Building(outrigger)
Instructure Responses for Acc. Range 3

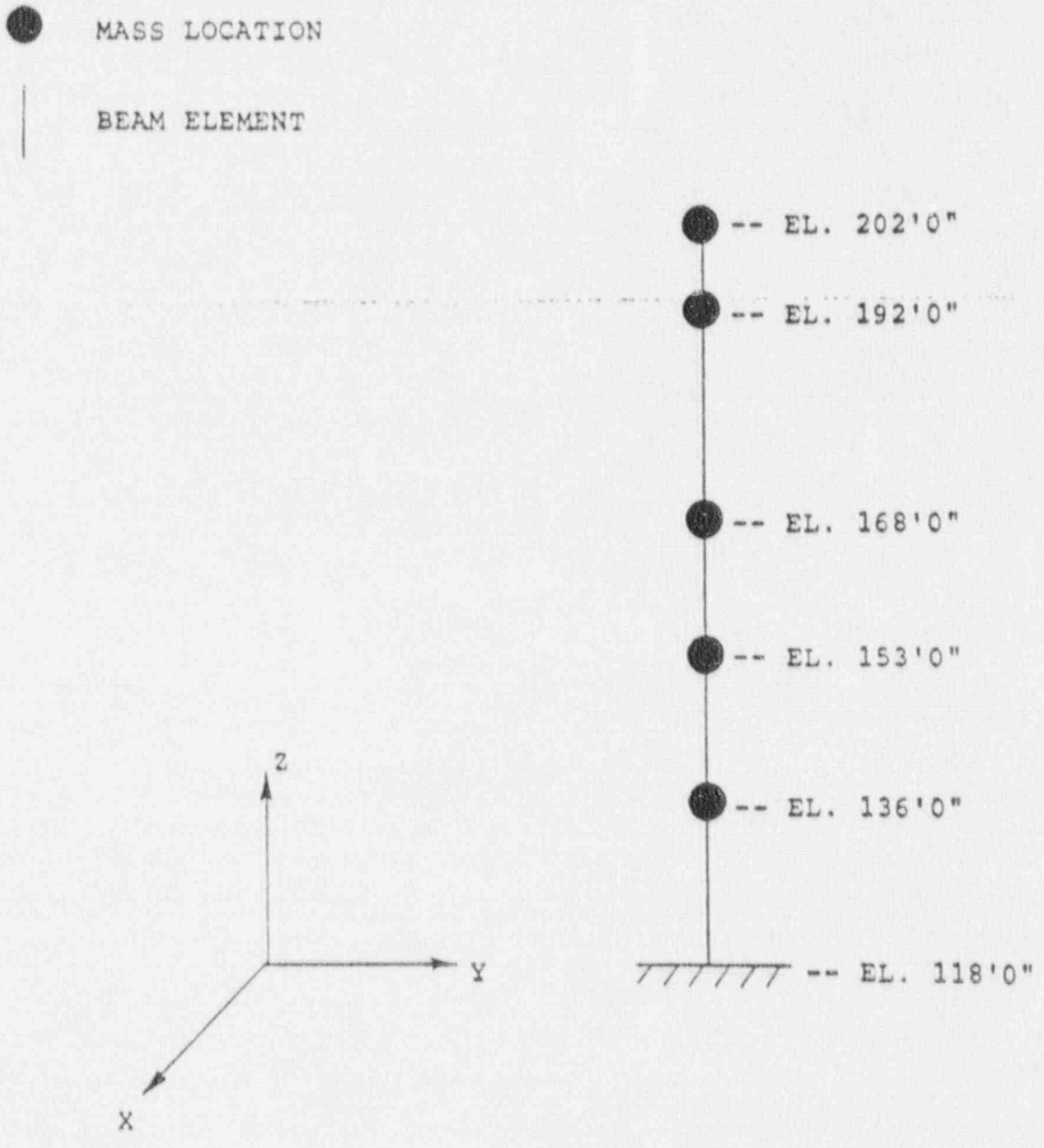

Fig. 5 Peach Bottom Power Station Emergency Cooling Tower

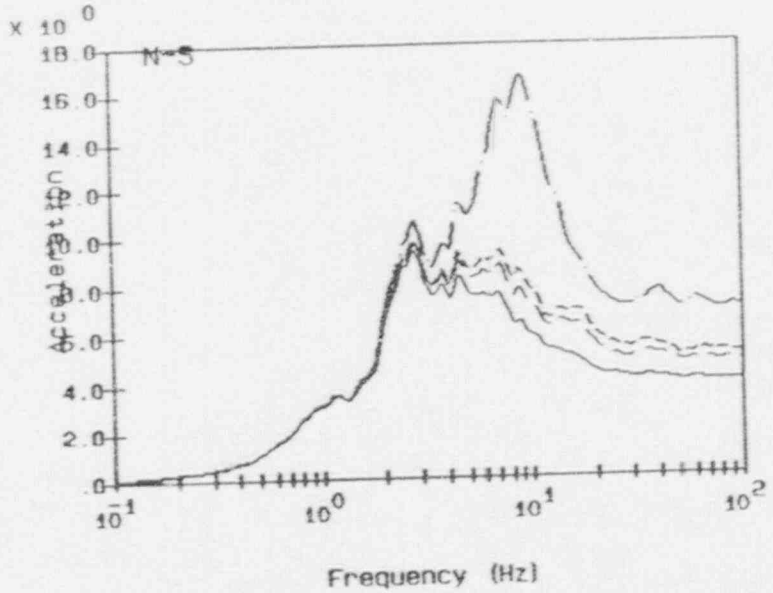

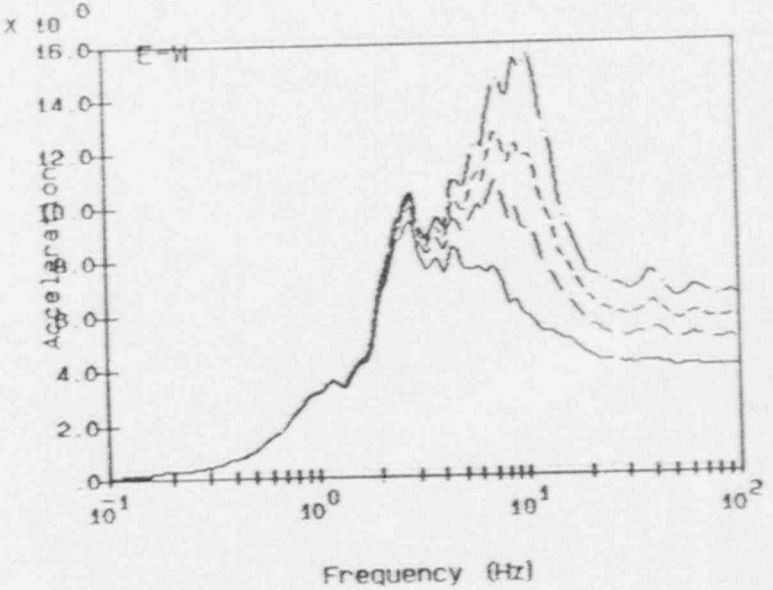

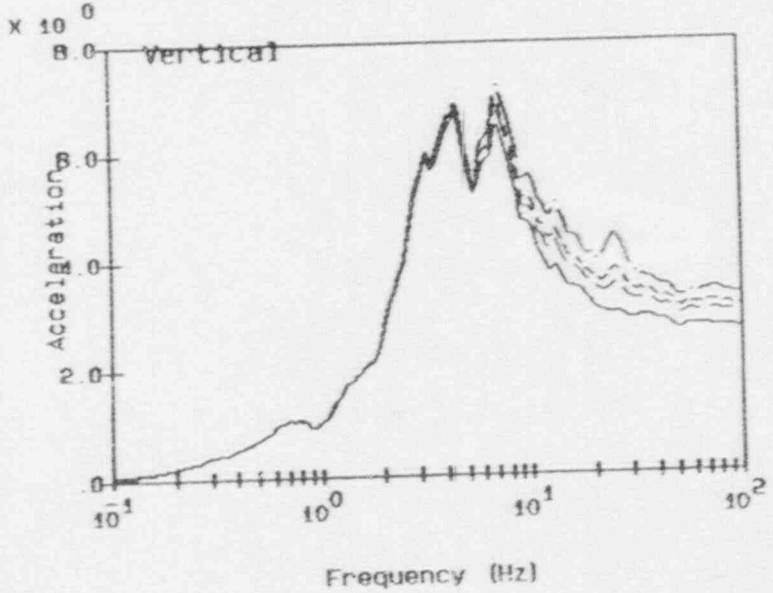

RSPLT V3.00 ect1.plt 07:40:07 04-20-88

Legend:

free-field

el 136'-0"

el 153'-0"

el 168'-0"

Notes:

accelerations in units of ft/s/s

spectra calculated at 5% damping

Fig. 6a Peach Bottom Atomic Power Station Emergency Cooling Towers
Instructure Responses Acc. Range 1

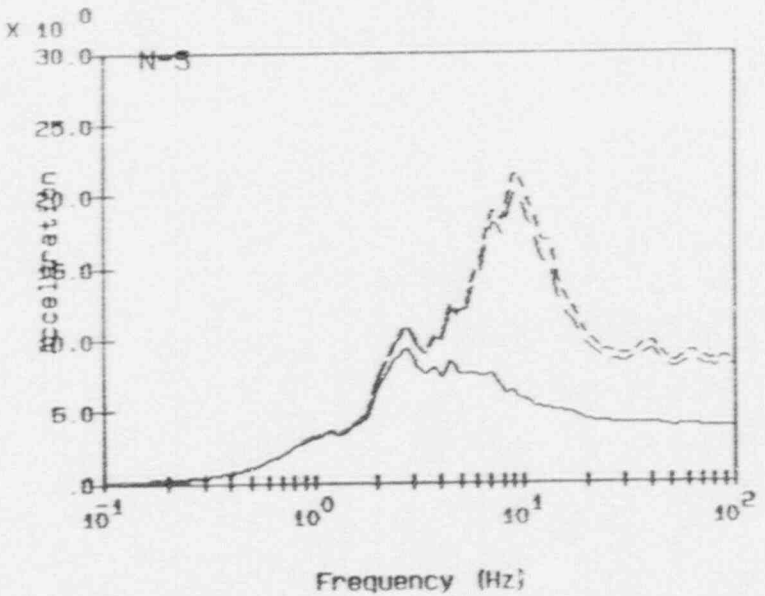

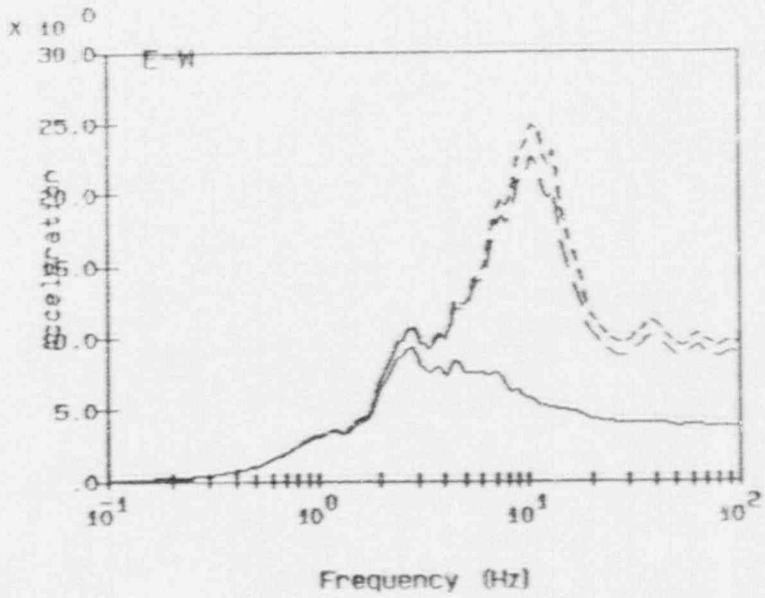

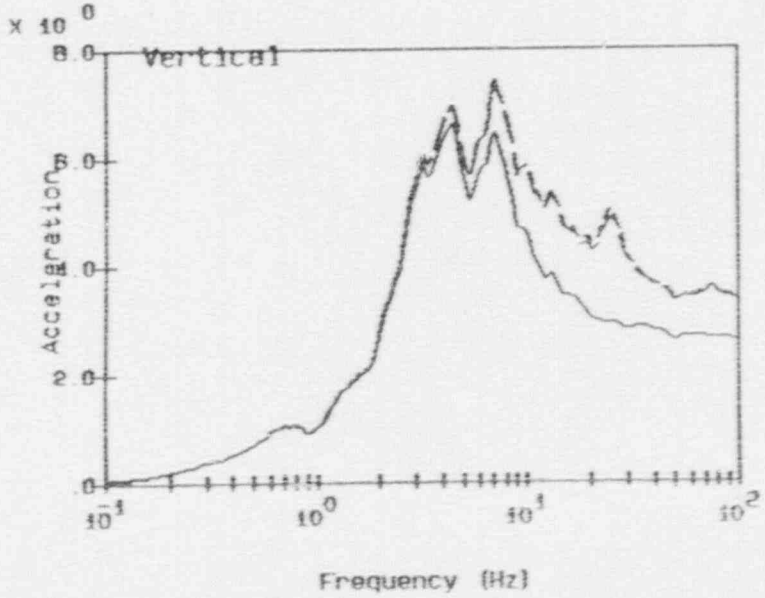

Legend:

free-field
el 192°-0°
el 202°-0°

Notes:

accelerations in units of ft/s/s
spectra calculated at 5% damping

RESPLT V3.00 ect2.plt 07:45:58 04-20-88

A-12

Fig. 6b Peach Bottom Atomic Power Station Emergency Cooling Towers
Instructure Responses Acc. Range 1

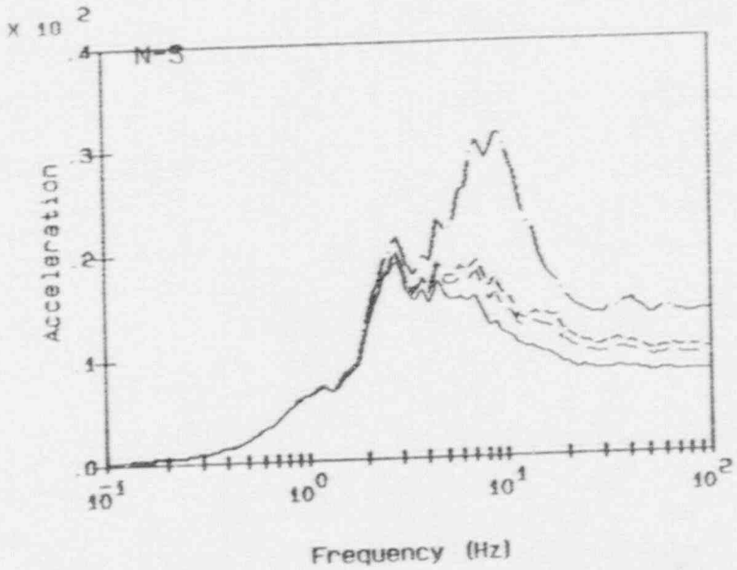

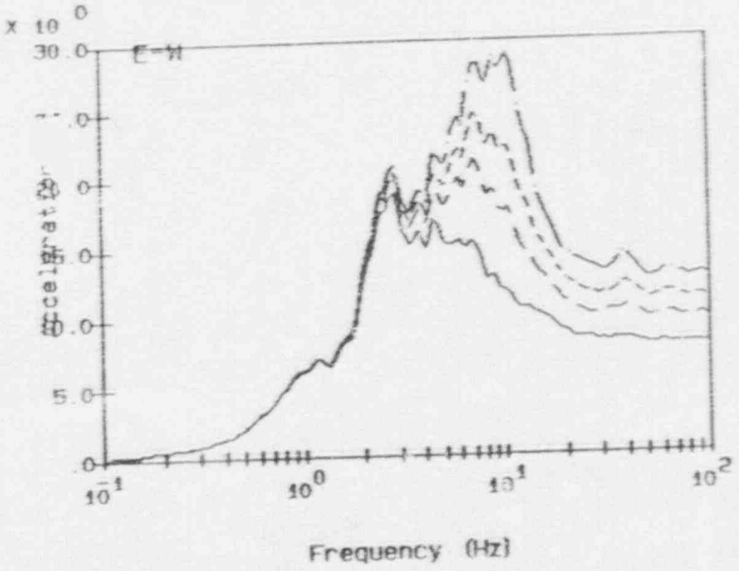

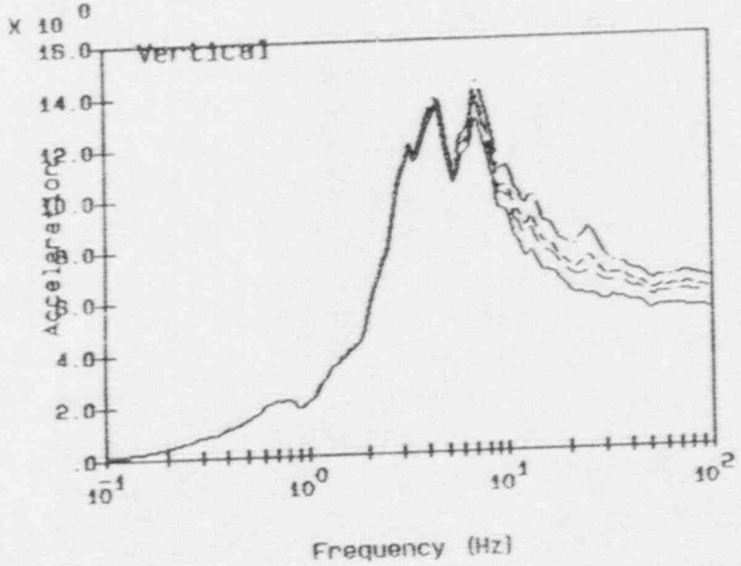

RSPLT V3.00 ect3.plt 07:54:29 04-20-88

Legend:

free-field
el 135°-0°
el 153°-0°
el 168°-0°

Notes:

accelerations in units of ft/s/s
spectra calculated at 5% damping

A-13

Fig. 7a Peach Bottom Atomic Power Station Emergency Cooling Towers
Instructure Responses Acc. Range 2

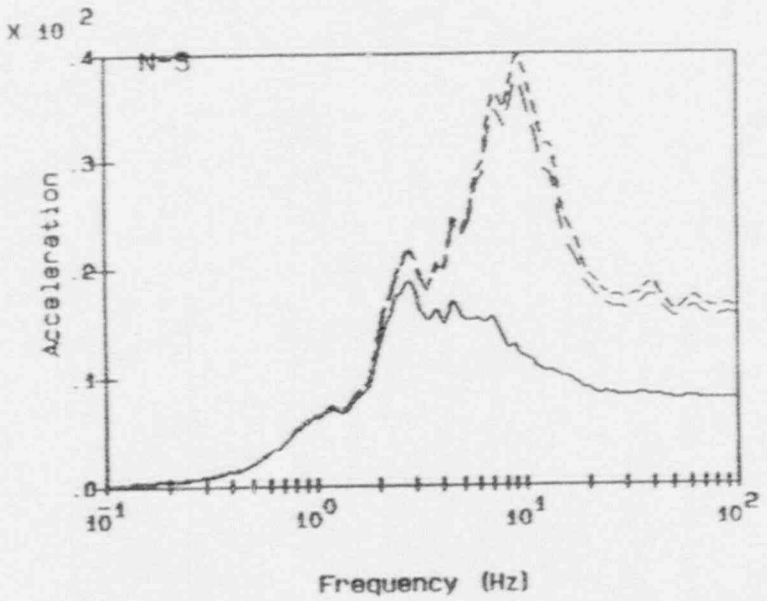

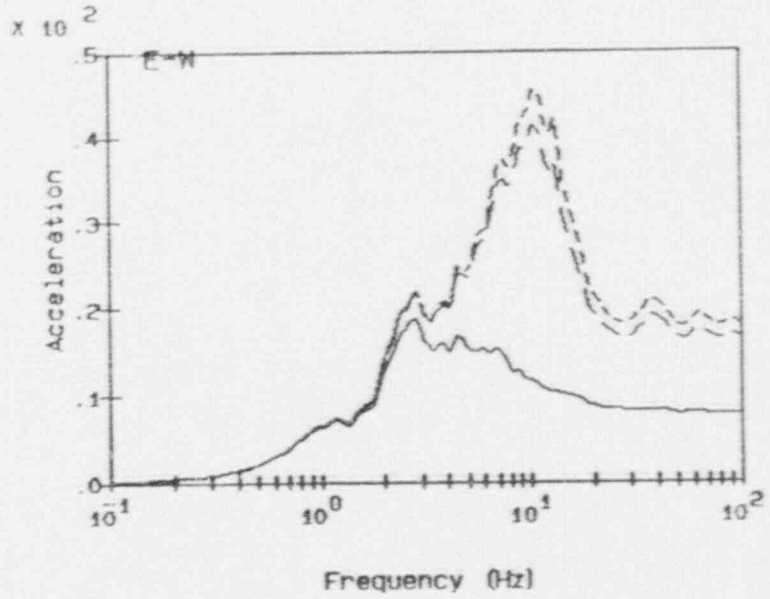

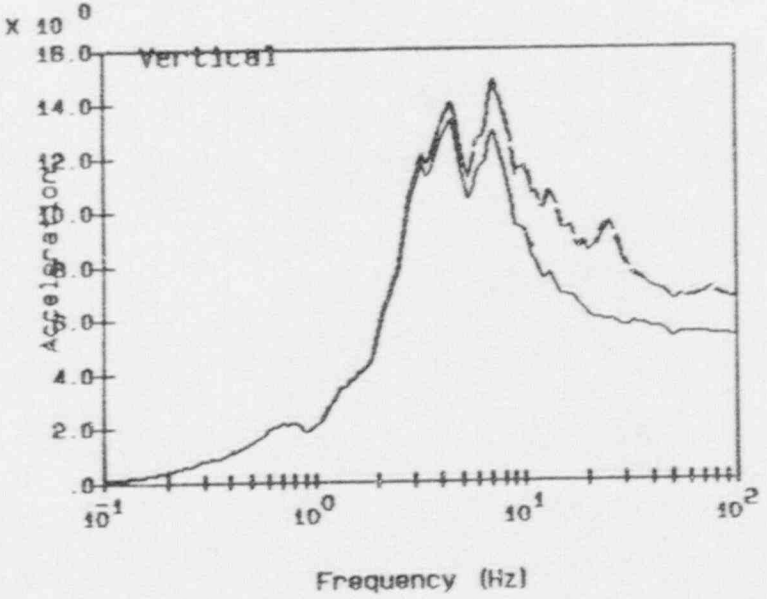

RSPLT V3.00 ect4.plt 07:55:05 04-20-88

Legend:

free-field

el 192°-0°

el 202°-0°

Notes:

accelerations in units of ft/s/s

spectra calculated at 5% damping

Fig. 7b Peach Bottom Atomic Power Station Emergency Cooling Towers
Instructure Responses Acc. Range 2

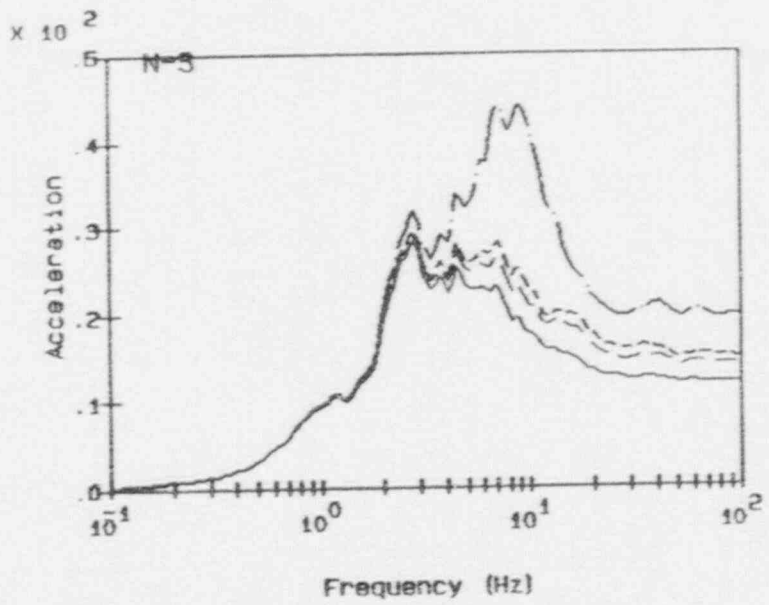

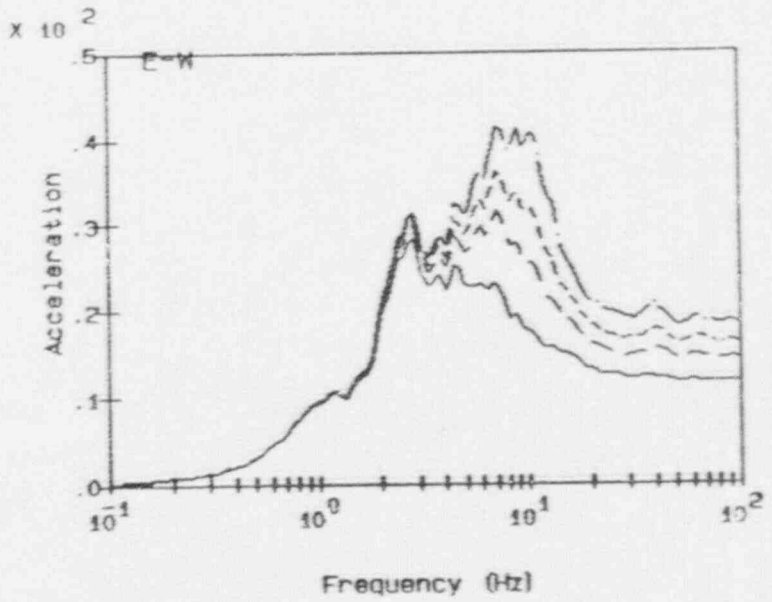

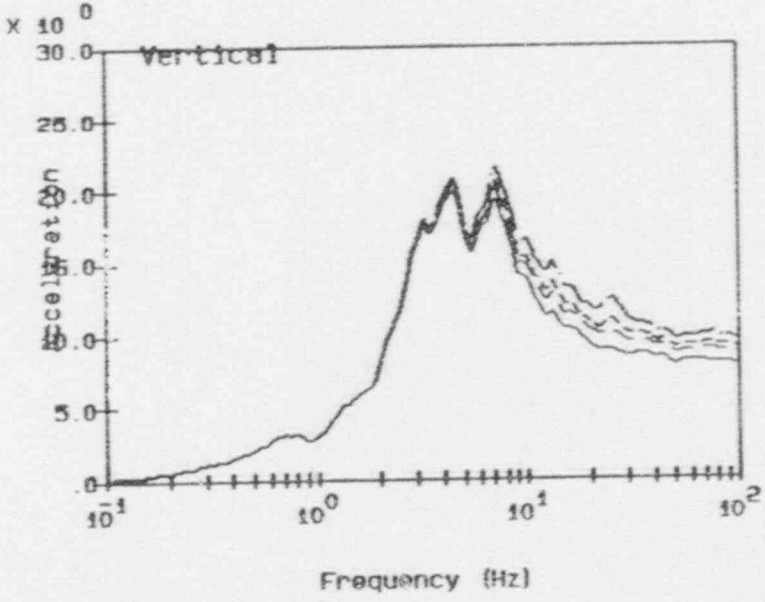

RSPLT V3.00 ect5.plt 07:59:13 04-20-88

Legend:

free-field
el 136°-0°
el 153°-0°
el 168°-0°

Notes:

accelerations in units of ft/s/s
spectra calculated at 5% damping

Fig. 8a Peach Bottom Atomic Power Station Emergency Cooling Towers
Instructure Responses Acc. Range 3

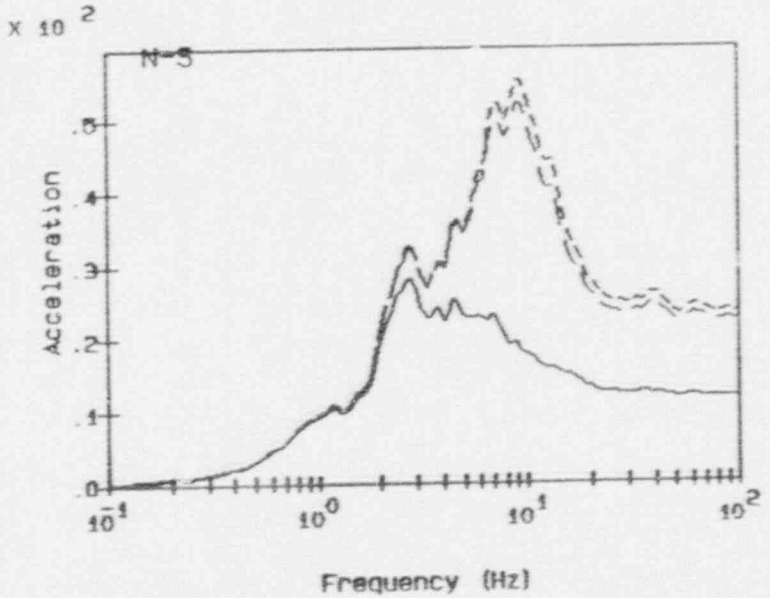

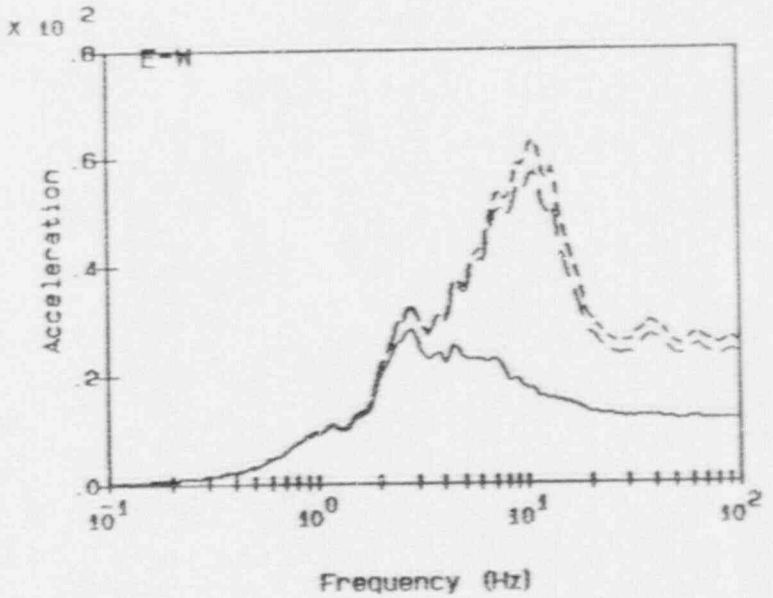

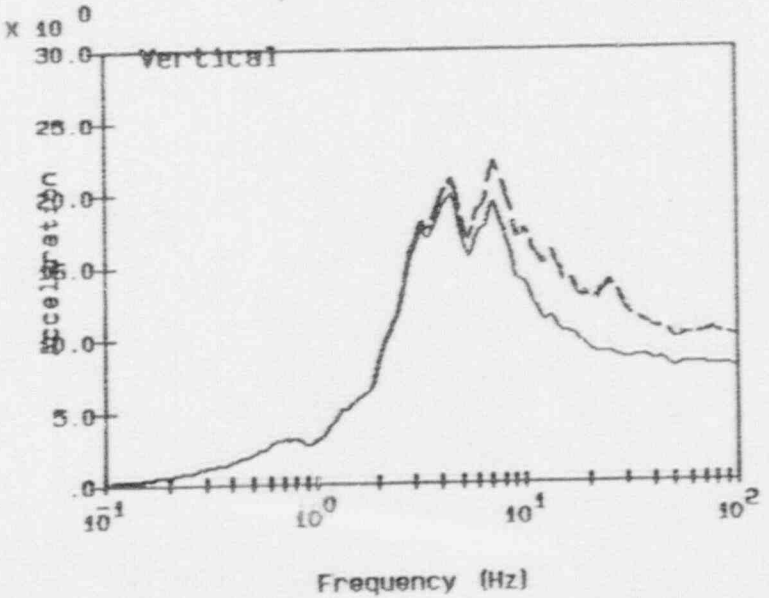

Legend:

free-field

el 192°-0°

el 202°-0°

Notes:

accelerations in units of ft/s/s

spectra calculated at 5% damping

BSPLT V3.00 ec16.plt 07:59:49 04-20-88

A-16

Fig. 8b Peach Bottom Atomic Power Station Emergency Cooling Towers
Instructure Responses Acc. Range 3

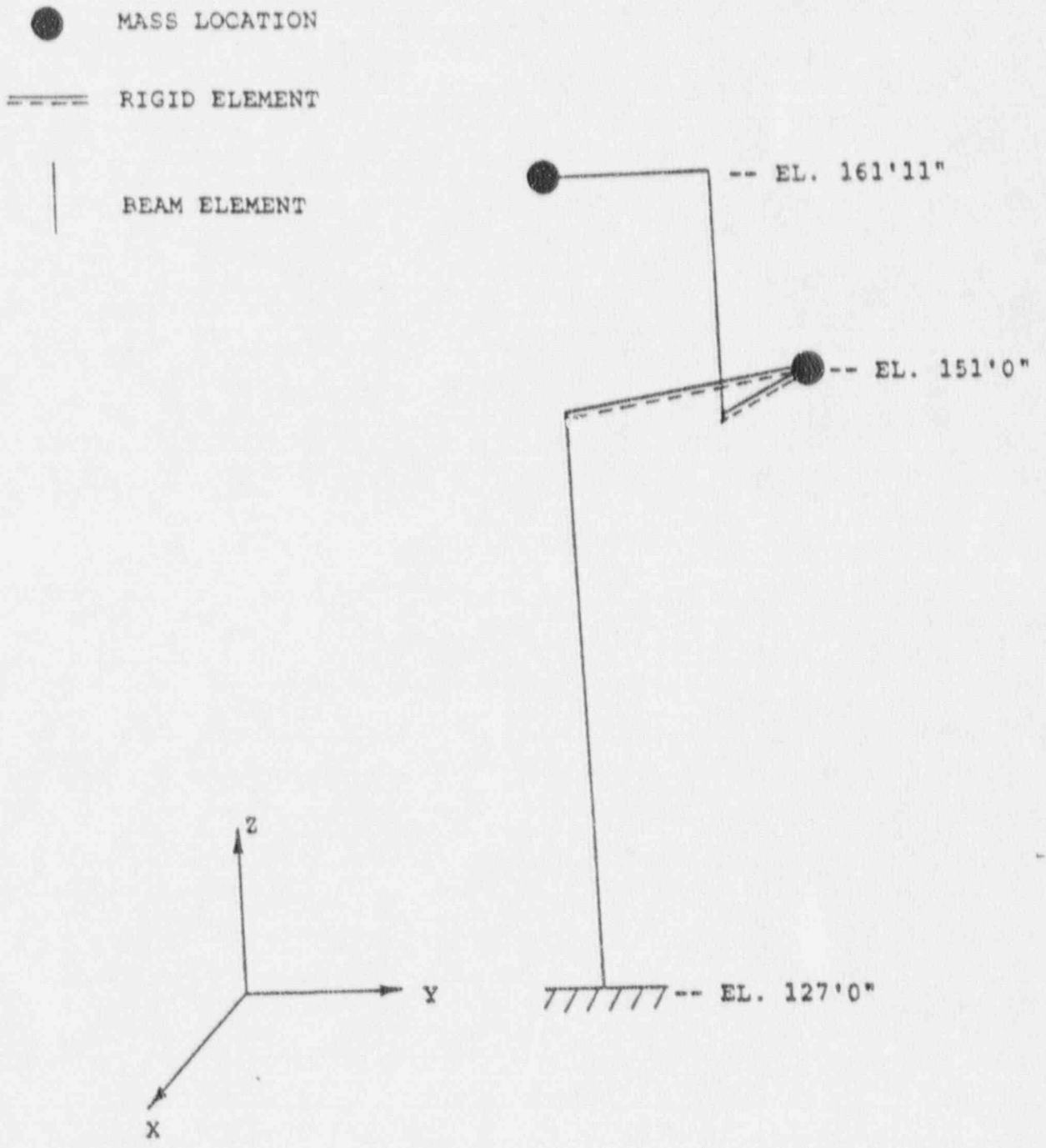

Fig. 9 Peach Bottom Power Station Diesel Generator Building

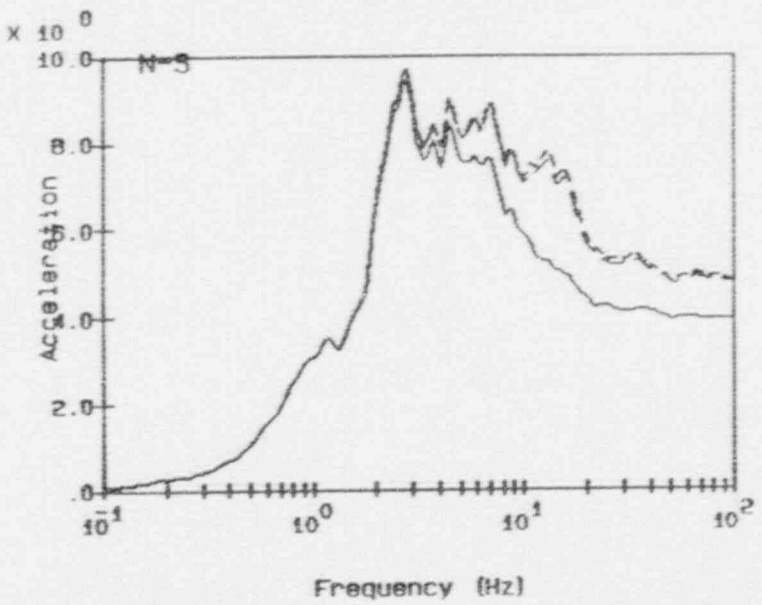

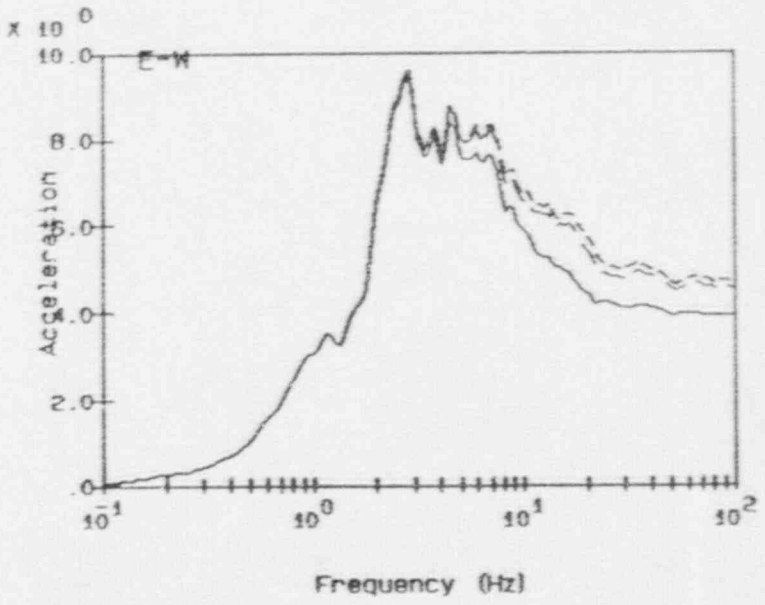

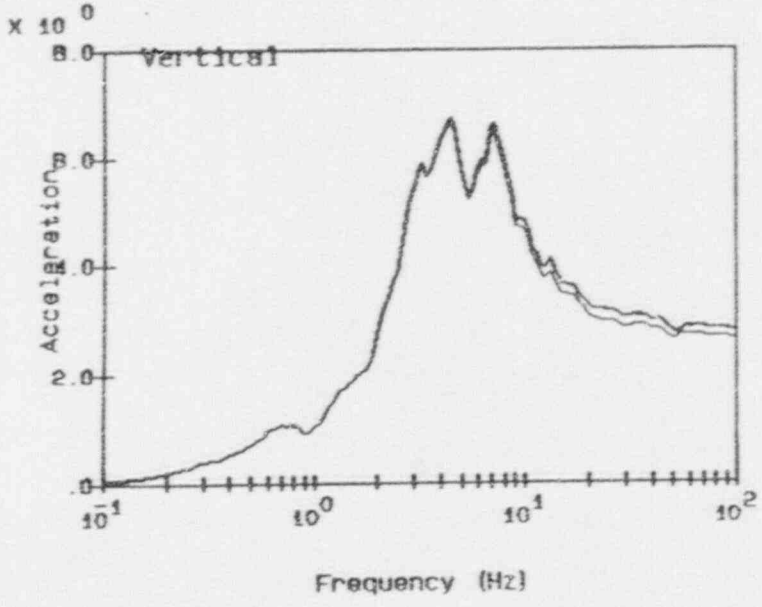

Legend:

free-field

el 151°-0°

el 161°-11°

Notes:

accelerations in units of ft/s/s

spectra calculated at 5% damping

RSPLT V3.00 dgb1.plt 08:34:11 04-20-88

Fig. 10 Peach Bottom Atomic Power Station Diesel Generator Building Instructure Responses for Acc. Range 1

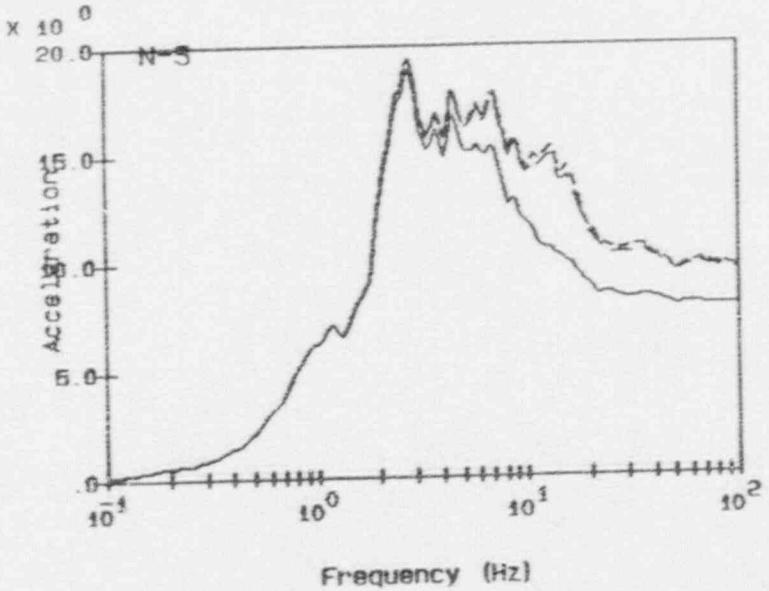

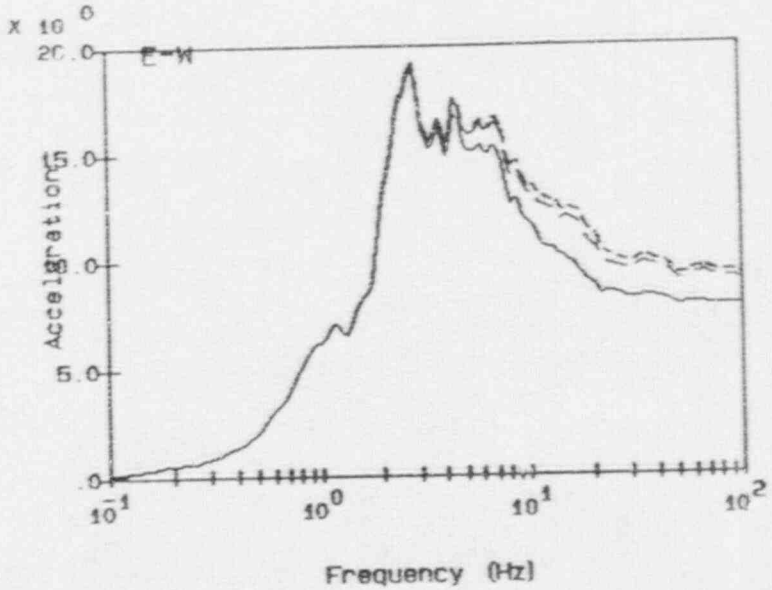

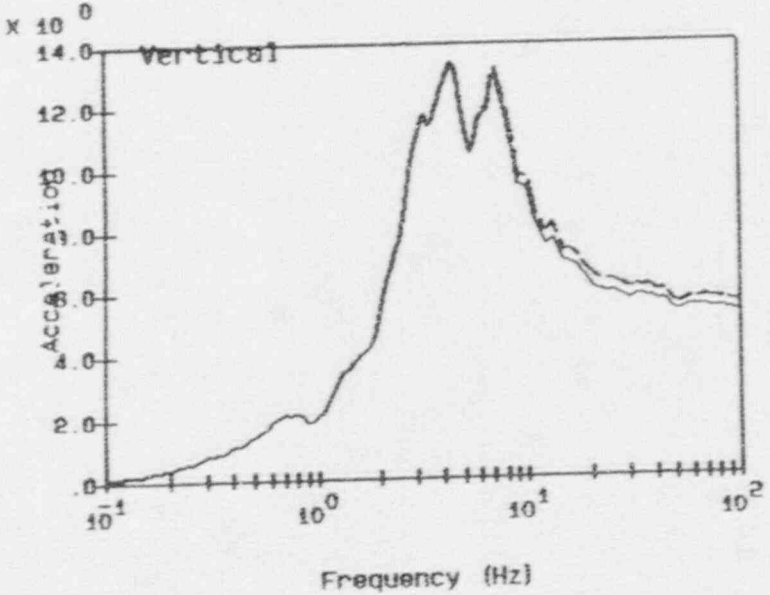

RSPLT V3.00 dgb2.plt 09:36:34 04-20-88

Legend:

free-field

el 151'-0"

el 161'-11"

Notes:

accelerations in units of ft/s/s

spectra calculated at 5% damping

A-19

Fig. 11 Peach Bottom Atomic Power Station Diesel Generator Building Instructure Responses for Acc. Range 2

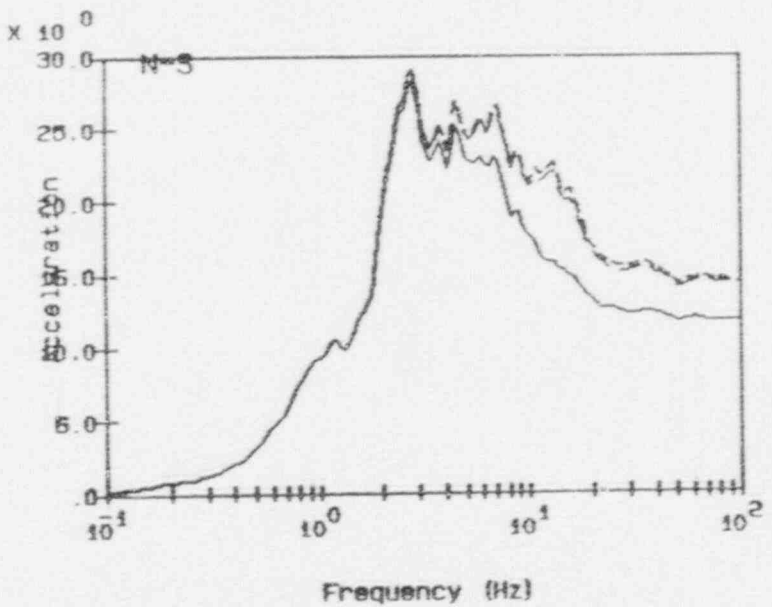

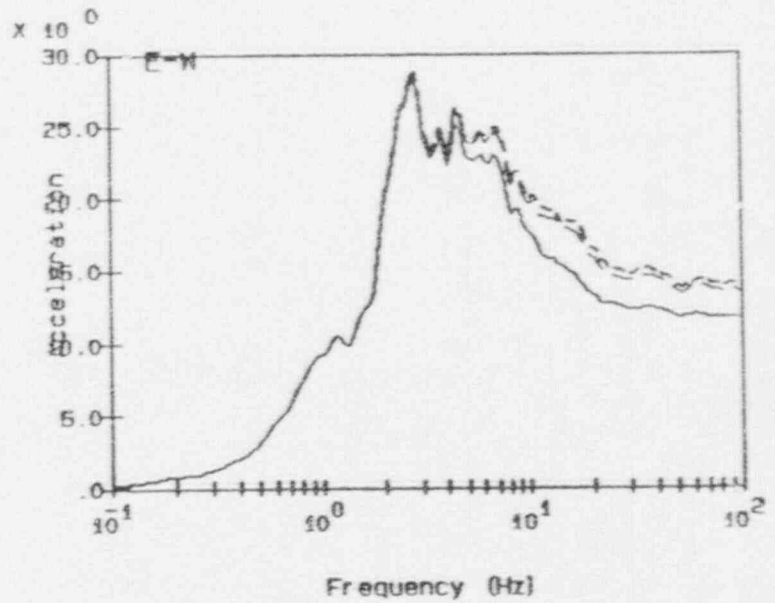

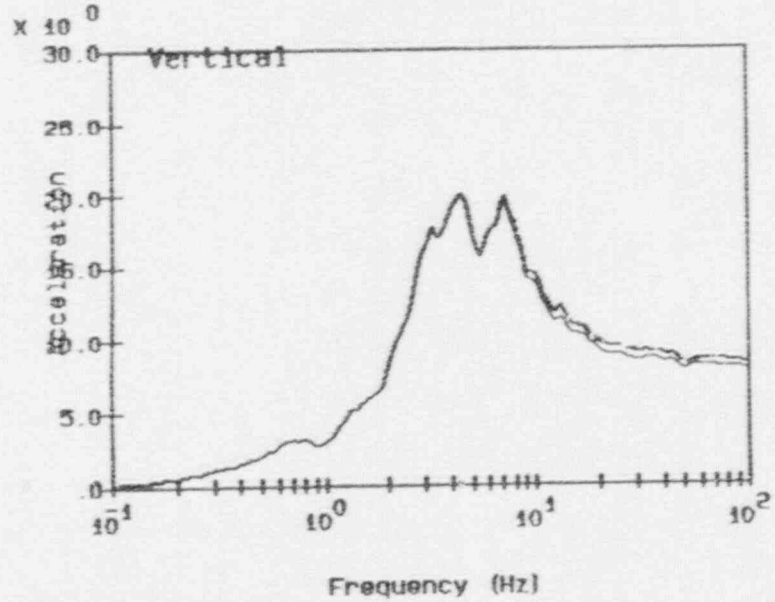

RSPLT V3.00 dgb3.plt 08:38:10 04-20-88

Legend:

free-field

el 151°-0°

el 161°-11°

Notes:

accelerations in units of ft/s/s

spectra calculated at 5% damping

Fig. 12 Peach Bottom Atomic Power Station Diesel Generator Building Instructure Responses for Acc. Range 3

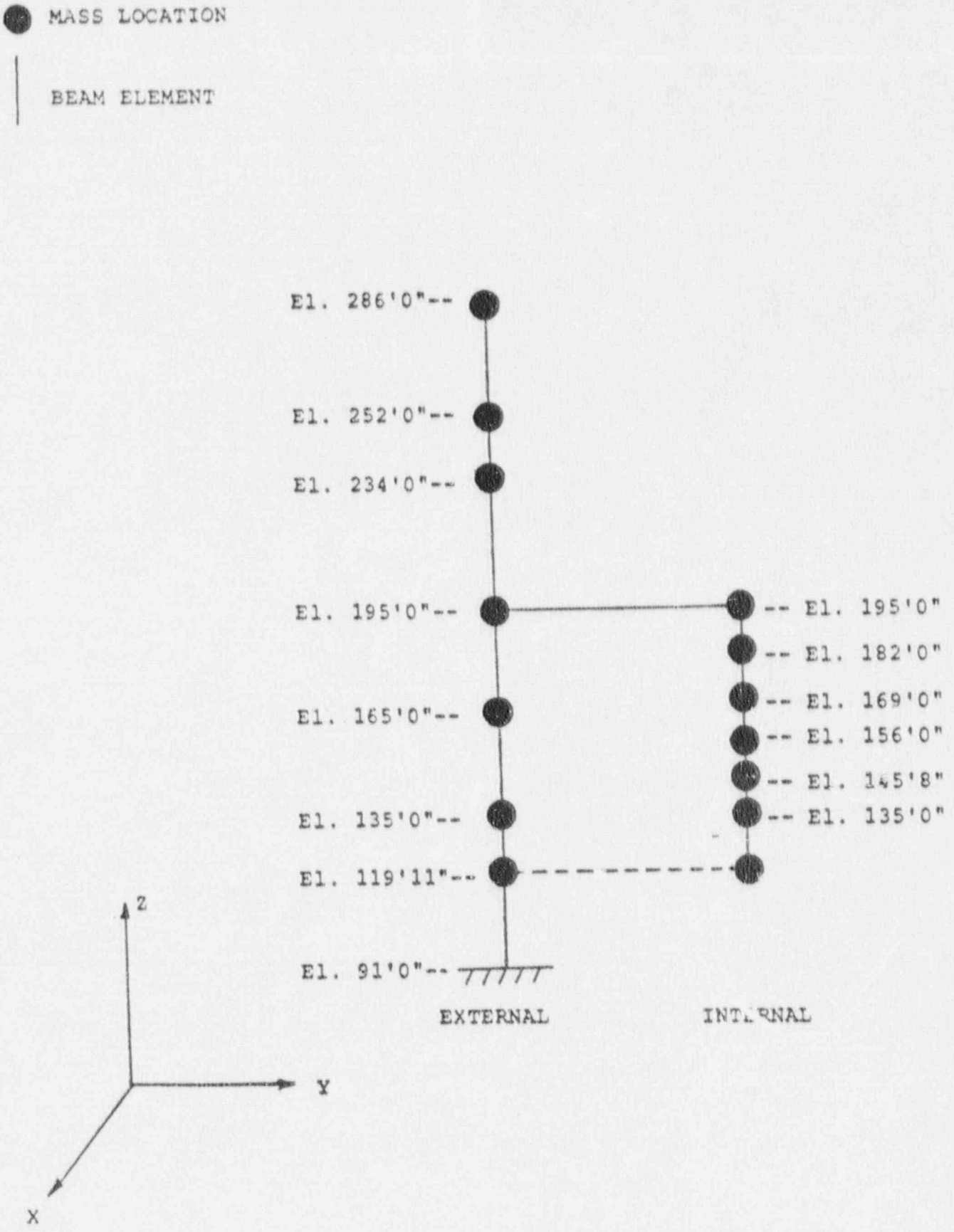

Peach Bottom Power Station Reactor Containment Building

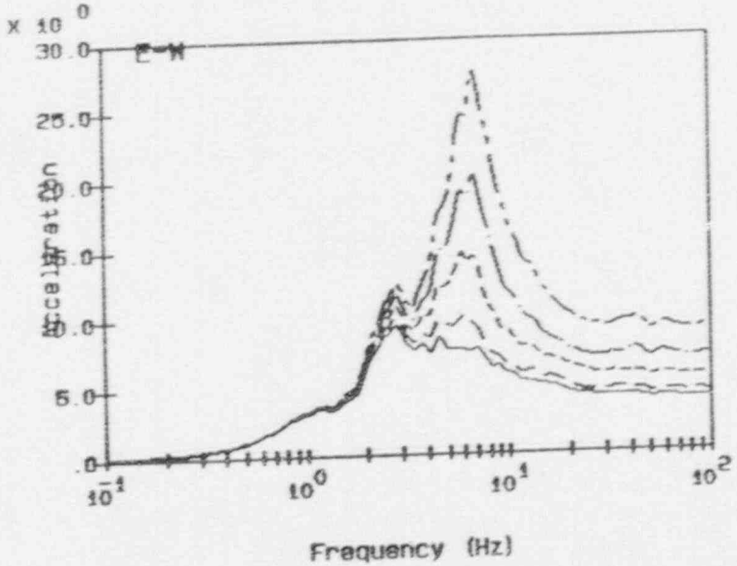

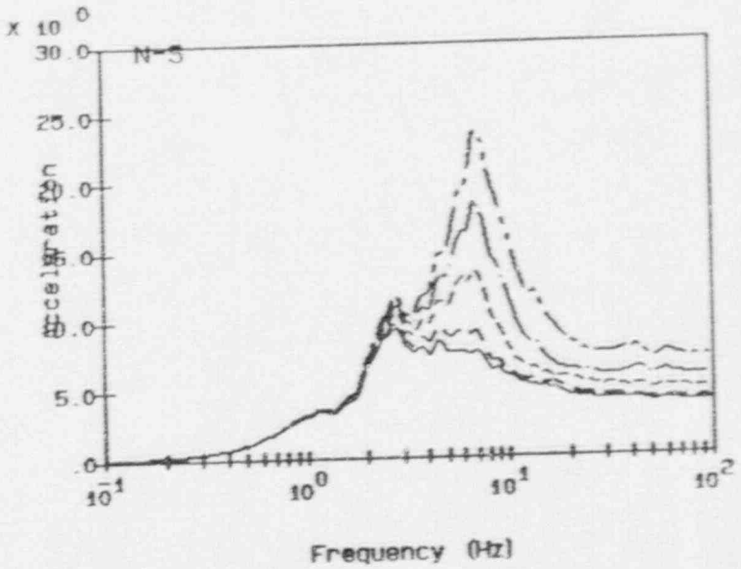

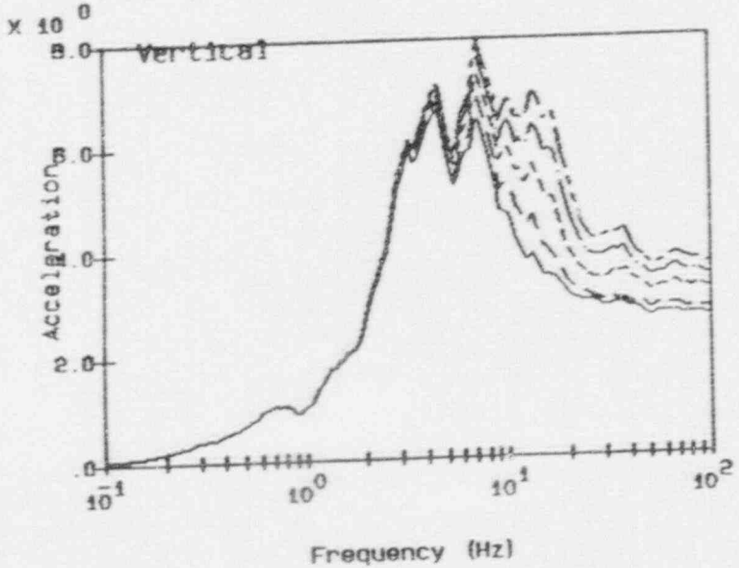

RSPLT V3.00 rb1.plt 12:30:21 04-20-88

Legend:

free-field
el 135°-0°
el 165°-0°
el 195°-0°
el 234°-0°

Notes:

accelerations in units of ft/s/s
spectra calculated at 5% damping

Fig. 14a Peach Bottom Atomic Power Station Reactor/Containment Bldg
Instructure Responses for Acc. Range 1

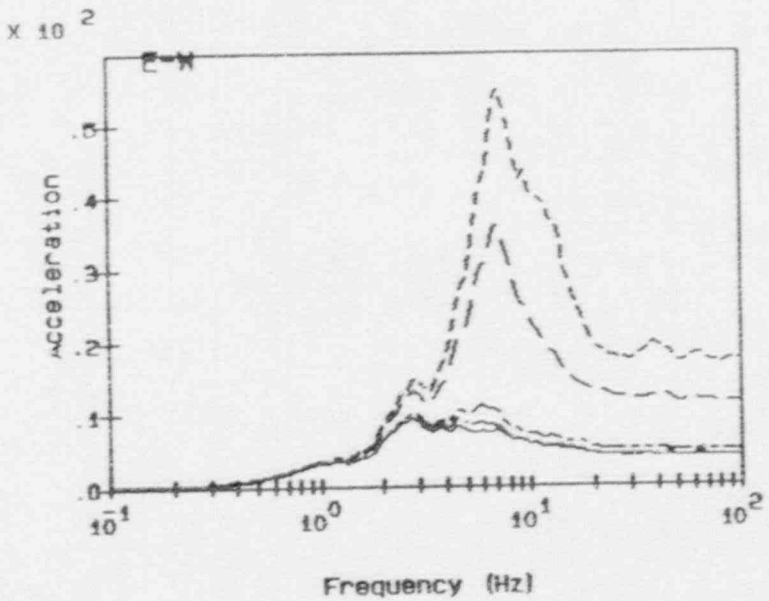

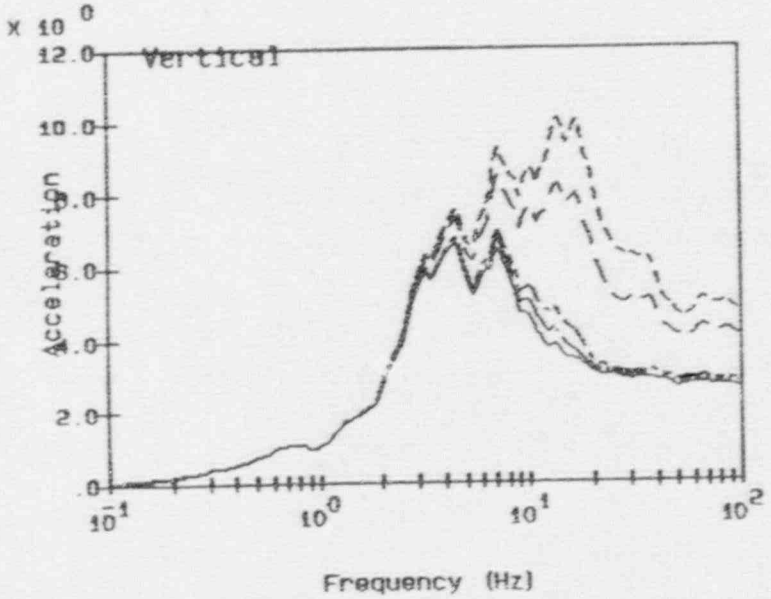

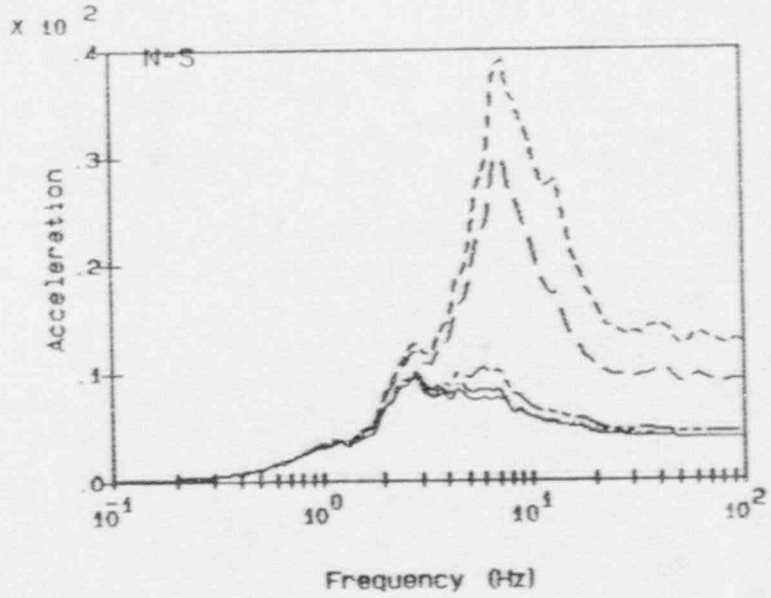

RESPLT V3.00 rb2.plt 12:32:12 04-20-88

Legend:

free-field
el 252°-0°
el 296°-0°
el 119°-11°
el 135°-0°

Notes:

accelerations in units of ft/s/s
spectra calculated at 5% damping

Fig. 14b Peach Bottom Atomic Power Station Reactor/Containment Bldg Instructure Responses for Acc. Range 1

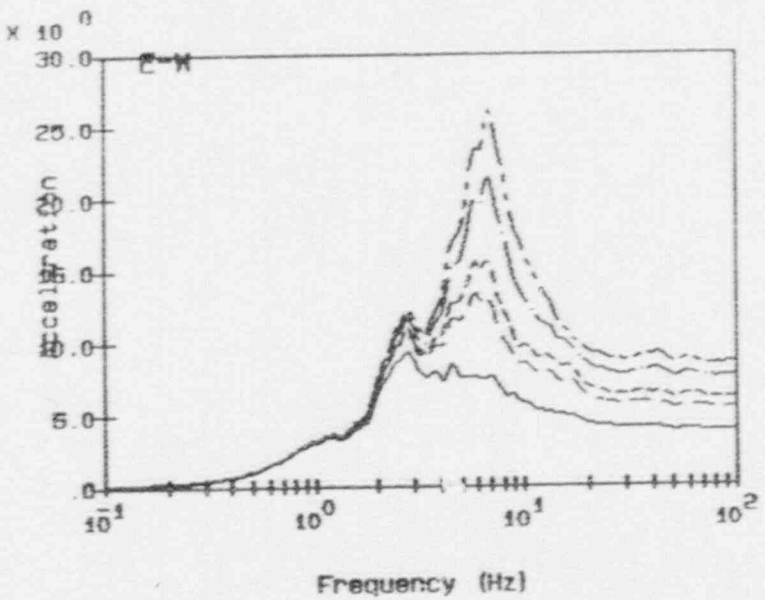

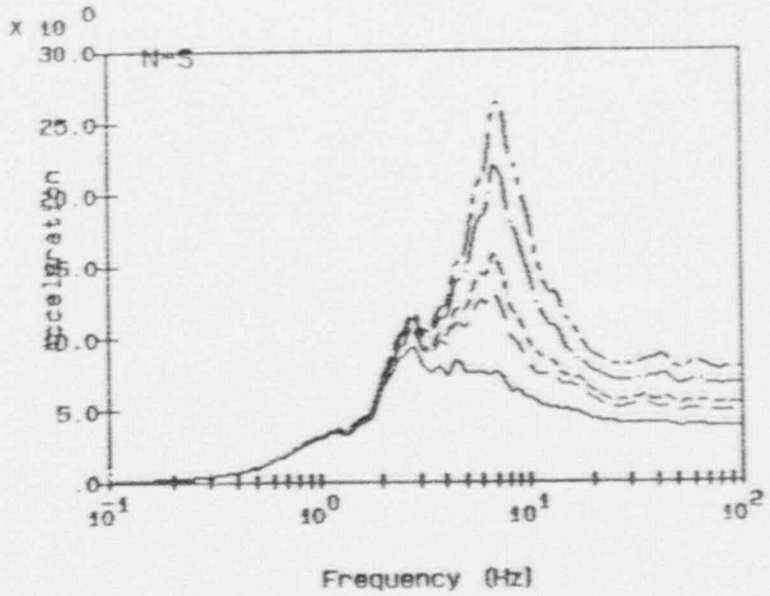

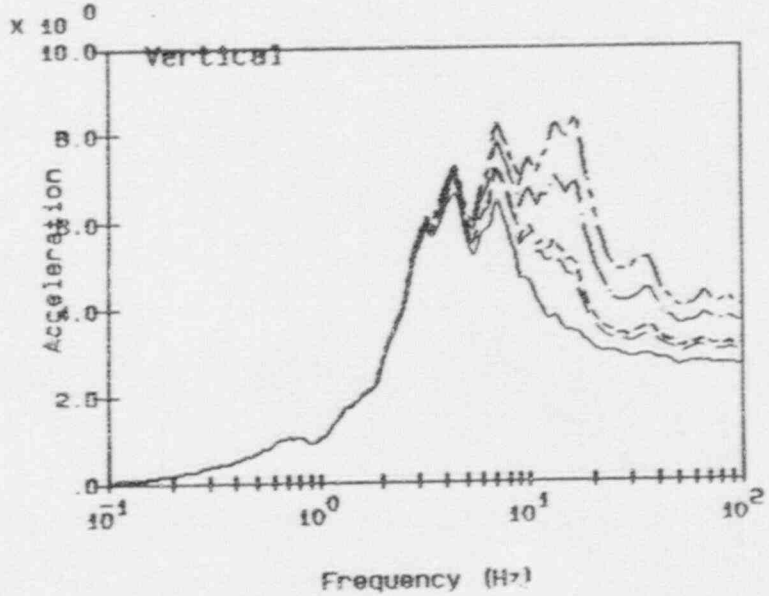

RSPLT V3.00 rb3.plt 12:33:02 04-20-88

Legend:

free-field
el 145'-9"
el 156'-0"
el 169'-0"
el 182'-0"

Notes:

accelerations in units of ft/s/s
spectra calculated at 5% damping

Fig. 14c Peach Bottom Atomic Power Station Reactor/Containment Bldg
Instructure Responses for Acc. Range 1

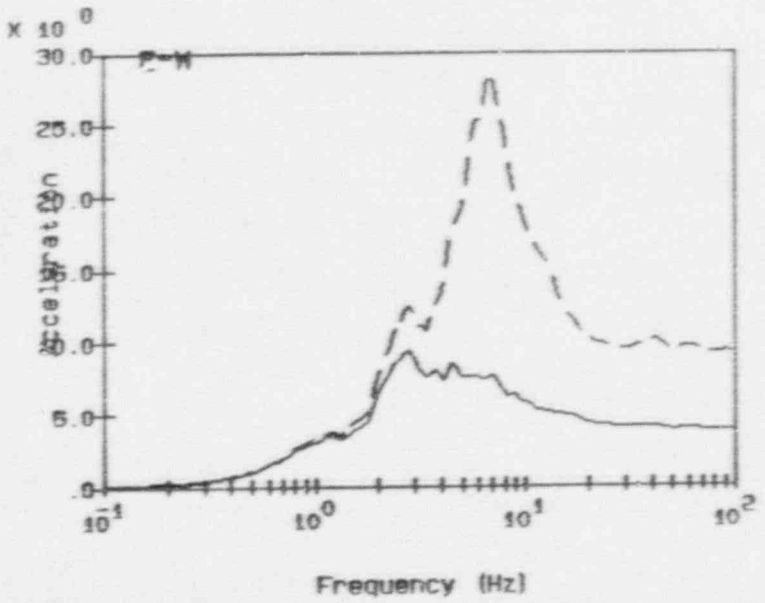

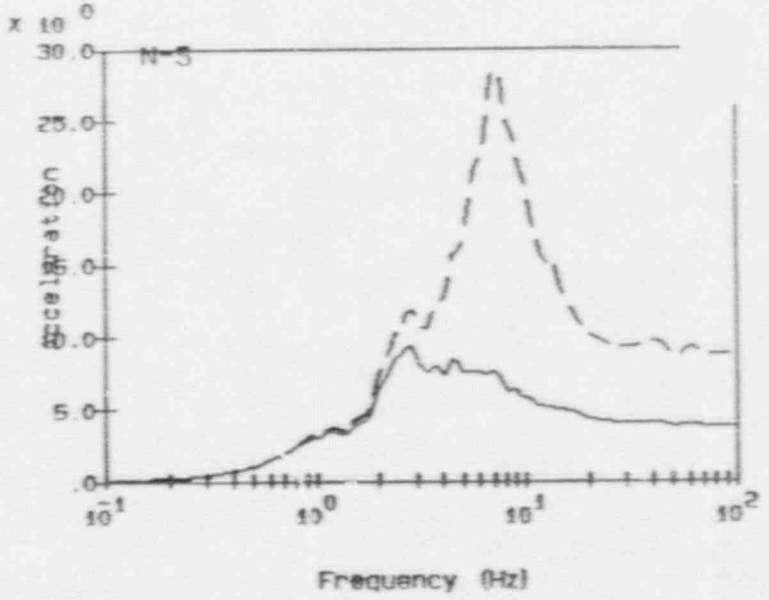

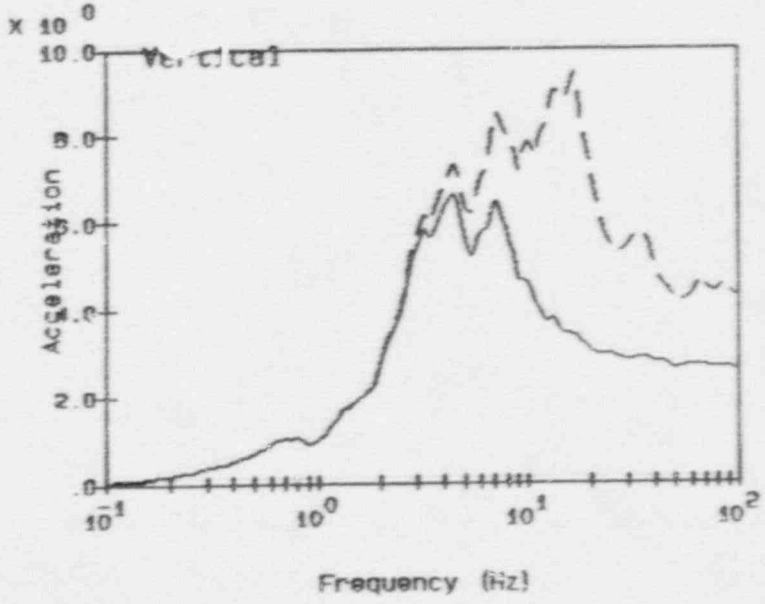

Legend:

free-field

el 195'-0"

Notes:

accelerations in units of ft/s/s

spectra calculated at 5% damping

RSFLT V3.00 rd4.plt 12:34:02 04-20-88

Fig. 14d Peach Bottom Atomic Power Station Reactor/Containment Bldg Instructure Responses for Acc. Range 1

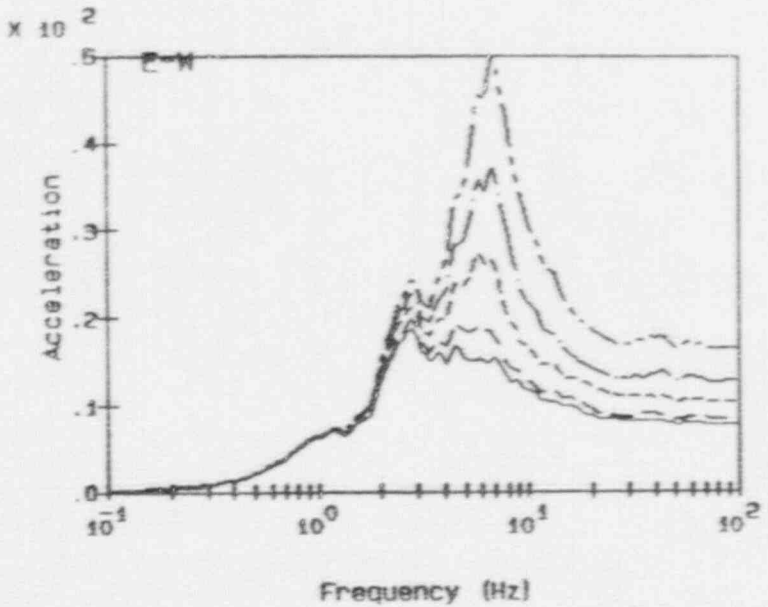

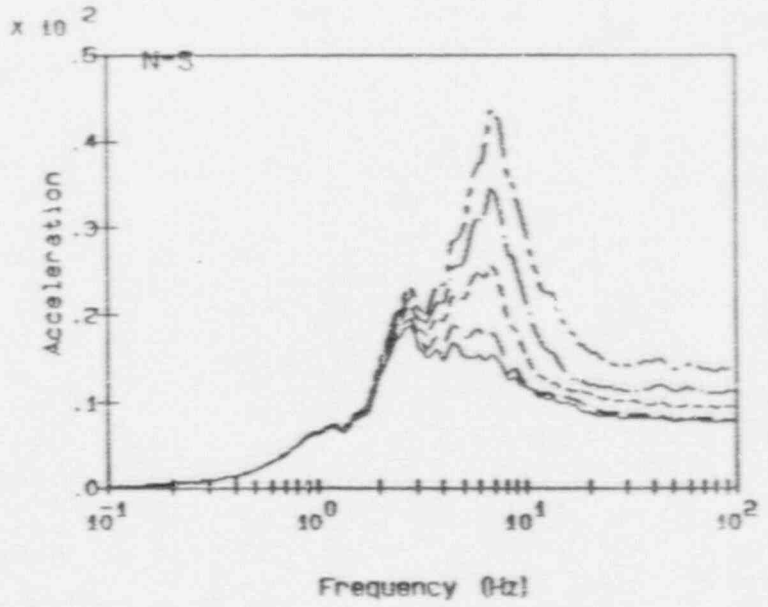

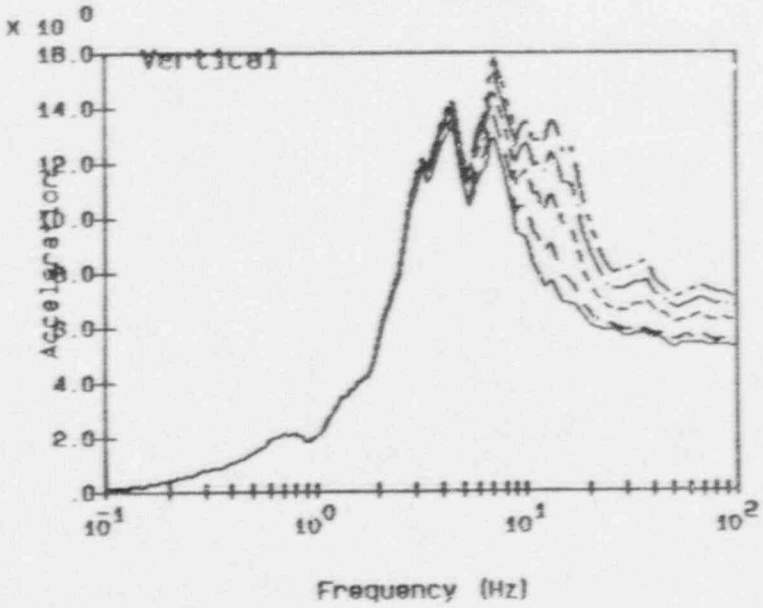

RSPLT V3.00 rb5.plt 13:05:16 04-20-88

Legend:

free-field
el 135°-0°
el 165°-0°
el 195°-0°
el 234°-0°

Notes:

accelerations in units of ft/s/s
spectra calculated at 5% damping

Fig. 15a Peach Bottom Atomic Power Station Reactor/Containment Bldg Instructure Responses for Acc. Range 2

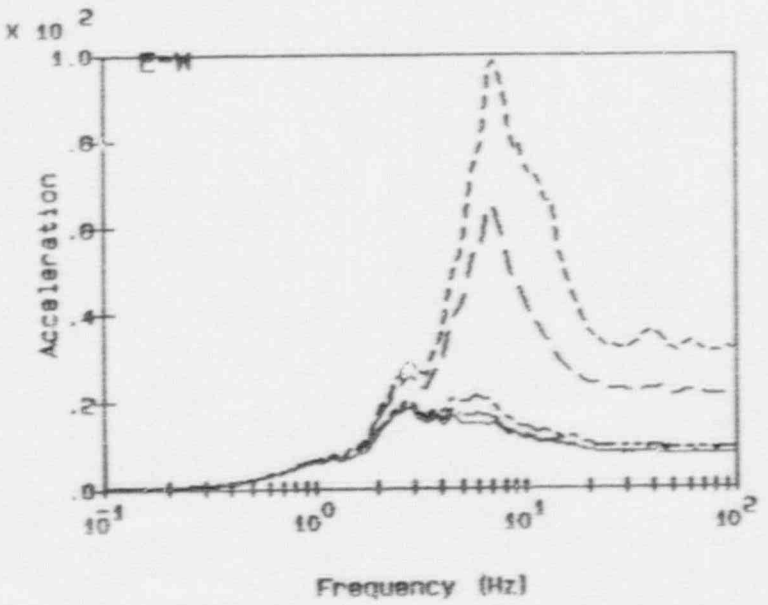

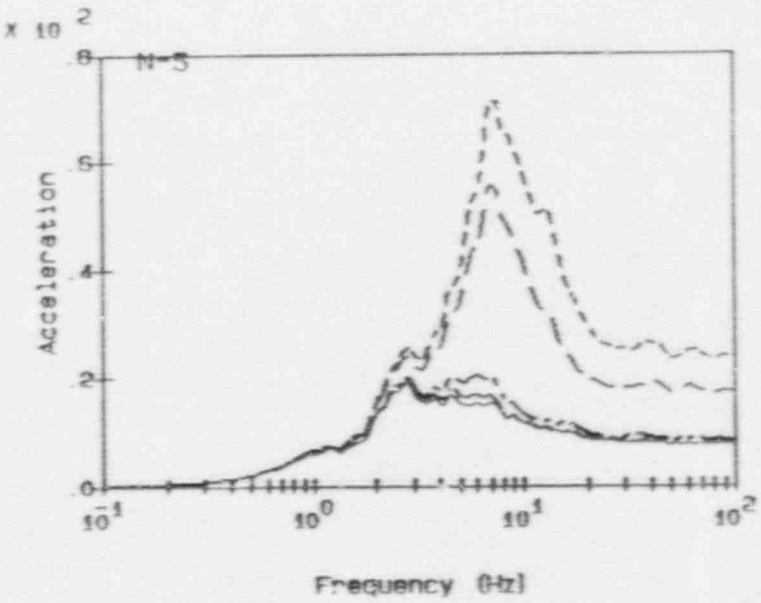

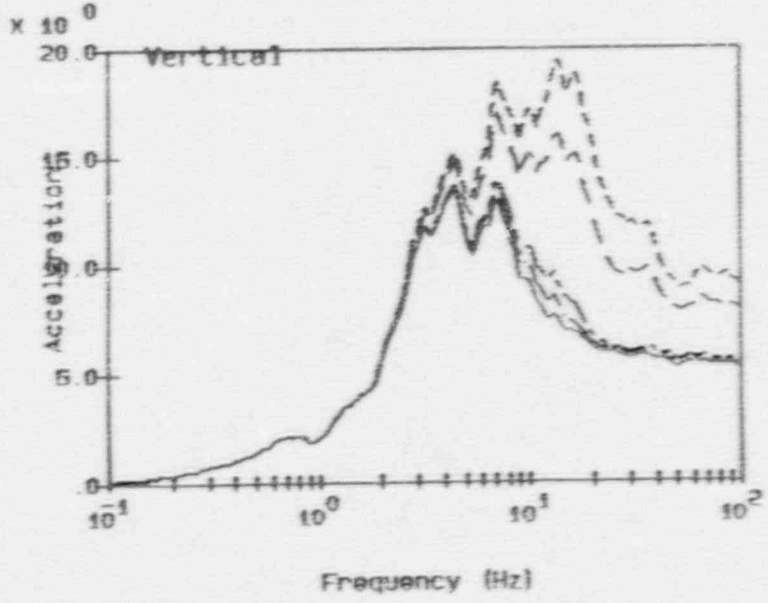

Legend:

free-field
el 252°-0°
el 286°-0°
el 119°-11°
el 135°-0°

Notes:

accelerations in units of ft/s/s
spectra calculated at 5% damping

RSPLT V3.00 FB6.plt 13:05:54 04-20-88

A-27

Fig. 15b Peach Bottom Atomic Power Station Reactor/Containment Bldg
Instructure Responses for Acc. Range 2

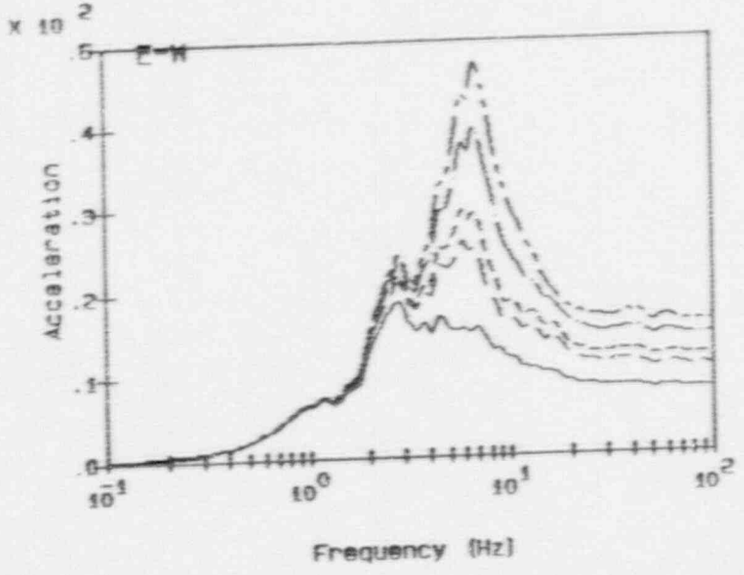

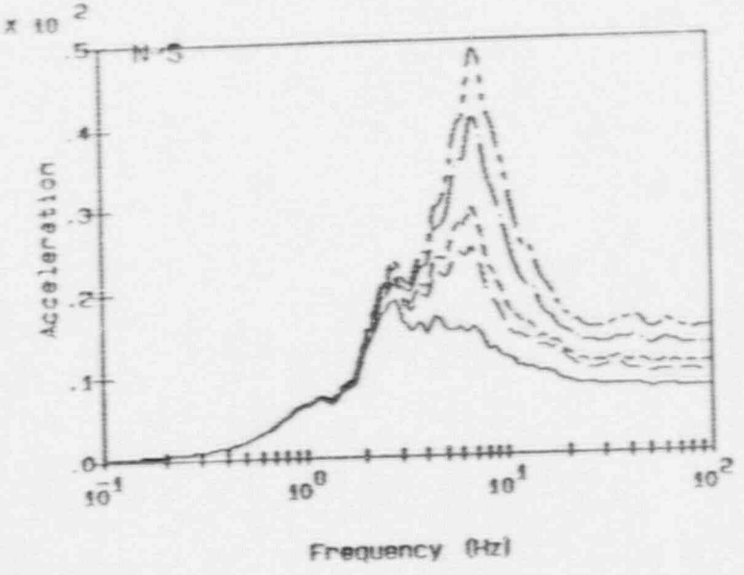

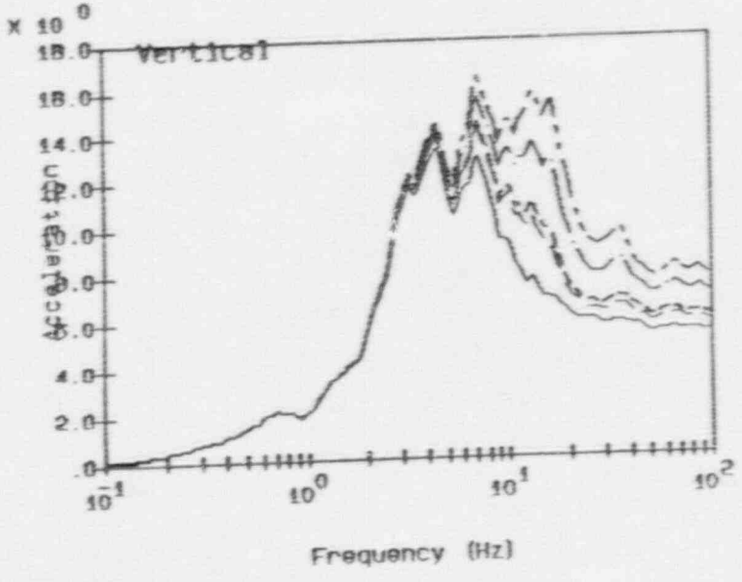

Legend:

free-field	———
el 145'-9"	— — — — — —
el 156'-0"	- - - - - - -
el 169'-0"	——— ——— ———
el 182'-0"	——— - - ——— - -

Notes:

accelerations in units of ft/s/s
spectra calculated at 5% damping

RSPLT V3.00 rb7.01t 13:06:43 04-20-89

A-28

Fig. 15c Peach Bottom Atomic Power Station Reactor/Containment Bldg
Instructure Responses for Acc. Range 2

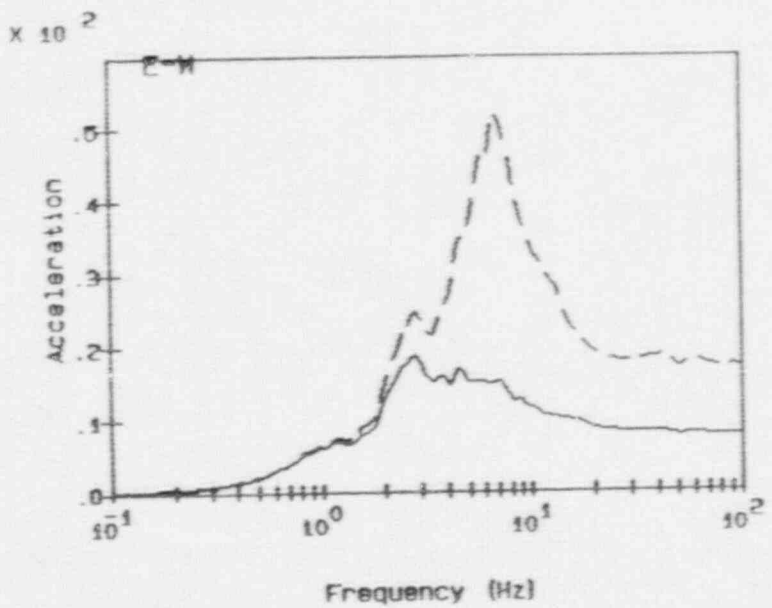

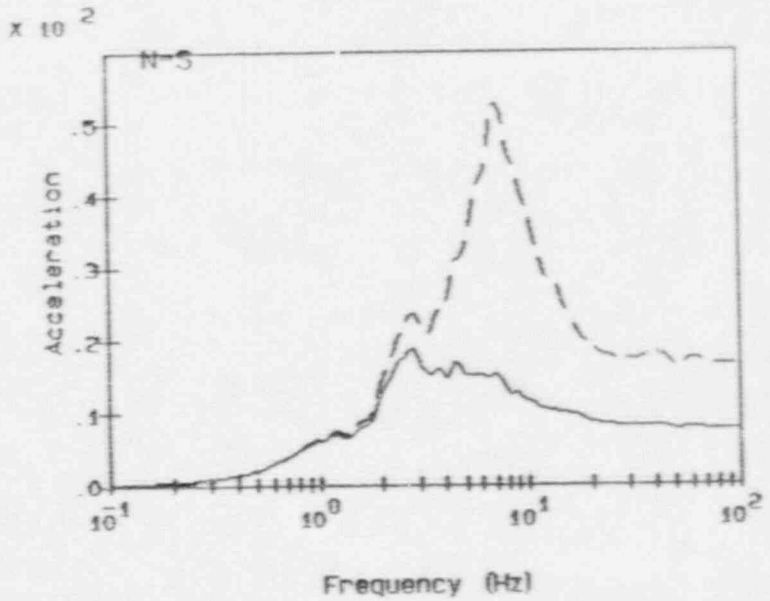

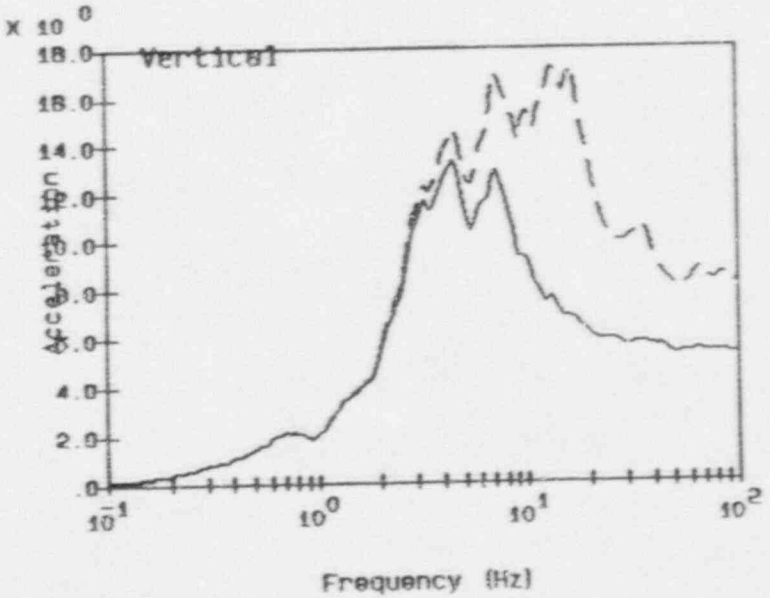

Legend:

free-field

el 195'-0"

Notes:

accelerations in units of ft/s/s

spectra calculated at 5% damping

RSPLT V3.00 rb8.plt 13:07:40 04-20-88

A-29

Fig. 15d Peach Bottom Atomic Power Station Reactor/Containment Bldg Instructure Responses for Acc. Range 2

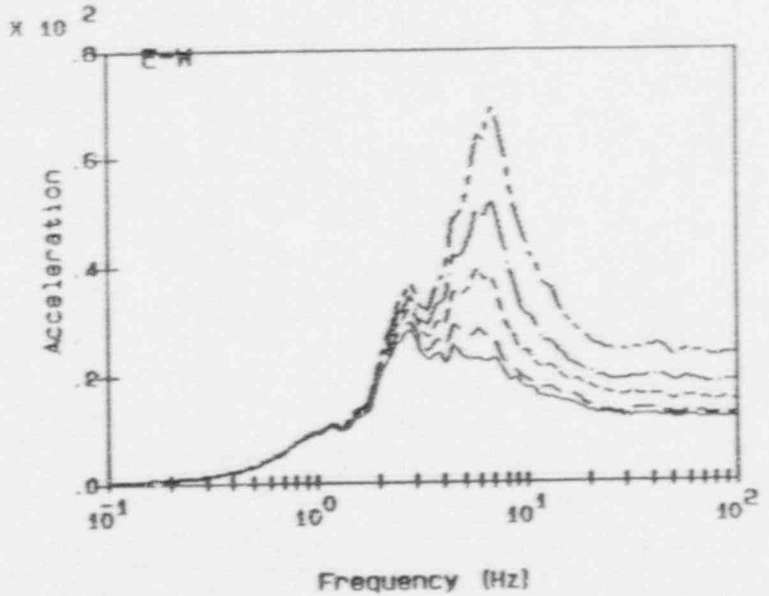

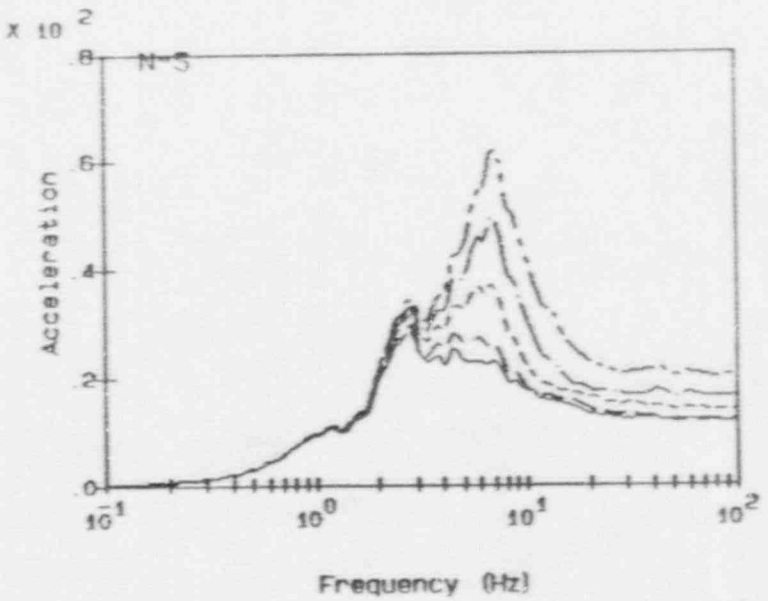

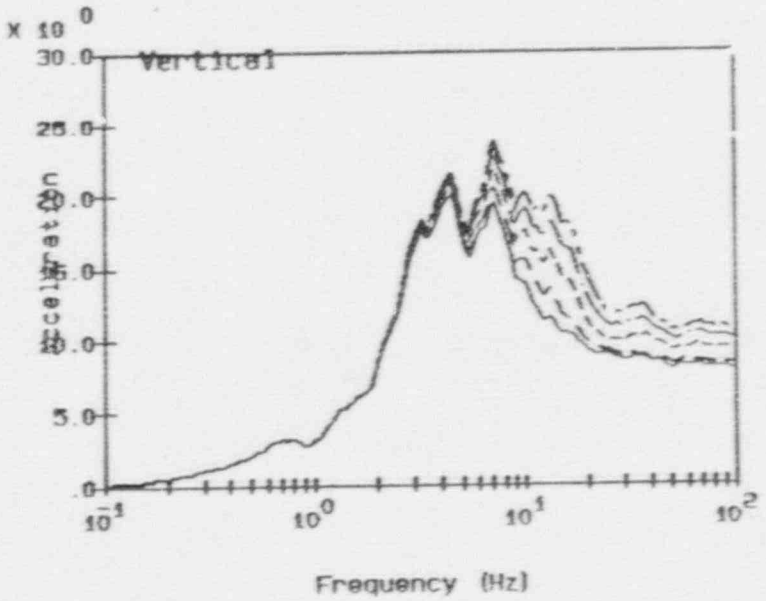

RESULT V3.00 rpb.plt 13:28:09 04-20-88

Legend:

free-field
el 135°-0°
el 165°-0°
el 195°-0°
el 234°-0°

Notes:

accelerations in units of ft/s/s
spectra calculated at 5% damping

Fig. 16a Peach Bottom Atomic Power Station Reactor/Containment Bldg Instructure Responses for Acc. Range 3

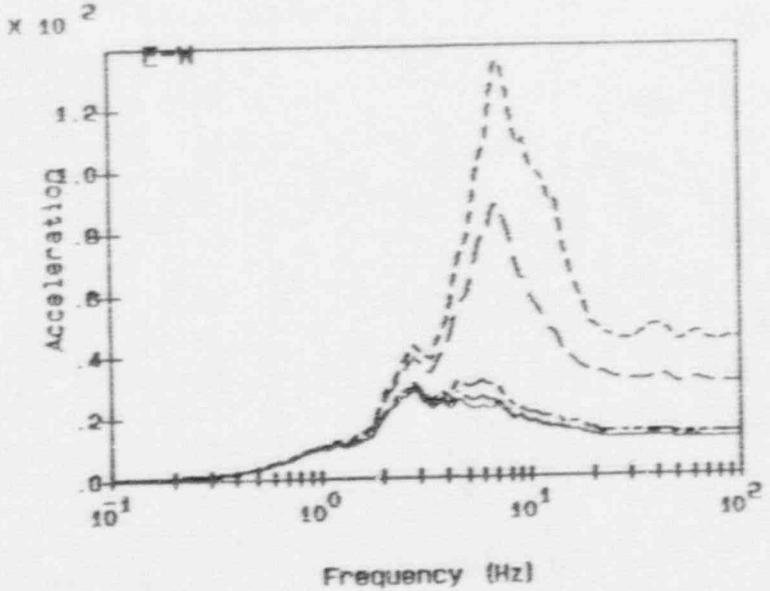

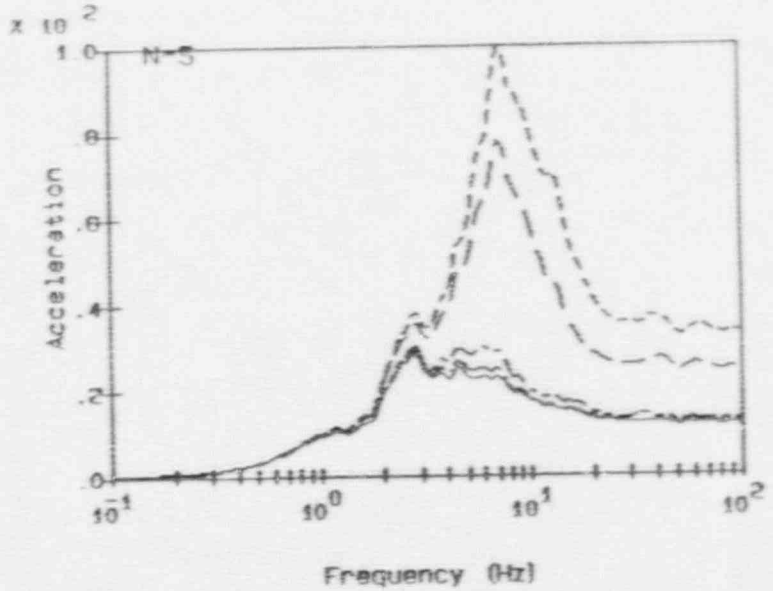

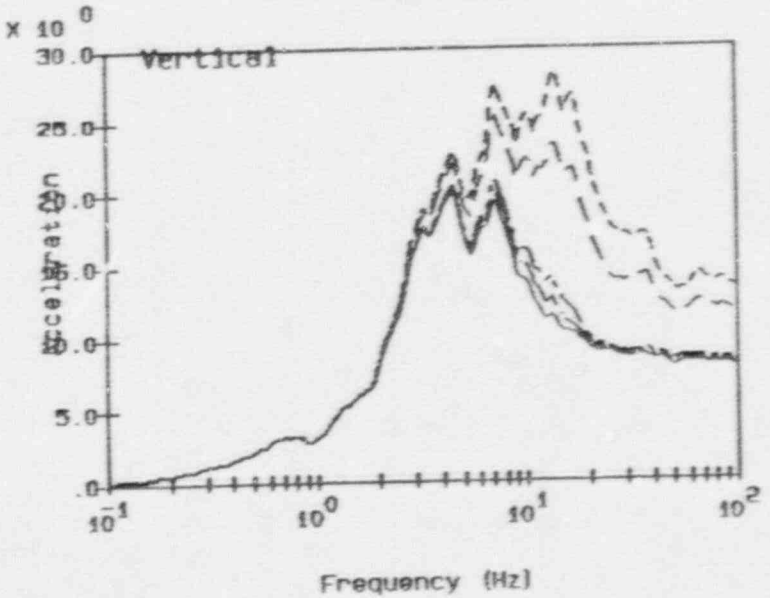

Legend:

free-field
el 252°-0°
el 286°-0°
el 119°-11°
el 135°-0°

Notes:

accelerations in units of ft/s/s
spectra calculated at 5% damping

RSPLT V3.00 FB10.P11 13:28:45 04-20-88

Fig. 16b Peach Bottom Atomic Power Station Reactor/Containment Bldg Instructure Responses for Acc. Range 3

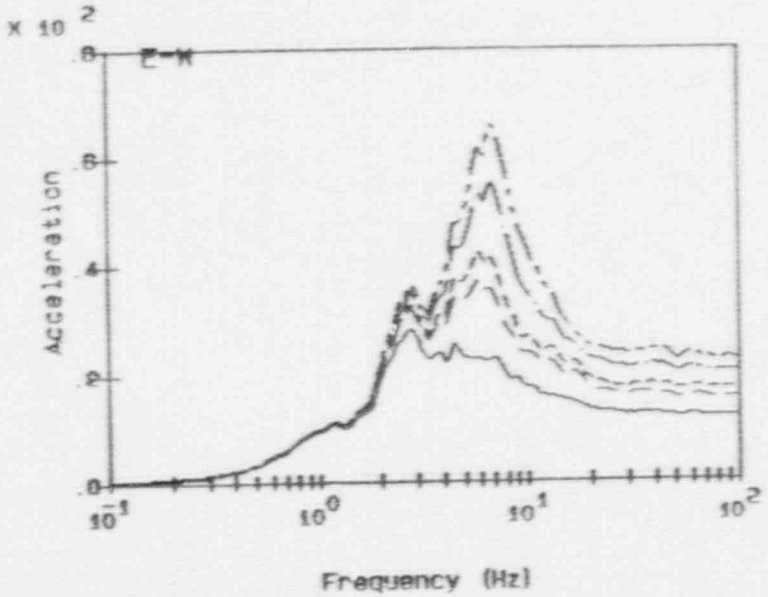

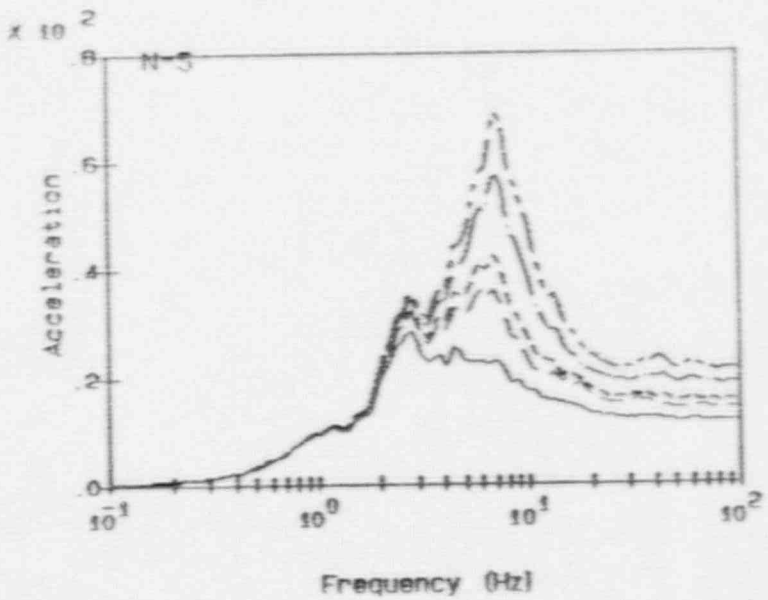

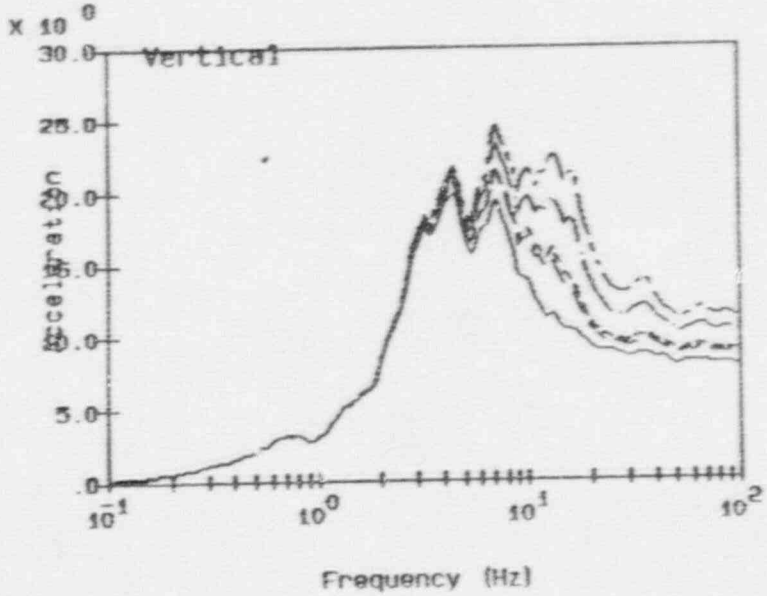

Legend:

free-field
el 145'-9"
el 156'-0"
el 169'-0"
el 182'-0"

Notes:

accelerations in units of ft/s/s
spectra calculated at 5% damping

RESULTS 13:00 Rfll.plt 13:28:30 04-20-88

Fig. 16c Peach Bottom Atomic Power Station Reactor/Containment Bldg
Instructure Responses for Acc. Range 3

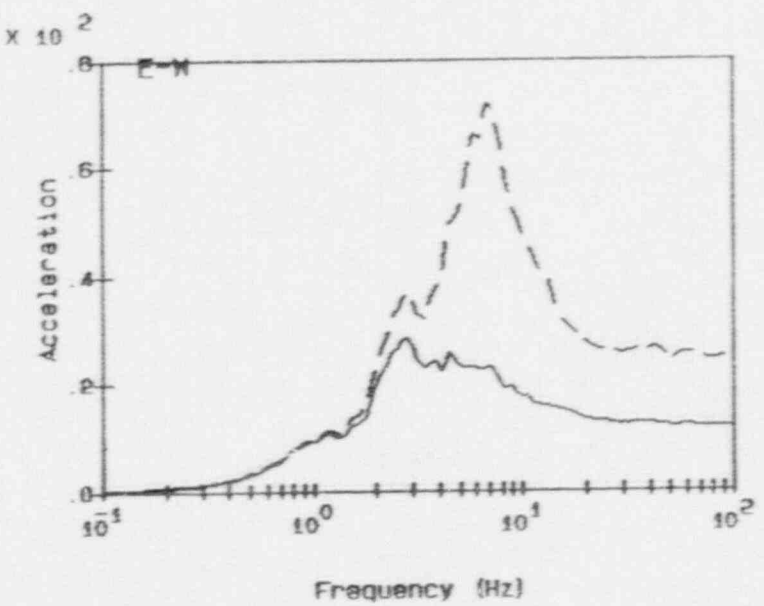

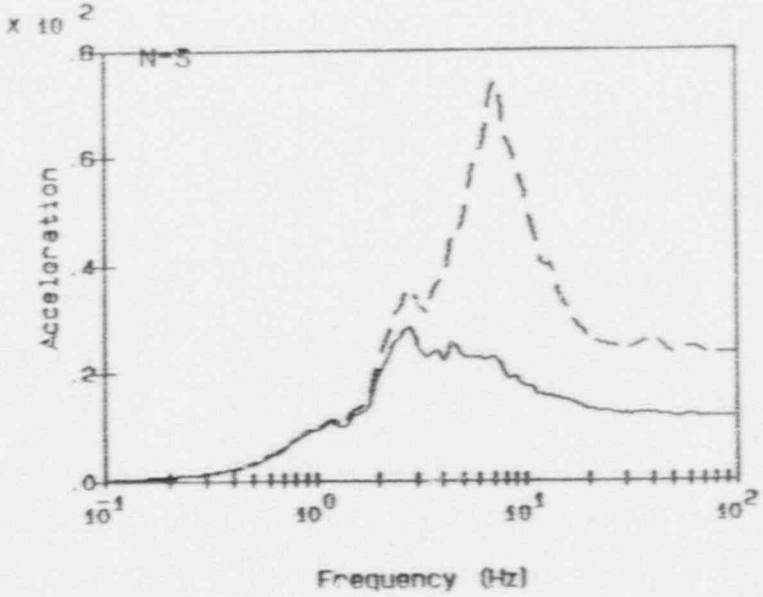

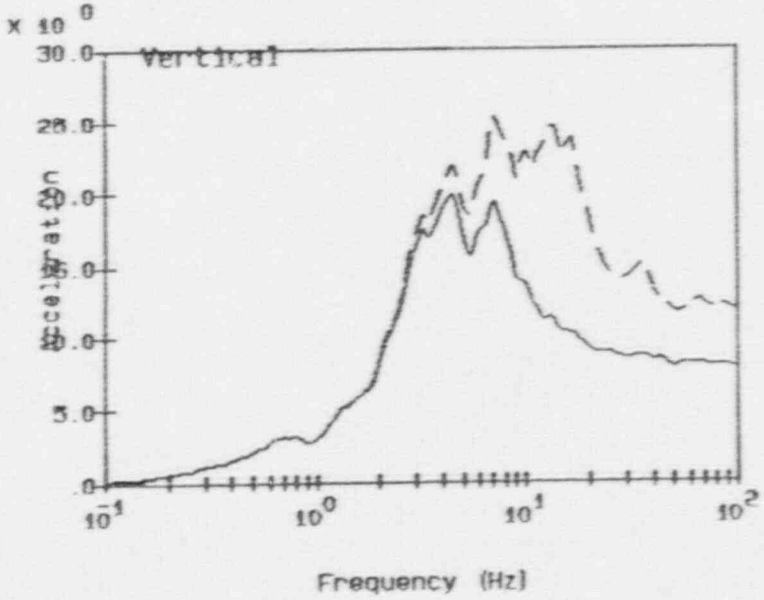

Legend:

free-field
el 195°-0°

Notes:

accelerations in units of ft/s/s
spectra calculated at 5% damping

RSPLT V3.00 rb12.plt 13:30:25 04-20-89

A-33

Fig. 16d Peach Bottom Atomic Power Station Reactor/Containment Bldg
Instructure Responses for Acc. Range 3

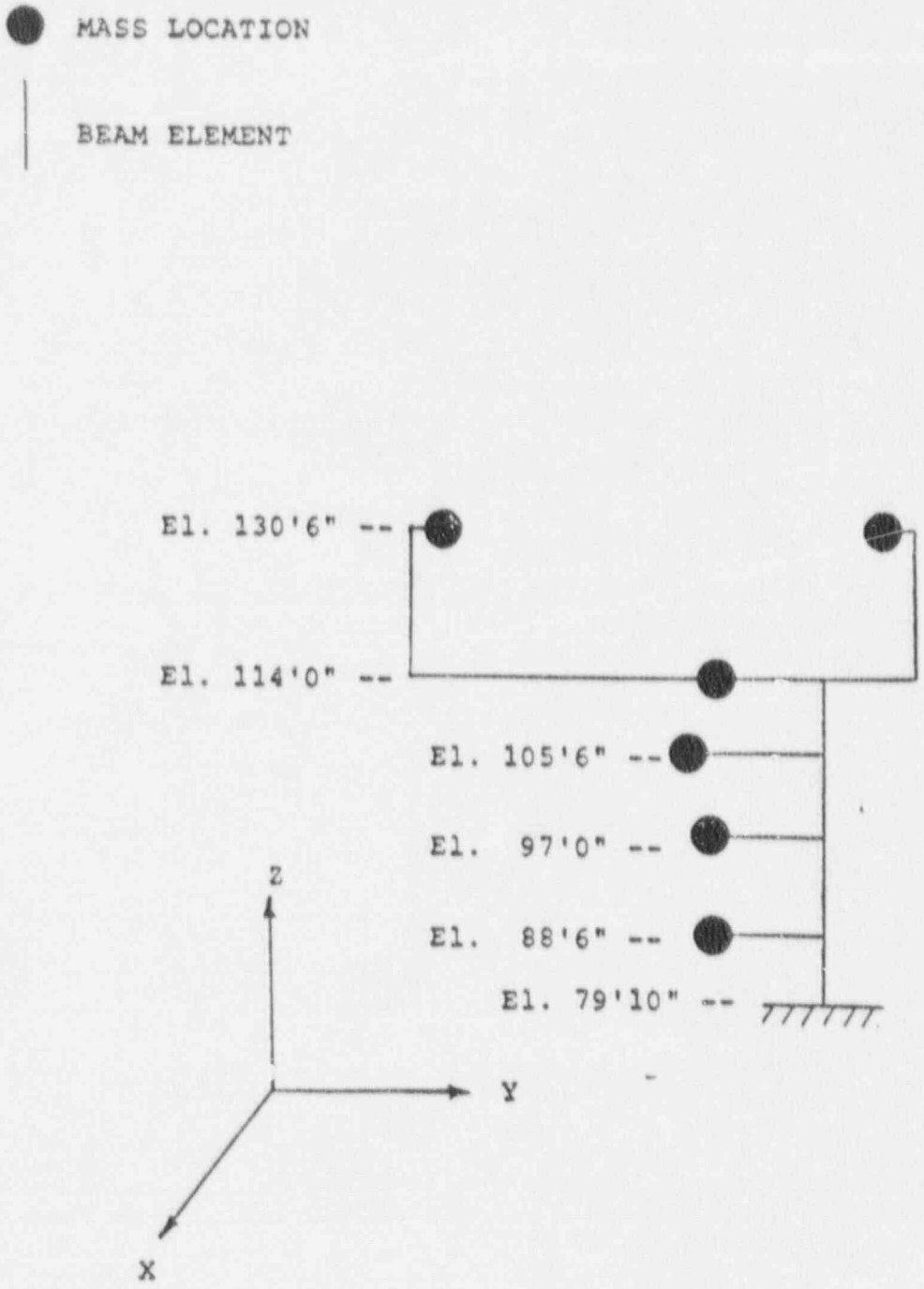

Fig. 17 Peach Bottom Power Station Circulating Water Pump Structure

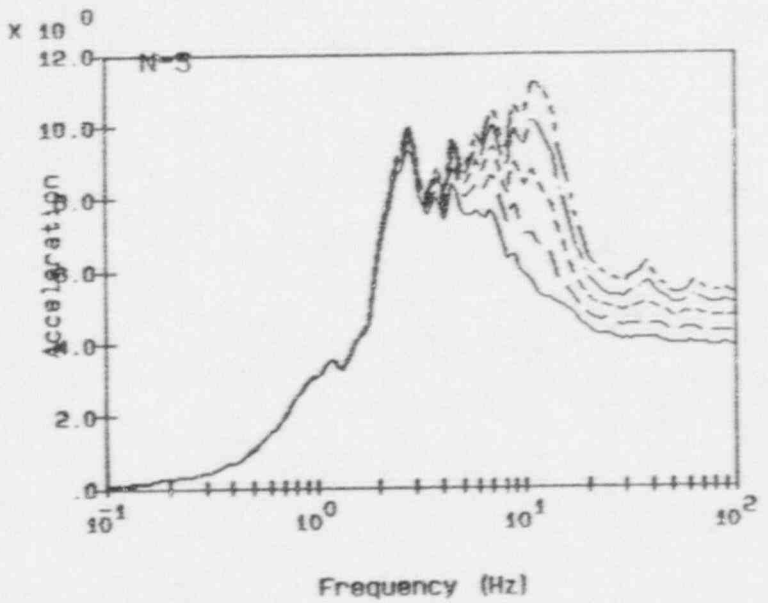

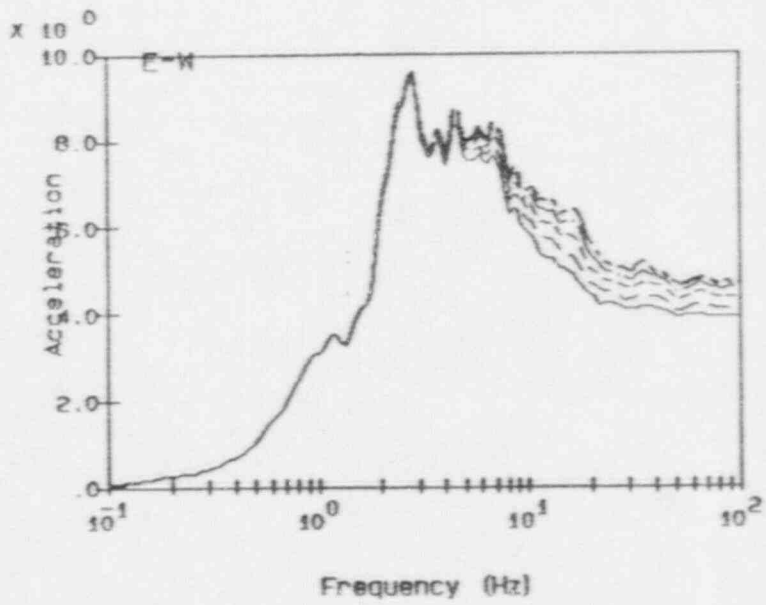

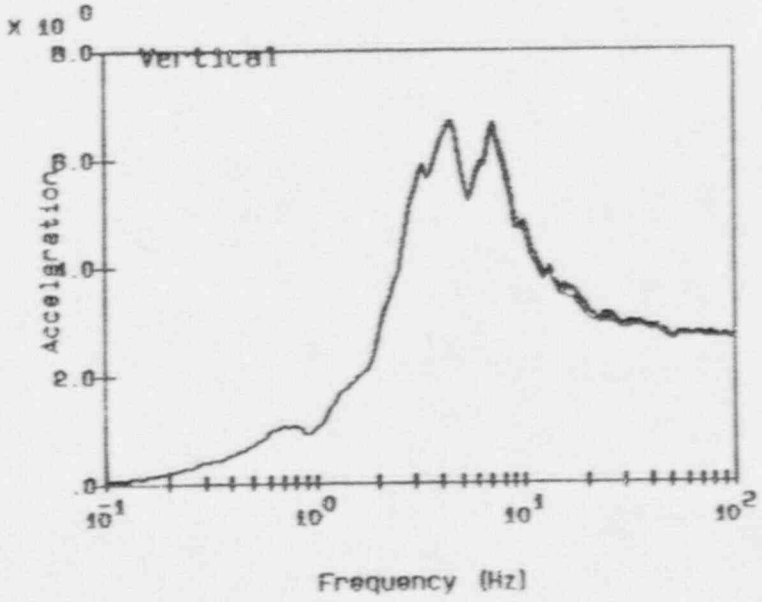

Legend:

free-field	
el 88'- 6"	
el 97' - 0"	
el 105' - 6"	
el 114' - 0"	

Notes:

accelerations in units of ft/s/s
spectra calculated at 5% damping

RSPLT V3.00 doble.plt 14:59:37 07-19-86

Fig. 18a Peach Bottom Atomic Power Station Circulating Water Pump Bldg
Instructure Responses for Acc. Range 1

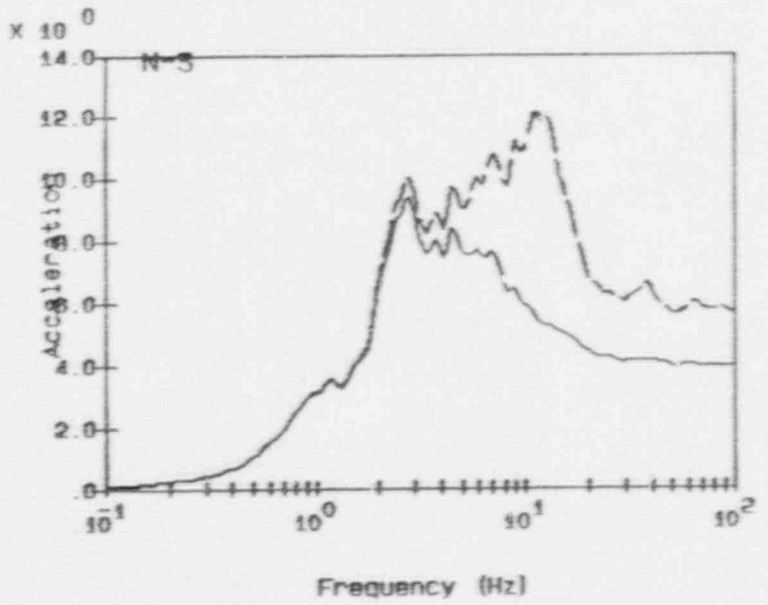

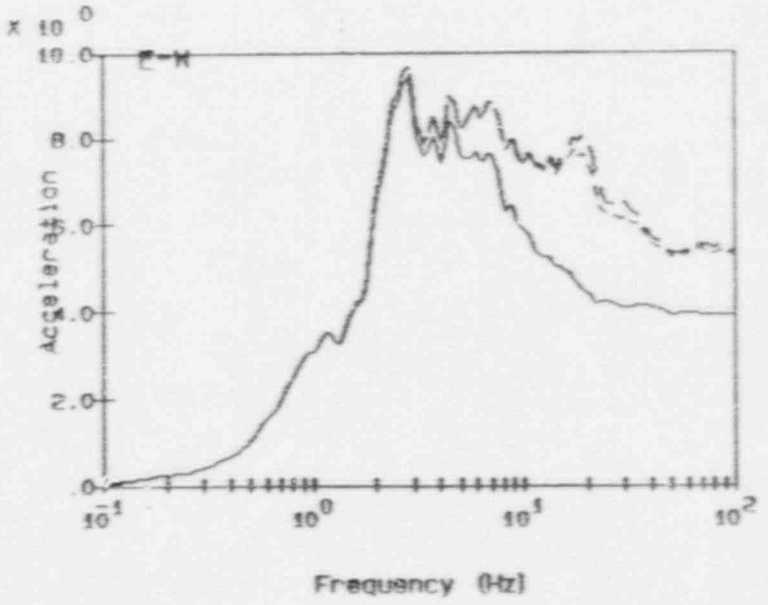

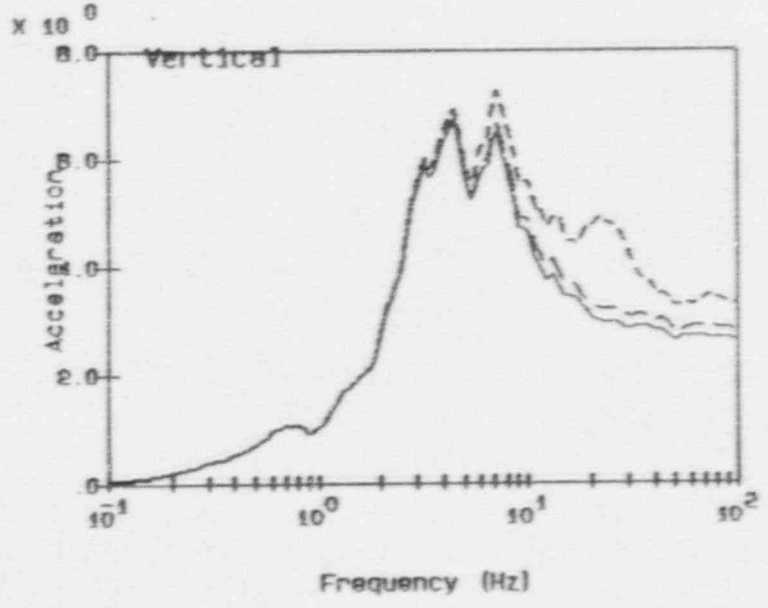

Legend:

free-field ———————————

el 130'6" (#17) — — — — — — —

el 130'6" (#20) - - - - - - - - - - - -

Notes:

accelerations in units of ft/s/s

spectra calculated at 5% damping

Fig. 18b Peach Bottom Atomic Power Station Circulating Water Pump Bldg Instructure Responses for Acc. Range 1

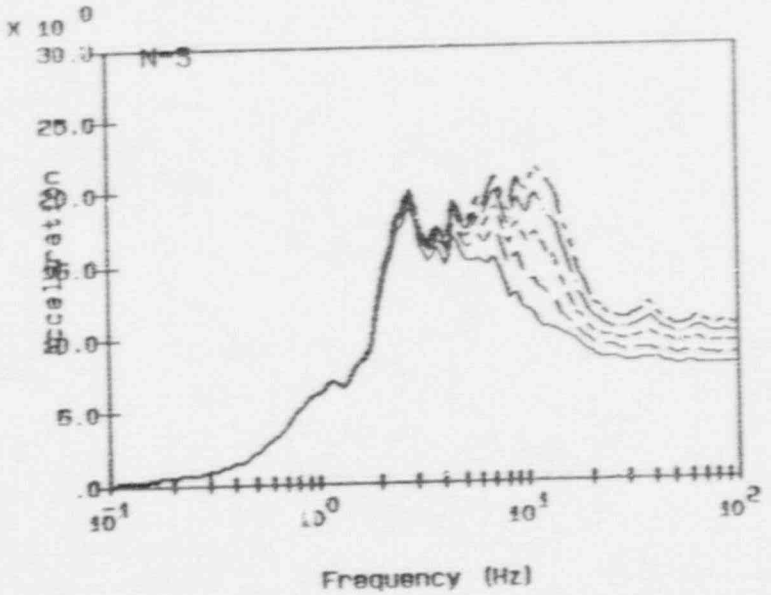

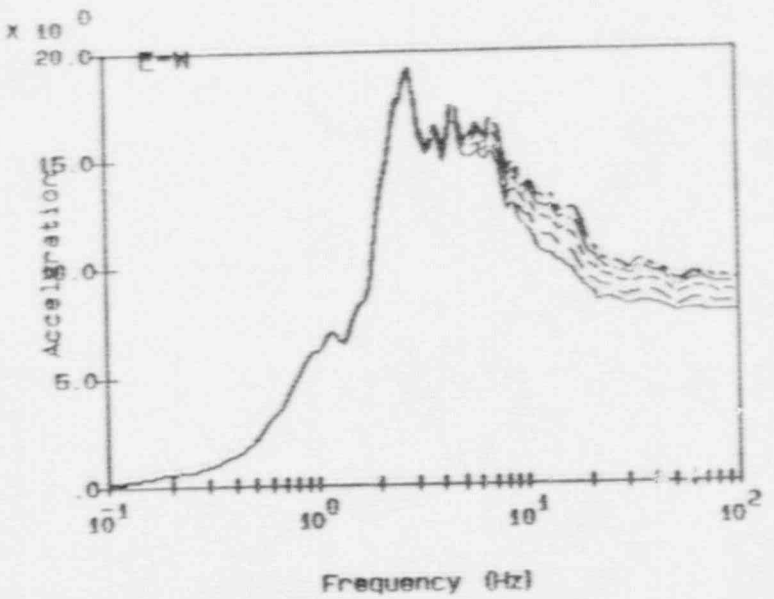

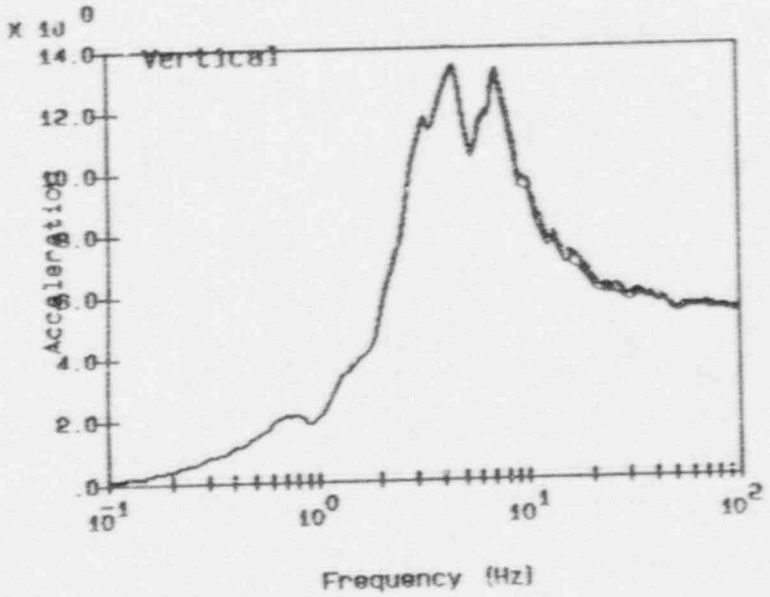

PSPLT V3.00 dgb2a.plt 15:04:45 07-19-88

Legend:

free-field
el 88° - 8°
el 97° - 0°
el 105° - 8°
el 114° - 0°

Notes:

accelerations in units of ft/s/s
spectra calculated at 5% damping

Fig. 19a Peach Bottom Atomic Power Station Circulating Water Pump Bldg
Instructure Responses for Acc. Range 2

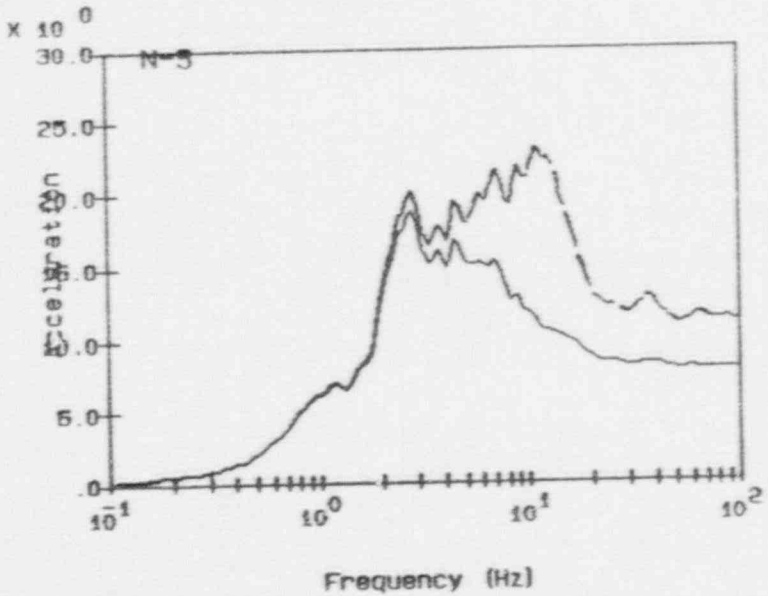

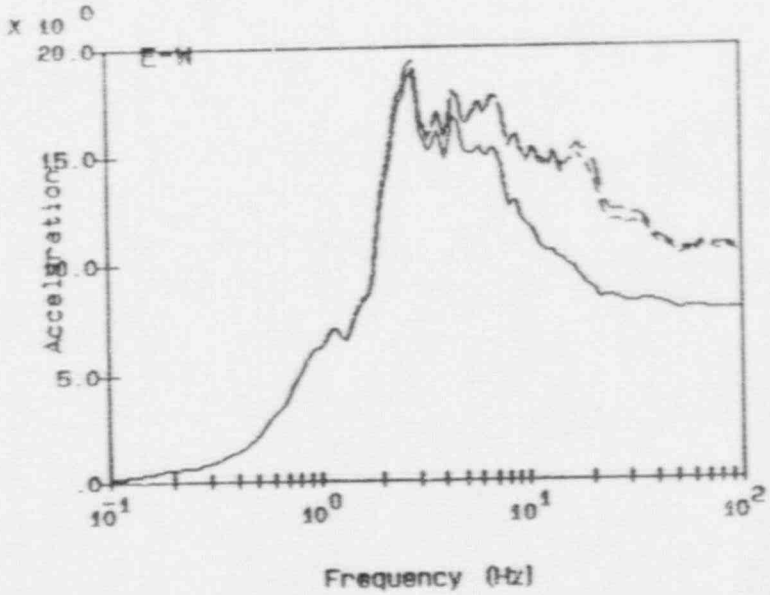

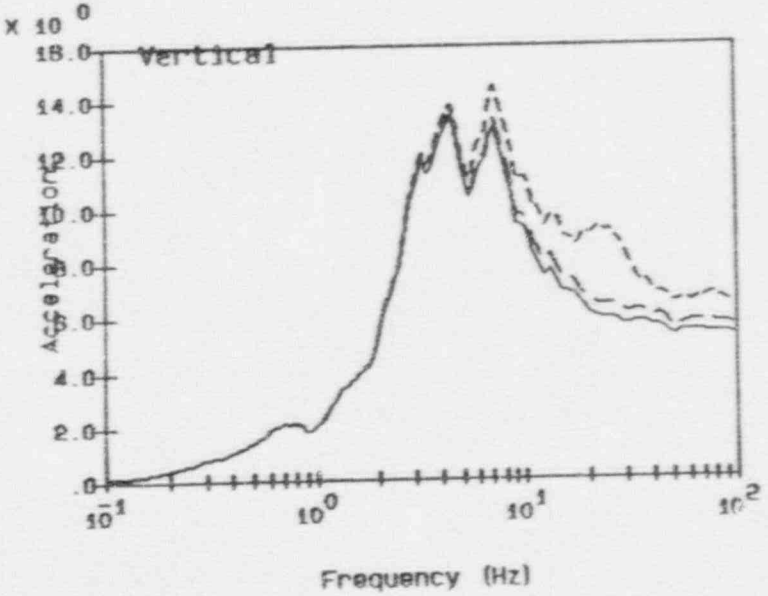

RSPLT V3.00 d00ZD.plt 15:05:12 07-19-88

Legend:

free-field

el 130'6" (#17)

el 130'6" (#20)

Notes:

accelerations in units of ft/s/s

spectra calculated at 5% damping

Fig. 19b Peach Bottom Atomic Power Station Circulating Water Pump Bldg Instructure Responses for Acc. Range 2

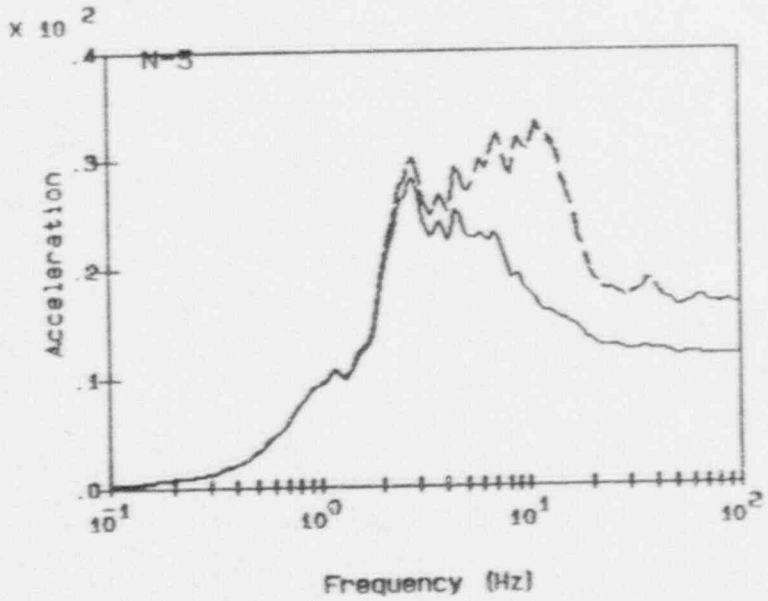

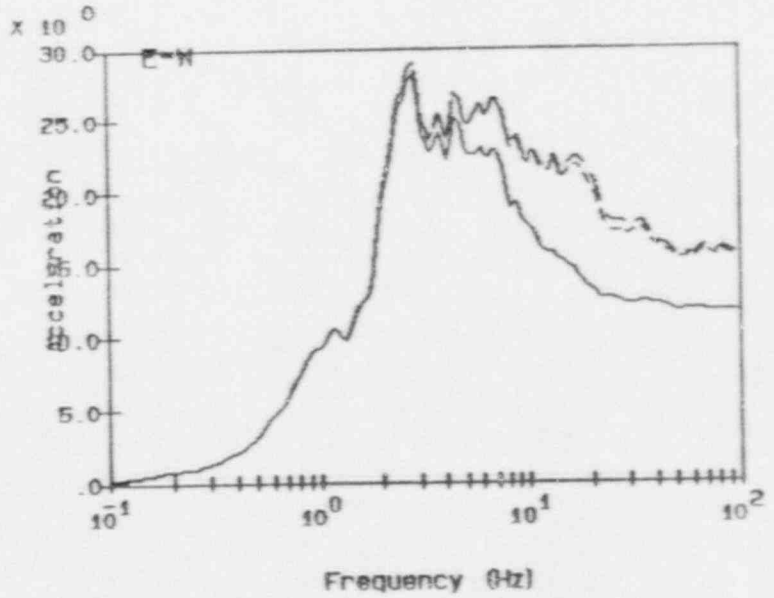

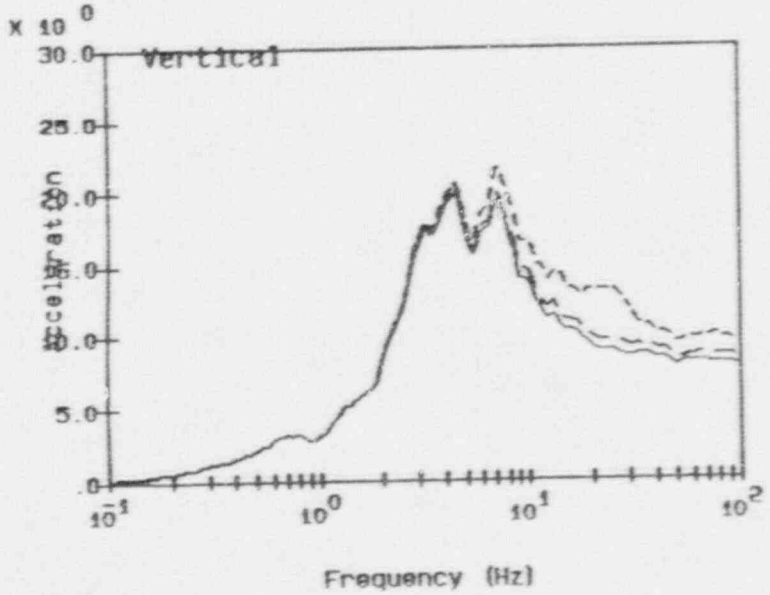

Legend:

free-field

el 130'6" (#17)

el 130'6" (#20)

Notes:

accelerations in units of ft/s/s

spectra calculated at 5% damping

RSPLT V3.00 08DEC88.PLT 15:30:59 07-19-89

A-39

Fig. 20a Peach Bottom Atomic Power Station Circulating Water Pump Bldg
Instructure Responses for Acc. Range 3

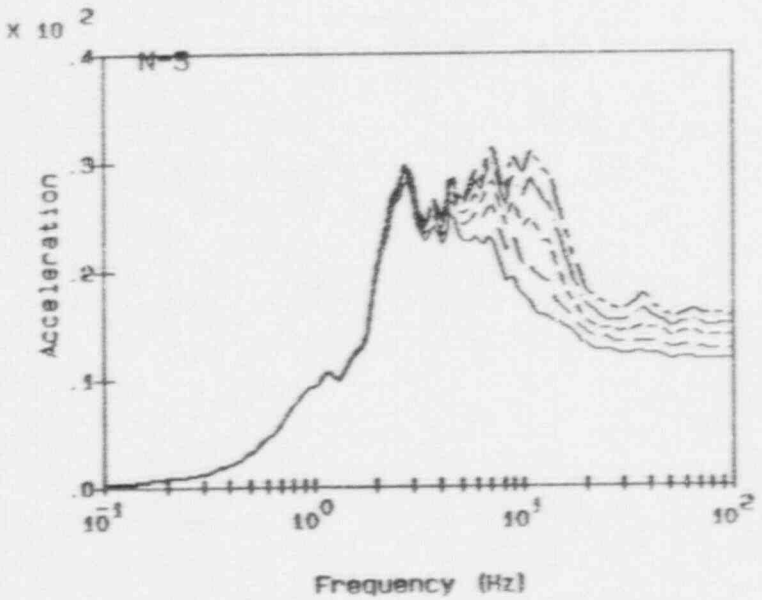

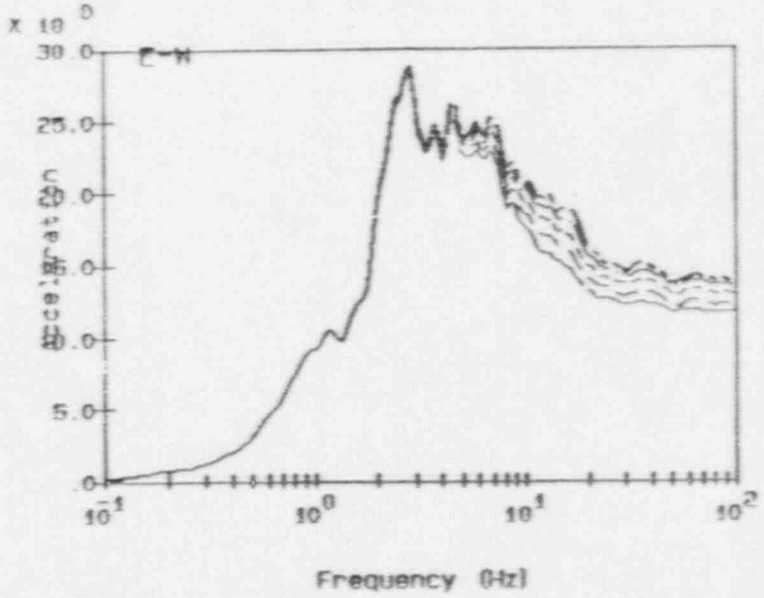

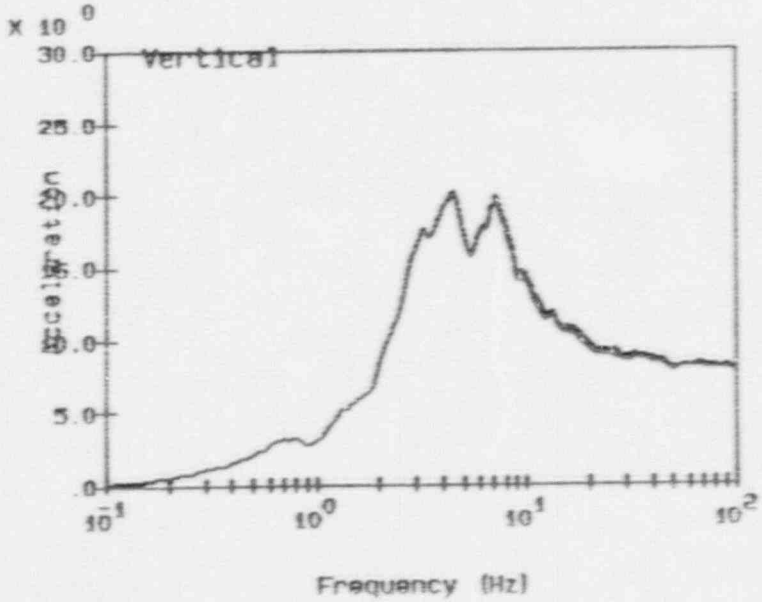

RSPLT V3.00 08B30.plt 15:30:34 07-19-88

Legend:

free-field

el 88' - 6"

el 97' - 0"

el 105' - 6"

el 114' - 0"

Notes:

accelerations in units of ft/s/s

spectra calculated at 5% damping

A-40

Fig. 20b Peach Bottom Atomic Power Station Circulating Water Pump Bldg
Instructure Responses for Acc. Range 3

APPENDIX B

NUMERICAL STRUCTURAL RESPONSES FOR PEACH BOTTOM

MEDIAN RESPONSE
CIRCULATING WATER PUMP STRUCTURE
ACCELERATION RANGE 1 (g)

el.	dir.	2-5 (Hz)	5-10 (Hz)	7 (Hz)	10 (Hz)	zpa
79'-10"	x	.25	.21	.23	.18	.12
79'-10"	y	.25	.21	.23	.18	.12
79'-10"	z	.16	.17	.19	.14	.08
88'-6"	x	.26	.25	.26	.22	.13
88'-6"	y	.25	.22	.24	.19	.13
88'-6"	z	.16	.17	.19	.14	.08
97'-0"	x	.26	.27	.28	.27	.15
97'-0"	y	.25	.23	.24	.20	.14
97'-0"	z	.16	.17	.19	.14	.08
105'-6"	x	.27	.29	.30	.30	.16
105'-6"	y	.25	.23	.25	.21	.14
105'-6"	z	.16	.17	.20	.14	.09
114'-0"	x	.27	.31	.31	.33	.17
114'-0"	y	.26	.24	.25	.21	.15
114'-0"	z	.16	.17	.20	.14	.09

EMERGENCY AND HIGH PRESSURE WATER PUMPS ENCLOSURE

el.	dir.	2-5 (Hz)	5-10 (Hz)	7 (Hz)	10 (Hz)	zpa
130'-6"	x	.27	.32	.32	.35	.17
130'-6"	y	.26	.25	.27	.24	.17
130'-6"	z	.16	.17	.20	.15	.09

TRAVELING WATER SCREEN ENCLOSURE

el.	dir.	2-5 (Hz)	5-10 (Hz)	7 (Hz)	10 (Hz)	zpa
130'-6"	x	.27	.32	.32	.35	.18
130'-6"	y	.26	.25	.27	.23	.16
130'-6"	z	.17	.19	.21	.17	.10

MEDIAN RESPONSE
CIRCULATING WATER PUMP STRUCTURE
ACCELERATION RANGE 2 (g)

el.	dir.	2-5 (Hz)	5-10 (Hz)	7 (Hz)	10 (Hz)	zpa
79'-10"	x	.50	.43	.46	.36	.25
79'-10"	y	.50	.43	.46	.36	.25
79'-10"	z	.33	.34	.38	.28	.17
88'-6"	x	.51	.49	.52	.44	.27
88'-6"	y	.50	.44	.47	.38	.25
88'-6"	z	.33	.34	.39	.28	.17
97'-0"	x	.53	.54	.56	.52	.29
97'-0"	y	.51	.46	.49	.40	.27
97'-0"	z	.33	.35	.39	.28	.17
105'-6"	x	.53	.58	.60	.59	.31
105'-6"	y	.51	.47	.50	.42	.28
105'-6"	z	.33	.35	.39	.29	.17
114'-0"	x	.54	.61	.62	.64	.33
114'-0"	y	.51	.48	.51	.43	.29
114'-0"	z	.33	.35	.39	.29	.17

EMERGENCY AND HIGH PRESSURE WATER PUMPS ENCLOSURE

el.	dir.	2-5 (Hz)	5-10 (Hz)	7 (Hz)	10 (Hz)	zpa
130'-6"	x	.55	.62	.64	.67	.34
130'-6"	y	.52	.51	.54	.47	.33
130'-6"	z	.33	.35	.39	.29	.18

TRAVELING WATER SCREEN ENCLOSURE

el.	dir.	2-5 (Hz)	5-10 (Hz)	7 (Hz)	10 (Hz)	zpa
130'-6"	x	.55	.63	.64	.68	.34
130'-6"	y	.52	.50	.53	.47	.32
130'-6"	z	.34	.38	.43	.33	.20

MEDIAN RESPONSE
CIRCULATING WATER PUMP STRUCTURE
ACCELERATION RANGE 3 (g)

el.	dir.	2-5 (Hz)	5-10 (Hz)	7 (Hz)	10 (Hz)	zpa
79'-10"	x	.74	.64	.69	.55	.37
79'-10"	y	.74	.64	.69	.55	.37
79'-10"	z	.49	.51	.58	.42	.25
88'-6"	x	.77	.73	.78	.65	.40
88'-6"	y	.75	.67	.71	.58	.38
88'-6"	z	.49	.51	.58	.42	.25
97'-0"	x	.79	.80	.84	.77	.44
97'-0"	y	.76	.69	.73	.60	.40
97'-0"	z	.49	.52	.58	.43	.25
105'-6"	x	.80	.86	.90	.86	.46
105'-6"	y	.76	.70	.75	.63	.42
105'-6"	z	.49	.52	.59	.43	.26
114'-0"	x	.81	.90	.93	.93	.49
114'-0"	y	.77	.72	.76	.64	.43
114'-0"	z	.49	.52	.59	.43	.26

EMERGENCY AND HIGH PRESSURE WATER PUMPS ENCLOSURE

el.	dir.	2-5 (Hz)	5-10 (Hz)	7 (Hz)	10 (Hz)	zpa
130'-6"	x	.82	.93	.96	.98	.51
130'-6"	y	.78	.76	.80	.70	.49
130'-6"	z	.49	.52	.59	.44	.26

TRAVELING WATER SCREEN ENCLOSURE

el.	dir.	2-5 (Hz)	5-10 (Hz)	7 (Hz)	10 (Hz)	zpa
130'-6"	x	.82	.93	.96	.99	.51
130'-6"	y	.78	.76	.80	.70	.48
130'-6"	z	.51	.57	.64	.50	.30

MEDIAN RESPONSE
REACTOR/CONTAINMENT BUILDING
ACCELERATION RANGE 1 (g)

REACTOR/CONTAINMENT BLDG

el.	dir.	2-5 (Hz)	5-10 (Hz)	7 (Hz)	10 (Hz)	zpa
91'-0"	x	.25	.21	.22	.18	.12
91'-0"	y	.25	.21	.22	.18	.12
91'-0"	z	.16	.17	.18	.14	.08
135'-0"	x	.27	.25	.26	.20	.14
135'-0"	y	.27	.24	.25	.19	.13
135'-0"	z	.17	.18	.19	.16	.09
165'-0"	x	.31	.35	.37	.27	.17
165'-0"	y	.30	.34	.36	.24	.15
165'-0"	z	.17	.19	.20	.18	.10
195'-0"	x	.35	.49	.52	.36	.22
195'-0"	y	.33	.46	.49	.34	.18
195'-0"	z	.17	.20	.21	.19	.11
234'-0"	x	.39	.67	.72	.51	.28
234'-0"	y	.35	.59	.63	.46	.23
234'-0"	z	.17	.21	.22	.21	.11
252'-0"	x	.43	.89	.94	.70	.36
252'-0"	y	.38	.77	.80	.66	.29
252'-0"	z	.18	.23	.23	.23	.13
286'-0"	x	.51	1.38	1.45	1.27	.54
286'-0"	y	.42	1.00	1.04	.95	.40
286'-0"	z	.18	.25	.25	.27	.14

REACTOR

el.	dir.	2-5 (Hz)	5-10 (Hz)	7 (Hz)	10 (Hz)	zpa
119'-11"	x	.26	.23	.24	.19	.13
119'-11"	y	.26	.23	.24	.18	.12
119'-11"	z	.17	.18	.18	.15	.09
135'-0"	x	.28	.28	.29	.22	.15
135'-0"	y	.28	.27	.28	.21	.14
135'-0"	z	.17	.18	.19	.16	.09
145'-9"	x	.30	.33	.35	.27	.17
145'-9"	y	.30	.33	.35	.26	.16
145'-9"	z	.17	.19	.19	.17	.09
156'-0"	x	.32	.39	.41	.30	.19
156'-0"	y	.31	.39	.42	.30	.17
156'-0"	z	.17	.19	.20	.18	.10
169'-0"	x	.36	.53	.57	.41	.24
169'-0"	y	.34	.55	.58	.43	.22
169'-0"	z	.17	.21	.21	.21	.11
182'-0"	x	.38	.65	.69	.50	.27
182'-0"	y	.36	.67	.70	.53	.25
182'-0"	z	.17	.22	.23	.23	.12
195'-0"	x	.40	.71	.76	.56	.29
195'-0"	y	.37	.72	.76	.59	.28
195'-0"	z	.18	.23	.23	.25	.13

MEDIAN RESPONSE
REACTOR/CONTAINMENT BUILDING
ACCELERATION RANGE 2 (g)

REACTOR/CONTAINMENT BLDG

el.	dir.	2-5 (Hz)	5-10 (Hz)	7 (Hz)	10 (Hz)	zpa
91'-0"	x	.50	.43	.44	.36	.25
91'-0"	y	.50	.43	.44	.36	.25
91'-0"	z	.33	.34	.35	.28	.17
135'-0"	x	.54	.49	.51	.39	.27
135'-0"	y	.53	.48	.50	.38	.25
135'-0"	z	.33	.36	.37	.31	.18
165'-0"	x	.62	.67	.70	.51	.33
165'-0"	y	.60	.65	.69	.47	.30
165'-0"	z	.34	.39	.40	.35	.19
195'-0"	x	.69	.91	.97	.67	.41
195'-0"	y	.65	.87	.92	.64	.36
195'-0"	z	.34	.41	.42	.39	.21
234'-0"	x	.77	1.24	1.32	.95	.52
234'-0"	y	.70	1.12	1.18	.87	.44
234'-0"	z	.34	.42	.43	.41	.22
252'-0"	x	.85	1.62	1.72	1.29	.67
252'-0"	y	.75	1.43	1.49	1.22	.55
252'-0"	z	.35	.46	.46	.46	.25
286'-0"	x	.99	2.51	2.62	2.31	.99
286'-0"	y	.82	1.86	1.92	1.75	.74
286'-0"	z	.36	.50	.50	.53	.28

REACTOR

el.	dir.	2-5 (Hz)	5-10 (Hz)	7 (Hz)	10 (Hz)	zpa
119'-11"	x	.52	.46	.47	.38	.25
119'-11"	y	.52	.45	.47	.37	.25
119'-11"	z	.33	.35	.37	.30	.17
135'-0"	x	.57	.54	.56	.44	.29
135'-0"	y	.56	.53	.55	.42	.27
135'-0"	z	.33	.37	.38	.32	.18
145'-9"	x	.60	.64	.67	.51	.33
145'-9"	y	.59	.64	.67	.49	.30
145'-9"	z	.33	.38	.39	.34	.18
156'-0"	x	.64	.74	.78	.58	.37
156'-0"	y	.62	.75	.79	.57	.34
156'-0"	z	.34	.38	.39	.35	.19
169'-0"	x	.71	.99	1.05	.75	.45
169'-0"	y	.68	1.03	1.09	.79	.41
169'-0"	z	.34	.42	.42	.41	.22
182'-0"	x	.75	1.20	1.27	.92	.50
182'-0"	y	.72	1.24	1.31	.98	.47
182'-0"	z	.35	.44	.45	.45	.24
195'-0"	x	.78	1.32	1.39	1.05	.55
195'-0"	y	.74	1.35	1.41	1.10	.52
195'-0"	z	.35	.46	.47	.48	.25

MEDIAN RESPONSE
REACTOR/CONTAINMENT BUILDING
ACCELERATION RANGE 3 (g)

REACTOR/CONTAINMENT BLDG

el.	dir.	2-5 (Hz)	5-10 (Hz)	7 (Hz)	10 (Hz)	zpa
91'-0"	x	.74	.64	.66	.54	.37
91'-0"	y	.74	.64	.66	.54	.37
91'-0"	z	.49	.51	.53	.41	.25
135'-0"	x	.81	.73	.75	.59	.39
135'-0"	y	.80	.71	.74	.57	.38
135'-0"	z	.50	.54	.56	.46	.26
165'-0"	x	.92	.96	1.01	.73	.48
165'-0"	y	.89	.94	.99	.69	.44
165'-0"	z	.51	.58	.60	.53	.29
195'-0"	x	1.02	1.29	1.37	.96	.59
195'-0"	y	.97	1.25	1.32	.91	.52
195'-0"	z	.51	.61	.62	.57	.31
234'-0"	x	1.14	1.75	1.85	1.34	.74
234'-0"	y	1.04	1.59	1.67	1.24	.64
234'-0"	z	.52	.63	.65	.61	.33
252'-0"	x	1.24	2.26	2.38	1.80	.94
252'-0"	y	1.12	2.01	2.10	1.71	.78
252'-0"	z	.53	.68	.69	.68	.36
286'-0"	x	1.44	3.45	3.60	3.16	1.38
286'-0"	y	1.22	2.60	2.69	2.43	1.03
286'-0"	z	.54	.74	.75	.78	.41

REACTOR

el.	dir.	2-5 (Hz)	5-10 (Hz)	7 (Hz)	10 (Hz)	zpa
119'-11"	x	.79	.69	.71	.56	.38
119'-11"	y	.78	.68	.70	.55	.37
119'-11"	z	.50	.53	.55	.45	.26
135'-0"	x	.85	.80	.82	.65	.43
135'-0"	y	.83	.78	.82	.62	.40
135'-0"	z	.50	.55	.57	.48	.27
145'-9"	x	.90	.93	.96	.74	.48
145'-9"	y	.88	.93	.98	.72	.45
145'-9"	z	.50	.57	.58	.51	.27
156'-0"	x	.95	1.06	1.11	.83	.53
156'-0"	y	.93	1.08	1.14	.82	.49
156'-0"	z	.50	.58	.59	.52	.28
169'-0"	x	1.05	1.40	1.48	1.07	.64
169'-0"	y	1.01	1.46	1.54	1.12	.60
169'-0"	z	.51	.62	.63	.60	.32
182'-0"	x	1.12	1.68	1.78	1.31	.72
182'-0"	y	1.07	1.75	1.84	1.38	.68
182'-0"	z	.52	.66	.67	.66	.35
195'-0"	x	1.15	1.85	1.95	1.47	.77
195'-0"	y	1.10	1.89	1.98	1.55	.74
195'-0"	z	.53	.69	.69	.71	.37

MEDIAN RESPONSE
RADWASTE/TURBINE BUILDING
ACCELERATION RANGE 1 (g)

MASS C.G.

el.	dir.	2-5 (Hz)	5-10 (Hz)	7 (Hz)	10 (Hz)	zpa
116'-0"	x	.25	.21	.22	.18	.12
116'-0"	y	.25	.21	.22	.18	.12
116'-0"	z	.16	.17	.18	.14	.08
135'-0"	x	.27	.29	.30	.24	.15
135'-0"	y	.26	.25	.26	.22	.13
135'-0"	z	.16	.17	.18	.15	.09
150'-0"	x	.29	.38	.38	.33	.18
150'-0"	y	.27	.30	.30	.28	.16
150'-0"	z	.17	.18	.19	.16	.09
165'-0"	x	.30	.44	.44	.40	.20
165'-0"	y	.28	.34	.34	.35	.18
165'-0"	z	.17	.19	.19	.16	.10

CONTROL ROOM

el.	dir.	2-5 (Hz)	5-10 (Hz)	7 (Hz)	10 (Hz)	zpa
135'-0"	x	.28	.34	.34	.28	.16
135'-0"	y	.26	.25	.26	.22	.13
135'-0"	z	.17	.19	.19	.16	.09
150'-0"	x	.29	.41	.41	.36	.19
150'-0"	y	.27	.30	.30	.28	.16
150'-0"	z	.17	.19	.20	.17	.10
165'-0"	x	.30	.45	.45	.41	.20
165'-0"	y	.28	.34	.34	.35	.18
165'-0"	z	.17	.19	.20	.18	.10

MEDIAN RESPONSE
RADWASTE/TURBINE BUILDING
ACCELERATION RANGE 2 (g)

MASS C.G.

el.	dir.	2-5 (Hz)	5-10 (Hz)	7 (Hz)	10 (Hz)	zpa
116'-0"	x	.50	.43	.46	.36	.25
116'-0"	y	.50	.43	.46	.36	.25
116'-0"	z	.33	.34	.38	.28	.17
135'-0"	x	.54	.57	.61	.49	.29
135'-0"	y	.52	.50	.53	.45	.27
135'-0"	z	.33	.35	.40	.29	.17
150'-0"	x	.58	.73	.78	.67	.35
150'-0"	y	.54	.58	.61	.57	.31
150'-0"	z	.33	.36	.41	.31	.19
165'-0"	x	.60	.84	.89	.81	.39
165'-0"	y	.56	.66	.69	.69	.35
165'-0"	z	.34	.38	.42	.33	.19

CONTROL ROOM

el.	dir.	2-5 (Hz)	5-10 (Hz)	7 (Hz)	10 (Hz)	zpa
135'-0"	x	.56	.65	.69	.58	.32
135'-0"	y	.52	.50	.53	.45	.27
135'-0"	z	.33	.37	.41	.32	.18
150'-0"	x	.58	.78	.83	.73	.36
150'-0"	y	.54	.58	.61	.57	.31
150'-0"	z	.34	.38	.42	.34	.19
165'-0"	x	.60	.86	.91	.83	.40
165'-0"	y	.56	.66	.69	.69	.35
165'-0"	z	.34	.39	.43	.35	.20

MEDIAN RESPONSE
RADWASTE/TURBINE BUILDING
ACCELERATION RANGE 3 (g)

MASS C.G.

el.	dir.	2-5 (Hz)	5-10 (Hz)	7 (Hz)	10 (Hz)	zpa
116'-0"	x	.74	.64	.69	.55	.37
116'-0"	y	.74	.64	.69	.55	.37
116'-0"	z	.49	.51	.58	.42	.25
135'-0"	x	.81	.84	.91	.71	.43
135'-0"	y	.78	.75	.80	.66	.40
135'-0"	z	.50	.53	.59	.44	.26
150'-0"	x	.86	1.06	1.14	.96	.51
150'-0"	y	.81	.86	.91	.82	.46
150'-0"	z	.50	.55	.62	.47	.28
165'-0"	x	.90	1.22	1.30	1.15	.58
165'-0"	y	.84	.97	1.02	.99	.51
165'-0"	z	.50	.56	.63	.49	.29

CONTROL ROOM

el.	dir.	2-5 (Hz)	5-10 (Hz)	7 (Hz)	10 (Hz)	zpa
135'-0"	x	.84	.95	1.02	.83	.46
135'-0"	y	.78	.73	.80	.66	.40
135'-0"	z	.50	.55	.62	.48	.27
150'-0"	x	.87	1.12	1.20	1.04	.54
150'-0"	y	.81	.86	.91	.82	.46
150'-0"	z	.50	.57	.64	.50	.28
165'-0"	x	.90	1.23	1.32	1.17	.58
165'-0"	y	.84	.97	1.02	.99	.51
165'-0"	z	.50	.58	.64	.52	.29

MEDIAN RESPONSE
DIESEL GENERATOR BUILDING
ACCELERATION RANGE 1 (g)

el.	dir.	2-5 (Hz)	5-10 (Hz)	7 (Hz)	10 (Hz)	zpa
127'-0"	x	.25	.21	.22	.18	.12
127'-0"	y	.25	.21	.22	.18	.12
127'-0"	z	.16	.17	.18	.14	.08
151'-0"	x	.26	.25	.25	.23	.15
151'-0"	y	.25	.23	.24	.21	.14
151'-0"	z	.16	.17	.18	.14	.09
161'-11"	x	.26	.25	.25	.23	.15
161'-11"	y	.26	.24	.24	.21	.15
161'-11"	z	.16	.17	.18	.14	.09

ACCELERATION RANGE 2 (g)

el.	dir.	2-5 (Hz)	5-10 (Hz)	7 (Hz)	10 (Hz)	zpa
127'-0"	x	.50	.43	.44	.36	.25
127'-0"	y	.50	.43	.44	.36	.25
127'-0"	z	.33	.34	.35	.28	.17
151'-0"	x	.52	.49	.50	.46	.29
151'-0"	y	.51	.46	.47	.41	.28
151'-0"	z	.33	.35	.36	.29	.17
161'-11"	x	.52	.50	.51	.47	.30
161'-11"	y	.51	.47	.48	.42	.29
161'-11"	z	.33	.35	.36	.29	.17

ACCELERATION RANGE 3 (g)

el.	dir.	2-5 (Hz)	5-10 (Hz)	7 (Hz)	10 (Hz)	zpa
127'-0"	x	.74	.64	.66	.54	.37
127'-0"	y	.74	.64	.66	.54	.37
127'-0"	z	.49	.51	.53	.41	.25
151'-0"	x	.77	.74	.76	.68	.44
151'-0"	y	.76	.70	.71	.62	.42
151'-0"	z	.49	.52	.54	.43	.26
161'-11"	x	.78	.75	.76	.69	.45
161'-11"	y	.77	.71	.72	.63	.43
161'-11"	z	.49	.52	.54	.43	.26

MEDIAN RESPONSE
EMERGENCY COOLING TOWERS
ACCELERATION RANGE 1 (g)

el.	dir.	2-5 (Hz)	5-10 (Hz)	7 (Hz)	10 (hz)	zpa
118'-0"	x	.25	.21	.22	.18	.12
118'-0"	y	.25	.21	.22	.18	.12
118'-0"	z	.16	.17	.18	.14	.08
136'-0"	x	.26	.25	.25	.22	.15
136'-0"	y	.27	.30	.31	.27	.15
136'-0"	z	.17	.18	.18	.15	.09
153'-0"	x	.26	.27	.27	.23	.16
153'-0"	y	.28	.36	.36	.34	.18
153'-0"	z	.17	.18	.19	.15	.10
168'-0"	x	.30	.45	.45	.45	.22
168'-0"	y	.29	.42	.42	.44	.20
168'-0"	z	.17	.19	.20	.17	.10
192'-0"	x	.31	.52	.52	.55	.25
192'-0"	y	.31	.54	.53	.64	.27
192'-0"	z	.17	.19	.20	.17	.11
202'-0"	x	.32	.55	.55	.59	.27
202'-0"	y	.32	.57	.56	.70	.30
202'-0"	z	.17	.20	.20	.18	.11

MEDIAN RESPONSE
EMERGENCY COOLING TOWERS
ACCELERATION RANGE 2 (g)

el.	dir.	2-5 (Hz)	5-10 (Hz)	7 (Hz)	10 (Hz)	zpa
118'-0"	x	.50	.43	.44	.36	.25
118'-0"	y	.50	.43	.44	.36	.25
118'-0"	z	.33	.34	.35	[illegible]	.17
136'-0"	x	.52	.50	.51	[illegible]	.29
136'-0"	y	.54	.59	.61	.53	.31
136'-0"	z	.33	.35	.37	.30	.18
153'-0"	x	.53	.53	.54	.46	[illegible]
153'-0"	y	.56	.70	.71	.65	.38
153'-0"	z	.33	.36	.37	.31	.19
168'-0"	x	.60	.87	.87	.84	.42
168'-0"	y	.59	.82	.82	.93	.39
168'-0"	z	.34	.38	.39	.33	.20
192'-0"	x	.62	1.00	1.00	1.02	.48
192'-0"	y	.62	1.02	1.01	1.18	.51
192'-0"	z	.34	.39	.40	.35	.21
202'-0"	x	.63	1.05	[illegible]5	1.10	.50
202'-0"	y	.63	1.09	[illegible]7	1.29	.56
202'-0"	z	.34	.39	[illegible]	.35	.21

MEDIAN RESPONSE
EMERGENCY COOLING TOWERS
ACCELERATION RANGE 3 (g)

el.	dir.	2-5 (Hz)	5-10 (Hz)	7 (Hz)	10 (Hz)	zpa
118'-0"	x	.74	.64	.66	.54	.37
118'-0"	y	.74	.64	.66	.54	.37
118'-0"	z	.49	.51	.53	.41	.25
136'-0"	x	.78	.74	.76	.64	.44
136'-0"	y	.81	.87	.90	.77	.46
136'-0"	z	.50	.53	.55	.45	.27
153'-0"	x	.79	.79	.81	.69	.46
153'-0"	y	.84	1.02	1.03	.94	.51
153'-0"	z	.50	.54	.56	.46	.28
168'-0"	x	.89	1.26	1.27	1.18	.61
168'-0"	y	.88	1.18	1.19	1.17	.58
168'-0"	z	.50	.57	.59	.50	.30
192'-0"	x	.93	1.44	1.44	1.44	.69
192'-0"	y	.93	1.46	1.45	1.64	.73
192'-0"	z	.51	.58	.60	.52	.31
202'-0"	x	.94	1.50	1.51	1.54	.72
202'-0"	y	.95	1.55	1.54	1.80	.79
202'-0"	z	.51	.59	.61	.53	.31

MEDIAN RESPONSE
CIRCULATING WATER PUMP STRUCTURE
ACCELERATION RANGE 1 (g)

el.	dir.	2-5 (Hz)	5-10 (Hz)	7 (Hz)	10 (Hz)	zpa
79'-10"	x	.25	.21	.23	.18	.12
79'-10"	y	.25	.21	.23	.18	.12
79'-10"	z	.16	.17	.19	.14	.08
88'-6"	x	.26	.25	.26	.22	.13
88'-6"	y	.25	.22	.24	.19	.13
88'-6"	z	.16	.17	.19	.14	.08
97'-0"	x	.26	.27	.28	.27	.15
97'-0"	y	.25	.23	.24	.20	.14
97'-0"	z	.16	.17	.19	.14	.08
105'-6"	x	.27	.29	.30	.30	.16
105'-6"	y	.25	.23	.25	.21	.14
105'-6"	z	.16	.17	.20	.14	.09
114'-0"	x	.27	.31	.31	.33	.17
114'-0"	y	.26	.24	.25	.21	.15
114'-0"	z	.16	.17	.20	.14	.09
130'-6"	x	.27	.32	.32	.35	.17
130'-6"	y	.26	.25	.27	.24	.17
130'-6"	z	.16	.17	.20	.15	.09
130'-6"	x	.27	.32	.32	.35	.18
130'-6"	y	.26	.25	.27	.23	.16
130'-6"	z	.17	.19	.21	.17	.10

MEDIAN RESPONSE
CIRCULATING WATER PUMP STRUCTURE
ACCELERATION RANGE 2 (g)

el.	dir.	2-5 (Hz)	5-10 (Hz)	7 (Hz)	10 (Hz)	zpa
79'-10"	x	.50	.43	.46	.36	.25
79'-10"	y	.50	.43	.46	.36	.25
79'-10"	z	.33	.34	.38	.28	.17
88'-6"	x	.51	.49	.52	.44	.27
88'-6"	y	.50	.44	.47	.38	.25
88'-6"	z	.33	.34	.39	.28	.17
97'-0"	x	.53	.54	.56	.52	.29
97'-0"	y	.51	.46	.49	.40	.27
97'-0"	z	.33	.35	.39	.28	.17
105'-6"	x	.53	.58	.60	.59	.31
105'-6"	y	.51	.47	.50	.42	.28
105'-6"	z	.33	.35	.39	.29	.17
114'-0"	x	.54	.61	.62	.64	.33
114'-0"	y	.51	.48	.51	.43	.29
114'-0"	z	.33	.35	.39	.29	.17
130'-6"	x	.55	.62	.64	.67	.34
130'-6"	y	.52	.51	.54	.47	.33
130'-6"	z	.33	.35	.39	.29	.18
130'-6"	x	.55	.63	.64	.68	.34
130'-6"	y	.52	.50	.53	.47	.32
130'-6"	z	.34	.38	.43	.33	.20

MEDIAN RESPONSE
CIRCULATING WATER PUMP STRUCTURE
ACCELERATION RANGE 3 (g)

el.	dir.	2-5 (Hz)	5-10 (Hz)	7 (Hz)	10 (Hz)	zpa
79'-10"	x	.74	.64	.69	.55	.37
79'-10"	y	.74	.64	.69	.55	.37
79'-10"	z	.49	.51	.58	.42	.25
88'-6"	x	.77	.73	.78	.65	.40
88'-6"	y	.75	.67	.71	.58	.38
88'-6"	z	.49	.51	.58	.42	.25
97'-0"	x	.79	.80	.84	.77	.44
97'-0"	y	.76	.69	.73	.60	.40
97'-0"	z	.49	.52	.58	.43	.25
105'-6"	x	.80	.86	.90	.86	.46
105'-6"	y	.76	.70	.75	.63	.42
105'-6"	z	.49	.52	.59	.43	.26
114'-0"	x	.81	.90	.93	.93	.49
114'-0"	y	.77	.72	.76	.64	.43
114'-0"	z	.49	.52	.59	.43	.26
130'-6"	x	.82	.93	.96	.98	.51
130'-6"	y	.78	.76	.80	.70	.49
130'-6"	z	.49	.52	.59	.44	.26
130'-6"	x	.82	.93	.96	.99	.51
130'-6"	y	.78	.76	.80	.70	.48
130'-6"	z	.51	.57	.64	.50	.30

MEDIAN RESPONSE
FREE-FIELD RESPONSE

ACCELERATION RANGE 1 (g)

dir.	2-5 (Hz)	5-10 (Hz)	7 (Hz)	10 (Hz)	zpa
x	.25	.21	.22	.18	.12
y	.25	.21	.22	.18	.12
z	.16	.17	.18	.14	.08

ACCELERATION RANGE 2 (g)

dir.	2-5 (Hz)	5-10 (Hz)	7 (Hz)	10 (Hz)	zpa
x	.50	.43	.46	.36	.24
y	.50	.43	.46	.36	.24
z	.33	.34	.38	.28	.16

ACCELERATION RANGE 3 (g)

dir.	2-5 (Hz)	5-10 (Hz)	7 (Hz)	10 (Hz)	zpa
x	.74	.64	.69	.55	.36
y	.74	.64	.69	.55	.36
z	.49	.51	.58	.42	.24

APPENDIX C

FILES FOR PEACH BOTTOM SEISMIC ANALYSIS

Fragility File

Response File

Accident Sequence Expressions

Cross-Reference File

PEACH BOTTOM FRAGILITIES FILE

No.	A_F	β_r	β_u	Category
1	0.25	0.25	.25	CERAMIC INSULATORS
2	4.00	0.48	.75	RELAY CHATTER
3	7.63	0.48	.74	CIRCUIT BREAKER TRIP
4	2.50	0.40	.39	BATTERIES
5	2.29	0.31	.39	BATTERY RACKS
6	2.00	0.26	.35	INVERTORS
7	8.80	0.28	.30	TRANSFORMERS
8	7.63	0.48	.74	MOTOR CONTROL CENTER
9	7.63	0.48	.66	AUX RELAY CABINET
10	6.43	0.29	.66	SWITCHGEAR
11	2.23	0.34	.19	CABLE TRAYS
12	11.50	0.46	.74	CONTROL PANELS AND RACKS
13	7.68	0.20	.35	LOCAL INSTRUMENTS
14	1.00	0.25	.31	DIESEL GENERATOR
15	12.10	0.27	.31	MOTORS-HORIZONTAL
16	2.80	0.25	.27	MOTOR-DRIVEN PUMPS & COMPRESSORS
17	2.21	0.22	.32	LG. VERT. M-D. CENTRIF PUMP
18	6.50	0.26	.60	LMOV
19	4.83	0.26	.60	SMALL MOV & AOVs
20	6.50	0.26	.34	LG. PNEUM/HYD VALVE
21	8.90	0.20	.35	LG. MANUAL,CHECK,RELIEF VALVE
22	12.50	0.33	.43	MISC. SMALL VALVES
23	3.00	0.30	.53	LG. HORIZ. VESSELS
24	1.84	0.25	.45	SM-MED HEAT EXCHANGERS & VESSELS
25	1.46	0.20	.35	LG. VERT VESSELS w/ FORMED HEADS
26	0.45	0.35	.29	LG. VERT. FLAT BOTTOMED TANKS
27	6.90	0.27	.31	AIR HANDLING UNITS
28	1.95	0.26	.28	BWR REACTOR SKIRT (GENERIC)
29	0.95892	0.50	.30	SLOCA FIT (SSMRP)
30	1.4967	0.4681	.30	MLOCA FIT (SSMRP)
31	1.26	0.35	.40	BWR RECIRC PUMP SUPPORT (GENERIC)
32	1.00	0.04	.17	DIKE AROUND CST AND RWST
33	0.55	0.11	.21	EMERGENCY COOLING TOWER (PEACH)
34	1.6	0.16	.27	REACTOR BLDG. SHEAR WALLS
35	1.2	0.10	.23	RADWASTE/TURBINE ROOF DIAPHRAGM
36	1.5	0.13	.25	RADWASTE/TURBINE SHEAR WALLS
37	0.50	0.11	.21	TURBINE BLDG.
38	1.5	0.13	.24	BLOCK WALLS-VARIOUS
39	99.0	0.3	.30	DUMMY EVENT-CAUSES NO SEISMIC FAILURE
40	0.01	0.3	.30	DUMMY EVENT-CAUSES FAILURE PF=1
41	3.30	0.15	.25	4KV BUSSES (PEACH BOTTOM)
42	0.95	0.15	.20	DG DAY TANKS
43	4.42	0.15	.25	HPCI ROOM COOLER

PEACH BOTTOM RESPONSE MULTIPLE FILE

No.	Mr/pga	βrr	βru	Response
1	1.00	0.25	.25	FREE-FIELD ZPA
2	2.08	0.45	.25	2-5 HZ
3	1.90	0.45	.25	5
4	1.78	0.35	.25	5-10
5	1.90	0.35	.25	"
6	1.20	0.35	.25	CS 135 ZPA
7	2.50	0.45	.25	5-10 HZ
8	1.40	0.35	.25	150 ZPA
9	3.00	0.45	.25	5-10
10	1.60	0.35	.25	165 ZPA
11	3.30	0.45	.25	5-10
12	1.00	0.35	.25	RB 91 ZPA
13	1.80	0.45	.25	5-10
14	1.80	0.45	.25	7
15	1.80	0.45	.25	5
16	1.10	0.35	.25	116 ZPA
17	2.10	0.45	.25	7
18	1.10	0.35	.25	135 ZPA
19	2.10	0.45	.25	7
20	1.30	0.35	.25	165 ZPA
21	3.00	0.45	.25	7
22	1.00	0.35	.25	DG 127 ZPA
23	1.80	0.45	.25	5-10
24	1.80	0.45	.25	5
25	1.00	0.35	.25	TB 116 ZPA
26	1.90	0.45	.25	7
27	1.30	0.35	.25	CWPS 114 ZPA
28	2.40	0.45	.25	7
29	1.40	0.35	.25	ECT 153 ZPA
30	2.60	0.45	.25	7
31	2.60	0.45	.25	5
32	1.00	0.00	.25	DUMMY RESPONSE FOR M & S LOCA

PEACH BOTTOM ACCIDENT SEQUENCES

```
LOSP = CERAMIC-INSULATORS
CBAR = 1.0
Q = 0.01
MBAR = 1.0
P1 = 0.096
P2 = 0.002
P3 = 0.0002
PBAR = 1.0-(P1+P2+P3)
BBAR = 1.0
X1BAR = 1.0

BOOLEAN 4 FAILS ALL ESW AND GIVEN LOSP, CAUSES SBO

BOOL(4) =
ACP-CCF-2-4KV * TURBINE-BLDG +
ACP-CCF-2-4KV * EMER-COOL-TOWER +
ACP-DGN-LP-EDGB * ACP-CCF-2-4KV +
ACP-DGN-LP-EDGD * ACP-CCF-2-4KV +
ACP-DGN-LP-EDGC * ACP-CCF-2-4KV +
ESW-MDP-FS-MDPA * ACP-BAC-LP-416C * TURBINE-BLDG +
ESW-MDP-FS-MDPB * ACP-BAC-LP-416B * TURBINE-BLDG +
ACP-BAC-LP-416D * ESW-CCF-PF-MDPS +
ACP-DGN-LP-EDGB * ACP-BAC-LP-416C * TURBINE-BLDG +
ACP-DGN-LP-EDGC * ACP-BAC-LP-416B * TURBINE-BLDG +
ESW-MDP-FS-MDPA * ACP-BAC-LP-416C * EMER-COOL-TOWER +
ESW-MDP-FS-MDPB * ACP-BAC-LP-416B * EMER-COOL-TOWER +
ACP-DGN-LP-EDGB * ACP-BAC-LP-416C * EMER-COOL-TOWER +
ACP-DGN-LP-EDGC * ACP-BAC-LP-416B * EMER-COOL-TOWER +
ESW-MDP-FS-MDPA * ESW-MDP-FS-ECW * ACP-BAC-LP-416C +
ESW-MDP-FS-MDPB * ESW-MDP-FS-ECW * ACP-BAC-LP-416B +
ACP-DGN-LP-EDGC * ESW-MDP-FS-ECW * ACP-BAC-LP-416B +
ACP-DGN-LP-EDGB * ESW-MDP-FS-ECW * ACP-BAC-LP-416C +
ACP-DGN-LP-EDGB * ESW-MDP-FS-MDPB * ACP-BAC-LP-416D +
ACP-DGN-LP-EDGD * ESW-MDP-FS-MDPB * ACP-BAC-LP-416B +
ACP-DGN-LP-EDGC * ESW-MDP-FS-MDPA * ACP-BAC-LP-416D +
ACP-DGN-LP-EDGD * ESW-MDP-FS-MDPA * ACP-BAC-LP-416C +
ESW-MDP-FS-ECW * ESW-CCF-PF-MDPS +
ESW-CCF-2-MDPS * TURBINE-BLDG +
ESW-CCF-2-MDPS * EMER-COOL-TOWER +
ACP-CCF-LP-DGS +
ACP-DGN-FR-EDGD * ACP-CCF-2-4KV +
ACP-DGN-FR-EDGB * ACP-CCF-2-4KV +
ACP-DGN-FR-EDGC * ACP-CCF-2-4KV +
ACP-CCF-2-DGS * ACP-BAC-LP-416D +
ACP-CCF-2-DGS * ACP-BAC-LP-416B +
```

BOOL(4) Cont'd

```
ACP-CCF-2-DGS * ACP-BAC-LP-416C +
ACP-DGN-LP-EDGC * ESW-MDP-FS-MDPA * TURBINE-BLDG +
ACP-DGN-LP-EDGB * ESW-MDP-FS-MDPB * TURBINE-BLDG +
ACP-DGN-LP-EDGD * ESW-CCF-PF-MDPS +
ACP-DGN-FR-EDGC * ACP-BAC-LP-416B * TURBINE-BLDG +
ACP-DGN-FR-EDGB * ACP-BAC-LP-416C * TURBINE-BLDG +
ACP-CCF-2-DGS * TURBINE-BLDG +
ACP-BAC-LP-416B * DCP-BDC-LP-125C * TURBINE-BLDG +
DCP-BDC-LP-125B * ACP-BAC-LP-416C * TURBINE-BLDG +
ACP-DGN-LP-EDGC * ESW-MDP-FS-MDPA * EMER-COOL-TOWER +
ACP-DGN-LP-EDGB * ESW-MDP-FS-MDPB * EMER-COOL-TOWER +
ACP-DGN-FR-EDGC * ACP-BAC-LP-416B * EMER-COOL-TOWER +
ACP-DGN-FR-EDGB * ACP-BAC-LP-416C * EMER-COOL-TOWER +
ACP-CCF-2-DGS * EMER-COOL-TOWER +
ACP-BAC-LP-416B * DCP-BDC-LP-125C * EMER-COOL-TOWER +
DCP-BDC-LP-125B * ACP-BAC-LP-416C * EMER-COOL-TOWER +
ACP-DGN-LP-EDGC * ESW-MDP-FS-MDPA * ESW-MDP-FS-ECW +
ACP-DGN-LP-EDGB * ESW-MDP-FS-MDPB * ESW-MDP-FS-ECW +
ACP-DGN-MA-EDGC * ACP-CCF-2-4KV +
ACP-DGN-MA-EDGD * ACP-CCF-2-4KV +
ACP-DGN-MA-EDGB * ACP-CCF-2-4KV +
DCP-BAT-LP-B2 * ACP-BAC-LP-416C * TURBINE-BLDG +
ACP-BAC-LP-416B * DCP-BAT-LP-C3 * TURBINE-BLDG +
DCP-BAT-LP-B2 * ACP-BAC-LP-416C * EMER-COOL-TOWER +
ACP-BAC-LP-416B * DCP-BAT-LP-C3 * EMER-COOL-TOWER +
ACP-CCF-2-4KV * ESW-TNK-LL-PS13 +
ACP-DGN-FR-EDGC * ESW-MDP-FS-ECW * ACP-BAC-LP-416B +
ACP-DGN-FR-EDGB * ESW-MDP-FS-ECW * ACP-BAC-LP-416C +
ACP-CCF-2-DGS * ESW-MDP-FS-ECW +
ACP-DGN-FR-EDGB * ESW-MDP-FS-MDPB * ACP-BAC-LP-416D +
ACP-DGN-FR-EDGC * ESW-MDP-FS-MDPA * ACP-BAC-LP-416D +
ACP-DGN-FR-EDGD * ESW-MDP-FS-MDPA * ACP-BAC-LP-416C +
ACP-DGN-FR-EDGD * ESW-MDP-FS-MDPB * ACP-BAC-LP-416B +
ACP-CCF-2-DGS * ESW-MDP-FS-MDPA +
ACP-CCF-2-DGS * ESW-MDP-FS-MDPB +
ACP-DGN-MA-EDGB * ACP-BAC-LP-416C * TURBINE-BLDG +
ACP-DGN-MA-EDGC * ACP-BAC-LP-416B * TURBINE-BLDG +
ACP-DGN-MA-EDGB * ACP-BAC-LP-416C * EMER-COOL-TOWER +
ACP-DGN-MA-EDGC * ACP-BAC-LP-416B * EMER-COOL-TOWER
```

```
BOOL 5 = BOOL 4 BUT NO DG'S

BOOL(5) =
ACP-CCF-2-4KV * TURBINE-BLDG +
ACP-CCF-2-4KV * EMER-COOL-TOWER +
ESW-MDP-FS-MDPA * ACP-BAC-LP-416C * TURBINE-BLDG +
ESW-MDP-FS-MDPB * ACP-BAC-LP-416B * TURBINE-BLDG +
ESW-MDP-FS-MDPA * ACP-BAC-LP-416C * EMER-COOL-TOWER +
ESW-MDP-FS-MDPB * ACP-BAC-LP-416B * EMER-COOL-TOWER +
ACP-BAC-LP-416B * ESW-CCF-PF-MDPS +
ESW-MDP-FS-MDPA * ESW-MDP-FS-ECW * ACP-BAC-LP-416C +
ESW-MDP-FS-MDPB * ESW-MDP-FS-ECW * ACP-BAC-LP-416B +
ESW-CCF-PF-MDPS * TURBINE-BLDG +
ESW-CCF-PF-MDPS * EMER-COOL-TOWER +
ESW-MDP-FS-ECW * ESW-CCF-PF-MDPS +
ACP-BAC-LP-416B * DCP-BDC-LP-125C * TURBINE-BLDG +
DCP-BDC-LP-125B * ACP-BAC-LP-416C * TURBINE-BLDG +
DCP-BAT-LP-B2 * ACP-BAC-LP-416C * TURBINE-BLDG +
ACP-BAC-LP-416B * DCP-BAT-LP-C3 * TURBINE-BLDG +
ACP-BAC-LP-416B * DCP-BDC-LP-125C * EMER-COOL-TOWER +
DCP-BDC-LP-125B * ACP-BAC-LP-416C * EMER-COOL-TOWER +
DCP-BAT-LP-B2 * ACP-BAC-LP-416C * EMER-COOL-TOWER +
ACP-BAC-LP-416B * DCP-BAT-LP-C3 * EMER-COOL-TOWER +
ACP-CCF-2-4KV * ESW-TNK-LL-PS13

BOOL 6 = BOOL 4 WITH 4KV-C BUT NO DG'S

BOOL(6) =
ACP-CCF-2-4KV * TURBINE-BLDG +
ACP-CCF-2-4KV * EMER-COOL-TOWER +
ESW-MDP-FS-MDPA * ACP-BAC-LP-416C * TURBINE-BLDG +
ESW-MDP-FS-MDPA * ACP-BAC-LP-416C * EMER-COOL-TOWER +
ESW-MDP-FS-MDPA * ESW-MDP-FS-ECW * ACP-BAC-LP-416C +
DCP-BDC-LP-125B * ACP-BAC-LP-416C * TURBINE-BLDG +
DCP-BAT-LP-B2 * ACP-BAC-LP-416C * TURBINE-BLDG +
DCP-BDC-LP-125B * ACP-BAC-LP-416C * EMER-COOL-TOWER +
DCP-BAT-LP-B2 * ACP-BAC-LP-416C * EMER-COOL-TOWER +
ACP-CCF-2-4KV * ESW-TNK-LL-PS13
```

```
BOOL 7 = BOOL 4 with TURBINE BLDG BUT NO DG'S

BOOL(7) =
ACP-CCF-2-4KV * TURBINE-BLDG +
ESW-MDP-FS-MDPA * ACP-BAC-LP-416C * TURBINE-BLDG +
ESW-MDP-FS-MDPB * ACP-BAC-LP-416B * TURBINE-BLDG +
ESW-CCF-2-MDPS * TURBINE-BLDG +
ACP-CCF-2-4KV * EMER-COOL-TOWER +
ESW-MDP-FS-MDPA * ACP-BAC-LP-416C * EMER-COOL-TOWER +
ESW-MDP-FS-MDPB * ACP-BAC-LP-416B * EMER-COOL-TOWER +
ESW-CCF-2-MDPS * EMER-COOL-TOWER



SEQUENCE 1 RVR-1
ACC(1) = IE(1)

SEQUENCE 2 ALOCA-17
ACC(2) = IE(2)*CBAR*NLOSP*BOOL(5)

SEQUENCE 3 ALOCA-30
ACC(3) = IE(2)*CBAR*LOSP*(BOOL(4)+RADWASTE/TB-ROOF)

SEQUENCE 4 S1LOCA-25
ACC(4) = IE(3)*CBAR*NLOSP*BOOL(6)

SEQUENCE 5  S1LOCA-70
ACC(5) = IE(3)*CBAR*LOSP*BOOL(4)

SEQUENCE 6 S1LOCA-80
ACC(6) = IE(3)*CBAR*LOSP*RADWASTE/TB-ROOF

SEQUENCE 7 S2LOCA-
ACC(7) = IE(4)*CBAR*NLOSP*BOOL(7)

SEQUENCE 8 S2LOCA-42
ACC(8) = IE(4)*CBAR*LOSP*RADWASTE/TB-ROOF

SEQUENCE 9 RWT-1
ACC(9) = IE(5)*CBAR*MBAR*PBAR

SEQUENCE 10 RWT-2
ACC(10) = IE(5)*CBAR*MBAR*P1

SEQUENCE 11 RWT-3
ACC(11) = IE(5)*CBAR*MBAR*P2
```

```
SEQUENCE 12 RWT-4
ACC(12) = IE(5)*CBAR*MBAR*P3

SEQUENCE 13  LOSP-SEQ5P
ACC(13) =  ACP-BAC-LP-416C *DCP-BDC-LP-125C*DCP-BDC-LP-125D
ACC(13) =  IE(6)*BBAR*X1BAR*ACC(13)

SEQUENCE #  14 LOSP-SEQ2P
ACC(14) =
ACP-CCF-2-4KV * ADS-LOG-HW-INHIB +
ACP-DGN-LP-EDGA * ACP-BAC-LP-416B * ADS-LOG-HW-INHIB +
ACP-DGN-LP-EDGB * ACP-BAC-LP-416A * ADS-LOG-HW-INHIB +
ACP-BAC-LP-416A * CRD-XHE-FO-BRKRS * ADS-LOG-HW-INHIB * HCI-TDP-FS-20S37 +
ACP-BAC-LP-416A * RBC-XHE-FO-SWCH * ADS-LOG-HW-INHIB * HCI-TDP-FS-20S37 +
ACP-BAC-LP-416A * ESF-XHE-FO-DEPRE * ADS-LOG-HW-INHIB * HCI-TDP-FS-20S37 +
ACP-BAC-LP-416B * CRD-XHE-FO-BRKRS * ADS-LOG-HW-INHIB * RCI-TDP-FS-20S38 +
ACP-BAC-LP-416B * RBC-XHE-FO-SWCH * ADS-LOG-HW-INHIB * RCI-TDP-FS-20S38 +
RBC-XHE-FO-LCVAL * ACP-BAC-LP-416B * ADS-LOG-HW-INHIB * RCI-TDP-FS-20S38 +
RBC-XHE-FO-LCVAL * ACP-BAC-LP-416A * ADS-LOG-HW-INHIB * HCI-TDP-FS-20S37 +
ACP-BAC-LP-416A * CRD-XHE-FO-BRKRS * ADS-LOG-HW-INHIB * HCI-TDP-FR-20S37 +
ACP-BAC-LP-416A * RBC-XHE-FO-SWCH * ADS-LOG-HW-INHIB * HCI-TDP-FR-20S37 +
RBC-XHE-FO-LCVAL * ACP-BAC-LP-416A * ADS-LOG-HW-INHIB * HCI-TDP-FR-20S37 +
ACP-BAC-LP-416A * ESF-XHE-FO-DEPRE * ADS-LOG-HW-INHIB * HCI-TDP-FR-20S37 +
ACP-BAC-LP-416B * CRD-XHE-FO-BRKRS * ADS-LOG-HW-INHIB * RCI-TDP-FR-20S38 +
ACP-BAC-LP-416B * RBC-XHE-FO-SWCH * ADS-LOG-HW-INHIB * RCI-TDP-FR-20S38 +
RBC-XHE-FO-LCVAL * ACP-BAC-LP-416B * ADS-LOG-HW-INHIB * RCI-TDP-FR-20S38
ACC(14) = IE(6)*BBAR*ACC(14)

SEQUENCE #  15 LOSP-SEQ1P
ACC(15) = IE(6)*CBAR*MBAR*PBAR*BOOL(4)

SEQUENCE # 16 T1S2-SEQ2P
ACC(16) = ACP-BAC-LP-416C * DCP-BDC-LP-125C * DCP-BDC-LP-125D
ACC(16) = IE(6)*P1*BBAR*X1BAR*ACC(16)
```

```
SEQUENCE # 17 T1S2-SEQ1P
ACC(17) =
ACP-CCF-2-4KV * ADS-LOG-HW-INHIB +
ACP-DGN-LP-EDGA * ACP-BAC-LP-416B * ADS-LOG-HW-INHIB +
ACP-DGN-LP-EDGB * ACP-BAC-LP-416A * ADS-LOG-HW-INHIB +
ACP-BAC-LP-416A * ESF-XHE-FO-DEPRE * ADS-LOG-HW-INHIB * HCI-TDP-FS-20S37 +
ACP-BAC-LP-416A * CRD-XHE-FO-BRKRS * ADS-LOG-HW-INHIB * HCI-TDP-FS-20S37 +
ACP-BAC-LP-416B * ESF-XHE-FO-DEPRE * ADS-LOG-HW-INHIB * RCI-TDP-FS-20S38 +
ACP-BAC-LP-416A * RBC-XHE-FO-SWCH * ADS-LOG-HW-INHIB * HCI-TDP-FS-20S37 +
RBC-XHE-FO-LCVAL * ACP-BAC-LP-416A * ADS-LOG-HW-INHIB * HCI-TDP-FS-20S37 +
ACP-BAC-LP-416B * CRD-XHE-FO-BRKRS * ADS-LOG-HW-INHIB * RCI-TDP-FS-20S38 +
ACP-BAC-LP-416B * RBC-XHE-FO-SWCH * ADS-LOG-HW-INHIB * RCI-TDP-FS-20S38 +
RBC-XHE-FO-LCVAL * ACP-BAC-LP-416B * ADS-LOG-HW-INHIB * RCI-TDP-FS-20S38 +
RBC-XHE-FO-LCVAL * ACP-BAC-LP-416A * ADS-LOG-HW-INHIB * HCI-TDP-FR-20S37 +
ACP-BAC-LP-416B * CRD-XHE-FO-BRKRS * ADS-LOG-HW-INHIB * RCI-TDP-FR-20S38 +
ACP-BAC-LP-416B * RBC-XHE-FO-SWCH * ADS-LOG-HW-INHIB * RCI-TDP-FR-20S38 +
ACP-BAC-LP-416A * ESF-XHE-FO-DEPRE * ADS-LOG-HW-INHIB * HCI-TDP-FR-20S37 +
ACP-BAC-LP-416A * CRD-XHE-FO-BRKRS * ADS-LOG-HW-INHIB * HCI-TDP-FR-20S37
ACC(17) = IE(6)*P1*BBAR*ACC(17)

SEQUENCE # 18 T1S1-SEQ2P
ACC(18) =    RHR-CCF-PF-MDPS * ACP-CCF-2-4KV
ACC(18) = IE(6)*P2*BBAR*X1BAR*ACC(18)

SEQUENCE # 19 T1S1-SEQ1P
ACC(19) =
ACP-CCF-2-4KV * ADS-LOG-HW-INHIB +
ACP-BAC-LP-416B * RBC-XHE-FO-SWCH * ADS-LOG-HW-INHIB +
RBC-XHE-FO-LCVAL * ACP-BAC-LP-416B * ADS-LOG-HW-INHIB +
ACP-BAC-LP-416B * CRD-XHE-FO-BRKRS * ADS-LOG-HW-INHIB +
ACP-BAC-LP-416B * ESF-XHE-FO-DEPRE * ADS-LOG-HW-INHIB +
ACP-DGN-LP-EDGA * ACP-BAC-LP-416B * ADS-LOG-HW-INHIB +
ACP-DGN-LP-EDGB * ACP-BAC-LP-416A * ADS-LOG-HW-INHIB
ACC(19) = IE(6)*P2*BBAR*ACC(19)

SEQUENCE #  20 A-SEQ1P
ACC(20) =
RHR-CCF-PF-MDPS * ACP-CCF-2-4KV +
RHR-CCF-PF-MDPS * ACP-CCF-2-4KV +
RHR-CCF-PF-MDPS * ACP-CCF-2-4KV
ACC(20) = IE(2)*BBAR*ACC(20)
```

```
SEQUENCE # 21   T3A-SEQ1P
ACC(21) =
ACP-CCF-2-4KV * ESF-XHE-FO-DEPRE * ADS-LOG-HW-INHIB +
ACP-CCF-3-4KV * TURBINE-BLDG * ESF-XHE-FO-DEPRE +
ACP-CCF-3-4KV * TURBINE-BLDG * ESF-XHE-FO-DEPRE +
ACP-CCF-2-4KV * TURBINE-BLDG * ESF-XHE-FO-DEPRE * CRD-XHE-FO-CRD +
ESW-MDP-FS-MDPB * ACP-CCF-2-4KV * TURBINE-BLDG * ESF-XHE-FO-DEPRE +
ESW-MDP-FS-MDPA * ACP-CCF-2-4KV * TURBINE-BLDG * ESF-XHE-FO-DEPRE +
ESW-MDP-FS-MDPA * ACP-CCF-2-4KV * TURBINE-BLDG * ESF-XHE-FO-DEPRE +
ESW-MDP-FS-MDPB * ACP-CCF-2-4KV * TURBINE-BLDG * ESF-XHE-FO-DEPRE +
ACP-CCF-3-4KV * EMER-COOL-TOWER * ESF-XHE-FO-DEPRE +
ACP-CCF-3-4KV * EMER-COOL-TOWER * ESF-XHE-FO-DEPRE +
ACP-CCF-2-4KV * EMER-COOL-TOWER * ESF-XHE-FO-DEPRE * CRD-XHE-FO-CRD +
ESW-MDP-FS-MDPB * ACP-CCF-2-4KV * EMER-COOL-TOWER * ESF-XHE-FO-DEPRE +
ESW-MDP-FS-MDPA * ACP-CCF-2-4KV * EMER-COOL-TOWER * ESF-XHE-FO-DEPRE +
ESW-MDP-FS-MDPA * ACP-CCF-2-4KV * EMER-COOL-TOWER * ESF-XHE-FO-DEPRE +
ESW-MDP-FS-MDPB * ACP-CCF-2-4KV * EMER-COOL-TOWER * ESF-XHE-FO-DEPRE
ACC(21) = IE(7)*CBAR*Q*MBAR*PBAR*ACC(21)

SEQUENCE #  22  T3A-SEQ2P
ACC(22) =
ACP-CCF-2-4KV * TURBINE-BLDG * CDS-SYS-FC-COND +
ACP-CCF-2-4KV * TURBINE-BLDG * IAS-PTF-HW-IAS +
ESW-MDP-FS-MDPA * ACP-BAC-LP-416C * TURBINE-BLDG * CDS-SYS-FC-COND +
ESW-MDP-FS-MDPB * ACP-CCF-2-4KV * TURBINE-BLDG * CDS-SYS-FC-COND +
ACP-CCF-2-4KV * EMER-COOL-TOWER * CDS-SYS-FC-COND +
ACP-CCF-2-4KV * EMER-COOL-TOWER * IAS-PTF-HW-IAS +
ESW-MDP-FS-MDPA * ACP-BAC-LP-416C * EMER-COOL-TOWER * CDS-SYS-FC-COND +
ESW-MDP-FS-MDPB * ACP-CCF-2-4KV * EMER-COOL-TOWER * CDS-SYS-FC-COND
ACC(22) = IE(7)*CBAR*Q*MBAR*PBAR*X1BAR*ACC(22)
```

PEACH BOTTOM CROSS REFERENCE FILE

Prandom	Basic Event	EF	Nfrag	Nresp	Ncorr	No.
2.000E-04	LOSP	3.0	1	1		1
1.610E-03	DGACTA		3	23		2
1.610E-03	DGACTB					3
1.610E-03	DGACTC					4
1.610E-03	DGACTD					5
1.000E-03	ESF-ACS-FC-MDPA		3	11		6
1.000E-03	ESF-ACS-FC-MDPB					7
1.610E-03	ADS-ACT-HW-DIV1					8
1.610E-03	ADS-ACT-HW-DIV2					9
1.610E-03	HCI-ACT-HW-HPCI					10
1.610E-03	HCI-ACT-HW-LOCST					11
1.610E-03	LCI-ACT-HW-DIV1					12
1.610E-03	LCI-ACT-HW-DIV2					13
1.610E-03	LCS-ACT-HW-LOOPA					14
1.610E-03	LCS-ACT-HW-LOOPB					15
1.000E-03	RCI-ACT-HW-LOCST					16
1.610E-03	RCI-ACT-HW-RCIC					17
5.000E-05	ESW-ACX-FC-HX1		24	12		18
5.000E-05	ESW-ACX-FC-HX10					19
5.000E-05	ESW-ACX-FC-HX12					20
5.000E-05	ESW-ACX-FC-HX13					21
5.000E-05	ESW-ACX-FC-HX15					22
5.000E-05	ESW-ACX-FC-HX16					23
5.000E-05	ESW-ACX-FC-HX18					24
5.000E-05	ESW-ACX-FC-HX19					25
5.000E-05	ESW-ACX-FC-HX2					26
5.000E-05	ESW-ACX-FC-HX21					27
5.000E-05	ESW-ACX-FC-HX22					28
5.000E-05	ESW-ACX-FC-HX24					29
5.000E-05	ESW-ACX-FC-HX25					30
5.000E-05	ESW-ACX-FC-HX27					31
5.000E-05	ESW-ACX-FC-HX28					32
5.000E-05	ESW-ACX-FC-HX3					33
5.000E-05	ESW-ACX-FC-HX4					34
5.000E-05	ESW-ACX-FC-HX6					35
5.000E-05	ESW-ACX-FC-HX7					36
5.000E-05	ESW-ACX-FC-HX9					37
3.750E-04	ESF-ADS-FC-LI13A		3	13		38
3.750E-04	ESF-ADS-FC-LI13B					39
3.750E-04	ESF-ADS-FC-LI13C					40
3.750E-04	ESF-ADS-FC-LI13D					41
1.000E-03	EHV-AOV-CC-AV25		19	22		42
1.000E-03	EHV-AOV-CC-AV27					43
1.000E-03	EHV-AOV-CC-AV28					44

Note: If number in column is blank, use next number above

Prandom	Basic Event	EF	Nfrag	Nresp	Ncorr	No.
1.000E-03	$ EHV-AOV-CC-AV30	$				45
1.000E-03	$ EHV-AOV-CC-AV31	$				46
1.000E-03	$ EHV-AOV-CC-AV33	$				47
1.000E-03	$ EHV-AOV-CC-AV34	$				48
1.000E-03	$ EHV-AOV-CC-AV36	$				49
1.000E-03	$ ESW-AOV-CC-0241A	$	19	12		50
1.000E-03	$ ESW-AOV-CC-0241B	$				51
1.000E-03	$ ESW-AOV-CC-0241C	$				52
1.000E-03	$ ESW-AOV-CC-0241D	$				53
1.000E-03	$ ESW-AOV-CC-AV1	$				54
1.000E-03	$ ESW-AOV-CC-AV10	$				55
1.000E-03	$ ESW-AOV-CC-AV11	$				56
1.000E-03	$ ESW-AOV-CC-AV12	$				57
1.000E-03	$ ESW-AOV-CC-AV13	$				58
1.000E-03	$ ESW-AOV-CC-AV14	$				59
1.000E-03	$ ESW-AOV-CC-AV15	$				60
1.000E-03	$ ESW-AOV-CC-AV16	$				61
1.000E-03	$ ESW-AOV-CC-AV17	$				62
1.000E-03	$ ESW-AOV-CC-AV18	$				63
1.000E-03	$ ESW-AOV-CC-AV19	$				64
1.000E-03	$ ESW-AOV-CC-AV2	$				65
1.000E-03	$ ESW-AOV-CC-AV20	$				66
1.000E-03	$ ESW-AOV-CC-AV3	$				67
1.000E-03	$ ESW-AOV-CC-AV4	$				68
1.000E-03	$ ESW-AOV-CC-AV5	$				69
1.000E-03	$ ESW-AOV-CC-AV6	$				70
1.000E-03	$ ESW-AOV-CC-AV7	$				71
1.000E-03	$ ESW-AOV-CC-AV8	$				72
1.000E-03	$ ESW-AOV-CC-AV9	$				73
2.000E-04	$ ESW-AOV-MA-0241A	$	0	0		74
2.000E-04	$ ESW-AOV-MA-0241B	$				75
2.000E-04	$ ESW-AOV-MA-0241C	$				76
2.000E-04	$ ESW-AOV-MA-0241D	$				77
2.000E-04	$ ESW-AOV-MA-AV1	$				78
2.000E-04	$ ESW-AOV-MA-AV10	$				79
2.000E-04	$ ESW-AOV-MA-AV11	$				80
2.000E-04	$ ESW-AOV-MA-AV12	$				81
2.000E-04	$ ESW-AOV-MA-AV13	$				82
2.000E-04	$ ESW-AOV-MA-AV14	$				83
2.000E-04	$ ESW-AOV-MA-AV15	$				84
2.000E-04	$ ESW-AOV-MA-AV16	$				85
2.000E-04	$ ESW-AOV-MA-AV17	$				86
2.000E-04	$ ESW-AOV-MA-AV18	$				87
2.000E-04	$ ESW-AOV-MA-AV19	$				88
2.000E-04	$ ESW-AOV-MA-AV2	$				89
2.000E-04	$ ESW-AOV-MA-AV20	$				90

Prandom		Basic Event		EF	Nfrag	Nresp	Ncorr	No.
2.000E-04	$	ESW-AOV-MA-AV3	$					91
2.000E-04	$	ESW-AOV-MA-AV4	$					92
2.000E-04	$	ESW-AOV-MA-AV5	$					93
2.000E-04	$	ESW-AOV-MA-AV6	$					94
2.000E-04	$	ESW-AOV-MA-AV7	$					95
2.000E-04	$	ESW-AOV-MA-AV8	$					96
2.000E-04	$	ESW-AOV-MA-AV9	$					97
1.000E-03	$	RBC-AOV-FT-A2352	$		19	16		98
1.000E-03	$	RBC-AOV-FT-A2354	$					99
1.000E-03	$	RBC-AOV-FT-A8154	$					100
1.000E-03	$	RBC-AOV-FT-A8156	$					101
2.000E-04	$	RBC-AOV-MA-A2352	$		0	0		102
2.000E-04	$	RBC-AOV-MA-A2354	$					103
2.000E-04	$	RBC-AOV-MA-A8154	$					104
2.000E-04	$	RBC-AOV-MA-A8156	$					105
3.000E-03	$	RBC-AOV-OO-2253	$		19	16		106
2.000E-04	$	RCI-AOV-MA-PCV23	$		0	0		107
3.000E-04	$	RCI-AOV-VF-PCV23	$		19	12		108
3.750E-04	$	ESF-ASD-FC-SC15A	$		13	13		109
3.750E-04	$	ESF-ASD-FC-SC15B	$					110
3.750E-04	$	ESF-ASD-FC-SC15C	$					111
3.750E-04	$	ESF-ASD-FC-SC15D	$					112
3.750E-04	$	ESF-ASD-FC-SDC17	$		13	11		113
3.750E-04	$	ESF-ASD-FC-SDC18	$					114
5.400E-04	$	ESF-ASL-FC-LT72A	$		13	21		115
5.400E-04	$	ESF-ASL-FC-LT72B	$					116
5.400E-04	$	ESF-ASL-FC-LT72C	$					117
5.400E-04	$	ESF-ASL-FC-LT72D	$					118
1.000E-03	$	ESF-ASL-FC-P101A	$					119
1.000E-03	$	ESF-ASL-FC-P101B	$					120
1.000E-03	$	ESF-ASL-FC-P101C	$					121
1.000E-03	$	ESF-ASL-FC-P101D	$					122
1.000E-03	$	ESF-ASL-HW-CSTL1	$		13	4		123
1.000E-03	$	ESF-ASL-HW-CSTL2	$					124
1.000E-03	$	ESF-ASL-HW-CSTL3	$					125
1.000E-03	$	ESF-ASL-HW-CSTL4	$					126
1.000E+00	$	ESF-ASL-LRXLEVEL	$		13	11		127
1.000E-03	$	ESF-ASL-NO-RSXDA	$		13	11		128
1.000E-03	$	ESF-ASL-NO-RSXDB	$					129
1.000E-03	$	ESF-ASP-FC-LH12A	$		13	11		130
1.000E-03	$	ESF-ASP-FC-LH12B	$					131
1.000E-03	$	ESF-ASP-FC-LH12C	$					132
1.000E-03	$	ESF-ASP-FC-LH12D	$					133
1.000E-03	$	ESF-ASP-FC-LSPHC	$		13	11		134
1.000E-03	$	ESF-ASP-FC-LSPRC	$					135
5.000E-04	$	ESF-ASP-FC-P100A	$					136
5.000E-04	$	ESF-ASP-FC-P100B	$					137

Prandom		Basic Event		EF	Nfrag	Nresp	Ncorr	No.
5.000E-04	$	ESF-ASP-FC-P100C	$					138
5.000E-04	$	ESF-ASP-FC-P100D	$					139
1.000E-03	$	ESF-ASP-FC-P101A	$					140
1.000E-03	$	ESF-ASP-FC-P101B	$					141
1.000E-03	$	ESF-ASP-FC-P101C	$					142
1.000E-03	$	ESF-ASP-FC-P101D	$					143
1.000E-03	$	ESF-ASP-FC-P128C	$					144
1.000E-03	$	ESF-ASP-FC-P128D	$					145
1.000E-03	$	ESF-ASP-FC-PL52A	$					146
1.000E-03	$	ESF-ASP-FC-PL52B	$					147
1.000E-03	$	ESF-ASP-FC-PL52C	$					148
1.000E-03	$	ESF-ASP-FC-PL52D	$					149
1.000E+00	$	ESF-ASP-HIDWPRES	$		13	11		150
1.000E-03	$	ESF-ASP-HW-EX72A	$		13	13		151
1.000E-03	$	ESF-ASP-HW-EX72B	$					152
1.000E+00	$	ESF-ASP-NOHDPEL	$		0	0		153
1.000E+00	$	ESF-ASP-NOHDPLT	$					154
5.000E-06	$	ACP-BAC-LP-416A	$	5.0	41	7		155
5.000E-06	$	ACP-BAC-LP-416B	$					156
5.000E-06	$	ACP-BAC-LP-416C	$					157
5.000E-06	$	ACP-BAC-LP-416D	$					158
1.080E-03	$	DCP-BAT-LP-A2	$	3.0	4	6		159
1.080E-03	$	DCP-BAT-LP-B2	$					160
1.080E-03	$	DCP-BAT-LP-C2	$					161
1.080E-03	$	DCP-BAT-LP-C3	$					162
1.080E-03	$	DCP-BAT-LP-D2	$					163
1.080E-03	$	DCP-BAT-LP-D3	$					164
5.000E-06	$	DCP-BDC-LP-125A	$	3.0	3	9		165
5.000E-06	$	DCP-BDC-LP-125B	$					166
5.000E-06	$	DCP-BDC-LP-125C	$					167
5.000E-06	$	DCP-BDC-LP-125D	$					168
3.900E-05	$	ACP-CCF-LP-DGS	$	3.0	42	22	3	169
1.500E-04	$	ADS-CCF-CC-ADSRV	$		20	20	4	170
1.200E-04	$	ADS-CCF-CC-NADSV	$		21	20	4	171
1.000E-04	$	ADS-CCF-LK-ACC	$					172
1.470E-04	$	CSS-CCF-LF-MOVS	$		19	12	4	173
2.500E-06	$	DCP-CCF-LP-BAT	$	10.	4	6	3	174
3.600E-05	$	EHV-CCF-LF-AOVS	$		19	22	3	175
5.500E-05	$	ESW-CCF-LF-AOVS	$		19	12	2	176
9.000E-09	$	ESW-CCF-MC-ECT	$		33	1		177
7.800E-05	$	ESW-CCF-PF-MDPS	$	10.	17	28	2	178
2.880E-05	$	HSW-CCF-LF-MDPS	$					179
9.600E-05	$	HSW-CCF-LF-MOVS	$		19	27	4	180
1.470E-04	$	LCI-CCF-LF-MOVS	$		19	27	2	181
1.470E-04	$	LCS-CCF-LF-MOVS	$		19	12	4	182
3.000E-04	$	LCS-CCF-PF-MDPS	$	10.	16	14	4	183
3.000E-04	$	RHR-CCF-PF-MDPS	$					184

Prandom		Basic Event		EF	Nfrag	Nresp	Ncorr	No.
6.300E-04	$	SLC-CCF-PF-MDPS	$	3.	0	0		185
1.470E-04	$	SPC-CCF-LF-MOVS	$		19	12	2	186
3.000E-03	$	ESW-CKV-CB-C515A	$		0	0		187
3.000E-03	$	ESW-CKV-CB-C515B	$					188
1.500E-02	$	ESW-CKV-CB-CV514	$					189
1.000E-04	$	ESW-CKV-HW-C515A	$		21	12		190
1.000E-04	$	ESW-CKV-HW-C515B	$					191
1.000E-04	$	ESW-CKV-HW-CV506	$					192
1.000E-04	$	ESW-CKV-HW-CV513	$					193
1.000E-04	$	ESW-CKV-HW-CV516	$					194
1.000E-04	$	HCI-CKV-HW-CV32	$					195
1.000E-04	$	HCI-CKV-HW-CV61	$					196
1.000E-04	$	HCI-CKV-HW-CV65	$					197
1.000E-04	$	HSW-CKV-HW-C502A	$		21	27		198
1.000E-04	$	HSW-CKV-HW-C502B	$					199
1.000E-04	$	HSW-CKV-HW-C502C	$					200
1.000E-04	$	HSW-CKV-HW-C502D	$					201
1.000E-04	$	HSW-CKV-HW-CV5	$					202
1.000E-04	$	LCI-CKV-HW-CV19A	$		21	12		203
1.000E-04	$	LCI-CKV-HW-CV19B	$					204
1.000E-04	$	LCI-CKV-HW-CV19C	$					205
1.000E-04	$	LCI-CKV-HW-CV19D	$					206
1.000E-04	$	LCI-CKV-HW-CV46A	$					207
1.000E-04	$	LCI-CKV-HW-CV46B	$					208
1.000E-04	$	LCI-CKV-HW-CV48A	$					209
1.000E-04	$	LCI-CKV-HW-CV48B	$					210
1.000E-04	$	LCI-CKV-HW-CV48C	$					211
1.000E-04	$	LCI-CKV-HW-CV48D	$					212
1.000E-04	$	LCS-CKV-HW-CV10A	$					213
1.000E-04	$	LCS-CKV-HW-CV10B	$					214
1.000E-04	$	LCS-CKV-HW-CV10C	$					215
1.000E-04	$	LCS-CKV-HW-CV10D	$					216
1.000E-04	$	LCS-CKV-HW-CV66A	$					217
1.000E-04	$	LCS-CKV-HW-CV66B	$					218
1.000E-04	$	LCS-CKV-HW-CV66C	$					219
1.000E-04	$	LCS-CKV-HW-CV66D	$					220
1.000E-04	$	RCI-CKV-HW-CV19	$					221
1.000E-04	$	RCI-CKV-HW-CV40	$					222
1.000E-04	$	RCI-CKV-HW-CV50	$					223
1.000E-04	$	SLC-CKV-HW-CV16	$		0	0		224
1.000E-04	$	SLC-CKV-HW-CV17	$					225
1.000E-04	$	SLC-CKV-HW-CV43A	$					226
1.000E-04	$	SLC-CKV-HW-CV43B	$					227
1.600E-02	$	ACP-DGN-FR-EDGA	$	10.	0	0		228
1.600E-02	$	ACP-DGN-FR-EDGB	$					229
1.600E-02	$	ACP-DGN-FR-EDGC	$					230
1.600E-02	$	ACP-DGN-FR-EDGD	$					231

Prandom	Basic Event	EF	Nfrag	Nresp	Ncorr	No.
3.000E-03 $	ACP-DGN-LP-EDGA $	3.0	42	22		232
3.000E-03 $	ACP-DGN-LP-EDGB $					233
3.000E-03 $	ACP-DGN-LP-EDGC $					234
3.000E-03 $	ACP-DGN-LP-EDGD $					235
6.000E-03 $	ACP-DGN-MA-EDGA $	10.	0	0		236
6.000E-03 $	ACP-DGN-MA-EDGB $					237
6.000E-03 $	ACP-DGN-MA-EDGC $					238
6.000E-03 $	ACP-DGN-MA-EDGD $					239
3.000E-04 $	ACP-DGN-RE-EDGA $	3.0	0			240
3.000E-04 $	ACP-DGN-RE-EDGB $					241
3.000E-04 $	ACP-DGN-RE-EDGC $					242
3.000E-04 $	ACP-DGN-RE-EDGD $					243
2.300E-03 $	ACP-DGN-TE-EDGA $					244
2.300E-03 $	ACP-DGN-TE-EDGB $					245
2.300E-03 $	ACP-DGN-TE-EDGC $					246
2.300E-03 $	ACP-DGN-TE-EDGD $					247
3.000E-03 $	SLC-EPV-HW-EV14A $					248
3.000E-03 $	SLC-EPV-HW-EV14B $					249
2.000E-04 $	SLC-EPV-MA-EV14A $					250
2.000E-04 $	SLC-EPV-MA-EV14B $					251
5.000E-04 $	EHV-FAN-FR-OAV64 $					252
5.000E-04 $	EHV-FAN-FR-OAV91 $					253
5.000E-04 $	EHV-FAN-FR-OBV64 $					254
5.000E-04 $	EHV-FAN-FR-OBV91 $					255
5.000E-04 $	EHV-FAN-FR-OCV64 $					256
5.000E-04 $	EHV-FAN-FR-OCV91 $					257
5.000E-04 $	EHV-FAN-FR-ODV64 $					258
5.000E-04 $	EHV-FAN-FR-ODV91 $					259
3.750E-04 $	EHV-FAN-FS-OAV64 $		27	24		260
3.750E-04 $	EHV-FAN-FS-OAV91 $					261
3.750E-04 $	EHV-FAN-FS-OBV64 $					262
3.750E-04 $	EHV-FAN-FS-OBV91 $					263
3.750E-04 $	EHV-FAN-FS-OCV64 $					264
3.750E-04 $	EHV-FAN-FS-OCV91 $					265
3.750E-04 $	EHV-FAN-FS-ODV64 $					266
3.750E-04 $	EHV-FAN-FS-ODV91 $					267
5.000E-04 $	ESW-FAN-FR-HX1 $		0	0		268
5.000E-04 $	ESW-FAN-FR-HX10 $					269
5.000E-04 $	ESW-FAN-FR-HX12 $					270
5.000E-04 $	ESW-FAN-FR-HX13 $					271
5.000E-04 $	ESW-FAN-FR-HX15 $					272
5.000E-04 $	ESW-FAN-FR-HX16 $					273
5.000E-04 $	ESW-FAN-FR-HX_8 $					274
5.000E-04 $	ESW-FAN-FR-HX19 $					275
5.000E-04 $	ESW-FAN-FR-HX2 $					276
5.000E-04 $	ESW-FAN-FR-HX21 $					277
5.000E-04 $	ESW-FAN-FR-HX22 $					278

Prandom	Basic Events	EF	Nfrag	Nresp	Ncorr	No.
5.000E-04	$ ESW-FAN-FR-HX24	$				279
5.000E-04	$ ESW-FAN-FR-HX25	$				280
5.000E-04	$ ESW-FAN-FR-HX27	$				281
5.000E-04	$ ESW-FAN-FR-HX28	$				282
5.000E-04	$ ESW-FAN-FR-HX3	$				283
5.000E-04	$ ESW-FAN-FR-HX4	$				284
5.000E-05	$ ESW-FAN-FR-HX6	$				285
5.000E-04	$ ESW-FAN-FR-HX7	$				286
5.000E-04	$ ESW-FAN-FR-HX9	$				287
3.750E-04	$ ESW-FAN-FS-HX1	$	27	15		288
3.750E-04	$ ESW-FAN-FS-HX10	$				289
3.750E-04	$ ESW-FAN-FS-HX12	$				290
3.750E-04	$ ESW-FAN-FS-HX13	$				291
3.750E-04	$ ESW-FAN-FS-HX15	$				292
3.750E-04	$ ESW-FAN-FS-HX16	$				293
3.750E-04	$ ESW-FAN-FS-HX18	$				294
3.750E-04	$ ESW-FAN-FS-HX19	$				295
3.750E-04	$ ESW-FAN-FS-HX2	$				296
3.750E-04	$ ESW-FAN-FS-HX21	$				297
3.750E-04	$ ESW-FAN-FS-HX22	$				298
3.750E-04	$ ESW-FAN-FS-HX24	$				299
3.750E-04	$ ESW-FAN-FS-HX25	$				300
3.750E-05	$ ESW-FAN-FS-HX27	$				301
3.750E-04	$ ESW-FAN-FS-HX28	$				302
3.750E-04	$ ESW-FAN-FS-HX3	$				303
3.750E-04	$ ESW-FAN-FS-HX4	$				304
3.750E-04	$ ESW-FAN-FS-HX6	$				305
3.750E-04	$ ESW-FAN-FS-HX7	$				306
3.750E-04	$ ESW-FAN-FS-HX9	$				307
1.860E-03	$ ESW-FAN-MA-HX1	$	0	0		308
1.860E-03	$ ESW-FAN-MA-HX10	$				309
1.860E-03	$ ESW-FAN-MA-HX12	$				310
1.860E-03	$ ESW-FAN-MA-HX13	$				311
1.860E-03	$ ESW-FAN-MA-HX15	$				312
1.860E-03	$ ESW-FAN-MA-HX16	$				313
1.860E-03	$ ESW-FAN-MA-HX18	$				314
1.860E-03	$ ESW-FAN-MA-HX19	$				315
1.860E-03	$ ESW-FAN-MA-HX2	$				316
1.860E-03	$ ESW-FAN-MA-HX21	$				317
1.860E-03	$ ESW-FAN-MA-HX22	$				318
1.860E-03	$ ESW-FAN-MA-HX24	$				319
1.860E-03	$ ESW-FAN-MA-HX25	$				320
1.860E-03	$ ESW-FAN-MA-HX27	$				321
1.860E-03	$ ESW-FAN-MA-HX28	$				322
1.860E-03	$ ESW-FAN-MA-HX3	$				323
1.860E-03	$ ESW-FAN-MA-HX4	$				324
1.860E-03	$ ESW-FAN-MA-HX6	$				325

Prandom		Basic Event		EF	Nfrag	Nresp	Ncorr	No.
1.860E-03	$	ESW-FAN-MA-HX7	$					326
1.860E-03	$	ESW-FAN-MA-HX9	$					327
2.660E-04	$	HSW-FAN-FR-ECTFA	$					328
2.660E-04	$	HSW-FAN-FR-ECTFB	$					329
2.660E-04	$	HSW-FAN-FR-ECTFC	$					330
3.500E-03	$	HSW-FAN-FS-ECTFA	$		27	31		331
3.500E-03	$	HSW-FAN-FS-ECTFB	$					332
3.500E-03	$	HSW-FAN-FS-ECTFC	$					333
1.860E-03	$	HSW-FAN-MA-ECTFA	$		0	0		334
1.860E-03	$	HSW-FAN-MA-ECTFB	$					335
1.860E-03	$	HSW-FAN-MA-ECTFC	$					336
2.280E-04	$	HSW-HTX-PG-HXA	$					337
2.280E-04	$	HSW-HTX-PG-HXB	$					338
2.280E-04	$	HSW-HTX-PG-HXC	$					339
2.280E-04	$	HSW-HTX-PG-HXD	$					340
1.200E-04	$	HSW-HTX-RP-HXA	$		25	27		341
1.200E-04	$	HSW-HTX-RP-HXB	$					342
1.200E-04	$	HSW-HTX-RP-HXC	$					343
1.200E-04	$	HSW-HTX-RP-HXD	$					344
1.250E-04	$	HCI-ICC-HW-FC108	$		3	9		345
1.250E-04	$	RCI-ICC-HW-FIC91	$		3	11		346
4.000E-03	$	DCP-INV-LP-24C	$	3.0	6	[illegible]		347
4.000E-03	$	DCP-INV-LP-24D	$					348
1.000E-05	$	ADS-LOG-HW-INHIB	$		0			349
1.610E-03	$	ESF-LOG-HW-RHRA	$					350
1.610E-03	$	ESF-LOG-HW-RHRB	$					351
7.200E-04	$	CRD-MDP-FR-PA	$		0	0		352
7.200E-04	$	CRD-MDP-FR-PB	$					353
3.000E-03	$	CRD-MDP-FS-PA	$		16	26		354
3.000E-03	$	CRD-MDP-FS-PB	$					355
1.200E-03	$	ESW-MDP-FR-ECW	$		0	0		356
1.200E-03	$	ESW-MDP-FR-MDPA	$					357
1.200E-03	$	ESW-MDP-FR-MDPB	$					358
3.000E-03	$	ESW-MDP-FS-ECW	$	10.	17	30		359
3.000E-03	$	ESW-MDP-FS-MDPA	$	10.	17	28		360
3.000E-03	$	ESW-MDP-FS-MDPB	$					361
2.000E-03	$	ESW-MDP-MA-ECW	$	10.	0	0		362
2.000E-03	$	ESW-MDP-MA-MDPA	$					363
2.000E-03	$	ESW-MDP-MA-MDPB	$					364
1.200E-03	$	HSW-MDP-FR-MDPA	$					365
1.200E-03	$	HSW-MDP-FR-MDPB	$					366
1.200E-03	$	HSW-MDP-FR-MDPC	$					367
1.200E-03	$	HSW-MDP-FR-MDPD	$					368
3.000E-03	$	HSW-MDP-FS-MDPA	$	10.	17	28		369
3.000E-03	$	HSW-MDP-FS-MDPB	$					370
3.000E-03	$	HSW-MDP-FS-MDPC	$					371
3.000E-03	$	HSW-MDP-FS-MDPD	$					372

Prandom	Basic Event	EF	Nfrag	Nresp	Ncorr	No.
2.000E-03	$ HSW-MDP-MA-MDPA	$ 3.0	0	0		373
2.000E-03	$ HSW-MDP-MA-MDPB	$				374
2.000E-03	$ HSW-MDP-MA-MDPC	$				375
2.000E-03	$ HSW-MDP-MA-MDPD	$				376
1.200E-03	$ LCI-MDP-FR-2AP35	$				377
1.200E-03	$ LCI-MDP-FR-2BP35	$				378
1.200E-03	$ LCI-MDP-FR-2CP35	$				379
1.200E-03	$ LCI-MDP-FR-2DP35	$				380
3.000E-03	$ LCI-MDP-FS-2AP35	$	16	14		381
3.000E-03	$ LCI-MDP-FS-2BP35	$				382
3.000E-03	$ LCI-MDP-FS-2CP35	$				383
3.000E-03	$ LCI-MDP-FS-2DP35	$				384
2.000E-03	$ LCI-MDP-MA-2AP35	$	0	0		385
2.000E-03	$ LCI-MDP-MA-2BP35	$				386
2.000E-03	$ LCI-MDP-MA-2CP35	$				387
2.000E-03	$ LCI-MDP-MA-2DP35	$				388
1.200E-03	$ LCS-MDP-FR-2AP37	$				389
1.200E-03	$ LCS-MDP-FR-2BP37	$				390
1.200E-03	$ LCS-MDP-FR-2CP37	$				391
1.200E-03	$ LCS-MDP-FR-2DP37	$				392
3.000E-03	$ LCS-MDP-FS-2AP37	$	16	14		393
3.000E-03	$ LCS-MDP-FS-2BP37	$				394
3.000E-03	$ LCS-MDP-FS-2CP37	$				395
3.000E-03	$ LCS-MDP-FS-2DP37	$				396
2.000E-03	$ LCS-MDP-MA-2AP37	$	0	0		397
2.000E-03	$ LCS-MDP-MA-2BP37	$				398
2.000E-03	$ LCS-MDP-MA-2CP37	$				399
2.000E-03	$ LCS-MDP-MA-2DP37	$				400
1.200E-03	$ RBC-MDP-FR-PA	$				401
1.200E-03	$ RBC-MDP-FR-PB	$				402
3.000E-03	$ RBC-MDP-FS-PA	$	16	17		403
3.000E-03	$ RBC-MDP-FS-PB	$				404
1.500E-05	$ SLC-MDP-FR-MDPA	$	0	0		405
1.500E-05	$ SLC-MDP-FR-MDPB	$				406
3.000E-03	$ SLC-MDP-FS-MDPA	$				407
3.000E-03	$ SLC-MDP-FS-MDPB	$				408
2.000E-03	$ SLC-MDP-MA-MDPA	$				409
1.200E-03	$ TBC-MDP-FR-PUMPA	$				10
1.200E-03	$ TBC-MDP-FR-PUMPB	$				411
3.000E-03	$ CSS-MOV-CC-MV26A	$	19	12		412
3.000E-03	$ CSS-MOV-CC-MV26B	$				413
3.000E-03	$ CSS-MOV-CC-MV31A	$				414
3.000E-03	$ CSS-MOV-CC-MV31B	$				415
2.000E-04	$ CSS-MOV-MA-MV26A	$	0	0		416
2.000E-04	$ CSS-MOV-MA-MV26B	$				417
3.000E-03	$ ESW-MOV-CC-M0841	$	19	22		418
2.000E-04	$ ESW-MOV-MA-M0841	$	0	0		419

Prandom	Basic Event	EF	Nfrag	Nresp	Ncorr	No.
2.000E-04	ESW-MOV-MA-MV1					420
4.000E-05	ESW-MOV-PG-M2972		19	22		421
3.000E-04	ESW-MOV-RE-M2972		0	0		422
3.000E-03	HCI-MOV-CC-MV14		19	12		423
3.000E-03	HCI-MOV-CC-MV19		19	18		424
3.000E-03	HCI-MOV-CC-MV57		19	12		425
3.000E-03	HCI-MOV-CC-MV58					426
4.000E-05	HCI-MOV-HW-MV15		19	16		427
4.000E-05	HCI-MOV-HW-MV20					428
2.000E-04	HCI-MOV-MA-MV14		0	0		429
2.000E-04	HCI-MOV-MA-MV17					430
2.000E-04	HCI-MOV-MA-MV20					431
2.000E-04	HCI-MOV-MA-MV57					432
2.000E-04	HCI-MOV-MA-PCV50					433
4.000E-05	HCI-MOV-PG-MV16		19	12		434
4.000E-05	HCI-MOV-PG-MV17					435
3.000E-03	HSW-MOV-CC-2344		19	27		436
3.000E-03	HSW-MOV-CC-2804A		19	29		437
3.000E-03	HSW-MOV-CC-2804B					438
3.000E-03	HSW-MOV-CC-M2803		19	22		439
3.000E-03	HSW-MOV-CC-M502C		19	29		440
3.000E-03	HSW-MOV-CC-MV174					441
3.000E-03	HSW-MOV-CC-MV176					442
3.000E-03	HSW-MOV-CC-MV89A		19	27		443
3.000E-03	HSW-MOV-CC-MV89B					444
3.000E-03	HSW-MOV-CC-MV89C					445
3.000E-03	HSW-MOV-CC-MV89D					446
2.000E-04	HSW-MOV-MA-2344		0	0		447
2.000E-04	HSW-MOV-MA-2804A					448
2.000E-04	HSW-MOV-MA-2804B					449
2.000E-04	HSW-MOV-MA-M2486					450
2.000E-04	HSW-MOV-MA-M2803					451
2.000E-04	HSW-MOV-MA-M502A					452
2.000E-04	HSW-MOV-MA-M502B					453
2.000E-04	HSW-MOV-MA-M502C					454
2.000E-04	HSW-MOV-MA-MV174					455
2.000E-04	HSW-MOV-MA-MV176					456
2.000E-04	HSW-MOV-MA-MV89A					457
2.000E-04	HSW-MOV-MA-MV89B					458
2.000E-04	HSW-MOV-MA-MV89C					459
2.000E-04	HSW-MOV-MA-MV89D					460
4.000E-05	HSW-MOV-PG-M2486		19	22		461
4.000E-05	HSW-MOV-PG-M502A		19	29		462
4.000E-05	HSW-MOV-PG-M502B					463
3.000E-04	HSW-MOV-RE-2344		0	0		464
3.000E-04	HSW-MOV-RE-M2803					465
3.000E-03	LCI-MOV-CC-MV25A		19	18		466

Prandom		Basic Event		EF	Nfrag	Nresp	Ncorr	No.
3.000E-03	$	LCI-MOV-CC-MV25B	$					467
4.000E-05	$	LCI-MOV-HW-MV13A	$		19	12		468
4.000E-05	$	LCI-MOV-HW-MV13B	$					469
4.000E-05	$	LCI-MOV-HW-MV13C	$					470
4.000E-05	$	LCI-MOV-HW-MV13D	$					471
2.000E-04	$	LCI-MOV-MA-154A	$		0	0		472
2.000E-04	$	LCI-MOV-MA-154B	$					473
2.000E-04	$	LCI-MOV-MA-2677A	$					474
2.000E-04	$	LCI-MOV-MA-2677D	$					475
2.000E-04	$	LCI-MOV-MA-M154A	$					476
2.000E-04	$	LCI-MOV-MA-M154B	$					477
2.000E-04	$	LCI-MOV-MA-MV16A	$					478
2.000E-04	$	LCI-MOV-MA-MV16B	$					479
2.000E-04	$	LCI-MOV-MA-MV16C	$					480
2.000E-04	$	LCI-MOV-MA-MV16D	$					481
4.000E-05	$	LCI-MOV-PG-154A	$		19	18		482
4.000E-05	$	LCI-MOV-PG-154B	$					483
4.000E-05	$	LCI-MOV-PG-2677A	$					484
4.000E-05	$	LCI-MOV-PG-2677D	$					485
4.000E-05	$	LCI-MOV-PG-MV16A	$		19	12		486
4.000E-05	$	LCI-MOV-PG-MV16B	$					487
4.000E-05	$	LCI-MOV-PG-MV16C	$					488
4.000E-05	$	LCI-MOV-PG-MV16D	$					489
1.200E-03	$	LCI-MOV-RE-154A	$		0	0		490
1.200E-03	$	LCI-MOV-RE-154B	$					491
3.000E-03	$	LCS-MOV-CC-MV12A	$		19	18		492
3.000E-03	$	LCS-MOV-CC-MV12B	$					493
1.800E-04	$	LCS-MOV-CO-MV26A	$		19	12		494
1.800E-04	$	LCS-MOV-CO-MV26B	$					495
4.500E-05	$	LCS-MOV-HW-MV7A	$					496
4.500E-05	$	LCS-MOV-HW-MV7B	$					497
4.500E-05	$	LCS-MOV-HW-MV7C	$					498
4.500E-05	$	LCS-MOV-HW-MV7D	$					499
2.000E-04	$	LCS-MOV-MA-MV11A	$		0	0		500
2.000E-04	$	LCS-MOV-MA-MV11B	$					501
2.000E-04	$	LCS-MOV-MA-MV5A	$					502
2.000E-04	$	LCS-MOV-MA-MV5B	$					503
2.000E-04	$	LCS-MOV-MA-MV5C	$					504
2.000E-04	$	LCS-MOV-MA-MV5D	$					505
4.000E-05	$	LCS-MOV-PG-MV11A	$		19	12		506
4.000E-05	$	LCS-MOV-PG-MV11B	$					507
4.000E-05	$	LCS-MOV-PG-MV5A	$					508
4.000E-05	$	LCS-MOV-PG-MV5B	$					509
4.000E-05	$	LCS-MOV-PG-MV5C	$					510
4.000E-05	$	LCS-MOV-PG-MV5D	$					511
1.500E-03	$	LCS-MOV-RE-MV11A	$		0	0		512
1.500E-03	$	LCS-MOV-RE-MV11B	$					513

Prandom	Basic Event	EF	Nfrag	Nresp	Ncorr	No.	
3.000E-03	$ RCI-MOV-CC-MV131	$	19	12		514	
3.000E-03	$ RCI-MOV-CC-MV132	$				515	
3.000E-03	$ RCI-MOV-CC-MV21	$	19	18		516	
3.000E-03	$ RCI-MOV-CC-MV39	$	19	12		517	
3.000E-03	$ RCI-MOV-CC-MV41	$				518	
4.000E-05	$ RCI-MOV-HW-MV20	$	19	20		519	
2.000E-04	$ RCI-MOV-MA-MV131	$	0	0		520	
2.000E-04	$ RCI-MOV-MA-MV132	$				521	
2.000E-04	$ RCI-MOV-MA-MV18	$				522	
2.000E-04	$ RCI-MOV-MA-MV20	$				523	
2.000E-04	$ RCI-MOV-MA-MV39	$				524	
4.000E-05	$ RCI-MOV-PG-MV15	$	19	20		525	
4.000E-05	$ RCI-MOV-PG-MV16	$				526	
4.000E-05	$ RCI-MOV-PG-MV18	$				527	
3.000E-03	$ RHR-MOV-CC-MV34A	$	19	12		528	
3.000E-03	$ RHR-MOV-CC-MV34B	$				529	
3.000E-03	$ RHR-MOV-CC-MV39A	$				530	
3.000E-03	$ RHR-MOV-CC-MV39B	$				531	
2.000E-04	$ RHR-MOV-MA-MV39A	$	0	0		532	
2.000E-04	$ RHR-MOV-MA-MV39B	$				533	
3.000E-03	$ SDC-MOV-CC-MV15A	$	19	12		534	
3.000E-03	$ SDC-MOV-CC-MV15B	$				535	
3.000E-03	$ SDC-MOV-CC-MV15C	$				536	
3.000E-03	$ SDC-MOV-CC-MV15D	$				537	
3.000E-03	$ SDC-MOV-CC-MV17	$				538	
3.000E-03	$ SDC-MOV-CC-MV18	$				539	
2.000E-04	$ SDC-MOV-MA-MV15A	$	0	0		540	
2.000E-04	$ SDC-MOV-MA-MV15B	$				541	
2.000E-04	$ SDC-MOV-MA-MV15C	$				542	
2.000E-04	$ SDC-MOV-MA-MV15D	$				543	
3.000E-03	$ SDC-MOV-OO-MV13A	$	19	12		544	
3.000E-03	$ SDC-MOV-OO-MV13B	$				545	
3.000E-03	$ SDC-MOV-OO-MV13C	$				546	
3.000E-03	$ SDC-MOV-OO-MV13D	$				547	
3.000E-03	$ SLC-MOV-OO-MV15	$				548	
3.000E-03	$ SLC-MOV-OO-MV18	$				549	
1.000E-03	$ ESF-PER-LCI3ACT	$	3	11		550	
5.000E-04	$ ESF-PER-LCI3ACT2	$				551	
1.000E+00	$ ESF-PER-LIA3TEST	$	0	0		552	
1.000E+00	$ ESF-PER-LIB3TEST	$				553	
1.000E+00	$ ESF-PER-LIC3TEST	$				554	
1.000E+00	$ ESF-PER-LID3TEST	$				555	
1.000E+00	$ ESF-PER-RXLNTMET	$				556	
7.000E-04	$ HSW-PFT-RE-MDPB	$				557	
1.000E-05	$ CST-PSF-CSTLOST	$	0			558	?SS?
1.000E+00	$ CST-PSF-DEPLETED	$	0	0		559	
4.000E-05	$ HCI-PSF-HW-COL13	$				560	

Prandom	Basic Event	EF	Nfrag	Nresp	Ncorr	No.
2.000E-03	$ SLC-PSF-MA-MDPB	$				561
1.000E-06	$ ADS-PTF-VF-ADSRV	$	20	20		562
1.000E-06	$ ADS-PTF-VF-NADSV	$	21	20		563
2.000E-03	$ CRD-PTF-MA-PB	$	0	0		564
2.000E-03	$ EHV-PTF-MA-OAV64	$				565
2.000E-03	$ EHV-PTF-MA-OAV91	$				566
2.000E-03	$ EHV-PTF-MA-OBV64	$				567
2.000E-03	$ EHV-PTF-MA-OBV91	$				568
2.000E-03	$ EHV-PTF-MA-OCV64	$				569
2.000E-03	$ EHV-PTF-MA-OCV91	$				570
2.000E-03	$ EHV-PTF-MA-ODV64	$				571
2.000E-03	$ EHV-PTF-MA-ODV91	$				572
9.000E-04	$ EHV-PTF-RE-OAV64	$				573
6.000E-04	$ EHV-PTF-RE-OAV91	$				574
9.000E-04	$ EHV-PTF-RE-OBV64	$				575
6.000E-04	$ EHV-PTF-RE-OBV91	$				576
9.000E-04	$ EHV-PTF-RE-OCV64	$				577
6.000E-04	$ EHV-PTF-RE-OCV91	$				578
9.000E-04	$ EHV-PTF-RE-ODV64	$				579
6.000E-04	$ EHV-PTF-RE-ODV91	$				580
1.000E-03	$ ESW-PTF-RE-DGA	$				581
1.000E-03	$ ESW-PTF-RE-DGB	$				582
1.000E-03	$ ESW-PTF-RE-DGC	$				583
1.000E-03	$ ESW-PTF-RE-DGD	$				584
7.000E-04	$ ESW-PTF-RE-ECW	$				585
7.000E-04	$ ESW-PTF-RE-HX1	$				586
7.000E-04	$ ESW-PTF-RE-HX10	$				587
7.000E-04	$ ESW-PTF-RE-HX12	$				588
7.000E-04	$ ESW-PTF-RE-HX13	$				589
7.000E-04	$ ESW-PTF-RE-HX15	$				590
7.000E-04	$ ESW-PTF-RE-HX16	$				591
7.000E-04	$ ESW-PTF-RE-HX18	$				592
7.000E-04	$ ESW-PTF-RE-HX19	$				593
7.000E-04	$ ESW-PTF-RE-HX2	$				594
7.000E-04	$ ESW-PTF-RE-HX21	$				595
7.000E-04	$ ESW-PTF-RE-HX22	$				596
7.000E-04	$ ESW-PTF-RE-HX24	$				597
7.000E-04	$ ESW-PTF-RE-HX25	$				598
7.000E-04	$ ESW-PTF-RE-HX27	$				599
7.000E-04	$ ESW-PTF-RE-HX28	$				600
7.000E-04	$ ESW-PTF-RE-HX3	$				601
7.000E-04	$ ESW-PTF-RE-HX4	$				602
0.000E-01	$ ESW-PTF-RE-HX5	$				603
7.000E-04	$ ESW-PTF-RE-HX6	$				604
7.000E-04	$ ESW-PTF-RE-HX7	$				605
7.000E-04	$ ESW-PTF-RE-HX9	$				606
7.000E-04	$ ESW-PTF-RE-MDPA	$				607

Prandom	Basic Event	EF	Nfrag	Nresp	Ncorr	No.
7.000E-04	$ ESW-PTF-RE-MDPB	$				608
1.000E-03	$ HCI-PTF-VF-NOSUC	$	19	12		609
1.200E-03	$ HSW-PTF-RE-ECTFA	$	0	0		610
1.200E-03	$ HSW-PTF-RE-ECTFB	$				611
1.200E-03	$ HSW-PTF-RE-ECTFC	$				612
1.200E-03	$ HSW-PTF-RE-HXA	$				613
1.200E-03	$ HSW-PTF-RE-HXB	$				614
1.200E-03	$ HSW-PTF-RE-HXC	$				615
1.200E-03	$ HSW-PTF-RE-HXD	$				616
7.000E-04	$ HSW-PTF-RE-MDPA	$				617
7.000E-04	$ HSW-PTF-RE-MDPB	$				618
7.000E-04	$ HSW-PTF-RE-MDPC	$				619
7.000E-04	$ HSW-PTF-RE-MDPD	$				620
6.000E-04	$ HSW-PTF-RE-PS10	$				621
9.000E-04	$ HSW-PTF-RE-PS18	$				622
9.000E-04	$ HSW-PTF-RE-PS20	$				623
1.000E-04	$ IAS-PTF-HW-IAS	$ 10.	16	26		624
1.500E-03	$ LCI-PTF-RE-2AP35	$	0	0		625
1.500E-03	$ LCI-PTF-RE-2BP35	$				626
1.500E-03	$ LCI-PTF-RE-2CP35	$				627
1.500E-03	$ LCI-PTF-RE-2DP35	$				628
1.200E-03	$ LCI-PTF-RE-LOOPA	$				629
1.200E-03	$ LCI-PTF-RE-LOOPB	$				630
1.500E-03	$ LCS-PTF-RE-2AP37	$				631
1.500E-03	$ LCS-PTF-RE-2BP37	$				632
1.500E-03	$ LCS-PTF-RE-2CP37	$				633
1.500E-03	$ LCS-PTF-RE-2DP37	$				634
2.000E-03	$ RBC-PTF-MA-PB	$				635
9.000E-04	$ RBC-PTF-RE-2352	$				636
9.000E-04	$ RBC-PTF-RE-2354	$				637
1.200E-03	$ RBC-PTF-RE-PB	$				638
3.000E-03	$ TBC-PTF-FS-PUMPB	$	16	26		639
2.000E-03	$ TBC-PTF-MA-PUMPB	$	0	0		640
1.200E-03	$ TBC-PTF-RE-PUMPB	$				641
1.000E-03	$ ESF-PWR-FC-4160A	$	2	7		642
1.000E-03	$ ESF-PWR-FC-4160B	$				643
1.000E-03	$ ESF-PWR-FC-4160C	$				644
1.000E-03	$ ESF-PWR-FC-4160D	$				645
8.000E-06	$ DCP-REC-LP-1	$	6	7		646
8.000E-06	$ DCP-REC-LP-2	$				647
8.000E-06	$ DCP-REC-LP-3	$				648
8.000E-06	$ DCP-REC-LP-4	$				649
1.000E-03	$ RBC-SOV-FT-S2352	$	20	16		650
1.000E-03	$ RBC-SOV-FT-S2354	$				651
2.000E-04	$ RBC-SOV-MA-S2352	$	0	0		652
2.000E-04	$ RBC-SOV-MA-S2354	$				653
3.000E-04	$ EHV-SRV-CC-RV1	$	21	6		654

Prandom		Basic Event		EF	Nfrag	Nresp	Ncorr	No.	
3.000E-04	$	EHV-SRV-CC-RV2	$					655	
3.000E-04	$	EHV-SRV-CC-RV3	$					656	
3.000E-04	$	EHV-SRV-CC-RV4	$					657	
3.000E-04	$	SLC-SRV-CC-RV39A	$		0	0		658	
3.000E-04	$	SLC-SRV-CC-RV39B	$					659	
1.000E-01	$	CDS-SYS-FC-COND	$	10.	16	26		660	
1.000E-01	$	NSW-SYS-FO-NSW	$					661	
1.000E-04	$	PCV-SYS-HW-SYSTM	$		19	20		662	
3.400E-03	$	SLC-SYS-TE-SLC	$		0	0		663	
1.000E-04	$	HCI-TCV-HW-TCV18	$		19	12		664	
1.000E-04	$	LCS-TCV-HW-TV13A	$					665	
1.000E-04	$	LCS-TCV-HW-TV13B	$					666	
1.000E-04	$	RCI-TCV-HW-TCV22	$					667	
5.000E-02	$	HCI-TDP-FR-20S37	$	10.	0	0		668	m.e.
3.000E-02	$	HCI-TDP-FS-20S37	$	10.	16	14		669	m.e.
1.000E-02	$	HCI-TDP-MA-20S37	$	10.	0	0		670	
5.000E-02	$	RCI-TDP-FR-20S38	$	10.				671	m.e.
3.000E-02	$	RCI-TDP-FS-20S38	$	10.	16	14		672	m.e.
1.000E-02	$	RCI-TDP-MA-20S38	$	10.	0	[illegible]		673	m.e.
1.000E-05	$	ESW-TNK-LL-PS13	$	10.	24	2[illegible]		674	m.e.
1.000E-05	$	HSW-TNK-LF-RESVR	$		0			675	
1.000E-06	$	ADS-TSW-FT-DC125	$		13	11		676	
1.250E-03	$	LCI-TSW-FT-ATOC	$		3	11		677	
1.250E-03	$	LCI-TSW-FT-BTOD	$					678	
1.000E-05	$	HSW-VFC-LF-PPBAY	$		0	0		679	
5.000E-01	$	CRD-XHE-FO-BRKRS	$	5.				680	
5.000E-01	$	CRD-XHE-FO-CRD	$	5.				681	
4.000E-04	$	CRD-XHE-RE-PB	$					682	
5.000E-01	$	ESF-XHE-FO-ADSBT	$					683	
5.000E-01	$	ESF-XHE-FO-DEPRE	$	5.				684	
5.000E-01	$	ESF-XHE-FO-DEPSD	$					685	
5.000E-01	$	ESF-XHE-FO-HCICL	$	5.				686	
5.000E-01	$	ESF-XHE-FO-HCIRL	$					687	
5.000E-01	$	ESF-XHE-FO-HPSAT	$					688	
5.000E-01	$	ESF-XHE-FO-HPSRL	$					689	
1.000E-01	$	ESF-XHE-FO-HSWIN	$	10.				690	
5.000E-01	$	ESF-XHE-FO-LPSAT	$					691	
5.000E-01	$	ESF-XHE-FO-OVRID	$					692	
5.000E-01	$	ESF-XHE-FO-RCICL	$					693	
5.000E-01	$	ESF-XHE-FO-RCICO	$					694	
5.000E-01	$	ESF-XHE-FO-RCIRL	$					695	
5.000E-01	$	ESF-XHE-FO-RHRAT	$					696	
2.500E-05	$	ESF-XHE-MC-CSTLV	$					697	
1.000E-04	$	ESF-XHE-MC-HDPRS	$					698	
2.000E-04	$	ESF-XHE-MC-PRES	$					699	
5.000E-05	$	ESF-XHE-MC-VSLVL	$					700	
9.000E-01	$	ESW-XHE-FO-EHS	$	10.				701	
5.000E-01	$	HSW-XHE-FO-PS9	$	5.				702	

Prandom		Basic Event		EF	Nfrag	Nresp	Ncorr	No.
5.000E-01	$	PCV-XHE-FO-PCV	$					703
5.000E-01	$	RBC-XHE-FO-LCVAL	$	5.0				704
5.000E-01	$	RBC-XHE-FO-SWCH	$	5.0				705
5.000E-01	$	SLC-XHE-FO-SLC	$					706
1.200E-02	$	SLC-XHE-RE-DIVER	$					707
3.000E-03	$	SLC-XHE-RE-EV14A	$					708
3.000E-03	$	SLC-XHE-RE-EV14B	$					709
1.000E-03	$	SLC-XHE-RE-MDPA	$					710
1.000E-03	$	SLC-XHE-RE-MDPB	$					711
2.000E-04	$	ESW-XVM-MA-XV517	$					712
4.000E-05	$	ESW-XVM-PG-D504A	$					713
4.000E-05	$	ESW-XVM-PG-D504B	$					714
4.000E-05	$	ESW-XVM-PG-D504C	$					715
4.000E-05	$	ESW-XVM-PG-D504D	$					716
4.000E-05	$	ESW-XVM-PG-D505A	$					717
4.000E-05	$	ESW-XVM-PG-D505B	$					718
4.000E-05	$	ESW-XVM-PG-D505C	$					719
4.000E-05	$	ESW-XVM-PG-D505D	$					720
4.000E-05	$	ESW-XVM-PG-D519A	$					721
4.000E-05	$	ESW-XVM-PG-D519B	$					722
4.000E-05	$	ESW-XVM-PG-D519C	$					723
4.000E-05	$	ESW-XVM-PG-D519D	$					724
4.000E-05	$	ESW-XVM-PG-X507A	$					725
4.000E-05	$	ESW-XVM-PG-X507B	$					726
4.000E-05	$	ESW-XVM-PG-XV13	$					727
4.000E-05	$	ESW-XVM-PG-XV15	$					728
4.000E-05	$	ESW-XVM-PG-XV16	$					729
4.000E-05	$	ESW-XVM-PG-XV17	$					730
4.000E-05	$	ESW-XVM-PG-XV18	$					731
4.000E-05	$	ESW-XVM-PG-XV19	$					732
4.000E-05	$	ESW-XVM-PG-XV20	$					733
4.000E-05	$	ESW-XVM-PG-XV21	$					734
4.000E-05	$	ESW-XVM-PG-XV22	$					735
4.000E-05	$	ESW-XVM-PG-XV23	$					736
4.000E-05	$	ESW-XVM-PG-XV24	$					737
4.000E-05	$	ESW-XVM-PG-XV25	$					738
4.000E-05	$	ESW-XVM-PG-XV26	$					739
4.000E-05	$	ESW-XVM-PG-XV27	$					740
4.000E-05	$	ESW-XVM-PG-XV28	$					741
4.000E-05	$	ESW-XVM-PG-XV29	$					742
4.000E-05	$	ESW-XVM-PG-XV30	$					743
4.000E-05	$	ESW-XVM-PG-XV31	$					744
4.000E-05	$	ESW-XVM-PG-XV32	$					745
4.000E-05	$	ESW-XVM-PG-XV33	$					746
4.000E-05	$	ESW-XVM-PG-XV34	$					747
4.000E-05	$	ESW-XVM-PG-XV35	$					748

Prandom	Basic Event	EF	Nfrag Nresp Ncorr	No.
4.000E-05	$ ESW-XVM-PG-XV36	$		749
4.000E-05	$ ESW-XVM-PG-XV37	$		750
4.000E-05	$ ESW-XVM-PG-XV38	$		751
4.000E-05	$ ESW-XVM-PG-XV39	$		752
4.000E-05	$ ESW-XVM-PG-XV40	$		753
4.000E-05	$ ESW-XVM-PG-XV41	$		754
4.000E-05	$ ESW-XVM-PG-XV42	$		755
4.000E-05	$ ESW-XVM-PG-XV43	$		756
4.000E-05	$ ESW-XVM-PG-XV44	$		757
4.000E-05	$ ESW-XVM-PG-XV45	$		758
4.000E-05	$ ESW-XVM-PG-XV46	$		759
4.000E-05	$ ESW-XVM-PG-XV47	$		760
4.000E-05	$ ESW-XVM-PG-XV48	$		761
4.000E-05	$ ESW-XVM-PG-XV49	$		762
4.000E-05	$ ESW-XVM-PG-XV50	$		763
4.000E-05	$ ESW-XVM-PG-XV502	$		764
4.000E-05	$ ESW-XVM-PG-XV506	$		765
4.000E-05	$ ESW-XVM-PG-XV509	$		766
4.000E-05	$ ESW-XVM-PG-XV51	$		767
4.000E-05	$ ESW-XVM-PG-XV510	$		768
4.000E-05	$ ESW-XVM-PG-XV517	$		769
4.000E-05	$ ESW-XVM-PG-XV52	$		770
4.000E-05	$ ESW-XVM-PG-XV53	$		771
4.000E-05	$ ESW-XVM-PG-XV54	$		772
4.000E-05	$ ESW-XVM-PG-XV55	$		773
4.000E-05	$ ESW-XVM-PG-XV56	$		774
4.000E-05	$ ESW-XVM-PG-XV57	$		775
4.000E-05	$ ESW-XVM-PG-XV58	$		776
4.000E-05	$ ESW-XVM-PG-XV59	$		777
4.000E-05	$ ESW-XVM-PG-XV60	$		778
4.000E-05	$ ESW-XVM-PG-XV61	$		779
4.000E-05	$ ESW-XVM-PG-XV62	$		780
4.000E-05	$ ESW-XVM-PG-XV63	$		781
4.000E-05	$ ESW-XVM-PG-XV64	$		782
4.000E-05	$ ESW-XVM-PG-XV65	$		783
4.000E-05	$ ESW-XVM-PG-XV66	$		784
4.000E-05	$ ESW-XVM-PG-XV67	$		785
4.000E-05	$ ESW-XVM-PG-XV68	$		786
4.000E-05	$ ESW-XVM-PG-XVA	$		787
4.000E-05	$ ESW-XVM-PG-XVB	$		788
4.000E-05	$ ESW-XVM-PG-XVC	$		789
4.000E-05	$ ESW-XVM-PG-XVD	$		790
4.000E-05	$ ESW-XVM-PG-XVE	$		791
4.000E-05	$ ESW-XVM-PG-XVF	$		792
4.000E-05	$ ESW-XVM-PG-XVG	$		793
4.000E-05	$ ESW-XVM-PG-XVH	$		794
4.000E-05	$ ESW-XVM-PG-XVI	$		795

Prandom	Basic Event	EF	Nfrag	Nresp	Ncorr	No.
4.000E-05	$ ESW-XVM-PG-XVJ	$				796
4.000E-05	$ ESW-XVM-PG-XVK	$				797
4.000E-05	$ ESW-XVM-PG-XVL	$				798
4.000E-05	$ ESW-XVM-PG-XVM	$				799
4.000E-05	$ ESW-XVM-PG-XVN	$				800
4.000E-05	$ ESW-XVM-PG-XVO	$				801
4.000E-05	$ ESW-XVM-PG-XVP	$				802
4.000E-05	$ ESW-XVM-PG-XVQ	$				803
4.000E-05	$ ESW-XVM-PG-XVR	$				804
4.000E-05	$ ESW-XVM-PG-XVS	$				805
4.000E-05	$ ESW-XVM-PG-XVT	$				806
3.000E-04	$ ESW-XVM-RE-XV517	$				807
0.000E-01	$ ESW-XVM-RE-XVA	$				808
9.000E-04	$ ESW-XVM-RE-XVAB	$				809
9.000E-04	$ ESW-XVM-RE-XVCD	$				810
9.000E-04	$ ESW-XVM-RE-XVEF	$				811
9.000E-04	$ ESW-XVM-RE-XVGH	$				812
9.000E-04	$ ESW-XVM-RE-XVIJ	$				813
9.000E-04	$ ESW-XVM-RE-XVKL	$				814
9.000E-04	$ ESW-XVM-RE-XVMN	$				815
9.000E-04	$ ESW-XVM-RE-XVOP	$				816
9.000E-04	$ ESW-XVM-RE-XVQR	$				817
9.000E-04	$ ESW-XVM-RE-XVST	$				818
4.000E-05	$ HCI-XVM-HW-CST01	$				819
4.000E-05	$ HCI-XVM-PG-XV12	$				820
4.000E-05	$ [illegible]I-XVM-PG-XV23	$				821
1.250E-04	$ HSW-XVM-OO-516A	$				822
4.000E-05	$ HSW-XVM-PG-X501A	$				823
4.000E-05	$ HSW-XVM-PG-X501B	$				824
4.000E-05	$ HSW-XVM-PG-X501C	$				825
4.000E-05	$ HSW-XVM-PG-X501D	$				826
4.000E-05	$ HSW-XVM-PG-X515B	$				827
4.000E-05	$ HSW-XVM-PG-XV11	$				828
4.000E-05	$ HSW-XVM-PG-XV5	$				829
4.000E-05	$ HSW-XVM-PG-XV6	$				830
4.000E-05	$ HSW-XVM-PG-XV7	$				831
4.000E-05	$ HSW-XVM-PG-XV8	$				832
4.000E-05	$ HSW-XVM-PG-XV9	$				833
4.000E-05	$ LCI-XVM-PG-XV81A	$				834
4.000E-05	$ LCI-XVM-PG-XV81B	$				835
4.000E-05	$ LCS-XVM-PG-XV14A	$				836
4.000E-05	$ LCS-XVM-PG-XV14B	$				837
4.000E-05	$ LCS-XVM-PG-XV63A	$				838
4.000E-05	$ LCS-XVM-PG-XV63B	$				839
4.000E-05	$ LCS-XVM-PG-XV63C	$				840
4.000E-05	$ LCS-XVM-PG-XV63D	$				841
4.000E-05	$ RCI-XVM-PG-XV17	$				842

Prandom		Basic Event		Ff	Nfrag	Nresp	Ncorr	No.
4.000E-05	$	RCI-XVM-PG-XV9	$					843
4.000E-05	$	SDC-XVM-PG-XV1	$					844
4.000E-05	$	SLC-XVM-PG-XV11	$					845
4.000E-05	$	SLC-XVM-PG-XV12A	$					846
4.000E-05	$	SLC-XVM-PG-XV12B	$					847
4.000E-05	$	SLC-XVM-PG-XV13A	$					848
4.000E-05	$	SLC-XVM-PG-XV13B	$					849
4.000E-05	$	SLC-XVM-PG-XV15	$					850
4.000E-05	$	SLC-XVM-PG-XV18	$					851
0.000E-00	$	SLOCA-FIT	$	3.0	29	32		852
0.000E-00	$	MLOCA-FIT	$	3.0	30	32		853
0.000E-00	$	RECIRC-PUMP	$	3.0	31	1		854
0.000E-00	$	VESSEL-SKIRT	$	3.0	28	1		855
5.000E-06	$	ACP-CCF-2-4KV	$	5.0	41	7	2	856
7.800E-05	$	ESW-CCF-2-MDPS	$	10.	17	28	2	857
3.900E-05	$	ACP-CCF-2-DGS	$	3.0	42	22	2	858
0.000E-00	$	DIKE-CST-RWST	$	3.0	32	1		859
0.000E-00	$	EMER-COOL-TOWER	$	3.0	33	1		860
0.000E-00	$	REACTOR-BLDG	$	3.0	34	1		861
0.000E-00	$	RADWASTE/TB-ROOF	$	3.0	35	1		862
0.000E-00	$	RADWASTE/TB-WALL	$	3.0	36	1		863
0.000E-00	$	TURBINE-BLDG	$	3.0	37	1		864
0.000E-00	$	BLOCK-WALLS-VAR	$	3.0	38	1		865
0.000E+00	$	RECIRC-PUMP-2CCF	$	3.0	31	1	2	866
5.000E-06	$	ACP-CCF-3-4KV	$	5.0	41	7	3	867

APPENDIX D

CRITICAL COMPONENTS BY FIRE AREA

Appendix D

Critical Components by Fire Area

Fire Area	Component Description
1	Unit 2--RHR Heat Exchangers (A and C); RHR Pumps A and C; RHR Pump Discharge Bypass Valves; RHR Heat Exchanger Discharge Valves; LPCI Suction Isolation Valves; RHR Shutdown Cooling Suction Valves; RHR Pump Room Cooling Fans (A-D).
2	Unit 2--RHR Heat Exchangers (B and D); RHR Pumps B and D; RHR Pump Discharge Bypass Valves; RHR Heat Exchanger Discharge Valves; LPCI Suction Isolation Valves; RHR Shutdown Cooling Suction Valves; RHR Pump Room Cooler Heat Exchanger; ESW Header Isolation Valve; HPCI Turbine; HPCI Pump Suction Valves From Torus; HPCI Pump Suction From CST; Outboard HPCI Pump Discharge Valve; HPCI Steam Line to Turbine; HPCI Minimum Recirc to Torus; Condensate Drain Pot Drain Valve; HPCI Pump Room Cooling Fans A and B; RCIC Turbine; RCIC Pump Suction Valves from Torus; RCIC Pump Suction from CST; Outboard RCIC Discharge Isolation Valve; RCIC Pump Room Cooling Fans;
3	Unit 3--RHR Heat Exchanger (A and C); RHR Pumps A and C; RHR Pump Discharge Bypass Valves; RHR Heat Exchanger Discharge Valves; LPCI Suction Isolation Valves; RHR Shutdown Cooling Suction Valves; RHR Pump Room Cooling Fans (A-D); RHR Service Water Crosstie Valves; HPCI Turbine; HPCI Pump Suction Valves From Torus; HPCI Pump Suction From CST; Outboard HPCI Pump Discharge Valve; HPCI Steam Line to Turbine; HPCI Minimum Recirc to Torus; HPCI Pump Room Cooling Fans A and B; RCIC Turbine; RCIC Pump Suction Valves From Torus; RCIC Pump Suction From CST; Outboard RCIC Discharge Isolation Valve; RCIC Steam to Turbine Isolation Valve; RCIC Lube Oil Cooler Isolation Valve; RCIC Pump Room Cooling Fans A and B.
4	There is currently no major safety-related equipment in Fire Area 4. The Unit 2 HPCI alternative control station will be located in Fire Area 4.
5	Unit 2--RHR Supply to Torus Valves (4); RHR Recirc Loops A and B Return Valves; Core Spray Pumps A-D; Core Spray Pump Suction Valves; Core Spray Minimum Bypass Valves; Core Spray Pump Room Cooling Fans (8); Core Spray Pump Room Cooler HXs (8).

Appendix D

Critical Components by Fire Area
(Continued)

Fire Area	Component Description
6N	RHR Shutdown Cooling Suction Valve; RHR Recirc Loop B Return Valve; RHR Drywell Spray Isolation Valves (B); Outboard and Inboard Core Spray Discharge Valves (B).
6S	RHR Recirc Loop A Return Valve; RHR Drywell Spray Isolation Valve (A); Outboard and Inboard Core Spray Discharge Valves (B).
17	Inboard RCIC Discharge Isolation Valve; Inboard HPCI Pump Discharge Valve.
18	RHR Shutdown Cooling Suction Valve; Inboard RCIC Steam Supply Isolation Valve; Inboard HPCI Steam Supply Isolation Valve.
19	Control Rod Drive Mechanisms.
25	Fire Area 25 contains the controls, instrumentation, and logic for all the plant's major safety-related systems.
30	Unit 3--Station Batteries B and D; Distribution Panel.
31	Unit 3--Station Batteries A and C; Distribution Panel.
32	Battery Chargers A and C; 3C Emergency Auxiliary Switchgear.
33	3A Emergency Auxiliary Switchgear; 3A Motor Control Center.
34	3D Emergency Auxiliary Switchgear; Battery Charger D; 125V dc Panel.
35	3B Emergency Auxiliary Switchgear; Battery Charger B.
36	Battery Chargers B and D; 2D Emergency Auxiliary Switchgear.
37	2B Emergency Auxiliary Switchgear.
38	2C Emergency Auxiliary Switchgear; Battery Chargers A, C.
39	2A Emergency Auxiliary Switchgear.

Appendix D

Critical Components by Fire Area
(Concluded)

Fire Area	Component Description
40	2B Station Battery; 2D Station Battery.
41	2A Station Battery; 2C Station Battery.
43	E4 DG Building Vent Supply; E4 DG Building Supply Fan; Distribution Panel; E4 Diesel Generator.
44	E3 DG Building Vent Supply; E3 DG Building Supply Fan; Distribution Panel; E3 Diesel Generator.
45	E2 DG Building Vent Supply; E2 DG Building Supply Fan; Distribution Panel; E2 Diesel Generator.
46	E1 DG Building Vent Supply; E1 DG Building Supply Fan; Distribution Panel; E1 Diesel Generator.
47	B ESW Pump.
48	A ESW Pump, HPSW Pumps A-D.
50	Condensate Storage Tank Water Level Transmitters (LT-2217, LT-3217, LT-9459).
51	Emergency Cooling Tower Fans A-C; Emergency Cooling Water Pump; Emergency Cooling Water Pump Discharge; ESW Discharge Valves A-C to Reservoir; HPSW Discharge to Reservoir.
54	ESW Discharge Valve; HPSW Discharge Valves (2) to Reservoir.

APPENDIX E

FIRE EVENT DATA

Appendix E. Peach Bottom Fire Event Data Table--Auxiliary Building Fires

Plant Name	Date of Occurrence	Plant Status	Fire Type	Remarks
San Onofre 1	2/7/68	Power Operation	Cable	Thermally overloaded 480 V cables caught fire - 55 cables damaged.
San Onofre 1	3/9/68	Power Operation	Cable	Thermally overloaded cables in switchgear room.
Palisades	6/25/71	Cold Shutdown	Air Dryer Filter	Low flow of air through air dryer resulted in temperature buildup and ignition of filter.
LaCrosse	7/15/72	Power Operation	Circulation Pump	Oil on pump lagging ignited by hot pump casing.
Turkey Point 3	12/16/72	Power Operation	Battery Charger	Battery charger overheated and a small fire occurred in the transformer winding insulation.
Robinson 2	4/19/74	Power Operation	Expansion Joint	Cigarette or welding slag from construction workers ignited combustible expansion joint material.
Robinson 2	4/19/74	Power Operation	Expansion Joint	Same type of event as previous event - occurred one week apart.

Appendix E. Peach Bottom Fire Event Data Table--Auxiliary Building Fires (Continued)

Plant Name	Date of Occurrence	Plant Status	Fire Type	Remarks
Turkey Point 3	5/75	Power Operation (100%)	Battery Charger	Transformer overheated igniting insulation. Similar to previous event on 12/14/72.
Millstone 2	3/24/76	Hot Shutdown	Motor Control Center	Fire resulted from arcing of a supply lead. Extinguished by de-energizing MCC.
Dresden 2	4/76	Cold Shutdown	Circuit Breaker	ECCS Jockey Pump control feed breaker caught fire from a burned-out contacter coil.
Fitzpatrick	6/11/76	Power Operation (93%)	Circuit Breaker	Overload in HPCI valve circuit breaker. Extinguished by de-energizing breaker.
Millstone 2	11/15/76	Hot Shutdown	Relay-MCC	Relay fire in motor control center.
Pilgrim 1	3/77	Hot Shutdown	Circuit Breaker	Circuit breaker under-voltage coil burnt due to high floating charge on station battery.
Fitzpatrick	4/4/77	Power Operation (88%)	Circuit Breaker	Coil failed by fire in HPCI test valve breaker and extinguished by de-energizing. Similar to 7/28/75 event.

Appendix E. Peach Bottom Fire Event Data Table--Auxiliary Building Fires (Continued)

Plant Name	Date of Occurrence	Plant Status	Fire Type	Remarks
Arnold	5/7/77	Refueling Outage	Circuit Breaker	Breaker relay failed, burning open and starting phase burner material above it on fire.
Salem 1	6/30/77	Power Operation	Relay - Cabinet	Fire detection instrumentation panel fire due to relay failure.
Unknown	4/13/78	Power Operation	Circuit Breaker - MCC	Failure breaker contact due to improper maintenance - occurred in motor control center.
Robinson 2	7/16/78	Power Operation	Battery	Resistance heating of terminal connection ignited plastic tops of two cells of a battery.
Unknown	7/27/78	Power Operation	Battery Terminal	Defective terminal or connections not secured.
Arkansas Nuclear One 1	8/16/78	Cold Shutdown	Pump Motor	LPSI pump motor on fire (being used for shutdown cooling) due to incorrect installation of motor bearings resulting in shorting of rotor with the stator.
Salem 1	1/79	Power Operation (95%)	Transformer	Moisture in the windings resulted in a short and subsequent fire.

Appendix E. Peach Bottom Fire Event Data Table--Auxiliary Building Fires (Continued)

Plant Name	Date of Occurrence	Plant Status	Fire Type	Remarks
Palisades	4/4/79	Power Operation (100%)	Battery	Battery burst due to internal explosion of hydrogen ignited by a test lead being used to measure voltage.
San Onofre 1	11/27/79	Power Operation (100%)	Switchgear	Rodents shorted two phases of a 480V bus in the switchgear room.
Hatch 2	4/80	Cold Shutdown	Cable	A loose connection resulted in a wire of an RPS motor generator set breaker burning.
Unknown BWR	4/15/80	Power Operation	Bus	Fire involving supply bus occurred in switchgear room.
Peach Bottom 1	6/3/80	Power Operation (100%)	Transformer	A filtering capacitor in a vital bus transformer caught fire damaging the transformer.
Unknown PWR	7/6/80	Power Operation	Circuit Breaker	Circuit breaker caught fire when it failed to close properly because contacts were out of adjustment.
Unknown PWR	10/2/80	Power Operation	Valve Motor	Air sample inlet valve motor issued smoke. Power was removed from motor.

Appendix E. Peach Bottom Fire Event Data Table--Auxiliary Building Fires (Continued)

Plant Name	Date of Occurrence	Plant Status	Fire Type	Remarks
Trojan	12/31/80	Power Operation (100%)	Circuit Breaker	Breaker stab misaligned causing ignition of plastic dust collector by arcing.
Palisades	1/24/81	Power Operation (98%)	Pump Motor	Component cooling water pump motor caught fire due to bearing failure from loss of lubricating oil.
San Onofre 1	7/17/81	Cold Shutdown	Gas Decay Tank	Explosion of H_2 in recombiner.
Indian Point 2	8/10/81	Power Operation (100%)	Pump Motor	Short circuit within SI pump caused fire and an overload trip of its supply breaker.
North Anna 1	11/11/81	Power Operation	Pump	Main feedwater pump fire.
Hatch 1	11/23/81	Cold Shutdown	Relay	Insulation breakdown caused fire in a reactor low-low RPS relay.
Point Beach 1	10/15/82	Power Operation (78%)	Circuit Breaker	Supply breaker for MG set caught fire.

Appendix E. Peach Bottom Fire Event Data Table--Auxiliary Building Fires (Continued)

Plant Name	Date of Occurrence	Plant Status	Fire Type	Remarks
Salem 1	11/9/82	Cold Shutdown	Relay	Relay failure resulted in a fire in a fire detection instrumentation panel. Fire detectors for switchgear rooms, battery room, and DG area were rendered inoperable.
Brunswick 1	11/27/82	Power Operation (68%)	Battery Charger	Resistor on charger amplifier board opened causing a voltage increase and capacitor failure.
Oconee 2	2/3/83	Power Operation (100%)	Pump Motor	Loss of lubrication oil resulted in high bearing temperature and smoke.
Brunswick 1	4/26/83	Refueling	Transformer	Following a loss of offsite power, a fire occurred in a transformer between emergency buses.
Oconee 3	5/25/83	Power Operation (100%)	Cable and Conduit	Welding operation started a fire in conduit surrounding a cable (letdown valve).

Appendix E. Peach Bottom Fire Event Data Table--Auxiliary Building Fires (Concluded)

Plant Name	Date of Occurrence	Plant Status	Fire Type	Remarks
Salem 2	6/20/83	Cold Shutdown	Transformer	Transformer breaker tripped on overcurrent and was reclosed. Fire occurred immediately thereafter.
Peach Bottom 1	9/9/83	Power Operation (100%)	Control Panel	Water entered a control room ventilation chiller control panel shorting motor starter contacters.
Yankee Rowe	8/2/84	Power Operation (100%)	Circuit Breaker	High resistance in the main disconnecting contacts of the center phase of the breaker caused an arc to propagate to outside phases.

Appendix E. Peach Bottom Fire Event Data Table--Reactor Building Fires

Plant Name	Date of Occurrence	Plant Status	Fire Type	Remarks
Quad Cities 1	12/10/72	Power Operation	Oil, Insul-ation	A small open flame was observed within a RHR service-water pump housing. Fire was set by welding sparks on oil soaked insulation.
Peach Bottom 1	12/22/72	Power Operation		The motor on a residual heat removal pump burst into flames due to insufficient lubrication to the lower bearing.
Monticello	5/15/74	Hot Shutdown	Hydrogen	An off-gas ignition occurred resulting in the rupture of both air ejector discharge line rupture discs.
Dresden 3	11/15/74	Power Operation	Hydrogen	An off-gas explosion occurred when the 3A recombiner outlet valve was opened.
Oconee 2	1/31/75	Hot Shutdown	Oil	A small oil fire occurred underneath a reactor coolant pump motor stand.
Brunswick 2	4/14/77	Power Operation	Hydrogen	A hydrogen flame was in the off-gas system at burning the flow orifice or in the jet air ejector.

Appendix E. Peach Bottom Fire Event Data Table--Reactor Building Fires (Continued)

Plant Name	Date of Occurrence	Plant Status	Fire Type	Remarks
Brunswick 2	6/15/77	Power Operation	Hydrogen	Following an off-gas over-pressurization, a hydrogen fire was detected downstream of the steam jet air ejectors.
Unknown BWR	2/10/78	Power Operation	Electrical	Smok[illegible]d coming from [illegible]wer.
Indian Point 2	9/4/79	Power Operation	Oil, Insulation	[illegible] the reactor coolant pump tube. Insulation was saturated with oil and ignited.
Robinson 2	9/30/79	Power Operation	Oil	[illegible]gging fire on cold leg piping. Fire caused by [illegible]bricating oil leak.
San Onofre 1	/16/80	Hot Shutdown	Oil, Insulation	Oil from leaking reactor coolant pump oil filter came in contact with the hot pump casing and ignited.
Nine Mile Point 1	4/22/80	Power Operation	Oil	Fire resulted from lube oil that leaked from a main turbine shaft-driven feed water pump.

Appendix E. Peach Bottom Fire Event Data Table--Reactor Building Fires (Concluded)

Plant Name	Date of Occurrence	Plant Status	Fire Type	Remarks
Pilgrim	2/24/81	Power Operation	Insu-lation	A fire was ignited by welded sparks falling on temporary foam rubber insulation.
Unknown PWR	11/7/81	Power Operation	Elec-trical	Wiring harness was pinched off inside a cabinet and electrically shorted out.
Unknown BWR	2/12/82	Cold Shutdown	Oil	Pipe vibrating loose leaked onto a hot turbine casing.

Appendix E. Peach Bottom Fire Event Data Table--Control Room Fires

Plant Name	Date of Occurrence	Plant Status	Fire Type	Remarks
Unknown	7/4/78	Power Operation	Diode	Zener diode failed in an RPS circuit.
Three Mile Island 2	7/12/79	Cold Shutdown	Circuit Board	Overheated resistor caused fire in a radiation monitoring readout panel. Extinguished immediately.
Hatch 1*	3/12/83	Power Operation (94%)	Relay	Low reactor water level RPS relay burned causing a 1/2 scram (failed safe). Extinguished by operators.
Hatch 1*	3/30/83	Power Operation (34%)	Relay	Scram discharge volume high level RPS relay burned a 1/2 scram (failed causing safe). Extinguished by operators. Same type of relay as in previous event.

*Counted as one event for quantification of fire frequency.

Appendix E. Peach Bottom Fire Event Data Table--Cable Spreading Room Fires

Plant Name	Date of Occurrence	Plant Status	Fire Type	Remarks
Browns Ferry 1&2	3/22/75	Power Operation (100%)	Cable Fire	Spread from cable spreading room to reactor building in Unit 1 and affected Unit 2.
Peach Bottom 3	4/18/77	Power Operation (25%)	Relay Fire	Fire in PCIS logic and RHR valve relay.

Appendix E. Peach Bottom Fire Event Data Table--Switchgear Room Fires

Plant Name	Date of Occurrence	Plant Status	Fire Type	Remarks
Unknown PWR	11/7/79	Power Operation	480 V Bus	Fire involved 480 V bus; short circuit caused by rodent bridging two energized phases.
Unknown BWR	4/15/80	Power Operation	Bus	Fire involved supply bus in switchgear room.
Unknown PWR	7/6/80	Power Operation	Circuit Breaker	Fire involving switchgear room breaker. Out of adjustment control circuit completed
Yankee Rowe	8/2/84	Power Operation (100%)	Circuit Breaker	A fault occurred in the 480 V supply ACB to bus 4-1; high resistance in the main disconnecting contacts caused an arc to propagate from the center phase to the outside phases.

Appendix E. Peach Bottom Fire Event Data Table--Battery Room Fires

Plant Name	Date of Occurrence	Plant Status	Fire Type	Remarks
Robinson 2	7/16/78	Power	Battery	Plastic tops of two Operation cells of a station battery caught fire caused by resistance heating of a terminal connection during the heavy dc load of the emergency oil pump.
Unknown	7/27/78	Power Operation	Battery	Fire caused by defective terminal or unsecured connections.
Palisades	4/4/79	Power Operation (100%)	Battery	A test lead being used to take battery voltage readings fell and struck a battery connector, causing a spark which ignited hydrogen gas.
Brunswick 1	11/27/82	Power Operation (68%)	Capacitor	Battery charger capacitor caught fire for unknown reason.

Appendix E. Peach Bottom Fire Event Data Table--Turbine Building Fires

Plant Name	Date of Occurrence	Plant Status	Fire Type	Remarks
Nine Mile Point	9/13/72	Power Operation	Oil, Insulation	Leak in oil supply line soaked insulation and ignited when it came in contact with hot pipe.
Yankee Rowe	6/15/73	Power Operation	Oil, Insulation	A fire started in oil soaked insulation around the high pressure turbine bearing casing.
Unknown PWR	8/15/73	Power Operation	Unknown	Fire around turbine area-unknown cause.
Unknown PWR	9/20/74	Power Operation	Ping Pong Balls	Cigarette ignited box of ping pong balls - automatic deluge system initiated.
Kewaunee	4/15/75	Power Operation	Bus	Bus fault resulted in cable insulation damage.
Unknown PWR	6/27/75	Power Operation	Oil	Leaking oil from a turbine oil purifier ignited when it contacted purifier heaters. Cables above the fire charred.
Haddam Neck	9/75	Power	Oil, Operation	Oil soaked insulation Insulation fire on gland steam lines under high pressure turbine.

Appendix E. Peach Bottom Fire Event Data Table--Turbine Building Fires (Continued)

Plant Name	Date of Occurrence	Plant Status	Fire Type	Remarks
Unknown PWR	4/3/77	Power Operation	Hydrogen	Leaking hydrogen at the generator ignited. Purged with CO_2 by shift personnel.
Saint Lucie 1	4/3/77	Power Operation	Hydrogen	Hydrogen leaked from turbine and ignited. Generator inerted with CO_2.
Oyster Creek 1	5/77	Refueling	Cable Insulation	Aluminum to copper bus terminal connecters resulted in high resistance and burned cable insulation.
Peach Bottom 3	9/77	Power Operation	Relays	Three relays in feedwater pump relay cabinet ignited. Since flame retardant cables were used in cabinet, fire did not propagate.
Unknown PWR	7/5/78	Power Operation	Auxiliary Boiler	Class B fire including the auxiliary boiler.
Cook 2	11/13/78	Power Operation	Hydrogen	Hydrogen fire under generator. Purged with CO_2.
Browns Ferry 1	1/21/80	Power Operation	Cable Insulation	Fire in cable tray beneath the turbine building operating floor.

Appendix E. Peach Bottom Fire Event Data Table--Turbine Building Fires (Concluded)

Plant Name	Date of Occurrence	Plant Status	Fire Type	Remarks
Cook 2	12/15/80	Power Operation	Electrical	Fire in generator pilot exciter.
Unknown BWR	7/24/81	Power Operation	Pump	Condensate booster pump binding overheated and caught fire.
Sequoyah 1	1/19/82	Cold Shutdown	Transformer	Neutral ground transformer exploded activating deluge system.
Unknown BWR	2/4/82	Power Operation	Hydrogen	Hydrogen leaked from a bad seal into the generator.
Rancho Seco	3/19/84	Power Operation	Hydrogen	Hydrogen explosion occurred following loss of H_2 side seal oil pump.
Indian Point 2	10/22/84	Power Operation	Insulation	Fire in insulation at the governor end of the high pressure turbine.
Arnold	11/4/84	Power Operation	Transformer	Transformer fire in yard propagated to the turbine building.

Appendix E. Peach Bottom Fire Event Data Table--Diesel Generator Room Fires

Plant Name	Date of Occurrence	Plant Status	Fire Type	Remarks
Three Mile Island 1	11/18/74	Power Operation	Oil	Leaking oil onto external surface of a diesel engine exhaust manifold ignited.
Three Mile Island 1	12/15/74	Power Operation	Oil	A small fire occurred in the lagging around the diesel engine exhaust inlet.
Unknown PWR	3/5/75	Power Operation	Cable	A fire started on a lift drive motor electrical cable left adjacent to the diesel generator exhaust stack.
Fitzpatrick	3/15/75	Power Operation	Oil	Back pressure in the exhaust manifold caused an explosion in the crankcase. Oil leaked from several locations and ignited on the exhaust manifold.
Millstone 2	9/15/75	Power Operation	Oil	Fire in a diesel exhaust manifold.
Duane Arnold	12/21/75	Power Operation	Oil	A small fire occurred on the surface of the exhaust manifold.
Duane Arnold	2/27/76	Refueling Outage	Oil	A small fire occurred on the exhaust manifold.

Appendix E. Peach Bottom Fire Event Data Table--Diesel Generator Room Fires (Continued)

Plant Name	Date of Occurrence	Plant Status	Fire Type	Remarks
Duane Arnold	3/17/76	Refueling Outage	Oil	The diesel flange gasket leaked exhaust gases with traces of oil onto the exterior of the flange. The oil was ignited by exhaust heat.
Duane Arnold	4/17/76	Power Operation	Oil	Oil leaked onto the diesel exhaust manifold and caught fire.
Millstone 2	9/15/76	Power Operation	Oil, Insulation	A small fire occurred on the exhaust manifold on the control end of the engine.
Zion 2	9/15/76	Power Operation		An operator disconnected a dc tie breaker, tripping the reactor and initiating safety injection. The main generator was overloaded, resulting in a fire.
Fitzpatrick	10/15/76	Power Operation	Oil	During testing a fire was discovered in the exhaust of the emergency diesel generator.
Duane Arnold	11/4/76	Power Operation	Oil	A hairline fracture in a fuel line fitting caused fuel to spray out and be ignited by heat from the exhaust header.

Appendix E. Peach Bottom Fire Event Data Table--Diesel Generator Room Fires (Continued)

Plant Name	Date of Occurrence	Plant Status	Fire Type	Remarks
Unknown PWR	12/4/76	Power Operation	Oil	During maintainence on the emergency diesel, a filter was ignited due to overheated oil.
Calvert Cliffs 1	7/11/77	Power Operation	Oil	A small fire developed when lube oil sprayed from the lube oil strainer and ignited on contact with the exhaust manifold.
Kewaunee	9/20/77	Power Operation	Carbon Buildup	A fire was caused by carbon residue buildup in the exhaust path through the turbocharger.
Unknown	12/28/77	Power Operation		Probable cause of fire was combustible materials left in close proximity to the diesel exhaust stack.
Arkansas Nuclear One 1	3/20/78	Refueling Outage	Oil	Failure of bearing oil seal allowed lubricating oil into the turbocharger of the diesel generator.
Arkansas Nuclear One 1	11/15/78	Refueling Outage	Oil	Fire in a diesel exhaust manifold during a test.

Appendix E. Peach Bottom Fire Event Data Table--Diesel Generator Room Fires (Continued)

Plant Name	Date of Occurrence	Plant Status	Fire Type	Remarks
Crystal River 3	7/24/79	Hot Shutdown	Oil, Carbon	A fire was caused in the exhaust manifold of an emergency diesel generator by an excessive fuel rich mixture aided by oil and carbon accumulation.
Unknown PWR	7/24/79	Power Operation	Elec-trical	A fire involved the exciter control cabinet of a diesel generator.
Crystal River 3	10/15/79	Hot Shutdown	Oil	Fire in the exhaust manifold fuel-oil mix rich on start (test).
Maine Yankee	10/15/79	Power Operaion	Oil	A diesel turbocharger failed which resulted in a fire within the exhaust system.
Calvert Cliffs 2	3/7/80	Power Operation		A small fire occurred in a diesel generator room.
Davis-Besse 1	7/15/80	Power Operation		Fire in a turbocharger.
Davis-Besse 1	7/23/80	Cold Shutdown	Oil	A diesel turbocharger failed which resulted in a fire in the exhaust pipe.

Appendix E. Peach Bottom Fire Event Data Table--Diesel Generator Room Fires (Continued)

Plant Name	Date of Occurrence	Plant Status	Fire Type	Remarks
Unknown PWR	3/9/81	Power Operation	Oil, Insulation	Fire involved exhaust manifold insulation.
North Anna 1	4/15/81	Power Operation	Oil	An oil leak in the area of the exhaust manifold started a small fire.
Unknown BWR	5/15/81	Power Operation	Electrical	Smoke filled diesel generator buiding.
Arkansas Nuclear One 2	6/30/81	Hot Shutdown	Oil, Insulation	Oil leaked through a diesel gasket onto insulation, igniting a fire.
San Onofre 1	7/14/81	Power Operation	Oil	Lube oil spraying from a cracked instrument line was ignited by hot exhaust piping above the diesel engine.
North Anna 1	7/16/81	Power Operation	Oil	An oil leak in the diesel exhaust manifold caused the fire.
Arkansas Nuclear One 1	7/27/81	Power Operation	Oil, Insulation	Fire on oil soaked insulation on a diesel engine.

Appendix E. Peach Bottom Fire Event Data Table--Diesel Generator Room Fires (Concluded)

Plant Name	Date of Occurrence	Plant Status	Fire Type	Remarks
Zion 1	8/15/81	Power Operation	Oil	Lube oil sprayed past a operation o-ring seal onto a hot exhaust manifold caused a fire.
Prairie Island 1	8/15/82	Power Operation	Oil	Turbocharger oil gasket filter failure sprayed lube oil on hot exhaust manifold and ignited.
Peach Bottom 2	9/7/83	Maintainence Outage	Oil	A diesel governor increased fuel flow as a result of a turbocharger failure. Excess fuel ignited in the exhaust.
Surry 1	12/18/84	Cold Shutdown	Oil	A diesel fire was caused by a leaking fitting on a fuel injector line.

DISTRIBUTION:

Frank Abbey
U. K. Atomic Energy Authority
Wigshaw Lane, Culcheth
Warrington, Cheshire, WA3 4NE
ENGLAND

Kiyoharu Abe
Department of Reactor Safety Research
Nuclear Safety Research Center
ToKai Research Establishment
JAERI
Tokai-mura, Naga-gun
Ibaraki-ken,
JAPAN

Ulvi Adalioglu
Nuclear Engineering Division
Cekmece Nuclear Research and Training Centre
P.K.1, Havaalani
Istanbul
TURKEY

Bharat Agrawal
USNRC-RES/AEB
MS: NL/N-344

Kiyoto Aizawa
Safety Research Group
Reactor Research and Development Project
PNC
9-13m 1-Chome Akasaka
Minatu-Ku
Tokyo
JAPAN

Oguz Akalin
Ontario Hydro
700 University Avenue
Toronto, Ontario
CANADA M5G 1X6

David Aldrich
Science Applications International Corporation
1710 Goodridge Drive
McLean, VA 22102

Agustin Alonso
University Politecnica De Madrid
J Gutierrez Abascal, 2
28006 Madrid
SPAIN

Christopher Amos
Science Applications International Corporation
2109 Air Park Road SE
Albuquerque, NM 87106

Richard C. Anoba
SAIC
4900 Motors Edge Drive, Suite 255
Raleigh, NC 27606

George Apostolakis
UCLA
Boelter Hall, Room 5532
Los Angeles, CA 90024

James W. Ashkar
Boston Edison Company
800 Boylston Street
Boston, MA 02199

Donald H. Ashton
Bechtel Power Corporation
P.O. Box 2166
Houston, TX 77252-2166

J. de Assuncao
Cabinete de Proteccao e Seguranca Nuclear
Secretario de Estado de Energia
Ministerio da Industria
av. da Republica, 45-6°
1000 Lisbon
PORTUGAL

Mark Averett
Florida Power Corporation
P.O. Box 14042
St. Petersburg, FL 33733

Raymond O. Bagley
Northeast Utilities
P.O. Box 270
Hartford, CT 06141-0270

Juan Bagues
Consejo de Seguridad Nucleare
Sarangela de la Cruz 3
28020 Madrid
SPAIN

George F. Bailey
Washington Public Power Supply System
P. O. Box 968
Richland, WA 99352

H. Bairiot
Belgonucleaire S A
Rue de Champ de Mars 25
B-1050 Brussels
BELGIUM

Louis Baker
Reactor Analysis and Safety Division
Building 207
Argonne National Laboratory
9700 South Cass Avenue
Argonne, IL 60439

H-P. Balfanz
TUV-Norddeutschland
Grosse Bahnstrasse 31,
2000 Hamburg 54
FEDERAL REPUBLIC OF GERMANY

Patrick Baranowsky
USNRC-NRR/OEAB
MS: 11E-22

H. Bargmann
Dept. de Mecanique
Inst. de Machines Hydrauliques et de Mecaniques des Fluides
Ecole Polytechnique de Lausanne
CH-1003 Lausanne
M.E. (ECUBLENS)
CH. 1015 Lausanne
SWITZERLAND

Robert A. Bari
Brookhaven National Laboratory
Building 130
Upton, NY 11973

Richard Barrett
USNRC-NRR/PRAB
MS: 10A-2

Kenneth S. Baskin
S. California Edison Company
P.O. Box 800
Rosemead, CA 91770

J. Basselier
Belgonucleaire S A
Rue du Champ de Mars 25, B-1050
Brussels
BELGIUM

Werner Bastl
Gesellschaft Fur Reaktorsicherheit
Forschungsgelande
D-8046 Garching
FEDERAL REPUBLIC OF GERMANY

Anton Bayer
BGA/ISH/ZDB
Postfach 1108
D-8042 Neuherberg
FEDERAL REPUBLIC OF GERMANY

Ronald Bayer
Virginia Electric Power Co.
P. O. Box 26666
Richmond, VA 23261

Eric S. Beckjord
Director
USNRC-RES
MS: NL/S-007

Bruce B. Beckley
Public Service Company
P.O. Box 330
Manchester, NH 03105

William Beckner
USNRC-RES/SAIB
MS: NL/S-324

Robert M. Bernero
Director
USNRC-NMSS
MS: 6A-4

Ronald Berryman [2]
Virginia Electric Power Co.
P. O. Box 26666
Richmond, VA 23261

Robert C. Bertucio
NUS Corporation
1301 S. Central Ave, Suite 202
Kent, WA 98032

John H. Bickel
EG&G Idaho
P.O. Box 1625
Idaho Falls, ID 83415

Peter Bieniarz
Risk Management Association
2309 Dietz Farm Road, NW
Albuquerque, NM 87107

Adolf Birkhofer
Gesellschaft Fur Reaktorsicherheit
Forschungsgelande
D-8046 Garching
FEDERAL REPUBLIC OF GERMANY

James Blackburn
Illinois Dept. of Nuclear Safety
1035 Outer Park Drive
Springfield, IL 62704

Dennis C. Bley
Pickard, Lowe & Garrick, Inc.
2260 University Drive
Newport Beach, CA 92660

Roger M. Blond
Science Applications Int. Corp.
20030 Century Blvd., Suite 201
Germantown, MD 20874

Simon Board
Central Electricity Generating
Board
Technology and Planning Research
Division
Berkeley Nuclear Laboratory
Berkeley Gloucestershire, GL139PB
UNITED KINGDOM

Mario V. Bonace
Northeast Utilities Service Company
P.O. Box 270
Hartford, CT 06101

Gary J. Boyd
Safety and Reliability Optimization
Services
9724 Kingston Pike, Suite 102
Knoxville, TN 37922

Robert J. Breen
Electric Power Research Institute
3412 Hillview Avenue
Palo Alto, CA 94303

Charles Brinkman
Combustion Engineering
7910 Woodmont Avenue
Bethesda, MD 20814

K. J. Brinkmann
Netherlands Energy Res. Fdtn.
P.O. Box 1
1755ZG Petten NH
NETHERLANDS

Allan R. Brown
Manager, Nuclear Systems and
Safety Department
Ontario Hydro
700 University Ave.
Toronto, Ontario M5G1X6
CANADA

Robert G. Brown
TENERA L.P.
1340 Saratoga-Sunnyvale Rd.
Suite 206
San Jose, CA 95129

Sharon Brown
EI Services
1851 So. Central Place, Suite 201
Kent, WA 98031

Ben Buchbinder
NASA, Code QS
600 Maryland Ave. SW
Was...agton, DC 20546

R. H. Buchholz
Nutech
6835 Via Del Oro
San Jose, CA 95119

Robert J. Budnitz
Future Resources Associates
734 Alameda
Berkeley, CA 94707

Gary R. Burdick
USNRC-RES/DSR
MS: NL/S-007

Arthur J. Buslik
USNRC-RES/PRAB
MS: NL/S-372

M. Bustraan
Netherlands Energy Res. Fdtn.
P.O. Box 1
1755ZG Petten NH
NETHERLANDS

Nigel E. Buttery
Central Electricity Generating Board
Booths Hall
Chelford Road, Knutsford
Cheshire, WA168QG
UNITED KINGDOM

Jose I. Calvo Molins
Probabilistic Safety Analysis Group
Consejo de Seguridad Nuclear
Sor Angela de la Cruz 3, Pl. 6
28020 Madrid
SPAIN

J. F. Campbell
Nuclear Installations Inspectorate
St. Peters House
Balliol Road, Bootle
Merseyside, L20 3LZ
UNITED KINGDOM

Kenneth S. Canady
Duke Power Company
422 S. Church Street
Charlotte, NC 28217

Lennart Carlsson
IAEA A-1400
Wagramerstrasse 5
P.O. Box 100
Vienna, 22
AUSTRIA

Annick Carnino
Electricite de France
32 Rue de Monceau 8EME
Paris, F5008
FRANCE

G. Caropreso
Dept. for Envir. Protect. & Hlth.
ENEA Cre Casaccia
Via Anguillarese, 301
00100 Roma
ITALY

James C. Carter, III
TENERA L.P.
Advantage Place
308 North Peters Road
Suite 280
Knoxville, TN 37922

Eric Cazzoli
Brookhaven National Laboratory
Building 130
Upton, NY 11973

John G. Cesare
SERI
Director Nuclear Licensing
5360 I-55 North
Jackson, MS 39211

S. Chakraborty
Radiation Protection Section
Div. De La Securite Des Inst. Nuc.
5303 Wurenlingen
SWITZERLAND

Sen-I Chang
Institute of Nuclear Energy Research
P.O. Box 3
Lungtan, 325
TAIWAN

J. R. Chapman
Yankee Atomic Electric Company
1671 Worcester Road
Framingham, MA 01701

Robert F. Christie
Tennessee Valley Authority
400 W. Summit Hill Avenue, W10D190
Knoxville, TN 37902

T. Cianciolo
BWR Assistant Director
ENEA DISP TX612167 ENEUR
Rome
ITALY

Thomas Cochran
Natural Resources Defense Council
1350 New York Ave. NW, Suite 300
Washington, D.C. 20005

Frank Coffman
USNRC-RES/HFB
MS: NL/N-316

Larry Conradi
NUS Corporation
16835 W. Bernardo Drive
Suite 202
San Diego, CA 92127

Peter Cooper
U.K. Atomic Energy Authority
Wigshaw Lane, Culcheth
Warrington, Cheshire, WA3 4NE
UNITED KINGDOM

C. Allin Cornell
110 Coquito Way
Portola Valley, CA 94025

Michael Corradini
University of Wisconsin
1500 Johnson Drive
Madison, WI 53706

E. R. Corran
Nuclear Technology Division
ANSTO Research Establishment
Lucas Heights Research Laboratories
Private Mail Bag 7
Menai, NSW 2234
AUSTRALIA

James Costello
USNRC-RES/SSEB
MS: NL/S-217A

George R. Crane
1570 E. Hobble Creek Dr.
Springville, UT 84663

Mat Crawford
SERI
5360 I-55 North
Jackson, MS 39211

Michael C. Cullingford
Nuclear Safety Division
IAEA
Wagramerstrasse, 5
P.O. Box 100
A-1400 Vienna
AUSTRIA

Garth Cummings
Lawrence Livermore Laboratory
L-91, Box 808
Livermore, CA 94526

Mark A. Cunningham
USNRC-RES/PRAB
MS: NL/S-372

James J. Curry
7135 Salem Park Circle
Mechanicsburg, PA 17055

Peter Cybulskis
Battelle Columbus Division
505 King Avenue
Columbus, OH 43201

Peter R. Davis
PRD Consulting
1935 Sabin Drive
Idaho Falls, ID 83401

Jose E. DeCarlos
Consejo de Seguridad Nuclear
Sor Angela de la Cruz 3, Pl. 8
28016 Madrid
SPAIN

M. Marc Decreton
Department Technologie
CEN/SCK
Boeretang 200
B-2400 Mol
BELGIUM

Richard S. Denning
Battelle Columbus Division
505 King Avenue
Columbus, OH 43201

Vernon Denny
Science Applications Int. Corp.
5150 El Camino Real, Suite 3
Los Altos, CA 94303

J. Devooget
Faculte des Sciences Appliques
Universite Libre de Bruxelles
av. Franklin Roosevelt
B-1050 Bruxelles
BELGIUM

R. A. Diederich
Supervising Engineer
Environmental Branch
Philadelphia Electric Co.
2301 Market St.
Philadelphia, PA 19101

Raymond DiSalvo
Battelle Columbus Division
505 King Avenue
Columbus, OH 43201

Mary T. Drouin
Science Applications International
Corporation
2109 Air Park Road S.E.
Albuquerque, NM 87106

Andrzej Drozd
Stone and Webster
Engineering Corp.
243 Summer Street
Boston, MA 02107

N. W. Edwards
NUTECH
145 Martinville Lane
San Jose, CA 95119

Ward Edwards
Social Sciences Research Institute
University of Southern California
Los Angeles, CA 90089-1111

Joachim Ehrhardt
Kernforschungszentrum Karlsruhe/INR
Postfach 3640
D-7500 Karlsruhe 1
FEDERAL REPUBLIC OF GERMANY

Adel A. El-Bassioni
USNRC-NRR/PRAB
MS: 10A-2

J. Mark Elliott
International Energy Associates,
Ltd., Suite 600
600 New Hampshire Ave., NW
Washington, DC 20037

Farouk Eltawila
USNRC-RES/AEB
MS: NL/N-344

Mike Epstein
Fauske and Associates
P. O. Box 1625
16W070 West 83rd Street
Burr Ridge, IL 60521

Malcolm L. Ernst
USNRC-RGN II

F. R. Farmer
The Long Wood, Lyons Lane
Appleton, Warrington
WA4 5ND
UNITED KINGDOM

P. Fehrenback
Atomic Energy of Canada, Ltd.
Chalk River Nuclear Laboratories
Chalk River Ontario, K0J1P0
CANADA

P. Ficara
ENEA Cre Casaccia
Department for Thermal Reactors
Via Anguillarese, 301
00100 ROMA
ITALY

A. Fiege
Kernforschungszentrum
Postfach 3640
D-7500 Karlsruhe
FEDERAL REPUBLIC OF GERMANY

John Flack
USNRC-RES/SAIB
MS: NLS-324

George F. Flanagan
Oak Ridge National Laboratory
P.O. Box Y
Oak Ridge, TN 37831

Karl N. Fleming
Pickard, Lowe & Garrick, Inc.
2260 University Drive
Newport Beach, CA 92660

Terry Foppe
Rocky Flats Plant
P. O. Box 464, Building T886A
Golden, CO 80402-0464

Joseph R. Fragola
Science Applications International Corporation
274 Madison Avenue
New York, NY 10016

Wiktor Frid
Swedish Nuclear Power Inspectorate
Division of Reactor Technology
P. O. Box 27106
S-102 52 Stockholm
SWEDEN

James Fulford
NUS Corporation
910 Clopper Road
Gaithersburg, MD 20878

Urho Fulkkinen
Technical Research Centre of Finland
Electrical Engineering Laboratory
Otakaari 7 B
SF-02150 Espoo 15
FINLAND

J. B. Fussell
JBF Associates, Inc.
1630 Downtown West Boulevard
Knoxville, TN 37919

John Garrick
Pickard, Lowe & Garrick, Inc.
2260 University Drive
Newport Beach, CA 92660

John Gaunt
British Embassy
3100 Massachusetts Avenue, NW
Washington, DC 20008

Jim Gieseke
Battelle Columbus Division
505 King Avenue
Columbus, OH 43201

Frank P. Gillespie
USNRC-NRR/PMAS
MS: 12G-18

Ted Ginsburg
Department of Nuclear Energy
Building 820
Brookhaven National Laboratory
Upton, NY 11973

James C. Glynn
USNRC-RES/PRAB
MS: NL/S-372

P. Govaerts
Departement de la Surete Nucleaire
Association Vincotte
avenue du Roi 157
B-1060 Bruxelles
BELGIUM

George Greene
Building 820M
Brookhaven National Laboratory
Upton, NY 11973

Carrie Grimshaw
Brookhaven National Laboratory
Building 130
Upton, NY 11973

H. J. Van Grol
Energy Technology Division
Energieonderzoek Centrum Nederland
Westerduinweg 3
Postbus 1
NL-1755 Petten ZG
NETHERLANDS

Sergio Guarro
Lawrence Livermore Laboratories
P. O. Box 808
Livermore, CA 94550

Sigfried Hagen
Kernforschungzentrum Karls. he
P. O. Box 3640
D-7500 Karlsruhe 1
FEDERAL REPUBLIC OF GERMANY

L. Hammar
Statens Karnkraftinspektion
P.O. Box 27106
S-10252 Stockholm
SWEDEN

Stephen Hanauer
Technical Analysis Corp.
6723 Whittier Avenue
Suite 202
McLean, VA 22101

Brad Hardin
USNRC-RES/TRAB
MS: NL/S-169

R. J. Hardwich, Jr.
Virginia Electric Power Co.
P.O. Box 26666
Richmond, Va 23261

Michael R. Haynes
UKAEA Harwell Laboratory
Oxfordshire
Didcot, Oxon., OX11 ORA
ENGLAND

Michael J. Hazzan
Stone & Webster
3 Executive Campus
Cherry Hill, NJ 08034

A. Hedgran
Royal Institute of Technology
Nuclear Safety Department
Bunellvagen 60
10044 Stockholm
SWEDEN

Sharif Heger
UNM Chemical and Nuclear
Engineering Department
Farris Engineering
Room 209
Albuquerque, NM 87131

Jon C. Helton
Dept. of Mathematics
Arizona State University
Tempe, AZ 85287

Robert E. Henry
Fauske and Associates, Inc.
16W070 West 83rd Street
Burr Ridge, IL 60521

P. M. Herttrich
Federal Ministry for the
Environment, Preservation of
Nature and Reactor Safety
Husarenstrasse 30
Postfach 120629
D-5300 Bonn 1
FEDERAL REPUBLIC OF GERMANY

F. Heuser
Giesellschaft Fur Reaktorsicherheit
Forschurgsgelande
D-8046 Garching
FEDERAL REPUBLIC OF GERMANY

E. F. Hicken
Giesellschaft Fur Reaktorsicherheit
Forschungsgelande
D-8046 Garching
FEDERAL REPUBLIC OF GERMANY

D. J. Higson
Radiological Support Group
Nuclear Safety Bureau
Australian Nuclear Science and
Technology Organisation
P.O. Box 153
Rosebery, NSW 2018
AUSTRALIA

Daniel Hirsch
University of California
A. Stevenson Program on
Nuclear Policy
Santa Cruz, CA 95064

H. Hirschmann
Hauptabteilung Sicherheit und
Umwelt
Swiss Federal Institute for
Reactor Research (EIR)
CH-5303 Wurenlingen
SWITZERLAND

Mike Hitchler
Westinghouse Electric Corp.
Savanna River Site
Aiken, SC 29808

Richard Hobbins
EG&G Idaho
P. O. Box 1625
Idaho Falls, ID 83415

Steven Hodge
Oak Ridge National Laboratory
P.O. Box Y
Oak Ridge, TN 37831

Lars Hoegberg
Office of Regulation and Research
Swedish Nuclear Power Inspectorate
P. O. Box 27106
S-102 52 Stockholm
SWEDEN

Lars Hoeghort
IAEA A-1400
Wagranerstraase 5
P.O. Box 100
Vienna, 22
AUSTRIA

Edward Hofer
Giesellschaft Fur Reaktorsicherheit
Forschurgsgelande
D-8046 Garching
FEDERAL REPUBLIC OF GERMANY

Peter Hoffmann
Kernforschingszentrum Karlsruhe
Institute for Material
Und Festkorperforsching I
Postfach 3640
D-7500 Karlsruhe 1
FEDERAL REPUBLIC OF GERMANY

N. J. Holloway
UKAEA Safety and Reliability
Directorate
Wigshaw Lane, Culcheth
Warrington, Cheshire, WA34NE
UNITED KINGDOM

Stephen C. Hora
University of Hawaii at Hilo
Division of Business Administration
and Economics
College of Arts and Sciences
Hilo, HI 96720-4091

J. Peter Hoseman
Swiss Federal Institute for
Reactor Research
CH-5303, Wurenlingen
SWITZERLAND

Thomas C. Houghton
KMC, Inc.
1747 Pennsylvania Avenue, NW
Washington, DC 20006

Dean Houston
USNRC-ACRS
MS: P-315

Der Yu Hsia
Taiwan Atomic Energy Council
67, Lane 144, Keelung Rd.
Sec. 4
Taipei
TAIWAN

Alejandro Huerta-Bahena
National Commission on Nuclear
Safety and Safeguards (CNSNS)
Insurgentes Sur N. 1776
Col. Florida
C. P. 04230 Mexico, D.F.
MEXICO

Kenneth Hughey [2]
SERI
5360 I-55 North
Jackson, MS 39211

Won-Guk Hwang
Kzunghee University
Yongin-Kun
Kyunggi-Do 170-23
KOREA

Michio Ichikawa
Japan Atomic Energy Research
Institute
Dept. of Fuel Safety Research
Tokai-Mura, Naka-Gun
Ibaraki-Ken, 319-1
JAPAN

Sanford Israel
USNRC-AEOD/ROAB
MS: MNBB-9715

Krishna R. Iyengar
Louisiana Power and Light
200 A Huey P. Long Avenue
Gretna, LA 70053

Jerry E. Jackson
USNRC-RES
MS: NL/S-302

R. E. Jaquith
Combustion Engineering, Inc.
1000 Prospect Hill Road
M/C 9490-2405
Windsor, CT 06095

S. E. Jensen
Exxon Nuclear Company
2101 Horn Rapids Road
Richland, WA 99352

Kjell Johannson
Studsvik Energiteknik AB
S-611 82, Nykoping
SWEDEN

Richard John
SSM, Room 102
927 W. 35th Place
USC, University Park
Los Angeles, CA 90089-0021

D. H. Johnson
Pickard, Lowe & Garrick, Inc.
2260 University Drive
Newport Beach, CA 92660

W. Reed Johnson
Department of Nuclear Engineering
University of Virginia
Reactor Facility
Charlottesville, VA 22901

Jeffery Julius
NUS Corporation
1301 S. Central Ave, Suite 202
Kent, WA 98032

H. R. Jun
Korea Adv. Energy Research Inst.
P.O. Box 7, Daeduk Danju
Chungnam 300-31
KOREA

Peter Kafka
Gesellschaft Fur Reaktorsicherheit
Forschungsgelande
D-8046 Garching
FEDERAL REPUBLIC OF GERMANY

Geoffrey D. Kaiser
Science Application Int. Corp.
1710 Goodridge Drive
McLean, VA 22102

William Kastenberg
UCLA
Boelter Hall, Room 5532
Los Angeles, CA 90024

Walter Kato
Brookhaven National Laboratory
Associated Universities, Inc.
Upton, NY 11973

M. S. Kazimi
MIT, 24-219
Cambridge, MA 02139

Ralph L. Keeney
101 Lombard Street
Suite 704W
San Francisco, CA 94111

Henry Kendall
Executive Director
Union of Concerned Scientists
Cambridge, MA

Frank King
Ontario Hydro
700 University Avenue
Bldg. H11 G5
Toronto
CANADA M5G1X6

Oliver D. Kingsley, Jr.
Tennessee Valley Authority
1101 Market Street
GN-38A Lookout Place
Chattanooga, TN 37402

Stephen R. Kinnersly
Winfrith Atomic Energy
Establishment
Reactor Systems Analysis Division
Winfrith, Dorchester
Dorset DT2 8DH
ENGLAND

Ryohei Kiyose
University of Tokyo
Dept. of Nuclear Engineering
7-3-1 Hongo Bunkyo
Tokyo 113
JAPAN

George Klopp
Commonwealth Edison Company
P.O. Box 767, Room 35W
Chicago, IL 60690

Klaus Koberlein
Gesellschaft Fur Reaktorsicherheit
Forschungsgelande
D-8046 Garching
FEDERAL REPUBLIC OF GERMANY

E. Kohn
Atomic Energy Canada Ltd.
Candu Operations
Mississauga
Ontario, L5K 1B2
CANADA

Alan M. Kolaczkowski
Science Applications International
Corporation
2109 Air Park Road, S.E.
Albuquerque, NM 87106

S. Kondo
Department of Nuclear Engineering
Facility of Engineering
University of Tokyo
3-1, Hongo 7, Bunkyo-ku
Tokyo
JAPAN

Herbert J. C. Kouts
Brookhaven National Laboratory
Building 179C
Upton, NY 11973

Thomas Kress
Oak Ridge National Laboratory
P.O. Box Y
Oak Ridge, TN 37831

W. Kroger
Institut iur Nukleare
Sicherheitsforschung
Kernforschungsanlage Julich GmbH
Postfach 1913
D-5170 Julich 1
FEDERAL REPUBLIC OF GERMANY

Greg Krueger [3]
Philadelphia Electric Co.
2301 Market St.
Philadelphia, PA 19101

Bernhard Kuczera
Kernforschungzentrum Karlsruhe
LWR Safety Project Group (PRS)
P. O. Box 3640
D-7500 Karlsruhe 1
FEDERAL REPUBLIC OF GERMANY

Jeffrey L. LaChance
Science Applications International
Corporation
2109 Air Park Road S.E.
Albuquerque, NM 87106

H. Larsen
Riso National Laboratory
Postbox 49
DK-4000 Roskilde
DENMARK

Wang L. Lau
Tennessee Valley Authority
400 West Summit Hill Avenue
Knoxville, TN 37902

Timothy J. Leahy
EI Services
1851 South Central Place, Suite 201
Kent, WA 98031

John C. Lee
University of Michigan
North Campus
Dept. of Nuclear Engineering
Ann Arbor, MI 48109

Tim Lee
USNRC-RES/RPSB
MS: NL/N-353

Mark T. Leonard
Science Applications International Corporation
2109 Air Park Road, SE
Albuquerque, NM 87106

Leo LeSage
Director, Applied Physics Div.
Argonne National Laboratory
Building 208, 9700 South Cass Ave.
Argonne, IL 60439

Milton Levenson
Bechtel Western Power Company
50 Beale St.
San Francisco, CA 94119

Librarian
NUMARC/USCEA
1776 I Street NW, Suite 400
Washington, DC 80006

Eng Lin
Taiwan Power Company
242, Roosevelt Rd., Sec. 3
Taipei
TAIWAN

N. J. Liparulo
Westinghouse Electric Corp.
P. O. Box 355
Pittsburgh, PA 15230

Y. H. (Ben) Liu
Department of Mechanical Engineering
University of Minnesota
Minneapolis, MN 55455

Bo Liwnang
IAEA A-1400
Swedish Nuclear Power Inspectorate
P.O. Box 27106
S-102 52 Stockholm
SWEDEN

J. P. Longworth
Central Electric Generating Board
Berkeley Gloucester
GL13 9PB
UNITED KINGDOM

Walter Lowenstein
Electric Power Research Institute
3412 Hillview Avenue
P. O. Box 10412
Palo Alto, CA 94303

William J. Luckas
Brookhaven National Laboratory
Building 130
Upton, NY 11973

Hans Ludewig
Brookhaven National Laboratory
Building 130
Upton, NY 11973

Robert J. Lutz, Jr.
Westinghouse Electric Corporation
Monroeville Energy Center
EC-E-371, P. O. Box 355
Pittsburgh, PA 15230-0355

Phillip E. MacDonald
EG&G Idaho, Inc.
P.O. Box 1625
Idaho Falls, ID 83415

Jim Mackenzie
World Resources Institute
1735 New York Ave. NW
Washington, DC 20006

Richard D. Fowler
Idaho Nat. Engineering Laboratory
P.O. Box 1625
Idaho Falls, ID 83415

A. P. Malinauskas
Oak Ridge National Laboratory
P.O. Box Y
Oak Ridge, TN 37831

Giuseppe Mancini
Commission European Comm.
CEC-JRC Eraton
Ispra Varese
ITALY

Lasse Mattila
Technical Research Centre of Finland
Lonnrotinkatu 37, P. O. Box 169
SF-00181 Helsinki 18
FINLAND

Roger J. Mattson
SCIENTECH Inc.
11821 Parklawn Dr.
Rockville, MD 20852

Donald McPherson
USNRC-NRR/DONRR
MS: 12G-18

Jim Metcalf
Stone and Webster Engineering Corporation
245 Summer St.
Boston, MA 02107

Mary Meyer
A-1, MS F600
Los Alamos National Laboratory
Los Alamos, NM 87545

Ralph Meyer
USNRC-RES/AEB
MS: NL/N-344

Charles Miller
8 Hastings Rd.
Momsey, NY 10952

Joseph Miller
Gulf States Utilities
P. O. Box 220
St. Francisville, LA 70775

William Mims
Tennessee Valley Authority
400 West Summit Hill Drive.
W10D199C-K
Knoxville, TN 37902

Jocelyn Mitchell
USNRC-RES/SAIB
MS: NL/S-324

Kam Mohktarian
CBI Na-Con Inc.
800 Jorie Blvd.
Oak Brook, IL 60521

James Moody
P.O. Box 641
Rye, NH 03870

S. Mori
Nuclear Safety Division
OECD Nuclear Energy Agency
38 Blvd. Suchet
75016 Paris
FRANCE

Walter B. Murfin
P.O. Box 550
Mesquite, NM 88048

Joseph A. Murphy
USNRC-RES/DSR
MS: NL/S-007

V. I. Nath
Safety Branch
Safety Engineering Group
Sheridan Park Research Community
Mississauga, Ontario L5K 1B2
CANADA

Susan J. Niemczyk
1545 18th St. NW, #112
Washington, DC 20036

Pradyot K. Niyogi
USDOE-Office of Nuclear Safety
Washington, DC 20545

Paul North
EG&G Idaho, Inc.
P. O. Box 1625
Idaho Falls, ID 83415

Edward P. O'Donnell
Ebasco Services, Inc.
2 World Trade Center, 89th Floor
New York, NY 10048

David Okrent
UCLA
Boelter Hall, Room 5532
Los Angeles, CA 90024

Robert L. Olson
Tennessee Valley Authority
400 West Summit Hill Rd.
Knoxville, TN 37902

Simon Ostrach
Case Western Reserve University
418 Glenman Bldg.
Cleveland, OH 44106

D. Paddleford
Westinghouse Electric Corporation
Savanna River Site
Aiken, SC 29808

Robert L. Palla, Jr.
USNRC-NRR/PRAB
MS: 10A-2

Chang K. Park
Brookhaven National Laboratory
Building 130
Upton, NY 11973

Michael C. Parker
Illinois Department of Nuclear Safety
1035 Outer Park Dr.
Springfield, IL 62704

Gareth Parry
NUS Corporation
910 Clopper Road
Gaithersburg, MD 20878

J. Pelce
Departement de Surete Nucleaire
IPSN
Centre d'Estudes Nucleaires du CEA
B.P. no. 6, Cedex
F-92260 Fontenay-aux-Roses
FRANCE

G. Petrangeli
ENEA Nuclear Energy ALT Disp
Via V. Brancati, 48
00144 Rome
ITALY

Marty Plys
Fauske and Associates
16W070 West 83rd St.
Burr Ridge, IL 60521

Mike Podowski
Department of Nuclear Engineering and Engineering Physics
RPI
Troy, NY 12180-3590

Robert D. Pollard
Union of Concerned Scientists
1616 P Street, NW, Suite 310
Washington, DC 20036

R. Potter
UK Atomic Energy Authority
Winfrith, Dorchester
Dorset, DT2 8DH
UNITED KINGDOM

William T. Pratt
Brookhaven National Laboratory
Building 130
Upton, NY 11973

M. Preat
Chef du Service Surete Nucleaire et Assurance Qualite
TRACTEBEL
Bd. du Regent 8
B-100 Bruxells
BELGIUM

David Pyatt
USDOE
MS: EH-332
Washington, DC 20545

William Raisin
NUMAEC
1726 M St. NW
Suite 904
Washington, DC 20036

Joe Rashid
ANATECH Research Corp.
3344 N. Torrey Pines Ct.
Suite 1320
La Jolla, CA 90237

Dale M. Rasmuson
USNRC-RES/PRAB
MS: NL/S-372

Ingvard Rasmussen
Riso National Laboratory
Postbox 49
DK-4000, Roskilde
DENMARK

Norman C. Rasmussen
Massachusetts Institute of
Technology
77 Massachusetts Avenue
Cambridge, MA 02139

John W. Reed
Jack R. Benjamin & Associates, Inc.
444 Castro St., Suite 501
Mountain View, CA 94041

David B. Rhodes
Atomic Energy of Canada, Ltd.
Chalk River Nuclear Laboratories
Chalk River, Ontario K0J1P0
CANADA

Dennis Richardon
Westinghouse Electric Corporation
P.O. Box 355
Pittsburgh, PA 15230

Doug Richeard
Virginia Electric Power Co.
P.O.Box 26666
Richmond, VA 23261

Robert Ritzman
Electric Power Research Institute
3412 Hillview Avenue
Palo Alto, CA 94304

Richard Robinson
USNRC-RES/PRAB
MS: NL/S-372

Jack E. Rosenthal
USNRC-AEOD/ROAB
MS: MNBB-9715

Denwood F. Ross
USNRC-RES
MS: NL/S-007

Frank Rowsome
9532 Fern Hollow Way
Gaithersburg, MD 20879

Wayne Russell
SERI
5360 I-55 North
Jackson, MS 39211

Jorma V. Sandberg
Finnish Ctr. Rad. Nucl. and Safety
Department of Nuclear Safety
P.O. Box 268
SF-00101 Helsinki
FINLAND

G. Saponaro
ENEA Nuclear Engineering Alt.
Zia V Brancati 4B
00144 ROME
ITALY

M. Sarran
United Engineers
P. O. Box 8223
30 S 17th Street
Philadelphia, PA 19101

Marty Sattison
EG&G Idaho
P. O. Box 1625
Idaho Falls, ID 83415

George D. Sauter
Electric Power Research Institute
3412 Hillview Avenue
Palo Alto, CA 94303

Jorge Schulz
Bechtel Western Power Corporation
50 Beale Street
San Francisco, CA 94119

B. R. Sehgal
Electric Power Research Institute
3412 Hillview Avenue
Palo Alto, CA 94303

Subir Sen
Bechtel Power Corp.
15740 Shady Grove Road
Location 1A-7
Gaithersburg, MD 20877

S. Serra
Ente Nazionale per l'Energia
Electtrica (ENEL)
via G. B. Martini 3
Rome
ITALY

Bonnie J. Shapiro
Science Applications International Corporation
360 Bay Street
Suite 200
Augusta, GA 30901

H. Shapiro
Licensing and Risk Branch
Atomic Energy of Canada Ltd.
Sheridan Park Research Community
Mississauga, Ontario L5K 1B2
CANADA

Dave Sharp
Westinghouse Savannah River Co.
Building 773-41A, P. O. Box 616
Aiken, SC 29802

John Sherman
Tennessee Environmental Council
1719 West End Avenue, Suite 227
Nashville, TN 37203

Brian Sheron
USNRC-RES/DSR
MS: NL/N-007

Rick Sherry
JAYCOR
P. O. Box 85154
San Diego, CA 92138

Steven C. Sholly
MHB Technical Associates
1723 Hamilton Avenue, Suite K
San Jose, CA 95125

Louis M. Shotkin
USNRC-RES/RPSB
MS: NL/N-353

M. Siebertz
Chef de la Section Surete' des Reacteurs
CEN/SCK
Boeretang, 200
B-2400 Mol
BELGIUM

Melvin Silberberg
USNRC-RES/DE/WNB
MS: NL/S-260

Gary Smith
SERI
5360 I-55 North
Jackson, MS 39211

Gary L. Smith
Westinghouse Electric Corporation
Hanford Site
Box 1970
Richland, WA 99352

Lanny N. Smith
Science Applications International Corporation
2109 Air Park Road SE
Albuquerque, NM 87106

K. Soda
Japan Atomic Energy Res. Inst.
Tokai-Mura Naka-Gun
Ibaraki-Ken 319-11
JAPAN

David Sommers
Virginia Electric Power Company
P. O. Box 26666
Richmond, VA 23261

Herschel Spector
New York Power Authority
123 Main Street
White Plains, NY 10601

Themis P. Speis
USNRC-RES
MS: NL/S-007

Klaus B. Stadie
OECD-NEA, 38 Bld. Suchet
75016 Paris
FRANCE

John Stetkar
Pickard, Lowe & Garrick, Inc.
2216 University Drive
Newport Beach, CA 92660

Wayne L. Stiede
Commonwealth Edison Company
P.O. Box 767
Chicago, IL 60690

William Stratton
Stratton & Associates
2 Acoma Lane
Los Alamos, NM 87544

Soo-Pong Suk
Korea Advanced Energy Research Institute
P. O. Box 7
Daeduk Danji, Chungnam 300-31
KOREA

W. P. Sullivan
GE Nuclear Energy
175 Curtner Ave., M/C 789
San Jose, CA 95125

Tony Taig
U.K. Atomic Energy Authority
Wigshaw Lane, Culcheth
Warrington, Cheshire, WA3 4NE
UNITED KINGDOM

John Taylor
Electric Power Research Institute
3412 Hillview Avenue
Palo Alto, CA 94303

Harry Teague
U.K. Atomic Energy Authority
Wigshaw Lane, Culcheth
Warrington, Cheshire, WA3 4NE
UNITED KINGDOM

Technical Library
Electric Power Research Institute
P.O. Box 10412
Palo Alto, CA 94304

Mark I. Temme
General Electric, Inc.
P.O. Box 3508
Sunnyvale, CA 94088

T. G. Theofanous
University of California, S.B.
Department of Chemical and Nuclear Engineering
Santa Barbara, CA 93106

David Teolis
Westinghouse-Bettis Atomic Power Laboratory
P. O. Box 79, ZAP 34N
West Mifflin, PA 15122-0079

Ashok C. Thadani
USNRC-NRR/SAD
MS: 7E-4

Garry Thomas
L-499 (Bldg. 490)
Lawrence Livermore National Laboratory
7000 East Ave.
P.O. Box 808
Livermore, CA 94550

Gordon Thompson
Institute for Research and Security Studies
27 Ellworth Avenue
Cambridge, MA 02139

Grant Thompson
League of Women Voters
1730 M. Street, NW
Washington, DC 20036

Arthur Tingle
Brookhaven National Laboratory
Building 130
Upton, NY 11973

Rich Toland
United Engineers and Construction
30 S. 17th St., MS 4V7
Philadelphia, PA 19101

Brian J. R. Tolley
DG/XII/D/1
Commission of the European Communities
Rue de la Loi, 200
B-1049 Brussels
BELGIUM

David R. Torgerson
Atomic Energy of Canada Ltd.
Whiteshell Nuclear Research Establishment
Pinawa, Manitoba, ROE 1LO
CANADA

Dr. Alfred F. Torri
1421 Hymettus Avenue
Leucadia, CA 92024

Klau Trambauer
Gesellschaft Fur Reaktorsicherheit
Forschungsgelande
D-8046 Garching
FERERAL REPUBLIC OF GERMANY

Nicholas Tsoulfanidis
Nuclear Engineering Dept.
University of Missouri-Rolla
Rolla, MO 65401-0249

Chao-Chin Tung
c/o H.B. Bengelsdorf
ERC Environmental Services Co.
P. O. Box 10130
Fairfax, VA 22030

Brian D. Turland
UKAEA Culham Laboratory
Abingdon, Oxon OX14 3DB
ENGLAND

Takeo Uga
Japan Institute of Nuclear Safety
Nuclear Power Engineering Test Center
3-6-2, Toranomon
Minato-ku, Tokyo 108
JAPAN

Stephen D. Unwin
Battelle Columbus Division
505 King Avenue
Columbus, OH 43201

A. Valeri
DISP
ENEA
Via Vitaliano Brancati, 48
I-00144 Rome
ITALY

Harold VanderMolen
USNRC-RES/PRAB
MS: NL/S-372

G. Bruce Varnado
ERC International
1717 Louisiana Blvd. NE, Suite 202
Albuquerque, NM 87110

Jussi K. Vaurio
Imatran Voima Oy
Loviisa NPS
SF-07900 Loviisa
FINLAND

William E. Vesely
Science Applications International Corporation
655 Metro Place South, Suite 745
Dubbin, OH 43017

J. I. Villadoniga Tallon
Div. of Analysis and Assessment
Consejo de Seguridad Nuclear
c/ Sor Angela de la Cruz, 3
28020 Madrid
SPAIN

Willem F. Vinck
Kapellestract 25
1980
Tervuren
BELGIUM

R. Virolainen
Office of Systems Integration
Finnish Centre for Radiation and Nuclear Safety
Department of Nuclear Safety
P.O. Box 268
Kumpulantie 7
SF-00520 Helsinki
FINLAND

Raymond Viskanta
School of Mechanical Engineering
Purdue University
West Lafayette, IN 47907

S. Visweswaran
General Electric Company
175 Curtner Avenue
San Jose, CA 95125

Truong Vo
Pacific Northwest Laboratory
Battelle Blvd.
Richland, WA 99352

Richard Vogel
Electric Power Research Institute
P. O. Box 10412
Palo Alto, CA 94303

G. Volta
Engineering Division
CEC Joint Research Centre
CP No. 1
I-21020 Ispra (Varese)
ITALY

Ian B. Wall
Electric Power Research Institute
3412 Hillview Avenue
Palo Alto, CA 94303

Adolf Walser
Sargent and Lundy Engineers
55 E. Monroe Street
Chicago, IL 60603

Edward Warman
Stone & Webster Engineering Corp.
P.O. Box 2325
Boston, MA 02107

Norman Weber
Sargent & Lundy Co.
55 E. Monroe Street
Chicago, IL 60603

Lois Webster
American Nuclear Society
555 N. Kensington Avenue
La Grange Park, IL 60525

Wolfgang Werner
Gesellschaft Fur Reaktorsicherheit
Forschungsgelande
D-8046 Garching
FEDERAL REPUBLIC OF GERMANY

Don Wesley
IMPELL
1651 East 4th Street
Suite 210
Santa Ana, CA 92701

Detlof von Winterfeldt
Institute of Safety and Systems Management
University of Southern California
Los Angeles, CA 90089-0021

Pat Worthington
USNRC-RES/AEB
MS: NL/N-344

John Wreathall
Science Applications International Corporation
655 Metro Place South, Suite 745
Dubbin, OH 43017

D. J. Wren
Atomic Energy of Canada Ltd.
Whiteshell Nuclear Research Establishment
Pinawa, Manitoba, ROE 1LO
CANADA

Roger Wyrick
Inst. for Nuclear Power Operations
1100 Circle 75 Parkway, Suite 1500
Atlanta, GA 30339

Kun-Joong Yoo
Korea Advanced Energy Research Institute
P. O. Box 7
Daeduk Danji, Chungnam 300-31
KOREA

Faith Young
Energy People, Inc.
Dixou Springs, TN 37057

Jonathan Young
R. Lynette and Associates
15042 Northeast 40th St.
Suite 206
Redmond, WA 98052

C. Zaffiro
Division of Safety Studies
Directorate for Nuclear Safety and Health Protection
Ente Nazionale Energie Alternative
Via Vitaliano Brancati, 48
I-00144 Rome
ITALY

Mike Zentner
Westinghouse Hanford Co.
P. O. Box 1970
Richland, WA 99352

X. Zikidis
Greek Atomic Energy Commission
Agia Paraskevi, Attiki
Athens
GREECE

Bernhard Zuczera
Kernforschungszentrum
Postfach 3640
D-7500 Karlsruhe
FEDERAL REPUBLIC OF GERMANY

1521 J. R. Weatherby
3141 S. A. Landenberger [5]
3151 W. I. Klein
5214 D. B. Clauss
6344 E. D. Gorham
6001 D. D. Carlson
6001 R. J. Breeding
6001 D. M. Kunsman
6400 D. J. McCloskey
6410 D. A. Dahlgren
6412 A. L. Camp
6412 S. L. Daniel
6412 T. M. Hake
6412 L. A. Miller
6412 D. B. Mitchell
6412 A. C. Payne, Jr.
6412 T. T. Sype
6412 T. A. Wheeler
6412 D. W. Whitehead
6413 T. D. Brown
6413 F. T. Harper [2]
6415 R. M. Cranwell
6415 W. R. Cramond [3]
6415 R. L. Iman
6418 J. E. Kelly
6418 K. J. Maloney
6419 M. P. Bohn
6419 J. A. Lambright
6422 D. A. Powers
6424 K. D. Bergeron
6424 J. J. Gregory
6424 D. R. Bradley
6424 D. C. Williams
6425 S. S. Dosanjh
6453 J. S. Philbin
6500 A. W. Snyder
6510 J. V. Walker
6517 M. Berman
6517 M. P. Sherman
6521 L. D. Bustard
6523 W. A. von Riesemann
8524 J. A. Wackerly

NRC FORM 335 (2-89) NRCM 1102, 3201, 3202

U.S. NUCLEAR REGULATORY COMMISSION

BIBLIOGRAPHIC DATA SHEET

(See instructions on the reverse)

1. REPORT NUMBER (Assigned by NRC, Add Vol., Supp., Rev., and Addendum Numbers, if any.)

NUREG/CR-4550
SAND86-2084
Vol. 4, Rev. 1, Part 3

2. TITLE AND SUBTITLE

Analysis of Core Damage Frequency: Peach Bottom, Unit 2
External Events

3. DATE REPORT PUBLISHED

MONTH: December
YEAR: 1990

4. FIN OR GRANT NUMBER

A-1228

5. AUTHOR(S)

J.A. Lambright, M.P. Bohn, S.L. Daniel, J.J. Johnson*,
M.K. Ravindra*, P.O. Hashimoto*, M.J. Mraz*, W.H. Tong*,
D.A. Brosseau**
*EQE, Incorporated
**ERCE, Inc.

6. TYPE OF REPORT

Technical

7. PERIOD COVERED (Inclusive Dates)

8. PERFORMING ORGANIZATION – NAME AND ADDRESS (If NRC, provide Division, Office or Region, U.S. Nuclear Regulatory Commission, and mailing address; if contractor, provide name and mailing address.)

Sandia National Laboratories
Albuquerque, NM 87185-5800

9. SPONSORING ORGANIZATION – NAME AND ADDRESS (If NRC, type "Same as above"; if contractor, provide NRC Division, Office or Region, U.S. Nuclear Regulatory Commission, and mailing address.)

Division of Systems Research
Office of Nuclear Regulatory Research
US Nuclear Regulatory Commission
Washington, DC 20555

10. SUPPLEMENTARY NOTES

11. ABSTRACT (200 words or less)

This report presents the analysis of external events (earthquakes, fires, floods, etc.) performed for the Peach Bottom Atomic Power Station as part of the USNRC-sponsored NUREG-1150 program. Both the internal and external events analyses make full use of recent insights and developments in risk assessment methods. In addition, the external event analyses make use of newly-developed simplified methods.

As a first step, a screening analysis was performed which showed that all external events were negligible except for fires and seismic events. Subsequent detailed analysis of fires resulted in a total (mean) core damage frequency of 1.95E-5 per year. The seismic analysis resulted in a total (mean) core damage frequency of 7.66E-5 per year using hazard curves developed by Lawrence Livermore National Laboratory and 3.09E-6 per year using hazard curves developed by the Electric Power Research Institute. Uncertainty analyses were performed, and dominant components and sources of uncertainty were identified.

12. KEY WORDS/DESCRIPTORS (List words or phrases that will assist researchers in locating the report.)

Probabilistic Risk Assessment (PRA)
External Hazards
safety analysis
uncertainty analysis
accident sequence analysis

13. AVAILABILITY STATEMENT

Unlimited

14. SECURITY CLASSIFICATION

(This Page) Unclassified
(This Report) Unclassified

15. NUMBER OF PAGES

16. PRICE

NRC FORM 335 (2-89)